



**Syntheses of 7-*O*-Methylnigrosporolide, Pestalotioprolide D,  
Nigrosporolide, Mutolide and (4*S*,7*S*,13*S*)-4,7-Dihydroxy-13-  
tetradeca-2,5,8-trienolide**

**Aticha Thiraporn**

**A Thesis Submitted in Partial Fulfillment of the Requirements for the  
Degree of Doctor of Philosophy in Chemistry (International Program)**

**Prince of Songkla University**

**2023**

**Copyright of Prince of Songkla University**



**Syntheses of 7-*O*-Methylnigrosporolide, Pestalotioprolide D,  
Nigrosporolide, Mutolide and (4*S*,7*S*,13*S*)-4,7-Dihydroxy-13-  
tetradeca-2,5,8-trienolide**

**Aticha Thiraporn**

**A Thesis Submitted in Partial Fulfillment of the Requirements for the  
Degree of Doctor of Philosophy in Chemistry (International Program)**

**Prince of Songkla University**

**2023**

**Copyright of Prince of Songkla University**

**Thesis Title**            Syntheses of 7-*O*-Methylnigrosporolide, Pestalotioprolide D, Nigrosporolide, Mutolide and (4*S*,7*S*,13*S*)-4,7-Dihydroxy-13-tetradeca-2,5,8-trienolide

**Author**                    Miss Aticha Thiraporn

**Major Program**        Chemistry

---

**Major Advisor**

.....  
 (Assoc. Prof. Dr. Kwanruthai Tadpetch)

**Examining Committee :**

.....Chairperson  
 (Prof. Dr. Tirayut Vilaivan)

.....Committee  
 (Assoc. Prof. Dr. Darunee Soorukram)

.....Committee  
 (Assoc. Prof. Dr. Kwanruthai Tadpetch)

.....Committee  
 (Assoc. Prof. Dr. Juthanat Kaeobamrung)

.....Committee  
 (Asst. Prof. Dr. Chittreeya Tansakul)

The Graduate School, Prince of Songkla University, has approved this thesis as partial fulfillment of the requirements for the Doctor of Philosophy Degree in Chemistry.

.....  
 (Asst. Prof. Dr. Thakerng Wongsirichot)

Acting Dean of Graduate School

This is to certify that the work here submitted is the result of the candidate's own investigations. Due acknowledgement has been made of any assistance received.

.....Signature  
(Assoc. Prof. Dr. Kwanruthai Tadpetch)  
Major Advisor

.....Signature  
(Miss Aticha Thiraporn)  
Candidate



I hereby certify that this work has not been accepted in substance for any degree, and is not being currently submitted in candidature for any degree.

.....Signature

(Miss Aticha Thiraporn)

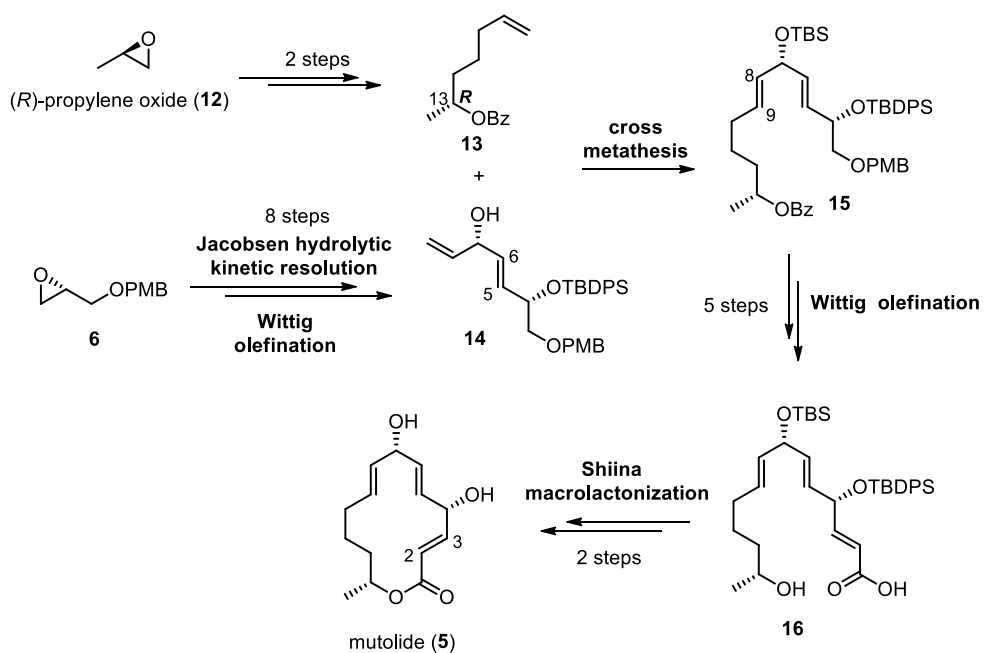
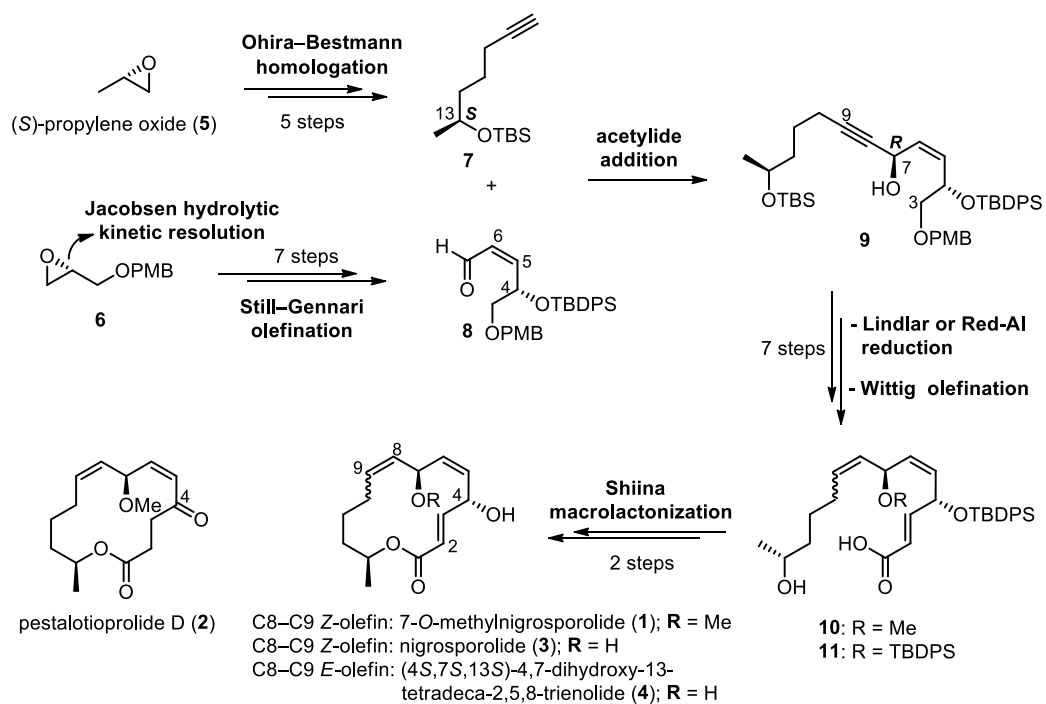
Candidate

ชื่อวิทยานิพนธ์	การสังเคราะห์ 7- <i>O</i> -methylnigrosporolide pestalotioprolide D nigrosporolide mutolide และ (4 <i>S</i> ,7 <i>S</i> ,13 <i>S</i> )-4,7-dihydroxy-13- tetradeca-2,5,8-trienolide
ผู้เขียน	นางสาวอริษา ธีระพร
สาขาวิชา	เคมี
ปีการศึกษา	2565

### บทคัดย่อ

7-*O*-methylnigrosporolide (1) pestalotioprolide D (2) nigrosporolide (3) (4*S*,7*S*,13*S*)-4,7-dihydroxy-13-tetradeca-2,5,8-trienolide (4) และ mutolide (5) เป็นสารผลิตภัณฑ์ธรรมชาติในกลุ่ม macrolide วง 14 เหลี่ยม ซึ่งแยกได้จากเชื้อราหลายชนิด โครงสร้างหลักของสาร 1 และ 3-5 ประกอบด้วยวงแลคโตน 14 เหลี่ยมที่มีพันธะคู่แบบ *E* ที่ตำแหน่ง 2-3 รวมถึงพันธะคู่แบบ *Z* หรือ *E* ที่ตำแหน่ง 5-6 และ 8-9 และมีไครัลคาร์บอนที่ตำแหน่ง 4 7 และ 13 ส่วนสาร 2 มีโครงสร้างคล้ายกับสาร 1 แต่ 2 มีหมู่คีโตนที่ตำแหน่ง 4 และพันธะเดี่ยวที่ตำแหน่ง 2-3 เนื่องจากสารผลิตภัณฑ์ธรรมชาติ 1-5 มีฤทธิ์ทางชีวภาพที่น่าสนใจและยังไม่เคยมีรายงานการสังเคราะห์ที่สมบูรณ์มาก่อน งานวิจัยนี้จึงเป็นการสังเคราะห์สาร 1-5 เพื่อยืนยันสเตอริโอเคมีสมบูรณ์ของสารผลิตภัณฑ์ธรรมชาติและเพื่อนำไปทดสอบฤทธิ์ทางชีวภาพอื่นเพิ่มเติม โดยปฏิกิริยาหลักที่สำคัญในการสังเคราะห์คือ Shiina macrolactonization เพื่อปิดวงแลคโตน 14 เหลี่ยมของสารสังเคราะห์ 1-5 สำหรับพันธะคู่แบบ *E* ที่ตำแหน่ง 2-3 ของสาร 1 และ 3-5 สร้างได้จากปฏิกิริยา Wittig olefination ส่วนพันธะคู่แบบ *Z* และ *E* ที่ตำแหน่ง 8-9 ของสาร 1-4 ทำได้จากปฏิกิริยา Lindlar และ Red-Al reduction ของ propargylic alcohol 9 ตามลำดับ ซึ่ง 9 สังเคราะห์ได้จากปฏิกิริยา acetylide addition ระหว่าง (*S*)-*tert*-butyl(hept-6-yn-2-yloxy)dimethylsilane (7) และ (*Z*)-enal 8 โดยในขั้นตอนนี้สามารถสร้างพันธะใหม่ที่ตำแหน่ง 7 และ 8 และสร้างไครัลคาร์บอนตำแหน่งที่ 7 ได้ สำหรับการสังเคราะห์ (*S*)-alkyne 7 ทำได้ใน 5 ขั้นตอนโดยใช้ (*S*)-propylene oxide (5) เป็นสารตั้งต้น ขณะที่ (*Z*)-enal 8 สามารถเตรียมได้ใน 7 ขั้นตอนโดยเริ่มจาก (*S*)-benzyl glycidyl ether (6) ซึ่งไครัลคาร์บอนตำแหน่งที่ 4 และพันธะคู่แบบ *Z* ที่ตำแหน่ง 5-6 ของสาร 8 สังเคราะห์ได้จากปฏิกิริยาหลักคือ Jacobsen hydrolytic kinetic resolution และ Still-Gennari olefination ตามลำดับ สำหรับการสังเคราะห์ mutolide (5) ทำได้โดยใช้แนวทางที่คล้ายกับสาร 4 แต่ใช้ปฏิกิริยา cross metathesis ระหว่าง (*R*)-hept-6-en-2-yl benzoate (13) และ chiral allylic alcohol 14 ในการสร้างพันธะคู่แบบ *E* ที่ตำแหน่ง 8-9 ซึ่งการสังเคราะห์ alkene 13 ทำได้ใน 2 ขั้นตอน

และใช้ (*R*)-propylene oxide (**12**) เป็นสารตั้งต้น ส่วน chiral allylic alcohol **14** สามารถเตรียมได้ใน 8 ขั้นตอนโดยเริ่มจากสาร **6** ซึ่งใช้ปฏิกิริยาหลักเดียวกันกับการสังเคราะห์ (*Z*)-enal **8** ยกเว้นการสร้างพันธะคู่แบบ *E* ที่ตำแหน่ง 5–6 ทำได้จากปฏิกิริยา Wittig olefination กลุ่มวิจัยของเราพบว่าหมู่ *tert*-butyldiphenylsilyl (TBDPS) ที่คาร์บอนตำแหน่งที่ 4 ของวงแลคโตน **14** เหลี่ยมเป็นหมู่ป้องกันที่เหมาะสมซึ่งสามารถกำจัดออกได้ง่ายในขั้นตอนสุดท้าย นอกจากนี้ยังพบว่า pestalotioprolide D (**2**) อาจเป็นอนุพันธ์ของ 7-*O*-methylnigrosporolide (**1**) โดยเกิดผ่านปฏิกิริยา 1,2-hydride shift สำหรับการสังเคราะห์สาร **1–4** เสร็จสมบูรณ์ได้ในทั้งหมด 22 ขั้นตอนและ 17 ขั้นตอนของเส้นทางที่ยาวที่สุดแบบเส้นตรงและได้ร้อยละผลิตภัณฑ์โดยรวมเป็น 1.7 2.6 1.8 และ 1.1 ตามลำดับ ส่วนการสังเคราะห์สาร **5** เสร็จสมบูรณ์ได้ในทั้งหมด 18 ขั้นตอนและ 16 ขั้นตอนของเส้นทางที่ยาวที่สุดแบบเส้นตรงโดยมีร้อยละผลิตภัณฑ์โดยรวมเป็น 1.5 จากการวิเคราะห์ข้อมูล <sup>1</sup>H และ <sup>13</sup>C NMR ค่ามวลของสารแบบความละเอียดสูงและค่าการหมุนระนาบแสงโพลาไรซ์ของสารสังเคราะห์ **1–5** เทียบกับสารผลิตภัณฑ์ธรรมชาติพบว่ามีค่าใกล้เคียงกันมาก ดังนั้นจึงสามารถยืนยันสเตอริโอเคมีสมบูรณ์ของสารผลิตภัณฑ์ธรรมชาติทุกตัวได้ จากการทดสอบฤทธิ์ความเป็นพิษต่อเซลล์มะเร็งในมนุษย์ 6 ชนิดของสารสังเคราะห์ **1** และ **2** ซึ่งประกอบด้วยเซลล์มะเร็งเต้านมชนิด MDA-MB-231 และ MCF-7 เซลล์มะเร็งปากมดลูกชนิด C33A HeLa และ SiHa รวมถึงเซลล์มะเร็งลำไส้ชนิด HCT116 พบว่า pestalotioprolide D (**2**) แสดงฤทธิ์ยับยั้งเซลล์มะเร็งทุกชนิดในระดับที่ดีกว่า 7-*O*-methylnigrosporolide (**1**) นอกจากนี้สาร **1** และ **2** ยังแสดงฤทธิ์ยับยั้งเซลล์มะเร็งปากมดลูกชนิด SiHa ได้ดีที่สุดเมื่อเทียบกับเซลล์มะเร็งชนิดอื่นๆที่ทดสอบด้วยค่า IC<sub>50</sub> เท่ากับ 35.17 ± 10.77 μM และ 8.90 ± 2.51 μM ตามลำดับ สำหรับสารสังเคราะห์ **3–5** ได้นำไปทดสอบฤทธิ์ความเป็นพิษต่อเซลล์มะเร็งในมนุษย์ทั้งหมด 3 ชนิด ซึ่งประกอบด้วยเซลล์ HCT116 MCF-7 และเซลล์มะเร็งปอดชนิด Calu-3 รวมถึงการทดสอบฤทธิ์ในการยับยั้งการหลั่งคลอไรด์ที่ใช้ cystic fibrosis transmembrane conductance regulator (CFTR) เป็นสื่อกลางในเซลล์เยื่อบุผิวในลำไส้ (T84) ของมนุษย์ พบว่า mutolide (**5**) แสดงฤทธิ์ยับยั้งเซลล์มะเร็งลำไส้ชนิด HCT116 อย่างมีนัยสำคัญด้วยค่า IC<sub>50</sub> ประมาณ 12 μM และมีฤทธิ์ในการยับยั้งการหลั่งคลอไรด์ที่ใช้ CFTR เป็นสื่อกลางในระดับที่ดีด้วยค่า IC<sub>50</sub> ประมาณ 1 μM แต่สาร **3** และ **4** ไม่แสดงฤทธิ์ความเป็นพิษต่อเซลล์มะเร็งในมนุษย์ที่ทดสอบทั้งหมด และมีฤทธิ์ในการยับยั้งการหลั่งคลอไรด์ใน CFTR ที่มีประสิทธิภาพน้อยกว่าสาร **5**

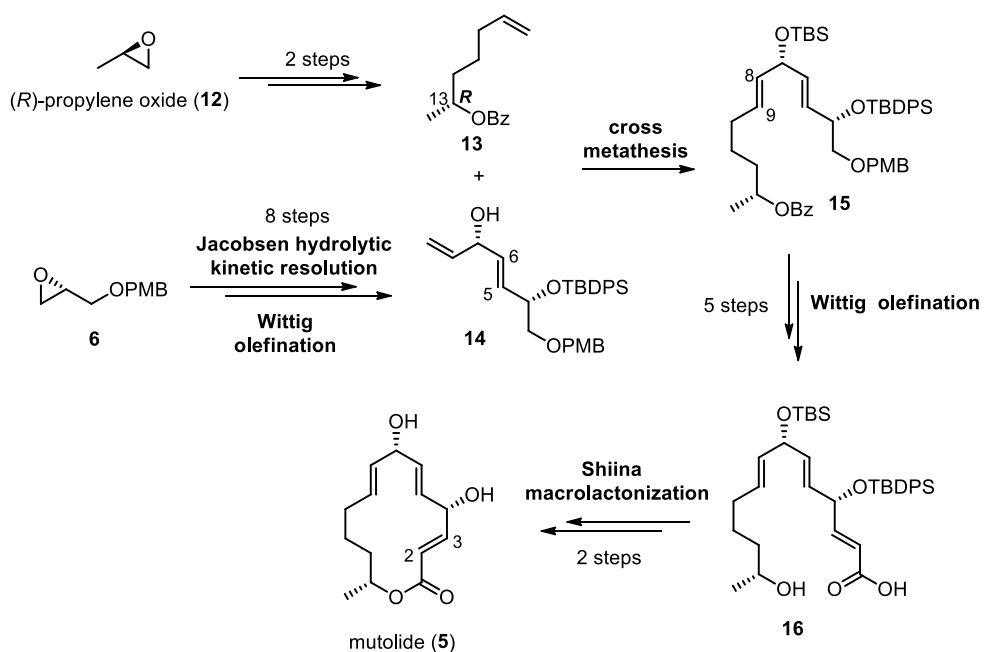
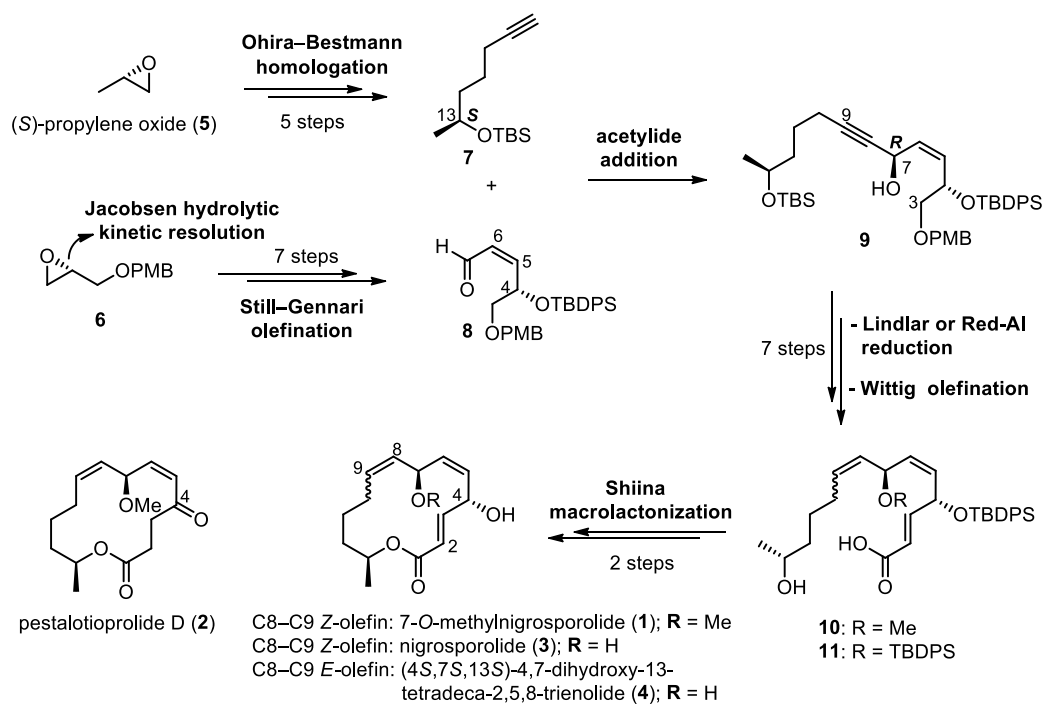


<b>Thesis Title</b>	Syntheses of 7- <i>O</i> -Methylnigrosporolide, Pestalotioprolide D, Nigrosporolide, Mutolide and (4 <i>S</i> ,7 <i>S</i> ,13 <i>S</i> )-4,7-Dihydroxy-13-tetradeca-2,5,8-trienolide
<b>Author</b>	Miss Aticha Thiraporn
<b>Major Program</b>	Chemistry
<b>Academic Year</b>	2022

### ABSTRACT

7-*O*-Methylnigrosporolide (**1**), pestalotioprolide D (**2**), nigrosporolide (**3**), (4*S*,7*S*,13*S*)-4,7-dihydroxy-13-tetradeca-2,5,8-trienolide (**4**) and mutolide (**5**) are 14-membered macrolides isolated from various strains of fungi. The core structure of compounds **1** and **3–5** consists of a 14-membered macrolactone with *E*-olefin at C2–C3 and *Z*- or *E*-double bond at C5–C6 and C8–C9 as well as three alcohol stereogenic centers at the 4, 7 and 13 positions. The structure of **2** is nearly identical to **1** but **2** contains one ketone functional group at the C4-position and saturation at C2–C3. Due to the promising biological activities of this class of natural products and unprecedented total syntheses of **1–5**, this work involves the syntheses of these natural products to confirm the absolute configurations as well as to further evaluation of biological activities. The key strategy of our synthesis relied on Shiina macrolactonization to assemble 14-membered macrolactone of targets **1–5**. The C2–C3 *E*-olefin moiety of macrolides **1** and **3–5** was constructed via Wittig olefination. The C8–C9 *Z*- and *E*-alkenes of **10** and **11** for the synthesis of **1–4** were generated from Lindlar and Red-Al reduction of propargylic alcohol **9**, respectively. Propargylic alcohol intermediate **9** was synthesized by addition of the corresponding acetylide of (*S*)-*tert*-butyl(hept-6-yn-2-yloxy)dimethylsilane (**7**) to (*Z*)-enal **8** to form the C7–C8 bond and install the C7 alcohol stereogenic center. The synthesis of (*S*)-alkyne **7** was accomplished in 5 steps from (*S*)-propylene oxide (**5**), while (*Z*)-enal **8** was prepared from (*S*)-benzyl glycidyl ether (**6**) in 7 steps using Jacobsen hydrolytic kinetic resolution (HKR) to install the stereogenic center at the C4-position and Still–Gennari olefination to generate C5–C6 *Z*-olefin as the key strategies. The synthesis of mutolide (**5**) was accomplished via the

similar synthetic procedure as that of **4** but the *E*-double bond at C8–C9 was constructed via cross metathesis between (*R*)-hept-6-en-2-yl benzoate (**13**) and chiral allylic alcohol **14**. Alkene **13** was synthesized in 2 steps from (*R*)-propylene oxide (**12**). Chiral allylic alcohol **14** was prepared in 8 steps via the similar synthetic sequence as (*Z*)-enal **8** except for the formation of *E*-alkene at C5–C6, which was achieved via Wittig olefination. Our research group found that the *tert*-butyldiphenylsilyl (TBDPS) group was a suitable protecting group for the C4 hydroxy group of the macrocyclic intermediates, which allowed for smooth final deprotection. In addition, our synthesis led to the hypothesis that macrolide pestalotioprolide D (**2**) might be an artifact from a facile 1,2-hydride shift of 7-*O*-methylnigrosporolide (**1**). The syntheses of macrolides **1–4** were accomplished in a longest linear sequence of 17 steps and total of 22 steps and 1.7%, 2.6%, 1.8%, 1.1% overall yields, respectively. The synthetic **5** was obtained in a longest linear sequence of 16 steps and a total of 18 steps in 1.5% overall yield. The <sup>1</sup>H and <sup>13</sup>C NMR spectroscopic data, HRMS data as well as specific rotation of synthetic compounds **1–5** were in excellent agreement with those reported, which confirmed the assigned absolute configurations of the natural products. Cytotoxic activities of synthetic 7-*O*-methylnigrosporolide (**1**) and pestalotioprolide D (**2**) against six human cancer cell lines consisting of two breast adenocarcinoma (MDA-MB-231 and MCF-7), three cervical carcinoma (C33A, HeLa and SiHa) and one colorectal carcinoma (HCT116) cell lines were evaluated. Compound **2** showed more potent cytotoxic activities against these cancer cell lines than **1**. Moreover, the SiHa cervical cancer cell line was the most sensitive cell line to synthetic **1** and **2** with IC<sub>50</sub> values of 35.17 ± 10.77 μM and 8.90 ± 2.51 μM, respectively. Synthetic compounds **3–5** were tested for their cytotoxic activities against three cancer cell lines, including HCT116, MCF-7 and Calu-3 lung adenocarcinoma cell lines as well as their inhibitory effect on cystic fibrosis transmembrane conductance regulator (CFTR)-mediated chloride secretion in human intestinal epithelial (T84) cells. Mutolide (**5**) showed significant cytotoxic activity against HCT116 colon cancer cells with an IC<sub>50</sub> value of ~12 μM. Moreover, **5** also exhibited potent CFTR inhibitory effect with an IC<sub>50</sub> value of ~1 μM. However, macrolides **3** and **4** displayed no cytotoxic effects on three cancer cell lines and showed inhibitory effects on the CFTR channels with less efficacy compared to **5**.



## ACKNOWLEDGEMENT

First and foremost, I would like to express my sincere gratitude to my advisor, Assoc. Prof. Dr. Kwanruthai Tadpetch, for her support, encouragement and constant guidance. I have benefited greatly from her wealth of knowledge. She gives me valuable experience and helps me grow both as an organic chemist and as a person.

Besides my advisor, I am extremely thankful to my dissertation committee members, Prof. Dr. Tirayut Vilaivan, Assoc. Prof. Dr. Darunee Soorukram, Assoc. Prof. Dr. Juthanat Kaeobamrung and Asst. Prof. Dr. Chittreeya Tansakul for taking the time to oversee my thesis and their helpful suggestion.

I also would like to thank Dr. Panata Iawsipo, Department of Biochemistry, Faculty of Science, Burapha University, and Prof. Dr. Chatchai Muanprasat of Chakri Naruebodindra Medical Institute, Faculty of Medicine Ramathibodi Hospital, Mahidol University for biological activities evaluation.

I would like to give special thanks to Assoc. Prof. Dr. Thitima Rujiralai, Department of Chemistry, Faculty of Science, Prince of Songkla University, for assistance in HPLC experiments.

I am very grateful to Science Achievement Scholarship of Thailand (SAST) for scholarship. The Graduate School, Prince of Songkla University and the Center of Excellence for Innovation in Chemistry (PERCH-CIC) as well as the Potential Scholars in Research and Innovation to Enhance the Economic, Social and Community Sectors (Talent Utilization) are appreciatively acknowledged for partial support.

Last, but not at least, I would like to collectively thank members of Ch416 and Ch418 laboratories, my family and friends who endured this long process with me, always offering support and love. This thesis would not have been possible without all of you. Thank you all for the strength you gave me.

Aticha Thiraporn



## CONTENTS

		<b>Page</b>
บทคัดย่อ		v
ABSTRACT		viii
ACKNOWLEDGEMENT		xi
CONTENTS		xii
LIST OF TABLES		xiv
LIST OF FIGURES		xvi
LIST OF SCHEMES		xxiii
LIST OF ABBREVIATIONS AND SYMBOLS		xxv
LIST OF PUBLICATION		xxviii
COPYRIGHT PERMISSION NOTICE		xxix
CHAPTER 1	INTRODUCTION	1
	1.1 Introduction	2
	1.2 Objectives	21
CHAPTER 2	SYNTHESES OF 7- <i>O</i> -METHYLNIGROSPOROLIDE, PESTALOTIOPROLIDE D AND NIGROSPOROLIDE	22
	2.1 Results and Discussion	23
	2.2 Conclusions	45
CHAPTER 3	SYNTHESES OF MUTOLIDE AND (4 <i>S</i> ,7 <i>S</i> ,13 <i>S</i> )-4,7- DIHYDROXY-13-TETRADECA-2,5,8-TRIENOLIDE AND BIOLOGICAL ACTIVITIES OF SYNTHETIC MACROLIDES	47
	3.1 Results and Discussion	48
	3.2 Conclusions	73
CHAPTER 4	EXPERIMENTAL	75
	4.1 General Information	76
	4.2 Experimentals and Characterization Data	77
	4.2.1 General procedure for epoxide ring opening/ TBS protection	77

**CONTENTS (Continued)**

	<b>Page</b>
4.2.2 General procedure for hydroboration-oxidation	77
4.2.3 General procedure for Ohira–Bestmann homologation	78
4.2.4 General procedure for acetylide addition	78
4.2.5 General procedure for MnO <sub>2</sub> oxidation	78
4.2.6 General procedure for PMB deprotection	78
4.2.7 General procedure for TEMPO/PhI(OAc) <sub>2</sub> - mediated oxidation	79
4.2.8 General procedure for Wittig olefination	79
4.2.9 General procedure for TBS deprotection	79
4.2.10 General procedure for hydrolysis	80
4.2.11 General procedure for Shiina macrolactonization	80
4.2.12 General procedure for global desilylation	80
4.2.13 General procedure for TBDPS protection	81
4.2.14 General procedures for Zn-mediated asymmetric alkynylation reaction	81
CYTOTOXICITY ASSAY	134
REFERENCES	136
APPENDIX	148
Publication	149
<sup>1</sup> H and <sup>13</sup> C NMR Spectra	164
HPLC trace	228
VITAE	231

## LIST OF TABLES

Table		Page
1	Screening of Zn-mediated asymmetric alkynylation reaction to assemble ( <i>S</i> )-alkyne <b>106</b> and ( <i>Z</i> )-enal <b>117</b>	31
2	Screening of stereoselective CBS reduction of ynone <b>160</b>	33
3	Screening for Mitsunobu inversion of propargylic alcohol <b>116S</b>	34
4	Screening for silyl deprotection conditions of <b>167</b>	39
5	Comparison of <sup>1</sup> H and <sup>13</sup> C NMR data for natural product and synthetic <b>19</b>	41
6	Comparison of <sup>1</sup> H and <sup>13</sup> C NMR data for natural product and synthetic <b>20</b>	42
7	Comparison of <sup>1</sup> H and <sup>13</sup> C NMR data for natural product and synthetic <b>21</b>	45
8	Comparison of <sup>1</sup> H and <sup>13</sup> C NMR data for natural product and synthetic <b>23</b>	53
9	Screening of Zn-mediated asymmetric alkynylation reaction to assemble ( <i>R</i> )-alkyne <i>epi</i> - <b>106</b> and ( <i>E</i> )-enal <b>180</b>	56
10	Screening of stereoselective CBS reduction of ynone <b>191</b>	58
11	Screening of Red-Al-mediated ( <i>E</i> )-selective reductions of alkyne <b>179R</b>	59
12	Screening of stereoselective CBS reduction of enone <b>198</b>	62
13	Screening of Mitsunobu inversion of chiral allylic alcohol <b>196R</b>	63
14	Comparison of <sup>1</sup> H and <sup>13</sup> C NMR data for natural product and synthetic <b>22</b>	66
15	Cytotoxic activity of 7- <i>O</i> -methylnigrosporolide ( <b>19</b> ) and pestalotioprolide D ( <b>20</b> ) against six human cancer cell lines	68
16	$\Delta\delta$ ( $\delta_S - \delta_R$ ) data for the ( <i>S</i> )- and ( <i>R</i> )-MTPA-Mosher esters of allylic alcohol <b>132</b>	87
17	$\Delta\delta$ ( $\delta_S - \delta_R$ ) data for the ( <i>S</i> )- and ( <i>R</i> )-MTPA-Mosher esters of propargylic alcohol <b>116R</b>	93

**LIST OF TABLES (Continued)**

<b>Table</b>		<b>Page</b>
<b>18</b>	$\Delta\delta$ ( $\delta_S - \delta_R$ ) data for the ( <i>S</i> )- and ( <i>R</i> )-MTPA-Mosher esters of propargylic alcohol <b>116S</b>	95
<b>19</b>	$\Delta\delta$ ( $\delta_S - \delta_R$ ) data for the ( <i>S</i> )- and ( <i>R</i> )-MTPA-Mosher esters of allylic alcohol <b>196S</b>	124
<b>20</b>	$\Delta\delta$ ( $\delta_S - \delta_R$ ) data for the ( <i>S</i> )- and ( <i>R</i> )-MTPA-Mosher esters of allylic alcohol <b>196R</b>	126

## LIST OF FIGURES

<b>Figure</b>		<b>Page</b>
<b>1</b>	Examples of 14-membered macrolides containing sugar moiety	4
<b>2</b>	Examples of 14-membered macrolides lacking sugar moiety	4
<b>3</b>	Structures of 7- <i>O</i> -methylnigrosporolide ( <b>19</b> ), pestalotioprolide D ( <b>20</b> ), nigrosporolide ( <b>21</b> ), mutolide ( <b>22</b> ) and (4 <i>S</i> ,7 <i>S</i> ,13 <i>S</i> )-4,7-dihydroxy-13-tetradeca-2,5,8-trienolide ( <b>23</b> )	7
<b>4</b>	Key bond formations in the syntheses of 14-membered unsaturated macrolides containing <i>E</i> -alkene at C2–C3 and <i>Z</i> - or <i>E</i> -double bonds at C5–C6 and C8–C9	8
<b>5</b>	Structures of 7- <i>O</i> -methylnigrosporolide ( <b>19</b> ), pestalotioprolide D ( <b>20</b> ), nigrosporolide ( <b>21</b> ), mutolide ( <b>22</b> ) and (4 <i>S</i> ,7 <i>S</i> ,13 <i>S</i> )-4,7-dihydroxy-13-tetradeca-2,5,8-trienolide ( <b>23</b> )	67
<b>6</b>	Viability of cells treated with synthetic compounds <b>21–23</b> or afatinib at 10 $\mu$ M for 24 h determined by the MTT assay. Results are shown in percentage of cell viability relative to untreated cells.	70
<b>7</b>	Viability of A) HCT116 cells, B) MCF-7 cells, C) Calu-3 cells and D) Vero cells treated with synthetic compounds <b>21–23</b> at indicated concentrations for 24 h determined by the MTT assay. *, **, *** and **** indicated the <i>p</i> -values of <0.05, <0.01, <0.005 and <0.001, respectively ( <i>n</i> =3) (One-way analysis of variance).	70
<b>8</b>	Viability of HCT116 cells treated with synthetic compounds <b>21–23</b> after A) 24 h, B) 48 h and C) 72 h of incubations at indicated concentrations for 24 h determined by the MTT assay. *, **, *** and **** indicated the <i>p</i> -values of <0.05, <0.01, <0.005 and <0.001, respectively ( <i>n</i> =3) (One-way analysis of variance).	71

## LIST OF FIGURES (Continued)

Figure		Page
9	Evaluation of effects of compounds <b>21–23</b> (5 $\mu$ M) on CFTR-mediated chloride secretion in T84 cells. Forskolin (20 $\mu$ M) was used to stimulate the CFTR-mediated chloride secretion. CFTRInh-172 (20 $\mu$ M) was used as a positive control. Representative tracings of 3 experiments are shown.	72
10	Evaluation of potency of synthetic mutolide ( <b>22</b> ) on CFTR-mediated chloride secretion on human intestinal epithelial (T84) cells. (Left) A representative current tracing of 3 experiments. (Right) Summary of the data. Data were fitted to Hill's equation.	73
11	$^1\text{H}$ NMR (300 MHz, $\text{CDCl}_3$ ) spectrum of compound <b>128</b>	164
12	$^{13}\text{C}$ NMR (75 MHz, $\text{CDCl}_3$ ) spectrum of compound <b>128</b>	164
13	$^1\text{H}$ NMR (300 MHz, $\text{CDCl}_3$ ) spectrum of compound <b>129</b>	165
14	$^{13}\text{C}$ NMR (75 MHz, $\text{CDCl}_3$ ) spectrum of compound <b>129</b>	165
15	$^1\text{H}$ NMR (300 MHz, $\text{CDCl}_3$ ) spectrum of compound <b>126</b>	166
16	$^{13}\text{C}$ NMR (75 MHz, $\text{CDCl}_3$ ) spectrum of compound <b>126</b>	166
17	$^1\text{H}$ NMR (300 MHz, $\text{CDCl}_3$ ) spectrum of compound <b>106</b>	167
18	$^{13}\text{C}$ NMR (75 MHz, $\text{CDCl}_3$ ) spectrum of compound <b>106</b>	167
19	$^1\text{H}$ NMR (300 MHz, $\text{CDCl}_3$ ) spectrum of compound <b>131</b>	168
20	$^{13}\text{C}$ NMR (75 MHz, $\text{CDCl}_3$ ) spectrum of compound <b>131</b>	168
21	$^1\text{H}$ NMR (300 MHz, $\text{CDCl}_3$ ) spectrum of compound <b>132</b>	169
22	$^{13}\text{C}$ NMR (75 MHz, $\text{CDCl}_3$ ) spectrum of compound <b>132</b>	169
23	$^1\text{H}$ NMR (300 MHz, $\text{CDCl}_3$ ) spectrum of ( <i>S</i> )-MTPA ester of ( <i>S</i> )- <b>132</b>	170
24	$^1\text{H}$ NMR (300 MHz, $\text{CDCl}_3$ ) spectrum of ( <i>R</i> )-MTPA ester of ( <i>S</i> )- <b>132</b>	170
25	$^1\text{H}$ NMR (300 MHz, $\text{CDCl}_3$ ) spectrum of compound <b>133</b>	171
26	$^{13}\text{C}$ NMR (75 MHz, $\text{CDCl}_3$ ) spectrum of compound <b>133</b>	171
27	$^1\text{H}$ NMR (300 MHz, $\text{CDCl}_3$ ) spectrum of compound <b>134</b>	172
28	$^{13}\text{C}$ NMR (75 MHz, $\text{CDCl}_3$ ) spectrum of compound <b>134</b>	172
29	$^1\text{H}$ NMR (300 MHz, $\text{CDCl}_3$ ) spectrum of compound <b>135</b>	173

## LIST OF FIGURES (Continued)

Figure		Page
30	$^{13}\text{C}$ NMR (75 MHz, $\text{CDCl}_3$ ) spectrum of compound <b>135</b>	173
31	$^1\text{H}$ NMR (300 MHz, $\text{CDCl}_3$ ) spectrum of compound <b>136</b>	174
32	$^{13}\text{C}$ NMR (75 MHz, $\text{CDCl}_3$ ) spectrum of compound <b>136</b>	174
33	$^1\text{H}$ NMR (300 MHz, $\text{CDCl}_3$ ) spectrum of compound <b>117</b>	175
34	$^{13}\text{C}$ NMR (75 MHz, $\text{CDCl}_3$ ) spectrum of compound <b>117</b>	175
35	$^1\text{H}$ NMR (300 MHz, $\text{CDCl}_3$ ) spectrum of compound <b>116S</b>	176
36	$^{13}\text{C}$ NMR (75 MHz, $\text{CDCl}_3$ ) spectrum of compound <b>116S</b>	176
37	$^1\text{H}$ NMR (300 MHz, $\text{CDCl}_3$ ) spectrum of compound <b>116R</b>	177
38	$^{13}\text{C}$ NMR (75 MHz, $\text{CDCl}_3$ ) spectrum of compound <b>116R</b>	177
39	$^1\text{H}$ NMR (300 MHz, $\text{CDCl}_3$ ) spectrum of ( <i>S</i> )-MTPA ester of ( <i>R</i> )- <b>116R</b>	178
40	$^1\text{H}$ NMR (300 MHz, $\text{CDCl}_3$ ) spectrum of ( <i>R</i> )-MTPA ester of ( <i>R</i> )- <b>116R</b>	178
41	$^1\text{H}$ NMR (300 MHz, $\text{CDCl}_3$ ) spectrum of compound <b>160</b>	179
42	$^1\text{H}$ NMR (300 MHz, $\text{CDCl}_3$ ) spectrum of compound <b>162</b>	179
43	$^{13}\text{C}$ NMR (75 MHz, $\text{CDCl}_3$ ) spectrum of compound <b>162</b>	180
44	$^1\text{H}$ NMR (300 MHz, $\text{CDCl}_3$ ) spectrum of compound <b>163</b>	180
45	$^{13}\text{C}$ NMR (75 MHz, $\text{CDCl}_3$ ) spectrum of compound <b>163</b>	181
46	$^1\text{H}$ NMR (300 MHz, $\text{CDCl}_3$ ) spectrum of compound <b>163a</b>	181
47	$^{13}\text{C}$ NMR (75 MHz, $\text{CDCl}_3$ ) spectrum of compound <b>163a</b>	182
48	$^1\text{H}$ NMR (300 MHz, $\text{CDCl}_3$ ) spectrum of compound <b>164</b>	182
49	$^{13}\text{C}$ NMR (75 MHz, $\text{CDCl}_3$ ) spectrum of compound <b>164</b>	183
50	$^1\text{H}$ NMR (300 MHz, $\text{CDCl}_3$ ) spectrum of compound <b>165</b>	183
51	$^{13}\text{C}$ NMR (75 MHz, $\text{CDCl}_3$ ) spectrum of compound <b>165</b>	184
52	$^1\text{H}$ NMR (300 MHz, $\text{CDCl}_3$ ) spectrum of compound <b>166</b>	184
53	$^{13}\text{C}$ NMR (75 MHz, $\text{CDCl}_3$ ) spectrum of compound <b>166</b>	185
54	$^1\text{H}$ NMR (300 MHz, $\text{CDCl}_3$ ) spectrum of compound <b>114</b>	185
55	$^{13}\text{C}$ NMR (75 MHz, $\text{CDCl}_3$ ) spectrum of compound <b>114</b>	186
56	$^1\text{H}$ NMR (300 MHz, $\text{CDCl}_3$ ) spectrum of compound <b>167</b>	186

## LIST OF FIGURES (Continued)

Figure		Page
57	$^{13}\text{C}$ NMR (75 MHz, $\text{CDCl}_3$ ) spectrum of compound <b>167</b>	187
58	$^1\text{H}$ NMR (300 MHz, $\text{CD}_3\text{OD}$ ) spectrum of 7- <i>O</i> -methylnigrosporolide ( <b>19</b> )	187
59	$^{13}\text{C}$ NMR (75 MHz, $\text{CD}_3\text{OD}$ ) spectrum of 7- <i>O</i> -methylnigrosporolide ( <b>19</b> )	188
60	$^1\text{H}$ NMR (300 MHz, $\text{CD}_3\text{OD}$ ) spectrum of pestalotioprolide D ( <b>20</b> )	188
61	$^{13}\text{C}$ NMR (75 MHz, $\text{CD}_3\text{OD}$ ) spectrum of pestalotioprolide D ( <b>20</b> )	189
62	$^1\text{H}$ NMR (300 MHz, $\text{CDCl}_3$ ) spectrum of compound <b>171</b>	189
63	$^{13}\text{C}$ NMR (75 MHz, $\text{CDCl}_3$ ) spectrum of compound <b>171</b>	190
64	$^1\text{H}$ NMR (300 MHz, $\text{CDCl}_3$ ) spectrum of compound <b>171a</b>	190
65	$^{13}\text{C}$ NMR (75 MHz, $\text{CDCl}_3$ ) spectrum of compound <b>171a</b>	191
66	$^1\text{H}$ NMR (300 MHz, $\text{CDCl}_3$ ) spectrum of compound <b>172</b>	191
67	$^{13}\text{C}$ NMR (75 MHz, $\text{CDCl}_3$ ) spectrum of compound <b>172</b>	192
68	$^1\text{H}$ NMR (300 MHz, $\text{CDCl}_3$ ) spectrum of compound <b>173</b>	192
69	$^{13}\text{C}$ NMR (75 MHz, $\text{CDCl}_3$ ) spectrum of compound <b>173</b>	193
70	$^1\text{H}$ NMR (300 MHz, $\text{CDCl}_3$ ) spectrum of compound <b>173a</b>	193
71	$^{13}\text{C}$ NMR (75 MHz, $\text{CDCl}_3$ ) spectrum of compound <b>173a</b>	194
72	$^1\text{H}$ NMR (300 MHz, $\text{CDCl}_3$ ) spectrum of compound <b>115</b>	194
73	$^{13}\text{C}$ NMR (75 MHz, $\text{CDCl}_3$ ) spectrum of compound <b>115</b>	195
74	$^1\text{H}$ NMR (300 MHz, $\text{CDCl}_3$ ) spectrum of compound <b>174</b>	195
75	$^{13}\text{C}$ NMR (75 MHz, $\text{CDCl}_3$ ) spectrum of compound <b>174</b>	196
76	$^1\text{H}$ NMR (500 MHz, $\text{CDCl}_3$ ) spectrum of nigrosporolide ( <b>21</b> )	196
77	$^{13}\text{C}$ NMR (75 MHz, $\text{CDCl}_3$ ) spectrum of nigrosporolide ( <b>21</b> )	197
78	$^1\text{H}$ NMR (300 MHz, $\text{CDCl}_3$ ) spectrum of compound <b>182</b>	197
79	$^{13}\text{C}$ NMR (75 MHz, $\text{CDCl}_3$ ) spectrum of compound <b>182</b>	198
80	$^1\text{H}$ NMR (300 MHz, $\text{CDCl}_3$ ) spectrum of compound <b>183</b>	198
81	$^{13}\text{C}$ NMR (75 MHz, $\text{CDCl}_3$ ) spectrum of compound <b>183</b>	199
82	$^1\text{H}$ NMR (300 MHz, $\text{CDCl}_3$ ) spectrum of compound <b>183a</b>	199
83	$^{13}\text{C}$ NMR (75 MHz, $\text{CDCl}_3$ ) spectrum of compound <b>183a</b>	200



## LIST OF FIGURES (Continued)

Figure		Page
84	<sup>1</sup> H NMR (300 MHz, CDCl <sub>3</sub> ) spectrum of compound <b>185</b>	200
85	<sup>13</sup> C NMR (75 MHz, CDCl <sub>3</sub> ) spectrum of compound <b>185</b>	201
86	<sup>1</sup> H NMR (300 MHz, CDCl <sub>3</sub> ) spectrum of compound <b>185a</b>	201
87	<sup>13</sup> C NMR (75 MHz, CDCl <sub>3</sub> ) spectrum of compound <b>185a</b>	202
88	<sup>1</sup> H NMR (300 MHz, CDCl <sub>3</sub> ) spectrum of compound <b>178</b>	202
89	<sup>13</sup> C NMR (75 MHz, CDCl <sub>3</sub> ) spectrum of compound <b>178</b>	203
90	<sup>1</sup> H NMR (300 MHz, CDCl <sub>3</sub> ) spectrum of compound <b>186</b>	203
91	<sup>13</sup> C NMR (75 MHz, CDCl <sub>3</sub> ) spectrum of compound <b>186</b>	204
92	<sup>1</sup> H NMR (300 MHz, CDCl <sub>3</sub> ) spectrum of (4 <i>S</i> ,7 <i>S</i> ,13 <i>S</i> )-4,7-dihydroxy-13-tetradeca-2,5,8-trienolide ( <b>23</b> )	204
93	<sup>13</sup> C NMR (75 MHz, CDCl <sub>3</sub> ) spectrum of (4 <i>S</i> ,7 <i>S</i> ,13 <i>S</i> )-4,7-dihydroxy-13-tetradeca-2,5,8-trienolide ( <b>23</b> )	205
94	<sup>1</sup> H NMR (300 MHz, CDCl <sub>3</sub> ) spectrum of compound <b>187</b>	205
95	<sup>1</sup> H NMR (300 MHz, CDCl <sub>3</sub> ) spectrum of compound <b>188</b>	206
96	<sup>1</sup> H NMR (300 MHz, CDCl <sub>3</sub> ) spectrum of compound <b>188a</b>	206
97	<sup>1</sup> H NMR (300 MHz, CDCl <sub>3</sub> ) spectrum of compound <i>epi</i> - <b>106</b>	207
98	<sup>1</sup> H NMR (300 MHz, CDCl <sub>3</sub> ) spectrum of compound <b>189</b>	207
99	<sup>13</sup> C NMR (75 MHz, CDCl <sub>3</sub> ) spectrum of compound <b>189</b>	208
100	<sup>1</sup> H NMR (300 MHz, CDCl <sub>3</sub> ) spectrum of compound <b>189a</b>	208
101	<sup>13</sup> C NMR (75 MHz, CDCl <sub>3</sub> ) spectrum of compound <b>189a</b>	209
102	<sup>1</sup> H NMR (300 MHz, CDCl <sub>3</sub> ) spectrum of compound <b>180</b>	209
103	<sup>13</sup> C NMR (75 MHz, CDCl <sub>3</sub> ) spectrum of compound <b>180</b>	210
104	<sup>1</sup> H NMR (300 MHz, CDCl <sub>3</sub> ) spectrum of compound <b>190</b>	210
105	<sup>13</sup> C NMR (75 MHz, CDCl <sub>3</sub> ) spectrum of compound <b>190</b>	211
106	<sup>1</sup> H NMR (300 MHz, CDCl <sub>3</sub> ) spectrum of compound <b>191</b>	211
107	<sup>1</sup> H NMR (300 MHz, CDCl <sub>3</sub> ) spectrum of compound <b>179R</b>	212
108	<sup>13</sup> C NMR (75 MHz, CDCl <sub>3</sub> ) spectrum of compound <b>179R</b>	212

**LIST OF FIGURES (Continued)**

<b>Figure</b>		<b>Page</b>
<b>109</b>	<sup>1</sup> H NMR (300 MHz, CDCl <sub>3</sub> ) spectrum of compound <b>193</b>	213
<b>110</b>	<sup>13</sup> C NMR (75 MHz, CDCl <sub>3</sub> ) spectrum of compound <b>193</b>	213
<b>111</b>	<sup>1</sup> H NMR (300 MHz, CDCl <sub>3</sub> ) spectrum of compound <b>195</b>	214
<b>112</b>	<sup>13</sup> C NMR (75 MHz, CDCl <sub>3</sub> ) spectrum of compound <b>195</b>	214
<b>113</b>	<sup>1</sup> H NMR (300 MHz, CDCl <sub>3</sub> ) spectrum of compound <b>196S</b>	215
<b>114</b>	<sup>13</sup> C NMR (75 MHz, CDCl <sub>3</sub> ) spectrum of compound <b>196S</b>	215
<b>115</b>	<sup>1</sup> H NMR (300 MHz, CDCl <sub>3</sub> ) spectrum of compound <b>196R</b>	216
<b>116</b>	<sup>13</sup> C NMR (75 MHz, CDCl <sub>3</sub> ) spectrum of compound <b>196R</b>	216
<b>117</b>	<sup>1</sup> H NMR (300 MHz, CDCl <sub>3</sub> ) spectrum of ( <i>S</i> )-MTPA ester of <b>196S</b>	217
<b>118</b>	<sup>1</sup> H NMR (300 MHz, CDCl <sub>3</sub> ) spectrum of ( <i>R</i> )-MTPA ester of <b>196S</b>	217
<b>119</b>	<sup>1</sup> H NMR (300 MHz, CDCl <sub>3</sub> ) spectrum of ( <i>S</i> )-MTPA ester of <b>196R</b>	218
<b>120</b>	<sup>1</sup> H NMR (300 MHz, CDCl <sub>3</sub> ) spectrum of ( <i>R</i> )-MTPA ester of <b>196R</b>	218
<b>121</b>	<sup>1</sup> H NMR (300 MHz, CDCl <sub>3</sub> ) spectrum of compound <b>198</b>	219
<b>122</b>	<sup>1</sup> H NMR (300 MHz, CDCl <sub>3</sub> ) spectrum of compound <b>199</b>	219
<b>123</b>	<sup>1</sup> H NMR (300 MHz, CDCl <sub>3</sub> ) spectrum of compound <b>202</b>	220
<b>124</b>	<sup>13</sup> C NMR (75 MHz, CDCl <sub>3</sub> ) spectrum of compound <b>202</b>	220
<b>125</b>	<sup>1</sup> H NMR (300 MHz, CDCl <sub>3</sub> ) spectrum of compound <b>194</b>	221
<b>126</b>	<sup>13</sup> C NMR (75 MHz, CDCl <sub>3</sub> ) spectrum of compound <b>194</b>	221
<b>127</b>	<sup>1</sup> H NMR (300 MHz, CDCl <sub>3</sub> ) spectrum of compound <b>194a</b>	222
<b>128</b>	<sup>13</sup> C NMR (75 MHz, CDCl <sub>3</sub> ) spectrum of compound <b>194a</b>	222
<b>129</b>	<sup>1</sup> H NMR (300 MHz, CDCl <sub>3</sub> ) spectrum of compound <b>203</b>	223
<b>130</b>	<sup>13</sup> C NMR (75 MHz, CDCl <sub>3</sub> ) spectrum of compound <b>203</b>	223
<b>131</b>	<sup>1</sup> H NMR (300 MHz, CDCl <sub>3</sub> ) spectrum of compound <b>204</b>	224
<b>132</b>	<sup>13</sup> C NMR (75 MHz, CDCl <sub>3</sub> ) spectrum of compound <b>204</b>	224
<b>133</b>	<sup>1</sup> H NMR (300 MHz, CDCl <sub>3</sub> ) spectrum of compound <b>204a</b>	225
<b>134</b>	<sup>13</sup> C NMR (75 MHz, CDCl <sub>3</sub> ) spectrum of compound <b>204a</b>	225
<b>135</b>	<sup>1</sup> H NMR (300 MHz, CDCl <sub>3</sub> ) spectrum of compound <b>205</b>	226

**LIST OF FIGURES (Continued)**

<b>Figure</b>		<b>Page</b>
<b>136</b>	$^{13}\text{C}$ NMR (75 MHz, $\text{CDCl}_3$ ) spectrum of compound <b>205</b>	226
<b>137</b>	$^1\text{H}$ NMR (300 MHz, acetone- $d_6$ ) spectrum of mutolide ( <b>22</b> )	227
<b>138</b>	$^{13}\text{C}$ NMR (75 MHz, acetone- $d_6$ ) spectrum of mutolide ( <b>22</b> )	227
<b>139</b>	Chromatogram of racemic benzoate ester <b>129a</b>	228
<b>140</b>	Chromatogram of ( <i>S</i> )-benzoate ester <b>129a</b>	228
<b>141</b>	Chromatogram of racemic benzoate ester <b>132a</b>	229
<b>142</b>	Chromatogram of ( <i>S</i> )-benzoate ester <b>132a</b>	229
<b>143</b>	Chromatogram of racemic alcohol <b>195a</b>	230
<b>144</b>	Chromatogram of ( <i>R</i> )-alcohol <b>195a</b>	230

## LIST OF SCHEMES

Scheme		Page
1	Aggarwal's key synthetic reactions of Sch 725674 ( <b>8</b> )	9
2	Kumar's key synthetic reactions of Sch 725674 ( <b>8</b> )	10
3	Krishna's key synthetic reactions of pestalotioprolide C ( <b>14</b> )	11
4	Kitahara's key synthetic reactions of cineromycin B ( <b>4</b> )	12
5	Zhai's key synthetic reactions of 5,6-dihydrocineromycin B ( <b>60</b> )	13
6	Tadpetch's key synthetic reactions of the proposed structure of pestalotioprolide A ( <b>68</b> )	14
7	Reddy and Sabitha's key synthetic reactions of Sch 725674 ( <b>8</b> )	15
8	Chatare and Andrade's key synthetic reactions of (–)-albocycline ( <b>7</b> )	16
9	Reddy and Sabitha's key synthetic reactions of pestalotioprolide C ( <b>14</b> )	17
10	Goswami's key synthetic reactions of pestalotioprolide E ( <b>15</b> ) and structural revision of pestalotioprolide F ( <b>16a</b> )	18
11	Narsaiah's key synthetic reactions towards the stereoselective synthesis of 7- <i>O</i> -methylnigrosporolide ( <b>19</b> )	20
12	Proposed syntheses of compounds <b>19–23</b>	21
13	Retrosynthetic analysis of 7- <i>O</i> -methylnigrosporolide ( <b>19</b> ), pestalotioprolide D ( <b>20</b> ) and nigrosporolide ( <b>21</b> )	24
14	Menezes or Wang's synthesis of alkynes <b>106</b> and <i>epi</i> - <b>106</b>	25
15	Narsaiah's synthesis of ( <i>S</i> )-alkyne <b>106</b>	25
16	Synthesis of ( <i>S</i> )-alkyne <b>106</b>	26
17	Synthesis of ( <i>Z</i> )-enal <b>117</b>	27
18	Examples of asymmetric alkyne addition to $\alpha,\beta$ -unsaturated aldehydes with (BINOL)-ZnEt <sub>2</sub> -Ti(O- <i>i</i> Pr) <sub>4</sub> catalyst system by Pu et al.	29
19	Examples of Zn-ProPhenol catalyzed asymmetric alkyne addition to $\alpha,\beta$ -unsaturated aldehydes by Trost and co-workers	29
20	Acetylide addition between ( <i>S</i> )-alkyne <b>106</b> and ( <i>Z</i> )-enal <b>117</b>	33

## LIST OF SCHEMES (Continued)

Scheme		Page
21	Synthesis the macrocycle <b>167</b>	36
22	Proposed mechanisms of the formation of pestalotioprolide D ( <b>20</b> )	39
23	Taylor's desilylation of $\gamma$ -silyloxy $\alpha,\beta$ -unsaturated ketone <b>168</b>	40
24	Rodrigo and Guan's desilylation of $\gamma$ -silyloxy $\alpha,\beta$ -unsaturated methyl ester <b>169</b>	40
25	Completion of the synthesis of nigrosporolide ( <b>21</b> )	44
26	Retrosynthetic analysis of mutolide ( <b>22</b> ) and (4 <i>S</i> ,7 <i>S</i> ,13 <i>S</i> )-4,7-dihydroxy-13-tetradeca-2,5,8-trienolide ( <b>23</b> )	50
27	Completion of the synthesis of (4 <i>S</i> ,7 <i>S</i> ,13 <i>S</i> )-4,7-dihydroxy-13-tetradeca-2,5,8-trienolide ( <b>23</b> )	52
28	Preparation of ( <i>R</i> )-alkyne <i>epi</i> - <b>106</b>	54
29	Synthesis of ( <i>E</i> )-enal <b>180</b>	55
30	Acetylide addition between ( <i>R</i> )-alkyne <i>epi</i> - <b>106</b> and ( <i>E</i> )-enal <b>180</b>	57
31	Revised retrosynthesis of mutolide ( <b>22</b> )	60
32	Preparation of ( <i>R</i> )-hept-6-en-2-yl benzoate ( <b>195</b> )	61
33	Preparation of chiral allylic alcohol <b>196S</b>	61
34	Completion of the synthesis of mutolide ( <b>22</b> )	65

## LIST OF ABBREVIATIONS AND SYMBOLS

[ $\alpha$ ]	=	specific rotation
Ac	=	acetyl
Acetone- $d_6$	=	hexadeuteroacetone
Ac <sub>2</sub> O	=	acetic anhydride
aq	=	aqueous
app	=	apparent (spectral)
br	=	broad (spectral)
brsm	=	based on recovered starting material
°C	=	degrees Celsius
<i>c</i>	=	concentration
cat	=	catalytic
cm <sup>-1</sup>	=	wavenumber(s)
CDCl <sub>3</sub>	=	deuteriochloroform
$\delta$	=	chemical shift in parts per million downfield from tetramethylsilane
d	=	doublet (spectral)
DDQ	=	2,3-dichloro-5,6-dicyano- <i>p</i> -benzoquinone
DIAD	=	diisopropyl azodicarboxylate
DEAD	=	diethyl azodicarboxylate
DIPEA	=	<i>N,N</i> -diisopropylethylamine
DMAP	=	4-( <i>N,N</i> -dimethylamino)pyridine
DMF	=	dimethylformamide
DMSO	=	dimethyl sulfoxide
ee	=	enantiomeric excess
equiv	=	equivalent
ESI	=	electrospray ionization
Et	=	ethyl
FT	=	Fourier transform

**LIST OF ABBREVIATIONS AND SYMBOLS (Continued)**

g	=	gram(s)
h	=	hour(s)
HPLC	=	high-performance liquid chromatography
HRMS	=	high-resolution mass spectrometry
Hz	=	hertz
IBX	=	2-iodoxybenzoic acid
IR	=	infrared
<i>J</i>	=	coupling constant (in NMR spectrometry)
L	=	liter(s)
μ	=	micro
m	=	multiplet (spectral); meter(s); milli
M	=	molar (moles per liter)
Me	=	methyl
MHz	=	megahertz
min	=	minute(s)
mol	=	mole
mol %	=	mole percent
mp	=	melting point
MTPA	=	methoxy trifluoromethyl phenyl acetate
<i>m/z</i>	=	mass-to-charge ratio
nm	=	nanometer(s)
NMR	=	nuclear magnetic resonance
Ph	=	phenyl
ppm	=	part(s) per million
<i>i</i> Pr	=	isopropyl
q	=	quartet (spectral)
<i>R<sub>f</sub></i>	=	retention factor (in chromatography)
rt	=	room temperature
s	=	singlet (spectral)
t	=	triplet (spectral)

**LIST OF ABBREVIATIONS AND SYMBOLS (Continued)**

TEMPO	=	2,2,6,6-tetramethylpiperidin-1-oxyl
TBS	=	<i>tert</i> -butyldimethylsilyl
TBDPS	=	<i>tert</i> -butyldiphenylsilyl
TBAF	=	tetrabutylammonium fluoride
TES	=	triethylsilyl ether
TLC	=	thin-layer chromatography
wt	=	weight



**LIST OF PUBLICATION**

- Thiraporn, A.; Iawsipo, P.; Tadpetch, K. 2022. Total Synthesis and Cytotoxic Activity of 7-*O*-Methylnigrosporolide and Pestalotioprolide D. *Synlett.* 33 (14), 1341–1346.
- Thiraporn, A.; Saikachain, N.; Khumjiang, R.; Muanprasat, C.; Tadpetch, K. 2022. Total Synthesis and Biological Evaluation of Mutolide and Analogues. *Chem. Asian J.* 17, e202200329.

**COPYRIGHT PERMISSION NOTICE**

Thiraporn, A.; Iawsipo, P.; Tadpetch, K. 2022. Total Synthesis and Cytotoxic Activity of 7-*O*-Methylnigrosporolide and Pestalotioprolide D. *Synlett*. 33 (14), 1341–1346.

Reproduced by permission of Georg Thieme Verlag KG.

Thiraporn, A.; Saikachain, N.; Khumjiang, R.; Muanprasat, C.; Tadpetch, K. 2022. Total Synthesis and Biological Evaluation of Mutolide and Analogues. *Chem. Asian J.* 17, e202200329.

Reproduced by permission of Wiley-VCH Verlag GmbH.

# **CHAPTER 1**

## **INTRODUCTION**

## CHAPTER 1

### INTRODUCTION

#### 1.1 Introduction

The 14-membered macrolides are an important class of polyketide metabolites that have received much attention from the scientific community due to their broad structural variations and prominent biological activities e.g. antibiotic, antifungal, antibacterial, phytotoxic and cytotoxic activities (Chu, 1995, Zhanel *et al.*, 2001 and 2002, Wang *et al.*, 2021). In this section, the selected examples of the structures, biological properties and synthetic strategies of these macrolides will be presented.

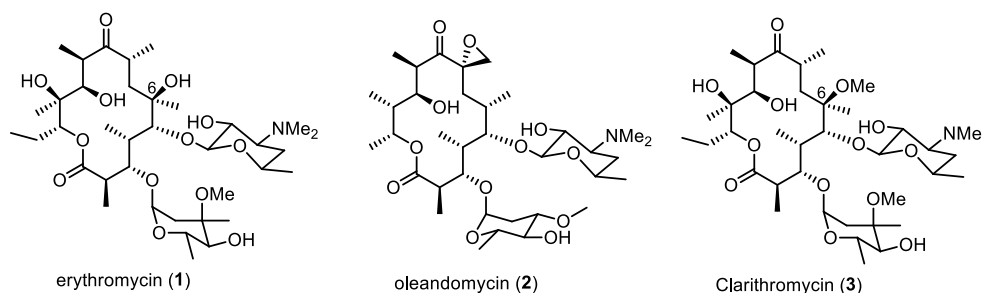
Fourteen-membered macrolides could be broadly classified into two groups based on the presence of a sugar moiety. The first group of 14-membered macrolactones is those containing two deoxy sugars. The selected examples of these macrolides are illustrated in **Figure 1**. Erythromycin (**1**) was originally isolated from the fungus *Streptomyces erythreus* by Mcguire and co-workers in 1952. Compound **1** was active against various gram-positive bacteria (*Staphylococcus aureus*, *Staphylococcus epidermidis*, *Streptococcus pneumonia* and *Streptococcus pyogenes*) and gram-negative bacteria e.g. *Legionella pneumonia*, *Campylobacter jejuni*, *Mycoplasma pneumoniae* and *Chlamydia trachomatis*. In addition, **1** was approved as an antibiotic medication for various diseases such as bronchitis, pneumonitis, diphtheria, carriers of pertussis, infections of the skin and soft tissues, and some sexually transmitted diseases (Washington and Wilson, 1985). In 1954, oleandomycin (**2**) was first discovered from the fungus *Streptomyces antibioticus* by Sobin and co-workers. Macrolide **2** was also used as antibacterial drug similar to **1** (Els *et al.*, 1958). Clarithromycin (**3**), C-6 methoxy derivative of **1**, was prepared and developed by Morimoto and co-workers in 1984. Compound **3** showed a broad antibacterial spectrum similar to **1**, however, **3** was two-fold more potent than **1** against most of aerobic and

anaerobic bacteria *in vitro* (Fernandes *et al.*, 1986, Ōmura *et al.*, 1992). Moreover, **3** displayed good activity against *Helicobacter pylori* and has been approved in a combination regimen for the treatment of peptic ulcer disease (Chu *et al.*, 1996).

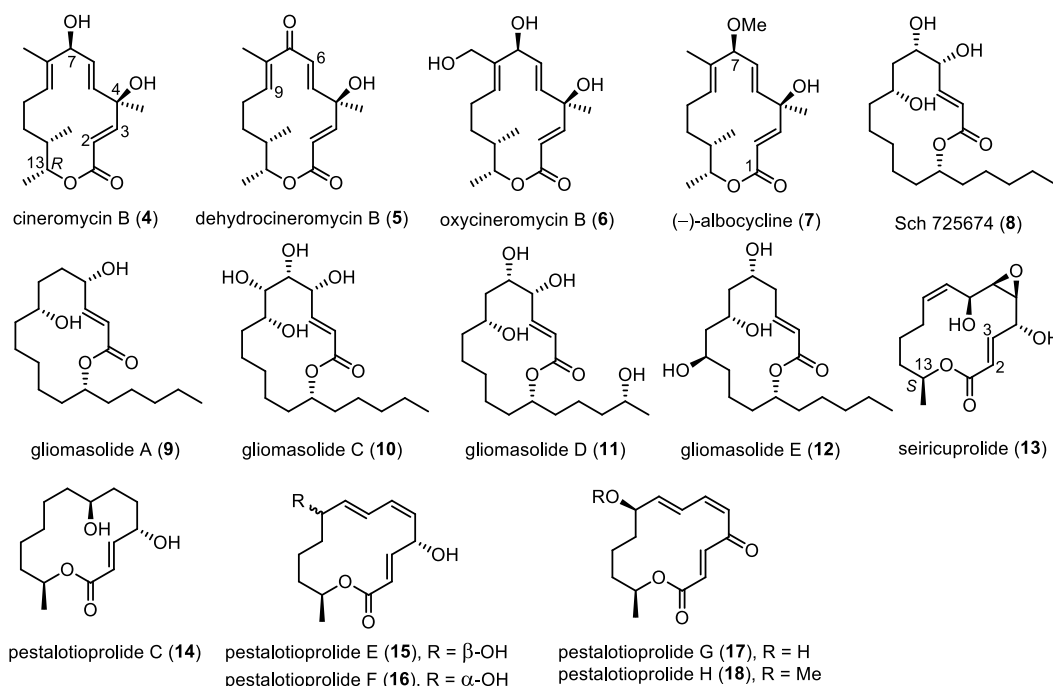
Another group of 14-membered macrolactones are those lacking the sugar moieties, which possess diverse structural features. Herein, only the 14-membered (*E*)- $\alpha,\beta$ -unsaturated lactone scaffolds will be discussed. This subclass of macrolides has been found to exhibit a significant and wide range of biological activities. The selected examples of this group of metabolites are shown in **Figure 2**. The cineromycin-family members (cineromycin B (**4**), dehydrocineromycin B (**5**) and oxycineromycin B (**6**)) were isolated from *Streptomyces cinerochromogenes*, *S. griseoviridis* and *S. sp.* Gö 40/10 (FH-S 1832) (Miyairi *et al.*, 1966, Burkhardt *et al.*, 1996 and Schiewe and Zeeck, 1999). The core structure of macrolides **4–6** also contains two *E*-alkenes at C5–C6 and C8–C9 as well as three or four stereogenic centers. Compounds **4–6** showed weak activity against methicillin-resistant *S. aureus* (MRSA) (Burkhardt *et al.*, 1996, Schneider *et al.*, 1996, Terekhova *et al.*, 2007 and Elleuch *et al.*, 2010). Albocycline (**7**), C7 methoxy derivative of **4**, was identified from *Streptomyces brunneogriseus*, *S. roseocitreus* and *S. roseochromogenes* var. *albocyclini* (Furumai *et al.*, 1968). Compound **7** inhibited the growth of MRSA with MIC values of 0.5–1.0  $\mu\text{g/mL}$  as potently as vancomycin, a glycopeptide antibiotic medication (Koyama *et al.*, 2013). Furthermore, **7** was found as a specific inhibitor of prolyl endopeptidases (PEP) isolated from human placenta with an  $\text{IC}_{50}$  value of 9.0  $\mu\text{M}$  (Christner *et al.*, 1998). Another group of the 14-membered unsaturated macrolides are those containing an unusual *n*-pentyl carbon chain at the C13-position as well as several alcohol stereogenic centers. Sch 725674 (**8**) was isolated from an *Aspergillus* sp. culture (SPRI-0836) by Yang and co-workers in 2005. Compound **8** displayed antifungal activity against *Saccharomyces cerevisiae* (PM503) and *Candida albicans* (C43) with MIC values of 8 and 32  $\mu\text{g/mL}$ , respectively. Gliomasolide A (**9**) and gliomasolides C–E (**10–12**) were isolated from the fungus *Gliomastix* sp. ZSDS1-F7-2 from the marine sponge *Phakellia fusca* Thiele by Zhang *et al.* in 2015. Among these compounds, gliomasolide A (**9**) was found to exhibit moderate *in vitro* inhibitory activity against human epithelial carcinoma (HeLa) cells with an  $\text{IC}_{50}$  value of 10.1  $\mu\text{M}$ . Moreover, 14-membered unsaturated macrolides containing the *S*-methyl lactone alcohol at the C13-

position have also been reported. Seiricuprolide (**13**) was isolated from the fungus *Seiridium cupressi* and showed phytotoxic activity, which causes canker in cypress trees (Ballio *et al.*, 1988). In 2016, Liu and co-workers reported the isolation of pestalotioprolide C (**14**) and pestalotioprolides E–H (**15–18**) from mangrove-derived endophytic fungus *Pestalotiopsis microspora*. Compounds **14–16** and **18** displayed cytotoxicity against the L5178Y murine lymphoma cell line with  $IC_{50}$  values of 39, 3.4, 3.9 and 11.0  $\mu\text{M}$ , respectively. Furthermore, macrolides **14–18** were also evaluated for their cytotoxic activity against the A2780 human ovarian cancer cell line, and only **15–17** showed cytotoxic activity against this cancer cell line with  $IC_{50}$  values of 1.2, 12.0 and 36.0  $\mu\text{M}$ , respectively.

**Figure 1** Examples of 14-membered macrolides containing sugar moiety



**Figure 2** Examples of 14-membered macrolides lacking sugar moiety



In addition to the isolation of compounds **14–18** by Liu and co-workers as shown above, two new 14-membered macrolides including 7-*O*-methylnigrosporolide (**19**) and pestalotioprolide D (**20**), along with a known compound, nigrosporolide (**21**), were also obtained from the same mangrove fungus (*P. microspora*) (**Figure 3a**). Compounds **19** and **20** showed significant cytotoxicity against the L5178Y murine lymphoma cells with respective IC<sub>50</sub> values of 0.7 and 5.6 μM, while **21** displayed mild cytotoxic activity against the same cell line with an IC<sub>50</sub> value of 21.0 μM. Moreover, **19** and **21** exhibited weak activity against the A2780 human ovarian cancer cells with IC<sub>50</sub> values of 28.0 and 43.0 μM, respectively. The core structures of these natural products are closely related. Compound **19** is a C7 methoxy derivative of **21** consisting of a C2–C3 *E*-double bond, two *Z*-alkenes at C5–C6 and C8–C9 as well as three alcohol stereogenic centers at 4, 7 and 13 positions. The core structure of **20** is nearly identical to **19** but **20** possesses one ketone functional group at the C4-position and two methylene groups at C2–C3 instead of *E*-alkene. The absolute configurations of crystalline **21** were determined by the Liu group for the first time to be 4*S*, 7*S* and 13*S* by single-crystal X-ray diffraction analysis. Based on the similarity of coupling constants, NOE correlations, ROESY and biogenetic relationships of natural products **19–21**, the absolute configurations of **19** and **20** were assigned to be identical to **21**.

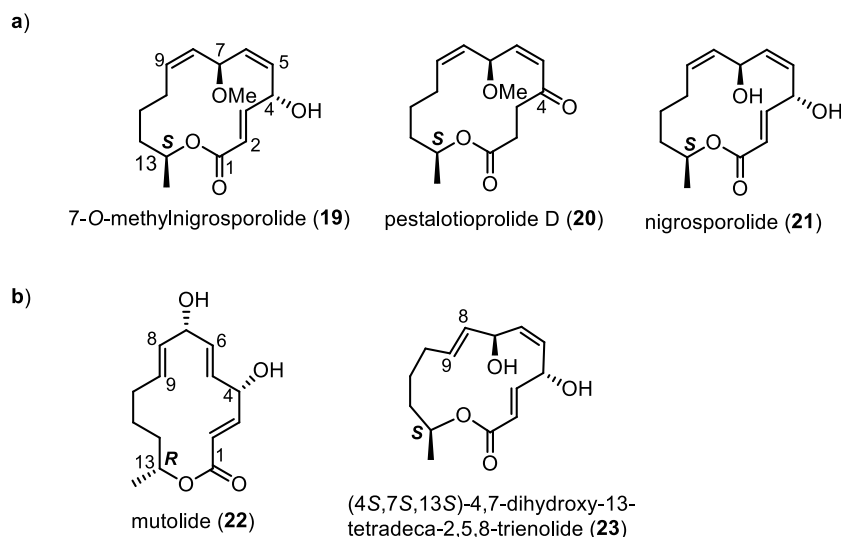
There are known natural analogues of nigrosporolide (**21**) namely mutolide (**22**) and (4*S*,7*S*,13*S*)-4,7-dihydroxy-13-tetradeca-2,5,8-trienolide (**23**), which will also be discussed herein (**Figure 3b**). Macrolide **22** differs from **21** by the absolute configuration at the C13-position and two *E*-alkenes at C5–C6 and C8–C9, while **23** has a core structure similar to **21** except for the presence of *E*-olefin at C8–C9. Mutolide (**22**) was originally isolated from the culture broth of a fungus strain obtained from UV mutagenesis of the fungus *Sphaeropsidales* sp. (strain F-24'707) by Bode et al. in 2000 and **22** showed weak antibacterial activity against *Bacillus subtilis* and *Escherichia coli*. Compound **22** was later found from the coprophilous fungus *Lepidosphaeria* sp. (PM0651419) by Shah and co-workers in 2015. This research demonstrated for the first time the anti-inflammatory effect of **22** via inhibition of nuclear factor kappa-light-chain-enhancer of activated B cells (NF-κB), which was the major transcription factor involved in the secretion of pro-inflammatory cytokines.

Recently, in 2020, **22** was identified from the endophytic fungus *Aplosporella javeedii* by Gao et al. and displayed a highly potent cytotoxic activity against the L5178Y mouse lymphoma cells with an IC<sub>50</sub> value of 0.4 μM after 72 hours of incubation. Moreover, **22** also showed significant cytotoxicity against the human leukemia (Jurkat J16) and lymphoma (Ramos) cell lines with IC<sub>50</sub> values of 5.8 and 4.4 μM, respectively after 24 hours of incubation. Interestingly though, after 72 hours of incubation, IC<sub>50</sub> values against human Jurkat J16 and Ramos cell lines of **22** dropped to 1.4 and 0.8 μM, respectively. The last natural compound of this group that will be presented is (4*S*,7*S*,13*S*)-4,7-dihydroxy-13-tetradeca-2,5,8-trienolide (**23**), which was originally obtained from the phytopathogen fungus *Colletotrichum acutatum* by Mancilla et al. in 2009. After that, **23** was reisolated from a marine-derived fungus *Diaporthaceae* sp. PSU-SP2/4 (Khamthong *et al.*, 2014). Macrolide **23** exhibited a low cytotoxic activity against human breast adenocarcinoma (MCF-7) cells with an IC<sub>50</sub> value of 30.76 μg/mL, and was non-cytotoxic to noncancerous Vero cells. In 2016, compound **23** was reisolated from the same mangrove fungus as compounds **19–21** (*P. microspora*) by Liu and co-workers and was shown to display weak activity against the L5178Y murine lymphoma cell line with an IC<sub>50</sub> value of 21.0 μM (Liu *et al.*, 2016). Notably, in 2011, macrolide **23** was synthesized as an intermediate in the total synthesis of aspergillide C by Kobayashi and co-workers.

Owing to the promising biological activities of this class of natural products and unprecedented total syntheses of **19–23**, we are interested in synthesizing such compounds in order to further examine their biological activities as well as to confirm the absolute configurations of the natural products.

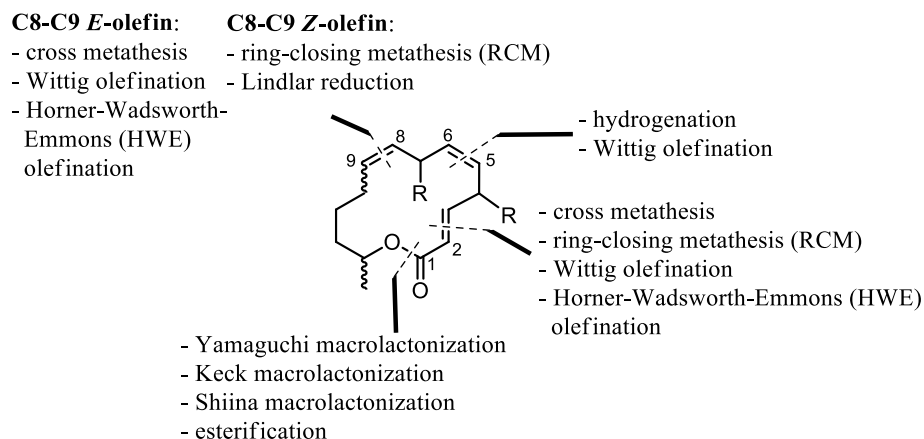


**Figure 3** Structures of 7-*O*-methylnigrosporolide (**19**), pestalotioprolide D (**20**), nigrosporolide (**21**), mutolide (**22**) and (4*S*,7*S*,13*S*)-4,7-dihydroxy-13-tetradeca-2,5,8-trienolide (**23**)



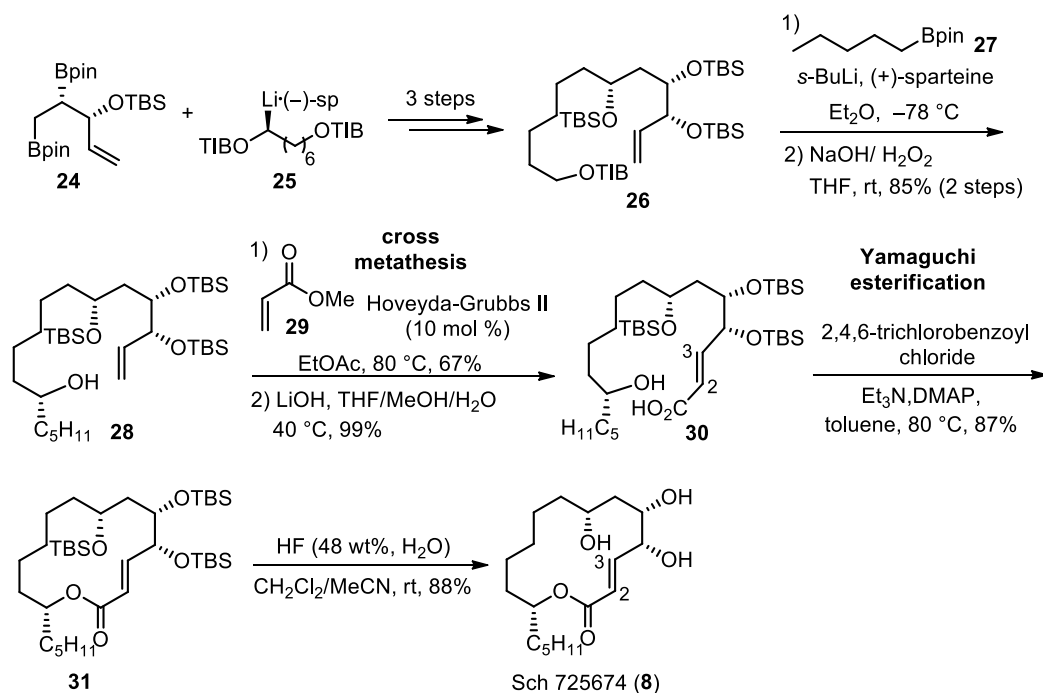
Currently, there are a number of research groups that have revealed the isolation and synthesis of 14-membered unsaturated macrolides containing *E*-alkene at C2–C3 similar to **19** and **21–23**. However, the reports on the synthetic approaches of fourteen-membered macrolactones containing *Z*- or *E*-double bond at C5–C6 and C8–C9 analogous to compounds **19–23** are limited. Therefore, this section will focus on literature precedents on syntheses of this class of 14-membered macrocycles possessing the core structure similar to **19** and **21–23** which is the *E*-double bond at C2–C3 and 14-membered macrolactone core. In previously reported syntheses of these macrolides, the key strategies to construct the C2–C3 *E*-double bond include cross metathesis, ring-closing metathesis (RCM), Wittig and Horner–Wadsworth–Emmons (HWE) olefinations. The synthetic approaches to form ester functionality together with 14-membered macrocyclic core were mostly achieved through Yamaguchi, Keck and Shiina macrolactonizations. Nevertheless, there are a few reports on the synthetic strategies to generate *Z*- or *E*-double bond at C5–C6 and C8–C9, which would also be reviewed in this section. Previously reported formation of *Z*- or *E*-alkenes at C5–C6 and C8–C9 was accomplished via olefination, metathesis reactions and selective reduction (**Figure 4**).

**Figure 4** Key bond formations in the syntheses of 14-membered unsaturated macrolides containing *E*-alkene at C2–C3 and *Z*- or *E*-double bond at C5–C6 and C8–C9

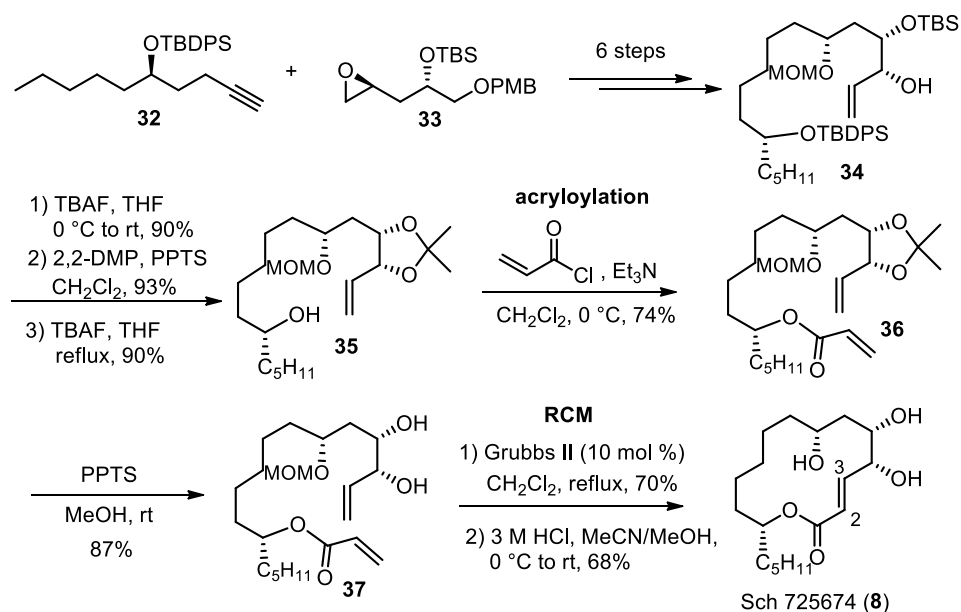


Firstly, selected examples of syntheses of 14-membered unsaturated macrolide derivatives highlighting the formation of C2–C3 *E*-double bond through metathesis reactions will be described. In 2016, the synthesis of Sch 725674 (**8**) was accomplished by Aggarwal and co-workers (**Scheme 1**). They presented the synthetic approach to form C2–C3 *E*-double bond by using cross metathesis. The synthesis commenced with the preparation of compound **26** from 1,2-bis(boronic ester) **24** and lithiated triisopropylbenzoate (**25-Li(-)-sp**) in 3 steps. The remaining triisopropylbenzoate of **26** was then treated with pentyl boronic ester **27** under selective deprotonation conditions (*s*-BuLi, (+)-sparteine in Et<sub>2</sub>O) and subsequent oxidation with NaOH/H<sub>2</sub>O<sub>2</sub> to give alcohol **28** in 85% yield over 2 steps. Cross metathesis between terminal alkene **28** and methyl acrylate (**29**) was performed using Hoveyda–Grubbs second generation catalyst (10 mol %) in EtOAc to afford exclusive (*E*)- $\alpha,\beta$ -unsaturated methyl ester in 67% yield, and then hydrolysis of methyl ester with LiOH in THF/MeOH/H<sub>2</sub>O gave seco acid **30** in 99% yield. In the final stage, Yamaguchi macrolactonization of acid **30** provided macrocycle **31** in 87% yield. Compound **31** was exposed to global deprotection of TBS groups to furnish Sch 725674 (**8**) in 88% yield.

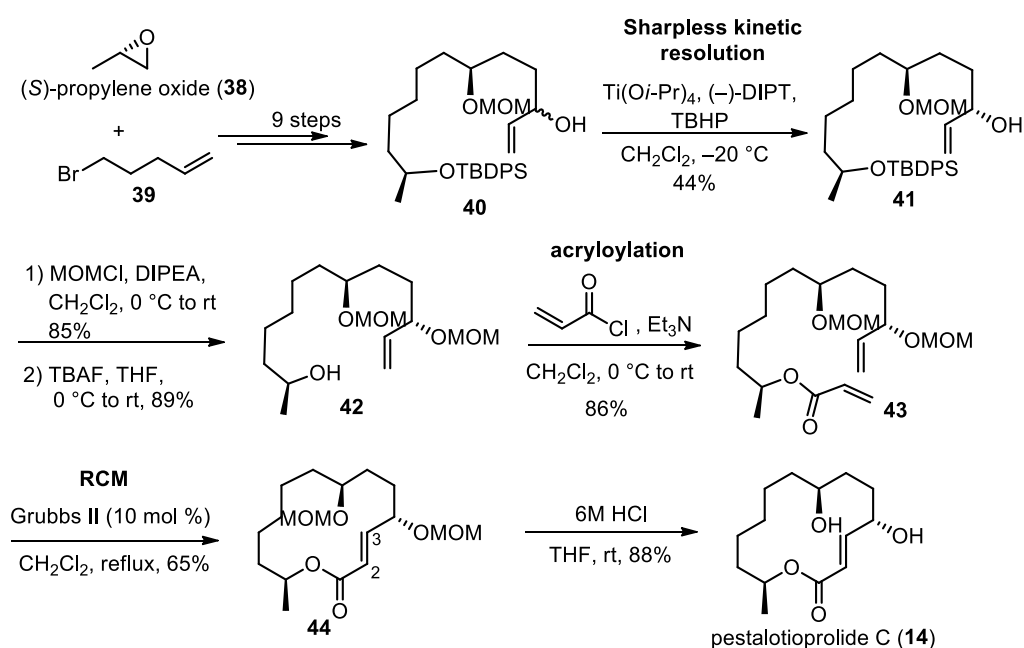
**Scheme 1** Aggarwal's key synthetic reactions of Sch 725674 (**8**)



The synthesis of Sch 725674 (**8**) was also disclosed by Kumar and co-workers in the same year as the Aggarwal group (**Scheme 2**). In this synthesis, ring-closing metathesis (RCM) was used as the key method to construct C2–C3 *E*-double bond together with 14-membered macrocyclic core of **8**. Kumar's process began with the synthesis of terminal alkene **34** from two key fragments **32** and **33** in 6 steps. Compound **34** was converted to alcohol **35** in 3 steps via TBS deprotection, acetonide protection and subsequent removal of TBDPS group. Esterification of alcohol **35** with acryloyl chloride led to diene **36** in 74% yield. After removal of the acetonide group of **36** with PPTS, diol **37** was treated with 10 mol % of second-generation Grubbs catalyst in refluxing  $\text{CH}_2\text{Cl}_2$  to generate the desired *E*-olefin at C2–C3 and form the macrocyclic core of target product in high yield as a single stereoisomer. Ultimately, deprotection of the remaining MOM group with 3M HCl yielded Sch 725674 (**8**) in 68% yield.

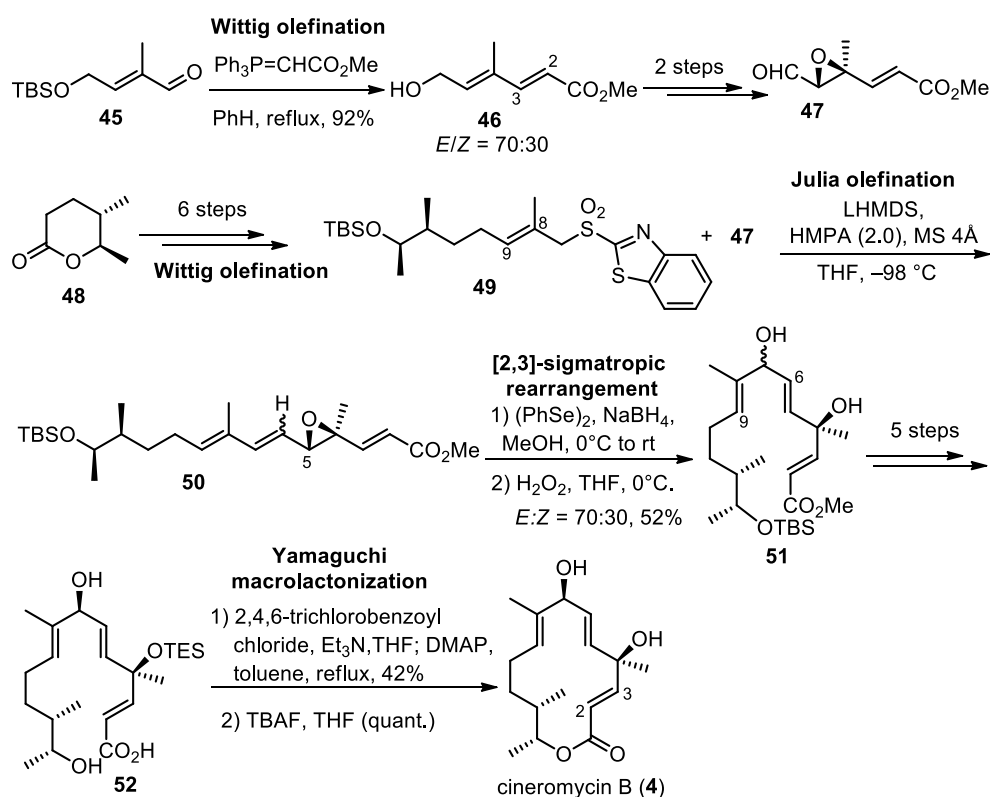
**Scheme 2** Kumar's key synthetic reactions of Sch 725674 (**8**)

Another example of utilization of ring-closing metathesis to form the *E*-double bond at C2–C3 as well as to assemble the macrolactone core was reported in the synthesis of pestalotioprolide C (**14**) by Krishna and co-workers in 2018 (**Scheme 3**). The synthesis started with preparation of racemic allylic alcohol **40** from (*S*)-propylene oxide (**38**) and 5-bromopent-1-ene (**39**) in 9 steps. The Sharpless kinetic resolution of **40** provided chiral alcohol **41** in 44% yield. Next, compound **41** was converted to alcohol **42** in 2 steps via protection of secondary alcohol as methoxymethyl (MOM) ether and subsequent removal of TBDPS group with TBAF. Acryloylation of alcohol **42** with acryloyl chloride and triethylamine in CH<sub>2</sub>Cl<sub>2</sub> installed the ester functional group of the RCM precursor **43** in 86% yield. Then, ring-closing metathesis of diene **43** using 10 mol % of second generation Grubbs catalyst in refluxing CH<sub>2</sub>Cl<sub>2</sub> yielded the macrocyclic core of **44** in 65% yield. This step exclusively provided the *E*-double bond at C2–C3. Finally, global deprotection of MOM protecting groups of **44** was accomplished upon treatment with 6M HCl to furnish pestalotioprolide C (**14**) in 88% yield.

**Scheme 3** Krishna's key synthetic reactions of pestalotioprolide C (**14**)

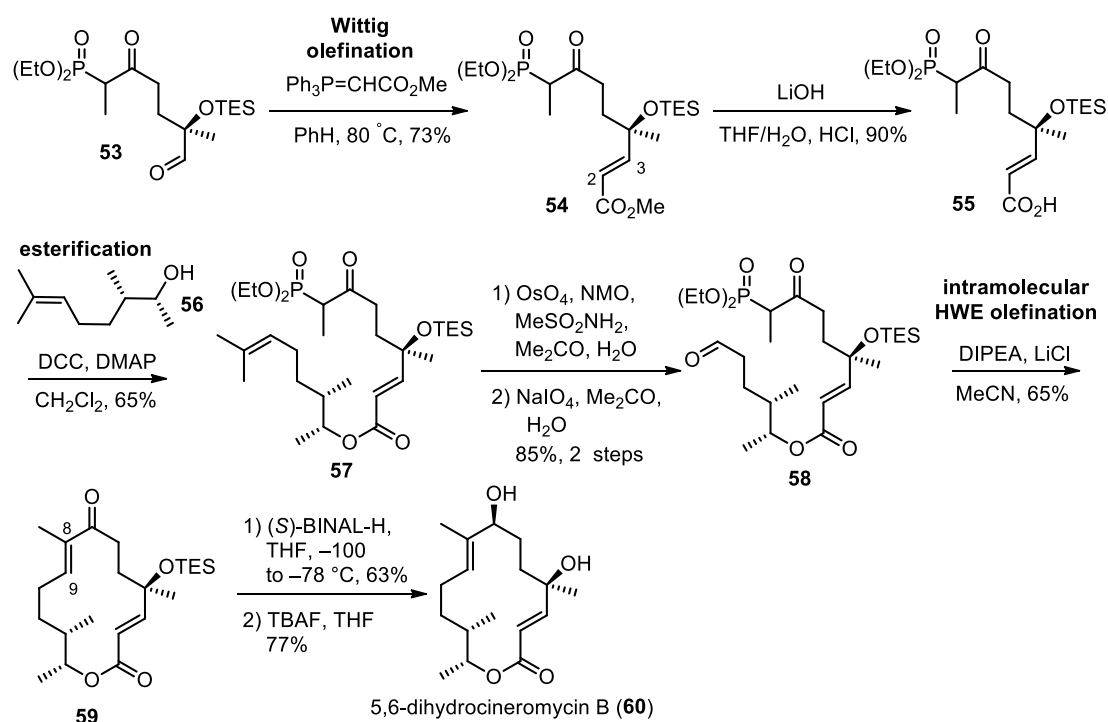
The Wittig olefination is another approach that is widely employed to form *E*-double bond at C2–C3. The first example was showcased in the synthesis of cineromycin B (**4**) by Kitahara and co-workers in 2003 (**Scheme 4**). They utilized Wittig olefination of aldehyde **45** with stabilized phosphonium ylide  $\text{Ph}_3\text{P}=\text{CHCO}_2\text{Me}$  to install C2–C3 *E*-double bond of **46** in 92% yield with good stereoselectivity (*E/Z* = 70:30). Compound **46** was then converted to epoxy aldehyde **47** in 2 steps. With the key fragment **47** in hand, their next goal was to synthesize sulfone **49** from lactone **48** in 6 steps by using Wittig olefination as the key step to generate *trans*-olefin at C8–C9. After that, the C6–C7 bond formation between aldehyde **47** and sulfone **49** was performed using Julia olefination and [2,3]-sigmatropic rearrangement as the key strategies to give diol **51**, which was transformed to seco acid **52** in 5 steps. In the final stage, Yamaguchi macrolactonization of **52** was used to form the ester functional group and close the 14-membered macrocyclic core, followed by removal of TES protecting group with TBAF to afford cineromycin B (**4**) in quantitative yield.

**Scheme 4** Kitahara's key synthetic reactions of cineromycin B (**4**)



In 2009, the synthesis of 5,6-dihydrocineromycin B (**60**) was disclosed by Zhai et al. (**Scheme 5**). The formation of the *E*-double bond at C2–C3 was also carried out via Wittig olefination of aldehyde **53** similar to Kitahara's method to produce unsaturated methyl ester **54** in 73% yield with exclusive *E*-selectivity. Methyl ester of **54** was then hydrolyzed with LiOH in THF/H<sub>2</sub>O to give carboxylic acid **55**. The formation of ester functionality was performed under different approach from Kitahara's synthesis. Acid **55** was coupled with alcohol **56** via esterification conditions (DCC, DMAP) to furnish ester **57** in 65% yield. The trisubstituted alkene moiety of **57** was transformed to aldehyde **58** in 2 steps under oxidative cleavage reaction. The intramolecular HWE olefination of **58** with DIPEA and LiCl was applied to construct the macrocycle and *trans*-olefin at C8–C9 of **59**. Next, the stereoselective reduction of ketone **59** by using (*S*)-BINAL-H in THF from –100 to –78 °C, followed by desilylation led to the final product **60** in 77% yield.

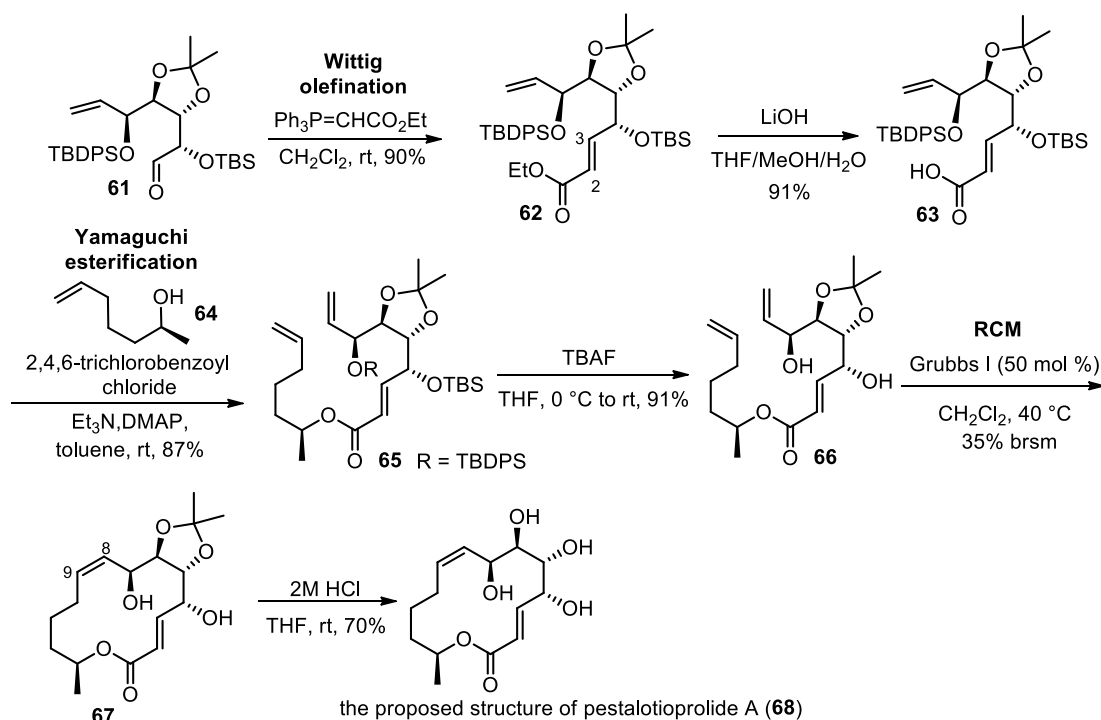
**Scheme 5** Zhai's key synthetic reactions of 5,6-dihydrocineromycin B (**60**)



In 2015, Tadpetch et al. reported the synthesis of the proposed structure of pestalotioprolide A (**68**), which also relied on Wittig olefination to generate the *E*-double bond at C2–C3 (**Scheme 6**). Aldehyde **61** was treated with stabilized phosphonium ylide  $\text{Ph}_3\text{P}=\text{CHCO}_2\text{Et}$  in  $\text{CH}_2\text{Cl}_2$  at room temperature to afford (*E*)- $\alpha,\beta$ -unsaturated acid **62** in 90% yield as a single stereoisomer. After basic hydrolysis of ester **62** with  $\text{LiOH}$ , the resultant carboxylic acid **63** was reacted with alcohol **64** via Yamaguchi esterification conditions to form the requisite ester **65**. Subsequent removal of TBS and TBDPS protecting groups of **65** with  $\text{TBAF}$  gave diol **66** in 91% yield. After diene precursor **66** was obtained, their next goal was to assemble the macrocycle and generate the C8–C9 *Z*-alkene through ring-closing metathesis (RCM). Reaction conditions using 10 mol % of second generation Grubbs (Grubb II) catalyst led to the undesired (*E*)-isomer as a major product. Interestingly, replacing the Grubb II catalyst with the less reactive first generation Grubbs (Grubbs I) catalyst (50 mol %) resulted in the formation of the desired macrocycle core of **67** with *Z*-olefin at C8–C9 as a major product. Ultimately, deprotection of acetonide

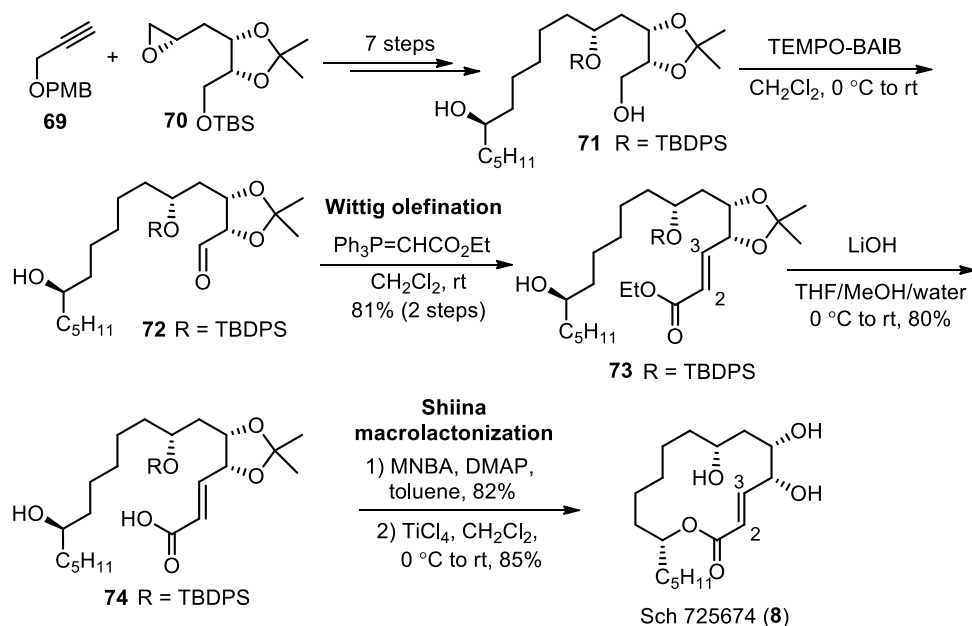
protecting group of **67** with 2M HCl in THF provided the desired target **68** in 70% yield.

**Scheme 6** Tadpetch's key synthetic reactions of the proposed structure of pestalotioprolide A (**68**)

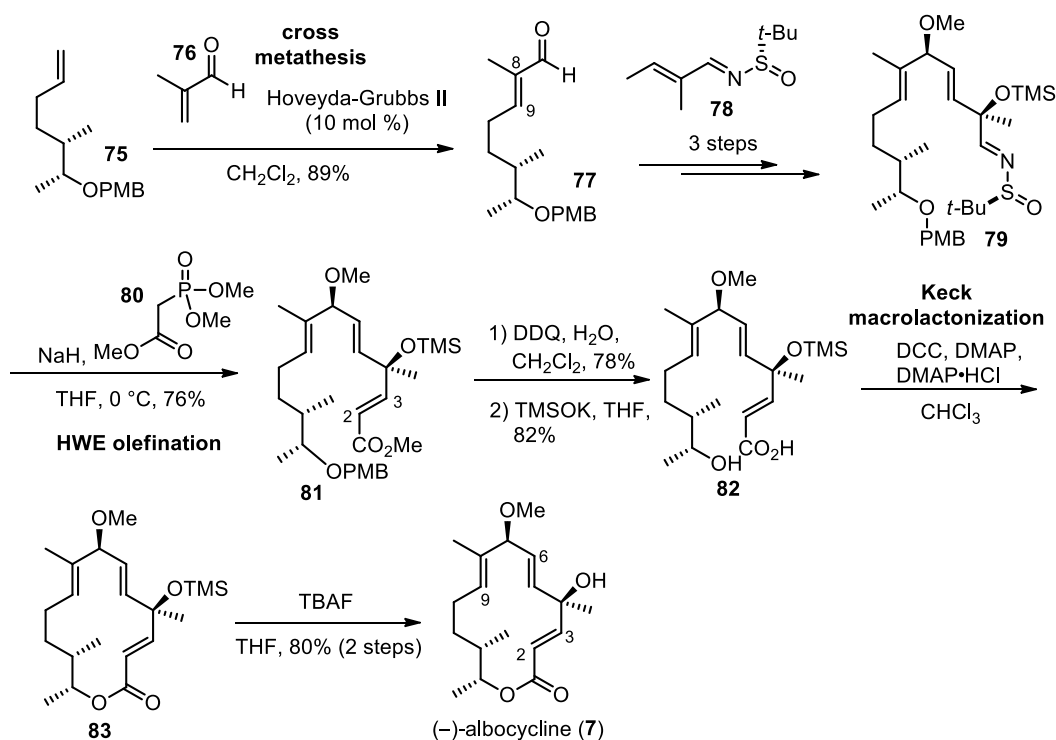


The last selected example of utilization of Wittig olefination to construct the *E*-double bond at C2–C3 was reported in the total synthesis of the Sch 725674 (**8**) by Reddy and Sabitha in 2016 (**Scheme 7**). The synthesis commenced with the preparation of alcohol **71** from alkyne **69** and epoxide **70** in 7 steps. Selective oxidation of primary alcohol **71** with TEMPO/BAIB gave aldehyde **72**, which was exposed to Wittig olefination by using the same conditions as Tadpetch's method to afford exclusive (*E*)- $\alpha,\beta$ -unsaturated ester **73** in 81% over 2 steps. Subsequently, hydrolysis of ethyl ester **73** with LiOH produced seco acid **74** in 80% yield. To access the final product, acid **74** was subjected to Shiina macrolactonization to assemble macrocyclic core of target product, and then global deprotection of the acetonide and TBDPS groups mediated by  $\text{TiCl}_4$  led to Sch 725674 (**8**) in 85% yield.

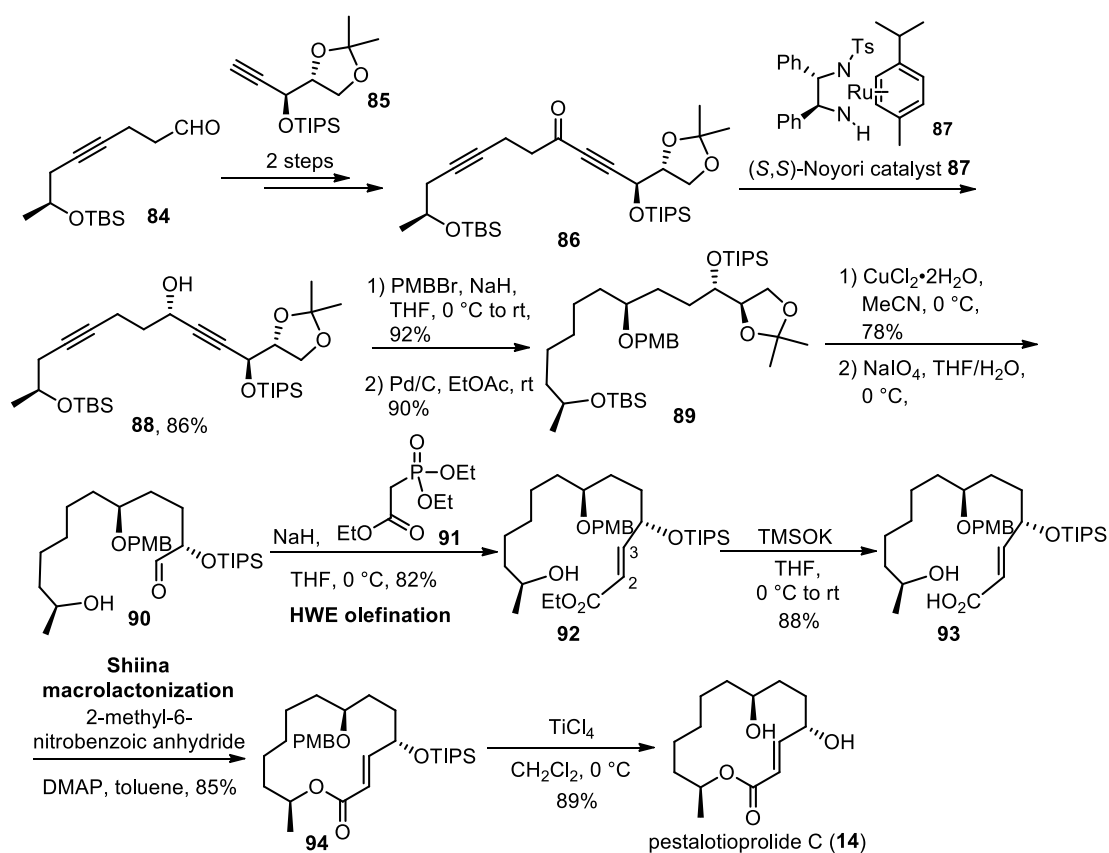


**Scheme 7** Reddy and Sabitha's key synthetic reactions of Sch 725674 (**8**)

Another approach to generate the *E*-double bond at C2–C3 that has been popularly utilized is HWE olefination. The first example is the synthesis of (–)-albacycline (**7**) by Chatare and Andrade in 2017 (**Scheme 8**). Cross metathesis between terminal alkene **75** and methacrolein (**76**) with Hoveyda–Grubbs second generation catalyst (10 mol %) in CH<sub>2</sub>Cl<sub>2</sub> was performed to generate *E*-alkene at C8–C9 of **77** in 89% yield as a sole stereoisomer. Then, aldehyde fragment **77** was converted to *N*-sulfinyl imine **79** in 3 steps. Intermolecular HWE olefination between *N*-sulfinyl imine **79** and phosphonate **80** in the presence of NaH was applied to form (*E*)- $\alpha,\beta$ -unsaturated acid **81** in 76% yield as a sole stereoisomer. Removal of PMB group of **81** with DDQ and subsequent hydrolysis of methyl ester with TMSOK provided seco acid **82** in 82% yield. Keck macrolactonization of **82** with DCC, DMAP and DMAP·HCl was employed to construct the ester functional group and the macrocycle **83**, which was subsequently exposed to TBAF in THF to produce the final product **7** in 80% yield over 2 steps.

**Scheme 8** Chatare and Andrade's key synthetic reactions of (-)-albacycline (**7**)

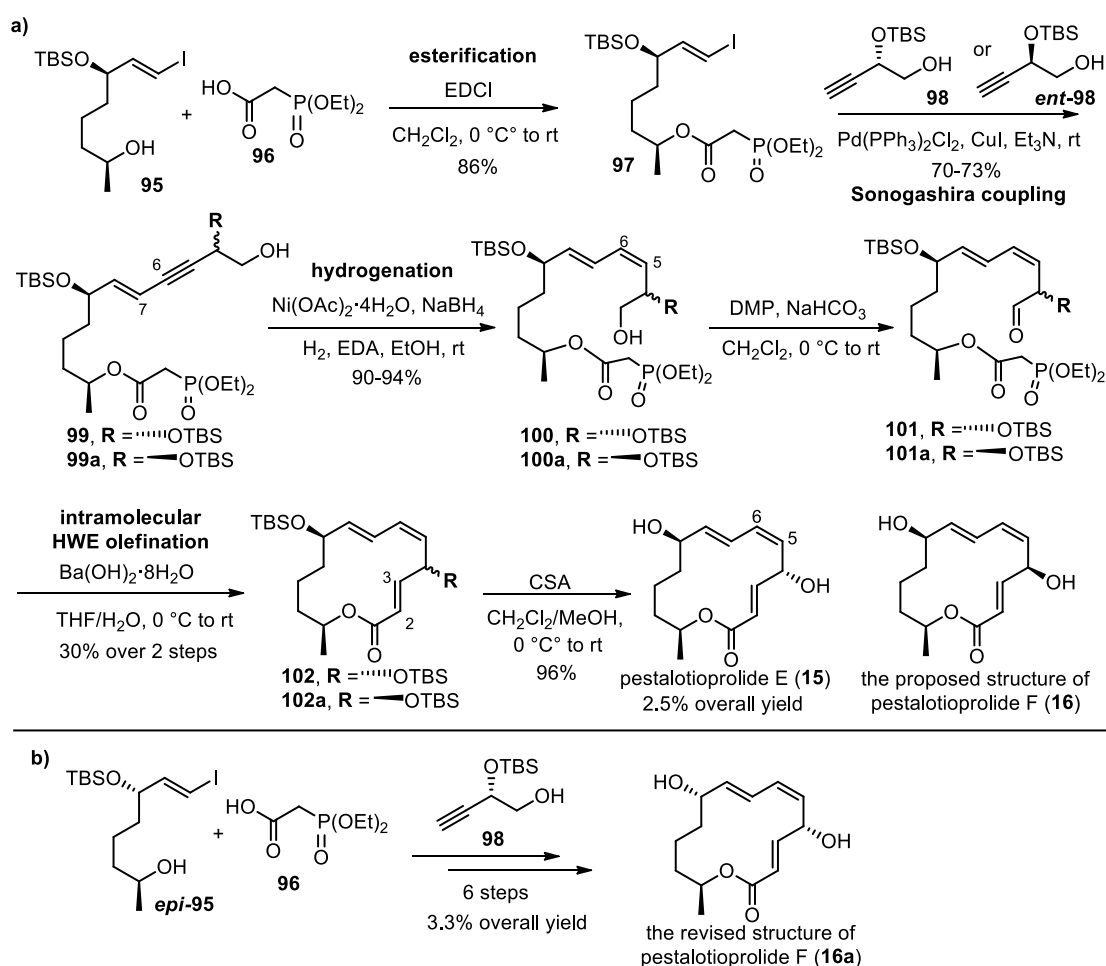
Pestalotioprolide C (**14**) was synthesized by Reddy and Sabitha in 2017 (**Scheme 9**). Their strategy also utilized HWE olefination to form *E*-double bond between C2–C3. The synthesis started with preparation of alkyne **86** from aldehyde **84** and alkyne **85** in 2 steps. Then, chiral alcohol **88** was installed via asymmetric transfer hydrogenation of ketone **86** using the (*S,S*)-Noyori catalyst **87**. After that, **88** was converted to aldehyde **90** in 4 steps consisting of PMB protection, hydrogenation, acetonide deprotection and oxidative cleavage. (*E*)- $\alpha,\beta$ -Unsaturated ester **92** was exclusively generated through intermolecular HWE olefination between aldehyde **90** and phosphonate **91**. Ethyl ester of **92** was hydrolyzed with TMSOK to provide seco acid **93**, which was subjected to Shiina macrolactonization to construct macrocycle product **94** in 85% yield. Finally, global deprotection of PMB and triisopropylsilyl (TIPS) groups of **94** were performed using  $\text{TiCl}_4$  to achieve the pestalotioprolide C (**14**) in 89% yield.

**Scheme 9** Reddy and Sabitha's key synthetic reactions of pestalotioprolide C (**14**)

One year after Reddy and Sabitha's synthesis of **14**, Goswami and co-workers disclosed the syntheses of pestalotioprolides E (**15**) and F (**16**), which utilized intramolecular HWE olefination to generate *E*-double bond between C2 and C3 (**Scheme 10a**). The synthesis commenced with the preparation of ester functionality of **97** via esterification between alcohol **95** and phosphonate **96** under the modified Steglich condition. The construction of the C6–C7 bond of enyne **99** (for **15**) and **99a** (for **16**) was carried out separately via Sonogashira coupling between vinyl iodide **97** and alkyne **98** or *ent*-**98** in the presence of Pd(PPh<sub>3</sub>)<sub>2</sub>Cl<sub>2</sub>, CuI and Et<sub>3</sub>N. Both alkyne **99** and **99a** were subjected to partial hydrogenation with Ni(OAc)<sub>2</sub>·4H<sub>2</sub>O/NaBH<sub>4</sub>/EDA to produce *Z*-alkene at C5–C6 of **100** and **100a** in high yield as a single stereoisomer. After oxidation of primary alcohol of **100** and **100a** with DMP, aldehyde **101** and **101a** were exposed to intramolecular HWE olefination to form the macrocycle **102** and **102a** in approximately 30% over 2 steps but with exclusive *E*-selectivity. Their next task toward the final product was performed via global deprotection of TBS groups of **102** and **102a** with CSA

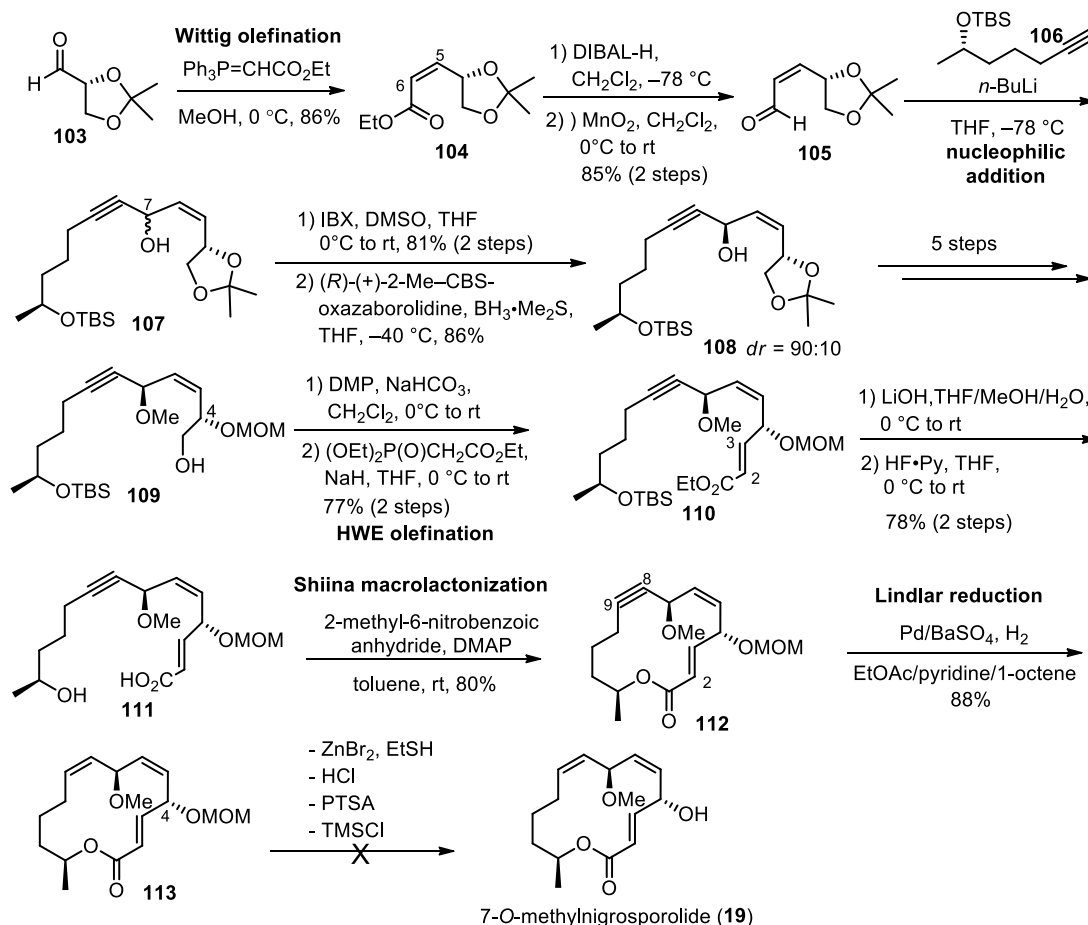
to provide pestalotioprolides E (**15**) and F (**16**), respectively. However, they discovered that the  $^1\text{H}$  and  $^{13}\text{C}$  NMR spectroscopic data as well as specific rotation of isolated pestalotioprolide F deviated considerably from the synthetic **16**. Therefore, this synthetic study led to the revision of the structure of pestalotioprolide F (**16a**), which was synthesized via the same synthetic procedure as that of **15** and **16** starting from the alcohol *epi*-**95** and phosphonate **96** (Scheme 10b).

**Scheme 10** Goswami's key synthetic reactions of pestalotioprolide E (**15**) and structural revision of pestalotioprolide F (**16a**)



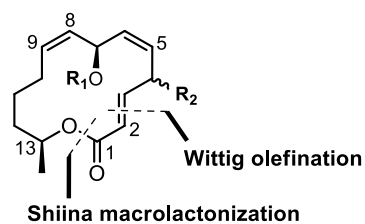
Recently, in 2019, Narsaiah and co-workers attempted to synthesize 7-*O*-methylnigrosporolide (**19**) (**Scheme 11**). The key strategy of their synthesis also relied on HWE olefination to construct an *E*-double bond between C2–C3. They started with the preparation of (*Z*)- $\alpha,\beta$ -unsaturated ester **104** from known aldehyde **103** via Wittig olefination using stabilized phosphonium ylide  $\text{Ph}_3\text{P}=\text{CHCO}_2\text{Et}$  to form C5–C6 *Z*-olefin with excellent selectivity. Ester **104** was transformed to aldehyde **105** in 2 steps via DIBAL-H reduction of ester group, followed by allylic oxidation of the corresponding primary alcohol with  $\text{MnO}_2$ . The racemic propargylic alcohol **107** was obtained from addition of the corresponding acetylide of known alkyne **106** to aldehyde **105**. After that, **107** was subjected to IBX oxidation and subsequent stereoselective reduction with (*R*)-Corey-Bakshi-Shibata reagent to generate chiral alcohol **108** in 86% yield with excellent diastereoselectivity (*dr* 90:10). Compound **108** was converted to alcohol **109** in 5 steps. The methoxymethyl (MOM) ether was chosen as a protecting group of C4-alcohol of compound **109**. Then, the construction of *E*-double bond between C2–C3 of **110** was conducted through DMP oxidation of primary alcohol **109** and subsequent HWE olefination of the corresponding aldehyde to exclusively afford (*E*)- $\alpha,\beta$ -unsaturated ester **110** in 81% yield. After hydrolysis of ester **110** with LiOH and deprotection of silyl ether with HF·Py, the resultant seco acid **111** was subjected to Shiina macrolactonization to assemble the macrocycle **112**. Lindlar reduction of **112** with Pd/BaSO<sub>4</sub> in EtOAc/pyridine/1-octene was utilized to generate exclusive *cis*-olefin at C8–C9 of **113**. In the last step, they attempted to remove the MOM protecting group at the C4-position of **113** under various acidic conditions. However, these conditions failed to yield the target molecule and led to decomposition of the starting material. Thus, a choice of C4 alcohol protecting group proved to be very crucial.

**Scheme 11** Narsaiah's key synthetic reactions towards the stereoselective synthesis of 7-*O*-methylnigrosporolide (**19**)

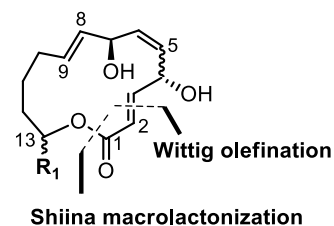


All of the aforementioned synthetic approaches suggested that Wittig and HWE olefinations are one of the most efficient methods for construction of (*E*)- $\alpha,\beta$ -unsaturated ester with high stereoselectivity and excellent yield. Moreover, Shiina and Yamaguchi macrolactonizations are also reliable methods to close the macrolactone core. Inspired by these reports, we envisioned that formation of C2–C3 *E*-olefin of macrolides **19** and **21–23** could be achieved by Wittig olefination, while the 14-membered macrocyclic core of **19–23** would be assembled via Shiina macrolactonization (**Scheme 12**).

### Scheme 12 Proposed syntheses of compounds 19–23



7-*O*-methylnigrosporolide (**19**);  $R_1 = \text{Me}$ ,  $R_2 = \text{HOH}$   
 pestalotioprolide D (**20**);  $R_1 = \text{Me}$ ,  $R_2 = \text{=O}$ ,  $-\text{CH}_2$  at C2–C3  
 nigrosporolide (**21**);  $R_1 = \text{H}$ ,  $R_2 = \text{HOH}$



mutolide (**22**): C5–C6 *E*-olefin;  $R_1 = \text{HOH}$   
 macrolide **23**: C5–C6 *Z*-olefin;  $R_1 = \text{Me}$

## 1.2 Objectives

1. To synthesize 7-*O*-methylnigrosporolide, pestalotioprolide D, nigrosporolide, mutolide and (4*S*,7*S*,13*S*)-4,7-dihydroxy-13-tetradeca-2,5,8-trienolide
2. To confirm the absolute configuration of the natural products
3. To provide materials for further evaluation of biological activities

## **CHAPTER 2**

**SYNTHESES OF 7-*O*-METHYLNIGROSPOROLIDE,  
PESTALOTIOPROLIDE D AND NIGROSPOROLIDE**



## CHAPTER 2

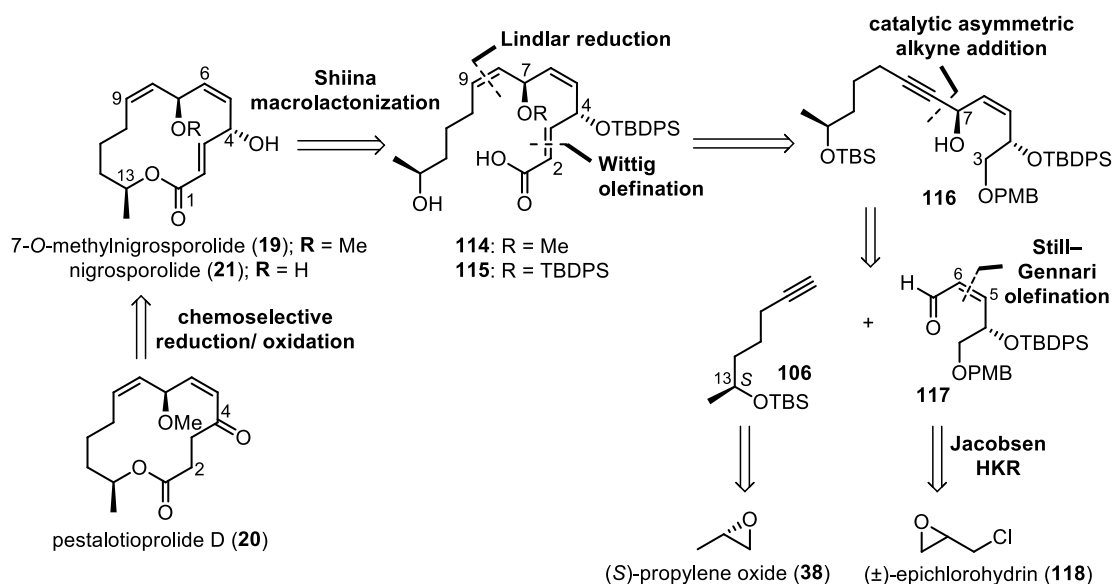
### SYNTHESES OF 7-*O*-METHYLNIGROSPOROLIDE, PESTALOTIOPROLIDE D AND NIGROSPOROLIDE

#### 2.1 Results and Discussion

Structurally, 7-*O*-methylnigrosporolide (**19**) is a C7 methoxy derivative of nigrosporolide (**21**) consisting of 14-membered ring lactone with two *Z*-double bonds at C5–C6 and C8–C9, C2–C3 *E*-olefin and three alcohol stereogenic centers at 4, 7 and 13 positions. The core skeleton of pestalotioprolide D (**20**) differs from **19** by the presence of ketone functional group at the C4-position and saturation at C2–C3. Since the core structures of compounds **19–21** are closely similar, it was envisioned that the synthesis of these macrolides would be achieved via the same synthetic strategy. The retrosynthetic analysis of **19–21** is outlined in **Scheme 13**. Macrolide **20** would be synthesized from **19** via chemoselective reduction of C2–C3 alkene, followed by oxidation of C4 alcohol to ketone functional group. The 14-membered macrocyclic core of targets **19–21** would be assembled by Shiina macrolactonization of seco acids **114** and **115**, respectively. Previous report by Narsaiah et al. has demonstrated that the choice of C4 alcohol protecting group is very crucial for the acid-sensitive final deprotection step (Narsaiah *et al.*, 2019). Therefore, the *tert*-butyldiphenylsilyl (TBDPS) group was chosen as a protecting group of C4 alcohol of **19** and **21** since it could be removed under mild and non-acidic conditions to avoid the decomposition of starting material. In addition, a TBDPS group would also be employed as a protecting group at C7 alcohol of seco acid **115** in the synthesis of nigrosporolide (**21**) to facilitate the global deprotection in the last step. The C2–C3 *E*-olefin moiety of seco acids **114** and **115** would be generated via Wittig olefination. The *cis*-olefin at C8–C9 of **114** and **115** would be prepared by Lindlar reduction of propargylic alcohol **116**, which would be constructed via asymmetric alkyne addition of known alkyne **106** to (*Z*)-enal **117** in order to form the C7–C8 bond and install the C7 alcohol stereogenic center. The

*p*-methoxybenzyl ether (PMB) group was selected as a protecting group at C3-alcohol of intermediate **116** due to its orthogonality to silyl protecting groups and selective deprotection in the presence of sensitive alkene functionality. (*S*)-Alkyne **106** would be synthesized from (*S*)-propylene oxide (**38**), while (*Z*)-enal **117** would be prepared from ( $\pm$ )-epichlorohydrin (**118**) through Jacobsen hydrolytic kinetic resolution (HKR) to install the stereogenic center at the C4-position and Still–Gennari olefination to form C5–C6 *Z*-olefin as the key strategies.

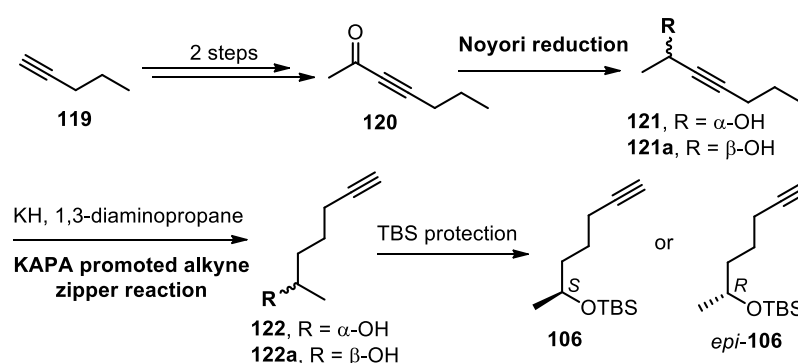
**Scheme 13** Retrosynthetic analysis of 7-*O*-methylnigrosporolide (**19**), pestalotioprolide D (**20**) and nigrosporolide (**21**)



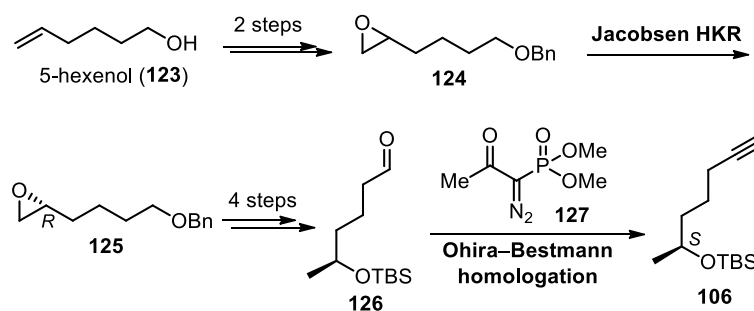
Our synthesis began with the preparation of (*S*)-alkyne **106**. The syntheses of alkynes **106** and *epi*-**106** have been reported by Wang *et al.* and Menezes *et al.*, respectively (Menezes *et al.*, 2008 and Wang *et al.*, 2016) (**Scheme 14**). Their synthetic approaches provided a good yield and high enantioselectivity using key Noyori reduction and alkyne zipper reaction with potassium 3-aminopropanamide (KAPA) reagent generated in situ from potassium hydride (KH) and 1,3-diaminopropane. However, the costliness of KH and difficulties with its safe laboratory handling led us to explore an alternative method to prepare (*S*)-alkyne **106** (Macaulay, 1980 and O'Doherty *et al.*, 2014). Later, in 2019, Narsaiah and co-workers reported a different approach for the synthesis of **106** (**Scheme 15**). Their synthesis started with the installation of chiral epoxide **125** from 5-hexenol (**123**) in 3 steps using the Jacobsen

HKR as the key strategy. After that, (*R*)-epoxide **125** was transformed to aldehyde precursor **126** in 4 steps. Finally, the homologation of aldehyde **126** with Ohira–Bestmann reagent (dimethyl 1-diazoacetylphosphonate, **127**) was performed to produce terminal alkyne of **106**. Although Narsaiah’s protocol would be compatible with our laboratory setup, it is quite lengthy and required 8 total steps with only 18% overall yield from racemic epoxide **124**.

#### Scheme 14 Menezes or Wang’s synthesis of alkynes **106** and *epi*-**106**



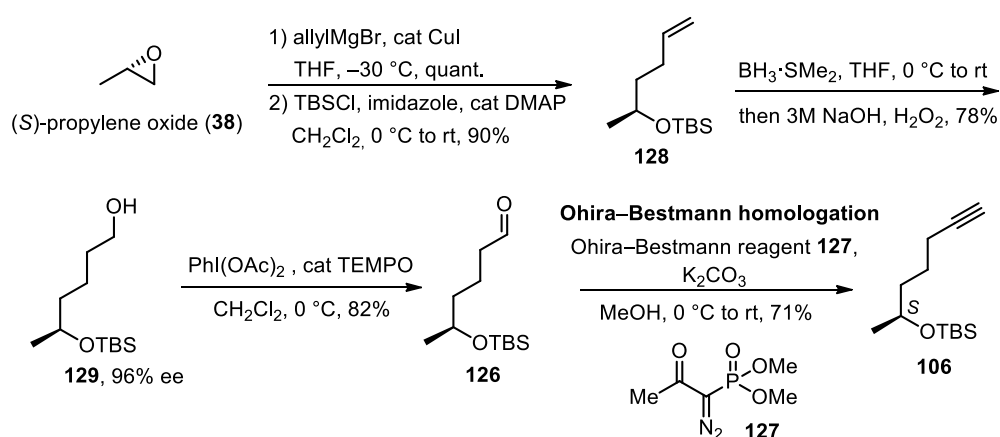
#### Scheme 15 Narsaiah’s synthesis of (*S*)-alkyne **106**



Inspired by Narsaiah’s report, we also planned to use Ohira–Bestmann homologation of aldehyde **126** as the key strategy to form (*S*)-alkyne **106**. However, a shorter synthetic sequence to deliver aldehyde **126** was performed in only 4 steps starting from commercially available (*S*)-propylene oxide (**38**) (Scheme 16). The process started with ring opening of (*S*)-epoxide **38** with allylmagnesium bromide in the presence of catalytic CuI to produce chiral alcohol, which was immediately protected with TBSCl to afford silyl ether **128** in 90% yield (Sasaki *et al.*, 2011 and Pandey *et al.*, 2018). Hydroboration of alkene **128** using borane dimethyl sulfide

( $\text{BH}_3 \cdot \text{SMe}_2$ ), followed by oxidation with hydrogen peroxide in 3M NaOH gave primary alcohol **129** in 78% yield (Sharma *et al.*, 2017). The enantiopurity of **129** was confirmed to be 96% ee by chiral HPLC of the corresponding benzoate derivative of **129**. After that, alcohol **129** was oxidized with  $\text{PhI}(\text{OAc})_2$  and catalytic TEMPO to deliver the requisite aldehyde **126** in 82% yield. Finally, treatment of **126** with Ohira–Bestmann reagent **127** and  $\text{K}_2\text{CO}_3$  in methanol provided the desired alkyne **106** in 71% yield (Marshall and Adams, 2002). Our method to synthesize (*S*)-alkyne **106** was accomplished in 5 steps and 40% overall yield, rendering a shorter synthetic sequence and higher overall yield compared with Narsaiah’s procedure.

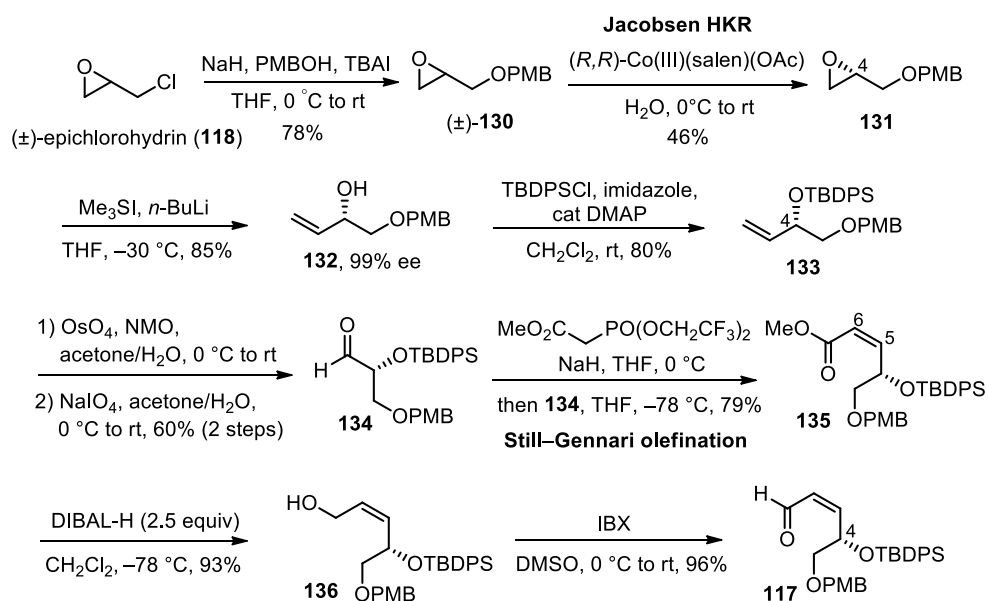
### Scheme 16 Synthesis of (*S*)-alkyne **106**



The synthesis of (*Z*)-enal **117** is shown in **Scheme 17**. The Jacobsen hydrolytic kinetic resolution (HKR) was utilized to install the stereogenic center at the C4-position. The synthetic sequence commenced with the preparation of known chiral epoxide **131** from commercially available ( $\pm$ )-epichlorohydrin (**118**) using a similar procedure to that described by Yadav and co-workers in 2014. Compound **118** was converted to *p*-methoxybenzyl glycidyl ether ( $\pm$ )-**130** by treatment of **118** with premixed *p*-methoxybenzyl alcohol (PMBOH) and NaH in the presence of tetrabutylammonium iodide (TBAI). The Jacobsen HKR of **130** using 0.5 mol % of (*R,R*)-Co(III)(salen)(OAc) catalyst afforded (*S*)-epoxide **131** in 46% yield. Next, nucleophilic epoxide ring opening of **131** with trimethylsulfonium ylide provided the chiral allylic alcohol **132** in 85% yield (Kim *et al.*, 2010 and Kumaraswamy and Sadaiah, 2012). The enantiopurity of **132** was determined to be 99% ee by chiral HPLC

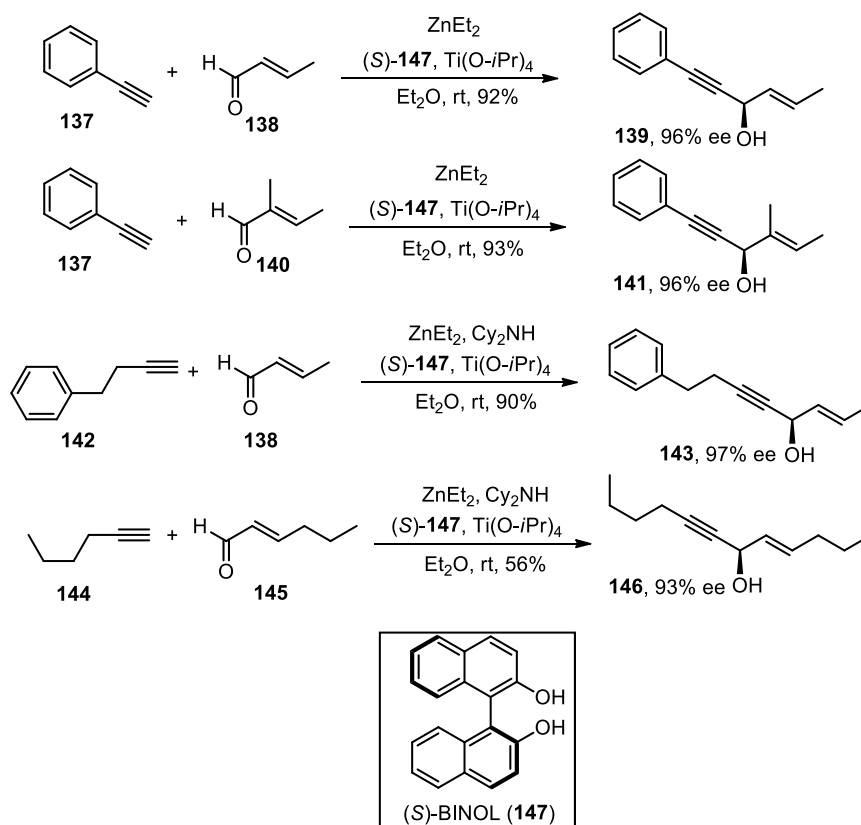
analysis of the corresponding benzoate derivative of **132**. The absolute configuration of the alcohol chiral center was confirmed to be *S* by Mosher's ester analysis. The C4 hydroxyl group of **132** was then protected with TBDPSCI to give silyl ether **133** in 80% yield. Subsequent oxidative cleavage of terminal alkene **133** using a modified Lemieux–Johnson reaction afforded aldehyde **134** in 60% yield over 2 steps. The next task was to generate C5–C6 *Z*-olefin of **135** through Still–Gennari olefination. Compound **134** was exposed to methyl bis(2,2,2-trifluoroethyl)phosphonoacetate and NaH in THF to give exclusive (*Z*)- $\alpha,\beta$ -unsaturated ester **135** in good yield (Mohapatra *et al.*, 2017). The *Z*-geometry of the newly created olefin was confirmed based on the coupling constant of 11.7 Hz between H5 and H6. After that, methyl ester of **135** was reduced with 1 equivalent of DIBAL-H in THF at  $-78$  °C. Nevertheless, these conditions led to the expected aldehyde **117** in only 48% yield along with 39% yield of allylic alcohol **136** based on recovered starting methyl ester **135**. It should be noted that reduction of the methyl ester moiety of **135** to alcohol **136** was very facile under these conditions. To circumvent the problems of incomplete consumption of starting ester **135**, excess (2.5 equivalents) DIBAL-H was required to produce allylic alcohol **136** in 93% yield as a single product, which was reoxidized with IBX to deliver the desired (*Z*)-enal **117** in 96% yield.

### Scheme 17 Synthesis of (*Z*)-enal **117**



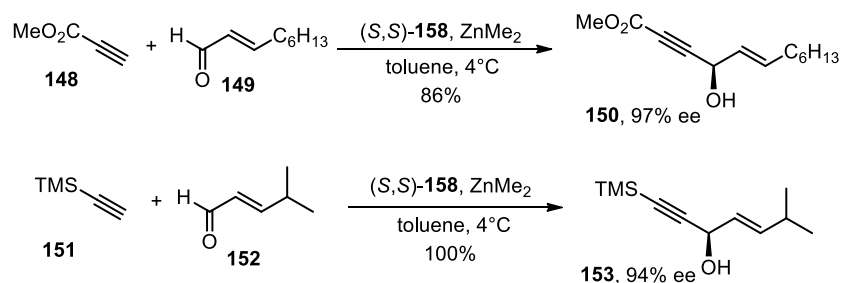
Having accomplished the synthesis of both alkyne **106** and  $\alpha,\beta$ -unsaturated aldehyde **117**, our next task was to assemble the two key fragments to form the C7–C8 bond and install the C7 alcohol stereogenic center of propargylic alcohol **116**. The catalytic enantioselective alkynylzinc addition to aldehydes is the widely employed method to construct chiral propargyl alcohol with high enantiomeric purity. In particular, asymmetric alkyne addition to  $\alpha,\beta$ -unsaturated aldehydes which have core structures similar to our enal substrate are also precedented. Previous reports by Pu and co-workers have demonstrated that the (*S*)-1,1'-bi-2-naphthol ((*S*)-BINOL **147**)-ZnEt<sub>2</sub>-Ti(O-*i*Pr)<sub>4</sub> catalyst system with or without dicyclohexylamine (Cy<sub>2</sub>NH) additive was effective for the alkyne addition to various types of aldehydes including  $\alpha,\beta$ -unsaturated aldehydes with high enantioselectivity as shown in **Scheme 18** (Pu *et al.*, 2002, 2010, 2013 and 2015). Furthermore, another highly efficient protocol to access high enantioselectivity and yield of chiral propargyl alcohols is Trost's asymmetric alkyne addition using ZnMe<sub>2</sub> and (*S,S*)-ProPhenol [2,6-bis({2-[hydroxy(diphenyl)methyl]pyrrolidin-1-yl}methyl)-4-methylphenol, **158**] as a chiral ligand (Trost *et al.*, 2006, 2012 and Bittman, *et al.*, 2010) (**Scheme 19a**). These conditions have enabled the total synthesis of a wide range of complex natural products. For example, in 2012, Trost and Bartlett reported the synthesis of aspergillide B (**157**) using the key Zn-ProPhenol catalyzed asymmetric alkyne addition between (*S*)-hept-6-yn-2-yl benzoate (**154**) and (*E*)-enal **155** to form propargylic alcohol **156** in 82% yield and 90% de (Trost and Bartlett, 2012) (**Scheme 19b**). The Trost group has also found that triphenylphosphine oxide (TPPO), a Lewis base additive significantly improved the enantioselectivity and yields of this reaction. They hypothesized that this Lewis basic group might coordinate with each of the zinc atoms and reinforce the chiral pocket created by the ProPhenol ligand (complex **159**) (Trost *et al.*, 2012). However, examples of the preparation of chiral propargylic alcohol via Zn-mediated asymmetric alkynylation of (*Z*)-enal by the Pu and Trost groups have never been reported.

**Scheme 18** Examples of asymmetric alkyne addition to  $\alpha,\beta$ -unsaturated aldehydes with (BINOL)-ZnEt<sub>2</sub>-Ti(O-*i*Pr)<sub>4</sub> catalyst system by Pu et al.

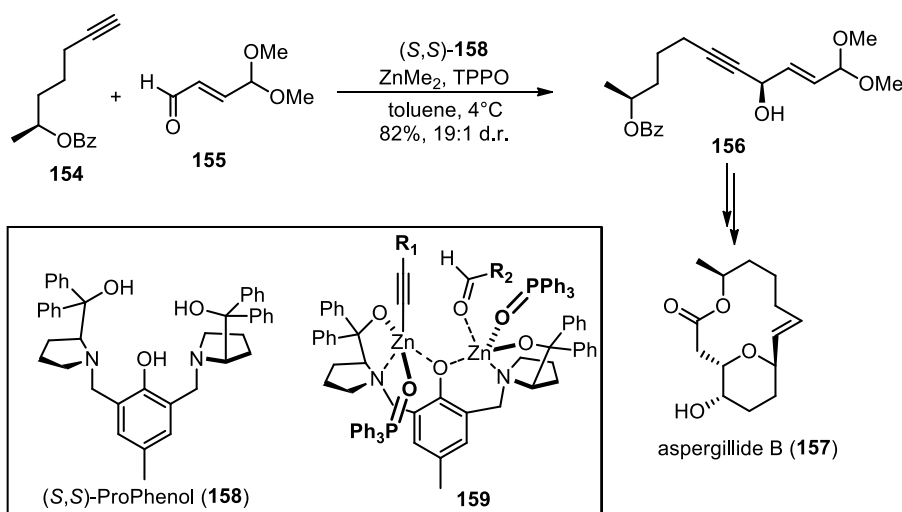


**Scheme 19** Examples of Zn-ProPhenol catalyzed asymmetric alkyne addition to  $\alpha,\beta$ -unsaturated aldehydes by Trost and co-workers

a)



b)

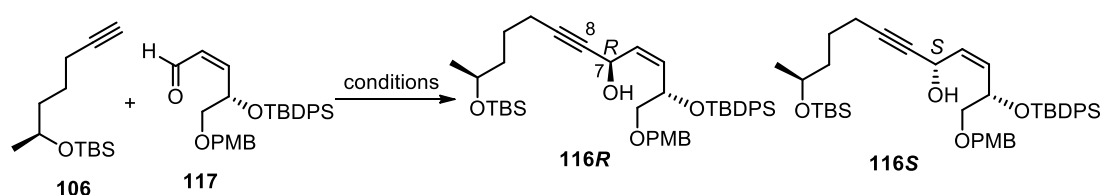


Owing to the effectiveness of the aforementioned Zn-mediated asymmetric alkynylation, the coupling of the key intermediates **106** and **117** to generate chiral propargylic alcohol **116** under these reactions was applied in our synthesis as shown in **Table 1**. Reaction conditions employing  $(S)$ -BINOL (20 mol %) as a chiral ligand in the presence of  $\text{ZnEt}_2$  (3 equiv),  $\text{Ti}(\text{O}-i\text{Pr})_4$  (20 mol %) and  $\text{Cy}_2\text{NH}$  (5 mol %) as an additive in  $\text{Et}_2\text{O}$  at room temperature were initially chosen (entry 1). Unfortunately, no desired product was obtained and the starting materials were recovered. After that, asymmetric alkynylzinc addition with Trost's protocol was attempted. The first conditions consisted of 1.5 equivalents of  $\text{ZnMe}_2$  and 10 mol % of  $(S,S)$ -ProPhenol ligand in toluene from  $0^\circ\text{C}$  to room temperature (entry 2). These conditions also failed to furnish any desired products and only the starting materials were observed. Increasing the amount of  $\text{ZnMe}_2$  to 3 equivalents under the same conditions also resulted in no reaction (entry 3). Further optimization of Trost's protocol was then performed by increasing the amount of  $\text{ZnMe}_2$  to 5 equivalents and  $(S,S)$ -ProPhenol to 20 mol % (entry 4). Gratifyingly, the requisite propargylic alcohol **116R** was formed under these conditions, however, the undesired **116S** was also obtained in a combined yield of only 33% as a 2:1 mixture of separable diastereomers. The absolute configuration of the C7 stereogenic centers of **116R** and **116S** were confirmed by the Mosher ester analysis. Similarly, 20 mol % of triphenylphosphine oxide (TPPO) additive did not improve this reaction as the separable propargylic alcohols **116R** and **116S** were also observed in only 20%



and 12% yields, respectively (entry 5). These unsuccessful results might be consistent with Pu and Trost's reports. Only the (*E*)-enal substrates might be compatible with Zn-mediated asymmetric alkylation to produce high enantioselectivity and yield of chiral propargylic alcohols.

**Table 1** Screening of Zn-mediated asymmetric alkylation reaction to assemble (*S*)-alkyne **106** and (*Z*)-enal **117**

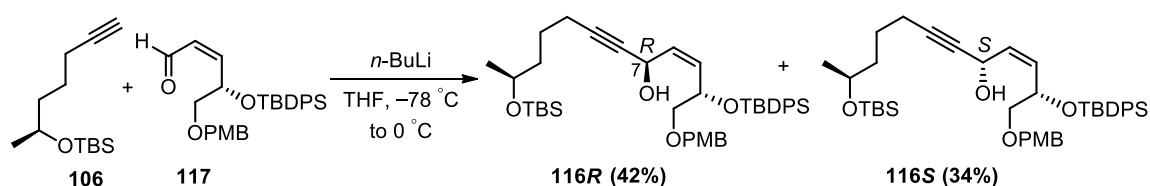


entry	reagents	solvent	temp	time (h)	results
1	ZnEt <sub>2</sub> (3.0 equiv), ( <i>S</i> )-BINOL (20 mol %), Ti(O- <i>i</i> Pr) <sub>4</sub> (20 mol %), Cy <sub>2</sub> NH (5 mol %)	Et <sub>2</sub> O	rt	19	no reaction
2	ZnMe <sub>2</sub> (1.5 equiv), ( <i>S,S</i> )-ProPhenol (10 mol %)	toluene	0 °C to rt	4	no reaction
3	ZnMe <sub>2</sub> (3.0 equiv), ( <i>S,S</i> )-ProPhenol (10 mol %)	toluene	0 °C to rt	7	no reaction
4	ZnMe <sub>2</sub> (5.0 equiv), ( <i>S,S</i> )-ProPhenol (20 mol %)	toluene	0 °C to rt	18	<b>116R</b> (22% yield), <b>116S</b> (11% yield),
5	ZnMe <sub>2</sub> (5.0 equiv), TPPO (20 mol %) ( <i>S,S</i> )-ProPhenol (20 mol %)	toluene	0 °C to rt	20	<b>116R</b> (20% yield), <b>116S</b> (12% yield),

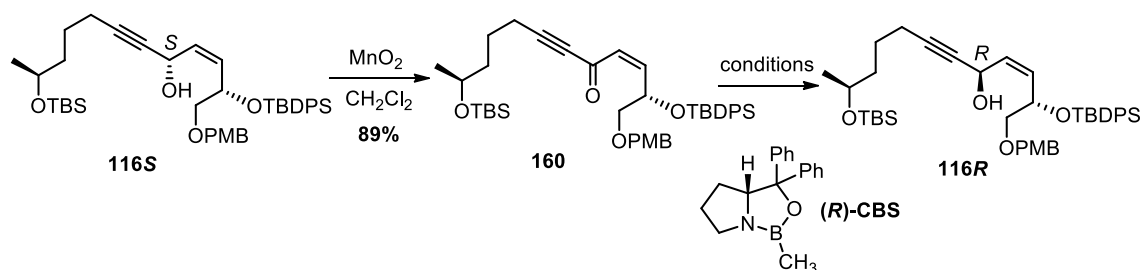
Due to the unsuccessful Zn-mediated asymmetric alkylation of enal **117** to form the desired propargylic alcohol **116R**, the assembling of known alkyne **106** and (*Z*)-enal **117** was then performed via an acetylide addition in the hope that the chiral elements in each fragment would possibly facilitate asymmetric induction in this step (**Scheme 20**). The acetylide anion generated in situ from deprotonation of

terminal alkyne **106** with *n*-BuLi was treated with chiral aldehyde **117** in THF from  $-78$  to  $0$  °C. These conditions led to the formation of the desired propargylic alcohols **116R** together with **116S** in 76% yield as a separable 1.2:1 mixture of diastereomers. Attempts to convert the undesired propargylic alcohol **116S** into **116R** were performed by stereoselective Corey-Bakshi-Shibata (CBS) reduction of ynone **160**, which was prepared from **116S** by MnO<sub>2</sub> oxidation (**Table 2**). Previous report by Yue et al. and Narsaiah et al. have demonstrated the stereoselective (*R*)-CBS reduction of ynone intermediates that have core structure similar to ynone **160** to produce chiral propargylic alcohols in high yield and stereoselectivity (Yue *et al.*, 2012 and Narsaiah *et al.*, 2019). Thus, stereoselective reduction of **160** was initially performed by employing 1.5 equivalents of (*R*)-CBS reagent and 2 equivalents of BH<sub>3</sub>·SMe<sub>2</sub> in THF from  $-78$  °C to  $-30$  °C (entry 1). Disappointingly, the desired **116R** was obtained as a minor product in only 35% yield whereas the undesired **116S** was formed in 41% yield based on recovered starting ketone **160**. In an attempt to ensure complete consumption of starting material, the reaction was performed at  $0$  °C to room temperature under the same conditions (entry 2). However, the starting ketone **160** was again recovered and the product yields of **116R** and **116S** decreased to 29% and 35%, respectively. Further optimization was then performed by changing the solvent to toluene owing to literature precedents on successful use of this solvent in stereoselective CBS reduction (Suenaga *et al.*, 2014, Wei *et al.*, 2016 and Yu *et al.*, 2017). Reaction conditions using (*R*)-CBS conditions in toluene at  $-30$  °C led to the formation of the requisite alcohol **116R** as a major product, but in only 42% yield together with the undesired **116S** in 25% yield based on recovered starting ynone **160** (entry 3). Elevating the reaction temperature to  $-15$  °C slightly increased the yield of the propargylic alcohol **116R** to 48%, however, the undesired **116S** as well as starting ynone **160** were also observed under these conditions (entry 4). Prolonged reaction time of 17 hours under these conditions did not improve the reaction although complete consumption of the starting ynone **160** was observed. In addition, propargylic alcohols **116R** and **116S** were obtained in low yields along with a multitude of unidentifiable products, which presumably formed upon decomposition of starting material (entry 5).

**Scheme 20** Acetylide addition between (*S*)-alkyne **106** and (*Z*)-enal **117**



**Table 2** Screening of stereoselective CBS reduction of ynone **160**

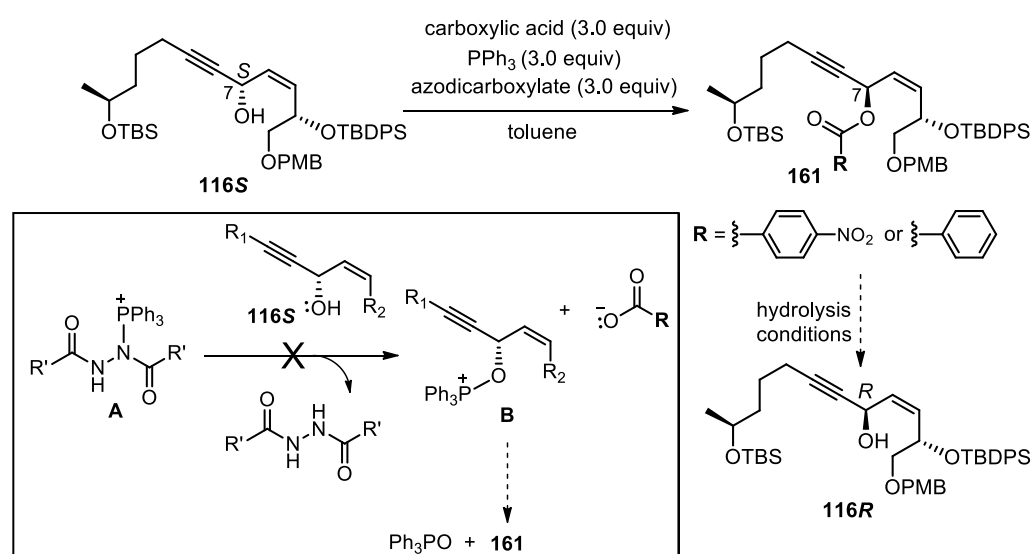


entry	reagent	solvent	temp	time (h)	results
1	$(R)\text{-CBS}$ (1.5 equiv) $\text{BH}_3\cdot\text{SMe}_2$ (2.0 equiv)	THF	$-78\text{ }^{\circ}\text{C}$ to $-30\text{ }^{\circ}\text{C}$	3.0	<b>116R</b> (35% brsm), <b>116S</b> (41% brsm)
2	$(R)\text{-CBS}$ (1.5 equiv) $\text{BH}_3\cdot\text{SMe}_2$ (2.0 equiv)	THF	$0\text{ }^{\circ}\text{C}$ to rt	3.5	<b>116R</b> (29% brsm), <b>116S</b> (35% brsm)
3	$(R)\text{-CBS}$ (1.5 equiv) $\text{BH}_3\cdot\text{SMe}_2$ (2.0 equiv)	toluene	$-30\text{ }^{\circ}\text{C}$	3	<b>116R</b> (42% brsm), <b>116S</b> (25% brsm)
4	$(R)\text{-CBS}$ (1.5 equiv) $\text{BH}_3\cdot\text{SMe}_2$ (2.0 equiv)	toluene	$-15\text{ }^{\circ}\text{C}$	9	<b>116R</b> (48% brsm), <b>116S</b> (23% brsm)
5	$(R)\text{-CBS}$ (1.5 equiv) $\text{BH}_3\cdot\text{SMe}_2$ (2.0 equiv)	toluene	$-15\text{ }^{\circ}\text{C}$	17	<b>116R</b> (25%), <b>116S</b> (12%), complex mixture

Due to unsatisfactory stereoselectivity of CBS reduction of ynone **160**, another method to improve stereoselective formation of (*R*)-alcohol **116** was investigated. Mitsunobu reaction is one of the effective methods to invert the stereochemistry of secondary alcohol chiral center. Therefore, the undesired diastereomer **116S** was then subjected to Mitsunobu conditions in order to invert the

absolute configuration of the C7 alcohol stereogenic center (Yadav *et al.*, 2008 and 2011, Prasad and Pawar, 2011 and Dudley *et al.*, 2013) (**Table 3**). Reaction conditions using 3 equivalents of 4-nitrobenzoic acid, diethyl azodicarboxylate (DEAD) and triphenylphosphine (PPh<sub>3</sub>) in toluene at room temperature were initially selected (entry 1). Disappointingly, these conditions resulted only in recovered starting alcohol **116S**. Increasing the reaction temperature to 60 °C or replacing DEAD with diisopropyl azodicarboxylate (DIAD) also led to the recovery of starting alcohol **116S** (entries 2 and 3). Further attempts were then performed by changing carboxylic acid nucleophile to benzoic acid under the same conditions used in entries 2 and 3 (entries 4 and 5). Similarly, no desired ester was obtained from any of these reactions and the starting material was recovered. To the best of our knowledge, there was no literature precedent on the inversion of the absolute stereochemistry of secondary alcohol chiral center that had the adjacent alkyne and Z-alkene moieties similar to alcohol **116S** via Mitsunobu reaction. It was assumed that the electronic effect from both alkyne and alkene groups might decrease nucleophilicity of the C7 alcohol, which might result in the failure to form oxyphosphonium ion **B**.

**Table 3** Screening for Mitsunobu inversion of propargylic alcohol **116S**

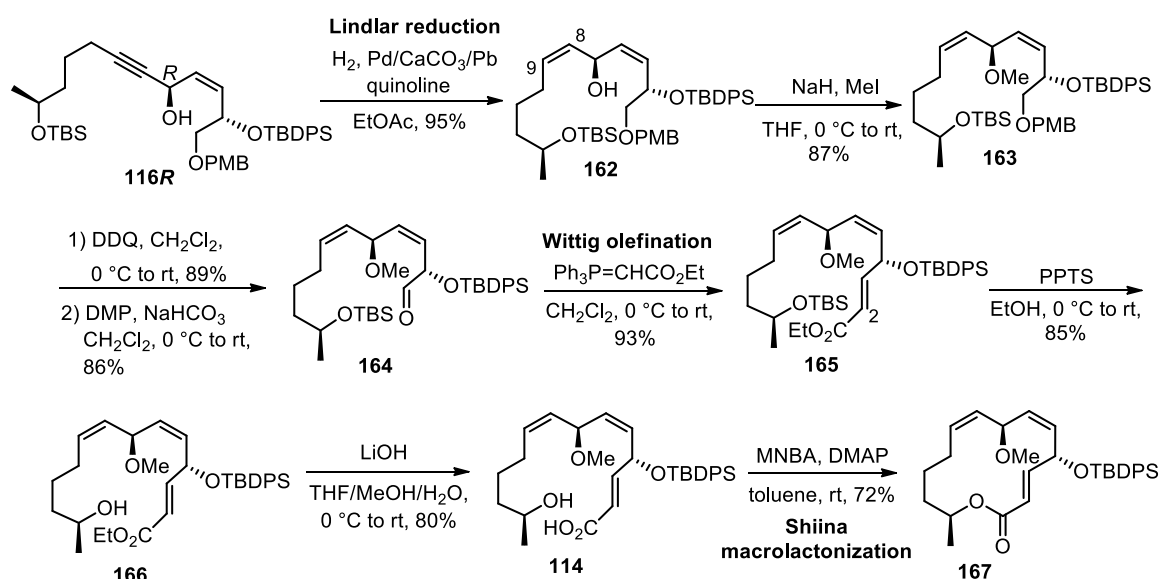


entry	carboxylic acid	azodicarboxylate	temp	time (h)	results
1	4-nitrobenzoic acid	DEAD	rt	20	no reaction
2	4-nitrobenzoic acid	DEAD	60 °C	16	no reaction
3	4-nitrobenzoic acid	DIAD	60 °C	19	no reaction
4	benzoic acid	DEAD	60 °C	18	no reaction
5	benzoic acid	DIAD	60 °C	18	no reaction

Owing to unsuccessful attempts to exclusively form chiral propargylic alcohol **116R** via the aforementioned strategies, an acetylide addition was chosen as the method to form **116R** because it was the most expedient way to access large amount of this substrate. Our next task was to reduce the alkyne moiety of **116R** to a *Z*-olefin via Lindlar reduction (**Scheme 21**). Alkyne **116R** was exposed to Pd/CaCO<sub>3</sub> poisoned with lead in the presence of quinoline in EtOAc under H<sub>2</sub> atmosphere to produce (*Z*)-olefin **162** in 95% yield (Ariza *et al.*, 2006). The *Z*-geometry of C8–C9 olefin was verified based on the coupling constant of 11.4 Hz between H8 and H9. The β-hydroxy group at C7 of **162** was methylated by treatment with iodomethane and NaH to afford the methoxy derivative **163** in 87% yield. Next, installation of the α,β-unsaturated ester to extend two-carbon fragment of the macrocycle from **163** was achieved in 3 steps starting with PMB deprotection of **163** using DDQ to provide the corresponding primary alcohol in 89% yield. Subsequent oxidation with DMP in the presence of NaHCO<sub>3</sub> in CH<sub>2</sub>Cl<sub>2</sub> gave aldehyde **164** in 86% yield (Tan *et al.*, 2014 and Walsh *et al.*, 2009). After that, Wittig olefination of **164** with (carbethoxymethylene)triphenylphosphorane in CH<sub>2</sub>Cl<sub>2</sub> afforded exclusive (*E*)-α,β-unsaturated ester **165** in 93% yield. The geometry of the newly created double bond was again confirmed to be *trans* by the coupling constant of 15.6 Hz between H2 and H3 of **165**. The next challenging task was to selectively remove the TBS protecting group of **165** in the presence of TBDPS group. Gratifyingly, when compound **165** was treated with 3 equivalents of pyridinium *p*-toluenesulfonate (PPTS) in ethanol, the secondary alcohol **166** was formed as a single product in excellent yield. After that, ethyl ester of **166** was then hydrolyzed

with LiOH in THF/MeOH/H<sub>2</sub>O to deliver seco acid **114** in 80% yield. To access the macrocycle product, compound **114** was then subjected to Shiina macrolactonization. Following the reaction conditions by Narsaiah *et al.*, 1.2 equivalents of 2-methyl-6-nitrobenzoic anhydride (MNBA) and 6 equivalents of DMAP in toluene were initially chosen (Narsaiah *et al.*, 2019). It should be noted that excess DMAP was required in these conditions as a bifunctional reagent to produce activated acyl carboxylate for macrocycle assembly via intramolecular nucleophilic substitution of hydroxyl group as well as to deprotonate acidic protons in the first and last steps. However, these conditions led to the formation of the desired macrocycle **167** in only 45% yield. Further optimization was then performed by decreasing the amount of MNBA or DMAP. It was found that decreasing the amount of DMAP did not improve the reaction whereas reducing the amount of MNBA led to the formation of **167** in higher yield. Thus, reaction conditions using 0.6 equivalents of MNBA and 6 equivalents of DMAP were the best conditions to smoothly produce the macrocycle **167** in 72% yield (Snider and Zhou, 2006 and Narsaiah *et al.*, 2019).

### Scheme 21 Synthesis the macrocycle **167**

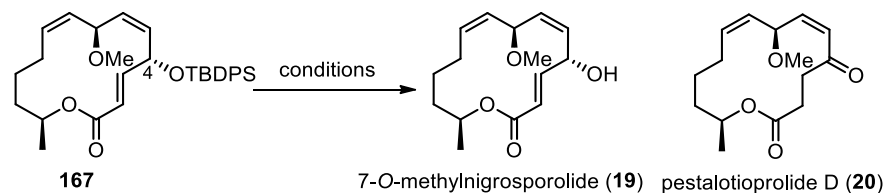


With the macrocycle **167** in hand, the next step was to remove of TBDPS protecting group of the C4 alcohol of **167** to access the final product (**Table 4**). There are previous reports by Kumar and Kauloorkar as well as Nanda and co-workers, which demonstrated the successful desilylation of the alcohol substrates containing adjacent

unsaturated ester by using ammonium fluoride ( $\text{NH}_4\text{F}$ ) in MeOH (Kauloorkar and Kumar, 2016 and Nanda *et al.*, 2010). However, when macrocycle **167** was treated with 10 equivalents of  $\text{NH}_4\text{F}$  in MeOH at 0 °C, the desired 7-*O*-methylnigrosporolide (**19**) was not observed and the starting material was recovered (entry 1). Similarly, silyl deprotection of **167** with PPTS or (1*S*)-(+)-camphor-10-sulfonic acid (CSA) resulted in no reaction (Prakash *et al.*, 1989 and Kalesse *et al.*, 2004) (entries 2 and 3). Further optimization was then undertaken by employing typical desilylation conditions with 3 equivalents of TBAF in anhydrous THF from 0 °C to room temperature (entry 4). To our surprise, pestalotioprolide D (**20**) was observed under these conditions albeit in only 48% yield and starting macrocycle **167** was recovered in 33% yield. Increasing the amount of TBAF to 5 equivalents under the same conditions resulted in complete consumption of the starting material but the yield of **20** increased to 75% (entry 5). Direct observation of compound **20** from macrocycle **167** instead of 7-*O*-methylnigrosporolide (**19**) under desilylation conditions mediated by TBAF suggested that **20** might be an artifact of **19**. Possible pathways for the formation of **20** from **167** under TBAF-mediated desilylation are proposed in **Scheme 22**. The first pathway as shown in **Scheme 22a**, treatment of compound **167** with large excess TBAF resulted in the formation of strongly basic tetrabutylammonium alkoxide **167a**. A 1,2-hydride shift of H-4 of **167a** to the adjacent electron-deficient olefin would deliver the thermodynamically more stable ketone moiety at C4-position of **20**. After the reaction work-up, macrolide **20** was formed as a sole product. Another possible pathway to form **20** from **167** under TBAF conditions is shown in **Scheme 22b**. When compound **167** was treated with large excess TBAF, enolate intermediate **167b** would be generated via enolization of acidic proton at C4 of **167** under basic conditions and subsequent desilylation. Then, pestalotioprolide D (**20**) was formed after the reaction work-up through tautomerization. To the best of our knowledge, there was no report on the  $\text{p}K_{\text{a}}$  value of an acidic proton at C4 of a similar macrocycle **167**. However, the H-4 of **167** is likely the most acidic proton based on the Web application of the  $\text{p}K_{\text{a}}$  predictor (<https://pka.allchemy.net/>, created and developed by Grzybowski and co-workers (Grzybowski *et al.*, 2019)) with a  $\text{p}K_{\text{a}}$  value of approximately 21. Recently, Taylor and co-workers have demonstrated the desilylation of a  $\gamma$ -silyloxy  $\alpha,\beta$ -unsaturated ketone **168** using 2 equivalents of TBAF in THF. However, these conditions led to the formation of unexpected 1,4-diketone **168b**. The

Taylor group proposed that compound **168b** was presumably obtained from air oxidation or silyl deprotection, followed by tautomerization (Taylor *et al.*, 2023) (**Scheme 23**). This report could support our second proposed mechanism for the construction of pestalotioprolide D (**20**) in **Scheme 22b**. Moreover, the phenomenon to deliver 1,4-dione product lacking the alkene moiety similar to our macrolide **20** has also been encountered in the removal of the silyl group of a similar  $\gamma$ -silyloxy  $\alpha,\beta$ -unsaturated methyl ester **169** using 2 equivalents of TBAF in THF reported by Rodrigo and Guan in 2012. Compound **170** was exclusively obtained under these conditions (**Scheme 24**). Under extremely basic conditions, we assumed that it might lead to the formation of **20** via possible pathways as mentioned in **Scheme 22**. To support these hypotheses, acetic acid was added to TBAF conditions as a buffer that mitigated the basicity of TBAF to prevent the 1,2-hydride shift (for **Scheme 22a**) or enolization of H-4 (for **Scheme 22b**). Gratifyingly, the modification of silyl deprotection conditions using 8 equivalents of TBAF buffered with acetic acid (5 mol %) in THF from 0 °C to 63 °C provided the desired 7-*O*-methylnigrosporolide (**19**) in 50% yield along with 31% of unreacted starting macrocycle **167**. Nonetheless, the formation of macrolide **20** was not observed under these conditions (entry 6) (Mohapatra *et al.*, 2010, Miller *et al.*, 2011 and Kanoh *et al.*, 2014). In an attempt to ensure complete consumption of macrocycle **167**, the amount of TBAF and acetic acid were increased to 15 equivalents and 10 mol %, respectively (entry 7). However, these conditions did not improve the reaction and starting macrocycle **167** was recovered once again. As such, silyl deprotection was further optimized by employing 15 equivalents of TBAF under the same amount of acetic acid as that of entry 6 in anticipation that compound **20** would not be formed (entry 8). Disappointingly, although starting **167** was not recovered under these conditions, the yield of targeted macrolactone **19** was decreased to 28%, and **20** was also obtained in 40% yield as a major product. Therefore, reaction conditions employing 8 equivalents of TBAF and 5 mol % of acetic acid in THF from 0 °C to 63 °C were the best conditions that led to the formation of 7-*O*-methylnigrosporolide (**19**) as a single product.

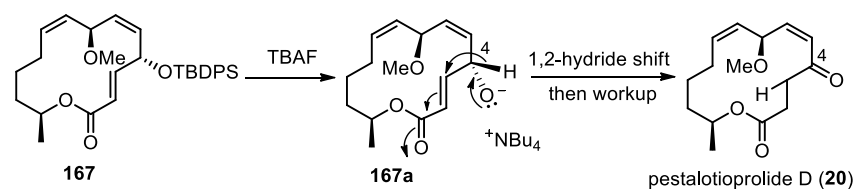


**Table 4** Screening for silyl deprotection conditions of **167**

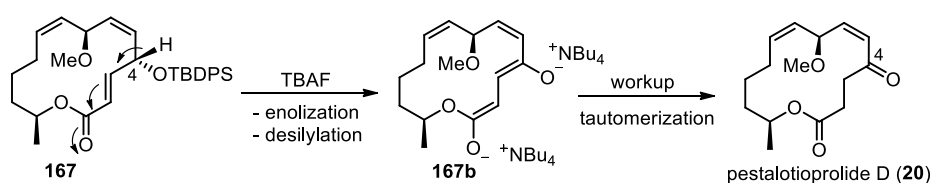
entry	reagent	solvent	temp	time (h)	results
1	NH <sub>4</sub> F (10 equiv)	MeOH	0 °C	8	no reaction
2	PPTS (5 equiv)	EtOH	0 °C to rt	17	no reaction
3	CSA (1 equiv)	CH <sub>2</sub> Cl <sub>2</sub> :MeOH	0 °C to rt	6	no reaction
4	TBAF (3 equiv)	THF	0 °C to rt	4	<b>20</b> (48% yield, 70% brsm)
5	TBAF (5 equiv)	THF	0 °C to rt	2.5	<b>20</b> (75% yield)
6	TBAF (8 equiv)/ AcOH (5 mol %)	THF	0 °C to 63 °C	10	<b>19</b> (50% yield, 72% brsm)
7	TBAF (15 equiv)/ AcOH (10 mol %)	THF	0 °C to 63 °C	15	<b>19</b> (45% yield, 70% brsm)
8	TBAF (15 equiv)/ AcOH (5 mol %)	THF	0 °C to 63 °C	9	<b>19</b> (28% yield) <b>20</b> (40% yield)

**Scheme 22** Proposed mechanisms for the formation of pestalotioprolide D (**20**)

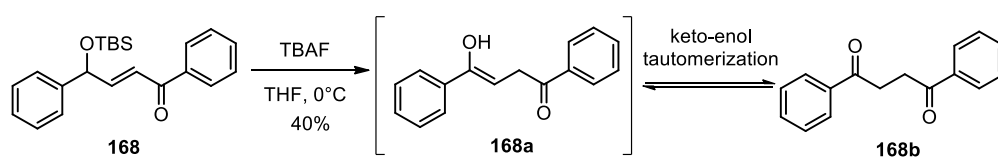
a)



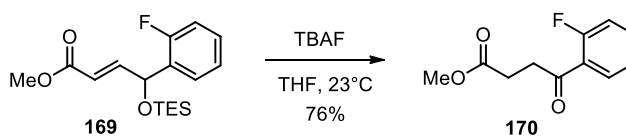
b)



**Scheme 23** Taylor's desilylation of  $\gamma$ -silyloxy  $\alpha,\beta$ -unsaturated ketone **168**



**Scheme 24** Rodrigo and Guan's desilylation of  $\gamma$ -silyloxy  $\alpha,\beta$ -unsaturated methyl ester **169**



The  $^1\text{H}$  and  $^{13}\text{C}$  NMR spectroscopic and HRMS data of synthetic **19** and **20** were in good agreement with those reported for the natural products **19** and **20** (Liu *et al.*, 2016) (**Table 5 and 6**). The specific rotation of synthetic **19** ( $[\alpha]_{\text{D}}^{25} +66.8$ ,  $c$  0.20, MeOH) was nearly identical to the reported value for the natural product **19** ( $[\alpha]_{\text{D}}^{25} +67.0$ ,  $c$  0.20, MeOH) by the Liu group. The specific rotation of synthetic **20** ( $[\alpha]_{\text{D}}^{26} -35.6$ ,  $c$  0.10, MeOH) was also in accordance with the reported value for the natural product **20** ( $[\alpha]_{\text{D}}^{20} -30.0$ ,  $c$  0.1, MeOH) (Liu *et al.*, 2016).

**Table 5** Comparison of  $^1\text{H}$  and  $^{13}\text{C}$  NMR data for natural product and synthetic **19**

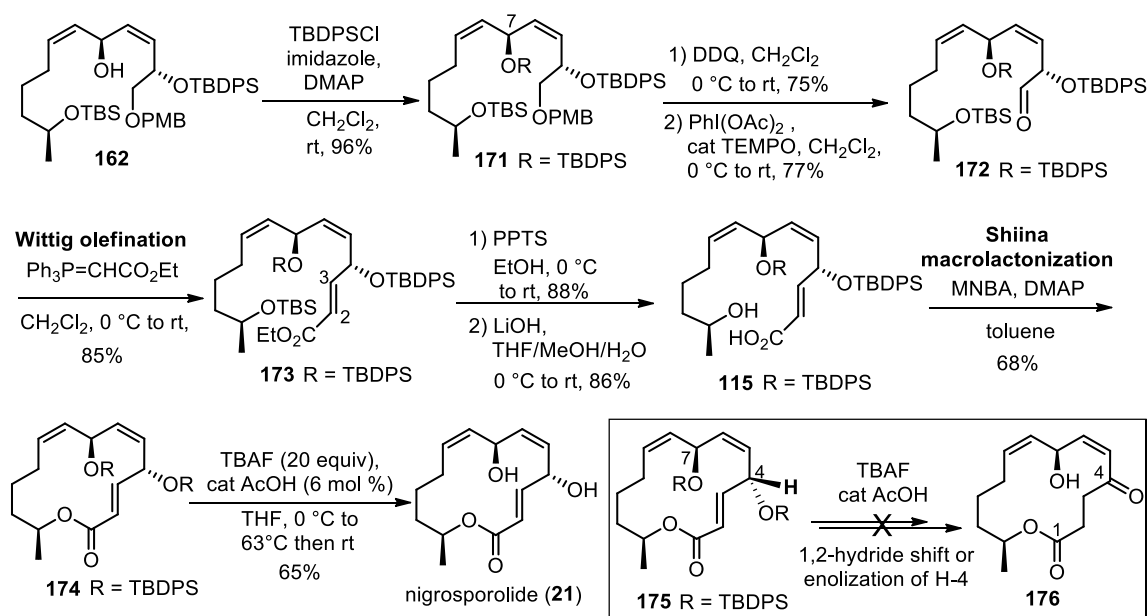
Position	$^1\text{H}$ NMR ( $\delta$ and $J$ in Hz)		$^{13}\text{C}$ NMR ( $\delta$ )	
	Natural (700 MHz) in $\text{CD}_3\text{OD}$	Synthetic (300 MHz) in $\text{CD}_3\text{OD}$	Natural (175 MHz) in $\text{CD}_3\text{OD}$	Synthetic (75 MHz) in $\text{CD}_3\text{OD}$
1	-	-	168.4	168.3
2	6.09, dd (15.5, 1.3)	6.08, d (15.6)	121.5	121.5
3	6.93, dd (15.5, 6.9)	6.93, dd (15.3, 6.9)	150.0	149.9
4	5.17, m	5.17, m	69.7	69.6
5	5.65, dd (11.4, 4.4)	5.65, dd (11.4, 4.5)	136.3	136.3
6	5.27, ddd (11.4, 10.1, 2.3)	5.27, td (11.7, 2.4)	130.4	130.4
7	4.70, dd (10.1, 9.5)	4.70, t (9.6)	73.4	73.4
8	5.14, m	5.13, m	128.6	128.6
9	5.49, ddd (11.0, 11.0, 3.4)	5.49, td (11.1, 3.3)	135.2	135.1
10	2.55, m/ 1.98, m	2.55, m/ 1.97, m	30.8	30.7
11	1.75, m/ 1.09, m	1.75, m/ 1.09, m	26.9	26.8
12	1.90, m/ 1.47, m	1.86, m/ 1.46, m	35.6	35.6
13	4.96, m	4.96, m	74.3	74.3
14	1.28, d (6.2)	1.28, d (6.3)	20.7	20.7
7-OMe	3.28, s	3.27, s	55.4	55.4

**Table 6** Comparison of  $^1\text{H}$  and  $^{13}\text{C}$  NMR data for natural product and synthetic **20**

Position	$^1\text{H}$ NMR ( $\delta$ and $J$ in Hz)		$^{13}\text{C}$ NMR ( $\delta$ )	
	Natural (600 MHz) in $\text{CD}_3\text{OD}$	Synthetic (300 MHz) in $\text{CD}_3\text{OD}$	Natural (150 MHz) in $\text{CD}_3\text{OD}$	Synthetic (75 MHz) in $\text{CD}_3\text{OD}$
1	-	-	174.7	174.6
2	2.80, ddd (15.0, 10.9, 2.8)/ 2.41, ddd (15.0, 6.7, 2.9)	2.79, ddd (15.0, 10.5, 2.7)/ 2.40, ddd (15.3, 6.9, 3.0)	30.0	30.0
3	2.96, ddd (17.8, 10.9, 2.9)/ 2.74, ddd (17.8, 6.7, 2.8)	2.96, ddd (17.4, 10.8, 2.7)/ 2.73, ddd (17.4, 6.6, 2.4)	41.0	40.9
4	-	-	201.5	201.5
5	6.32, dd (11.5, 0.9)	6.31, d (11.1)	127.4	127.4
6	5.90, dd (11.5, 9.6)	5.89, dd (11.1, 9.6)	145.5	145.5
7	5.79, m	5.79, app t (9.6)	73.0	73.0
8	5.23, m	5.22, app t (9.6)	129.8	129.8
9	5.67, m	5.67, m	135.0	134.9
10	2.12, m/ 1.85, m	2.12, m/ 1.86, m	30.0	29.9
11	1.31, m/ 0.92, m	1.32, m/ 0.91, m	28.3	28.2
12	1.64, m/ 1.54, m	1.65, m/ 1.54, m	37.4	37.3
13	4.90, m	4.91, m	73.1	73.2
14	1.24, d (6.4)	1.24, d (6.3)	20.4	20.3
7-OMe	3.30, s	3.29, s	56.1	56.0

Having achieved the syntheses of 7-*O*-methylnigrosporolide (**19**) and pestalotioprolide D (**20**), the synthesis of nigrosporolide (**21**), C7 hydroxy analogue of **19**, was undertaken following the same synthetic sequence as that of **19** (Scheme 25). The synthesis started with protection of C7 alcohol of **162** as TBDPS group to give silyl ether **171** in 96% yield. As mentioned earlier, the TBDPS protecting group was selected for the purpose of final global deprotection. Next, conversion of intermediate **171** to aldehyde **172** was achieved in 2 steps via PMB deprotection with DDQ and subsequent oxidation of the corresponding primary alcohol with  $\text{PhI}(\text{OAc})_2$  in the presence of catalytic TEMPO. It should be noted that this primary alcohol substrate was inert to DMP oxidizing agent, which was previously employed in the synthesis of 7-*O*-methylnigrosporolide (**19**). Therefore, a suitable oxidizing reagent was sought in this step. To our delight, when this primary alcohol substrate was exposed to  $\text{PhI}(\text{OAc})_2/\text{TEMPO}$ , the desired aldehyde **172** was obtained in 77% yield. After that, aldehyde **172** was subjected to Wittig olefination using the same conditions employed in the synthesis of **164** to afford the exclusive (*E*)- $\alpha,\beta$ -unsaturated ester **173** in 85% yield. The *E*-geometry of the newly created C2–C3 olefin was also verified by the  $^1\text{H}$ - $^1\text{H}$  coupling constant of 15.3 Hz. Then, compound **173** was transformed to macrocyclic product **174** in 3 steps via the same synthetic procedure employed in the synthesis of **19**. Ultimately, the global deprotection of both TBDPS groups of **174** was smoothly accomplished upon treatment with large excess TBAF (20 equiv) buffered with acetic acid (6 mol %) in THF from 0 °C to 63 °C to provide nigrosporolide (**21**) in 65% yield as a single product with complete consumption of starting macrocycle **174**. Notably, the formation of the corresponding 1,4-dione **176** via the 1,2-hydride shift or enolization of H-4 was not observed under these conditions. It was assumed that the bulky TBDPS group at the C7-position might cause a change in macrocycle **175** conformation that presumably led to the suppression of the 1,2-hydride shift or enolization of H-4 pathway.

**Scheme 25** Completion of the synthesis of nigrosporolide (**21**)



The  $^1\text{H}$  and  $^{13}\text{C}$  NMR spectroscopic data as well as HRMS data of **21** were in excellent agreement with those reported for the natural product **21** (Harwood *et al.*, 1995) (**Table 7**). The specific rotation of synthetic **21** was obtained to be  $[\alpha]_{\text{D}}^{26} +89.0$  ( $c$  0.90, MeOH), which was closely similar to the reported value for the natural product **21** ( $[\alpha]_{\text{D}}^{20} +81.0$ ,  $c$  0.90, MeOH) (Liu *et al.*, 2016).

**Table 7** Comparison of  $^1\text{H}$  and  $^{13}\text{C}$  NMR data for natural product and synthetic **21**

Position	$^1\text{H}$ NMR ( $\delta$ and $J$ in Hz)		$^{13}\text{C}$ NMR ( $\delta$ )	
	Natural (400 MHz) in $\text{CDCl}_3$	Synthetic (500 MHz) in $\text{CDCl}_3$	Natural (100 MHz) in $\text{CDCl}_3$	Synthetic (75 MHz) in $\text{CDCl}_3$
1	-	-	166.4	166.8
2	6.08, dd (15.6, 1.0)	6.07, d (16.0)	121.3	120.9
3	6.93, dd (15.6, 7.1)	6.93, dd (15.5, 7.0)	147.3	148.0
4	5.25, m	5.22, m	69.1	68.8
5	5.59, dd (11.4, 4.3)	5.57, dd (11.5, 4.0)	133.0	132.8
6	5.45, dd (11.4, 2.2)	5.43, dd (11.5, 1.5)	131.5	131.5
7	5.12, bm	5.10, t (9.5)	63.7	63.6
8	5.32, bdd (10.6, 2.0)	5.31, m	129.3	129.6
9	5.37, dd (10.6, 3.5)	5.37, dd (10.5, 3.5)	133.2	133.3
10	2.48, m/ 1.98, m	2.48, m/ 1.98, m	29.5	29.6
11	1.72, m/ 1.15, m	1.71, m/ 1.13, m	25.6	25.7
12	1.87, m/ 1.45, m	1.87, m/ 1.45, m	34.5	34.7
13	4.99, m	4.97, m	73.0	73.2
14	1.27, d (6.3)	1.29, d (6.5)	20.4	20.5

## 2.2 Conclusions

In summary, we have completed the convergent total synthesis of 7-*O*-methylnigrosporolide (**19**), pestalotioprolide D (**20**) and nigrosporolide (**21**) starting from (*S*)-propylene oxide (**38**) and (*S*)-benzyl glycidyl ether (**131**). The synthetic **19–21** were accomplished in 17 longest linear steps and 22 total steps in 1.7, 2.6 and 1.8% overall yields, respectively. The key synthetic reactions involved the Jacobsen hydrolytic kinetic resolution (HKR) to install the stereogenic center at the C4-

position and Still–Gennari olefination to establish C5–C6 *cis*-olefin. Moreover, the C7–C8 bond and the C7 alcohol stereogenic center of targeted products were constructed via acetylide addition to provide a large amount of chiral propargylic alcohol **116R** since Zn-mediated asymmetric alkynylation, the stereoselective Corey–Bakshi–Shibata (CBS) reduction and Mitsunobu inversion failed to exclusively produce the requisite **116R**. Our approach also exploited Lindlar reduction and Wittig olefination as the key strategies to generate C8–C9 *Z*-olefin and *E*-alkene at C2–C3, respectively. The 14-membered macrocyclic core of targets **19–21** was assembled by the key Shiina macrolactonization. It was found that the TBDPS group proved to be the suitable protecting group for the C4 hydroxy group of the macrocyclic intermediates, which were smoothly removed under TBAF buffered with acetic acid conditions in the final step to produce 7-*O*-methylnigrosporolide (**19**) and nigrosporolide (**21**). Upon treatment of C7 methoxy-substituted macrocycle intermediate with large excess TBAF, pestalotioprolide D (**20**) was formed. Therefore, our synthesis led to the hypothesis that macrolide **20** might be an artifact from a facile 1,2-hydride shift or enolization of H-4 of compound **19**.



## CHAPTER 3

SYNTHESES OF MUTOLIDE AND (4*S*,7*S*,13*S*)-4,7-  
DIHYDROXY-13-TETRADECA-2,5,8-TRIENOLIDE  
AND BIOLOGICAL ACTIVITIES OF  
SYNTHETIC MACROLIDES

## CHAPTER 3

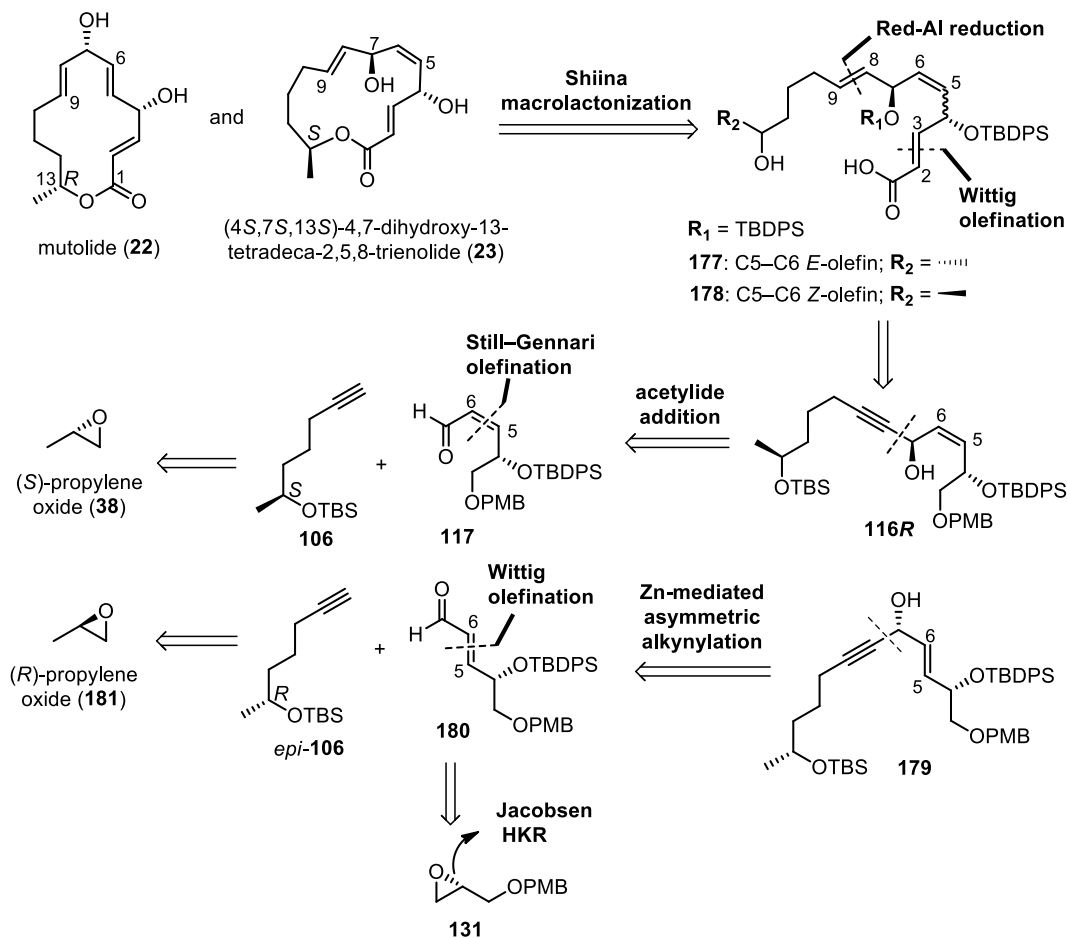
### SYNTHESES OF MUTOLIDE AND (4*S*,7*S*,13*S*)-4,7-DIHYDROXY-13-TETRADECA-2,5,8-TRIENOLIDE AND BIOLOGICAL ACTIVITIES OF SYNTHETIC MACROLIDES

#### 3.1 Results and Discussion

The syntheses of 7-*O*-methylnigrosporolide (**19**), nigrosporolide (**21**) and pestalotioprolide D (**20**), 14-membered (*E*)- $\alpha,\beta$ -unsaturated lactones with two *Z*-alkenes at C5–C6 and C8–C9, have been accomplished as mentioned in the previous chapter. This chapter will focus on the synthesis of the other two analogues of nigrosporolide (**21**) that contain C8–C9 *E*-olefin i.e. mutolide (**22**) and (4*S*,7*S*,13*S*)-4,7-dihydroxy-13-tetradeca-2,5,8-trienolide (**23**). The structure of macrolide **23** is identical to **21** except for the presence of *E*-olefin at C8–C9. Compound **22** differs from **23** by the configuration of alkene at C5–C6 and the absolute configuration of C13 alcohol stereogenic center. Due to the structural relationship of macrolides **21–23**, the synthesis of compounds **22** and **23** would be accomplished following the same key bond formation strategies as that of nigrosporolide (**21**) previously discussed in Chapter 2. The retrosynthetic analysis of macrolides **22** and **23** is illustrated in **Scheme 26**. The construction of the macrocyclic core and the *E*-double bond at C2–C3 of **22** and **23** would be conducted through Shiina macrolactonization and Wittig olefination, the same key strategies employed in the syntheses of **19–21**. The C8–C9 *E*-olefin of seco acids **177** (for **22**) and **178** (for **23**) would be generated via *E*-selective reduction of propargylic alcohol **179** or **116R** mediated by sodium bis(2-methoxyethoxy)aluminum hydride (Red-Al). To form the C7–C8 bond and install the C7 alcohol stereogenic center of targeted macrolactones **22** and **23**, the known compound **116R** required for the synthesis of **23** would be assembled via the key acetylide addition of (*S*)-alkyne **106** and (*Z*)-enal **117** due to unsuccessful Zn-mediated asymmetric alkynylation of (*Z*)-enal **117** by Pu or Trost's protocol to exclusively form chiral propargylic alcohol **116R**

previously discussed. However, there are previous reports by the Pu and the Trost groups that have demonstrated the successful catalytic enantioselective alkynylzinc addition to (*E*)-enal substrates to produce chiral propargylic alcohols with high enantioselectivity and yields (Pu *et al.*, 2002, 2010, 2013, 2015, Trost *et al.*, 2006, 2012 and Trost and Bartlett, 2012). Thus, chiral propargylic alcohol **179** necessitated for the synthesis of **22** would be constructed from (*R*)-alkyne *epi*-**106** and (*E*)-enal **180** by employing this strategy. The alkynes **106** (for **23**) and *epi*-**106** (for **22**) would be prepared from commercially available (*S*)-(**38**) and (*R*)-propylene oxides (**181**), respectively. (*S*)-Benzyl glycidyl ether (**131**) would be employed as a starting material to synthesize (*Z*)-**117** and (*E*)-enals **180**. The preparation of (*Z*)-enal **117** would be constructed via the same synthetic sequence as described in the previous chapter using Still–Gennari olefination as the key strategy to generate *Z*-alkene at C5–C6, while the C5–C6 *E*-olefin of **180** needed for the synthesis of **22** would be formed through Wittig olefination.

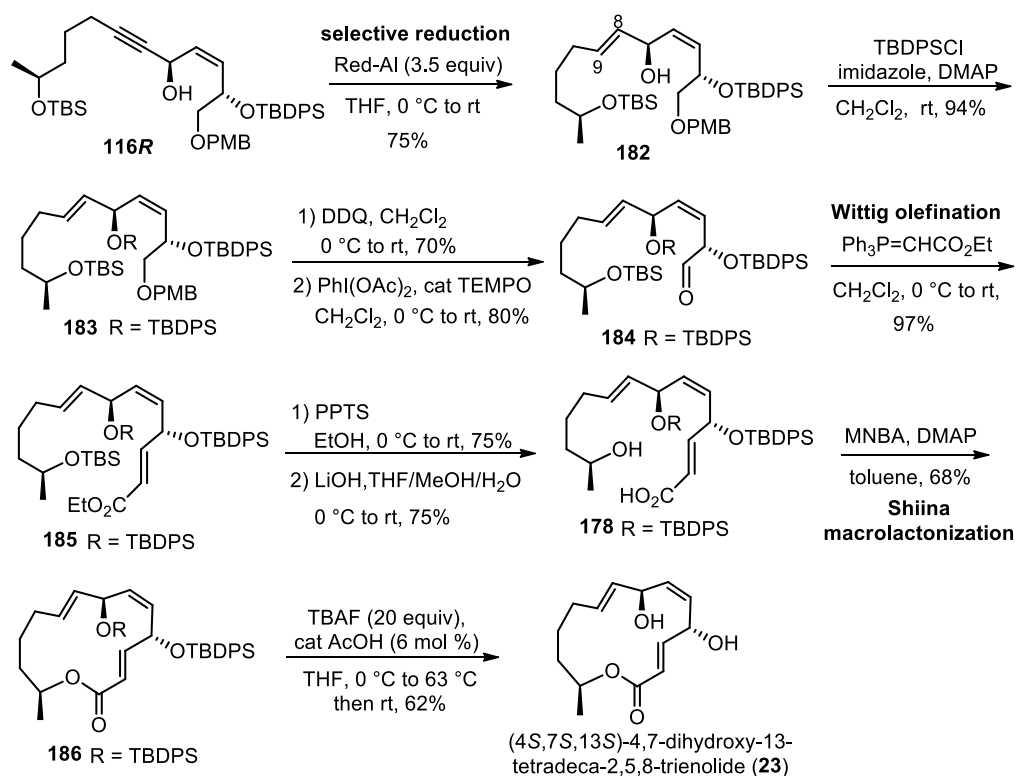
**Scheme 26** Retrosynthetic analysis of mutolide (**22**) and (4*S*,7*S*,13*S*)-4,7-dihydroxy-13-tetradeca-2,5,8-trienolide (**23**)



Firstly, the synthesis of (4*S*,7*S*,13*S*)-4,7-dihydroxy-13-tetradeca-2,5,8-trienolide (**23**) will be discussed since it was carried out via the similar synthetic procedure as that of nigrosporolide (**21**) starting from the known propargylic alcohol **116R** described in the previous chapter (**Scheme 27**). The stereoselective reduction of the propargylic alcohols mediated by Red-Al to give allylic alcohols with high *E*-selectivity has been achieved by many research groups (Alami *et al.*, 1999, Spino *et al.*, 2008, Yajima *et al.*, 2009 and Akai *et al.*, 2012). Therefore, alkyne **116R** was exposed to 3.5 equivalents of Red-Al in THF from 0 °C to room temperature. These conditions smoothly generated C8–C9 *E*-olefin of **182** in 75% yield and were not detrimental to another alkene functional group at C5–C6. The *E*-geometry of the newly created C8–C9 olefin was verified by the  $^1\text{H}$ - $^1\text{H}$  coupling constant of 15.3 Hz. After that, alcohol **182** was

transformed to aldehyde **184** in 3 steps via TBDPS protection at C7 alcohol, removal of PMB group with DDQ to give the corresponding primary alcohol and subsequent oxidation with  $\text{PhI}(\text{OAc})_2$  in the presence of catalytic TEMPO to produce aldehyde **184** in 80% yield. Two-carbon extension of **184** by Wittig olefination using (carbethoxymethylene)triphenylphosphorane in  $\text{CH}_2\text{Cl}_2$  afforded (*E*)- $\alpha,\beta$ -unsaturated ester **185** in 97% yield. The geometry of the newly formed double bond was also confirmed to be *trans* by the coupling constant of 15.6 Hz between H2 and H3 of **185**. The next task toward the core macrocyclic intermediate **186** was conducted through the same fashion employed in the synthesis of **21**. Selective removal of TBS protecting group of **185** in the presence of TBDPS group using pyridinium *p*-toluenesulfonate (PPTS) exclusively delivered the secondary alcohol, which was subjected to basic hydrolysis of the ethyl ester functional group to give seco acid **178** in 75% yield. Subsequently, Shiina macrolactonization of **178** using 2-methyl-6-nitrobenzoic anhydride (MNBA) and DMAP in toluene smoothly furnished the requisite macrocycle **186** in 68% yield (Snider and Zhou, 2006 and Narsaiah *et al.*, 2019). Finally, global deprotection of the TBDPS groups of **186** using large excess TBAF (20 equiv) buffered with acetic acid (6 mol %) in THF from 0 °C to 63 °C exclusively afforded targeted macrolactone **23** in 62% yield.

**Scheme 27** Completion of the synthesis of (4*S*,7*S*,13*S*)-4,7-dihydroxy-13-tetradeca-2,5,8-trienolide (**23**)



The  $^1\text{H}$  and  $^{13}\text{C}$  NMR spectroscopic data as well as HRMS data of synthetic **23** were in good agreement with those reported for Shishido's intermediate (Shishido *et al.*, 2011) (**Table 8**). The specific rotation of synthetic **23** ( $[\alpha]_{\text{D}}^{24} +148.8$ ,  $c$  0.68,  $\text{CHCl}_3$ ) was consistent with the reported value for the natural product **23** ( $[\alpha]_{\text{D}}^{25} +156.0$ ,  $c$  0.68,  $\text{CHCl}_3$ ) (Rukachaisirikul *et al.*, 2014).

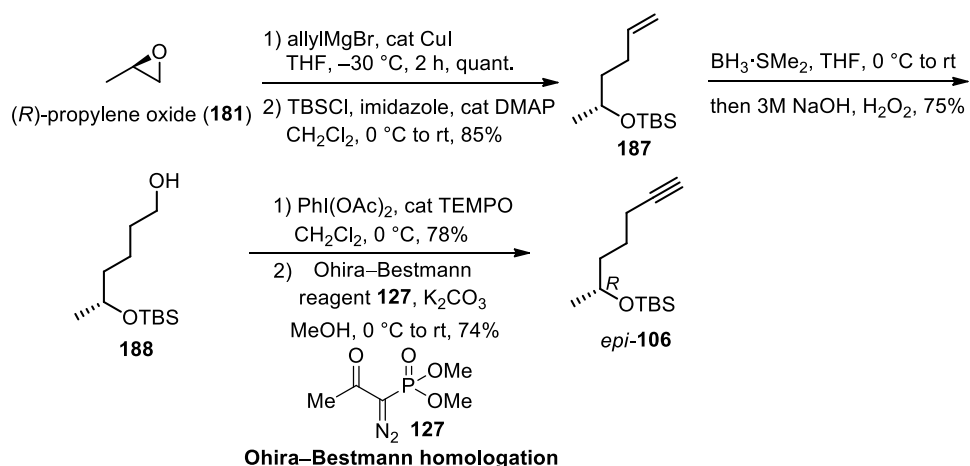
**Table 8** Comparison of  $^1\text{H}$  and  $^{13}\text{C}$  NMR data for natural product and synthetic **23**

Position	$^1\text{H}$ NMR ( $\delta$ and $J$ in Hz)		$^{13}\text{C}$ NMR ( $\delta$ )	
	Natural (400 MHz) in $\text{CDCl}_3$	Synthetic (300 MHz) in $\text{CDCl}_3$	Natural (100 MHz) in $\text{CDCl}_3$	Synthetic (75 MHz) in $\text{CDCl}_3$
1	-	-	166.1	166.3
2	5.90, dd (15.6, 2.0)	5.91, dd (15.6, 1.5)	118.3	118.3
3	7.03, dd (15.6, 4.4)	7.03, dd (15.6, 4.2)	148.3	148.5
4	5.26, m	5.27, m	70.6	70.6
5	5.54, dd (11.2, 4.4)	5.54, dd (11.1, 4.2)	132.1	132.2
6	5.46, ddd (10.8, 9.6, 2.4)	5.46, dd (10.8, 9.5)	131.2	131.3
7	4.82, t (8.4)	4.82, t (8.1)	68.4	68.5
8	5.49, dd (15.2, 7.6)	5.49, m	130.3	130.4
9	5.86, ddd (15.6, 9.2, 5.6)	5.86, ddd (15.6, 9.6, 5.4)	134.4	134.4
10	2.13, m/ 1.95, m	2.14, m/ 1.92, m	32.8	32.9
11	1.73, m/ 1.15, m	1.75, m/ 1.12, m	24.4	24.4
12	1.87, m/1.48, m	1.86, m/1.50, m	34.5	34.6
13	4.75 (dtd, 16.0, 6.0, 2.0)	4.74, m	72.0	72.2
14	1.26, d (6.0)	1.26, d (6.0)	20.2	20.3

Having achieved the synthesis of (4*S*,7*S*,13*S*)-4,7-dihydroxy-13-tetradeca-2,5,8-trienolide (**23**), the synthesis of mutolide (**22**) was then performed using the same key strategies. The process started with preparation of two key fragments (*R*)-alkyne *epi*-**106** and (*E*)-enal **180**. Chiral alkyne *epi*-**106** was elaborated from commercially available (*R*)-propylene oxide (**181**) in 5 steps using our previously described approach for the synthesis of (*S*)-alkyne **106** (Scheme 28). Ring opening of (*R*)-epoxide **181** with allylmagnesium bromide in the presence of catalytic

CuI and subsequent TBS protection afforded the TBS ether **187** in 85% yield. Terminal alkene **187** was transformed to primary alcohol **188** via hydroboration using borane dimethyl sulfide ( $\text{BH}_3\cdot\text{SMe}_2$ ), followed by oxidation with hydrogen peroxide in 3M NaOH. After that, alcohol **188** was subjected to oxidation with  $\text{PhI}(\text{OAc})_2$  and catalytic TEMPO to give the corresponding aldehyde, which was immediately treated with Ohira–Bestmann reagent **127** and  $\text{K}_2\text{CO}_3$  in methanol furnished the desired (*R*)-alkyne *epi*-**106** in 74% yield.

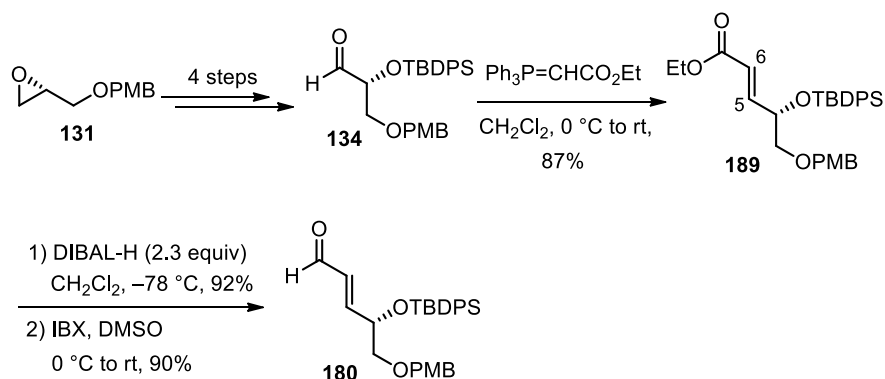
**Scheme 28** Preparation of (*R*)-alkyne *epi*-**106**



Synthesis of (*E*)-enal **180** was achieved in 3 steps from our previously reported aldehyde intermediate **134** (**Scheme 29**). The *E*-double bond at C5–C6 of mutolide (**22**) was constructed via Wittig olefination of **134** mediated with (carbethoxymethylene)triphenylphosphorane in  $\text{CH}_2\text{Cl}_2$  to afford exclusive (*E*)- $\alpha,\beta$ -unsaturated ester **189** in 87% yield. The *E*-geometry of the newly generated olefin was confirmed by its  $^1\text{H}$ - $^1\text{H}$  coupling constant of 15.6 Hz. Then, ethyl ester **189** was exposed to excess (2.3 equivalents) DIBAL-H to aid the complete consumption of the starting material and produce the corresponding primary alcohol as a single product. Lastly, this primary alcohol was oxidized with IBX to furnish (*E*)-enal **180** in 90% yield.



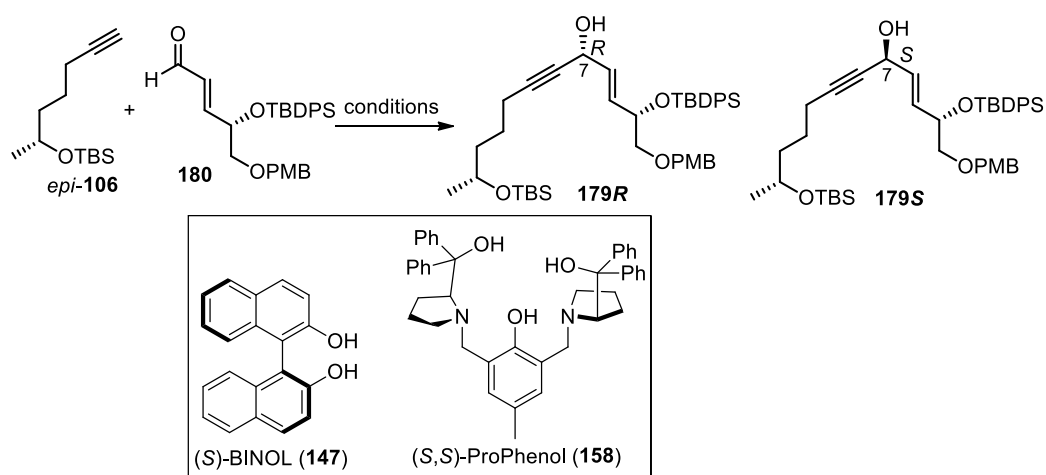
**Scheme 29** Synthesis of (*E*)-enal **180**



With the key (*R*)-alkyne *epi*-**106** and (*E*)-enal **180** intermediates in hand, the stage was then set for union of the two fragments to construct the C7–C8 bond of the core structure and to install the C7 alcohol stereogenic center of propargylic alcohol **179**. The reports on catalytic enantioselective alkynylzinc addition to (*E*)-enal by the Pu and Trost groups as mentioned in previous chapter provided excellent selectivity and yields of chiral propargyl alcohols (Pu *et al.*, 2002, 2010, 2013, 2015, Trost *et al.*, 2006, 2012 and Trost and Bartlett, 2012). Thus, their conditions were then utilized in our synthesis to assemble alkyne *epi*-**106** and (*E*)-enal **180** (Table 9). Our initial attempt was performed by employing  $\text{ZnEt}_2$  (3 equiv),  $\text{Ti}(\text{O}-i\text{Pr})_4$  (20 mol %) and dicyclohexylamine ( $\text{C}_6\text{H}_{11}\text{N}$ ) additive (5 mol %) in the presence of (*S*)-BINOL **147** (20 mol %) as a chiral ligand in  $\text{Et}_2\text{O}$  at room temperature (entry 1). Disappointingly, these conditions gave none of the desired product and the starting alkyne *epi*-**106** and aldehyde **180** were recovered. Increasing the amount of  $\text{ZnEt}_2$  to 5 equivalents and  $\text{C}_6\text{H}_{11}\text{N}$  to 10 mol % under the same conditions and prolonged reaction time of 18 hours also led to the recovery of starting materials (entry 2). Owing to the failure of both cases, attempts to assemble *epi*-**106** and **180** by Trost's protocol were applied in this reaction. The first conditions consisted of 5 equivalents of  $\text{ZnMe}_2$  and 20 mol % of (*S,S*)-ProPhenol ligand in toluene from  $0\text{ }^\circ\text{C}$  to room temperature (entry 3). It was found that propargylic alcohols **179R** and **179S** were obtained under these conditions in only 48% yield as an inseparable 1.1:1 mixture of diastereomers and a multitude of unidentifiable products were observed, which presumably formed upon decomposition of starting materials. Further optimization was then carried out by addition of triphenylphosphine oxide (TPPO) (20 mol %) with the intention to improve the enantioselectivity and yields (entry 4). Unfortunately, these

conditions led to an unidentified complex mixture once again along with an inseparable mixture of propargylic alcohols **179R** and **179S** (1.1:1) in only 30% isolated yield. These results indicated that Zn-mediated asymmetric alkylation reaction might be incompatible with our substrates. Hence, another strategy to stereoselectively synthesize **179R** was pursued.

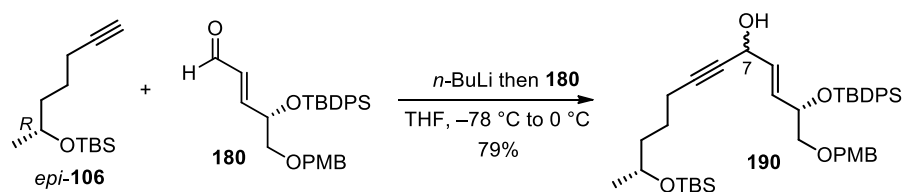
**Table 9** Screening of Zn-mediated asymmetric alkylation reaction to assemble (*R*)-alkyne *epi*-**106** and (*E*)-enal **180**

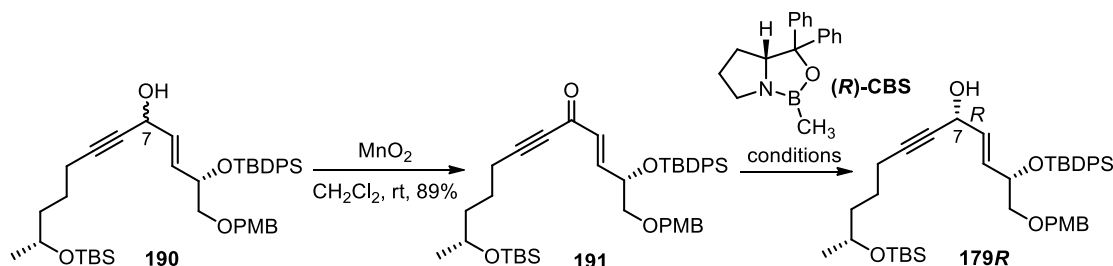


entry	reagents	solvent	temp	time (h)	results
1	ZnEt <sub>2</sub> (3.0 equiv), ( <i>S</i> )-BINOL (20 mol %), Ti(O- <i>i</i> Pr) <sub>4</sub> (20 mol %) Cy <sub>2</sub> NH (5 mol %)	Et <sub>2</sub> O	rt	9	no reaction
2	ZnEt <sub>2</sub> (5.0 equiv), ( <i>S</i> )-BINOL (20 mol %), Ti(O- <i>i</i> Pr) <sub>4</sub> (20 mol %), Cy <sub>2</sub> NH (10 mol %)	Et <sub>2</sub> O	rt	18	no reaction
3	ZnMe <sub>2</sub> (5.0 equiv), ( <i>S,S</i> )-ProPhenol (20 mol %)	toluene	0 °C to rt	8	<b>179R</b> and <b>179S</b> (48% yield) complex mixture
4	ZnMe <sub>2</sub> (5.0 equiv), TPPO (20 mol %) ( <i>S,S</i> )-ProPhenol (20 mol %)	toluene	0 °C to rt	23	<b>179R</b> and <b>179S</b> (30% yield), complex mixture

Owing to the failure to exclusively generate propargylic alcohol **179R** through Zn-mediated asymmetric alkynylation reaction, attempts to form **179R** via the stereoselective Corey-Bakshi-Shibata (CBS) reduction of ynone **191** were then undertaken. The process started with preparation of propargylic alcohol **190** via acetylide addition. Addition of the acetylide generated in situ by deprotonation of alkyne *epi*-**106** with *n*-BuLi to (*E*)-enal **180** yielded propargylic alcohol **190** as an inseparable mixture of diastereomers in 79% yield (**Scheme 30**). Nevertheless, separation of diastereomeric products of **190** was not necessary as the C7 alcohol stereogenic center was subsequently oxidized with MnO<sub>2</sub> to provide the corresponding ynone **191** in 89% yield. After that, compound **191** was subjected to the stereoselective CBS reduction using similar conditions to that of ynone **160** previously mentioned in Chapter 2. Reaction conditions employing 1.5 equivalents of (*R*)-CBS reagent and 2 equivalents of BH<sub>3</sub>·SMe<sub>2</sub> in THF from -78 °C to -30 °C were initially selected (entry 1). Unfortunately, only starting ynone **191** was recovered under these conditions. Increasing the reaction temperature to -15 °C until room temperature resulted in the formation of diastereomeric mixture of propargylic alcohols **190** in 55% yield (entry 2). Changing the solvent to toluene in the presence of 1 equivalent of (*R*)-CBS reagent and 2 equivalents of BH<sub>3</sub>·SMe<sub>2</sub> at -30 °C was then applied in this reaction (entry 3). To our delight, the expected propargylic alcohol **179R** was exclusively generated under these conditions albeit in only 45% yield based on recovered starting ynone **191**. To ensure complete consumption of starting **191**, the temperature was increased to -15 °C under the same conditions (entry 4). Gratifyingly, these conditions led to the desired alcohol **179R** as a single product in 65% yield, and starting ynone **191** was completely consumed.

**Scheme 30** Acetylide addition between (*R*)-alkyne *epi*-**106** and (*E*)-enal **180**



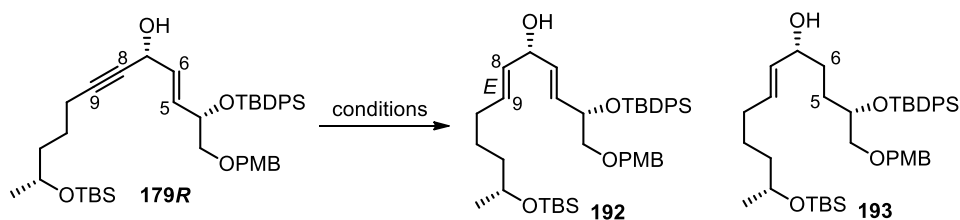
**Table 10** Screening of stereoselective CBS reduction of ynone **191**

entry	reagent	solvent	temp	time (h)	results
1	$(R)$ -CBS (1.5 equiv) $\text{BH}_3 \cdot \text{SMe}_2$ (2.0 equiv)	THF	$-78\text{ }^\circ\text{C}$ to $-30\text{ }^\circ\text{C}$	3	no reaction
2	$(R)$ -CBS (1.5 equiv) $\text{BH}_3 \cdot \text{SMe}_2$ (2.0 equiv)	THF	$-15\text{ }^\circ\text{C}$ to rt	5	<b>190</b> (55% yield)
3	$(R)$ -CBS (1.0 equiv) $\text{BH}_3 \cdot \text{SMe}_2$ (2.0 equiv)	toluene	$-30\text{ }^\circ\text{C}$	2	<b>179R</b> (45% brsm)
4	$(R)$ -CBS (1.0 equiv) $\text{BH}_3 \cdot \text{SMe}_2$ (2.0 equiv)	toluene	$-15\text{ }^\circ\text{C}$	3.5	<b>179R</b> (65% yield)

After the requisite propargylic alcohol **179R** was obtained, the next task was to form the C8–C9 *E*-olefin of **22** via selective reduction of the alkyne moiety of **179R** as shown in **Table 11**. Unfortunately, Red-Al reduction of **179R** under the same conditions employed with **116R** (3.5 equivalents of Red-Al in THF from  $0\text{ }^\circ\text{C}$  to room temperature) failed to furnish the desired allylic alcohol **192** and the starting material was recovered (entry 1). Further attempt was then undertaken by increasing the amount of Red-Al from 3.5 to 5 equivalents under the same conditions (entry 2). THF was still employed as a solvent under these conditions because it led to the successful selective reduction of the alkyne moiety of **116R**. Disappointingly, these conditions did not improve the reaction and only starting propargylic alcohol **179R** was recovered once again. Elevating the reaction temperature to  $50\text{ }^\circ\text{C}$  in the presence of 4 equivalents of Red-Al in THF also gave no desired product and the

starting propargylic alcohol **179R** remained (entry 3). Further optimization was then performed by changing the solvent to toluene in the presence of 3 equivalents of Red-Al from 0 °C to room temperature (Kobayashi and Morita, 2018) (entry 4). Although these conditions resulted in the formation of *E*-olefin at C8–C9, the *E*-alkene at C5–C6 was also reduced leading to the undesired overreduced product **193** in 40% yield. In addition, starting alkyne **179R** was recovered in 42% under these conditions. In an attempt to circumvent the problem of overreduction, the temperature was decreased to –15 °C under the same conditions (Phillips and Keaton, 2008) (entry 5). However, the undesired **193** was still obtained in 29% yield (65% yield based on recovered starting material). It should be noted that reduction of the alkene functional group at C5–C6 of propargylic alcohol **179R** was very facile under these conditions compared to the alkyne moiety at C8–C9.

**Table 11** Screening of Red-Al-mediated (*E*)-selective reductions of alkyne **179R**

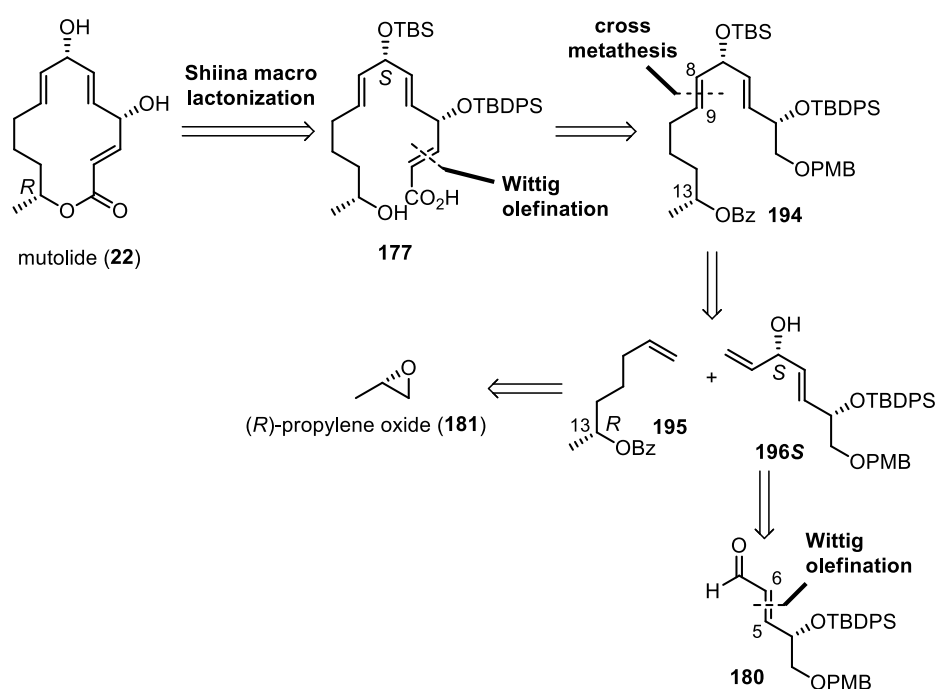


entry	Red-Al (equiv)	solvent	temp	time (h)	results
1	3.5	THF	0 °C to rt	5	no reaction
2	5.0	THF	0 °C to rt	18	no reaction
3	4.0	THF	0 °C to 50 °C	8	no reaction
4	3.0	toluene	0 °C to rt	3	<b>193</b> (40% yield, 58% brsm)
5	3.0	toluene	–15 °C	6	<b>193</b> (29% yield, 65% brsm)

The construction of the C8–C9 *E*-alkene of **192** from alkyne intermediate **179R** via selective reduction mediated by Red-Al proved to be problematic. Although, the alkyne moiety at C8–C9 of **179R** could be reduced to *E*-olefin under these conditions, the other *E*-alkene at C5–C6 was concurrently reduced in this step. These results led us to

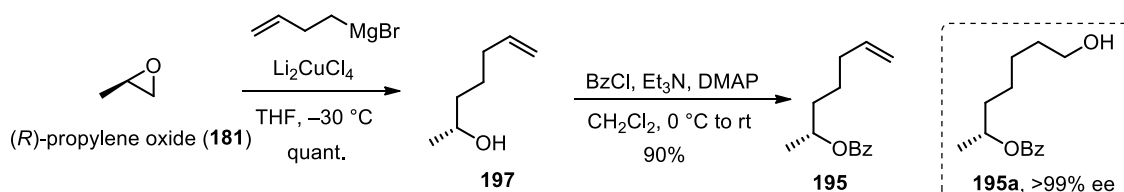
revise retrosynthetic strategy of mutolide (**22**) as shown in **Scheme 31**. Our synthesis would still rely on Shiina macrolactonization of seco acid **177** to assemble the 14-membered macrocyclic core and Wittig olefination to generate C2–C3 *E*-olefin. Cross metathesis is one of the most widely employed methods to construct carbon-carbon double bond with high *E*-selectivity and yield. There are literature precedents on the successful use of the second-generation Grubbs catalyst (Grubbs II) or Hoveyda–Grubbs second generation catalyst (Hoveyda–Grubbs II) on *E*-selective cross metathesis in the presence of allylic alcohol substrate (Nolen *et al.*, 2005, Bittman *et al.*, 2011 and Ramana *et al.*, 2012). Consequently, the *E*-double bond at C8–C9 of macrolide **22** was envisioned to derive from cross metathesis between (*R*)-hept-6-en-2-yl benzoate (**195**) and chiral allylic alcohol **196S**, which would be prepared from (*R*)-propylene oxide (**181**) and previously synthesized (*E*)-enal **180**, respectively. The benzoyl group (Bz) would be used as a protecting group at C13 alcohol of **195** instead of TBS group since Bz group could be simultaneously removed in the hydrolysis step in order to form seco acid **177**, rendering a shorter synthetic sequence.

**Scheme 31** Revised retrosynthesis of mutolide (**22**)

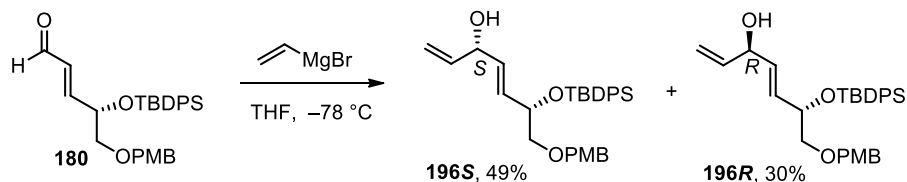


The synthesis of mutolide (**22**) commenced with preparation of cross metathesis alkene precursors **195** and **196S**. Synthesis of (*R*)-benzoate **195** was achieved in 2 steps starting from commercially available (*R*)-propylene oxide (**181**) (**Scheme 32**). Epoxide ring opening of **181** with 3-butenylmagnesium bromide in the presence of catalytic dilithium copper (II) chloride ( $\text{Li}_2\text{CuCl}_4$ ) yielded chiral alcohol **197**, which was immediately protected with benzoyl chloride (BzCl) in the presence of triethylamine and DMAP to deliver (*R*)-hept-6-en-2-yl benzoate (**195**) in 90% yield. The enantiopurity of **195** was confirmed to be >99% ee by chiral HPLC of the corresponding alcohol derivative ((*R*)-7-hydroxyheptan-2-yl benzoate (**195a**)). Then, the requisite chiral allylic alcohol **196S** was prepared via vinylation of (*E*)-enal **180** using vinylmagnesium bromide in THF at  $-78\text{ }^\circ\text{C}$  (**Scheme 33**). The desired chiral allylic alcohol **196S** was obtained as a major product in 49% yield together with the undesired **196R** in 30% yield as separable diastereomers. The absolute configuration of the alcohol chiral center of each diastereomer was determined by Mosher ester analysis.

**Scheme 32** Preparation of (*R*)-hept-6-en-2-yl benzoate (**195**)



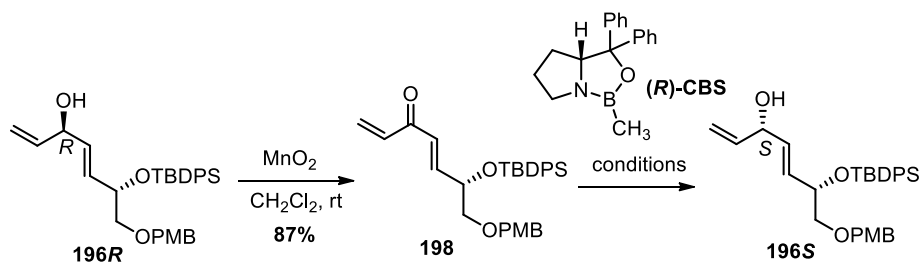
**Scheme 33** Preparation of chiral allylic alcohol **196S**



To convert the undesired allylic alcohol **196R** into **196S**, stereoselective CBS reduction of enone **198** was performed in our synthesis (**Table 12**). Compound **196R** was treated with  $\text{MnO}_2$  in  $\text{CH}_2\text{Cl}_2$  at room temperature to deliver enone **198** in 87% yield. Reduction conditions using 1.5 equivalents of (*R*)-CBS reagent and 2 equivalents of  $\text{BH}_3\cdot\text{SMe}_2$  in THF at  $-78\text{ }^\circ\text{C}$  or from  $0\text{ }^\circ\text{C}$  to room temperature provided

no desired chiral alcohol product and the starting ketone **198** was recovered (entries 1 and 2). Further optimization was then performed by changing the solvent to toluene in the presence of 1 equivalent of (*R*)-CBS reagent and 2 equivalents of  $\text{BH}_3\cdot\text{SMe}_2$  at  $-78$  °C (entry 3). However, both chiral allylic alcohols **196S** and **196R** were formed under these conditions in 40% and 30% yields, respectively. Obviously, this reaction provided the product yield of the requisite allylic alcohol **196S** lower than that produced from vinylation of (*E*)-enal **180**. Therefore, treatment of (*E*)-enal **180** with vinylmagnesium bromide as shown in **Scheme 32** was still the best alternative for preparation of chiral allylic alcohol **196S** compared to CBS reduction of enone **198**.

**Table 12** Screening of stereoselective CBS reduction of enone **198**



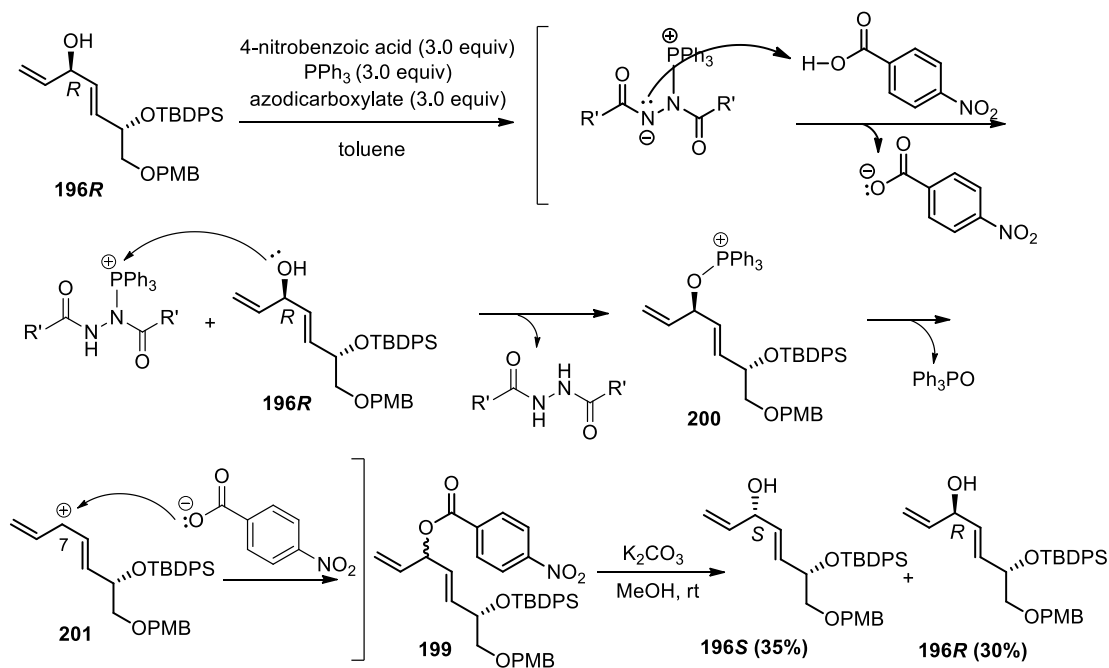
entry	reagent	solvent	temp	time (h)	results
1	( <i>R</i> )-CBS (1.5 equiv) $\text{BH}_3\cdot\text{SMe}_2$ (2.0 equiv)	THF	$-78$ °C	1.5	no reaction
2	( <i>R</i> )-CBS (1.5 equiv) $\text{BH}_3\cdot\text{SMe}_2$ (2.0 equiv)	THF	$0$ °C to rt	2.0	no reaction
3	( <i>R</i> )-CBS (1.0 equiv) $\text{BH}_3\cdot\text{SMe}_2$ (2.0 equiv)	toluene	$-78$ °C	3.5	<b>196R</b> (30% yield), <b>196S</b> (40% yield)

Since the CBS reduction of enone **198** provided unsatisfactory results, another approach i.e. Mitsunobu reaction to convert the undesired allylic alcohol **196R** into **196S** was undertaken as shown in **Table 13**. Attempts employing 3 equivalents of 4-nitrobenzoic acid, DIAD and  $\text{PPh}_3$  in toluene at room temperature or  $60$  °C failed to furnish the desired ester product, and only the starting allylic alcohol **196R** was observed (entries 1 and 2). After that, replacing DIAD with DEAD under the same conditions used in entry 2 was performed (entry 3). Unfortunately, epimerized ester



product **199** was formed under these conditions in 53% yield, which was observed from two sets of overlapping signals of some  $^1\text{H}$  NMR signals. As anticipated, upon treatment of **199** with 1.2 equivalents of  $\text{K}_2\text{CO}_3$  in MeOH resulted in the formation of the expected allylic alcohol **196S** together with the undesired **196R** in 35% yield and 30% yield, respectively. Moreover, the epimerization of similar allylic alcohol substrates under Mitsunobu conditions has also been encountered in the previous report by Shull and co-workers (Shull *et al.*, 1997). Therefore, epimerized ester product **199** might be formed through intermediate **201**. The loss of chirality at C7-position of **201** led to the formation of an inseparable mixture of 4-nitrobenzoate ester **199**.

**Table 13** Screening of Mitsunobu inversion of chiral allylic alcohol **196R**

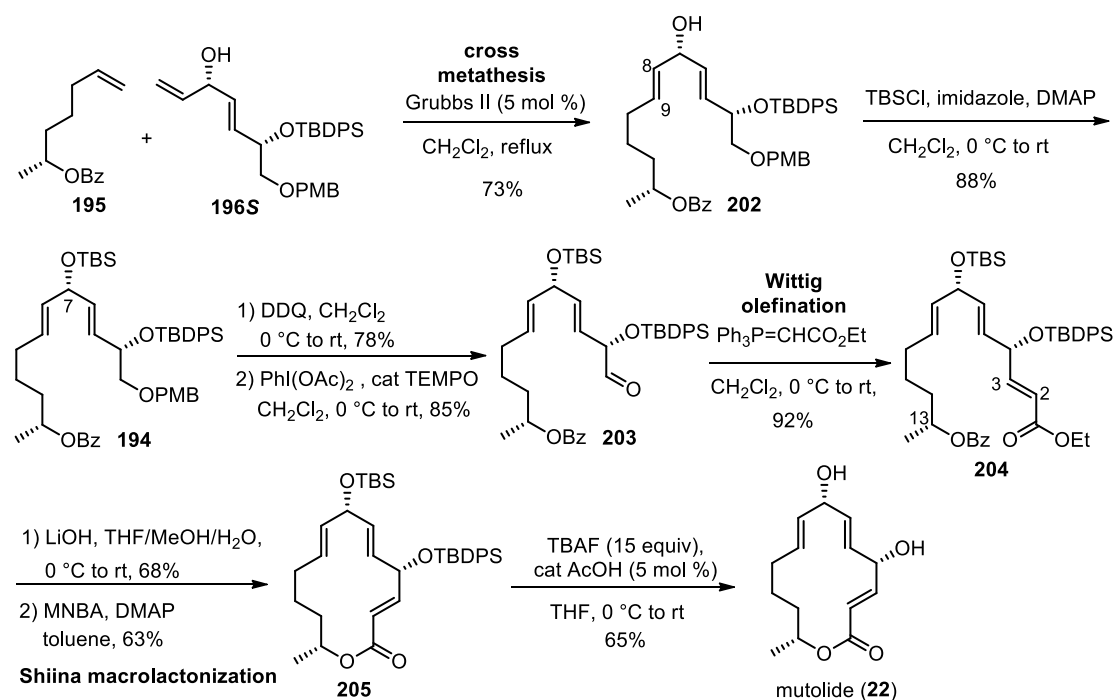


entry	azodicarboxylate	temp	time (h)	results
1	DIAD	rt	16	no reaction
2	DIAD	60 °C	19	no reaction
3	DEAD	60 °C	18	<b>199</b> (53% yield)

Attempts to generate exclusive chiral allylic alcohol **196S** via stereoselective CBS reduction and Mitsunobu inversion described above were unsuccessful. Therefore, vinylation of (*E*)-enal **180** was the best method to produce

large amount of the requisite allylic alcohol **196S**. Then, both key fragments (*R*)-hept-6-en-2-yl benzoate (**195**) and chiral allylic alcohol **196S** were carried to the next step to complete the synthesis mutolide (**22**) (**Scheme 34**). Cross metathesis between terminal alkene **195** and allylic alcohol **196S** using 5 mol % of second-generation Grubbs catalyst in refluxing CH<sub>2</sub>Cl<sub>2</sub> (0.1 M) smoothly and exclusively produced the desired *E*-alkene **202** in 73% yield. Remarkably, these conditions were not detrimental to alkene functional group at C5–C6. The *E*-geometry of the newly formed C8–C9 olefin was confirmed based on the coupling constant of 15.6 Hz between H8 and H9. Next, the C7 alcohol of **202** was protected with TBSCl to give silyl ether **194** in 88% yield. The TBS group was selected as a protecting group in this case for the purpose of the ease in global desilylation. As mentioned earlier in the synthesis of nigrosporolide (**21**) and (4*S*,7*S*,13*S*)-4,7-dihydroxy-13-tetradeca-2,5,8-trienolide (**23**), removal of both TBDPS groups was relatively sluggish and required the use of large amount of TBAF (20 equivalents). Our next task was to install C2–C3 *E*-olefin of **204**, which was smoothly accomplished in 3 steps from intermediate **194** using the same synthetic sequence employed in the synthesis of **185** to deliver (*E*)- $\alpha,\beta$ -unsaturated ester **204** in 92% yield as a single stereoisomer. The newly generated *E*-alkene was again verified by the coupling constant of 15.6 Hz between H2 and H3. After that, diester **204** was treated with 4 equivalents of LiOH in THF and aqueous methanol to simultaneously remove ethyl ester and the benzoyl groups and produced the corresponding seco acid in good yield. The corresponding seco acid was then exposed to Shiina macrolactonization conditions to afford macrocycle **205** in 63% yield. Finally, global deprotection of both silyl protecting groups of **205** using 15 equivalents of TBAF buffered with acetic acid (5 mol %) in THF from 0 °C to room temperature smoothly furnished mutolide (**22**) in 65% yield as a sole product.

**Scheme 34** Completion of the synthesis of mutolide (**22**)



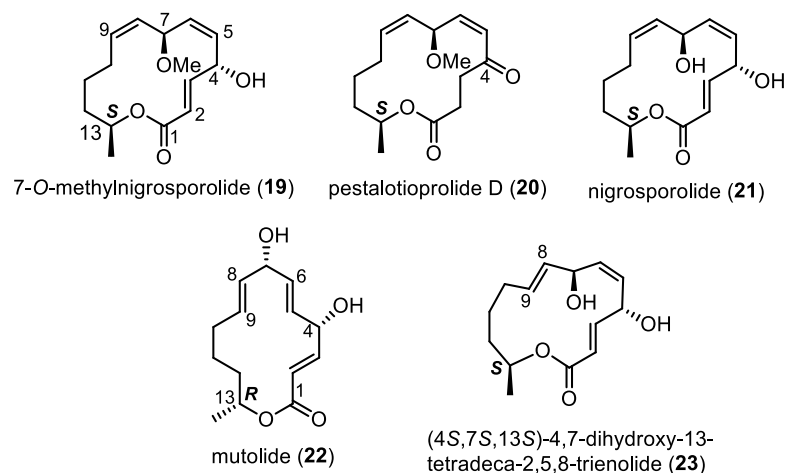
The  $^1\text{H}$  and  $^{13}\text{C}$  NMR spectroscopic data as well as HRMS data of synthetic mutolide (**22**) were in excellent agreement with those reported for the natural product **22** except for the chemical shift of H5 (Kulkarni-Almeida *et al.*, 2015 and Zeeck *et al.*, 2000) (**Table 14**). The proton NMR chemical shift at the 5-position of the synthetic **22** appears at 5.63 ppm, while natural **22** shows at 5.41 ppm. From personal communication with Prof. Axel Zeeck, the report on the chemical shift of H5 is a typographical error. As such, all of the spectroscopic data for synthetic **22** were still consistent with those reported for natural **22**. Moreover, the specific rotation of the synthetic **22** ( $[\alpha]_{\text{D}}^{25} -59.8, c 1.79, \text{CH}_3\text{CN}$ ) was nearly identical to the natural **22** ( $[\alpha]_{\text{D}}^{25} -61.0, c 1.79, \text{CD}_3\text{CN}$ ) reported by Zeeck and co-workers. Thus, the structure of synthetic **22** could be confirmed by these  $^1\text{H}$  and  $^{13}\text{C}$  NMR spectroscopic and HRMS data as well as the specific rotation.

**Table 14** Comparison of  $^1\text{H}$  and  $^{13}\text{C}$  NMR data for natural product and synthetic **22**

Position	$^1\text{H}$ NMR ( $\delta$ and $J$ in Hz)		$^{13}\text{C}$ NMR ( $\delta$ )	
	Natural (300 MHz) in acetone- $d_6$	Synthetic (300 MHz) in acetone- $d_6$	Natural (75.5 MHz) in acetone- $d_6$	Synthetic (75 MHz) in acetone- $d_6$
1	-	-	168.6	167.0
2	5.81 (dd, 16.0, 1.0)	5.81 (d, 15.9, 0.9)	118.8	118.2
3	6.70 (dd, 16.0, 7.0)	6.72 (dd, 15.9, 6.9)	152.9	152.5
4	4.89 (m)	4.89 (m)	70.8	70.2
5	5.41 (m)	5.63 (dd, 15.6, 4.2)	131.1	130.5
6	5.77 (ddd, 16.0, 7.0, 1.0)	5.78 (dd, 15.9, 6.6, 0.9)	135.0	135.4
7	4.62 (s, br)	4.62 (s, br)	73.0	72.4
8	5.57 (m)	5.58 (m)	135.6	135.8
9	5.41 (m)	5.41 (m)	132.6	131.1
10	1.94 (m)	1.95 (m)	31.7	31.2
11	1.40 (m)	1.39 (m)	25.0	24.5
12	1.52 (m)	1.53 (m)	35.5	35.0
13	4.98 (m)	4.98 (m)	72.8	71.3
14	1.18 (d, 6.5)	1.20 (d, 6.6)	18.9	18.7
	4.50 (s, br, 4-OH)	-		
	3.96 (s, br, 7-OH)	4.05 (s, br, 7-OH)		

### 3.2 Biological activities evaluation of synthetic macrolides 19–23

**Figure 5** Structures of 7-*O*-methylnigrosporolide (**19**), pestalotioprolide D (**20**), nigrosporolide (**21**), mutolide (**22**) and (4*S*,7*S*,13*S*)-4,7-dihydroxy-13-tetradeca-2,5,8-trienolide (**23**)



Our attention initially focused on cytotoxic activities evaluation of 14-membered macrolactones containing C7 methoxy group and two *Z*-olefins at C5–C6 and C8–C9 i.e. 7-*O*-methylnigrosporolide (**19**) and pestalotioprolide D (**20**). In 2016, these compounds were reported to show significant cytotoxicity against the L5178Y murine lymphoma cells (Liu *et al.*, 2016). Thus, the synthetic **19** and **20** were evaluated for their cytotoxic activities against other human cancer cell lines, including two breast adenocarcinoma (MDA-MB-231 and MCF-7), three cervical carcinoma (C33A, HeLa and SiHa) and one colorectal carcinoma (HCT116) cell lines as well as monkey kidney non-cancerous (Vero) cells using an MTT [3-(4,5-dimethylthiazol-2-yl)-2,5-diphenyltetrazolium bromide] assay by the laboratory of Dr. Panata Iawsipo, Burapha University (**Table 15**). It was observed that both compounds exhibited weak cytotoxic activity against all cancer cell lines with  $IC_{50}$  ranges of 35.17–69.13  $\mu$ M for compound **19** and 8.90–53.25  $\mu$ M for compound **20**. Notably, pestalotioprolide D (**20**) showed a stronger cytotoxic activity against all cancer cell lines tested than **19**. Among the six cell lines tested, the SiHa cell line was the most sensitive cell line to synthetic **19** and **20** with  $IC_{50}$  values of  $35.17 \pm 10.77 \mu$ M and  $8.90 \pm 2.51 \mu$ M, respectively. These results were inconsistent with the Liu and

Proksch group that macrolide **19** displayed higher antiproliferative effect compared to **20** (Liu *et al.*, 2016). Although both compounds **19** and **20** showed much lower cytotoxicity compared to standard drugs cisplatin and doxorubicin, they were relatively non-cytotoxic to Vero cells. Our cytotoxic activity results suggested a preliminary structure-activity relationship that the presence of ketone functional group at the C4-position and absence of double bond at C2–C3 in pestalotioprolide D (**20**) apparently increased the cytotoxicity compared to 7-*O*-methylnigrosporolide (**19**)

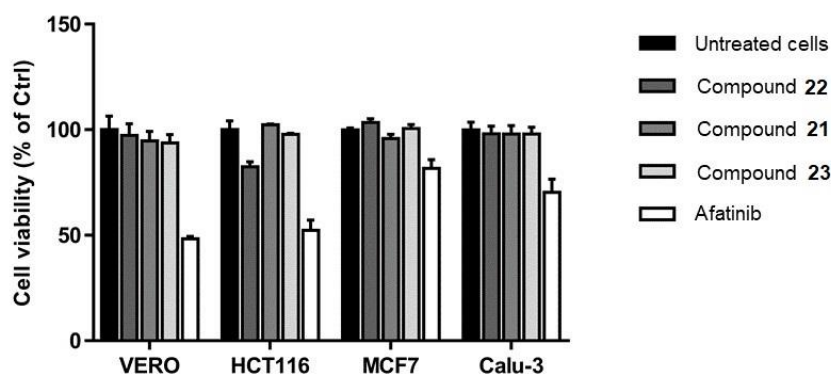
**Table 15** Cytotoxic activity of 7-*O*-methylnigrosporolide (**19**) and pestalotioprolide D (**20**) against six human cancer cell lines

cell lines	cytotoxicity, IC <sub>50</sub> (μM)			
	<b>19</b>	<b>20</b>	cisplatin	doxorubicin
MDA-MB-231	60.75 ± 1.50	21.10 ± 4.04	17.00 ± 1.46	0.16 ± 0.01
MCF-7	61.61 ± 5.01	53.25 ± 5.15	17.98 ± 2.97	0.24 ± 0.03
C33A	57.38 ± 9.51	22.00 ± 4.92	6.50 ± 0.76	0.22 ± 0.02
HeLa	69.13 ± 16.87	33.76 ± 13.23	8.20 ± 0.90	0.33 ± 0.08
SiHa	35.17 ± 10.77	8.90 ± 2.51	6.10 ± 0.85	0.51 ± 0.08
HCT116	54.25 ± 2.47	13.75 ± 0.35	11.75 ± 3.89	0.15 ± 0.01
Vero	74.13 ± 10.41	42.50 ± 3.07	14.42 ± 3.86	>1

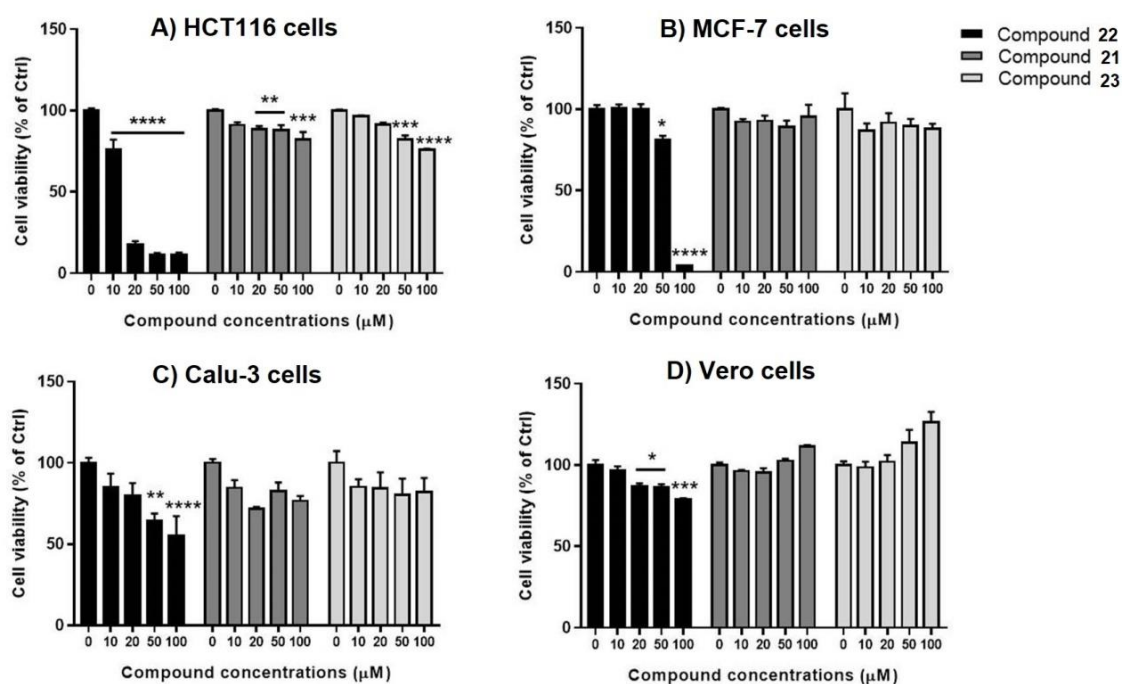
Furthermore, the remaining three synthetic macrolides, nigrosporolide (**21**), mutolide (**22**) and (4*S*,7*S*,13*S*)-4,7-dihydroxy-13-tetradeca-2,5,8-trienolide (**23**), were tested for their *in vitro* cytotoxic activity against three human cancer cell lines, including HCT116, MCF-7 and Calu-3 lung adenocarcinoma as well as Vero cells using an MTT assay by the laboratory of Prof. Dr. Chatchai Muanprasat of Chakri Naruebodindra Medical Institute, Faculty of Medicine Ramathibodi Hospital, Mahidol University (**Figure 6**). Viability of these cells was treated with 10 μM of synthetic **21–23** for 24 hours, and it was measured and compared with untreated cells using afatinib as a positive control. It was found that macrolides **21–23** were non-cytotoxic to Vero cells and compounds **21** and **23** showed no cytotoxic effects on the

three cancer cell lines tested at this concentration. Nevertheless, synthetic mutolide (**22**) exclusively exhibited inhibition of viability of HCT116 cells at 10  $\mu\text{M}$  to approximately 18%, albeit in lower extent compared to afatinib (~48%). Further dose-response experiments were then performed by treating the three cancer cell lines at 0, 10, 20, 50 and 100  $\mu\text{M}$  concentrations of **21–23** at 24 hours of incubation (**Figure 7**). It was observed that only mutolide (**22**) displayed significant cytotoxic activity against HCT116 cells. The percentage of HCT116 cell viability dropped to ~18% at 20 M and further dropped to ~11% at 50 and 100  $\mu\text{M}$  (**Figure 7A**). These results indicated that macrolactone **22** inhibited the viability of HCT116 cells in a concentration-dependent manner with an  $\text{IC}_{50}$  value of ~12  $\mu\text{M}$ . Mutolide (**22**) also showed inhibition of the viability of MCF-7, Calu-3 and Vero cells in a concentration-dependent manner with less efficacy compared to the HCT116 cells ( $\text{IC}_{50} > 50 \mu\text{M}$ ) (**Figures 7B–7C**). However, the dose-response experiments of compounds **21** and **23** at all concentrations did not show significant results to inhibit cell viability in all cell lines. These biological activity profiles of **21–23** are in accordance with Liu and Proksch's reports that **22** showed more potent inhibition of the proliferation of the L5178Y murine lymphoma cells than **21** and **23** (Liu *et al.*, 2016 and 2020). Moreover, viability of HCT116 cells treated with synthetic compounds **21–23** at prolonged incubation for 48 and 72h was also examined but the results were relatively unchanged, indicating that a longer incubation period did not significantly affect the potency of mutolide (**22**) on inhibition of HCT116 cells (**Figure 8**). Structure-activity relationships of macrolides **21–23** could be roughly concluded that two *E*-alkenes at C5–C6 and C8–C9 as well as the *R* methyl lactone alcohol at the C13-position in **22** resulted in total increment of cytotoxicity compared to presence of *Z*-olefin at C5–C6 with *Z*- or *E*-double bond at C8–C9 and the *S* configuration of the C13 stereogenic center in **21** and **23**.

**Figure 6** Viability of cells treated with synthetic compounds **21–23** or afatinib at 10  $\mu\text{M}$  for 24 h determined by the MTT assay. Results are shown in percentage of cell viability relative to untreated cells.

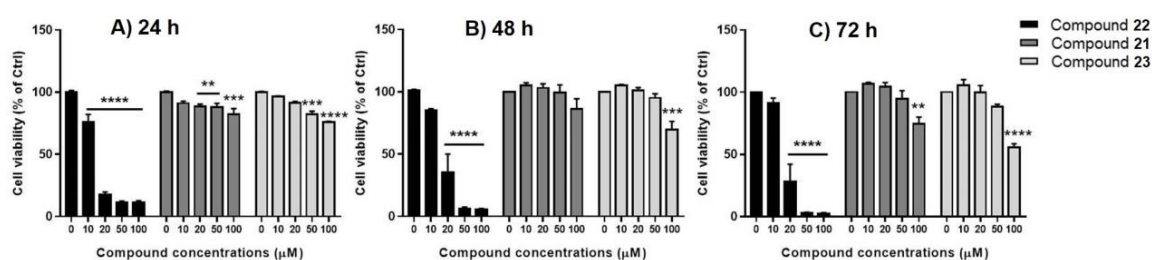


**Figure 7** Viability of A) HCT116 cells, B) MCF-7 cells, C) Calu-3 cells and D) Vero cells treated with synthetic compounds **21–23** at indicated concentrations for 24 h determined by the MTT assay. \*, \*\*, \*\*\* and \*\*\*\* indicated the  $p$ -values of  $<0.05$ ,  $<0.01$ ,  $<0.005$  and  $<0.001$ , respectively ( $n=3$ ) (One-way analysis of variance).





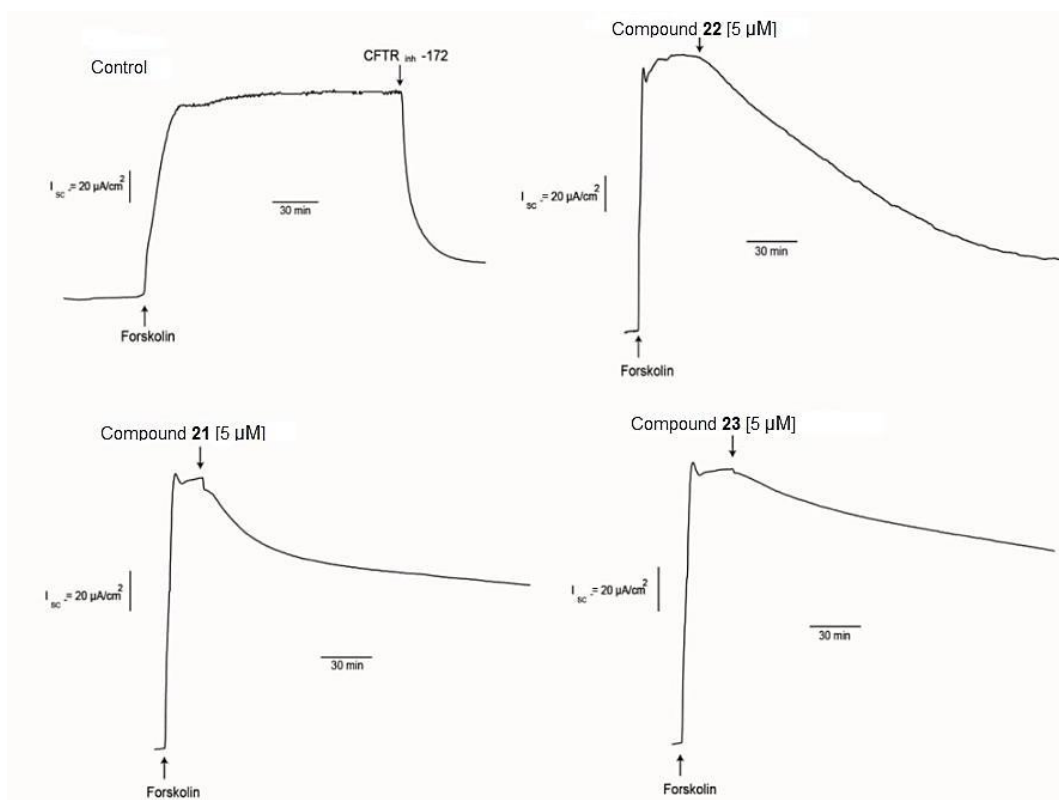
**Figure 8** Viability of HCT116 cells treated with synthetic compounds **21–23** after A) 24 h, B) 48 h and C) 72 h of incubations at indicated concentrations for 24 h determined by the MTT assay. \*, \*\*, \*\*\* and \*\*\*\* indicated the *p*-values of <0.05, <0.01, <0.005 and <0.001, respectively (*n*=3) (One-way analysis of variance)



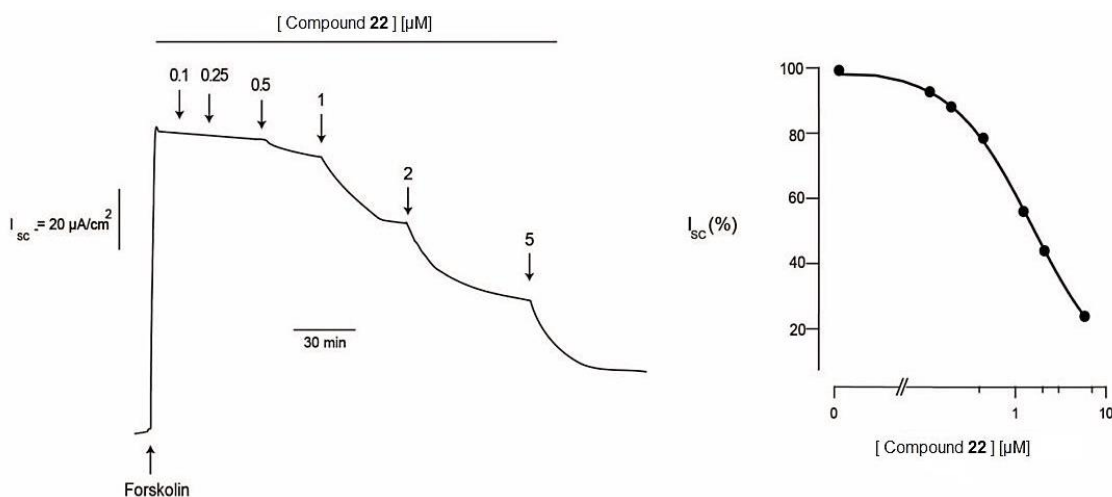
In addition to the evaluation of cytotoxic activity against human cancer cell lines as mentioned above of macrolides **21–23**, inhibition of cystic fibrosis transmembrane conductance regulator (CFTR)-mediated chloride secretion in human intestinal epithelial (T84) cells of synthetic **21–23** was also assessed by the laboratory of Prof. Dr. Chatchai Muanprasat of Chakri Naruebodindra Medical Institute, Faculty of Medicine Ramathibodi Hospital, Mahidol University (**Figure 9**). Overstimulation of CFTR-mediated chloride secretion in T84 cells is one of the important roles in the pathogenesis of secretory diarrhea, which is one of the major health problems that cause morbidity and mortality worldwide. Interestingly, in 2018, Muanprasat and co-workers have demonstrated that zearalenone, the 14-membered resorcylic acid lactone fungal metabolite, is a highly potent CFTR inhibitor in T84 cells with an  $IC_{50}$  of  $\sim 0.5 \mu\text{M}$ . As such, the three synthetic 14-membered macrolides lacking resorcylic acid moieties **21–23** were also screened for their inhibitory effects on the CFTR channels using short-circuit current ( $I_{SC}$ ) measurements. It was observed that at  $5 \mu\text{M}$ , only mutolide (**22**) showed the most significant inhibition ( $\sim 70\%$  inhibition) compared to its analogues **21** (40% inhibition) and **23** (30% inhibition). Therefore, macrolide **22** was further evaluated in concentration-inhibition studies. Synthetic compound **22** was found to inhibit CFTR-mediated chloride secretion in T84 cells stimulated by forskolin (a cyclic adenosine 3',5'-monophosphate (cAMP) donor) in a concentration-dependent manner with an  $IC_{50}$  of  $\sim 1 \mu\text{M}$  (**Figure 10**).

Thus, these results suggested that the two *E*-olefins at C5–C6 and C8–C9 as well as the *R* configuration of the C13 stereogenic center in **22** thus increased the CFTR inhibitory effect compared to **21** and **23**. Obviously, mutolide (**22**) had anti-diarrheal efficacy comparable to that of zearalenone. These findings suggested that further development of this subclass of macrolides might lead to drug candidates for the treatment of secretory diarrheas.

**Figure 9** Evaluation of effects of compounds **21–23** (5  $\mu\text{M}$ ) on CFTR-mediated chloride secretion in T84 cells. Forskolin (20  $\mu\text{M}$ ) was used to stimulate the CFTR-mediated chloride secretion. CFTR<sub>Inh</sub>-172 (20  $\mu\text{M}$ ) was used as a positive control. Representative tracings of 3 experiments are shown.



**Figure 10** Evaluation of potency of synthetic mutolide (**22**) on CFTR-mediated chloride secretion on human intestinal epithelial (T84) cells. (Left) A representative current tracing of 3 experiments. (Right) Summary of the data. Data were fitted to Hill's equation.



### 3.3 Conclusions

In conclusion, we have accomplished the total synthesis of mutolide (**22**) and (4*S*,7*S*,13*S*)-4,7-dihydroxy-13-tetradeca-2,5,8-trienolide (**23**) starting from commercially available (*S*)- (**38**) (for **23**) or (*R*)-propylene oxide (**181**) (for **22**) and known (*S*)-benzyl glycidyl ether (**131**) described in the previous chapter. The synthetic **22** was achieved in a longest linear sequence of 16 steps and a total of 18 steps in 1.5% overall yield, whereas **23** was obtained in a longest linear sequence of 17 steps and a total of 22 steps in 1.1% overall yield. The construction of 14-membered macrocyclic core and C2–C3 *trans*-olefin of targets **22** and **23** still utilized the key Shiina macrolactonization and Wittig olefination, respectively. The synthesis of macrolide **23** was accomplished via the similar synthetic procedure as that of nigrosporolide (**21**) from the known propargylic alcohol **116R** using selective reduction of propargylic alcohol mediated by Red-Al as a key strategy to form *E*-olefin at C8–C9. However, in the synthesis of mutolide (**22**), Red-Al reduction was not compatible with chiral propargylic alcohol **179R** which differs from **116R** by the configuration of alkene at C5–C6, and resulted in the formation of an undesired overreduced product. Therefore,

the retrosynthetic strategy of **22** was revised using cross metathesis to effect the formation of exclusive C8–C9 *E*-alkene.

Furthermore, cytotoxic activities against various human cancers cell lines of the synthetic 7-*O*-methylnigrosporolide (**19**), pestalotioprolide D (**20**), nigrosporolide (**21**), mutolide (**22**) and (4*S*,7*S*,13*S*)-4,7-dihydroxy-13-tetradeca-2,5,8-trienolide (**23**) were evaluated. Synthetic pestalotioprolide D (**20**) showed a stronger cytotoxic activity against MDA-MB-231, MCF-7, C33A, HeLa, SiHa and HCT116 cell lines than synthetic **19**. Among the six cancer cell lines tested, the SiHa cervical cancer cell line was the most sensitive to both macrolides **19** and **20** with IC<sub>50</sub> values of 35.17 ± 10.77 μM and 8.90 ± 2.51 μM, respectively. The three synthetic macrolides **21–23** were evaluated for their cytotoxic activity against HCT116, MCF-7 and Calu-3 cell lines as well as their inhibitory effect on CFTR-mediated chloride secretion in human intestinal epithelial (T84) cells. Mutolide (**22**) displayed significant cytotoxic activity against HCT116 colon cancer cells with an IC<sub>50</sub> of ~12 μM and also exhibited potent CFTR inhibitory effect with an IC<sub>50</sub> value of ~1 μM. Nevertheless, compounds **21** and **23** showed no significant cytotoxic activity against three human cancer cell lines and displayed inhibitory effects on the CFTR channels with less efficacy compared to **22**. Preliminary structure-activity relationships of macrolides **19–23** suggested that the presence of one ketone functional group at the C4-position and two methylene groups at C2–C3 of **20** or two *trans*-olefins at C5–C6 and C8–C9 as well as the *R* methyl lactone alcohol at the C13-position of **22** led to an improvement in biological activities.

## **CHAPTER 4**

### **EXPERIMENTAL**

## CHAPTER 4

### EXPERIMENTAL

#### 4.1. General Information

Unless otherwise stated, all reactions were conducted under a nitrogen or argon atmosphere in oven- or flamed-dried glassware. Solvents were used as received from suppliers or distilled prior to use using standard procedures. All other reagents were obtained from commercial sources and used without further purification. Column chromatography was performed on Silica gel 60 (0.063-0.200 mm, Merck). Thin-layer chromatography (TLC) was performed on Silica gel 60 F<sub>254</sub> (Merck). <sup>1</sup>H, <sup>13</sup>C and 2D NMR spectroscopic data were recorded on 300 and 500 MHz Bruker FTNMR Ultra Shield spectrometer. <sup>1</sup>H NMR spectra are reported in ppm on the  $\delta$  scale and referenced to the internal tetramethylsilane. The data are presented as follows: chemical shift, multiplicity (s = singlet, d = doublet, t = triplet, q = quartet, m = multiplet, br = broad, app = apparent), coupling constant(s) in hertz (Hz), and integration. Infrared (IR) spectra were recorded on a Perkin Elmer 783 FTS165 FT-IR spectrometer. High-resolution mass spectra were obtained on a Ultra-Performance Liquid Chromatography–High Resolution Mass Spectrometer (Agilent LC-QTOF 6500 system), Mae Fah Luang University and Liquid Chromatograph-Quadrupole Time-of-Flight Mass Spectrometer (LC-QTOF MS), Prince of Songkla University. Melting points were measured using an Electrothermal IA9200 melting point apparatus and are uncorrected. The optical rotations were recorded on a JASCO P-2000 polarimeter. Enantiopurity was determined using HPLC on an Agilent series 1200 equipped with a diode array UV detector using either CHIRALCEL<sup>®</sup> OD-H column (15 cm) or CHIRALPAK<sup>®</sup> AS-H column (15 cm) and a guard column (1 cm).

## 4.2. Experimentals and Characterization Data

### 4.2.1 General procedure for epoxide ring opening/ TBS protection

To a suspension of CuI (0.3 equiv) in anhydrous THF (1.73 M) at  $-30\text{ }^{\circ}\text{C}$  was added allylmagnesium bromide (*ca.* 1 M solution in diethyl ether, 2.0 equiv). After stirring at  $-30\text{ }^{\circ}\text{C}$  for 1 h, a solution of (*S*)- or (*R*)-propylene oxide (1.0 equiv) in anhydrous THF (0.8 M) was slowly added. The reaction mixture was stirred at the same temperature for 1 h, then quenched with  $\text{NH}_4\text{Cl}$  and extracted with  $\text{CH}_2\text{Cl}_2$  (x3). The combined organic layers were washed with brine, dried over anhydrous  $\text{Na}_2\text{SO}_4$  and concentrated *in vacuo* to give (*S*)- or (*R*)-hex-5-en-2-ol which was used in the next step without further purification.

To a solution of (*S*)- or (*R*)-hex-5-en-2-ol (1.0 equiv) in  $\text{CH}_2\text{Cl}_2$  (0.5 M) were added DMAP (0.33 equiv) and imidazole (3.0 equiv), followed by TBSCl (2.0 equiv) and stirred from  $0\text{ }^{\circ}\text{C}$  to room temperature overnight. The reaction was quenched with  $\text{H}_2\text{O}$  and extracted with  $\text{CH}_2\text{Cl}_2$  (x3). The combined organic layers were washed with brine, dried over anhydrous  $\text{Na}_2\text{SO}_4$  and concentrated under reduced pressure. The crude product was purified by column chromatography to give (*S*)- or (*R*)-silyl ether (Sasaki *et al.*, 2011 and Pandey *et al.*, 2018).

### 4.2.2 General procedure for hydroboration-oxidation

To a solution of olefin derivative (1.0 equiv) in anhydrous THF (0.35 M) at  $0\text{ }^{\circ}\text{C}$  was added borane dimethyl sulfide ( $\text{BH}_3\cdot\text{SMe}_2$ ) (1.7 equiv). The reaction mixture was stirred at  $0\text{ }^{\circ}\text{C}$  for 2 h, then treated with 3 M aq NaOH (0.4 M) and 30%  $\text{H}_2\text{O}_2$  (0.4 M). After stirring from  $0\text{ }^{\circ}\text{C}$  to  $25\text{ }^{\circ}\text{C}$  for 4 h, the mixture was diluted with  $\text{H}_2\text{O}$  and extracted with EtOAc (x3). The combined organic layers were washed with brine, dried over anhydrous  $\text{Na}_2\text{SO}_4$  and concentrated *in vacuo*. Purification of the crude residue by column chromatography yielded the alcohol derivative (Sharma *et al.*, 2017).

#### 4.2.3 General procedure for Ohira–Bestmann homologation

To a suspension of  $K_2CO_3$  (2.3 equiv) in MeOH (0.1 M) was added dimethyl (1-diazo-2-oxopropyl) phosphonate (1.4 equiv) at 0 °C. After stirring at 0 °C for 1 h, a solution of aldehyde derivative (1.0 equiv) in MeOH (0.2 M) was slowly added and stirred from 0 °C to room temperature overnight. The reaction mixture was concentrated under reduced pressure and purified by column chromatography to give alkyne derivative (Marshall and Adams, 2002).

#### 4.2.4 General procedure for acetylide addition

To a solution of alkyne derivative (1.5 equiv) in anhydrous THF (0.23 M) was added *n*-BuLi (*ca.* 1.6 M solution in hexane, 1.5 equiv) dropwise at –78 °C. After stirring at –78 °C for 1 h, a solution of (*Z*)- or (*E*)-enal (1.0 equiv) in anhydrous THF (0.35 M) was slowly added. The reaction mixture was stirred from –78 °C to approximately 0 °C over 3 h. The reaction was quenched with saturated aqueous  $NH_4Cl$  and extracted with EtOAc (x3). The combined organic layer were washed with brine, dried over anhydrous  $Na_2SO_4$  and concentrated *in vacuo*. Purification of the crude residue by column chromatography yielded the propargylic alcohol derivative.

#### 4.2.5 General procedure for $MnO_2$ oxidation

To a solution of propargylic or allylic alcohol derivative (1.0 equiv) in anhydrous  $CH_2Cl_2$  (0.1 M) was added  $MnO_2$  (15 equiv). The reaction mixture was stirred at room temperature overnight, then filtered through a pad of Celite, washed with EtOAc and concentrated *in vacuo*. Purification of the crude residue by column chromatography yielded ketone derivative.

#### 4.2.6 General procedure for PMB deprotection

To a solution of PMB ether derivative (1.0 equiv) in  $CH_2Cl_2$  (0.06 M) at 0 °C was added DDQ (1.3 equiv). After being stirred from 0 °C to room temperature for 3 h, the reaction mixture was then quenched with saturated aqueous  $NaHCO_3$ . The resulting solution was extracted with  $CH_2Cl_2$  (x3). The combined organic layers were



washed with brine, dried over anhydrous Na<sub>2</sub>SO<sub>4</sub> and concentrated under reduced pressure. Purification of the crude residue by column chromatography yielded the primary alcohol derivative (Walsh *et al.*, 2009).

#### 4.2.7 General procedure for TEMPO/PhI(OAc)<sub>2</sub>-mediated oxidation

To a solution of alcohol derivative (1.0 equiv) in anhydrous CH<sub>2</sub>Cl<sub>2</sub> (0.05 M) at 0 °C were added PhI(OAc)<sub>2</sub> (1.2 equiv) and TEMPO (0.2 equiv). The reaction mixture was stirred from 0 °C to 25 °C for 4 h, and then quenched with saturated aqueous NH<sub>4</sub>Cl. The aqueous phase was extracted with CH<sub>2</sub>Cl<sub>2</sub> (x3). The combined organic phases were washed with brine, dried over anhydrous Na<sub>2</sub>SO<sub>4</sub> and concentrated *in vacuo*. The crude residue was purified by column chromatography to afford the aldehyde derivative.

#### 4.2.8 General procedure for Wittig olefination

To a solution of aldehyde derivative (1.0 equiv) in anhydrous CH<sub>2</sub>Cl<sub>2</sub> (0.05 M) at 0 °C was added (carbethoxymethylene)triphenylphosphorane (2.1 equiv). The reaction mixture was stirred from 0 °C to room temperature for 2.5 h before being concentrated under reduced pressure. The crude product was purified by column chromatography to afford (*E*)-α,β-unsaturated ester derivative.

#### 4.2.9 General procedure for TBS deprotection

To a solution of silyl ether derivative (1.0 equiv) in EtOH (0.05 M) at 0 °C was added pyridinium *p*-toluenesulfonate (PPTS, 3.0 equiv). The reaction mixture was stirred from 0 °C to room temperature overnight. The reaction mixture was quenched with H<sub>2</sub>O and the aqueous phase was extracted with EtOAc (x3). The combined organic layers were washed with brine, dried over anhydrous Na<sub>2</sub>SO<sub>4</sub> and concentrated *in vacuo*. Purification of the crude residue by column chromatography yielded the secondary alcohol derivative.

#### 4.2.10 General procedure for hydrolysis

To a solution of ester derivative (1.0 equiv) in THF:MeOH:H<sub>2</sub>O (1:1:2, 0.08 M) at 0 °C was added LiOH (4.0 equiv) and stirred from 0 °C to room temperature overnight. The reaction mixture was acidified with 1 M HCl until the pH reached 7. The resulting solution was extracted with EtOAc (x4). The combined organic layers were washed with brine, dried over anhydrous Na<sub>2</sub>SO<sub>4</sub> and concentrated *in vacuo*. The crude product was purified by column chromatography to give seco acid derivative.

#### 4.2.11 General procedure for Shiina macrolactonization

To a solution of 2-methyl-6-nitrobenzoic anhydride (0.6 equiv) in anhydrous toluene (0.0021 M) was added DMAP (6.0 equiv). The solution of seco acid derivative (1.0 equiv) in anhydrous toluene (0.0105 M) was slowly added by syringe pump at room temperature for 12 h. The reaction mixture was concentrated under reduced pressure and purified by column chromatography to give macrolactone derivative (Snider and Zhou, 2006 and Narsaiah *et al.*, 2019).

#### 4.2.12 General procedure for global desilylation

To a solution of macrolactone derivative (1.0 equiv) in anhydrous THF (0.035 M) were added AcOH (0.06 equiv) and TBAF (1 M solution in THF, 20 equiv) dropwise at 0 °C. The reaction mixture was stirred from 0 °C to 63 °C for 3 h and then cooled to room temperature for 15 h. The reaction was quenched with saturated aqueous NaHCO<sub>3</sub> and H<sub>2</sub>O. The organic phase was extracted with EtOAc (x4), washed with brine and dried over anhydrous Na<sub>2</sub>SO<sub>4</sub>. Purification of the crude residue by column chromatography yielded diol derivative (Mohapatra *et al.*, 2010, Miller *et al.*, 2011 and Kanoh *et al.*, 2014).

#### 4.2.13 General procedure for TBDPS protection

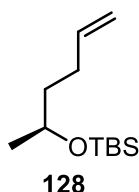
To a solution of alcohol derivative (1.0 equiv) in anhydrous  $\text{CH}_2\text{Cl}_2$  (0.2 M) was added DMAP (0.33 equiv) and imidazole (2.5 equiv), followed by TBDPSCl (1.3 equiv). The reaction mixture was stirred at room temperature overnight. The reaction was then quenched with  $\text{H}_2\text{O}$  and extracted with  $\text{CH}_2\text{Cl}_2$  (x3). The combined organic layers were washed with brine, dried over anhydrous  $\text{Na}_2\text{SO}_4$  and concentrated *in vacuo*. The crude product was purified by column chromatography to give silyl ether derivative.

#### 4.2.14 General procedures for Zn-mediated asymmetric alkylation reaction

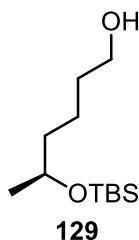
Pu's protocol: To a stirred suspension of (*S*)-BINOL (20 mol %) in  $\text{Et}_2\text{O}$  (0.08 M) were added a solution of alkyne derivative (3.0 equiv) in  $\text{Et}_2\text{O}$  (0.5 M) and  $\text{Cy}_2\text{NH}$  (5 or 10 mol %), followed by  $\text{ZnEt}_2$  (3.0 or 5.0 equiv) and stirred at room temperature overnight. Then, the reaction mixture were added  $\text{Ti}(\text{O}-i\text{Pr})_4$  (20 mol %) and a solution of aldehyde derivative (1.0 equiv) in  $\text{Et}_2\text{O}$  (0.4 or 0.7 M). After stirring for 9–19 h, the reaction was quenched with saturated aqueous  $\text{NH}_4\text{Cl}$ , the organic layer was separated and the aqueous phase was extracted with  $\text{CH}_2\text{Cl}_2$  (x3). The combined organic layers were washed with brine, dried over anhydrous  $\text{Na}_2\text{SO}_4$  and concentrated *in vacuo*. The crude product was purified by column chromatography (Pu *et al.*, 2002, 2010, 2013 and 2015).

Trost's protocol: To a solution of alkyne derivative (2.0 equiv) in anhydrous toluene (0.8 or 1.0 M) was added (*S,S*)-ProPhenol (10 or 20 mol %) with or without triphenylphosphine oxide (TPPO, 20 mol %), followed by  $\text{ZnMe}_2$  (1.5, 3.0 or 5.0 equiv) at 0 °C. The reaction mixture was stirred from 0 °C to room temperature for 2–4 h before addition of a solution of aldehyde derivative (1 equiv) in anhydrous toluene (0.8 M) at 0 °C. The reaction was stirred from 0 °C to room temperature for 4–23 h, then quenched with saturated aqueous  $\text{NH}_4\text{Cl}$  and extracted with  $\text{EtOAc}$  (x3). The combined organic layer were washed with brine, dried over anhydrous  $\text{Na}_2\text{SO}_4$

and concentrated under reduced pressure. The crude residue was purified by column chromatography (Trost *et al.*, 2006, 2012 and Trost and Bartlett, 2012).

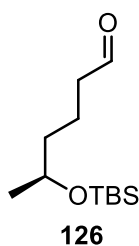


**(S)-tert-Butyl(hex-5-en-2-yloxy)dimethylsilane (128)**: Silyl ether **128** was prepared from (*S*)-propylene oxide (**38**) (2.5 mL, 35.7 mmol) using the general procedure for epoxide ring opening/TBS protection. The crude residue was purified by column chromatography (100% hexanes–5% EtOAc/hexanes) to give (*S*)-tert-butyl(hex-5-en-2-yloxy)dimethylsilane (**128**) as a colorless oil (6.64 g, 90%):  $R_f = 0.75$  (10% EtOAc/hexanes);  $[\alpha]_D^{26} = +12.9$  ( $c$  1.0,  $\text{CHCl}_3$ );  $^1\text{H NMR}$  (300 MHz,  $\text{CDCl}_3$ )  $\delta$  5.89–5.76 (m, 1H), 5.04–4.93 (m, 2H), 3.85–3.79 (m, 1H), 2.18–2.01 (m, 2H), 1.60–1.44 (m, 2H), 1.14 (d,  $J = 6.0$  Hz, 3H), 0.90 (s, 9H), 0.06 (s, 6H);  $^{13}\text{C NMR}$  (75 MHz,  $\text{CDCl}_3$ )  $\delta$  139.0, 114.4, 68.2, 39.1, 30.2, 26.1, 23.9, 18.3, –4.2, –4.6. The spectral data of **128** matched those previously described (She *et al.*, 2009).

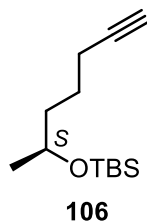


**(S)-5-((tert-Butyldimethylsilyl)oxy)hexan-1-ol (129)**: Alcohol **129** was prepared from olefin **128** (5.90 g, 27.5 mmol) using the general procedure for hydroboration-oxidation. The combined organic layers were washed with brine, dried over anhydrous  $\text{Na}_2\text{SO}_4$  and concentrated *in vacuo*. Purification of the crude residue by column chromatography (10–20% EtOAc/hexanes) yielded (*S*)-5-((tert-butyl dimethylsilyl)oxy)hexan-1-ol (**129**) as a colorless oil (4.97 g, 78%):  $R_f = 0.36$  (20% EtOAc/hexanes);  $[\alpha]_D^{25} = +11.9$  ( $c$  1.3,  $\text{CHCl}_3$ );  $^1\text{H NMR}$  (300 MHz,  $\text{CDCl}_3$ )  $\delta$  3.82–3.76 (m, 1H), 3.64 (t,  $J = 6.3$  Hz, 2H), 1.57–1.29 (m, 6H), 1.12 (d,  $J = 6.0$  Hz, 3H), 0.88 (s, 9H), 0.05 (s, 6H);  $^{13}\text{C NMR}$  (75

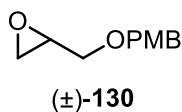
MHz, CDCl<sub>3</sub>)  $\delta$  68.7, 63.1, 39.5, 32.9, 26.0, 23.9, 22.0, 18.3, -4.3, -4.6; IR (thin film) 3346, 2931, 1462, 1255, 1059, 835 cm<sup>-1</sup>. The spectral data of **129** matched those previously described (She *et al.*, 2009). The enantiomeric excess of **129** was determined to be 96% ee from the corresponding benzoate ester, (*S*)-6-(benzyloxy)hexan-2-yl benzoate (**129a**), by HPLC analysis using CHIRALPAK<sup>®</sup> AS-H column eluting with 98:2 hexane/isopropanol (flow rate = 0.2 mL/min, pressure = 7.62 bar, temp = 25-28 °C): retention time = 15.251 min, retention time of (*R*)-enantiomer = 16.327 min.



**(*S*)-5-((*tert*-Butyldimethylsilyl)oxy)hexanal (**126**):** To a solution of alcohol **129** (4.35 g, 18.7 mmol) in anhydrous CH<sub>2</sub>Cl<sub>2</sub> (32 mL, 0.57 M) at 0 °C was added PhI(OAc)<sub>2</sub> (7.23 g, 22.4 mmol, 1.2 equiv), followed by TEMPO (292.3 mg, 1.9 mmol, 0.1 equiv). The reaction mixture was stirred from 0 °C to room temperature for 2 h and then quenched with saturated aqueous NH<sub>4</sub>Cl (20 mL). The aqueous phase was extracted with CH<sub>2</sub>Cl<sub>2</sub> (3x15 mL). The combined organic phases were washed with brine, dried over anhydrous Na<sub>2</sub>SO<sub>4</sub> and concentrated *in vacuo*. The crude residue was purified by column chromatography (100% hexanes–10% EtOAc/hexanes) to afford aldehyde **126** as a light yellow oil (3.55 g, 82%):  $R_f$  = 0.53 (10% EtOAc/hexanes); <sup>1</sup>H NMR (300 MHz, CDCl<sub>3</sub>)  $\delta$  9.72 (t,  $J$  = 1.8 Hz, 1H), 3.82–3.72 (m, 1H), 2.39 (td,  $J$  = 7.2, 1.5 Hz, 2H), 1.76–1.53 (m, 2H), 1.43–1.38 (m, 2H), 1.10 (d,  $J$  = 6.3 Hz, 3H), 0.85 (s, 9H), 0.01 (s, 6H); <sup>13</sup>C NMR (75 MHz, CDCl<sub>3</sub>)  $\delta$  202.7, 68.2, 43.9, 39.0, 25.9, 23.8, 18.4, 18.2, -4.3, -4.7. The spectral data of **126** matched those previously described (Anderson and Miller *et al.*, 2011).

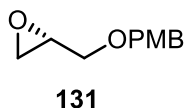


**(S)-tert-Butyl(hept-6-yn-2-yloxy)dimethylsilane (106):** Alkyne **106** was prepared from aldehyde **126** (3.00 g, 13.0 mmol) using the general procedure for Ohira–Bestmann homologation. Purification of the crude residue by column chromatography (100% hexanes) afforded alkyne **106** as a light yellow oil (2.09 g, 71%):  $R_f = 0.62$  (3% EtOAc/hexanes);  $[\alpha]_D^{25} = +13.8$  ( $c$  7.0,  $\text{CH}_2\text{Cl}_2$ );  $^1\text{H NMR}$  (300 MHz,  $\text{CDCl}_3$ )  $\delta$  3.85–3.75 (m, 1H), 2.20–2.16 (m, 2H), 1.93 (t,  $J = 2.7$  Hz, 1H), 1.64–1.48 (m, 4H), 1.13 (d,  $J = 6.0$  Hz, 3H), 0.88 (s, 9H), 0.04 (s, 6H);  $^{13}\text{C NMR}$  (75 MHz,  $\text{CDCl}_3$ )  $\delta$  84.7, 68.3, 68.3, 38.8, 26.0, 24.9, 23.9, 18.6, 18.3, –4.2, –4.6. The spectral data of **106** matched those previously described (Suh *et al.*, 2002).

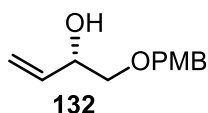


**2-(((4-Methoxybenzyl)oxy)methyl)oxirane (130):** To a suspension of NaH (60% dispersion in mineral oil, 12.97 g, 324.3 mmol, 1.5 equiv) in anhydrous THF (115 mL, 1.85 M) at 0 °C was added 4-methoxybenzyl alcohol (32.85 g, 237.8 mmol, 1.1 equiv) in anhydrous THF (80 mL, 2.7 M) at 0 °C. After stirring from 0 °C to room temperature for 1.5 h,  $(\text{Bu})_4\text{NI}$  (638.8 mg, 1.7 mmol, 0.008 equiv) and (±)-epichlorohydrin (**118**) (20.01 g, 216.2 mmol) in anhydrous THF (40 mL, 4.45 M) were added at 0 °C. The reaction mixture was stirred from 0 °C to room temperature for 14 h, then quenched with saturated aqueous  $\text{NH}_4\text{Cl}$  (80 mL) and extracted with EtOAc (3x50 mL). The combined organic layers were washed with brine, dried over anhydrous  $\text{Na}_2\text{SO}_4$  and concentrated under reduced pressure. Purification of the crude residue by column chromatography (10–20% EtOAc/hexanes) yielded racemic epoxide **130** (32.5 g, 78%) as a yellow oil:  $R_f = 0.20$  (10% EtOAc/hexanes);  $^1\text{H NMR}$  (300 MHz,  $\text{CDCl}_3$ )  $\delta$  7.27 (d,  $J = 8.4$  Hz, 2H), 6.88 (d,  $J = 8.7$  Hz, 2H), 4.51 (dd,  $J = 18.9, 11.4$  Hz, 2H), 3.80 (s, 3H), 3.72 (dd,  $J = 11.4, 3.3$  Hz, 1H), 3.41 (dd,  $J = 11.4, 5.7$  Hz, 1H), 3.20–3.14 (m, 1H), 2.79 (t,  $J = 4.5$  Hz, 1H), 2.60 (dd,  $J = 5.1, 2.7$  Hz,

1H);  $^{13}\text{C}$  NMR (75 MHz,  $\text{CDCl}_3$ )  $\delta$  159.2, 129.9, 129.3, 113.7, 72.9, 70.5, 55.2, 50.8, 44.2. The spectral data of racemic epoxide **130** matched those previously described (Kumar and Reddy, 2012).

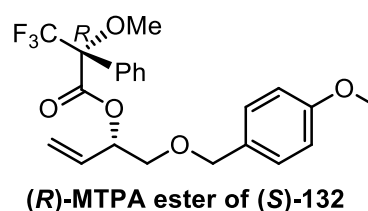
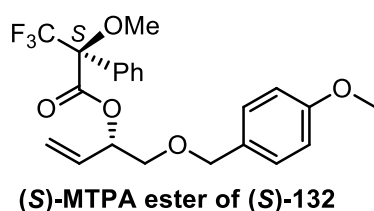


**(S)-2-((4-Methoxybenzyl)oxy)methyl oxirane (131)**: To a flame-dried flask was added (*R,R*)-cobalt(II) salen (331.0 mg, 0.5 mmol, 0.005 equiv) and toluene (2.2 mL, 50 M). The reaction mixture was treated with AcOH (135  $\mu\text{L}$ , 2.18 mmol, 0.02 equiv) and stirred open to air at room temperature for 30 min over which time the color changed from orange-red to dark brown. The solution was concentrated under reduced pressure to give a brown solid before the racemic epoxide **130** (21.25 g, 109.4 mmol) was added in one portion. The reaction was cooled to 0  $^\circ\text{C}$  and  $\text{H}_2\text{O}$  (1.3 mL, 0.60 equiv) was added dropwise and stirred from 0  $^\circ\text{C}$  to room temperature overnight. The crude residue was purified by column chromatography (10% EtOAc/hexanes–100% EtOAc) to give chiral epoxide **131** (9.77 g, 46%) as a yellow oil:  $R_f$  = 0.20 (10% EtOAc/hexanes);  $[\alpha]_D^{25} = -2.8$  ( $c$  1.0,  $\text{CHCl}_3$ );  $^1\text{H}$  NMR (300 MHz,  $\text{CDCl}_3$ )  $\delta$  7.25 (d,  $J$  = 8.7 Hz, 2H), 6.86 (d,  $J$  = 8.7 Hz, 2H), 4.48 (dd,  $J$  = 18.3, 11.4 Hz, 2H), 3.76 (s, 3H), 3.70 (dd,  $J$  = 11.4, 3.0 Hz, 1H), 3.37 (dd,  $J$  = 11.4, 6.0 Hz, 1H), 3.16–3.11 (m, 1H), 2.75 (t,  $J$  = 4.5 Hz, 1H), 2.56 (dd,  $J$  = 5.1, 2.7 Hz, 1H);  $^{13}\text{C}$  NMR (75 MHz,  $\text{CDCl}_3$ )  $\delta$  159.2, 129.9, 129.3, 113.7, 72.8, 70.4, 55.1, 50.7, 44.1. The spectral data of **131** matched those previously described (Chandankar and Raghavan, 2019).



**(S)-1-((4-Methoxybenzyl)oxy)but-3-en-2-ol (132)**: To a solution of trimethylsulfonium iodide (23.01 g, 112.2 mmol, 2.5 equiv) in anhydrous THF (150 mL, 0.3 M) was added *n*-BuLi (*ca.* 1.6 M solution in hexane, 100 mL, 157.1 mmol, 3.5 equiv) at  $-30$   $^\circ\text{C}$ . After stirring at the same temperature for 1 h, chiral epoxide **131** (8.72 g, 44.9 mmol) in anhydrous THF (70 mL, 0.65 M) was added dropwise and stirred for 1.5 h. The reaction mixture was quenched with saturated aqueous  $\text{NH}_4\text{Cl}$  (70 mL) and

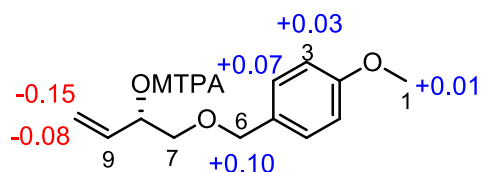
extracted with EtOAc (3x50 mL). The combined organic layers were washed with brine, dried over anhydrous Na<sub>2</sub>SO<sub>4</sub> and concentrated *in vacuo*. Purification of the crude residue by column chromatography (10–30% EtOAc/hexanes) yielded allylic alcohol **132** as a light yellow oil (7.95 g, 85%):  $R_f = 0.24$  (20% EtOAc/hexanes);  $[\alpha]_D^{25} = -2.3$  ( $c$  2.0, CHCl<sub>3</sub>); <sup>1</sup>H NMR (300 MHz, CDCl<sub>3</sub>)  $\delta$  7.26 (d,  $J = 8.4$  Hz, 2H), 6.88 (d,  $J = 8.7$  Hz, 2H), 5.82 (ddd,  $J = 16.8, 10.5, 5.7$  Hz, 1H), 5.35 (d,  $J = 17.4$  Hz, 1H), 5.18 (d,  $J = 10.8$  Hz, 1H), 4.50 (s, 2H), 4.33 (brs, 1H), 3.80 (s, 3H), 3.51 (dd,  $J = 9.6, 3.3$  Hz, 1H), 3.37–3.31 (m, 1H); <sup>13</sup>C NMR (75 MHz, CDCl<sub>3</sub>)  $\delta$  159.3, 136.7, 129.9, 129.5, 116.4, 113.9, 73.7, 73.0, 71.5, 55.3; IR (thin film) 3435, 2859, 1612, 1513, 1248, 1034 cm<sup>-1</sup>. The spectral data of **132** matched those previously described (Haug and Kirsch, 2010). The enantiomeric excess of **132** was determined to be 99% ee from the corresponding benzoate ester, (*S*)-1-((4-methoxybenzyl)oxy)but-3-en-2-yl benzoate (**132a**), by HPLC analysis using CHIRALCEL<sup>®</sup> OD-H column eluting with 98:2 hexane/isopropanol (flow rate = 1.0 mL/min, pressure = 31.02 bar, temp = 25–27 °C): retention time = 6.560 min, retention time of (*R*)-enantiomer = 7.805 min. The absolute configuration was determined to be *S* by Mosher's method using the corresponding (*S*)-MTPA and (*R*)-MTPA esters.



**(S)-MTPA ester of allylic alcohol 132:** <sup>1</sup>H NMR (300 MHz, CDCl<sub>3</sub>)  $\delta$  7.57 (d,  $J = 7.2$  Hz, 2H), 7.39–7.29 (m, 3H), 7.22 (d,  $J = 8.4$  Hz, 2H), 6.86 (d,  $J = 8.7$  Hz, 2H), 5.80–5.68 (m, 2H), 5.28 (d,  $J = 16.8$  Hz, 1H), 5.24 (d,  $J = 9.6$  Hz, 1H), 4.50 (d,  $J = 4.5$  Hz, 2H), 3.80 (s, 3H), 3.61–3.58 (m, 2H), 3.57 (s, 3H).

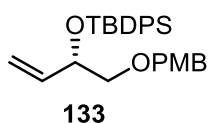
**(R)-MTPA ester of allylic alcohol 132:** <sup>1</sup>H NMR (300 MHz, CDCl<sub>3</sub>)  $\delta$  7.54 (d,  $J = 6.9$  Hz, 2H), 7.38–7.32 (m, 3H), 7.15 (d,  $J = 8.4$  Hz, 2H), 6.83 (d,  $J = 8.4$  Hz, 2H), 5.91–5.72 (m, 2H), 5.43 (d,  $J = 16.8$  Hz, 1H), 5.32 (d,  $J = 10.2$  Hz, 1H), 4.40 (d,  $J = 4.2$  Hz, 2H), 3.79 (s, 3H), 3.59–3.55 (m, 2H), 3.52 (s, 3H).





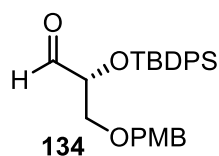
**Table 16**  $\Delta\delta$  ( $\delta_S - \delta_R$ ) data for the (*S*)- and (*R*)-MTPA-Mosher esters of allylic alcohol **132**

position	$\delta_{S\text{-ester}}$ (ppm)	$\delta_{R\text{-ester}}$ (ppm)	$\Delta\delta$ ( $\delta_S - \delta_R$ ) (ppm)
1	3.80	3.79	+0.01
3	6.86	6.83	+0.03
4	7.22	7.15	+0.07
6	4.50	4.40	+0.10
10	5.28	5.43	-0.15
	5.24	5.32	-0.08



**(*S*)-tert-Butyl((1-((4-methoxybenzyl)oxy)but-3-en-2-yl)oxy)diphenylsilane (133):** To a solution of allylic alcohol **132** (7.53 g, 36.1 mmol) in  $\text{CH}_2\text{Cl}_2$  (120 mL, 0.3 M) were added DMAP (1.32 g, 10.8 mmol, 0.3 equiv) and imidazole (4.92 g, 72.3 mmol, 2.0 equiv), followed by TBDPSCl (11.0 mL, 43.4 mmol, 1.2 equiv) and stirred at room temperature overnight. The reaction mixture was quenched with  $\text{H}_2\text{O}$  (50 mL) and extracted with  $\text{CH}_2\text{Cl}_2$  (3x40 mL). The combined organic layers were washed with brine, dried over anhydrous  $\text{Na}_2\text{SO}_4$  and concentrated *in vacuo*. The crude residue was purified by column chromatography (5–10% EtOAc/hexanes) to give silyl ether **133** (12.9 g, 80%) as a colorless oil:  $R_f = 0.73$  (20% EtOAc/hexanes);  $[\alpha]_D^{25} = -29.0$  ( $c$  1.7,  $\text{CHCl}_3$ );  $^1\text{H}$  NMR (300 MHz,  $\text{CDCl}_3$ )  $\delta$  7.69–7.62 (m, 4H), 7.42–7.29 (m, 6H), 7.10 (d,  $J = 8.4$  Hz, 2H), 6.80 (d,  $J = 8.4$  Hz, 2H), 5.87 (ddd,  $J = 17.1, 10.5, 5.7$  Hz, 1H), 5.16 (dt,  $J = 17.1, 1.5$  Hz, 1H), 5.06 (dt,  $J = 10.5, 1.5$  Hz, 1H), 4.33–4.30 (m, 3H), 3.79 (s, 3H), 3.36 (qd,  $J = 9.9, 5.7$  Hz, 2H), 1.06 (s, 9H);  $^{13}\text{C}$  NMR (75 MHz,  $\text{CDCl}_3$ )  $\delta$  159.1, 138.4, 136.1, 136.0, 134.3, 133.9, 130.4, 129.6, 129.2, 127.5, 115.5,

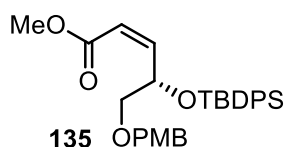
113.7, 74.4, 73.4, 72.8, 55.2, 27.1, 19.4. The spectral data of **133** matched those previously described (Kumaraswamy and Sadaiah, 2012).



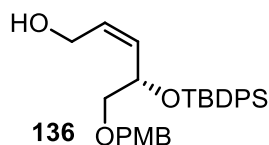
**(R)-2-((tert-Butyldiphenylsilyloxy)-3-((4-methoxybenzyl)oxy)propanal (134):** To a solution of alkene **133** (11.63 g, 26.0 mmol) in acetone/water (4:1, 260 mL, 0.1 M) at 0 °C was added *N*-methylmorpholine *N*-oxide (50 wt% in H<sub>2</sub>O, 12 mL, 52.1 mmol, 2.0 equiv), followed by OsO<sub>4</sub> (4 wt% in H<sub>2</sub>O, 1.6 mL, 0.3 mmol, 1 mol %) and stirred from 0 °C to room temperature overnight. The reaction mixture was then concentrated under reduced pressure, diluted with H<sub>2</sub>O (50 mL) and EtOAc (40 mL). The aqueous phase was separated and further extracted with EtOAc (4x40 mL). The combined organic phases were washed with brine, dried over anhydrous Na<sub>2</sub>SO<sub>4</sub> and concentrated *in vacuo*. The crude residue was purified by column chromatography (20–50% EtOAc/hexanes) to give the corresponding diol (7.51 g, 60%) as a colorless oil: *R*<sub>f</sub> = 0.30 (40% EtOAc/hexanes); <sup>1</sup>H NMR (300 MHz, CDCl<sub>3</sub>) δ 7.67–7.64 (m, 4H), 7.45–7.34 (m, 6H), 7.05 (d, *J* = 8.4 Hz, 2H), 6.80 (d, *J* = 8.4 Hz, 2H), 4.23–4.12 (m, 2H), 3.92–3.87 (m, 2H), 3.85–3.76 (m, 4H), 3.69 (brs, 2H), 3.51–3.36 (m, 2H), 1.05 (s, 9H); <sup>13</sup>C NMR (75 MHz, CDCl<sub>3</sub>) δ 159.3, 136.0, 135.8, 133.8, 132.8, 130.1, 129.9, 129.5, 129.5, 127.9, 127.7, 113.8, 74.1, 73.0, 72.7, 71.1, 63.3, 55.3, 27.0, 19.4.

To a solution of the corresponding diol (7.40 g, 15.3 mmol) in acetone/H<sub>2</sub>O (5:1, 55 mL, 0.285 M) at 0 °C was added NaIO<sub>4</sub> (3.94 g, 18.4 mmol, 1.2 equiv). After stirring from 0 °C to room temperature for 2 h, the reaction mixture was concentrated under reduced pressure and diluted with H<sub>2</sub>O (40 mL). The aqueous phase was separated and further extracted with CH<sub>2</sub>Cl<sub>2</sub> (4x20 mL). The combined organic phases were washed with brine, dried over anhydrous Na<sub>2</sub>SO<sub>4</sub> and concentrated *in vacuo*. Purification of the crude residue by column chromatography (10–20% EtOAc/hexanes) yielded aldehyde **134** (5.30 g, 61%) as a light yellow oil: *R*<sub>f</sub> = 0.26 (10% EtOAc/hexanes); <sup>1</sup>H NMR (300 MHz, CDCl<sub>3</sub>) δ 9.65 (s, 1H), 7.67–7.62 (m, 4H), 7.42–7.31 (m, 6H), 7.15 (d, *J* = 8.1 Hz, 2H), 6.84 (d, *J* = 8.4 Hz, 2H), 4.37 (s, 2H), 4.16–4.13 (m, 1H), 3.79 (s, 3H), 3.64 (dd, *J* = 10.2, 4.8 Hz, 1H), 3.56 (dd, *J* =

10.2, 4.2 Hz, 1H), 1.11 (s, 9H);  $^{13}\text{C}$  NMR (75 MHz,  $\text{CDCl}_3$ )  $\delta$  202.6, 159.3, 135.9, 135.8, 133.2, 132.7, 130.1, 130.0, 129.9, 129.3, 127.9, 127.8, 113.8, 77.9, 73.1, 70.8, 55.3, 27.0, 19.4.

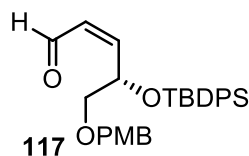


**(S,Z)-Methyl 4-((tert-butyldiphenylsilyl)oxy)-5-((4-methoxybenzyl)oxy)pent-2-enoate (135):** To a solution of methyl *P,P*-bis(2,2,2-trifluoroethyl)phosphonoacetate (5.39 g, 16.1 mmol, 1.1 equiv) in anhydrous THF (100 mL, 0.14 M) at 0 °C was added NaH (60% dispersion in mineral oil, 647.3 mg, 16.2 mmol, 1.1 equiv). After stirring at 0 °C for 1 h, the solution of aldehyde **134** (6.6 g, 14.7 mmol) in anhydrous THF (60 mL, 0.25 M) was slowly added. The reaction mixture was stirred at -78 °C for 1 h. The reaction was quenched with saturated aqueous  $\text{NH}_4\text{Cl}$  (60 mL) and extracted with EtOAc (3x40 mL). The combined organic layers were washed with brine, dried over anhydrous  $\text{Na}_2\text{SO}_4$  and concentrated *in vacuo*. The crude residue was purified by column chromatography (10% EtOAc/hexanes) to give (*Z*)- $\alpha,\beta$ -unsaturated ester **135** (5.86 g, 79%) as a light yellow oil:  $R_f$  = 0.33 (10% EtOAc/hexanes);  $[\alpha]_D^{25} = -23.2$  ( $c$  1.0,  $\text{CHCl}_3$ );  $^1\text{H}$  NMR (300 MHz,  $\text{CDCl}_3$ )  $\delta$  7.70–7.61 (m, 4H), 7.41–7.27 (m, 6H), 7.19 (d,  $J = 8.4$  Hz, 2H), 6.83 (d,  $J = 8.4$  Hz, 2H), 6.22 (dd,  $J = 11.7, 7.8$  Hz, 1H), 5.58 (dd,  $J = 11.7, 0.9$  Hz, 1H), 5.54–5.51 (m, 1H), 4.42 (s, 2H), 3.77 (s, 3H), 3.57 (dd,  $J = 10.5, 5.4$  Hz, 1H), 3.49–3.45 (m, 4H), 1.08 (s, 9H);  $^{13}\text{C}$  NMR (75 MHz,  $\text{CDCl}_3$ )  $\delta$  165.8, 159.1, 149.8, 136.0, 135.9, 133.9, 130.7, 129.6, 129.6, 129.2, 127.5, 127.5, 119.0, 113.7, 73.8, 72.7, 69.5, 55.3, 51.1, 27.0, 19.3; IR (thin film) 2951, 2857, 1721, 1248, 1112, 702  $\text{cm}^{-1}$ ; HRMS (ESI)  $m/z$  calcd for  $\text{C}_{30}\text{H}_{36}\text{NaO}_5\text{Si}$  ( $\text{M} + \text{Na}$ ) $^+$  527.2230, found 527.2224.



**(*S,Z*)-4-((*tert*-Butyldiphenylsilyl)oxy)-5-((4-methoxybenzyl)oxy)pent-2-en-1-ol (**136**):**

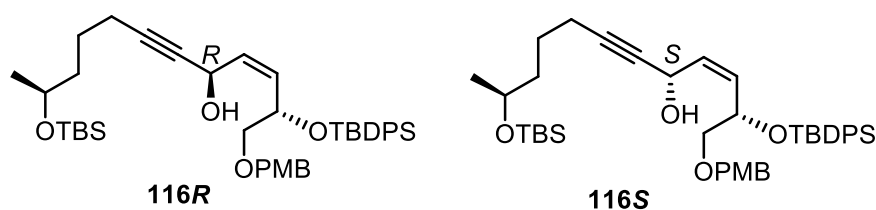
To a solution of *Z*-ester **135** (3.05 g, 5.9 mmol) in anhydrous CH<sub>2</sub>Cl<sub>2</sub> (60 mL, 0.1 M) at -78 °C was added DIBAL-H (1 M in THF, 15 mL, 14.8 mmol, 2.5 equiv) dropwise and stirred at -78 °C for 1 h. The reaction mixture was quenched with saturated aqueous potassium sodium tartrate solution (100 mL) and stirred for 1 h. The aqueous phase was extracted with CH<sub>2</sub>Cl<sub>2</sub> (3×50 mL). The combined organic layers were washed with brine, dried over anhydrous Na<sub>2</sub>SO<sub>4</sub> and concentrated under reduced pressure. Purification of the crude residue by column chromatography (20–30% EtOAc/hexanes) yielded allylic alcohol **136** (2.63 g, 93%) as a colorless oil: *R*<sub>f</sub> = 0.22 (20% EtOAc/hexanes); [α]<sub>D</sub><sup>25</sup> = -48.33 (*c* 1.0, CHCl<sub>3</sub>); <sup>1</sup>H NMR (300 MHz, CDCl<sub>3</sub>) δ 7.64 (t, *J* = 7.5 Hz, 4H), 7.41–7.31 (m, 6H), 7.14 (d, *J* = 8.1 Hz, 2H), 6.82 (d, *J* = 8.4 Hz, 2H), 5.66–5.51 (m, 2H), 4.63–4.56 (m, 1H), 4.35 (s, 2H), 3.76 (s, 3H), 3.58 (d, *J* = 6.3 Hz, 2H), 3.51 (dd, *J* = 9.0, 5.1 Hz, 1H), 3.33–3.27 (m, 1H), 1.04 (s, 9H); <sup>13</sup>C NMR (75 MHz, CDCl<sub>3</sub>) δ 159.4, 136.0, 135.9, 134.0, 133.9, 133.8, 130.3, 129.8, 129.4, 127.6, 127.5, 113.9, 73.3, 73.1, 68.4, 57.9, 55.3, 27.0, 19.2; IR (thin film) 3434, 2932, 2857, 1513, 1248, 1111 cm<sup>-1</sup>; HRMS (ESI) *m/z* calcd for C<sub>29</sub>H<sub>36</sub>NaO<sub>4</sub>Si (M + Na)<sup>+</sup> 499.2281, found 499.2280.



**(*S,Z*)-4-((*tert*-Butyldiphenylsilyl)oxy)-5-((4-methoxybenzyl)oxy)pent-2-enal (**117**):**

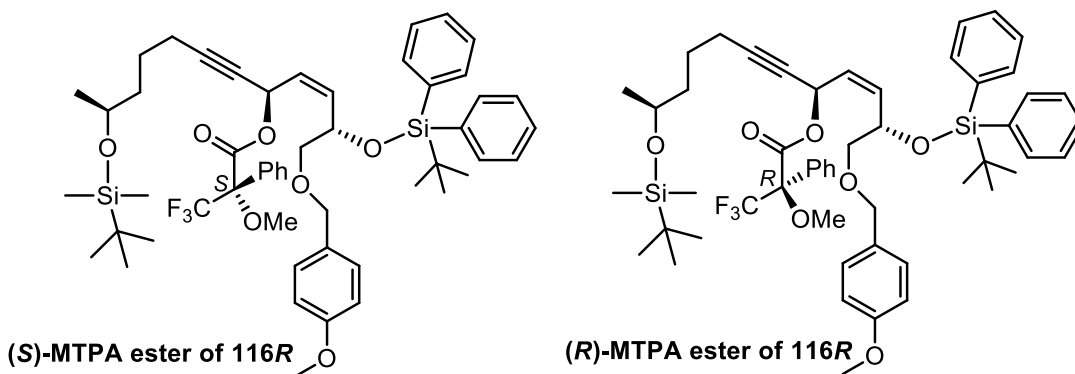
To a solution of alcohol **136** (2.0 g, 4.2 mmol) in DMSO (8.5 mL, 0.5 M) at 0 °C was added IBX (3.52 g, 12.6 mmol, 3.0 equiv) and stirred from 0 °C to room temperature for 1.5 h. The reaction was then added H<sub>2</sub>O (10 mL), filtered through a pad of Celite and washed with EtOAc. The mixture was extracted with EtOAc (3×10 mL), washed with brine, dried over anhydrous Na<sub>2</sub>SO<sub>4</sub> and concentrated *in vacuo*. The crude residue was purified by column chromatography (20% EtOAc/hexanes) to give (*Z*)-

enal **117** (1.91 g, 96%) as a light yellow oil:  $R_f = 0.26$  (10% EtOAc/hexanes);  $[\alpha]_D^{25} = -22.17$  ( $c$  1.0,  $\text{CHCl}_3$ );  $^1\text{H NMR}$  (300 MHz,  $\text{CDCl}_3$ )  $\delta$  9.44 (d,  $J = 7.8$  Hz, 1H), 7.62 (dd,  $J = 15.9, 6.9$  Hz, 4H), 7.45–7.30 (m, 6H), 7.11 (d,  $J = 8.4$  Hz, 2H), 6.82 (d,  $J = 8.4$  Hz, 2H), 6.48 (dd,  $J = 11.4, 8.7$  Hz, 1H), 5.78 (dd,  $J = 11.4, 7.8$  Hz, 1H), 5.08–5.03 (m, 1H), 4.36 (s, 2H), 3.78 (s, 3H), 3.57 (dd,  $J = 9.6, 5.1$  Hz, 1H), 3.42 (dd,  $J = 9.6, 6.6$  Hz, 1H), 1.06 (s, 9H);  $^{13}\text{C NMR}$  (75 MHz,  $\text{CDCl}_3$ )  $\delta$  190.9, 159.3, 150.5, 135.9, 135.8, 133.2, 133.0, 130.1, 130.0, 129.9, 129.8, 129.2, 127.8, 113.8, 73.2, 73.0, 68.5, 55.2, 26.9, 19.2; IR (thin film) 2932, 2857, 1688, 1248, 1111, 702  $\text{cm}^{-1}$ ; HRMS (ESI)  $m/z$  calcd for  $\text{C}_{29}\text{H}_{34}\text{NaO}_4\text{Si}$  ( $\text{M} + \text{Na}$ ) $^+$  497.2124, found 497.2104.



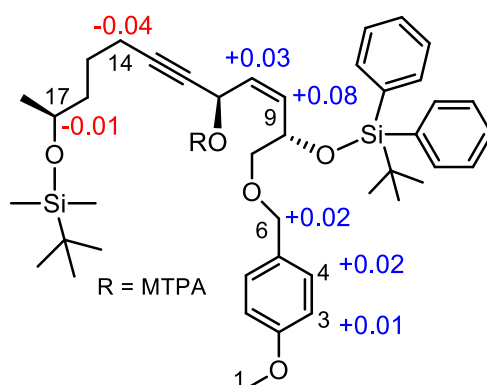
**Propargylic alcohols 116R and 116S:** Propargylic alcohols **116R** and **116S** were prepared from alkyne **106** (1.07 g, 4.7 mmol, 1.5 equiv) and (*Z*)-enal **117** (1.50 g, 3.2 mmol, 1.0 equiv) using the general procedure for acetylide addition. The crude residue was purified by column chromatography (100% hexanes–20% EtOAc/hexanes) to give **116R** and **116S**. The absolute configuration was determined by Mosher's method using the corresponding (*S*)-MTPA and (*R*)-MTPA esters.

**Propargylic alcohol 116R:** light yellow oil (930.5 mg, 42%):  $R_f = 0.46$  (20% EtOAc/hexanes);  $[\alpha]_D^{25} = -51.46$  ( $c$  1.0,  $\text{CHCl}_3$ );  $^1\text{H NMR}$  (300 MHz,  $\text{CDCl}_3$ )  $\delta$  7.71–7.64 (m, 4H), 7.45–7.31 (m, 6H), 7.19 (d,  $J = 8.7$  Hz, 2H), 6.84 (d,  $J = 8.7$  Hz, 2H), 5.52–5.40 (m, 2H), 4.71–4.65 (m, 2H), 4.41 (s, 2H), 3.80 (s, 3H), 3.76–3.70 (m, 1H), 3.49 (dd,  $J = 9.9, 5.7$  Hz, 1H), 3.36 (dd,  $J = 9.9, 5.1$  Hz, 1H), 2.07–2.02 (m, 2H), 1.61–1.38 (m, 4H), 1.09–1.05 (m, 12H), 0.86 (s, 9H), 0.02 (s, 3H), 0.01 (s, 3H);  $^{13}\text{C NMR}$  (75 MHz,  $\text{CDCl}_3$ )  $\delta$  159.2, 136.2, 136.0, 133.9, 131.5, 131.3, 130.3, 129.9, 129.8, 129.3, 127.7, 127.6, 113.8, 85.6, 79.5, 73.9, 73.0, 69.1, 68.2, 58.5, 55.3, 38.9, 27.0, 26.0, 24.8, 23.8, 19.3, 18.9, 18.2, -4.2, -4.5; IR (thin film) 3441, 2931, 1513, 1249, 1106, 834  $\text{cm}^{-1}$ ; HRMS (ESI)  $m/z$  calcd for  $\text{C}_{42}\text{H}_{60}\text{NaO}_5\text{Si}_2$  ( $\text{M} + \text{Na}$ ) $^+$  723.3877, found 723.3836.



**(S)-MTPA ester of propargylic alcohol 116R:**  $^1\text{H}$  NMR (300 MHz,  $\text{CDCl}_3$ )  $\delta$  7.64 (dd,  $J = 16.5, 7.5$  Hz, 4H), 7.56–7.29 (m, 11H), 7.11 (d,  $J = 8.4$  Hz, 2H), 6.81 (d,  $J = 8.1$  Hz, 2H), 5.99 (d,  $J = 8.7$  Hz, 1H), 5.72 (dd,  $J = 10.8, 7.8$  Hz, 1H), 5.53 (t,  $J = 10.8$  Hz, 1H), 4.74–4.68 (m, 1H), 4.30 (s, 2H), 3.79 (s, 3H), 3.70 (q,  $J = 6.0$  Hz, 1H), 3.42 (s, 3H), 3.38 (d,  $J = 6.0$  Hz, 1H), 3.32 (dd,  $J = 9.6, 5.6$  Hz, 1H), 2.03 (t,  $J = 6.3$  Hz, 2H), 1.75–1.18 (m, 4H), 1.06 (s, 3H), 1.03 (s, 9H), 0.85 (s, 9H), 0.01 (s, 6H).

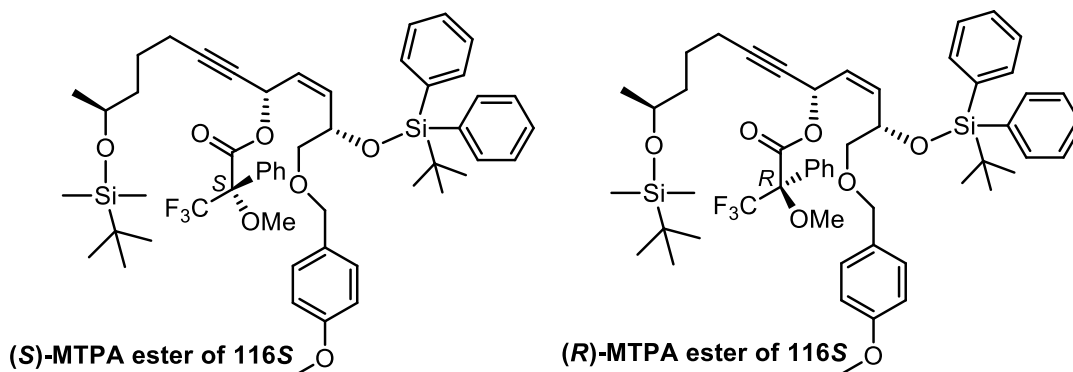
**(R)-MTPA ester of propargylic alcohol 116R:**  $^1\text{H}$  NMR (300 MHz,  $\text{CDCl}_3$ )  $\delta$  7.65 (dd,  $J = 16.8, 6.6$  Hz, 4H), 7.56–7.27 (m, 11H), 7.09 (d,  $J = 8.7$  Hz, 2H), 6.80 (d,  $J = 8.4$  Hz, 2H), 6.04 (d,  $J = 8.7$  Hz, 1H), 5.69 (dd,  $J = 10.8, 8.1$  Hz, 1H), 5.45 (t,  $J = 10.5$  Hz, 1H), 4.77–4.70 (m, 1H), 4.28 (s, 2H), 3.79 (s, 3H), 3.71 (q,  $J = 6.0$  Hz, 1H), 3.52 (s, 3H), 3.38 (dd,  $J = 9.9, 6.0$  Hz, 1H), 3.32 (dd,  $J = 9.6, 5.4$  Hz, 1H), 2.07 (t,  $J = 6.3$  Hz, 2H), 1.75–1.22 (m, 4H), 1.06 (s, 3H), 1.04 (s, 9H), 0.85 (s, 9H), 0.01 (s, 6H).



**Table 17**  $\Delta\delta$  ( $\delta_S - \delta_R$ ) data for the (*S*)- and (*R*)-MTPA-Mosher esters of propargylic alcohol **116R**

position	$\delta_{S\text{-ester}}$ (ppm)	$\delta_{R\text{-ester}}$ (ppm)	$\Delta\delta$ ( $\delta_S - \delta_R$ ) (ppm)
3	6.81	6.80	+0.01
4	7.11	7.09	+0.02
6	4.30	4.28	+0.02
9	5.53	5.45	+0.08
10	5.72	5.69	+0.03
14	2.03	2.07	-0.04
17	3.70	3.71	-0.01

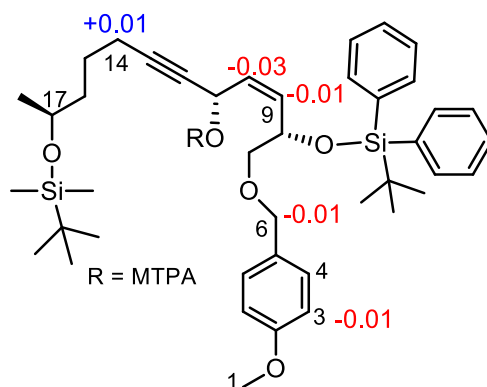
**Propargylic alcohol 116S:** light yellow oil (740.7 mg, 34%):  $R_f = 0.40$  (20% EtOAc/hexanes);  $^1\text{H}$  NMR (300 MHz,  $\text{CDCl}_3$ )  $\delta$  7.63–7.58 (m, 4H), 7.45–7.32 (m, 6H), 7.12 (d,  $J = 8.4$  Hz, 2H), 6.82 (d,  $J = 8.7$  Hz, 2H), 5.69 (dd,  $J = 10.8, 8.4$  Hz, 1H), 5.53 (t,  $J = 10.8$  Hz, 1H), 4.59–4.51 (m, 1H), 4.40–4.38 (m, 1H), 4.32 (s, 2H), 3.85–3.78 (m, 4H), 3.48 (dd,  $J = 8.4, 4.5$  Hz, 1H), 3.27 (t,  $J = 8.7$  Hz, 1H), 2.20–2.16 (m, 2H), 1.60–1.48 (m, 4H), 1.13 (d,  $J = 6.0$  Hz, 3H), 1.03 (s, 9H), 0.88 (s, 9H) 0.05 (s, 6H);  $^{13}\text{C}$  NMR (75 MHz,  $\text{CDCl}_3$ )  $\delta$  159.5, 135.8, 135.7, 134.2, 133.6, 133.3, 132.6, 129.9, 129.7, 128.9, 127.7, 127.7, 113.9, 85.2, 80.0, 73.2, 72.5, 68.3, 68.0, 57.7, 55.2, 38.9, 26.9, 24.9, 23.9, 19.2, 18.9, 18.2, -4.2, -4.5.



**(S)-MTPA ester of propargylic alcohol 116S:**  $^1\text{H}$  NMR (300 MHz,  $\text{CDCl}_3$ )  $\delta$  7.66 (ddd,  $J = 12.6, 7.8, 1.2$  Hz, 4H), 7.43–7.25 (m, 11H), 7.11 (d,  $J = 8.7$  Hz, 2H), 6.81 (d,  $J = 8.7$  Hz, 2H), 5.77 (d,  $J = 9.3$  Hz, 1H), 5.73 (dd,  $J = 10.6, 9.0$  Hz, 1H), 5.45 (t,  $J = 10.2$  Hz, 1H), 4.63–4.57 (m, 1H), 4.27 (s, 2H), 3.79 (s, 3H), 3.77–3.75 (m, 1H), 3.49 (s, 3H), 3.24 (d,  $J = 4.8$  Hz, 2H), 2.14 (t,  $J = 5.1$  Hz, 2H), 1.58–1.44 (m, 4H), 1.11 (d,  $J = 6.0$  Hz, 3H), 1.04 (s, 9H), 0.88 (s, 9H), 0.04 (s, 3H), 0.03 (s, 3H).

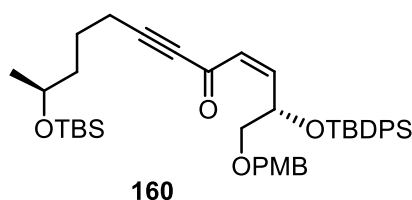
**(R)-MTPA ester of propargylic alcohol 116S:**  $^1\text{H}$  NMR (300 MHz,  $\text{CDCl}_3$ )  $\delta$  7.67 (dd,  $J = 13.2, 7.5$  Hz, 4H), 7.45–7.34 (m, 11H), 7.11 (d,  $J = 8.4$  Hz, 2H), 6.82 (d,  $J = 8.7$  Hz, 2H), 5.85 (d,  $J = 9.0$  Hz, 1H), 5.76 (dd,  $J = 11.1, 8.7$  Hz, 1H), 5.55 (t,  $J = 10.2$  Hz, 1H), 4.73–4.67 (m, 1H), 4.28 (s, 2H), 3.81 (s, 3H), 3.78–3.76 (m, 1H), 3.43 (s, 3H), 3.36 (dd,  $J = 9.9, 5.7$  Hz, 1H), 3.29 (dd,  $J = 9.9, 5.1$  Hz, 1H), 2.13 (t,  $J = 5.4$  Hz, 2H), 1.77–1.45 (m, 4H), 1.12 (d,  $J = 6.0$  Hz, 3H), 1.06 (s, 9H), 0.90 (s, 9H), 0.07 (s, 3H), 0.06 (s, 3H).



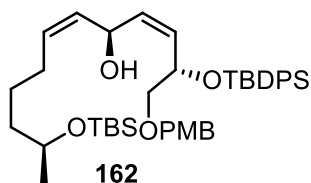


**Table 18**  $\Delta\delta$  ( $\delta_S - \delta_R$ ) data for the (*S*)- and (*R*)-MTPA-Mosher esters of propargylic alcohol **116S**

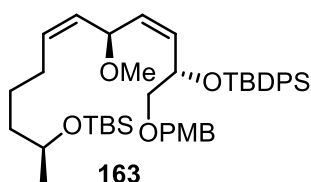
position	$\delta_{S\text{-ester}}$ (ppm)	$\delta_{R\text{-ester}}$ (ppm)	$\Delta\delta$ ( $\delta_S - \delta_R$ ) (ppm)
3	6.81	6.82	-0.01
6	4.27	4.28	-0.01
9	5.45	5.55	-0.01
10	5.73	5.76	-0.03
14	2.14	2.13	+0.01



**Ynone 160:** Ynone **160** was prepared from propargylic alcohol **116S** (650 mg, 0.92 mmol) using the general procedure for  $\text{MnO}_2$  oxidation. Purification of the crude residue by column chromatography (10–20% EtOAc/hexanes) yielded ketone **160** (572.5 mg, 89%) as a light yellow oil:  $R_f = 0.58$  (20% EtOAc/hexanes);  $^1\text{H NMR}$  (300 MHz,  $\text{CDCl}_3$ )  $\delta$  7.71–7.63 (m, 4H), 7.43–7.32 (m, 6H), 7.23 (d,  $J = 8.4$  Hz, 2H), 6.87 (d,  $J = 8.4$  Hz, 2H), 6.23 (dd,  $J = 11.7, 7.8$  Hz, 1H), 5.98 (d,  $J = 11.7$  Hz, 1H), 5.58–5.53 (m, 1H), 4.46 (s, 2H), 3.83 (s, 3H), 3.83–3.79 (m, 1H), 3.61 (dd,  $J = 10.5, 5.4$  Hz, 1H), 3.52 (dd,  $J = 10.5, 3.6$  Hz, 1H), 2.30–2.62 (m, 2H), 1.64–1.48 (m, 4H), 1.15 (d,  $J = 6.0$  Hz, 3H), 1.11 (s, 9H), 0.92 (s, 9H), 0.08 (s, 3H), 0.07 (s, 3H).

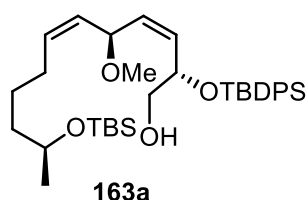


**(Z)-Olefin 162:** To a solution of alkyne **116R** (760.2 mg, 1.08 mmol) in EtOAc (11 mL, 0.1 M) were added quinoline (260  $\mu$ L, 2.16 mmol, 2.0 equiv) and Pd/CaCO<sub>3</sub> poisoned with lead (Lindlar's catalyst, 5 wt.%, 459.7 mg, 0.216 mmol 20 mol %). The reaction mixture was stirred at room temperature under H<sub>2</sub> atmosphere until the starting material was completely consumed (monitored by <sup>1</sup>H NMR), then filtered through a pad of Celite and washed with EtOAc. The organic layers were washed successively with 1 M HCl then brine, dried over anhydrous Na<sub>2</sub>SO<sub>4</sub> and concentrated *in vacuo*. The crude product was purified by column chromatography (10–20% EtOAc/hexanes) to afford (Z)-olefin **162** (854.9 mg, 95%) as a light yellow oil:  $R_f$  = 0.48 (20% EtOAc/hexanes);  $[\alpha]_D^{25} = -3.16$  ( $c$  1.0, CHCl<sub>3</sub>); <sup>1</sup>H NMR (300 MHz, CDCl<sub>3</sub>)  $\delta$  7.74–7.68 (m, 4H), 7.45–7.31 (m, 6H), 7.17 (d,  $J$  = 8.7 Hz, 2H), 6.84 (d,  $J$  = 8.4 Hz, 2H), 5.44 (dd,  $J$  = 11.4, 8.7 Hz, 1H), 5.35–5.23 (m, 2H), 5.17–5.11 (m, 1H), 4.73–4.59 (m, 2H), 4.41 (s, 2H), 3.79 (s, 3H), 3.73–3.68 (m, 1H), 3.47 (dd,  $J$  = 9.6, 6.0 Hz, 1H), 3.29 (dd,  $J$  = 9.6, 5.1 Hz, 1H), 1.90–1.66 (m, 2H), 1.38–1.26 (m, 4H), 1.08–1.05 (m, 12H), 0.87 (s, 9H), 0.03 (s, 3H), 0.02 (s, 3H); <sup>13</sup>C NMR (75 MHz, CDCl<sub>3</sub>)  $\delta$  159.2, 136.2, 136.1, 134.1, 134.0, 133.0, 132.0, 130.6, 130.5, 130.1, 129.9, 129.8, 129.2, 127.7, 127.6, 113.8, 74.2, 73.0, 69.3, 68.6, 64.3, 55.3, 39.4, 27.7, 27.0, 26.0, 25.7, 23.9, 19.4, 18.2, -4.2, -4.5; IR (thin film) 3432, 2931, 1611, 1249, 1111, 823 cm<sup>-1</sup>; HRMS (ESI)  $m/z$  calcd for C<sub>42</sub>H<sub>62</sub>NaO<sub>5</sub>Si<sub>2</sub> (M + Na)<sup>+</sup> 725.4033, found 725.3997.



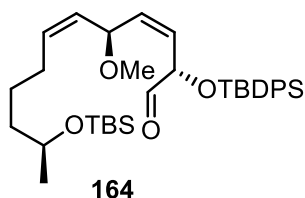
**Methyl ether 163:** To a suspension of NaH (60% dispersion in mineral oil, 147 mg, 3.67 mmol, 3.5 equiv) in anhydrous THF (3.5 mL, 0.3 M) at 0 °C was added a solution alcohol **162** (740 mg, 1.05 mmol) in anhydrous THF (5.3 mL, 0.2 M). After

stirring at 0 °C for 1 h, the mixture was added iodomethane (165  $\mu$ L, 2.62 mmol, 2.5 equiv) and allowed to stir at room temperature for 18 h. The reaction was then recooled to 0 °C, added H<sub>2</sub>O (10 mL) and extracted with EtOAc (3x10 mL). The combined organic layers were washed with brine, dried over anhydrous Na<sub>2</sub>SO<sub>4</sub> and concentrated *in vacuo*. The crude residue was purified by column chromatography (5% EtOAc/hexanes) to give methyl ether **163** (655.1 mg, 87%) as a light yellow oil:  $R_f$  = 0.44 (10% EtOAc/hexanes);  $[\alpha]_D^{25}$  = -8.56 (*c* 1.0, CHCl<sub>3</sub>); <sup>1</sup>H NMR (300 MHz, CDCl<sub>3</sub>)  $\delta$  7.72–7.67 (m, 4H), 7.43–7.30 (m, 6H), 7.13 (d, *J* = 8.4 Hz, 2H), 6.82 (d, *J* = 8.4 Hz, 2H), 5.64–5.57 (m, 1H), 5.38–5.28 (m, 2H), 5.10–5.04 (m, 1H), 4.57–4.51 (m, 1H), 4.35 (s, 2H), 4.10 (t, *J* = 8.7 Hz, 1H), 3.79 (s, 3H), 3.71 (q, *J* = 5.7 Hz, 1H), 3.39 (dd, *J* = 9.6, 6.6 Hz, 1H), 3.25 (dd, *J* = 9.9, 3.3 Hz, 1H), 2.91 (s, 3H), 1.84–1.59 (m, 2H), 1.39–1.12 (m, 4H), 1.08–1.05 (m, 12H), 0.88 (s, 9H), 0.03 (s, 3H), 0.02 (s, 3H); <sup>13</sup>C NMR (75 MHz, CDCl<sub>3</sub>)  $\delta$  159.1, 136.2, 136.1, 134.2, 133.9, 133.0, 131.7, 131.4, 130.7, 129.6, 129.6, 128.3, 127.5, 113.6, 74.5, 72.9, 72.6, 69.9, 68.5, 55.3, 55.2, 39.3, 27.6, 27.1, 26.0, 25.6, 23.9, 19.4, 18.2, -4.2, -4.5; IR (thin film) 2930, 1513, 1249, 1111, 823, 702 cm<sup>-1</sup>; HRMS (ESI) *m/z* calcd for C<sub>43</sub>H<sub>64</sub>NaO<sub>5</sub>Si<sub>2</sub> (M + Na)<sup>+</sup> 739.4190, found 739.4156.

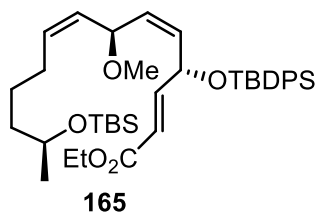


**Alcohol 163a:** Alcohol **163a** was prepared from PMB ether **163** (600 mg, 0.8 mmol) using the general procedure for PMB deprotection. Purification of the crude residue by column chromatography (5–20% EtOAc/hexanes) afforded **163a** (440.9 mg, 89%) as a light yellow oil:  $R_f$  = 0.57 (20% EtOAc/hexanes);  $[\alpha]_D^{25}$  = -1.03 (*c* 1.0, CHCl<sub>3</sub>); <sup>1</sup>H NMR (300 MHz, CDCl<sub>3</sub>)  $\delta$  7.70 (d, *J* = 6.3 Hz, 4H), 7.45–7.38 (m, 6H), 5.55 (dd, *J* = 11.1, 9 Hz, 1H), 5.43–5.34 (m, 2H), 5.08–5.01 (m, 1H), 4.48–4.42 (m, 1H), 4.10–4.05 (m, 1H), 3.74 (dd, *J* = 11.4, 5.7 Hz, 1H), 3.50–3.34 (m, 2H), 2.93 (s, 3H), 1.99 (t, *J* = 6.3 Hz, 1H), 1.82–1.74 (m, 1H), 1.39–1.27 (m, 4H), 1.11–1.08 (m, 12H), 0.89 (s, 9H), 0.05 (s, 3H), 0.04 (s, 3H); <sup>13</sup>C NMR (75 MHz, CDCl<sub>3</sub>)  $\delta$  136.1, 135.8, 133.9, 133.5, 133.3, 132.5, 130.9, 129.9, 129.9, 128.2, 127.9, 127.7, 72.7, 71.3, 68.6, 66.7,

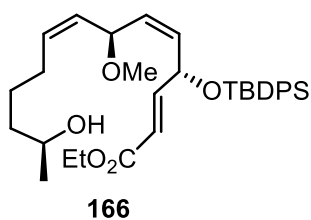
55.2, 39.3, 27.6, 27.1, 26.0, 25.6, 23.8, 19.4, 18.2, -4.2, -4.5; IR (thin film) 3467, 2930, 1601, 1253, 1106, 702  $\text{cm}^{-1}$ ; HRMS (ESI)  $m/z$  calcd for  $\text{C}_{35}\text{H}_{56}\text{NaO}_4\text{Si}_2$  ( $\text{M} + \text{Na}$ )<sup>+</sup> 619.3615, found 619.3586.



**Aldehyde 164:** To a solution of alcohol **163a** (390.5 mg, 0.6 mmol) in anhydrous  $\text{CH}_2\text{Cl}_2$  (30 mL, 0.02 M) at 0 °C were added  $\text{NaHCO}_3$  (109.2 mg, 1.3 mmol, 2.0 equiv) and Dess–Martin periodinane (DMP) (689.2 mg, 1.62 mmol, 2.5 equiv). The reaction mixture was stirred from 0 °C to room temperature for 4 h, then quenched with saturated aqueous  $\text{NaHCO}_3$  (20 mL) and extracted with EtOAc (3x10 mL). The combined organic layers were washed with brine, dried over anhydrous  $\text{Na}_2\text{SO}_4$  and concentrated *in vacuo*. The crude product was purified by column chromatography (10–20% EtOAc/hexanes) to afford aldehyde **164** (334.7 mg, 86%) as a light yellow oil:  $R_f = 0.70$  (20% EtOAc/hexanes);  $[\alpha]_{\text{D}}^{25} = +25.33$  ( $c$  1.0,  $\text{CHCl}_3$ );  $^1\text{H}$  NMR (300 MHz,  $\text{CDCl}_3$ )  $\delta$  9.41 (s, 1H), 7.71–7.68 (m, 4H), 7.48–7.37 (m, 6H), 5.67 (dd,  $J = 11.1, 7.5$  Hz, 1H), 5.52–5.41 (m, 2H), 5.11 (t,  $J = 10.8$  Hz, 1H), 4.84 (d,  $J = 8.7$  Hz, 1H), 4.24 (t,  $J = 8.7$  Hz, 1H), 3.77–3.71 (m, 1H), 2.97 (s, 3H), 1.88–1.70 (m, 2H), 1.43–1.18 (m, 4H), 1.12–1.09 (m, 12H), 0.89 (s, 9H), 0.05 (s, 3H), 0.04 (s, 3H);  $^{13}\text{C}$  NMR (75 MHz,  $\text{CDCl}_3$ )  $\delta$  197.9, 135.9, 135.4, 133.9, 133.0, 130.1, 130.0, 127.9, 127.8, 127.6, 126.1, 76.6, 73.1, 68.5, 55.3, 39.3, 27.7, 26.9, 26.0, 25.5, 23.9, 19.4, 18.2, -4.2, -4.6; IR (thin film) 2931, 1733, 1472, 1254, 1113, 701  $\text{cm}^{-1}$ ; HRMS (ESI)  $m/z$  calcd for  $\text{C}_{35}\text{H}_{54}\text{NaO}_4\text{Si}_2$  ( $\text{M} + \text{Na}$ )<sup>+</sup> 617.3458, found 617.3453.

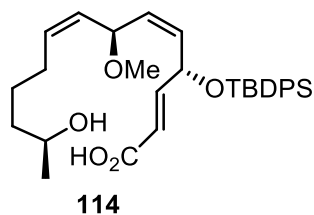


**(E)- $\alpha,\beta$ -Unsaturated ester 165:** Ester **165** was prepared from aldehyde **164** (335.1 mg, 0.56 mmol) using the general procedure for Wittig olefination. The crude product was purified by column chromatography (10–20% EtOAc/hexanes) to afford ester **165** (348.2 mg, 93%) as a light yellow oil:  $R_f = 0.47$  (10% EtOAc/hexanes);  $[\alpha]_D^{25} = +66.2$  ( $c$  1.0,  $\text{CHCl}_3$ );  $^1\text{H NMR}$  (300 MHz,  $\text{CDCl}_3$ )  $\delta$  7.71–7.65 (m, 4H), 7.46–7.35 (m, 6H), 6.71 (dd,  $J = 15.6, 4.2$  Hz, 1H), 6.05 (dd,  $J = 15.6, 1.5$  Hz, 1H), 5.46–5.36 (m, 2H), 5.09–4.96 (m, 2H), 4.22–4.14 (m, 2H), 4.02 (dd,  $J = 9.6, 6.0$  Hz, 1H), 3.75–3.69 (m, 1H), 2.91 (s, 3H), 1.81–1.62 (m, 2H), 1.31–1.26 (m, 4H), 1.10–1.08 (m, 12H), 0.89 (s, 9H), 0.04 (s, 3H), 0.03 (s, 3H);  $^{13}\text{C NMR}$  (75 MHz,  $\text{CDCl}_3$ )  $\delta$  166.6, 148.0, 136.0, 135.9, 133.3, 133.3, 133.2, 131.6, 130.7, 130.0, 129.9, 127.9, 127.8, 127.7, 120.0, 72.8, 69.6, 68.5, 60.4, 55.2, 39.3, 27.6, 27.0, 26.0, 25.5, 23.8, 19.4, 18.2, 14.3, –4.2, –4.6; IR (thin film) 2932, 1723, 1273, 1110, 836, 702  $\text{cm}^{-1}$ ; HRMS (ESI)  $m/z$  calcd for  $\text{C}_{39}\text{H}_{60}\text{NaO}_5\text{Si}_2$  ( $\text{M} + \text{Na}$ ) $^+$  687.3877, found 687.3850.

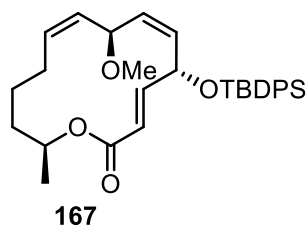


**Alcohol 166:** Alcohol **166** was prepared from TBS ether **165** (350.2 mg, 0.53 mmol) using the general procedure for TBS deprotection. The crude product was purified by column chromatography (20–30% EtOAc/hexanes) to give alcohol **166** (248.1 mg, 85%) as a colorless oil:  $R_f = 0.15$  (20% EtOAc/hexanes);  $[\alpha]_D^{25} = +67.1$  ( $c$  1.0,  $\text{CHCl}_3$ );  $^1\text{H NMR}$  (300 MHz,  $\text{CDCl}_3$ )  $\delta$  7.70–7.65 (m, 4H), 7.44–7.34 (m, 6H), 6.69 (d,  $J = 15.6, 4.2$  Hz, 1H), 6.05 (dd,  $J = 15.6, 1.5$  Hz, 1H), 5.47–5.32 (m, 3H), 5.11–5.05 (m, 1H), 4.99 (ddd,  $J = 7.8, 4.2, 1.5$  Hz, 1H), 4.21–4.14 (m, 2H), 4.05 (dd,  $J = 9.3, 7.5$  Hz, 1H), 3.68 (q,  $J = 6.0$  Hz, 1H), 2.89 (s, 3H), 1.86–1.68 (m, 2H), 1.42–1.26 (m, 7H), 1.14 (d,  $J = 6.3$  Hz, 3H), 1.08 (s, 9H);  $^{13}\text{C NMR}$  (75 MHz,  $\text{CDCl}_3$ )  $\delta$  166.8,

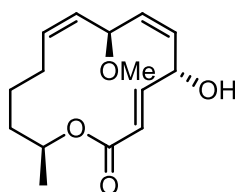
148.1, 136.0, 135.9, 133.2, 133.1, 131.4, 130.9, 130.0, 129.9, 128.0, 127.8, 127.7, 119.9, 72.6, 69.5, 67.8, 60.5, 55.2, 38.8, 27.5, 26.9, 25.5, 23.5, 19.4, 14.3; IR (thin film) 3494, 2932, 1721, 1274, 1111, 702  $\text{cm}^{-1}$ ; HRMS (ESI)  $m/z$  calcd for  $\text{C}_{33}\text{H}_{46}\text{NaO}_5\text{Si}$  ( $\text{M} + \text{Na}$ )<sup>+</sup> 573.3012, found 573.2998.



**Seco acid 114:** To a solution of ester **166** (247.1 mg, 0.45 mmol) in THF:MeOH:H<sub>2</sub>O (1:1:2, 1.5 mL, 1.5 mL, 3 mL, 0.08 M) at 0 °C was added LiOH (75.6 mg, 3.15 mmol, 7.0 equiv) and stirred from 0 °C to room temperature for 5 h. The reaction mixture was added 1M HCl until the pH reached 7. The resulting solution was extracted with EtOAc (4x10 mL). The combined organic layers were washed with brine, dried over anhydrous Na<sub>2</sub>SO<sub>4</sub> and concentrated *in vacuo*. The crude product was purified by column chromatography (50–80% EtOAc/hexanes) to give seco acid **114** (188.1 mg, 80%) as a light yellow oil:  $R_f = 0.24$  (50% EtOAc/hexanes);  $[\alpha]_D^{25} = +66.3$  ( $c$  1.0, CHCl<sub>3</sub>); <sup>1</sup>H NMR (300 MHz, CDCl<sub>3</sub>)  $\delta$  7.70–7.65 (m, 4H), 7.46–7.36 (m, 6H), 6.76 (dd,  $J = 15.3, 4.2$  Hz, 1H), 6.06 (dd,  $J = 15.6, 1.5$  Hz, 1H), 5.49–5.34 (m, 3H), 5.09 (t,  $J = 10.8$  Hz, 1H), 5.02–4.98 (m, 1H), 4.07 (t,  $J = 8.4$  Hz, 1H), 3.71 (q,  $J = 6.0$  Hz, 1H), 2.89 (s, 3H), 1.87–1.68 (m, 2H), 1.41–1.23 (m, 4H), 1.14 (d,  $J = 6.0$  Hz, 3H), 1.08 (s, 9H); <sup>13</sup>C NMR (75 MHz, CDCl<sub>3</sub>)  $\delta$  170.7, 150.0, 136.0, 135.8, 133.2, 133.1, 131.5, 130.8, 130.0, 129.9, 127.9, 127.9, 127.7, 119.6, 72.6, 69.5, 68.1, 55.2, 38.6, 27.5, 26.9, 25.5, 23.2, 19.4; IR (thin film) 3424, 2932, 1699, 1271, 1111, 702  $\text{cm}^{-1}$ ; HRMS (ESI)  $m/z$  calcd for  $\text{C}_{31}\text{H}_{42}\text{NaO}_5\text{Si}$  ( $\text{M} + \text{Na}$ )<sup>+</sup> 545.2699, found 545.2694.



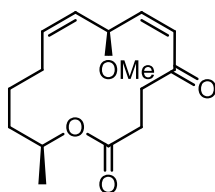
**Macrolactone 167:** Macrolactone **167** was prepared from seco acid **114** (112.4 mg, 0.2 mmol) using the general procedure for Shiina macrolactonization. Purification of the crude residue by column chromatography (10–20% EtOAc/hexanes) gave compound **167** (76.0 mg, 72%) as a light yellow oil:  $R_f = 0.50$  (20% EtOAc/hexanes);  $[\alpha]_D^{25} = +5.03$  ( $c$  1.0,  $\text{CHCl}_3$ );  $^1\text{H NMR}$  (300 MHz,  $\text{CDCl}_3$ )  $\delta$  7.68–7.62 (m, 4H), 7.45–7.34 (m, 6H), 6.94 (dd,  $J = 15.6, 6.0$  Hz, 1H), 5.94 (dd,  $J = 15.6, 1.2$  Hz, 1H), 5.73 (dd,  $J = 11.4, 4.5$  Hz, 1H), 5.37 (td,  $J = 10.8, 3.6$  Hz, 1H), 5.15–5.02 (m, 3H), 4.94–4.84 (m, 1H), 4.31 (t,  $J = 9.6$  Hz, 1H), 2.79 (s, 3H), 2.45–2.31 (m, 1H), 1.98–1.62 (m, 4H), 1.46–1.35 (m, 1H), 1.28 (d,  $J = 6.0$  Hz, 3H), 1.09 (s, 9H);  $^{13}\text{C NMR}$  (75 MHz,  $\text{CDCl}_3$ )  $\delta$  166.6, 147.9, 136.1, 136.0, 136.0, 133.4, 133.2, 133.1, 130.0, 128.5, 127.9, 127.8, 120.3, 73.0, 72.3, 70.7, 55.0, 34.7, 30.1, 27.0, 25.8, 20.6, 19.4; IR (thin film) 2931, 1721, 1254, 1112, 1073, 701  $\text{cm}^{-1}$ ; HRMS (ESI)  $m/z$  calcd for  $\text{C}_{31}\text{H}_{40}\text{NaO}_4\text{Si}$  ( $M + \text{Na}$ ) $^+$  527.2594, found 527.2576.



7-O-methylnigrosporolide (**19**)

**7-O-Methylnigrosporolide (19):** To a solution of macrolactone **167** (60 mg, 0.12 mmol) in anhydrous THF (3 mL, 0.04 M) were added AcOH (340  $\mu\text{L}$ , 0.006 mmol, 0.05 equiv) followed by TBAF (1 M solution in THF, 250  $\mu\text{L}$ , 0.96 mmol, 8.0 equiv) dropwise at 0  $^\circ\text{C}$ . The reaction mixture was stirred from 0  $^\circ\text{C}$  to room temperature for 1 h and then heated at 63  $^\circ\text{C}$  for 9 h. The reaction mixture was then cooled to room temperature and quenched with saturated aqueous  $\text{NaHCO}_3$  (5 mL) and  $\text{H}_2\text{O}$  (3 mL). The organic phase was extracted with EtOAc (4x5 mL), washed with brine and dried over with anhydrous  $\text{Na}_2\text{SO}_4$ . Purification of the crude residue by column

chromatography (10–30% EtOAc/hexanes) yielded 7-*O*-methylnigrosporolide (**19**) (17.3 mg, 50%, 72% brsm) as a colorless oil:  $R_f = 0.12$  (40% EtOAc/hexanes);  $[\alpha]_D^{25} = +66.8$  ( $c$  0.2, MeOH);  $^1\text{H NMR}$  (300 MHz,  $\text{CD}_3\text{OD}$ )  $\delta$  6.93 (dd,  $J = 15.3, 6.9$  Hz, 1H), 6.08 (d,  $J = 15.6$  Hz, 1H), 5.65 (dd,  $J = 11.4, 4.5$  Hz, 1H), 5.49 (td,  $J = 11.1, 3.3$  Hz, 1H), 5.27 (td,  $J = 11.7, 2.4$  Hz, 1H), 5.17–5.10 (m, 2H), 5.01–4.91 (m, 1H), 4.70 (t,  $J = 9.6$  Hz, 1H), 3.27 (s, 3H), 2.62–2.48 (m, 1H), 2.04–1.85 (m, 2H), 1.81–1.67 (m, 1H), 1.51–1.40 (m, 1H), 1.28 (d,  $J = 6.3$  Hz, 3H), 1.11–1.06 (m, 1H);  $^{13}\text{C NMR}$  (75 MHz,  $\text{CD}_3\text{OD}$ )  $\delta$  168.3, 149.9, 136.3, 135.1, 130.4, 128.6, 121.5, 74.3, 73.4, 69.6, 55.4, 35.6, 30.7, 26.8, 20.7; IR (thin film) 3422, 2929, 1717, 1255, 1062, 948  $\text{cm}^{-1}$ ; HRMS (ESI)  $m/z$  calcd for  $\text{C}_{15}\text{H}_{22}\text{NaO}_4$  ( $\text{M} + \text{Na}$ ) $^+$  289.1416, found 289.1410.

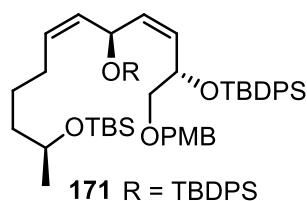


pestalotioprolide D (**20**)

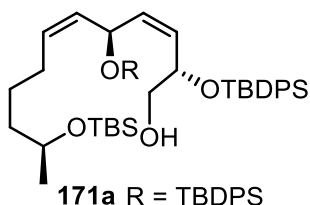
**Pestalotioprolide D (20):** To a solution of macrolactone **167** (15 mg, 0.03 mmol) in anhydrous THF (1.2 mL, 0.025 M) was added TBAF (1 M solution in THF, 150  $\mu\text{L}$ , 0.15 mmol, 5.0 equiv) dropwise at 0  $^\circ\text{C}$ . The reaction mixture was stirred from 0  $^\circ\text{C}$  to room temperature for 1.5 h. The reaction was quenched with saturated aqueous  $\text{NaHCO}_3$  (3 mL) and  $\text{H}_2\text{O}$  (2 mL). The aqueous phase was extracted with EtOAc (4x5 mL), washed with brine and dried over with anhydrous  $\text{Na}_2\text{SO}_4$ . Purification of the crude residue by column chromatography yielded pestalotioprolide D (**20**) (5.8 mg, 75%) as a colorless oil:  $R_f = 0.21$  (20% EtOAc/hexanes);  $[\alpha]_D^{26} = -35.6$  ( $c$  0.1, MeOH);  $^1\text{H NMR}$  (300 MHz,  $\text{CD}_3\text{OD}$ )  $\delta$  6.31 (d,  $J = 11.1$  Hz, 1H), 5.89 (dd,  $J = 11.1, 9.6$  Hz, 1H), 5.79 (app t,  $J = 9.6$  Hz, 1H), 5.71–5.63 (m, 1H), 5.22 (app t,  $J = 9.6$ , 1H), 4.94–4.90 (m, 1H), 3.29 (s, 3H), 2.96 (ddd,  $J = 17.4, 10.8, 2.7$ , 1H), 2.79 (ddd,  $J = 15.0, 10.5, 2.7$ , 1H), 2.73 (ddd,  $J = 17.4, 6.6, 2.4$  Hz, 1H), 2.40 (ddd,  $J = 15.3, 6.9, 3.0$  Hz, 1H), 2.19–2.05 (m, 1H), 1.91–1.79 (m, 1H), 1.70–1.61 (m, 1H), 1.59–1.47 (m, 1H), 1.38–1.26 (m, 1H), 1.24 (d,  $J = 6.3$  Hz, 3H), 0.98–0.83 (m, 1H);  $^{13}\text{C NMR}$  (75 MHz,  $\text{CD}_3\text{OD}$ )  $\delta$  201.5, 174.6, 145.5, 134.9, 129.8, 127.4, 73.2, 73.0, 56.0, 40.9, 37.3,



30.0, 29.9, 28.2, 20.3; IR (thin film) 2931, 1724, 1406, 1237, 1085, 953  $\text{cm}^{-1}$ ; HRMS (ESI)  $m/z$  calcd for  $\text{C}_{15}\text{H}_{22}\text{NaO}_4$  ( $\text{M} + \text{Na}$ )<sup>+</sup> 289.1416, found 289.1410.

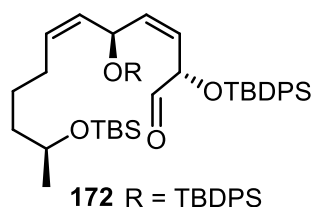


**Silyl ether 171:** Silyl ether **171** was prepared from alcohol **162** (751.4 mg, 1.06 mmol) using the general procedure for TBDPS protection. The crude residue was purified by column chromatography (5–10% EtOAc/hexanes) to give silyl ether **171** (965.3 mg, 96%) as a colorless oil:  $R_f = 0.40$  (10% EtOAc/hexanes);  $[\alpha]_D^{25} = -4.70$  ( $c$  1.04,  $\text{CHCl}_3$ );  $^1\text{H}$  NMR (300 MHz,  $\text{CDCl}_3$ )  $\delta$  7.63–7.54 (m, 8H), 7.39–7.33 (m, 4H), 7.30–7.19 (m, 8H), 7.03 (d,  $J = 8.1$  Hz, 2H), 6.80 (d,  $J = 8.1$  Hz, 2H), 5.68 (dd,  $J = 11.4, 6.6$  Hz, 1H), 5.59–5.53 (m, 1H), 5.22–5.15 (m, 1H), 4.92–4.81 (m, 2H), 4.46–4.42 (m, 1H), 4.21 (s, 2H), 3.8 (s, 3H), 3.59 (q,  $J = 5.7$  Hz, 1H), 3.25 (dd,  $J = 9.6, 6.9$  Hz, 1H), 3.15–3.12 (m, 1H), 1.23–1.06 (m, 6H), 1.03 (s, 9H), 0.99–0.96 (m, 12H), 0.90 (s, 9H), 0.05 (s, 3H), 0.04 (s, 3H);  $^{13}\text{C}$  NMR (75 MHz,  $\text{CDCl}_3$ )  $\delta$  158.9, 136.1, 136.0, 135.8, 134.3, 134.2, 133.8, 130.7, 130.6, 129.8, 129.5, 129.4, 129.2, 127.6, 127.5, 127.4, 113.5, 74.4, 72.7, 70.3, 68.7, 66.8, 55.3, 39.5, 27.1, 27.0, 26.0, 25.6, 24.0, 19.4, 19.3, 18.2, -4.2, -4.5; IR (thin film) 2930, 1513, 1111, 822, 702  $\text{cm}^{-1}$ ; HRMS (ESI)  $m/z$  calcd for  $\text{C}_{58}\text{H}_{80}\text{NaO}_5\text{Si}_3$  ( $\text{M} + \text{Na}$ )<sup>+</sup> 963.5211, found 963.5206.

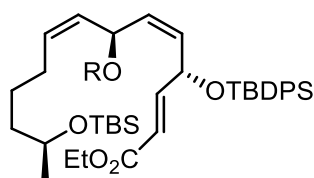


**Alcohol 171a:** Alcohol **171a** was prepared from PMB ether **171** (835.2 mg, 0.89 mmol) using the general procedure for PMB deprotection. Purification of the crude residue by column chromatography (5–10% EtOAc/hexanes) afforded **171a** (546.5 mg, 75%) as a light yellow oil:  $R_f = 0.67$  (20% EtOAc/hexanes);  $[\alpha]_D^{25} = +2.83$  ( $c$  1.08,  $\text{CHCl}_3$ );  $^1\text{H}$  NMR (300 MHz,  $\text{CDCl}_3$ )  $\delta$  7.61–7.50 (m, 8H), 7.38–7.34 (m, 4H),

7.27–7.18 (m, 8H), 5.69 (dd,  $J = 11.4, 6.6$  Hz, 1H), 5.49 (dd,  $J = 11.4, 8.7$  Hz, 1H), 5.20–5.13 (m, 1H), 4.95–4.88 (m, 1H), 4.81–4.76 (m, 1H), 4.36–4.30 (m, 1H), 3.62–3.56 (m, 1H), 3.33–3.23 (m, 2H), 1.14–1.00 (m, 15H), 0.95–0.93 (m, 12H), 0.87 (s, 9H), 0.02 (s, 3H), 0.01 (s, 3H);  $^{13}\text{C}$  NMR (75 MHz,  $\text{CDCl}_3$ )  $\delta$  136.1, 136.0, 135.8, 134.8, 134.3, 134.1, 133.9, 133.7, 130.7, 129.92, 129.88, 129.7, 129.6, 129.4, 127.9, 127.8, 127.6, 127.5, 71.5, 68.7, 67.0, 66.8, 39.5, 27.3, 27.2, 27.0, 26.1, 25.5, 23.9, 19.4, 19.3, 18.3,  $-4.2, -4.5$ ; IR (thin film) 3698, 2930, 1427, 1111, 701  $\text{cm}^{-1}$ ; HRMS (ESI)  $m/z$  calcd for  $\text{C}_{50}\text{H}_{72}\text{NaO}_4\text{Si}_3$  ( $\text{M} + \text{Na}$ ) $^+$  843.4636, found 843.4628.

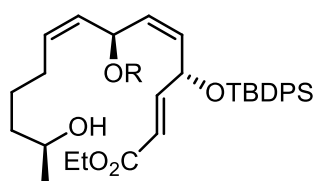


**Aldehyde 172:** Aldehyde **172** was prepared from alcohol **171a** (472.0 mg, 0.57 mmol) using the general procedure for TEMPO/ $\text{PhI}(\text{OAc})_2$ -mediated oxidation. The crude residue was purified by column chromatography (100% hexanes–10% EtOAc/hexanes) to afford aldehyde **172** (361.5 mg, 77%) as a light yellow oil:  $R_f = 0.73$  (20% EtOAc/hexanes);  $[\alpha]_{\text{D}}^{25} = +95.5$  ( $c$  1.01,  $\text{CHCl}_3$ );  $^1\text{H}$  NMR (300 MHz,  $\text{CDCl}_3$ )  $\delta$  9.15 (s, 1H), 7.61–7.57 (m, 4H), 7.52–7.50 (m, 4H), 7.41–7.34 (m, 4H), 7.29–7.18 (m, 8H), 5.94 (dd,  $J = 11.4, 6.9$  Hz, 1H), 5.40–5.30 (m, 1H), 5.26–5.19 (m, 1H), 4.99–4.94 (m, 1H), 4.91–4.85 (m, 1H), 4.79–4.77 (m, 1H), 3.62–3.56 (m, 1H), 1.07 (s, 9H), 1.04–0.98 (m, 9H), 0.93 (s, 9H), 0.88 (s, 9H), 0.03 (s, 3H), 0.01 (s, 3H);  $^{13}\text{C}$  NMR (75 MHz,  $\text{CDCl}_3$ )  $\delta$  197.0, 137.8, 136.1, 136.0, 135.8, 134.0, 133.8, 133.5, 133.1, 130.3, 130.1, 130.0, 129.7, 129.6, 127.9, 127.7, 127.5, 124.2, 68.7, 67.5, 39.5, 27.4, 27.0, 26.9, 26.1, 25.5, 23.9, 19.5, 19.3, 18.3,  $-4.2, -4.5$ ; IR (thin film) 2931, 1743, 1427, 1112, 701  $\text{cm}^{-1}$ ; HRMS (ESI)  $m/z$  calcd for  $\text{C}_{50}\text{H}_{70}\text{NaO}_4\text{Si}_3$  ( $\text{M} + \text{Na}$ ) $^+$  841.4480, found 841.4467.



**173** R = TBDPS

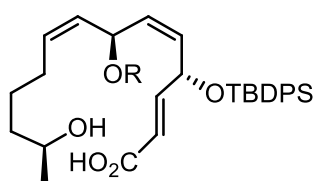
**(E)- $\alpha,\beta$ -Unsaturated ester 173:** Ester **173** was prepared from aldehyde **172** (374.2 mg, 0.46 mmol) using the general procedure for Wittig olefination. The crude product was purified by column chromatography (10–20% EtOAc/hexanes) to afford ester **173** (347.6 mg, 85%) as a light yellow oil:  $R_f = 0.71$  (20% EtOAc/hexanes);  $[\alpha]_D^{25} = +64.8$  ( $c$  1.06,  $\text{CHCl}_3$ );  $^1\text{H NMR}$  (300 MHz,  $\text{CDCl}_3$ )  $\delta$  7.63 (d,  $J = 6.9$  Hz, 2H), 7.57 (d,  $J = 6.9$  Hz, 2H), 7.52 (d,  $J = 7.5$  Hz, 4H), 7.38–7.34 (m, 4H), 7.28–7.20 (m, 8H), 6.64 (dd,  $J = 15.3, 3.9$  Hz, 1H), 5.94 (dd,  $J = 15.3, 1.5$  Hz, 1H), 5.64 (dd,  $J = 11.4, 6.3$  Hz, 1H), 5.40–5.33 (m, 1H), 5.17–5.10 (m, 1H), 4.98–4.89 (m, 2H), 4.81–4.76 (m, 1H), 4.17–4.06 (m, 2H), 3.61–3.56 (m, 1H), 1.22 (t,  $J = 7.0$  Hz, 3H), 1.06–0.99 (m, 15H), 0.94 (s, 9H), 0.89 (m, 9H), 0.04 (s, 3H), 0.02 (s, 3H);  $^{13}\text{C NMR}$  (75 MHz,  $\text{CDCl}_3$ )  $\delta$  166.7, 148.1, 136.1, 135.93, 135.87, 135.85, 134.1, 134.0, 133.7, 133.6, 133.4, 130.4, 129.9, 129.59, 129.57, 129.50, 127.8, 127.7, 127.6, 127.5, 119.8, 69.7, 68.7, 67.3, 60.3, 39.5, 27.3, 27.1, 27.0, 26.1, 25.5, 23.9, 19.5, 19.3, 18.3, 14.3, –4.2, –4.5; IR (thin film) 2931, 1722, 1427, 1112, 822  $\text{cm}^{-1}$ ; HRMS (ESI)  $m/z$  calcd for  $\text{C}_{54}\text{H}_{76}\text{NaO}_5\text{Si}_3$  ( $\text{M} + \text{Na}$ ) $^+$  911.4898, found 911.4892.



**173a** R = TBDPS

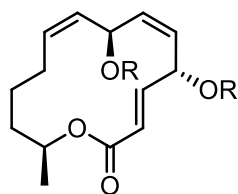
**Alcohol 173a:** Alcohol **173a** was prepared from TBS ether **173** (354.9 mg, 0.40 mmol) using the general procedure for TBS deprotection. The crude product was purified by column chromatography (20–30% EtOAc/hexanes) to give alcohol **173a** (267.1 mg, 88%) as a colorless oil:  $R_f = 0.51$  (40% EtOAc/hexanes);  $[\alpha]_D^{25} = +63.4$  ( $c$  1.01,  $\text{CHCl}_3$ );  $^1\text{H NMR}$  (300 MHz,  $\text{CDCl}_3$ )  $\delta$  7.63–7.49 (m, 8H), 7.38–7.33 (m, 4H), 7.27–7.17 (m, 8H), 6.58 (dd,  $J = 15.6, 3.9$  Hz, 1H), 5.91 (dd,  $J = 15.6, 1.5$  Hz, 1H), 5.65 (dd,  $J = 11.1, 6.6$  Hz, 1H), 5.38 (dd,  $J = 11.1, 8.1$  Hz, 1H), 5.19–5.13 (m, 1H),

4.97–4.89 (m, 2H), 4.79–4.74 (m, 1H), 4.15–4.06 (m, 2H), 3.54–3.49 (m, 1H), 1.21 (t,  $J = 6.9$  Hz, 3H), 1.16–0.95 (m, 18H), 0.92 (s, 9H);  $^{13}\text{C}$  NMR (75 MHz,  $\text{CDCl}_3$ )  $\delta$  166.8, 148.1, 136.1, 135.92, 135.88, 134.1, 133.7, 133.6, 133.4, 130.6, 129.9, 129.7, 129.6, 129.5, 129.4, 127.8, 127.7, 127.6, 127.5, 119.8, 69.7, 67.9, 67.0, 60.4, 38.9, 27.1, 27.0, 25.2, 23.4, 19.4, 19.3, 14.3; IR (thin film) 3427, 2931, 1719, 1111, 701  $\text{cm}^{-1}$ ; HRMS (ESI)  $m/z$  calcd for  $\text{C}_{48}\text{H}_{62}\text{NaO}_5\text{Si}_2$  ( $\text{M} + \text{Na}$ ) $^+$  797.4033, found 797.4028.



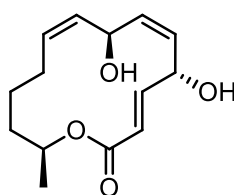
**115** R = TBDPS

**Seco acid 115:** Seco acid **115** was prepared from ester **173a** (180.2 mg, 0.23 mmol) using the general procedure for hydrolysis. The crude product was purified by column chromatography (50–80% EtOAc/hexanes) to afford compound **115** (147.5 mg, 86%) as a colorless oil:  $R_f = 0.20$  (50% EtOAc/hexanes);  $[\alpha]_{\text{D}}^{25} = +50.7$  ( $c$  1.09,  $\text{CHCl}_3$ );  $^1\text{H}$  NMR (300 MHz,  $\text{CDCl}_3$ )  $\delta$  7.61–7.47 (m, 8H), 7.37–7.33 (m, 4H), 7.27–7.16 (m, 8H), 6.61 (dd,  $J = 15.6, 4.2$  Hz, 1H), 5.85 (dd,  $J = 15.6, 1.2$  Hz, 1H), 5.66 (dd,  $J = 11.1, 7.2$  Hz, 1H), 5.39 (dd,  $J = 11.1, 8.1$  Hz, 1H), 5.20–5.14 (m, 1H), 4.97–4.89 (m, 1H), 4.86–4.82 (m, 1H), 4.77–4.71 (m, 1H), 3.55–3.49 (m, 1H), 1.26 (t,  $J = 7.2$  Hz, 3H), 1.05–0.97 (m, 15H), 0.91 (s, 9H);  $^{13}\text{C}$  NMR (75 MHz,  $\text{CDCl}_3$ )  $\delta$  170.9, 150.2, 136.1, 135.9, 135.9, 135.0, 134.1, 134.0, 133.5, 133.3, 130.6, 130.0, 129.9, 129.8, 129.62, 129.57, 129.2, 127.83, 127.77, 127.6, 127.5, 119.3, 69.7, 68.1, 66.9, 38.8, 27.1, 27.0, 25.2, 23.3, 19.4, 19.3, 14.3; IR (thin film) 3424, 2931, 1697, 1112, 701  $\text{cm}^{-1}$ ; HRMS (ESI)  $m/z$  calcd for  $\text{C}_{46}\text{H}_{58}\text{NaO}_5\text{Si}_2$  ( $\text{M} + \text{Na}$ ) $^+$  769.3720, found 769.3713.



**174** R = TBDPS

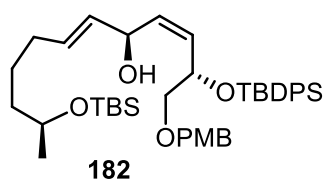
**Macrolactone 174:** Macrolactone **174** was prepared from seco acid **115** (90.6 mg, 0.12 mmol) using the general procedure for Shiina macrolactonization. Purification of the crude residue by column chromatography (5–20% EtOAc/hexanes) yielded compound **174** (61.2 mg, 68%) as a colorless oil:  $R_f = 0.45$  (20% EtOAc/hexanes);  $[\alpha]_D^{25} = +2.60$  ( $c$  1.06,  $\text{CHCl}_3$ );  $^1\text{H NMR}$  (300 MHz,  $\text{CDCl}_3$ )  $\delta$  7.62–7.50 (m, 4H), 7.47–7.39 (m, 6H), 7.34–7.24 (m, 6H), 7.19–7.14 (m, 2H), 7.09–7.04 (m, 2H), 6.46 (dd,  $J = 15.6, 6.9$  Hz, 1H), 5.55 (dd,  $J = 11.7, 3.3$  Hz, 1H), 5.41 (dd,  $J = 11.7, 2.1$  Hz, 1H), 5.28–5.20 (m, 2H), 5.06–4.99 (m, 1H), 4.88–4.82 (m, 1H), 4.65–4.59 (m, 2H), 1.70–1.53 (m, 4H), 1.46–1.28 (m, 2H), 1.18 (d,  $J = 6.2$  Hz, 3H), 1.03 (s, 9H), 0.91 (s, 9H);  $^{13}\text{C NMR}$  (75 MHz,  $\text{CDCl}_3$ )  $\delta$  166.6, 147.9, 136.1, 135.9, 135.8, 134.1, 134.0, 133.6, 133.4, 132.7, 131.6, 131.0, 130.1, 129.93, 129.90, 129.7, 129.6, 127.8, 127.75, 127.71, 127.6, 120.4, 72.2, 70.5, 65.4, 34.6, 29.4, 27.0, 26.9, 25.4, 20.7, 19.3, 19.3; IR (thin film) 2931, 1722, 1427, 1112, 701  $\text{cm}^{-1}$ ; HRMS (ESI)  $m/z$  calcd for  $\text{C}_{46}\text{H}_{57}\text{O}_4\text{Si}_2$  ( $\text{M} + \text{H}$ ) $^+$  729.3795, found 729.3786.



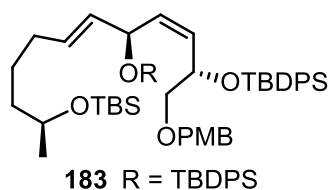
nigrosporolide (**21**)

**Nigrosporolide (21):** Compound **21** was prepared from macrolactone **174** (59.4 mg, 0.08 mmol) using the general procedure for global desilylation. Purification of the crude residue by column chromatography (20–50% EtOAc/hexanes) yielded nigrosporolide (**21**) (13.5 mg, 65%) as a white solid:  $R_f = 0.17$  (50% EtOAc/hexanes); mp 141.5–142.8  $^\circ\text{C}$ .  $[\alpha]_D^{26} = +89.0$  ( $c$  0.90, MeOH);  $^1\text{H NMR}$  (500 MHz,  $\text{CDCl}_3$ )  $\delta$  6.93 (dd,  $J = 15.5, 7.0$  Hz, 1H), 6.07 (d,  $J = 16.0$  Hz, 1H), 5.57 (dd,  $J = 11.0, 4.0$  Hz, 1H), 5.44–5.36 (m, 2H), 5.31–5.27 (m, 1H), 5.23–5.20 (m, 1H), 5.10 (t,  $J = 9.5$  Hz,

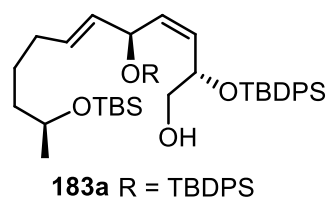
1H), 4.99–4.93 (m, 1H), 2.53–2.44 (m, 1H), 1.98–1.84 (m, 2H), 1.74–1.66 (m, 1H), 1.48–1.41 (m, 1H), 1.29 (d,  $J = 6.5$  Hz, 3H), 1.17–1.11 (m, 1H);  $^{13}\text{C}$  NMR (75 MHz,  $\text{CDCl}_3$ )  $\delta$  167.0, 148.0, 133.4, 132.8, 131.5, 129.6, 120.9, 73.2, 68.8, 63.6, 34.7, 29.7, 25.8, 20.5; IR (thin film) 3429, 2929, 1721, 1038, 702  $\text{cm}^{-1}$ ; HRMS (ESI)  $m/z$  calcd for  $\text{C}_{14}\text{H}_{20}\text{NaO}_4$  ( $\text{M} + \text{Na}$ ) $^+$  275.1259, found 275.1253.



**(E)-Olefin 182:** To a solution of alkyne **116R** (720.3 mg, 1.07 mmol) in anhydrous THF (22 mL, 0.05 M) were added sodium bis(2-methoxyethoxy)aluminium hydride (Red-Al) (3.6 M solution in toluene, 1.1 mL, 3.74 mmol, 3.5 equiv). After being stirred from 0 °C to room temperature for 5 h, the reaction mixture was quenched with saturated aqueous potassium sodium tartrate solution (30 mL). The aqueous phase was extracted with EtOAc (3×20 mL). The combined organic layers were washed with brine, dried over anhydrous  $\text{Na}_2\text{SO}_4$  and concentrated under reduced pressure. Purification of the crude residue by column chromatography (10–30% EtOAc/hexanes) afforded (*E*)-olefin **182** (561.5 mg, 75%) as a colorless oil:  $R_f = 0.53$  (30% EtOAc/hexanes);  $[\alpha]_D^{26} = -25.9$  ( $c$  1.03,  $\text{CHCl}_3$ );  $^1\text{H}$  NMR (300 MHz,  $\text{CDCl}_3$ )  $\delta$  7.76–7.71 (m, 4H), 7.48–7.35 (m, 6H), 7.22 (d,  $J = 8.7$  Hz, 2H), 6.87 (d,  $J = 8.7$  Hz, 2H), 5.47 (dd,  $J = 10.8, 9.0$  Hz, 1H), 5.42 (dd,  $J = 15.3, 6.0$  Hz, 1H), 5.26 (dd,  $J = 10.8, 9.0$  Hz, 1H), 5.22 (dd,  $J = 15.3, 6.0$  Hz, 1H), 4.72–4.69 (m, 1H), 4.44 (s, 2H), 4.34–4.29 (m, 1H), 3.82 (s, 3H), 3.76–3.72 (m, 1H), 3.53 (dd,  $J = 9.6, 6.0$  Hz, 1H), 3.35 (dd,  $J = 9.6, 5.4$  Hz, 1H), 1.89–1.85 (m, 2H), 1.43–1.25 (m, 4H), 1.11–1.09 (m, 12H), 0.90 (s, 9H), 0.06 (s, 3H), 0.05 (s, 3H);  $^{13}\text{C}$  NMR (75 MHz,  $\text{CDCl}_3$ )  $\delta$  159.2, 136.3, 136.1, 134.9, 134.2, 134.0, 132.9, 131.6, 130.8, 130.5, 130.4, 129.8, 129.2, 127.6, 127.5, 113.8, 74.1, 73.0, 69.1, 68.6, 68.5, 55.3, 39.3, 32.3, 27.0, 26.0, 25.2, 23.8, 19.3, 18.2, –4.2, –4.5; IR (thin film) 3447, 2930, 1716, 1249, 773  $\text{cm}^{-1}$ ; HRMS (ESI)  $m/z$  calcd for  $\text{C}_{42}\text{H}_{62}\text{NaO}_5\text{Si}_2$  ( $\text{M} + \text{Na}$ ) $^+$  725.4033, found 725.4015.

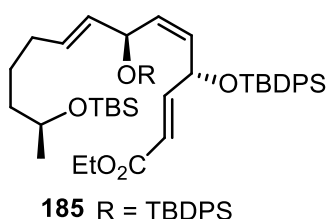


**Silyl ether 183:** Silyl ether **183** was prepared from alcohol **182** (530.0 mg, 0.75 mmol) using the general procedure for TBDPS protection. The crude residue was purified by column chromatography (5–10% EtOAc/hexanes) to give silyl ether **183** (700.5 mg, 94%) as a colorless oil:  $R_f = 0.42$  (10% EtOAc/hexanes);  $[\alpha]_D^{26} = -13.0$  ( $c$  1.08,  $\text{CHCl}_3$ );  $^1\text{H NMR}$  (300 MHz,  $\text{CDCl}_3$ )  $\delta$  7.59–7.56 (m, 8H), 7.39–7.34 (m, 4H), 7.31–7.20 (m, 8H), 7.00 (d,  $J = 8.7$  Hz, 2H), 6.79 (d,  $J = 8.7$  Hz, 2H), 5.65 (dd,  $J = 11.7, 6.9$  Hz, 1H), 5.57 (dd,  $J = 11.7, 7.5$  Hz, 1H), 5.17 (dd,  $J = 15.3, 6.9$  Hz, 1H), 4.84 (dd,  $J = 15.3, 6.9$  Hz, 1H), 4.55 (t,  $J = 6.9$  Hz, 1H), 4.49–4.44 (m, 1H) 4.13 (s, 2H), 3.80 (s, 3H), 3.73–3.67 (m, 1H), 3.25 (dd,  $J = 10.2, 6.9$  Hz, 1H), 3.12 (dd,  $J = 10.2, 3.3$  Hz, 1H), 1.67–1.62 (m, 2H), 1.32–1.15 (m, 4H), 1.09 (d,  $J = 6.0$  Hz, 3H), 1.02 (s, 9H), 1.00 (s, 9H), 1.92 (s, 9H), 0.07 (s, 3H), 0.05 (s, 3H);  $^{13}\text{C NMR}$  (75 MHz,  $\text{CDCl}_3$ )  $\delta$  159.0, 136.0, 135.8, 134.4, 134.2, 133.7, 131.7, 131.3, 130.7, 129.8, 129.5, 129.4, 129.0, 127.6, 127.5, 127.4, 113.6, 74.4, 72.4, 71.7, 69.8, 68.5, 55.3, 39.3, 32.1, 27.2, 27.1, 26.0, 25.0, 23.9, 19.4, 19.3, 18.2, -4.2, -4.5; IR (thin film) 2930, 1508, 1249, 1112, 701  $\text{cm}^{-1}$ ; HRMS (ESI)  $m/z$  calcd for  $\text{C}_{58}\text{H}_{80}\text{NaO}_5\text{Si}_3$  ( $\text{M} + \text{Na}$ )<sup>+</sup> 963.5211, found 963.5205.



**Alcohol 183a:** Alcohol **183a** was prepared from PMB ether **183** (700.2 mg, 0.74 mmol) using the general procedure for PMB deprotection. Purification of the crude residue by column chromatography (5–10% EtOAc/hexanes) afforded alcohol **183a** (428.6 mg, 70%) as a light yellow oil:  $R_f = 0.72$  (20% EtOAc/hexanes);  $[\alpha]_D^{26} = -9.60$  ( $c$  1.08,  $\text{CHCl}_3$ );  $^1\text{H NMR}$  (300 MHz,  $\text{CDCl}_3$ )  $\delta$  7.58–7.50 (m, 8H), 7.38–7.33 (m, 4H), 7.28–7.18 (m, 8H), 5.65 (dd,  $J = 11.4, 6.9$  Hz, 1H), 5.49 (dd,  $J = 11.4, 8.7$  Hz, 1H), 5.15 (dd,  $J = 15.3, 7.5$  Hz, 1H), 4.80 (dd,  $J = 15.3, 6.9$  Hz, 1H), 4.45 (t,  $J = 7.2$

Hz, 1H), 4.36–4.30 (m, 1H), 3.72–3.62 (m, 1H), 3.27–3.22 (m, 2H), 1.69–1.62 (m, 2H), 1.28–1.14 (m, 4H), 1.05 (d,  $J = 6.0$  Hz, 3H), 1.01 (s, 9H), 0.95 (s, 9H), 0.87 (s, 9H), 0.03 (s, 3H), 0.01 (s, 3H);  $^{13}\text{C}$  NMR (75 MHz,  $\text{CDCl}_3$ )  $\delta$  136.0, 135.9, 135.8, 134.6, 134.3, 134.2, 133.9, 133.6, 131.9, 131.7, 129.8, 129.5, 129.2, 127.8, 127.7, 127.5, 127.4, 72.0, 71.1, 68.5, 66.8, 39.3, 32.1, 27.1, 27.0, 26.0, 25.0, 23.9, 19.3, 19.2, 18.2, -4.2, -4.5; IR (thin film) 3447, 2930, 1541, 1112, 701  $\text{cm}^{-1}$ ; HRMS (ESI):  $m/z$  calcd for  $\text{C}_{50}\text{H}_{72}\text{NaO}_4\text{Si}_3$  ( $\text{M} + \text{Na}$ ) $^+$  843.4636, found 843.4630.

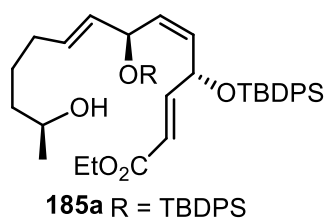


**(E)- $\alpha,\beta$ -Unsaturated ester 185:** To a solution of alcohol **183a** (420.0 mg, 0.51 mmol) in anhydrous  $\text{CH}_2\text{Cl}_2$  (11 mL, 0.05 M) at 0 °C were added  $\text{PhI}(\text{OAc})_2$  (197.3 mg, 0.61 mmol, 1.2 equiv) and TEMPO (16.2 mg, 0.10 mmol, 0.2 equiv). The reaction mixture was stirred from 0 °C to room temperature for 5 h, then quenched with saturated aqueous  $\text{NH}_4\text{Cl}$  (15 mL) and the aqueous phase was extracted with  $\text{CH}_2\text{Cl}_2$  (3x10 mL). The combined organic phases were washed with brine, dried over anhydrous  $\text{Na}_2\text{SO}_4$  and concentrated *in vacuo*. The crude residue was purified by column chromatography (100% hexanes–10% EtOAc/hexanes) to afford unstable aldehyde **184** (335.7 mg, 80%) as a light yellow oil:  $R_f = 0.53$  (10% EtOAc/hexanes) which was used immediately in the next step.

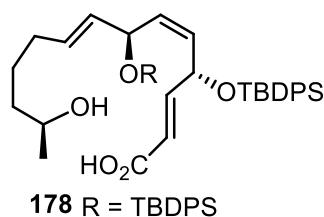
Ester **185** was prepared from aldehyde **184** (330.2 mg, 0.40 mmol) using the general procedure for Wittig olefination. The crude product was purified by column chromatography (10–20% EtOAc/hexanes) to afford ester **185** (345.6 mg, 97%) as a colorless oil:  $R_f = 0.50$  (10% EtOAc/hexanes);  $[\alpha]_{\text{D}}^{26} = +27.4$  ( $c = 1.04$  in  $\text{CHCl}_3$ );  $^1\text{H}$  NMR (300 MHz,  $\text{CDCl}_3$ )  $\delta$  7.60–7.52 (m, 8H), 7.39–7.34 (m, 4H), 7.27–7.21 (m, 8H), 6.59 (dd,  $J = 15.6, 4.8$  Hz, 1H), 5.71 (dd,  $J = 15.6, 1.2$  Hz, 1H), 5.64 (dd,  $J = 11.1, 7.8$  Hz, 1H), 5.41 (dd,  $J = 11.1, 8.4$  Hz, 1H), 5.15 (dd,  $J = 15.3, 7.8$  Hz, 1H), 4.87–4.82 (m, 1H), 4.76 (dt,  $J = 15.3, 6.6$  Hz, 1H), 4.44 (t,  $J = 7.2$  Hz, 1H), 4.11 (q,  $J = 7.2$  Hz, 2H), 3.73–3.67 (m, 1H), 1.72–1.65 (m, 2H), 1.23 (t,  $J = 7.2$  Hz, 3H), 1.18–



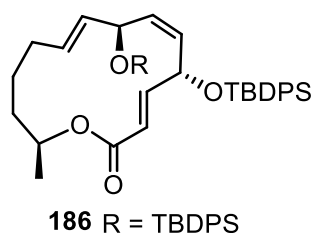
1.12 (m, 4H), 1.07 (d,  $J = 6.0$  Hz, 3H), 1.03 (s, 9H), 0.97 (s, 9H), 0.91 (s, 9H), 0.0 (s, 3H), 0.04 (s, 3H);  $^{13}\text{C}$  NMR (75 MHz,  $\text{CDCl}_3$ )  $\delta$  166.5, 147.7, 136.0, 135.9, 135.8, 134.2, 134.1, 133.9, 133.5, 133.3, 132.2, 131.0, 129.8, 129.6, 129.5, 129.2, 127.7, 127.5, 127.4, 119.9, 72.2, 69.6, 68.5, 60.2, 39.3, 32.0, 27.0, 26.0, 24.9, 23.8, 19.3, 19.2, 18.2, 14.3, -4.2, -4.5; IR (thin film) 2931, 1716, 1541, 1112, 772  $\text{cm}^{-1}$ ; HRMS (ESI)  $m/z$  calcd for  $\text{C}_{54}\text{H}_{77}\text{O}_5\text{Si}_3$  ( $\text{M} + \text{H}$ ) $^+$  889.5079, found 889.5040.



**Alcohol 185a:** Alcohol **185a** was prepared from TBS ether **185** (360.5 mg, 0.40 mmol) using the general procedure for TBS deprotection. The crude product was purified by column chromatography (20–30% EtOAc/hexanes) to give alcohol **185a** (240.2 mg, 75%) as a light yellow oil:  $R_f = 0.30$  (30% EtOAc/hexanes);  $[\alpha]_{\text{D}}^{26} = +30.0$  ( $c$  1.01,  $\text{CHCl}_3$ );  $^1\text{H}$  NMR (300 MHz,  $\text{CDCl}_3$ )  $\delta$  7.59–7.48 (m, 8H), 7.39–7.34 (m, 4H), 7.27–7.21 (m, 8H), 6.57 (ddd,  $J = 15.6, 4.8, 1.5$  Hz, 1H), 5.75 (dd,  $J = 15.6, 1.5$  Hz, 1H), 5.65 (dd,  $J = 11.1, 6.9$  Hz, 1H), 5.40 (dd,  $J = 11.1, 8.1$  Hz, 1H), 5.14 (dd,  $J = 15.3, 7.8$  Hz, 1H), 4.83–4.79 (m, 1H), 4.68 (dd,  $J = 15.3, 8.1$  Hz, 1H), 4.43 (t,  $J = 7.2$  Hz, 1H), 4.10 (q,  $J = 7.2$  Hz, 2H), 4.83–4.79 (m, 1H), 1.69–1.63 (m, 2H), 1.23 (t,  $J = 7.2$  Hz, 3H), 1.20–1.16 (m, 4H), 1.10 (d,  $J = 6.3$  Hz, 3H), 1.03 (s, 9H), 0.95 (s, 9H);  $^{13}\text{C}$  NMR (75 MHz,  $\text{CDCl}_3$ )  $\delta$  166.8, 148.0, 136.0, 135.8, 134.1, 134.0, 133.9, 133.4, 133.3, 132.0, 131.3, 129.8, 129.5, 129.2, 127.7, 127.5, 127.3, 119.7, 72.1, 69.5, 67.8, 60.4, 38.9, 31.8, 27.0, 26.9, 24.9, 23.2, 19.3, 19.2, 14.3; IR (thin film) 3447, 2931, 1716, 1112, 701  $\text{cm}^{-1}$ ; HRMS (ESI)  $m/z$  calcd for  $\text{C}_{48}\text{H}_{62}\text{NaO}_5\text{Si}_2$  ( $\text{M} + \text{Na}$ ) $^+$  797.4033, found 797.4026.

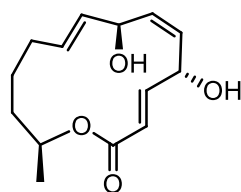


**Seco acid 178:** Seco acid **178** was prepared from ester **185a** (230.6 mg, 0.30 mmol) using the general procedure for hydrolysis. The crude residue was purified by column chromatography (50–80% EtOAc/hexanes) to give seco acid **178** (165.5 mg, 75%) as a light yellow oil:  $R_f = 0.25$  (50% EtOAc/hexanes);  $[\alpha]_D^{26} = +29.2$  ( $c$  1.00,  $\text{CHCl}_3$ );  $^1\text{H}$  NMR (300 MHz,  $\text{CDCl}_3$ )  $\delta$  7.59–7.48 (m, 8H), 7.38–7.33 (m, 4H), 7.27–7.17 (m, 8H), 6.60 (dd,  $J = 15.6, 4.8$  Hz, 1H), 5.70 (dd,  $J = 15.6, 1.5$  Hz, 1H), 5.65 (dd,  $J = 11.1, 7.5$  Hz, 1H), 5.42 (dd,  $J = 11.1, 7.5$  Hz, 1H), 5.17 (dd,  $J = 15.3, 7.5$  Hz, 1H), 4.79–4.74 (m, 1H), 4.70 (dd,  $J = 15.3, 6.9$  Hz, 1H), 4.41 (t,  $J = 7.2$  Hz, 1H), 3.72–3.66 (m, 1H), 1.76–1.64 (m, 2H), 1.24–1.08 (m, 4H), 1.09 (d,  $J = 6.0$  Hz, 3H), 1.03 (s, 9H), 0.96 (s, 9H);  $^{13}\text{C}$  NMR (75 MHz,  $\text{CDCl}_3$ )  $\delta$  169.9, 149.8, 136.0, 135.8, 134.1, 133.8, 133.4, 133.2, 132.1, 131.3, 131.0, 130.5, 129.9, 129.6, 129.3, 127.7, 127.5, 127.4, 119.1, 71.9, 69.6, 68.2, 38.6, 31.9, 27.0, 25.0, 23.0, 19.3, 19.2; IR (thin film) 3446, 2930, 1711, 1115, 770  $\text{cm}^{-1}$ ; HRMS (ESI)  $m/z$  calcd for  $\text{C}_{46}\text{H}_{58}\text{NaO}_5\text{Si}_2$  ( $M + \text{Na}$ ) $^+$  769.3720, found 769.3715.



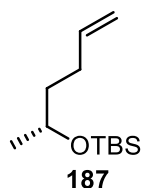
**Macrolactone 186:** Macrolactone **186** was prepared from seco acid **178** (70.6 mg, 0.09 mmol) using the general procedure for Shiina macrolactonization. The crude product was purified by column chromatography (5–20% EtOAc/hexanes) to give compound **186** (47.4 mg, 68%) as a colorless oil:  $R_f = 0.52$  (20% EtOAc/hexanes);  $[\alpha]_D^{26} = +34.8$  ( $c$  1.07 in  $\text{CHCl}_3$ );  $^1\text{H}$  NMR (300 MHz,  $\text{CDCl}_3$ )  $\delta$  7.64–7.62 (m, 2H), 7.55–7.49 (m, 4H), 7.44–7.36 (m, 4H), 7.33–7.24 (m, 6H), 7.21–7.14 (m, 2H), 7.05–7.00 (m, 2H), 6.65 (dd,  $J = 15.3, 4.2$  Hz, 1H), 5.81 (dd,  $J = 15.3, 1.5$  Hz, 1H), 5.47–5.45 (m, 2H), 5.30 (dd,  $J = 15.3, 6.9$  Hz, 1H), 5.21–5.12 (m, 1H), 4.82 (brs, 1H),

4.68–4.59 (m, 1H), 4.42 (t,  $J = 7.2$  Hz, 1H), 1.96–1.87 (m, 1H), 1.75–1.57 (m, 3H), 1.28–1.25 (m, 2H), 1.17 (d,  $J = 6.3$  Hz, 3H), 1.06 (s, 9H), 0.94 (s, 9H);  $^{13}\text{C}$  NMR (75 MHz,  $\text{CDCl}_3$ )  $\delta$  166.4, 148.6, 136.0, 135.8, 135.7, 134.0, 133.8, 133.6, 133.2, 131.7, 131.2, 130.9, 129.9, 129.6, 127.8, 127.6, 127.4, 118.0, 71.9, 71.8, 69.9, 34.5, 32.8, 27.0, 24.4, 20.3, 19.3, 19.2; IR (thin film) 2931, 1716, 1507, 1112, 772  $\text{cm}^{-1}$ ; HRMS (ESI)  $m/z$  calcd for  $\text{C}_{46}\text{H}_{57}\text{O}_4\text{Si}_2$  ( $\text{M} + \text{H}$ ) $^+$  729.3795, found 729.3784.

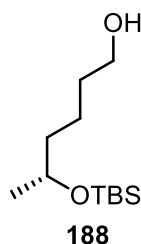


(4S,7S,13S)-4,7-dihydroxy-13-tetradeca-2,5,8-trienolide (**23**)

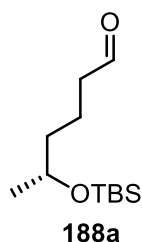
**(4S,7S,13S)-4,7-Dihydroxy-13-tetradeca-2,5,8-trienolide (23)**: Compound **23** was prepared from macrolactone **186** (46.5 mg, 0.07 mmol) using the general procedure for global desilylation. Purification of the crude residue by column chromatography (20–60% EtOAc/hexanes) yielded compound **23** (11.5 mg, 62%) as a white powder:  $R_f = 0.15$  (50% EtOAc/hexanes);  $[\alpha]_{\text{D}}^{26} = +148.8$  ( $c$  0.68,  $\text{CHCl}_3$ );  $^1\text{H}$  NMR (300 MHz,  $\text{CDCl}_3$ )  $\delta$  7.03 (dd,  $J = 15.6, 4.2$  Hz, 1H), 5.91 (dd,  $J = 15.6, 1.5$  Hz, 1H), 5.86 (ddd,  $J = 15.6, 9.6, 5.4$  Hz, 1H), 5.54 (dd,  $J = 11.1, 4.2$  Hz, 1H), 5.49–5.46 (m, 1H), 5.49–5.46 (m, 1H), 5.46 (dd,  $J = 10.8, 9.5$  Hz, 1H), 5.29–5.24 (m, 1H), 4.82 (t,  $J = 8.1$  Hz, 1H), 4.75–4.72 (m, 1H), 2.14–1.71 (m, 4H), 1.60–1.48 (m, 1H), 1.26 (d,  $J = 6.0$  Hz, 3H), 1.16–1.06 (m, 1H);  $^{13}\text{C}$  NMR (75 MHz,  $\text{CDCl}_3$ )  $\delta$  166.3, 148.5, 134.4, 132.2, 131.3, 130.4, 118.3, 72.2, 70.6, 68.5, 34.6, 32.9, 24.4, 20.3; IR (thin film) 3390, 2936, 1702, 1255, 940  $\text{cm}^{-1}$ ; HRMS (ESI)  $m/z$  calcd for  $\text{C}_{14}\text{H}_{20}\text{NaO}_4$  ( $\text{M} + \text{Na}$ ) $^+$  275.1259, found 275.1249.



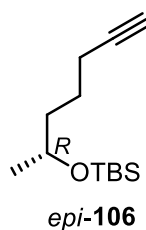
**(R)-tert-Butyl(hex-5-en-2-yloxy)dimethylsilane (187):** Silyl ether **187** was prepared from (*R*)-propylene oxide (**181**) (4.0 mL, 57.1 mmol) using the general procedure for epoxide ring opening/TBS protection. The crude residue was purified by column chromatography (100% hexanes–5% EtOAc/hexanes) to give (*R*)-tert-butyl(hex-5-en-2-yloxy)dimethylsilane (**187**) as a colorless oil (10.4 g, 85%):  $R_f = 0.76$  (10% EtOAc/hexanes);  $[\alpha]_D^{26} = -58.5$  ( $c$  0.76,  $\text{CHCl}_3$ );  $^1\text{H NMR}$  (300 MHz,  $\text{CDCl}_3$ )  $\delta$  5.89–5.76 (m, 1H), 5.04–4.93 (m, 2H), 3.79 (q,  $J = 6.0$  Hz, 1H), 2.18–2.01 (m, 2H), 1.57–1.43 (m, 2H), 1.14 (d,  $J = 6.0$  Hz, 3H), 0.90 (s, 9H), 0.06 (s, 6H). The spectral data of **187** matched those previously described (Sharma *et al.*, 2009 and Kim *et al.*, 2022).



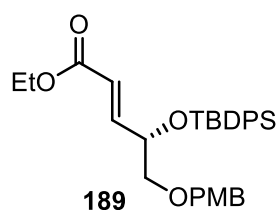
**(R)-5-((tert-Butyldimethylsilyl)oxy)hexan-1-ol (188):** Alcohol **188** was prepared from olefin **187** (6.55 g, 30.5 mmol) using the general procedure for hydroboration-oxidation. Purification of the crude residue by column chromatography (10–20% EtOAc/hexanes) yielded (*R*)-5-((tert-butyl dimethylsilyl)oxy)hexan-1-ol (**188**) as a colorless oil (5.32 g, 75%):  $R_f = 0.38$  (20% EtOAc/hexanes);  $[\alpha]_D^{26} = -13.8$  ( $c$  1.0,  $\text{CHCl}_3$ );  $^1\text{H NMR}$  (300 MHz,  $\text{CDCl}_3$ )  $\delta$  3.84–3.73 (m, 1H), 3.63 (t,  $J = 6.0$  Hz, 2H), 1.59–1.30 (m, 6H), 1.11 (d,  $J = 6.0$  Hz, 3H), 0.87 (s, 9H), 0.03 (s, 6H). The spectral data of **188** matched those previously described (Takemoto *et al.*, 2003 and Yadav *et al.*, 2007).



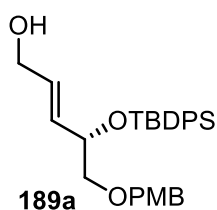
**(R)-5-((tert-Butyldimethylsilyl)oxy)hexanal (188a):** To a solution of alcohol **188** (4.32 g, 18.6 mmol) in anhydrous  $\text{CH}_2\text{Cl}_2$  (33 mL, 0.57 M) at 0 °C was added  $\text{PhI}(\text{OAc})_2$  (7.75 g, 24.1 mmol, 1.3 equiv), followed by TEMPO (581.2 mg, 3.72 mmol, 0.2 equiv). The reaction mixture was stirred from 0 °C to room temperature for 3 h and then quenched with saturated aqueous  $\text{NH}_4\text{Cl}$  (20 mL). The aqueous phase was extracted with  $\text{CH}_2\text{Cl}_2$  (3x15 mL). The combined organic phases were washed with brine, dried over anhydrous  $\text{Na}_2\text{SO}_4$  and concentrated *in vacuo*. The crude residue was purified by column chromatography (100% hexanes–10% EtOAc/hexanes) to afford aldehyde **188a** as a light yellow oil (3.34 g, 78%):  $R_f = 0.55$  (10% EtOAc/hexanes);  $^1\text{H NMR}$  (300 MHz,  $\text{CDCl}_3$ )  $\delta$  9.74 (t,  $J = 1.8$  Hz, 1H), 3.84–3.76 (m, 1H), 2.41 (td,  $J = 7.2, 1.8$  Hz, 2H), 1.76–1.55 (m, 2H), 1.48–1.37 (m, 2H), 1.11 (d,  $J = 6.0$  Hz, 3H), 0.86 (s, 9H), 0.04 (s, 6H). The spectral data of **188a** matched those previously described (Takemoto *et al.*, 2003).



**(R)-tert-Butyl(hept-6-yn-2-yloxy)dimethylsilane (epi-106):** Alkyne **epi-106** was prepared from aldehyde **188a** (2.95 g, 12.8 mmol) using the general procedure for Ohira–Bestmann homologation. Purification of the crude residue by column chromatography (100% hexanes) afforded alkyne **epi-106** as a colorless oil (2.14 g, 74%):  $R_f = 0.63$  (3% EtOAc/hexanes);  $[\alpha]_D^{26} = -14.4$  ( $c$  7.0,  $\text{CH}_2\text{Cl}_2$ );  $^1\text{H NMR}$  (300 MHz,  $\text{CDCl}_3$ )  $\delta$  3.85–3.75 (m, 1H), 2.20–2.16 (m, 2H), 1.93 (t,  $J = 2.7$  Hz, 1H), 1.63–1.49 (m, 4H), 1.12 (d,  $J = 6.0$  Hz, 3H), 0.88 (s, 9H), 0.04 (s, 6H).

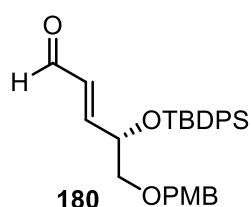


**(*S,E*)-Ethyl-4-((*tert*-butyldiphenylsilyl)oxy)-5-((4-methoxybenzyl)oxy)pent-2-enoate (**189**):** To a solution of aldehyde **134** (7.55 g, 16.7 mmol) in anhydrous CH<sub>2</sub>Cl<sub>2</sub> (300 mL, 0.05 M) was added (carbethoxymethylene)triphenylphosphorane (12.2 g, 35.0 mmol, 2.1 equiv). The reaction mixture was stirred at room temperature for 5 h before being concentrated under reduced pressure. The crude product was purified by column chromatography (10–20% EtOAc/hexanes) to afford (*E*)- $\alpha,\beta$ -unsaturated ester **189** (7.35 g, 87%) as a light yellow oil:  $R_f$  = 0.6 (10% EtOAc/hexanes);  $[\alpha]_D^{26}$  =  $-7.86$  ( $c$  1.03, CHCl<sub>3</sub>); <sup>1</sup>H NMR (300 MHz, CDCl<sub>3</sub>)  $\delta$  7.67–7.58 (m, 4H), 7.44–7.29 (m, 6H), 7.06 (d,  $J$  = 8.7 Hz, 2H), 6.95 (dd,  $J$  = 15.6, 4.5 Hz, 1H), 6.80 (d,  $J$  = 8.7 Hz, 2H), 6.04 (dd,  $J$  = 15.6, 1.5 Hz, 1H), 4.49–4.45 (m, 1H), 4.25 (s, 2H), 4.21–4.14 (m, 2H), 3.78 (s, 3H), 3.40–3.28 (m, 2H), 1.28 (t,  $J$  = 7.2 Hz, 3H), 1.07 (s, 9H); <sup>13</sup>C NMR (75 MHz, CDCl<sub>3</sub>)  $\delta$  166.5, 159.2, 147.9, 136.0, 135.9, 133.8, 133.1, 130.1, 129.9, 129.8, 129.3, 127.7, 127.6, 127.5, 121.3, 113.7, 73.4, 72.9, 71.7, 60.4, 55.3, 27.1, 19.4, 14.3; IR (thin film) 2932, 1719, 1248, 1112, 702 cm<sup>-1</sup>; HRMS (ESI)  $m/z$  calcd for C<sub>31</sub>H<sub>38</sub>NaO<sub>5</sub>Si (M + Na)<sup>+</sup> 541.2386, found 541.2394.



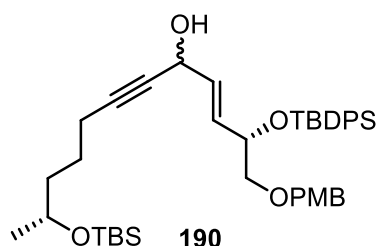
**(*S,E*)-4-((*tert*-Butyldiphenylsilyl)oxy)-5-((4-methoxybenzyl)oxy)pent-2-en-1-ol (**189a**):** To a solution of *E*-ester **189** (10.52 g, 20.2 mmol) in anhydrous CH<sub>2</sub>Cl<sub>2</sub> (200 mL, 0.1 M) at  $-78$  °C was added DIBAL-H (1 M in THF, 46 mL, 46.4 mmol, 2.3 equiv) dropwise. After being stirred at  $-78$  °C for 1 h, the reaction mixture was then quenched with saturated aqueous potassium sodium tartrate solution (200 mL) and stirred for 1 h. The aqueous phase was extracted with CH<sub>2</sub>Cl<sub>2</sub> (3 $\times$ 50 mL). The combined organic layers were washed with brine, dried over anhydrous Na<sub>2</sub>SO<sub>4</sub> and

concentrated under reduced pressure. Purification of the crude residue by column chromatography (20–30% EtOAc/hexanes) yielded alcohol **189a** (8.72 g, 92%) as a colorless oil:  $R_f = 0.30$  (20% EtOAc/hexanes);  $[\alpha]_D^{26} = -11.6$  ( $c$  1.05,  $\text{CHCl}_3$ );  $^1\text{H}$  NMR (300 MHz,  $\text{CDCl}_3$ )  $\delta$  7.69–7.63 (m, 4H), 7.40–7.30 (m, 6H), 7.12 (d,  $J = 8.7$  Hz, 2H), 6.81 (d,  $J = 8.7$  Hz, 2H), 5.64 (dd,  $J = 15.6, 4.5$  Hz, 1H), 5.61–5.53 (m, 1H), 4.36–4.33 (m, 3H), 3.93 (brs, 2H), 3.77 (s, 3H), 3.43 (dd,  $J = 9.9, 5.7$  Hz, 1H), 3.35 (dd,  $J = 9.9, 5.7$  Hz, 1H), 1.06 (s, 9H);  $^{13}\text{C}$  NMR (75 MHz,  $\text{CDCl}_3$ )  $\delta$  159.2, 136.1, 136.0, 134.2, 131.7, 130.7, 130.4, 129.6, 129.3, 127.6, 127.5, 113.7, 74.4, 72.9, 72.7, 63.0, 55.3, 27.1, 19.4; IR (thin film) 3421, 2856, 1513, 1111, 701  $\text{cm}^{-1}$ ; HRMS (ESI)  $m/z$  calcd for  $\text{C}_{29}\text{H}_{36}\text{NaO}_4\text{Si}$  ( $M + \text{Na}$ ) $^+$  499.2281, found 499.2289.

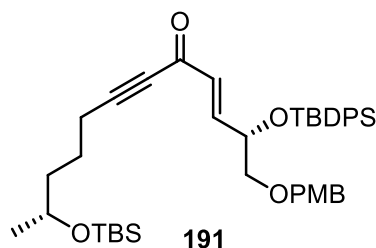


**(*S,E*)-4-((*tert*-Butyldiphenylsilyloxy)-5-((4-methoxybenzyl)oxy)pent-2-enal (**180**):**

To a solution of alcohol **189a** (8.02 g, 16.7 mmol) in DMSO (30 mL, 0.5 M) at 0 °C was added 2-iodoxybenzoic acid (IBX, 14.0 g, 50.1 mmol, 3.0 equiv). The reaction mixture was stirred from 0 °C to room temperature for 3 h. The reaction was then added  $\text{H}_2\text{O}$  (15 mL), filtered through a pad of Celite and washed with EtOAc. The mixture was extracted with EtOAc (3x10 mL), washed with brine, dried over anhydrous  $\text{Na}_2\text{SO}_4$  and concentrated *in vacuo*. The crude residue was purified by column chromatography (20% EtOAc/hexanes) to give (*E*)-enal **180** (7.13 g, 90%) as a light yellow oil:  $R_f = 0.30$  (10% EtOAc/hexanes);  $[\alpha]_D^{26} = -10.9$  ( $c$  1.08,  $\text{CHCl}_3$ );  $^1\text{H}$  NMR (300 MHz,  $\text{CDCl}_3$ )  $\delta$  9.48 (d,  $J = 8.1$  Hz, 1H), 7.67–7.57 (m, 4H), 7.45–7.30 (m, 6H), 7.07 (d,  $J = 8.7$  Hz, 2H), 6.83 (dd,  $J = 15.6, 4.2$  Hz, 1H), 6.81 (d,  $J = 8.7$  Hz, 2H), 6.32 (ddd,  $J = 15.6, 7.8, 1.2$  Hz, 1H), 4.60–4.54 (m, 1H), 4.27 (d,  $J = 2.7$  Hz, 2H), 3.77 (s, 3H), 3.43 (dd,  $J = 9.6, 6.6$  Hz, 1H), 3.35 (dd,  $J = 9.6, 6.6$  Hz, 1H), 1.08 (s, 9H);  $^{13}\text{C}$  NMR (75 MHz,  $\text{CDCl}_3$ )  $\delta$  193.5, 159.3, 157.1, 135.8, 133.4, 132.8, 131.6, 130.1, 130.0, 129.8, 129.3, 127.8, 127.7, 113.8, 73.1, 73.0, 71.6, 55.3, 27.0, 19.3; IR (thin film) 2857, 1691, 1513, 1112, 702  $\text{cm}^{-1}$ ; HRMS (ESI)  $m/z$  calcd for  $\text{C}_{29}\text{H}_{34}\text{NaO}_4\text{Si}$  ( $M + \text{Na}$ ) $^+$  497.2124, found 497.2120.



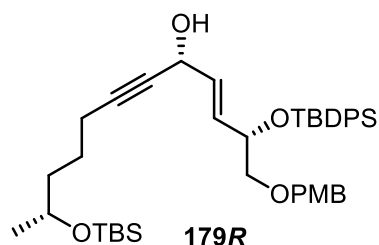
**Propargylic alcohol 190:** Propargylic alcohol **190** were prepared from alkyne *epi*-**106** (1.34 g, 5.94 mmol, 1.5 equiv) and (*E*)-enal **180** (1.88 g, 3.97 mmol, 1.0 equiv) using the general procedure for acetylide addition. The crude residue was purified by column chromatography (100% hexanes–20% EtOAc/hexanes) to give **190** (2.18 g, 79%) as a light yellow oil:  $R_f = 0.38$  (20% EtOAc/hexanes);  $[\alpha]_D^{25} = -0.13$  ( $c$  1.00,  $\text{CHCl}_3$ );  $^1\text{H}$  NMR (300 MHz,  $\text{CDCl}_3$ )  $\delta$  7.71–7.67 (m, 4H), 7.44–7.36 (m, 6H), 7.16 (d,  $J = 8.4$  Hz, 2H), 6.85 (d,  $J = 8.4$  Hz, 2H), 5.92–5.82 (m, 1H), 5.69–5.60 (m, 1H), 4.74–4.71 (m, 1H), 4.41–4.39 (m, 1H), 4.37 (s, 2H), 3.81–3.80 (m, 4H), 3.48 (dd,  $J = 9.6, 5.1$  Hz, 1H), 3.39 (dd,  $J = 9.6, 5.4$  Hz, 1H), 2.26–2.22 (m, 2H), 1.71–1.52 (m, 4H), 1.17–1.11 (m, 12H), 0.92 (s, 9H), 0.08 (s, 6H).  $^{13}\text{C}$  NMR (75 MHz,  $\text{CDCl}_3$ )  $\delta$  159.1, 136.2, 136.0, 134.1, 133.9, 132.3, 132.2, 131.1, 130.4, 129.7, 129.3, 127.5, 113.7, 86.8, 86.7, 79.3, 79.2, 74.3, 72.9, 72.4, 68.2, 62.7, 62.5, 55.3, 38.9, 27.1, 26.0, 24.9, 23.9, 19.4, 18.9, 18.2, –4.3, –4.6.



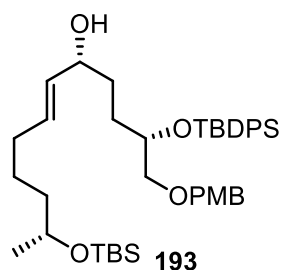
**Ynone 191:** Ynone **191** was prepared from propargylic alcohol **190** (460 mg, 0.65 mmol) using the general procedure for  $\text{MnO}_2$  oxidation. Purification of the crude residue by column chromatography (10–20% EtOAc/hexanes) yielded ketone **191** (404.5 mg, 89%) as a light yellow oil:  $R_f = 0.62$  (20% EtOAc/hexanes);  $^1\text{H}$  NMR (300 MHz,  $\text{CDCl}_3$ )  $\delta$  7.67–7.58 (m, 4H), 7.45–7.30 (m, 6H), 7.13–7.06 (m, 3H), 6.81 (d,  $J = 8.4$  Hz, 2H), 6.31 (d,  $J = 15.3$  Hz, 1H), 4.55–4.50 (m, 1H), 4.28 (s, 2H), 3.83–3.79 (m, 4H), 3.42 (dd,  $J = 9.6, 5.7$  Hz, 1H), 3.35 (dd,  $J = 9.6, 6.0$  Hz, 1H), 2.41–2.37 (m,



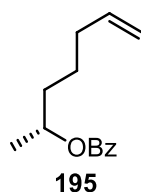
2H), 1.70–1.65 (m, 2H), 1.55–1.50 (m, 2H), 1.12 (d,  $J = 6.0$  Hz, 3H), 1.08 (s, 9H), 0.88 (s, 9H), 0.04 (s, 3H), 0.03 (s, 3H).



**Propargylic alcohol 179R:** To a solution of (*R*)-Corey-Bakshi-Shibata (CBS) (1 M solution in toluene, 500  $\mu$ L, 0.50 mmol, 1.0 equiv) in anhydrous toluene (2.5 mL, 0.2 M) at  $-15$   $^{\circ}$ C was added a solution of  $\text{BH}_3\cdot\text{SMe}_2$  (90  $\mu$ L, 1.0 mmol, 2.0 equiv) in anhydrous toluene (400  $\mu$ L, 2.5 M). The reaction mixture was stirred at  $-15$   $^{\circ}$ C for 1 h before a solution of ynone **191** (350 mg, 0.50 mmol) in anhydrous toluene (1.5 mL, 0.3 M) was slowly added. The reaction mixture was stirred at same temperature for 3.5 h, then quenched with MeOH (3 mL) and concentrated *in vacuo*. The crude residue was purified by column chromatography (5–20% EtOAc/hexanes) to give **179R** (226.5 mg, 65%) as a light yellow oil:  $R_f = 0.36$  (20% EtOAc/hexanes);  $[\alpha]_D^{25} = -7.5$  ( $c$  1.00,  $\text{CHCl}_3$ );  $^1\text{H}$  NMR (300 MHz,  $\text{CDCl}_3$ )  $\delta$  7.71–7.65 (m, 4H), 7.44–7.25 (m, 6H), 7.14 (d,  $J = 8.7$  Hz, 2H), 6.83 (d,  $J = 8.7$  Hz, 2H), 5.90–5.80 (m, 1H), 5.67–5.58 (m, 1H), 4.73–4.71 (m, 1H), 4.39–4.37 (m, 1H), 4.35 (s, 2H), 3.81–3.79 (m, 4H), 3.46 (dd,  $J = 9.9, 5.7$  Hz, 1H), 3.37 (dd,  $J = 9.9, 5.7$  Hz, 1H), 2.25–2.22 (m, 2H), 1.62–1.51 (m, 4H), 1.14 (d,  $J = 6.3$  Hz, 3H), 1.08 (s, 9H), 0.89 (s, 9H), 0.06 (s, 3H), 0.05 (s, 3H).  $^{13}\text{C}$  NMR (75 MHz,  $\text{CDCl}_3$ )  $\delta$  159.2, 136.3, 136.1, 134.2, 134.1, 132.4, 132.2, 131.2, 130.5, 129.7, 129.3, 127.6, 113.8, 86.9, 79.3, 74.4, 72.9, 72.5, 68.3, 62.6, 55.4, 38.9, 27.2, 26.0, 24.9, 23.9, 19.4, 18.9, 18.2,  $-4.2$ ,  $-4.6$ .



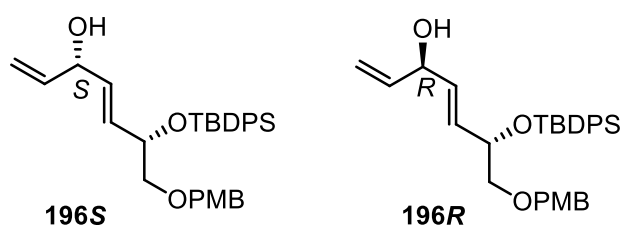
**The undesired overreduced product 193:** To a solution of alkyne **179R** (250 mg, 0.36 mmol) in anhydrous toluene (8 mL, 0.05 M) were added sodium bis(2-methoxyethoxy)aluminium hydride (Red-Al) (3.6 M solution in toluene, 300  $\mu$ L, 1.08 mmol, 3.0 equiv). After being stirred from 0  $^{\circ}$ C to room temperature for 3 h, the reaction mixture was quenched with saturated aqueous potassium sodium tartrate solution (15 mL). The aqueous phase was extracted with EtOAc (3 $\times$ 10 mL). The combined organic layers were washed with brine, dried over anhydrous Na<sub>2</sub>SO<sub>4</sub> and concentrated under reduced pressure. Purification of the crude residue by column chromatography (10–20% EtOAc/hexanes) afforded compound **193** (100.5 mg, 40%, 58% brsm) as a light yellow oil:  $R_f$  = 0.45 (30% EtOAc/hexanes); <sup>1</sup>H NMR (300 MHz, CDCl<sub>3</sub>)  $\delta$  7.69–7.64 (m, 4H), 7.41–7.31 (m, 6H), 7.14 (d,  $J$  = 8.7 Hz, 2H), 6.82 (d,  $J$  = 8.7 Hz, 2H), 5.66–5.52 (m, 1H), 5.47 (dd,  $J$  = 15.6, 6.3 Hz, 1H), 5.32 (dd,  $J$  = 15.6, 6.3 Hz, 1H), 4.38–4.35 (m, 3H), 3.80 (s, 3H), 3.78–3.75 (m, 1H), 3.46 (dd,  $J$  = 9.9, 6.0 Hz, 1H), 3.36 (dd,  $J$  = 9.9, 5.7 Hz, 1H), 2.03–1.96 (m, 2H), 1.40–1.21 (m, 8H), 1.10 (d,  $J$  = 6.3 Hz, 3H), 1.06 (s, 9H), 0.88 (s, 9H), 0.04 (s, 3H), 0.03 (s, 3H). <sup>13</sup>C NMR (75 MHz, CDCl<sub>3</sub>)  $\delta$  159.3, 136.3, 136.1, 134.4, 134.3, 133.4, 132.5, 131.2, 131.1, 130.7, 129.7, 129.3, 127.6, 127.5, 113.8, 74.6, 72.9, 68.6, 68.3, 55.4, 39.4, 32.4, 27.2, 26.1, 25.4, 23.9, 19.4, 18.3, –4.2, –4.5.



**(R)-Hept-6-en-2-yl benzoate (195):** To a solution of (*R*)-propylene oxide (**181**) (1.7 mL, 25.8 mmol) in anhydrous THF (50 mL, 0.5 M) at  $-30\text{ }^{\circ}\text{C}$  was added dilithium copper(II) chloride (*ca.* 0.1 M solution in THF, 26 mL, 2.58 mmol, 0.1 equiv), followed by 3-butenylmagnesium bromide (*ca.* 0.5 M solution in THF, 80 mL, 3.9 mmol, 1.5 equiv). The reaction mixture was stirred at same temperature for 2 h, then quenched with  $\text{NH}_4\text{Cl}$  (50 mL) and extracted with  $\text{CH}_2\text{Cl}_2$  (3x30 mL). The combined organic layers were washed with brine, dried over anhydrous  $\text{Na}_2\text{SO}_4$  and concentrated *in vacuo* to give (*R*)-hept-6-en-2-ol (**197**) which was used in the next step without further purification.

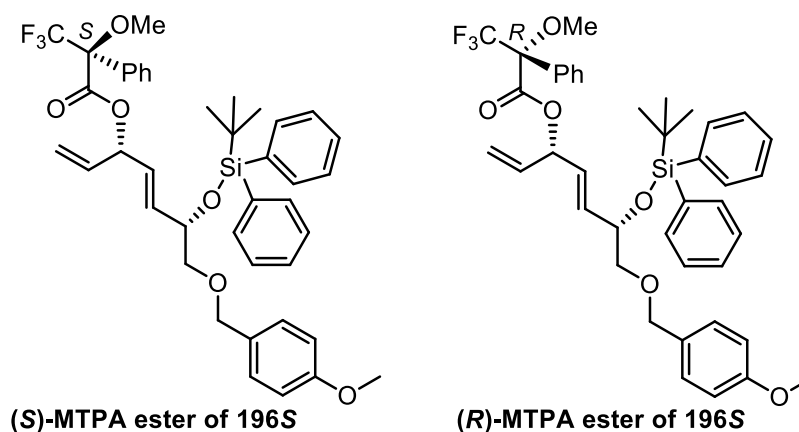
To a solution of (*R*)-hept-6-en-2-ol (**197**) (2.62 g, 22.7 mmol) in  $\text{CH}_2\text{Cl}_2$  (75 mL, 0.3 M) were added DMAP (920 mg, 7.5 mmol, 0.33 equiv) and triethylamine (9 mL, 68.1 mmol, 3.0 equiv), followed by benzoyl chloride (3.2 mL, 27.2 mmol, 1.2 equiv). The reaction mixture was stirred from  $0\text{ }^{\circ}\text{C}$  to room temperature overnight. The reaction mixture was then quenched with  $\text{NH}_4\text{Cl}$  (60 mL) and extracted with  $\text{CH}_2\text{Cl}_2$  (3x30 mL). The combined organic layers were washed with brine, dried over anhydrous  $\text{Na}_2\text{SO}_4$  and concentrated under reduced pressure. The crude product was purified by column chromatography (100% hexanes–5% EtOAc/hexanes) to give (*R*)-hept-6-en-2-yl benzoate (**195**) as a light yellow oil (4.51 g, 90%):  $R_f = 0.70$  (10% EtOAc/hexanes);  $[\alpha]_{\text{D}}^{26} = -33.1$  (*c* 1.05,  $\text{CHCl}_3$ );  $^1\text{H NMR}$  (300 MHz,  $\text{CDCl}_3$ )  $\delta$  8.05–8.03 (m, 2H), 7.56–7.52 (m, 1H), 7.50–7.39 (m, 2H), 5.86–5.72 (m, 1H), 5.22–5.12 (m, 1H), 5.03 (dd,  $J = 15.6, 1.5$  Hz, 1H), 4.96 (dd,  $J = 11.4, 1.5$  Hz, 1H), 2.12–2.05 (m, 2H), 1.76–1.68 (m, 1H), 1.66–1.59 (m, 1H), 1.58–1.50 (m, 2H), 1.34 (d,  $J = 6.3$  Hz, 3H);  $^{13}\text{C NMR}$  (75 MHz,  $\text{CDCl}_3$ )  $\delta$  166.2, 138.4, 132.7, 130.9, 129.5, 128.3, 114.8, 71.5, 35.5, 33.5, 24.7, 20.1; IR (thin film) 2937, 1716, 1274, 1113, 772  $\text{cm}^{-1}$ ; The enantiopurity of **195** was determined to be >99% ee from the corresponding alcohol derivative, (*R*)-7-hydroxyheptan-2-yl benzoate (**195a**), by HPLC analysis using CHIRALPAK<sup>®</sup> AS-H column eluting with 99:1 hexane/isopropanol (flow rate

= 0.8 mL/min, pressure = 28.6 bar, temp = 26-29 °C): retention time of (*R*)-enantiomer = 24.85 min.



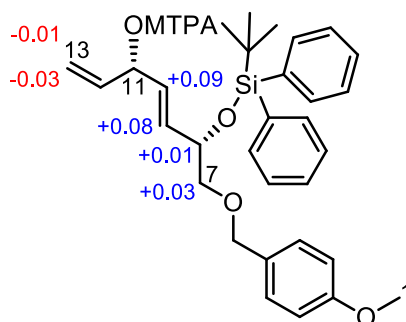
**Allylic alcohols 196S and 196R:** To a solution of (*E*)-enal **180** (3.24 g, 6.74 mmol) in anhydrous THF (26 mL, 0.25 M) was added vinylmagnesium bromide (*ca.* 1 M solution in THF, 10 mL, 10.0 mmol, 1.5 equiv) dropwise at  $-78$  °C. The reaction mixture was stirred from  $-78$  °C to approximately  $-30$  °C for 2 h. The reaction was quenched with saturated aqueous  $\text{NH}_4\text{Cl}$  (20 mL) and extracted with EtOAc (3x20 mL). The combined organic layer were washed with brine, dried over anhydrous  $\text{Na}_2\text{SO}_4$  and concentrated *in vacuo*. The crude residue was purified by column chromatography (100% hexanes–10% EtOAc/hexanes) to give **196S** and **196R**. The absolute configuration was determined by Mosher's method using the corresponding (*S*)-MTPA and (*R*)-MTPA esters.

**Allylic alcohol 196S:** light yellow oil (1.61 g, 49%):  $R_f = 0.51$  (20% EtOAc/hexanes);  $[\alpha]_D^{26} = -3.90$  ( $c$  1.03,  $\text{CHCl}_3$ );  $^1\text{H NMR}$  (300 MHz,  $\text{CDCl}_3$ )  $\delta$  7.68–7.61 (m, 4H), 7.42–7.29 (m, 6H), 7.12 (d,  $J = 8.7$  Hz, 2H), 6.81 (d,  $J = 8.7$  Hz, 2H), 5.75 (dd,  $J = 17.1, 10.5$  Hz, 1H), 5.66 (dd,  $J = 15.6, 6.0$  Hz, 1H), 5.50 (dd,  $J = 15.6, 6.0$  Hz, 1H), 5.15 (dd,  $J = 17.1, 1.2$  Hz, 1H), 5.06 (dd,  $J = 10.5, 1.2$  Hz, 1H), 4.46 (t,  $J = 5.7$  Hz, 1H), 4.37–4.34 (m, 1H), 4.33 (s, 2H), 3.77 (s, 3H), 3.41 (dd,  $J = 9.6, 6.0$  Hz, 1H), 3.38 (dd,  $J = 9.6, 6.0$  Hz, 1H), 1.06 (s, 9H);  $^{13}\text{C NMR}$  (75 MHz,  $\text{CDCl}_3$ )  $\delta$  159.1, 139.2, 136.1, 136.0, 134.1, 132.7, 131.4, 130.4, 129.6, 129.3, 127.5, 115.0, 113.7, 74.4, 73.0, 72.8, 72.6, 27.1, 19.4; IR (thin film) 3447, 2857, 1513, 1111, 702  $\text{cm}^{-1}$ ; HRMS (ESI)  $m/z$  calcd for  $\text{C}_{31}\text{H}_{38}\text{NaO}_4\text{Si}$  ( $\text{M} + \text{Na}$ ) $^+$  525.2437, found 525.2433.



**(S)-MTPA ester of allylic alcohol 196S:**  $^1\text{H NMR}$  (300 MHz,  $\text{CDCl}_3$ )  $\delta$  7.66–7.56 (m, 4H), 7.50–7.29 (m, 11H), 7.07 (d,  $J = 8.4$  Hz, 2H), 6.80 (d,  $J = 8.4$  Hz, 2H), 5.91–5.80 (m, 2H), 5.73 (dd,  $J = 16.0, 6.6$  Hz, 1H), 5.63 (dd,  $J = 16.0, 6.6$  Hz, 1H), 5.28 (d,  $J = 16.8$  Hz, 1H), 5.20 (d,  $J = 10.8$  Hz, 1H), 4.38–4.30 (m, 1H), 4.27 (s, 2H), 3.77 (s, 3H), 3.48 (s, 3H), 3.39 (dd,  $J = 9.6, 5.7$  Hz, 1H), 3.29 (dd,  $J = 9.6, 5.7$  Hz, 1H), 1.05 (s, 9H).

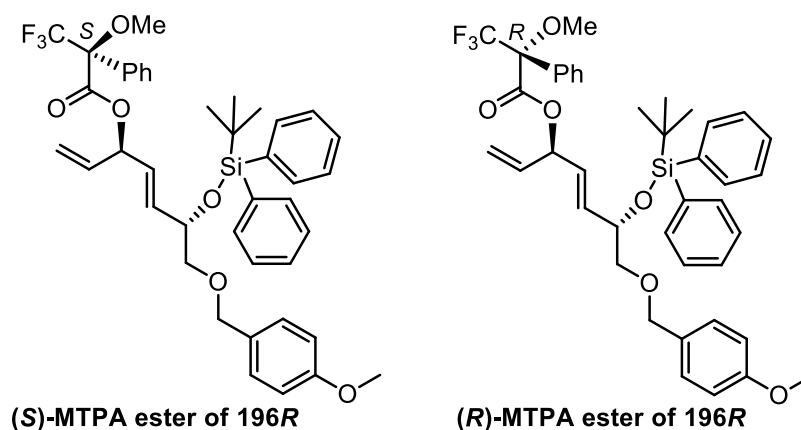
**(R)-MTPA ester of allylic alcohol 196S:**  $^1\text{H NMR}$  (300 MHz,  $\text{CDCl}_3$ )  $\delta$  7.66–7.55 (m, 4H), 7.50–7.26 (m, 11H), 7.07 (d,  $J = 8.4$  Hz, 2H), 6.80 (d,  $J = 8.4$  Hz, 2H), 5.89–5.74 (m, 2H), 5.64 (dd,  $J = 16.0, 6.3$  Hz, 1H), 5.55 (dd,  $J = 16.0, 6.3$  Hz, 1H), 5.29 (d,  $J = 16.8$  Hz, 1H), 5.23 (d,  $J = 10.8$  Hz, 1H), 4.36–4.30 (m, 1H), 4.26 (s, 2H), 3.78 (s, 3H), 3.48 (s, 3H), 3.36 (dd,  $J = 9.6, 5.7$  Hz, 1H), 3.26 (dd,  $J = 9.6, 5.7$  Hz, 1H), 1.03 (s, 9H).



**Table 19**  $\Delta\delta$  ( $\delta_S - \delta_R$ ) data for the (*S*)- and (*R*)-MTPA-Mosher esters of allylic alcohol **196S**

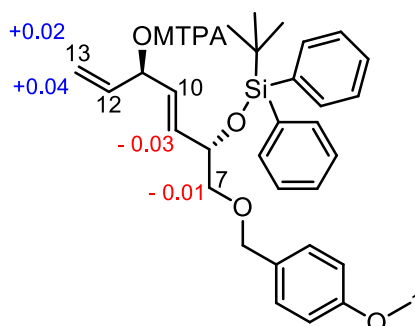
position	$\delta_{S\text{-ester}}$ (ppm)	$\delta_{R\text{-ester}}$ (ppm)	$\Delta\delta$ ( $\delta_S - \delta_R$ ) (ppm)
7	3.39	3.36	+0.03
	3.29	3.26	+0.03
8	4.34	4.33	+0.01
9	5.63	5.55	+0.08
10	5.73	5.64	+0.09
13	5.28	5.29	-0.01
	5.20	5.23	-0.03

**Allylic alcohol 196R**: light yellow oil (1.02 g, 30%):  $R_f = 0.53$  (20% EtOAc/hexanes);  $[\alpha]_D^{26} = +2.30$  ( $c$  1.06,  $\text{CHCl}_3$ );  $^1\text{H NMR}$  (300 MHz,  $\text{CDCl}_3$ )  $\delta$  7.69–7.63 (m, 4H), 7.43–7.29 (m, 6H), 7.13 (d,  $J = 8.4$  Hz, 2H), 6.82 (d,  $J = 8.4$  Hz, 2H), 5.73 (dd,  $J = 17.4, 10.5$  Hz, 1H), 5.65 (dd,  $J = 15.6, 6.3$  Hz, 1H), 5.48 (dd,  $J = 15.6, 6.3$  Hz, 1H), 5.15 (dd,  $J = 17.4$  Hz, 1H), 5.06 (dd,  $J = 10.5$  Hz, 1H), 4.43 (t,  $J = 5.7$  Hz, 1H), 4.38–4.36 (m, 1H), 4.34 (s, 2H), 3.77 (s, 3H), 3.45 (dd,  $J = 9.6, 5.7$  Hz, 1H), 3.35 (dd,  $J = 9.6, 5.7$  Hz, 1H), 1.06 (s, 9H);  $^{13}\text{C NMR}$  (75 MHz,  $\text{CDCl}_3$ )  $\delta$  159.7, 139.1, 136.2, 136.0, 134.1, 132.6, 131.7, 130.4, 129.6, 129.2, 127.5, 115.0, 113.7, 74.4, 73.1, 72.8, 72.7, 55.3, 27.1, 19.3; IR (thin film) 3447, 2857, 1513, 1111, 702  $\text{cm}^{-1}$ .



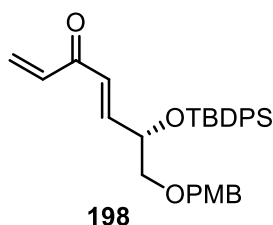
**(S)-MTPA ester of allylic alcohol 196R:**  $^1\text{H}$  NMR (300 MHz,  $\text{CDCl}_3$ )  $\delta$  7.68–7.58 (m, 4H), 7.51–7.26 (m, 11H), 7.10 (d,  $J = 8.4$  Hz, 2H), 6.83 (d,  $J = 8.4$  Hz, 2H), 5.91–5.71 (m, 3H), 5.61 (dd,  $J = 15.6, 6.3$  Hz, 1H), 5.31 (d,  $J = 17.1$  Hz, 1H), 5.25 (d,  $J = 10.2$  Hz, 1H), 4.35–4.32 (m, 1H), 4.29 (s, 2H), 3.80 (s, 3H), 3.51 (s, 3H), 3.37 (dd,  $J = 9.6, 6.3$  Hz, 1H), 3.29 (dd,  $J = 9.6, 6.3$  Hz, 1H), 1.05 (s, 9H).

**(R)-MTPA ester of allylic alcohol 196R:**  $^1\text{H}$  NMR (300 MHz,  $\text{CDCl}_3$ )  $\delta$  7.66–7.56 (m, 4H), 7.50–7.24 (m, 11H), 7.07 (d,  $J = 8.7$  Hz, 2H), 6.80 (d,  $J = 8.7$  Hz, 2H), 5.89–5.72 (m, 3H), 5.64 (dd,  $J = 16.0, 6.3$  Hz, 1H), 5.29 (d,  $J = 17.1$  Hz, 1H), 5.21 (d,  $J = 10.8$  Hz, 1H), 4.35–4.31 (m, 1H), 4.27 (s, 2H), 3.78 (s, 3H), 3.49 (s, 3H), 3.38 (dd,  $J = 9.6, 5.7$  Hz, 1H), 3.30 (dd,  $J = 9.6, 5.7$  Hz, 1H), 1.03 (s, 9H).



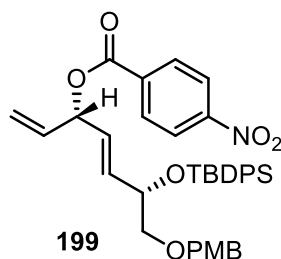
**Table 20**  $\Delta\delta$  ( $\delta_S - \delta_R$ ) data for the (*S*)- and (*R*)-MTPA-Mosher esters of allylic alcohol **196R**

position	$\delta_{S\text{-ester}}$ (ppm)	$\delta_{R\text{-ester}}$ (ppm)	$\Delta\delta$ ( $\delta_S - \delta_R$ ) (ppm)
7	3.37	3.38	-0.01
	3.29	3.30	-0.01
9	5.61	5.64	-0.03
13	5.31	5.29	+0.02
	5.25	5.21	+0.04

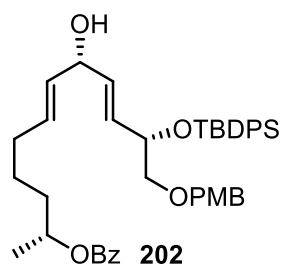


**Enone 198:** Enone **198** was prepared from allylic alcohol **196R** (600 mg, 1.19 mmol) using the general procedure for  $\text{MnO}_2$  oxidation. Purification of the crude residue by column chromatography (10–20% EtOAc/hexanes) yielded enone **198** (518.4 mg, 87%) as a colorless oil:  $R_f = 0.58$  (20% EtOAc/hexanes);  $^1\text{H NMR}$  (300 MHz,  $\text{CDCl}_3$ )  $\delta$  7.70–7.62 (m, 4H), 7.47–7.31 (m, 6H), 7.11 (d,  $J = 8.7$  Hz, 2H), 6.91 (dd,  $J = 15.6, 4.5$  Hz, 1H), 6.83 (d,  $J = 8.7$  Hz, 2H), 6.58 (dd,  $J = 15.6, 1.2$  Hz, 1H), 6.53 (dd,  $J = 17.4, 10.8$  Hz, 1H), 6.19 (dd,  $J = 17.4, 0.9$  Hz, 1H), 5.81 (dd,  $J = 10.8, 0.9$  Hz, 1H), 4.58–4.53 (m, 1H), 4.31 (s, 2H), 3.80 (s, 3H), 3.46 (dd,  $J = 9.6, 5.7$  Hz, 1H), 3.39 (dd,  $J = 9.6, 6.0$  Hz, 1H), 1.11 (s, 9H).



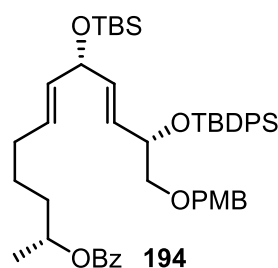


**4-Nitrobenzoate ester 199:** To a suspension of  $\text{PPh}_3$  (141.8 mg, 0.54 mmol, 3.0 equiv) in anhydrous toluene (1.0 mL, 0.5 M) at 0 °C was added diethyl azodicarboxylate (DEAD) (*ca.* 2.2 M solution in toluene, 260  $\mu\text{L}$ , 0.54 mmol, 3.0 equiv). After stirring at 0 °C for 1 h, a solution of allylic alcohol **196R** (90 mg, 0.18 mmol) in anhydrous toluene (1.2 mL, 0.15 M) and 4-nitrobenzoic acid (65.8 mg, 0.54 mmol, 3.0 equiv) were added. The reaction mixture was stirred from 0 °C to 60 °C for 18 h, then diluted with EtOAc (5 mL), quenched with  $\text{H}_2\text{O}$  (5 mL) and extracted with EtOAc (3x5 mL). The combined organic layers were washed with brine, dried over anhydrous  $\text{Na}_2\text{SO}_4$  and concentrated *in vacuo*. Purification of the crude residue by column chromatography yielded ester **199** (62.3 mg, 53%) as a light yellow oil:  $R_f = 0.65$  (20% EtOAc/hexanes);  $^1\text{H NMR}$  (300 MHz,  $\text{CDCl}_3$ )  $\delta$  8.30–8.26 (m, 2H), 8.19–8.14 (m, 2H), 7.67–7.60 (m, 4H), 7.42–7.27 (m, 6H), 7.10 (d,  $J = 8.7$  Hz, 2H), 6.79 (d,  $J = 8.7$  Hz, 2H), 5.92–5.77 (m, 3H), 5.71–5.63 (m, 1H), 5.30 (d,  $J = 15.9$  Hz, 1H), 5.26–5.23 (m, 1H), 4.40–4.34 (m, 1H), 4.32 (s, 2H), 3.78 (s, 3H), 3.46 (dd,  $J = 9.6, 5.4$  Hz, 1H), 3.36 (dd,  $J = 9.6, 6.0$  Hz, 1H), 1.05 (s, 9H).



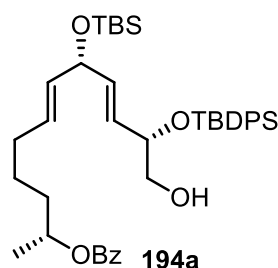
**(E)-Alkene 202:** To a solution of both key fragments **195** (628.4 mg, 2.86 mmol) and **196S** (720.5 mg, 1.43 mmol) in anhydrous  $\text{CH}_2\text{Cl}_2$  (15 mL, 0.1 M) was added 2nd generation Grubbs catalyst (61 mg, 0.07 mmol, 5 mol %). The reaction mixture was purged with argon for 5 min before being heated at reflux for 2 h. The reaction mixture was then cooled to room temperature and concentrated *in vacuo*. The crude

residue was purified by column chromatography (10–20% EtOAc/hexanes) to give (*E*)-alkene **202** (840.5 mg, 73%) as a light yellow oil:  $R_f = 0.30$  (30% EtOAc/hexanes);  $[\alpha]_D^{26} = +3.63$  ( $c$  1.07,  $\text{CHCl}_3$ );  $^1\text{H NMR}$  (300 MHz,  $\text{CDCl}_3$ )  $\delta$  8.03 (d,  $J = 7.8$  Hz, 2H), 7.67–7.61 (m, 4H), 7.53–7.48 (m, 1H), 7.42–7.22 (m, 8H), 7.12 (d,  $J = 8.7$  Hz, 2H), 6.81 (d,  $J = 8.7$  Hz, 2H), 5.64 (dd,  $J = 15.6, 6.0$  Hz, 1H), 5.56 (dd,  $J = 15.6, 7.5$  Hz, 1H), 5.49 (dd,  $J = 15.6, 6.0$  Hz, 1H), 5.34 (dd,  $J = 15.6, 6.3$  Hz, 1H), 5.19–5.13 (m, 1H), 4.41 (t,  $J = 6.0$  Hz, 1H), 4.37–4.33 (m, 1H), 4.32 (s, 2H), 3.76 (s, 3H), 3.43 (dd,  $J = 9.9, 6.0$  Hz, 1H), 3.35 (dd,  $J = 9.9, 6.0$  Hz, 1H), 2.07–2.01 (m, 2H), 1.80–1.45 (m, 4H), 1.32 (d,  $J = 6.3$  Hz, 3H), 1.04 (s, 9H);  $^{13}\text{C NMR}$  (75 MHz,  $\text{CDCl}_3$ )  $\delta$  166.2, 159.1, 136.0, 134.1, 133.4, 132.7, 131.6, 131.5, 130.8, 130.4, 129.5, 129.2, 128.3, 127.4, 113.7, 74.4, 72.8, 72.7, 71.5, 55.2, 35.6, 32.0, 27.0, 24.9, 20.1, 19.3; IR (thin film) 3503, 2857, 1716, 1275, 708  $\text{cm}^{-1}$ ; HRMS (ESI)  $m/z$  calcd for  $\text{C}_{43}\text{H}_{52}\text{NaO}_6\text{Si}$  ( $\text{M} + \text{Na}$ ) $^+$  715.3431, found 715.3423.



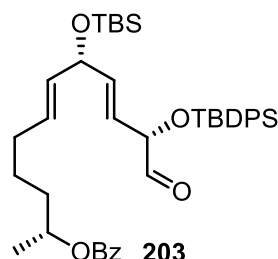
**Silyl ether 194:** To a solution of (*E*)-alkene **202** (820.6 mg, 1.18 mmol) in anhydrous  $\text{CH}_2\text{Cl}_2$  (6 mL, 0.2 M) were added DMAP (48.5 mg, 0.39 mmol, 0.33 equiv), imidazole (245.6 mg, 3.54 mmol, 3.0 equiv), followed by TBSCl (360.8 mg, 2.36 mmol, 2.0 equiv). The reaction mixture was stirred from 0 °C to room temperature overnight. The reaction was then quenched with  $\text{H}_2\text{O}$  (50 mL) and extracted with  $\text{CH}_2\text{Cl}_2$  (3x30 mL). The combined organic layers were washed with brine, dried over anhydrous  $\text{Na}_2\text{SO}_4$  and concentrated under reduced pressure. The crude product was purified by column chromatography (100% hexanes–5% EtOAc/hexanes) to give silyl ether **194** (840.2 mg, 88%) as a colorless oil:  $R_f = 0.60$  (20% EtOAc/hexanes);  $[\alpha]_D^{26} = +3.93$  ( $c$  1.02,  $\text{CHCl}_3$ );  $^1\text{H NMR}$  (300 MHz,  $\text{CDCl}_3$ )  $\delta$  8.04 (d,  $J = 7.8$  Hz, 2H), 7.69–7.61 (m, 4H), 7.54–7.52 (m, 1H), 7.45–7.26 (m, 8H), 7.10 (d,  $J = 8.7$  Hz, 2H), 6.81 (d,  $J = 8.7$  Hz, 2H), 5.66 (dd,  $J = 15.3, 6.0$  Hz, 1H), 5.48 (dd,  $J = 15.0, 7.2$  Hz, 1H), 5.46 (dd,  $J = 15.0, 5.0$  Hz, 1H), 5.29 (dd,  $J = 15.3, 6.3$  Hz, 1H), 5.19–5.13 (m,

1H), 4.50 (t,  $J = 5.4$  Hz, 1H), 4.36–4.32 (m, 1H), 4.30 (s, 2H), 3.80 (s, 3H), 3.42 (dd,  $J = 9.9, 6.0$  Hz, 1H), 3.32 (dd,  $J = 9.9, 6.0$  Hz, 1H), 2.07–2.01 (m, 2H), 1.78–1.39 (m, 4H), 1.34 (d,  $J = 6.3$  Hz, 3H), 1.04 (s, 9H), 0.88 (s, 9H), 0.02 (s, 6H);  $^{13}\text{C}$  NMR (75 MHz,  $\text{CDCl}_3$ )  $\delta$  166.3, 159.1, 136.1, 136.0, 134.4, 134.1, 134.0, 132.8, 130.9, 130.6, 129.8, 129.6, 129.5, 129.2, 128.4, 127.4, 113.7, 76.7, 74.7, 73.6, 72.8, 71.6, 55.3, 35.6, 32.0, 27.1, 26.0, 25.1, 20.2, 19.4, 18.4, –4.4; IR (thin film) 2857, 1716, 1508, 1112, 710  $\text{cm}^{-1}$ ; HRMS (ESI)  $m/z$  calcd for  $\text{C}_{49}\text{H}_{66}\text{NaO}_6\text{Si}_2$  ( $\text{M} + \text{Na}$ ) $^+$  829.4296, found 829.4299.

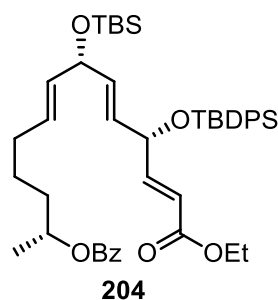


**Alcohol 194a:** To a solution of PMB ether **194** (740.5 mg, 0.91 mmol) in  $\text{CH}_2\text{Cl}_2:\text{H}_2\text{O}$  (4:1, 23 mL, 0.04 M) at 0 °C was added DDQ (330.6 mg, 1.45 mmol, 1.6 equiv). After being stirred from 0 °C to room temperature for 1.5 h, the reaction mixture was then quenched with saturated aqueous  $\text{NaHCO}_3$ . The resulting solution was extracted with  $\text{CH}_2\text{Cl}_2$  (3x10 mL). The combined organic layers were washed with brine, dried over anhydrous  $\text{Na}_2\text{SO}_4$  and concentrated under reduced pressure. Purification of the crude residue by column chromatography (5–20% EtOAc/hexanes) yielded alcohol **194a** (490.2 mg, 78%) as a colorless oil:  $R_f = 0.62$  (20% EtOAc/hexanes);  $[\alpha]_D^{26} = +15.6$  ( $c$  1.01,  $\text{CHCl}_3$ );  $^1\text{H}$  NMR (300 MHz,  $\text{CDCl}_3$ )  $\delta$  8.09 (dd,  $J = 8.4, 1.5$  Hz, 2H), 7.73–7.68 (m, 4H), 7.60–7.55 (m, 1H), 7.48–7.36 (m, 8H), 5.65 (d,  $J = 15.3, 6.6$  Hz, 1H), 5.57–5.50 (m, 1H), 5.47 (d,  $J = 15.3, 5.4$  Hz, 1H), 5.29 (d,  $J = 15.6, 6.0$  Hz, 1H), 5.25–5.19 (m, 1H), 4.51 (t,  $J = 5.4$  Hz, 1H), 4.33–4.27 (m, 1H), 3.53 (d,  $J = 2.7$  Hz, 2H), 2.08 (q,  $J = 6.9$  Hz, 2H), 1.83–1.47 (m, 4H), 1.39 (d,  $J = 6.0$  Hz, 3H), 1.11 (s, 9H), 0.93 (s, 9H), 0.06 (s, 6H);  $^{13}\text{C}$  NMR (75 MHz,  $\text{CDCl}_3$ )  $\delta$  166.2, 136.0, 135.8, 135.6, 133.9, 133.6, 132.8, 132.4, 130.9, 130.0, 129.9, 129.7, 129.6, 128.3, 128.0, 127.8, 127.6, 74.8, 73.4, 71.6, 67.0, 35.6, 31.9, 27.1, 25.9, 25.0,

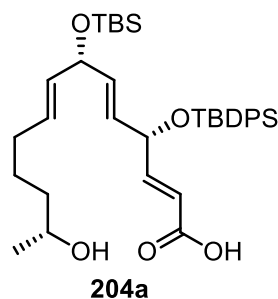
20.2, 19.4, 18.4, -4.4, -4.5; IR (thin film) 3439, 2932, 1716, 1112, 709  $\text{cm}^{-1}$ ; HRMS (ESI)  $m/z$  calcd for  $\text{C}_{41}\text{H}_{58}\text{NaO}_5\text{Si}_2$  ( $\text{M} + \text{Na}$ )<sup>+</sup> 709.3720, found 709.3710.



**Aldehyde 203:** Aldehyde **203** was prepared from **194a** (475.0 mg, 0.69 mmol) using the general procedure for TEMPO/ $\text{PhI}(\text{OAc})_2$ -mediated oxidation. The crude residue was purified by column chromatography (100% hexanes–10% EtOAc/hexanes) to afford aldehyde **203** (402.8 mg, 85%) as a light yellow oil:  $R_f = 0.60$  (20% EtOAc/hexanes);  $[\alpha]_D^{26} = +4.33$  ( $c$  1.01,  $\text{CHCl}_3$ );  $^1\text{H NMR}$  (300 MHz,  $\text{CDCl}_3$ )  $\delta$  9.40 (d,  $J = 1.2$  Hz, 1H), 8.04 (d,  $J = 7.2$  Hz, 2H), 7.64–7.60 (m, 4H), 7.56–7.52 (m, 1H), 7.45–7.35 (m, 8H), 5.83 (dd,  $J = 15.3, 4.8$  Hz, 1H), 5.59 (dd,  $J = 15.6, 5.4$  Hz, 1H), 5.53 (dd,  $J = 15.3, 6.9$  Hz, 1H), 5.33 (dd,  $J = 15.6, 6.3$  Hz, 1H), 5.16 (q,  $J = 6.0$  Hz, 1H), 4.60–4.57 (m, 1H), 4.52 (d,  $J = 5.4$  Hz, 1H), 2.10–2.03 (m, 2H), 1.76–1.47 (m, 4H), 1.33 (d,  $J = 6.3$  Hz, 3H), 1.11 (s, 9H), 0.89 (s, 9H), 0.04 (s, 3H), 0.03 (s, 3H);  $^{13}\text{C NMR}$  (75 MHz,  $\text{CDCl}_3$ )  $\delta$  199.7, 166.2, 137.1, 135.8, 132.9, 132.8, 132.1, 130.9, 130.5, 130.1, 130.0, 129.6, 128.3, 127.9, 127.8, 123.4, 79.0, 73.3, 71.5, 35.6, 31.9, 26.9, 25.9, 25.0, 20.2, 19.4, 18.4, -4.5, -4.6; IR (thin film) 2931, 1716, 1275, 1113, 773  $\text{cm}^{-1}$ ; HRMS (ESI)  $m/z$  calcd for  $\text{C}_{41}\text{H}_{56}\text{NaO}_5\text{Si}_2$  ( $\text{M} + \text{Na}$ )<sup>+</sup> 707.3564, found 707.3560.

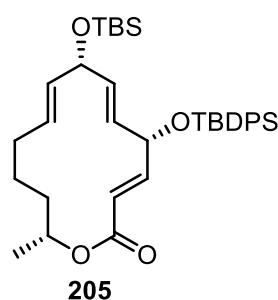


**(E)- $\alpha,\beta$ -Unsaturated ester 204:** Ester **204** was prepared from aldehyde **203** (390.2 mg, 0.56 mmol) using the general procedure for Wittig olefination. The crude product was purified by column chromatography (10–20% EtOAc/hexanes) to afford ester **204** (389.4 mg, 92%) as a light yellow oil:  $R_f = 0.51$  (20% EtOAc/hexanes);  $[\alpha]_D^{26} = +25.8$  ( $c$  1.08,  $\text{CHCl}_3$ );  $^1\text{H NMR}$  (300 MHz,  $\text{CDCl}_3$ )  $\delta$  8.06 (d,  $J = 7.5$  Hz, 2H), 7.76–7.64 (m, 4H), 7.58–7.53 (m, 1H), 7.46–7.33 (m, 8H), 6.83 (dd,  $J = 15.6, 4.8$  Hz, 1H), 6.01 (d,  $J = 15.6$  Hz, 1H), 5.56–5.44 (m, 2H), 5.35 (dd,  $J = 15.3, 4.8$  Hz, 1H), 5.26 (dd,  $J = 15.3, 6.0$  Hz, 1H), 5.21–5.15 (m, 1H), 4.78–4.74 (m, 1H), 4.50 (t,  $J = 5.4$  Hz, 1H), 4.20 (q,  $J = 6.9$  Hz, 2H), 2.05 (q,  $J = 6.9$  Hz, 2H), 1.79–1.47 (m, 1H), 1.35 (d,  $J = 6.3$  Hz, 3H), 1.30 (t,  $J = 6.9$  Hz, 3H), 1.09 (s, 9H), 0.89 (s, 9H), 0.02 (s, 6H);  $^{13}\text{C NMR}$  (75 MHz,  $\text{CDCl}_3$ )  $\delta$  166.4, 166.0, 148.7, 135.8, 135.7, 134.7, 134.5, 133.3, 133.2, 132.6, 132.1, 130.7, 129.9, 129.6, 129.5, 129.3, 128.2, 128.1, 127.5, 127.4, 119.6, 73.1, 71.3, 60.1, 35.4, 31.7, 26.8, 25.7, 24.8, 19.9, 19.2, 18.2, 14.1, –4.6, –4.8; IR (thin film) 2932, 1716, 1521, 1274, 710  $\text{cm}^{-1}$ ; HRMS (ESI)  $m/z$  calcd for  $\text{C}_{45}\text{H}_{62}\text{NaO}_6\text{Si}_2$  ( $\text{M} + \text{Na}$ ) $^+$  777.3983, found 777.3976.

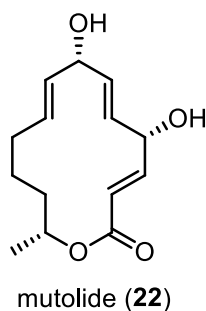


**Seco acid 204a:** Seco acid **204a** was prepared from ester **204** (205.1 mg, 0.27 mmol) using the general procedure for hydrolysis. The crude product was purified by column chromatography (50–80% EtOAc/hexanes) to give compound **204a** (120.6 mg, 68%) as a colorless oil:  $R_f = 0.25$  (60% EtOAc/hexanes);  $[\alpha]_D^{26} = +35.1$  ( $c$  1.03,  $\text{CHCl}_3$ );  $^1\text{H}$

NMR (300 MHz, CDCl<sub>3</sub>)  $\delta$  7.66–7.62 (m, 4H), 7.45–7.33 (m, 6H), 6.91 (dd,  $J$  = 15.6, 4.5 Hz, 1H), 5.97 (d,  $J$  = 15.6 Hz, 1H), 5.56–5.44 (m, 2H), 5.39 (dd,  $J$  = 15.6, 4.5 Hz, 1H), 5.28–5.21 (m, 1H), 4.79–4.77 (m, 1H), 4.47–4.46 (m, 1H), 3.81 (q,  $J$  = 5.7 Hz, 1H), 2.03–2.01 (m, 1H), 1.52–1.36 (m, 5H), 1.19 (d,  $J$  = 6.3 Hz, 3H), 1.09 (s, 9H), 0.88 (s, 9H), 0.02 (s, 6H); <sup>13</sup>C NMR (75 MHz, CDCl<sub>3</sub>)  $\delta$  171.3, 151.3, 136.0, 135.9, 135.1, 133.5, 133.3, 132.1, 130.4, 129.9, 129.8, 128.1, 127.7, 127.6, 119.3, 73.3, 73.2, 68.1, 38.7, 32.1, 27.0, 25.9, 25.3, 23.4, 19.4, 18.4, –4.4, –4.5; IR (thin film) 3414, 2931, 1698, 1112, 701 cm<sup>-1</sup>; HRMS (ESI)  $m/z$  calcd for C<sub>36</sub>H<sub>54</sub>NaO<sub>5</sub>Si<sub>2</sub> (M + Na)<sup>+</sup> 645.3407, found 645.3400.



**Macrolactone 205:** Macrolactone **205** was prepared from seco acid **204a** (75.5 mg, 0.12 mmol) using the general procedure for Shiina macrolactonization. The crude product was purified by column chromatography (5–20% EtOAc/hexanes) to give compound **205** (45.6 mg, 63%) as a colorless oil:  $R_f$  = 0.62 (10% EtOAc/hexanes);  $[\alpha]_D^{26}$  = –15.2 ( $c$  1.03, CHCl<sub>3</sub>); <sup>1</sup>H NMR (300 MHz, CDCl<sub>3</sub>)  $\delta$  7.69–7.62 (m, 4H), 7.43–7.33 (m, 6H), 6.71 (dd,  $J$  = 15.9, 6.9 Hz, 1H), 5.86 (dd,  $J$  = 15.9, 6.9 Hz, 1H), 5.59 (d,  $J$  = 15.6 Hz, 1H), 5.52 (dd,  $J$  = 15.6, 4.5 Hz, 1H), 5.51 (dd,  $J$  = 15.6, 6.0 Hz, 1H), 5.40–5.30 (m, 1H), 5.05–5.00 (m, 1H), 4.80–4.76 (m, 1H), 4.63 (t,  $J$  = 5.4 Hz, 1H), 2.08–1.88 (m, 2H), 1.61–1.29 (m, 4H), 1.24 (d,  $J$  = 6.3 Hz, 3H), 1.08 (s, 9H), 0.90 (s, 9H), 0.06 (s, 6H); <sup>13</sup>C NMR (75 MHz, CDCl<sub>3</sub>)  $\delta$  167.0, 150.8, 135.8, 135.3, 134.6, 133.6, 133.4, 131.0, 129.9, 129.7, 127.7, 117.8, 73.1, 71.6, 71.0, 34.7, 30.7, 26.9, 26.0, 23.8, 19.4, 18.7, 18.4, –4.4, –4.6; IR (thin film) 2931, 1716, 1541, 1257, 774 cm<sup>-1</sup>; HRMS (ESI)  $m/z$  calcd for C<sub>36</sub>H<sub>52</sub>NaO<sub>4</sub>Si<sub>2</sub> (M + Na)<sup>+</sup> 627.3302, found 627.3289.



**Mutolide (22):** To a solution of macrolactone **205** (45.3 mg, 0.07 mmol) in anhydrous THF (2 mL, 0.04 M) were added AcOH (200  $\mu$ L, 0.0035 mmol, 0.05 equiv) and TBAF (1.0 M solution in THF, 1.1 mL, 1.05 mmol, 15 equiv) dropwise at 0 °C. The reaction mixture was stirred from 0 °C room temperature overnight. The reaction was quenched with saturated aqueous NaHCO<sub>3</sub> (2 mL) and H<sub>2</sub>O (5 mL). The organic phase was extracted with EtOAc (4x5 mL), washed with brine and dried over with anhydrous Na<sub>2</sub>SO<sub>4</sub>. Purification of the crude residue by column chromatography (30–50% EtOAc/hexanes) yielded mutolide (**22**) (11.3 mg, 65%) as a white solid:  $R_f$  = 0.14 (60% EtOAc/hexanes); mp 167–169 °C;  $[\alpha]_D^{25} = -59.8$  ( $c$  1.79, CH<sub>3</sub>CN); <sup>1</sup>H NMR (300 MHz, acetone-*d*<sub>6</sub>)  $\delta$  6.72 (dd,  $J$  = 15.9, 6.9 Hz, 1H), 5.81 (dd,  $J$  = 15.9, 0.9 Hz, 1H), 5.78 (ddd,  $J$  = 15.9, 6.6, 0.9 Hz, 1H), 5.63 (dd,  $J$  = 15.6, 4.2 Hz, 1H), 5.59–5.57 (m, 1H), 5.45–5.36 (m, 1H), 5.03–4.95 (m, 1H), 4.90–4.87 (m, 1H), 4.62 (brs, 1H), 4.05 (brs, 1H, 7-OH), 1.99–1.92 (m, 2H), 1.59–1.48 (m, 2H), 1.47–1.30 (m, 2H), 1.20 (s,  $J$  = 6.6 Hz, 3H); <sup>13</sup>C NMR (75 MHz, acetone-*d*<sub>6</sub>)  $\delta$  167.0, 152.5, 135.8, 135.4, 131.1, 130.5, 118.2, 72.4, 71.3, 70.2, 35.0, 31.2, 24.5, 18.7; IR (thin film) 3360, 1710, 1624, 1110, 702 cm<sup>-1</sup>; HRMS (ESI)  $m/z$  calcd for C<sub>14</sub>H<sub>20</sub>NaO<sub>4</sub> (M + Na)<sup>+</sup> 275.1259, found 275.1250.

## CYTOTOXICITY ASSAY

Cytotoxic activity of synthetic **19** and **20** were evaluated against six human cancer cell lines including two breast adenocarcinoma (MDA-MB-231 and MCF-7), three cervical carcinoma (C33A, HeLa and SiHa) and one colorectal carcinoma (HCT116) cells as well as one monkey kidney non-cancerous cell line using 3-(4,5-dimethyl-2-thiazolyl)-2,5-diphenyl-2Htetrazolium bromide (MTT) assay by the laboratory of Dr. Panata Iawsipo, Burapha University using the general procedure previously described (Ponglikitmongkol *et al.*, 2012 and Tadpetch *et al.*, 2017). Cancer cells were exposed to various concentrations of compounds **19** and **20** (0–25  $\mu$ M; 0.2% (v/v) DMSO). Vero cells were exposed to 0–50  $\mu$ M of **19** and **20**. Each experiment was performed in triplicate and was repeated three times. Data was expressed as IC<sub>50</sub> values (the concentration needed for 50% cell growth inhibition) relative to the untreated cells (0.2% (v/v) DMSO) (means  $\pm$  SD). Cisplatin (0–50  $\mu$ M) and doxorubicin (0–1  $\mu$ M) (Pfizer, Australia) were used as positive controls.

Synthetic **21–23** were tested for their *in vitro* cytotoxic activity against three human cancer cell lines, including HCT116, MCF-7 and Calu-3 lung adenocarcinoma as well as Vero cells. Cell viability was measured using MTT assay by the laboratory of Prof. Dr. Chatchai Muanprasat of Chakri Naruebodindra Medical Institute, Faculty of Medicine Ramathibodi Hospital, Mahidol University. Three cancer cell lines and Vero cells were plated on 96-well plates at a density of  $1 \times 10^5$  cells/well and grown overnight, before 24-h exposure to culture media containing DMSO (control) or test compounds at indicated concentrations. After culture media were removed, cells were treated with MTT reagent (5 mg/ml) for 4 h at 37 °C and the reaction was stopped by addition of an aliquot of DMSO (100  $\mu$ l). Thirty minutes later, an absorbance at 540 nm was determined using a spectrophotometer.



## SHORT-CIRCUIT CURRENT ANALYSIS

Synthetic macrolides **21–23** were also evaluated for inhibitory effect on cystic fibrosis transmembrane conductance regulator (CFTR)-mediated chloride secretion in human intestinal epithelial (T84) cells by the laboratory of Prof. Dr. Chatchai Muanprasat of Chakri Naruebodindra Medical Institute, Faculty of Medicine Ramathibodi Hospital, Mahidol University. T84 cells were seeded onto inserts at a density of 500,000 cells/insert and cultured for 14 days. Inserts containing T84 cells (with transepithelial electrical resistance  $> 1,000 \Omega \cdot \text{cm}^2$ ) were then mounted in Ussing chambers filled with Kreb's solution containing (pH 7.3) 120 mM NaCl, 25 mM  $\text{NaHCO}_3$ , 3.3 mM  $\text{KH}_2\text{PO}_4$ , 0.8 mM  $\text{K}_2\text{HPO}_4$ , 1.2 mM  $\text{MgCl}_2$ , 1.2 mM  $\text{CaCl}_2$  and 10 mM glucose. The solutions were bubbled continuously with 95%  $\text{O}_2$ /5%  $\text{CO}_2$  and maintained at 37 °C. Short-circuit current was recorded using a DVC-1000 voltage-clamp (World Precision Instruments, Sarasota, Florida, USA) with Ag/AgCl electrode and 3M KCl agar bridge.

## REFERENCES

- Ariza, X.; Garcia, J.; Georges, Y.; Vicente, M. 2006. 1-Phenylprop-2-ynyl Acetate: A Useful Building Block for the Stereoselective Construction of Polyhydroxylated Chains. *Org. Lett.* 8 (20), 4501–4504.
- Avocetien, K.; Li, Y.; O'Doherty, G. A. 2014. The Alkyne Zipper Reaction in Asymmetric Synthesis. In Book: *Modern Alkyne Chemistry: Catalytic and Atom-Economic Transformations*. DOI 10.1002/9783527677894, 365–394.
- Avocetien, K. F.; Li, J. J.; Liu, X.; Wang, Y.; Xing, Y.; O'Doherty, G. A. 2016. *De Novo* Asymmetric Synthesis of Phoracantholide. *J. Org. Lett.* 18, 4970–4973.
- Ballio, A.; Evidente, A.; Graniti, A.; Randazzo, G.; Sparapano, L. 1988. Seiricuprolide, a New Phytotoxic Macrolide from a Strain of *Seiridium Cupressi* Infecting Cypress. *Phytochemistry*. 27 (10), 3117–3121.
- Burkhardt, K.; Fiedler, H. P.; Grabley, S.; Thiericke, R.; Zeeck, A. 1996. New Cineromycins and Musacins Obtained by Metabolite Pattern Analysis of *Streptomyces griseoviridis* (FH-S 1832). I. Taxonomy, Fermentation, Isolation and Biological Activity. *J. Antibiot.* 49, 432–437.
- Bode, H. B.; Walker, M.; Zeeck, A. 2000. Structure and Biosynthesis of Mutolide, a Novel Macrolide from a UV Mutant of the Fungus F-24'707. *Eur. J. Org. Chem.* 1451–1456.
- Baikadi, K.; Talakokkula, A.; Narsaiah, V. 2019. Studies Towards the Stereoselective Total Synthesis of 7-*O*-methylnigrosporolide. *ChemistrySelect*. 4, 5531–5534.
- Babcock, E. G.; Rahman, Md. S.; Taylor, J. E. 2023. Brønsted acid-catalysed desilylative heterocyclisation to form substituted furans. *Org. Biomol. Chem.* 21, 163–168.

- Chu, D. T. W. 1995. Section Review Anti-Infectives: Recent Developments in 14- and 15- Membered Macrolides. *Expert Opin. Invest. Drugs*. 4 (2), 65–94.
- Chu, D. T. W.; Plattner, J. J.; Katz, L. 1996. New Directions in Antibacterial Research. *J. Med. Chem.* 39 (20), 3853–3874.
- Christner, C.; Kullertz, G.; Fischer, G.; Zerlin, M.; Grabley, S.; Thiericke, R.; Taddei, A.; Zeeck, A. 1998. Albocycline- and Carbomycin-type Macrolides, Inhibitors of Human Prolyl Endopeptidases. *J. Antibiot.* 51 (3), 368–371.
- Crousse, B.; Mladenova, M.; Ducept, P.; Alami, M.; Linstrumelle, G. 1999. Stereoselective Approaches to (*E,E,E*) and (*Z,E,E*)- $\alpha$ -Chloro- $\omega$ -Substituted Hexatrienes: Synthesis of *all E* Polyenes. *Tetrahedron*. 55 (14), 4353–4368.
- Chatare, V. K.; Andrade, R. B. 2017. Total Synthesis of (–)-Albocycline. *Angew. Chem. Int. Ed.* 56, 5909–5911.
- Chen, W.; Tay, J.-H.; Ying, J.; Yu, X.-Q.; Pu, L. 2013. Catalytic Asymmetric Enyne Addition to Aldehydes and Rh(I)-Catalyzed Stereoselective Domino Pauson–Khand/[4+2] Cycloaddition. *J. Org. Chem.* 78, 2256–2265.
- Das, T.; Jana, N.; Nanda, S. 2010. Asymmetric Synthesis of (+)-Chloriolide. *Tetrahedron Lett.* 51 (19), 2644–2647.
- Dermenci, A.; Selig, P. S.; Domoal, R. A.; Spasov, K. A.; Anderson, K. S.; Miller, S. J. 2011. Quasi-Biomimetic Ring Contraction Promoted by a Cysteine-Based Nucleophile: Total Synthesis of Sch-642305, Some Analogs and Their Putative Anti-HIV Activities. *Chem. Sci.* 2, 1568–1572.
- Dey, P.; Chatterjee, S.; Gamre, S. S.; Chattopadhyay, S.; Sharma, A. 2017. An Enantioselective Synthesis of (5*S*, 6*R*, 11*S*, 14*R*)-Acremodiol. *Synthesis*. 49, 5231–5237.

- Els, H.; Celmer, W. D.; Murai, K. 1958. Oleandomycin (PA-105). II. Chemical Characterization (I). *J. Am. Chem. Soc.* 80, 3777–3782.
- Elleuch, L.; Shaaban, M.; Smaoui, S.; Mellouli, L.; Karray-Rebai, I.; Fguira, L. F. B.; Shaaban, K. A.; Laatsch, H. 2010. Bioactive Secondary Metabolites from a New Terrestrial *Streptomyces* sp. TN262. *Appl Biochem Biotechnol.* 162, 579–593.
- Ebine, M.; Fuwa, H.; Sasaki, M. 2011. Total Synthesis of (–)-Brevenal: A Streamlined Strategy for Practical Synthesis of Polycyclic Ethers. *Chem. Eur. J.* 17, 13754–13761.
- Egi, M.; Kawai, T.; Umemura, M.; Akai, S. 2012. Heteropolyacid-Catalyzed Direct Deoxygenation of Propargyl and Allyl Alcohols. *J. Org. Chem.* 77 (16), 7092–7097.
- Furumai, T.; Nagahama, N.; Okuda, T. 1968. Studies on a New Antibiotic, Albocycline. II. Taxonomic Studies on Albocycline-Producing Strains. *J. Antibiot.* 21, 85–90.
- Fernandes, P. B.; Bailer, R.; Swanson, R.; Hanson, C. W.; McDonald, E.; Ramer, N.; Hardy, D.; Shipkowitz, N.; Bower, R.; Gade, E. 1986. In Vitro and In Vivo Evaluation of A-56268 (TE-031), a New Macrolide. *Antimicrob. Agents Chemother.* 30, 865–873.
- Fawcett, A.; Nitsch, D.; Ali, M.; Bateman, J. M.; Myers, E. L.; Aggarwal, V. K. 2016. Regio- and Stereoselective Homologation of 1,2-Bis(Boronic Esters): Stereocontrolled Synthesis of 1,3-Diols and Sch725674. *Angew. Chem. Int. Ed.* 55, 14663–14667.
- Gao, G.; Moore, D.; Xie, R. G.; Pu, L. 2002. Highly Enantioselective Phenylacetylene Additions to Both Aliphatic and Aromatic Aldehydes. *Org. Lett.* 4 (23), 4143–4146.

- Gao, Y.; Stuhldreier, F.; Schmitt, L.; Wesselborg, S.; Wang, L.; Müller, W. E. G.; Kalscheuer, R.; Guo, Z.; Zou, K.; Liu, Z.; Proksch, P. 2020. Sesterterpenes and macrolide derivatives from the endophytic fungus *Aplosporella javeedii*. *Fitoterapia*. 146, 104652.
- Harwood, J.; Cutler, H. G.; Jacyno, J. M. 1995. Nigrosporolide, a Plant Growth-Inhibiting Macrolide from the Mould *Nigrospora sphaerica*. *Nat. Prod. Lett.* 6, 181–185.
- Jeong, W.; Kim, M. J.; Kim, H.; Kim, S.; Kim, D.; Shin, K. J. 2010. Substrate-Controlled Asymmetric Total Synthesis and Structure Revision of (+)-Itomanallene A. *Angew. Chem.* 122, 764–768.
- Joe, C. L.; Blaisdell, T. P.; Geoghan, A. F.; Tan, K. L. 2014. Distal-Selective Hydroformylation using Scaffolding Catalysis. *J. Am. Chem. Soc.* 136, 8556–8559.
- Keaton, K. A.; Phillips, A. J. 2008. Toward the Synthesis of Spirastrellolide B: A Synthesis of the C1–C23 Subunit. *Org. Lett.* 10 (6), 1083–1086.
- Kerrigan, M. H.; Jeon, S.-J.; Chen, Y. K.; Salvi, L.; Carroll, P. J.; Walsh, P. J. 2009. One-Pot Multicomponent Coupling Methods for the Synthesis of Diastereo- and Enantioenriched (*Z*)-Trisubstituted Allylic Alcohols. *J. Am. Chem. Soc.* 131, 8434–8445.
- Kobayashi, H.; Kanematsu, M.; Yoshida, M.; Shishido, K. 2011. Efficient Access to a Dihydropyran-Containing Macrolide via a Transannular Oxy-Michael Reaction: Total Synthesis of (+)-Aspergillide C. *Chem. Commun.* 47, 7440–7442.
- Kumaraswamy, G.; Sadaiah, K. 2012. Flexible Organocatalytic Enantioselective Synthesis of Heptadeca-1-Ene-4,6-Diyne-3*S*,8*R*,9*S*,10*S*-Tetrol and Its Congeners. *Tetrahedron*. 68, 262–271.

- Koyama, N.; Yotsumoto, M.; Onaka, H.; Tomoda, H. 2013. New Structural Scaffold 14-Membered Macrocyclic Lactone Ring for Selective Inhibitors of Cell Wall Peptidoglycan Biosynthesis in *Staphylococcus aureus*. *J. Antibiot.* 66, 303–304.
- Khamthong, N.; Rukachaisirikul, V.; Phongpaichit, S.; Preedanon, S.; Sakayaroj, J. 2014. An Antibacterial Cytochalasin Derivative from the Marine-Derived Fungus *Diaporthaceae* sp. PSU-SP2/4. *Phytochem. Lett.* 10, 5–9.
- Kanoh, N.; Kawamata, A.; Itagaki, T.; Miyazaki, Y.; Yahata, K.; Kwon, E.; Iwabuchi, Y. 2014. A Concise and Unified Strategy for Synthesis of the C1–C18 Macrolactone Fragments of FD-891, FD-892 and Their Analogues: Formal Total Synthesis of FD-891. *Org. Lett.* 16 (19), 5216–5219.
- Kenneth, J. Y.; Brown, K. B.; Sandridge, M. J.; Hering, B. A.; Sabat, M.; Pu, L. 2015. Rh(I)-Catalyzed Chemo- and Stereoselective Domino Cycloaddition of Optically Active Propargyl 2,4-Hexadienyl Ethers. *J. Org. Chem.* 80, 3195–3202.
- Kauloorkar, S. V.; Kumar, P. 2016. Total Synthesis of (–)-(6*R*,11*R*,14*S*)-Colletalol via Proline Catalyzed  $\alpha$ -Aminooxylation and Yamaguchi Macrolactonization. *RSC Adv.* 6, 63607–63612.
- Kundoor, G. R.; Battina, S. K.; Krishna, P. R. 2018. A Concise and Stereoselective Total Synthesis of Pestalotioprolide C Using Ring-Closing Metathesis. *Synthesis.* 50, 1152–1158.
- Kaur, A.; Prakash, R.; Pandey, S. K. 2018. An Asymmetric Synthesis of ((3*R*,6*R*)-6-Methylpiperidine-3-yl) methanol; A Piperidine Core Unit of Potent Dual Orexin Receptor Antagonist MK-6096. *ChemistrySelect.* 3, 12164–12166.

- Lauzon, S.; Tremblay, F.; Gagnon, D.; Godbout, C.; Chabot, C.; Mercier-Shanks, C.; Perreault, S.; DeSève, H.; Spino, C. 2008. Sterically Biased 3,3-Sigmatropic Rearrangement of Chiral Allylic Azides: Application to the Total Syntheses of Alkaloids. *J. Org. Chem.* 73, 6239–6250.
- Li, G. Z.; Yang, X. X.; Zhai, H. B. 2009. Total Synthesis of (–)-5,6-Dihydrocineromycin B. *J. Org. Chem.* 74 (3), 1356–1359.
- Liu, Z.; Byun, H. S.; Bittman, R. 2010. Asymmetric Synthesis of *D-ribo*-Phytosphingosine from 1-Tetradecyne and (4-Methoxyphenoxy)acetaldehyde. *J. Org. Chem.* 75, 4356–4364.
- Liu, Z.; Byun, H. -S.; Bittman, R. 2011. Total Synthesis of  $\alpha$ -1C-Galactosylceramide, an Immunostimulatory C-Glycosphingolipid, and Confirmation of the Stereochemistry in the First-Generation Synthesis. *J. Org. Chem.* 76, 8588–8598.
- Lisboa, M. P.; Jones, D. M.; Dudley, G. B. 2013. Formal Synthesis of Palmerolide A, Featuring Alkynogenic Fragmentation and *syn*-Selective Vinylogous Aldol Chemistry. *Org. Lett.* 15 (4), 886–889.
- Liu, S.; Dai, H.; Makhloufi, G.; Heering, C.; Janiak, C.; Hartmann, R.; Mándi, A.; Kurtán, T.; Müller, W. E. G.; Kassack, M. U.; Lin, W.; Liu, Z.; Proksch, P. 2016. Cytotoxic 14-Membered Macrolides from a Mangrove-Derived Endophytic Fungus, *Pestalotiopsis microspora*. *J. Nat. Prod.* 79, 2332–2340.
- McGuire, J. M.; Bunch, R. L.; Anderson, R. C.; Boaz, H. E.; Flynn, E. H.; Powell, H. M.; Smith, J. W. 1952. Ilotycin, a New Antibiotic. *Antibiot. Chemother.* 2, 281–283.
- Miyairi, N.; Takashima, M.; Shimizu, K.; Sakai, H. 1966. Studies on New Antibiotics, Cineromycins A and B. *J. Antibiot.* 19, 56–62.

- Macaulay, S. R. 1980. Isomerization of Internal Triple Bonds of Alkyn-1-ols with Sodium Hydride in 1,3-Diaminopropane. *J. Org. Chem.* 45, 735–737.
- Morimoto, S.; Takahashi, Y.; Watanabe, Y.; Omura, S. 1984. Chemical Modification of Erythromycins. I. Syntheses and Antibacterial Activity of 6-*O*-Methylerythromycin A. *J. Antibiot.* 37, 187–189.
- Marshall, J. A.; Adams, N. D. 2002. Total Synthesis of Bafilomycin V<sub>1</sub>: A Methanolysis Product of the Macrolide Bafilomycin C<sub>2</sub>. *J. Org. Chem.* 67 (3), 733–740.
- Mancilla, G.; Jiménez-Teja, D.; Femenía-Ríos, M.; Macías-Sánchez, A. J.; Collado, I. G.; Hernández-Galán, R. 2009. Novel Macrolide from Wild Strains of the Phytopathogen Fungus *Colletotrichum acutatum*. *Nat. Prod. Commun.* 4 (3), 395–398.
- Mohapatra, D. K.; Das, P. P.; Pattanayak, M. R.; Gayatri, G.; Sastry, G. N.; Yadav, J. S. 2010. Protecting-Group Directed Stereoselective Intramolecular Nozaki–Hiyama–Kishi Reaction: A Concise and Efficient Total Synthesis of Amphidinolactone A. *Eur. J. Org. Chem.* 4775–4784.
- Mao, Z. -Y.; Si, C.-M.; Liu, Y. -W.; Dong, H. -Q.; Wei, B. -G.; Lin, G. -Q. 2016. Asymmetric Synthesis of Apratoxin E. *J. Org. Chem.* 81, 9903–9911.
- Maity, S.; Kanikarapu, S.; Marumudi, K.; Kunwar, A. C.; Yadav, J. S.; Mohapatra, D. K. 2017. Asymmetric Total Synthesis of the Putative Structure of Diplopyrone. *J. Org. Chem.* 82, 4561–4568.
- Morita, M.; Kobayashi, Y. 2018. Stereocontrolled Synthesis of Resolvin D4. *J. Org. Chem.* 83 (7), 3906–3914.



- Muangnil, P.; Satitsri, S.; Tadpetch, K.; Saparpakorn, P.; Chatsudthipong, V.; Hannongbua, S.; Rukachaisirikul, V.; Muanprasat, C. 2018. A Fungal Metabolite Zearalenone as a CFTR Inhibitor and Potential Therapy of Secretory Diarrheas. *Biochem. Pharmacol.* 150, 293–304.
- Nolen, E. G.; Kurish, A. J.; Potter, J. M.; Donahue, L. A.; Orlando, M. D. 2005. Stereoselective Synthesis of  $\alpha$ -C-Glucosyl Serine and Alanine via a Cross-Metathesis/ Cyclization Strategy. *Org. Lett.* 7 (15), 3383–3386.
- Omura, S.; Morimoto, S.; Nagate, T.; Adachi, T.; Kohno, Y. 1992. Research and Development of Clarithromycin. *Yakugaku zasshi.* 112, 593–614.
- Oliveira, R. A.; Oliveira, J. M.; Rahmeier, L. H. S.; Comasseto, J. V.; Marino, J. P.; Menezes, P. H. 2008. Synthesis of the C7–C24 fragment of (–)-Macrolactin F. *Tetrahedron Lett.* 49, 5759–5761.
- Prakash, C.; Saleh, S.; Blair, I. A. 1989. Selective De-Protection of Silyl Ethers. *Tetrahedron Lett.* 30 (1), 19–22.
- Prasad, K. R.; Pawar, A. B. 2011. Enantioselective Formal Synthesis of Palmerolide A. *Org. Lett.* 13 (16), 4252–4255.
- Patil, R. S.; Ahire, K. M.; Ramana, C. V. 2012. Stereospecific Synthesis of C-Arabinofuranosides and Carba-Disaccharide Analogues of Motif C of Cell Wall AG Complex of *Mtb*. *Tetrahedron Lett.* 53, 6347–6350.
- Paul, D.; Saha, S.; Goswami, R. K. 2018. Total Synthesis of Pestalotioprolide E and Structural Revision of Pestalotioprolide F. *Org. Lett.* 20, 4606–4609.

- Rodrigo, S. K.; Guan, H. 2012. Quick Installation of a 1,4-Difunctionality via Regioselective Nickel-Catalyzed Reductive Coupling of Ynoates and Aldehydes. *J. Org. Chem.* 77 (18), 8303–8309.
- Reddy, Y.; Sabitha, G. 2016. Total Synthesis of Antifungal Macrolide Sch 725674. *ChemistrySelect.* 1, 2156–2158.
- Reddy, K. S. N.; Sabitha, G. 2017. First Total Synthesis of Pestalotioprolide C and its C7 Epimer. *Tetrahedron Lett.* 58 (12), 1198–1201.
- Roszak, R.; Beker, W.; Molga, K.; Grzybowski, B. A. 2019. Rapid and Accurate Prediction of  $pK_a$  Values of C–H Acids Using Graph Convolutional Neural Networks. *J. Am. Chem. Soc.* 141 (43), 17142–17149.
- Sobin, B. A.; English A. R.; Celmer, W. D. 1954–1955. PA 105, a New Antibiotic. In: Welch H., Marti-Ibanez F., Editors. *Antibiotics Annual*. Medical Encyclopedia, Inc., New York. 827–830.
- Schneider, A.; Spath, J.; Breiding-Mack, S.; Zeeck, A.; Grabley, S.; Thiericke, R. 1996. New Cineromycins and Musacins Obtained by Metabolite Pattern Analysis of *Streptomyces griseoviridis* (FH-S 1832). II. Structure Elucidation. *J. Antibiot.* 49, 438–446.
- Schiewe, H. J.; Zeeck, A. 1999. Cineromycins,  $\gamma$ -Butyrolactones and Ansamycins by Analysis of the Secondary Metabolite Pattern Created by a Single Strain of *Streptomyces*. *J. Antibiot.* 52 (7), 635–642.
- Stellfeld, T.; Bhatt, U.; Kalesse, M. 2004. Synthesis of the A,B,C-Ring System of Hexacyclinic Acid. *Org. Lett.* 6 (22), 3889–3892.


- Snider, B. B.; Zhou, J. 2006. Synthesis of (+)-Sch 642305 by a Biomimetic Transannular Michael Reaction. *Org. Lett.* 8 (7), 1283–1286.
- Shah, M.; Deshmukh, S. K.; Verekar, S. A.; Gohil, A.; Kate, A. S.; Rekha, V.; Kulkarni-Almeida, A. 2015. Anti-Inflammatory Properties of Mutolide Isolated from the Fungus *Lepidosphaeria* Species (PM0651419). *Springerplus.* 4, 706, DOI 10.1186/s40064-015-1493-6.
- Sharma, B. M.; Gontala, A.; Kumar, P. 2016. Enantioselective Modular Total Synthesis of Macrolides Sch725674 and C-4-*epi*-Sch725674. *Eur. J. Org. Chem.* 1215–1226.
- Takahashi, T.; Watanabe, H.; Kitahara, T. 2003. Enantioselective Total Synthesis of Cineromycin B. *Tetrahedron Lett.* 44 (51), 9219–9222.
- Trost, B. M.; Weiss, A. H.; von Wangelin A. J. 2006. Dinuclear Zn-Catalyzed Asymmetric Alkynylation of Unsaturated Aldehydes. *J. Am. Chem. Soc.* 128 (1), 8–9.
- Trost, B. M.; Weiss, A. H. 2006. Catalytic Enantioselective Synthesis of Adociacetylene B. *Org. Lett.* 8 (20), 4461–4464.
- Terekhova, L. P.; Galatenko, O. A.; Kulyaeva, V. V.; Malkina, N. D.; Boikova, Yu. V.; Katrukha, G. S.; Shashkov, A. S.; Gerbst, A. G.; Nifantiev, N. E. 2007. Isolation, NMR Spectroscopy, and Conformational Analysis of the Antibiotic INA 2770 (Cineromycin B) Produced by *Streptomyces* Strain. *Russ. Chem. Bull., Int. Ed.* 56 (4), 815–818.
- Turlington, M.; Yue, Y.; Yu, X.-Q.; Pu, L. 2010. Catalytic Asymmetric Synthesis of Chiral Propargylic Alcohols for the Intramolecular Pauson–Khand Cycloaddition. *J. Org. Chem.* 75, 6941–6952.

- Trost, B. M.; Bartlett, M. J.; Weiss, A. H.; von Wangelin, A. J.; Chan, V. S. 2012. Development of Zn-ProPhenol-Catalyzed Asymmetric Alkyne Addition: Synthesis of Chiral Propargylic Alcohols. *Chem. Eur. J.* 18, 16498–16509.
- Trost, B. M.; Bartlett, M. J. 2012. Transition-Metal-Catalyzed Synthesis of Aspergillide B: An Alkyne Addition Strategy. *Org. Lett.* 14(5), 1322–1325.
- Tanabe, Y.; Sato, E.; Nakajima, N.; Ohkubo, A.; Ohno, O.; Suenaga, K. 2014. Total Synthesis of Biselyngbyolide A. *Org. Lett.* 16, 2858–2861.
- Tadpetch, K.; Jeanmard, L.; Rukachaisirikul, V. 2015. Total Synthesis of the Proposed Structure of Pestalotioprolide A. *Tetrahedron:Asymmetry.* 26 (17), 918–923.
- Washington, J. A.; Wilson, W. R. 1985. Erythromycin: a Microbial and Clinical Perspective After 30 Years of Clinical Use. *Mayo Clin Proc.* 60, 189–203 and 271–278.
- Yang, S. W.; Chan, T. M.; Terracciano, J.; Loebenberg, D.; Patel, M.; Chu, M. 2005. Structure Elucidation of Sch 725674 from *Aspergillus* sp. *J. Antibiot.* 58 (8), 535–538.
- Yadav, J. S.; Ather, H.; Gayathri, K. U.; Rao, N. V.; Prasad, A. R. 2008. Stereoselective Formal Synthesis of Herbarumin III via Prins Cyclization. *Synthesis.* 24, 3945–3950.
- Yajima, A.; Oona, Y.; Nakagawa, R.; Nukada, T.; Yabuta, G. 2009. A Simple Synthesis of Four Stereoisomers of Roseoside and Their Inhibitory Activity on Leukotriene Release from Mice Bone Marrow-Derived Cultured Mast Cells. *Bioorg. Med. Chem.* 17, 189–194.

- Yadav, J. S.; Rao, C. V.; Prasad, A. R.; Ghamdi, A. A. K. A. 2011. Syntheses of Aggregation Pheromones of the Palm Weevils *Rhyncophorus vulneratus* and *R. phoenicis* and of (+)-*trans*-Whiskey Lactone. *Synthesis*. 23, 3894–3898.
- Yadav, J. S.; Swamy, T.; Subba Reddy, B. V.; Ravinder, V. 2014. Stereoselective Synthesis of C19–C27 fragment of bryostatin 11. *Tetrahedron Lett.* 55, 4054–4056.
- Yang, J.; Xu, W.; Cui, Q.; Fan, X.; Wang, L. -N.; Yu, Z. -X. 2017. Asymmetric Total Synthesis of (–)-Clovan-2,9-dione Using Rh(I)-Catalyzed [3+2+1] Cycloaddition of 1-Yne-vinylcyclopropane and CO. *Org. Lett.* 19, 6040–6043.
- Zhanel, G. G.; Dueck, M.; Hoban, D. J.; Vercaigne, L. M.; Embil, J. M.; Gin, A. S.; Karlowsky, J. A. 2001. Review of Macrolides and Ketolides: Focus on Respiratory Tract Infections. *Drugs*. 61 (4), 443–498.
- Zhanel, G. G.; Walters, M.; Noreddin, A.; Vercaigne, L. M.; Wierzbowski, A.; Embil, J. M.; Gin, A. S.; Douthwaite, S.; Hoban, D. J. 2002. The Ketolides: a Critical Review. *Drugs*. 62 (12), 1771–1804.
- Zhang, B.; Wang, Y.; Yang, S.-P.; Zhou, Y.; Wu, W.-B.; Tang, W.; Zuo, J.-P.; Li, Y.; Yue, J.-M. 2012. Ivorenolide A, an Unprecedented Immunosuppressive Macrolide from *Khaya ivorensis*: Structural Elucidation and Bioinspired Total Synthesis. *J. Am. Chem. Soc.* 134 (51), 20605–20608.
- Zhang, J.; Lin, X. P.; Li, L. C.; Zhong, B. L.; Liao, X. J.; Liu, Y. H.; Xu, S. H. 2015. Gliomasolides A–E, Unusual Macrolides from a Sponge-Derived Fungus *Gliomastix* sp. ZSDS1-F7-2. *RSC Adv.* 5, 54645–54648.
- Zhang, H.; Zou, J.; Yan, X.; Chen, J.; Cao, X.; Wu, J.; Liu, Y.; Wang, T. 2021. Marine-Derived Macrolides 1990–2020: An Overview of Chemical and Biological Diversity. *Mar. Drugs*. 19, 180.

## **APPENDIX**

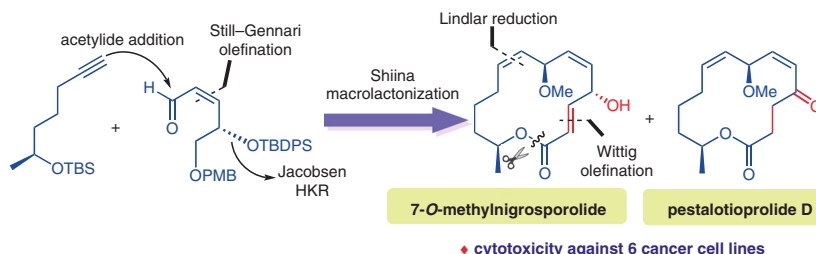
# Total Synthesis and Cytotoxic Activity of 7-O-Methylnigrosporolide and Pestalotioprolide D

Aticha Thiraporn<sup>a</sup>Panata lawsipo<sup>b</sup>Kwanruthai Tadpetch<sup>a</sup> 

<sup>a</sup> Division of Physical Science and Center of Excellence for Innovation in Chemistry, Faculty of Science, Prince of Songkla University, Hat Yai, Songkhla 90110 Thailand  
kwanruthai.t@psu.ac.th

<sup>b</sup> Department of Biochemistry and Center of Excellence for Innovation in Chemistry, and Research Unit of Natural Bioactive Compounds for Healthcare Products Development, Faculty of Science, Burapha University, Chonburi 20131, Thailand

Published as part of the Cluster  
*Organic Chemistry in Thailand*



Received: 30.01.2022

Accepted after revision: 09.03.2022

Published online: 09.03.2022

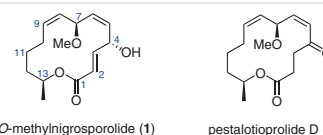
DOI: 10.1055/a-1792-8402; Art ID: st-2022-u0050-c

**Abstract** A convergent total synthesis of 7-*O*-methylnigrosporolide and pestalotioprolide D has been accomplished in 17 linear steps and overall yields of 1.7% and 2.6%, respectively, starting from (*S*)-propylene oxide and (*S*)-benzyl glycidyl ether. Our synthesis exploited an acetylide addition and a Shiina macrolactonization to assemble the macrocycle, a Lindlar reduction, and Wittig and Still–Gennari olefinations to construct the three alkene groups, as well as a Jacobsen hydrolytic kinetic resolution to install the stereogenic center. The selection of the silyl protecting group of the C-4 alcohol was crucial for the final deprotection step. Our synthesis also led to a hypothesis that pestalotioprolide D might be an artifact of 7-*O*-methylnigrosporolide. The cytotoxic activities of the two synthetic compounds against six human cancer cell lines were evaluated. Synthetic pestalotioprolide D showed more potent cytotoxic activity than 7-*O*-methylnigrosporolide against all the cancer cell lines tested, and the SiHa cervical cancer cell line was the most sensitive to both synthetic compounds.

**Key words** total synthesis, cytotoxicity, macrolactones, 7-*O*-methylnigrosporolide, pestalotioprolide D

Fourteen-membered macrolides are an important class of polyketide metabolites that attract considerable attention due to their diverse structures and prominent biological properties.<sup>1–5</sup> 7-*O*-methylnigrosporolide (**1**) and pestalotioprolide D (**2**) are new 14-membered macrolactones isolated along with seven other analogues from the mangrove-derived endophytic fungus *Pestalotiopsis microspora* by the research groups of Liu and Proksch (Figure 1).<sup>6</sup> Structurally, compound **1** is a 14-membered macrolide containing an (*E*)- $\alpha,\beta$ -unsaturated ester, two (*Z*)-olefin groups at C5–C6 and C8–C9, and three stereogenic centers. Compound **2** is structurally very similar to **1** except for the presence of a carbonyl group at the 4-position and saturation of the C2–C3 atoms. Compound **1** exhibited a potent cytotoxic activity against the L5178Y mouse lymphoma

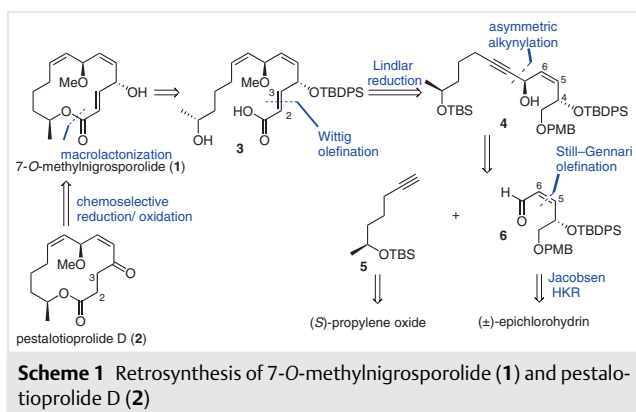
cells with an IC<sub>50</sub> value of 0.7  $\mu$ M, whereas compound **2** was less active (IC<sub>50</sub> = 5.6  $\mu$ M). Note that the cytotoxicity of **1** was greater than that of the positive control kahalalide F (IC<sub>50</sub> = 4.3  $\mu$ M). Moreover, compound **1** displayed additional cytotoxic effect against the A2780 human ovarian cancer cells with an IC<sub>50</sub> value of 28  $\mu$ M, whereas compound **2** was inactive. To verify the stereochemistry of the natural products and because of the promising biological activities of this group of macrolides, we began a program to synthesize selected compounds of this class. Here, we report a convergent total synthesis of 7-*O*-methylnigrosporolide (**1**) and pestalotioprolide D (**2**), as well as an evaluation of their cytotoxic activities against six human cancer cell lines.



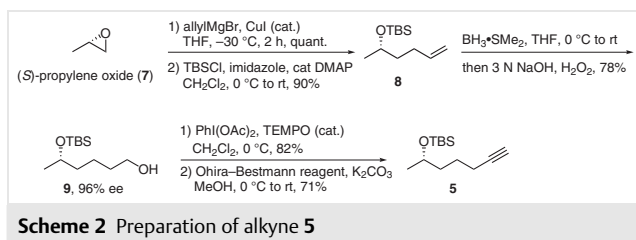
**Figure 1** Structures of 7-*O*-methylnigrosporolide (**1**) and pestalotioprolide D (**2**)

In 2019, Narsaiah et al. reported the studies toward a stereoselective total synthesis of **1**,<sup>7</sup> which our research group had already pursued with similar key synthetic strategies. Their key synthetic features involved acetylide addition and macrolactonization starting from *D*-mannitol and hex-5-en-1-ol; however, their synthesis suffered from an unsuccessful final removal of a MOM protecting group on the C4-hydroxy group to give the natural product. We therefore decided to continue with our synthesis to obtain synthetic **1**. Our retrosynthesis is outlined in Scheme 1. Macrolide **2** would be derived from **1** by chemoselective reduction of alkene at C2–C3, followed by oxidation of the C4-alcohol group to a ketone functional group. Macrolactonization of seco acid **3** would also be used to construct the

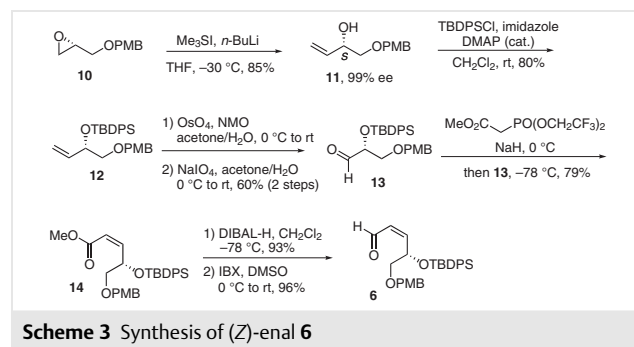
macrocycle. The (*E*)-olefin at C2–C3 would be elaborated from **4** through Wittig olefination. Asymmetric alkynylation would be exploited to install the C-7 alcohol stereogenic center and to assemble the key intermediates alkyne **5** and (*Z*)-enal **6**, which would be prepared from (*S*)-propylene oxide and ( $\pm$ )-epichlorohydrin, respectively. Since a protecting group of the hydroxy group at C4 is crucial for the final deprotection step, we selected *tert*-butyldiphenylsilyl (TBDPS) as the protecting group of choice in our synthesis because it can be removed under mild and nonacidic conditions.



Our synthesis commenced with the preparation of chiral alkyne **5** (Scheme 2). Although a few reports on the synthesis of **5** have appeared, some of the reagents needed are relatively expensive and some of the reactions were incompatible with our laboratory setup. We therefore chose to use a key Ohira–Bestmann homologation, similar to Narsiah's strategy, but with slight modification to shorten the synthetic sequence and to give a higher enantiopurity of the intermediate. Ring opening of commercially available (*S*)-propylene oxide (**7**) by allylmagnesium bromide in the presence of catalytic CuI furnished the corresponding chiral alcohol, which was protected with a TBS group to give the TBS ether **8** in 90% yield.<sup>8</sup> Hydroboration with  $\text{BH}_3\cdot\text{SMe}_2$  in THF led, after oxidative workup, to the formation of chiral alcohol **9** in 78% yield and 96% ee (determined by chiral HPLC).<sup>9</sup> Subsequent oxidation of alcohol **9** with  $\text{PhI}(\text{OAc})_2$  in the presence of catalytic TEMPO furnished the corresponding aldehyde, which was then treated with Ohira–Bestmann reagent (dimethyl 1-diazoacetylphosphonate) and  $\text{K}_2\text{CO}_3$  in methanol to afford the requisite alkyne **5** in 71% yield.<sup>10</sup>



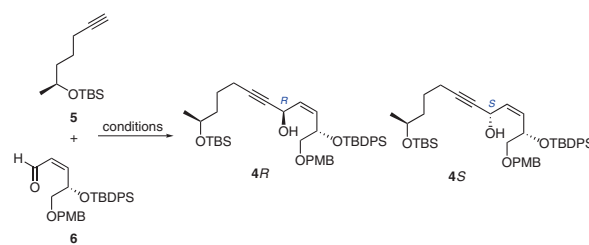
Our preparation of the requisite (*Z*)-enal **6** is shown in Scheme 3. Regioselective one-carbon homologation of the known chiral epoxide **10** [prepared in two steps from ( $\pm$ )-epichlorohydrin by Jacobsen hydrolytic kinetic resolution]<sup>11</sup> with trimethylsulfonium ylide gave the chiral allylic alcohol **11** in 85% yield.<sup>12</sup> The enantiopurity of **10** was confirmed to be 99% ee by chiral HPLC analysis of the corresponding benzoate derivative of **11**. The absolute configuration of the alcohol stereogenic center was confirmed by a Mosher's ester analysis. Subsequent protection of **11** with a TBDPS group gave the silyl ether **12**, which was subjected to oxidative cleavage to furnish aldehyde **13**. The next task was to install the (*Z*)-olefin, which was accomplished by Still–Gennari olefination with methyl bis(2,2,2-trifluoroethyl)phosphonoacetate and NaH to give the (*Z*)- $\alpha,\beta$ -unsaturated ester **14** in good yield.<sup>13</sup> The *Z*-geometry of the newly generated olefin was confirmed by its  $^1\text{H}$ – $^1\text{H}$  coupling constant of  $J = 11.7$  Hz. Finally, ester **14** was converted into the desired (*Z*)-enal **6** in excellent yield by DIBAL-H reduction followed by IBX oxidation.



We next attempted to assemble the key intermediates **5** and **6** by a Zn-mediated asymmetric alkynylation (Table 1). Our initial attempt employing (*S*)-BINOL as a chiral ligand under previously reported conditions<sup>14</sup> yielded none of the desired product, and the starting materials were recovered (Table 1, entry 1). Trost's protocol using 1.5 or 3 equivalents of  $\text{ZnMe}_2$  and 10 mol% of (*S,S*)-ProPhenol [(*S,S*)-2,6-bis(2-[hydroxy(diphenyl)methyl]pyrrolidin-1-yl)methyl]-4-methylphenol] as a chiral ligand in toluene<sup>15</sup> also failed to furnish any of the desired product, and again only the starting materials were observed (entries 2 and 3). To our delight, increasing the amount of  $\text{ZnMe}_2$  to 5.0 equivalents and that of (*S,S*)-ProPhenol to 20 mol% resulted in the formation of the propargylic alcohols **4R** and **4S** as a 2:1 mixture of separable diastereomers albeit in a combined yield of only 33% (entry 4). The absolute configurations of **4R** and **4S** were determined by Mosher's ester analyses.

Because of the unsatisfactory results of the Zn-mediated asymmetric alkynylation, we decided to assemble the key intermediates **5** and **6** by an acetylide addition in the hope that the chiral entities in each fragment would somehow facilitate asymmetric induction in this step (Scheme 4).

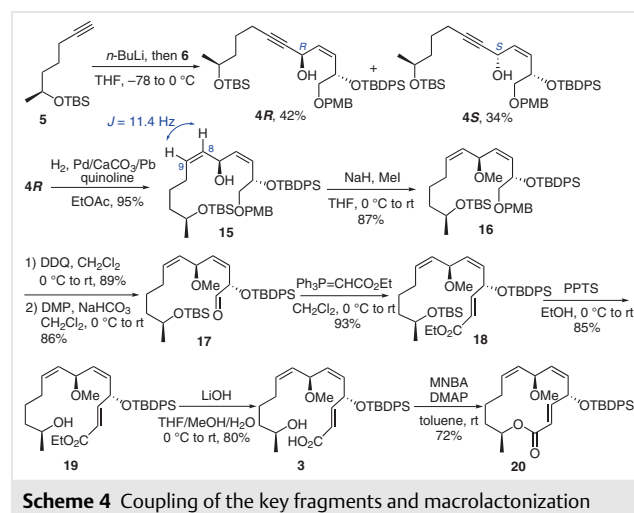


**Table 1** Screening of the Zn-Mediated Asymmetric Alkynylation


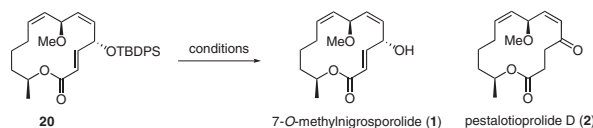
Entry	Reagents	Solvent	Temp	Time (h)	Products (yield)
1	ZnEt <sub>2</sub> (3.0 equiv), (S)-BINOL (20 mol%), Ti(O- <i>i</i> Pr) <sub>4</sub> (20 mol%), Cy <sub>2</sub> NH (5 mol%)	Et <sub>2</sub> O	rt	19	no reaction
2	ZnMe <sub>2</sub> (1.5 equiv), (S,S)-ProPhenol (10 mol%)	toluene	0 °C to rt	4	no reaction
3	ZnMe <sub>2</sub> (3.0 equiv), (S,S)-ProPhenol (10 mol%)	toluene	0 °C to rt	7	no reaction
4	ZnMe <sub>2</sub> (5.0 equiv), (S,S)-ProPhenol (20 mol%)	toluene	0 °C to rt	18	<b>4R</b> (22%), <b>4S</b> (11%)

Treatment of the acetylide generated in situ by BuLi deprotonation of alkyne **5** with (*Z*)-enal **6** in THF at  $-78$  to  $0$  °C provided the propargylic alcohols **4R** (42%) and **4S** (34%); these were separable by column chromatography on silica gel. The absolute configuration of the newly formed stereogenic center of each diastereomer was confirmed by a Mosher's ester analysis (See Supporting Information). Attempts to convert the undesired diastereomer **4S** into **4R** by oxidation followed by stereoselective reduction with CBS oxazaborolidine<sup>16</sup> were unsuccessful, as no preferential formation of **4R** was observed. At this stage, we chose to reduce the alkyne moiety of **4R** to a (*Z*)-olefin. This transformation was smoothly accomplished by hydrogenation with Lindlar's catalyst in ethyl acetate, which resulted in the formation of (*Z*)-olefin **15** in 95% yield.<sup>17</sup> The *Z*-geometry of the olefin was again confirmed by the coupling constant of  $J = 11.4$  Hz between H8 and H9. Next, the hydroxy group at C-7 was methylated by treatment with iodomethane and NaH as a base to provide the methoxy derivative **16** in 87% yield. The next task was to install the  $\alpha,\beta$ -unsaturated ester, which was accomplished in three steps. Removal of the *p*-methoxybenzyl (PMB) protecting group was smoothly accomplished by treatment with DDQ<sup>18</sup> to give the corresponding primary alcohol, which was then subjected to oxidation with Dess–Martin periodinane in the presence of NaHCO<sub>3</sub> in CH<sub>2</sub>Cl<sub>2</sub> to give aldehyde **17** in 86% yield. Wittig olefination of **17** with (carbethoxymethylene)triphenylphosphorane delivered the (*E*)- $\alpha,\beta$ -unsaturated ester **18** in 93% yield. The geometry of the newly generated double bond was confirmed by its <sup>1</sup>H–<sup>1</sup>H coupling constant of  $J =$

15.6 Hz. The next challenging task was to selectively remove the TBS protecting group in the presence of the TBDPS group. To our delight, this was cleanly accomplished by using pyridinium *p*-toluenesulfonate (PPTS) in ethanol to furnish the secondary alcohol **19** as a single product in 85% yield. Subsequent hydrolysis of the ester with LiOH in THF and aqueous methanol<sup>19</sup> afforded the seco acid **3** in good yield; this was then subjected to Shiina macrolactonization with 2-methyl-6-nitrobenzoic anhydride (MNBA) and DMAP in toluene to give the macrocycle **20** in 72% yield.<sup>7</sup>



With the macrocyclic core of **1** in hand, the final, yet challenging, task was to remove the TBDPS protecting group from the C-4 alcohol (Table 2). NH<sub>4</sub>F was initially chosen as a reagent, as it has been shown to be successful in silyl-group deprotections of similar substrates containing adjacent  $\alpha,\beta$ -unsaturated ester groups.<sup>20</sup> Disappointingly, no desilylations were observed under the initial conditions (Table 2, entry 1). Replacement of the desilylating agents with PPTS<sup>21</sup> or (1*S*)-(+)-camphor-10-sulfonic acid (CSA)<sup>22</sup> also resulted in no reaction (entries 2 and 3). We then attempted to employ typical silyl deprotection conditions with TBAF (3 equiv) in THF from  $0$  °C to room temperature (entry 4). To our surprise, these conditions led to the formation of pestalotioprolide D (**2**) in 48% yield (70% based on recovered **20**). Upon increasing the amount of TBAF to five equivalents, compound **2** was obtained in 75% yield and the starting **20** was completely consumed (entry 5). Gratifyingly, deprotection conditions using a large excess of TBAF buffered with acetic acid (5 mol%) in THF at an elevated temperature<sup>23</sup> (entry 6) delivered the desired 7-*O*-methyl-nigrosporolide (**1**) in 50% yield (72% yield based on recovered starting material). The <sup>1</sup>H and <sup>13</sup>C NMR spectroscopic data as well as HRMS data for synthetic **1** and **2** were in good agreement with those reported for natural **1** and **2** (see Tables 1 and 2 in the Supporting Information). The specific rotation of synthetic **1** ( $[\alpha]_D^{25} +66.8$ ;  $c$  0.20, MeOH) was

**Table 2** Screening for Silyl Deprotection of **20**

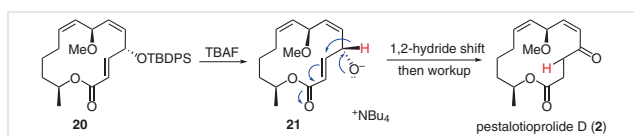
Entry	Reagent	Solvent	Temp	Time	Product	Yield (%)
1	NH <sub>4</sub> F (10 equiv)	MeOH	0 °C	8	nr <sup>a</sup>	–
2	PPTS (5 equiv)	EtOH	0 °C to rt	17	nr	–
3	CSA (1 equiv)	CH <sub>2</sub> Cl <sub>2</sub> :MeOH	0 °C to rt	6	nr	–
4	TBAF (3 equiv)	THF	0 °C to rt	4	<b>2</b>	48 (70) <sup>b</sup>
5	TBAF (5 equiv)	THF	0 °C to rt	2.5	<b>2</b>	75
6	TBAF (8 equiv) + AcOH (5 mol%)	THF	0–63 °C	10	<b>1</b>	50 (72) <sup>b</sup>

<sup>a</sup> nr = No reaction.

<sup>b</sup> Yield based on recovered starting material.

in good agreement with the reported value for the natural product **1** ( $[\alpha]_D^{25} +67.0$ ,  $c$  0.20, MeOH). The specific rotation of synthetic **2** was  $[\alpha]_D^{26} -35.6$  ( $c$  0.10, MeOH), which was similar to that of the natural product **2** ( $[\alpha]_D^{20} -30.0$ ,  $c$  0.10, MeOH).

The direct formation of pestalotioprolide D (**2**) under typical TBAF desilylation conditions for **20** suggested that **2** might be an artifact of 7-*O*-methylnigrosporolide (**1**). We proposed that **2** is formed by TBAF-mediated desilylation of **20** (Scheme 5). Treatment of **20** with TBAF generates strongly basic tetrabutylammonium alkoxide **21**. A 1,2-hydride shift of H-4 to the adjacent electron-deficient olefin delivers the C-4 ketone moiety of **2**, which upon workup

**Scheme 5** Proposed mechanism for the formation of pestalotioprolide D (**2**)

leads to pestalotioprolide D (**2**). This phenomenon has also been observed by Rodrigo and Guan in a silyl deprotection of a similar  $\gamma$ -silyloxy  $\alpha,\beta$ -unsaturated ester scaffold with TBAF.<sup>24</sup> This proposed mechanism was supported by the fact that the addition of acetic acid as a buffer mitigated the basicity of TBAF and suppressed the 1,2-hydride shift pathway, thereby furnishing the requisite desilylation product 7-*O*-methylnigrosporolide (**1**).

The synthetic 7-*O*-methylnigrosporolide (**1**) and pestalotioprolide D (**2**) were evaluated for their cytotoxic activities against six human cancer cell lines: two breast adenocarcinoma cell lines (MDA-MB-231 and MCF-7), three cervical carcinoma cell lines (C33A, HeLa and SiHa), and one colorectal carcinoma cell line (HCT116), as well as one monkey kidney noncancerous (Vero) cell line (Table 3). Our results showed that compound **1** displayed a very low cytotoxic activity against all cancer cell lines tested, with IC<sub>50</sub> values in the range 35.17–69.13  $\mu$ M, whereas compound **2** exhibited a significantly stronger cytotoxic activity against all cell lines compared to **1** (IC<sub>50</sub> range 8.90–53.25  $\mu$ M). Among the six cell lines tested, the SiHa cell line was the

**Table 3** Cytotoxic Activities of 7-*O*-Methylnigrosporolide (**1**) and Pestalotioprolide D (**2**) against Six Human Cancer Cell Lines

Cell line	Cytotoxicity, IC <sub>50</sub> ( $\mu$ M)			
	<b>1</b>	<b>2</b>	Cisplatin	Doxorubicin
MDA-MB-231	60.75 $\pm$ 1.50	21.10 $\pm$ 4.04	17.00 $\pm$ 1.46	0.16 $\pm$ 0.01
MCF-7	61.61 $\pm$ 5.01	53.25 $\pm$ 5.15	17.98 $\pm$ 2.97	0.24 $\pm$ 0.03
C33A	57.38 $\pm$ 9.51	22.00 $\pm$ 4.92	6.50 $\pm$ 0.76	0.22 $\pm$ 0.02
HeLa	69.13 $\pm$ 16.87	33.76 $\pm$ 13.23	8.20 $\pm$ 0.90	0.33 $\pm$ 0.08
SiHa	35.17 $\pm$ 10.77	8.90 $\pm$ 2.51	6.10 $\pm$ 0.85	0.51 $\pm$ 0.08
HCT116	54.25 $\pm$ 2.47	13.75 $\pm$ 0.35	11.75 $\pm$ 3.89	0.15 $\pm$ 0.01
Vero	74.13 $\pm$ 10.41	42.50 $\pm$ 3.07	14.42 $\pm$ 3.86	>1

most sensitive to both compounds. Both synthetic **1** and **2** showed a much lower cytotoxicity than the standard drugs cisplatin and doxorubicin; however, they were relatively nontoxic to noncancerous Vero cells.

In summary, we have completed a convergent total synthesis of 7-*O*-methylnigrosporolide (**1**) and pestalotioprolide D (**2**),<sup>25</sup> starting from (*S*)-propylene oxide and (*S*)-benzyl glycidyl ether. The target compounds **1** and **2** were obtained in 17 longest linear steps and 22 total steps in overall yields of 1.7% and 2.6%, respectively. The key features of our synthesis include acetylde addition and a Shiina macrolactonization to assemble the macrocycle, Lindlar reduction, Wittig and Still–Gennari olefinations to construct the three olefins, and a Jacobsen hydrolytic kinetic resolution to install the stereogenic center. The TBDPS group proved to be a suitable protecting group for the C4 hydroxy group, permitting a smooth final deprotection. Our synthesis led to the hypothesis that **2** might be an artifact of **1**. Synthetic **1** and **2** were tested for their cytotoxic activity against six human cancer cell lines. **2** showed greater cytotoxic activity than **1** against all cell lines, and the SiHa cervical cancer cell line was the most sensitive to both synthetic compounds.

## Conflict of Interest

The authors declare no conflict of interest.

## Funding Information

This work was financially supported by Prince of Songkla University (Grant No. SCI610438S) and the Faculty of Science Research Fund. We also acknowledge partial support from Thailand Science Research and Innovation, supported through the Direct Basic Research Grant (DBG6280007), the Center of Excellence for Innovation in Chemistry (PERCH-CIC), the Ministry of Higher Education, Science, Research and Innovation. Additional support was generously provided by the Graduate School, Prince of Songkla University, the Science Achievement Scholarship of Thailand (SAST), and a Thesis Research Grant under the Scholarship Support for Potential Scholars in Research and Innovation to Enhance the Economic, Social and Community Sectors (Talent Utilization) for A.T.

## Supporting Information

Supporting information for this article is available online at <https://doi.org/10.1055/a-1792-8402>.

## References and Notes

- (1) (a) Chu, D. T. W. *Expert Opin. Invest. Drugs* **1995**, *4*, 65. (b) Zhanel, G. G.; Dueck, M.; Hoban, D. J.; Vercaigne, L. M.; Embil, J. M.; Gin, A. S.; Karlowsky, J. A. *Drugs* **2001**, *61*, 443.
- (2) Yang, S.-W.; Chan, T.-M.; Terracciano, J.; Loebenber, D.; Patel, M.; Chu, M. J. *Antibiot.* **2005**, *58*, 535.
- (3) Bode, H. B.; Walker, M.; Zeeck, A. *Eur. J. Org. Chem.* **2000**, 1451.
- (4) (a) Ballio, A.; Evidente, A.; Graniti, A.; Randazzo, G.; Sparapano, L. *Phytochemistry* **1988**, *27*, 3117. (b) Bartolucci, C.; Cerrini, S.; Lamba, D. *Acta Crystallogr., Sect. C* **1992**, *48*, 83.
- (5) Kito, K.; Ookura, R.; Yoshida, S.; Namikoshi, M.; Ooi, T.; Kusumi, T. *Org. Lett.* **2008**, *10*, 225.
- (6) Liu, S.; Dai, H.; Makhoulfi, G.; Heering, C.; Janiak, C.; Hartmann, R.; Mándi, A.; Kurtán, T.; Müller, W. E. G.; Kassack, M. U.; Lin, W.; Liu, Z.; Proksch, P. *J. Nat. Prod.* **2016**, *79*, 2332.
- (7) Baikadi, K.; Talakokkula, A.; Narsaiah, V. *ChemistrySelect* **2019**, *4*, 5531.
- (8) (a) Ebine, M.; Fuwa, H.; Sasaki, M. *Chem. Eur. J.* **2011**, *17*, 13754. (b) Kaur, A.; Prakash, R.; Pandey, S. K. *ChemistrySelect* **2018**, *3*, 12164.
- (9) Dey, P.; Chatterjee, S.; Gamre, S. S.; Chattopadhyay, S.; Sharma, A. *Synthesis* **2017**, *49*, 5231.
- (10) Marshall, J. A.; Adams, N. D. *J. Org. Chem.* **2002**, *67*, 733.
- (11) Yadav, J. S.; Swamy, T.; Subba Reddy, B. V.; Ravinder, V. *Tetrahedron Lett.* **2014**, *55*, 4054.
- (12) (a) Jeong, W.; Kim, M. J.; Kim, H.; Kim, S.; Kim, D.; Shin, K. J. *Angew. Chem.* **2010**, *122*, 764. (b) Kumaraswamy, G.; Sadaiah, K. *Tetrahedron* **2012**, *68*, 262.
- (13) Maity, S.; Kanikarapu, S.; Marumudi, K.; Kunwar, A. C.; Yadav, J. S.; Mohapatra, D. K. *J. Org. Chem.* **2017**, *82*, 4561.
- (14) (a) Turlington, M.; Yue, Y.; Yu, X.-Q.; Pu, L. *J. Org. Chem.* **2010**, *75*, 6941. (b) Chen, W.; Tay, J.-H.; Ying, J.; Yu, X.-Q.; Pu, L. *J. Org. Chem.* **2013**, *78*, 2256. (c) Kenneth, J. Y.; Brown, K. B.; Sandridge, M. J.; Hering, B. A.; Sabat, M.; Pu, L. *J. Org. Chem.* **2015**, *80*, 3195.
- (15) (a) Trost, B. M.; Weiss, A. H.; von Wangelin, A. J. *J. Am. Chem. Soc.* **2006**, *128*, 8. (b) Trost, B. M.; Weiss, A. H. *Org. Lett.* **2006**, *8*, 4461. (c) Liu, Z.; Byun, H.-S.; Bittman, R. *J. Org. Chem.* **2010**, *75*, 4356. (d) Trost, B. M.; Bartlett, M. J.; Weiss, A. H.; von Wangelin, A. J.; Chan, V. S. *Chem. Eur. J.* **2012**, *18*, 16498.
- (16) (a) Meiries, S.; Bartoli, A.; Decostanzi, M.; Parrain, J. L.; Commeiras, L. *Org. Biomol. Chem.* **2013**, *11*, 4882. (b) Duymaz, A.; Korber, J.; Hofmann, C.; Gerlach, D.; Nubbemeyer, U. *Synthesis* **2018**, *50*, 1246. (c) Majetich, G.; Zhang, Y.; Tian, X.; Britton, J. E.; Li, Y.; Phillips, R. *Tetrahedron* **2011**, *67*, 10129. (d) Zhang, B.; Wang, Y.; Yang, S.-P.; Zhou, Y.; Wu, W.-B.; Tang, W.; Zuo, J.-P.; Li, Y.; Yue, J.-M. *J. Am. Chem. Soc.* **2012**, *134*, 20605. (e) Parker, K.; Katsoulis, I. A. *Org. Lett.* **2004**, *6*, 1413.
- (17) Ariza, X.; Garcia, J.; Georges, Y.; Vicente, M. *Org. Lett.* **2006**, *8*, 4501.
- (18) (a) Joe, C. L.; Blaisdell, T. P.; Geoghan, A. F.; Tan, K. L. *J. Am. Chem. Soc.* **2014**, *136*, 8556. (b) Kerrigan, M. H.; Jeon, S.-J.; Chen, Y. K.; Salvi, L.; Carroll, P. J.; Walsh, P. J. *J. Am. Chem. Soc.* **2009**, *131*, 8434.
- (19) Snider, B. B.; Zhou, J. *Org. Lett.* **2006**, *8*, 1283.
- (20) (a) Kauloorkar, S. V.; Kumar, P. *RSC Adv.* **2016**, *6*, 63607. (b) Das, T.; Jana, N.; Nanda, S. *Tetrahedron Lett.* **2010**, *51*, 2644.
- (21) Prakash, C.; Saleh, S.; Blair, I. A. *Tetrahedron Lett.* **1989**, *30*, 19.
- (22) Stellfeld, T.; Bhatt, U.; Kalesse, M. *Org. Lett.* **2004**, *6*, 3889.
- (23) (a) Mohapatra, D. K.; Das, P. P.; Pattanayak, M. R.; Gayatri, G.; Sastry, G. N.; Yadav, J. S. *Eur. J. Org. Chem.* **2010**, 4775. (b) Dermenci, A.; Selig, P. S.; Domaol, R. A.; Spasov, K. A.; Anderson, K. S.; Miller, S. J. *Chem. Sci.* **2011**, *2*, 1568. (c) Kanoh, N.; Kawamata, A.; Itagaki, T.; Miyazaki, Y.; Yahata, K.; Kwon, E.; Iwabuchi, Y. *Org. Lett.* **2014**, *16*, 5216.
- (24) Rodrigo, S. K.; Guan, H. *J. Org. Chem.* **2012**, *77*, 8303.
- (25) **7-O-Methylnigrosporolide (1)**: AcOH (340  $\mu$ L, 0.006 mmol, 0.05 equiv) and a 1.0 M solution of TBAF in THF (250  $\mu$ L, 0.96 mmol, 8.0 equiv) were sequentially added dropwise to a solution of macrolactone **20** (60 mg, 0.12 mmol) in anhyd THF (3 mL, 0.04 M) at 0 °C. The mixture was

stirred at 0 °C to rt for 1 h and then heated at 63 °C for 9 h. The mixture then cooled to rt and the reaction was quenched with sat. aq NaHCO<sub>3</sub> (5 mL) and H<sub>2</sub>O (3 mL). The organic phase was extracted with EtOAc (4 × 5 mL), washed with brine, and dried (Na<sub>2</sub>SO<sub>4</sub>). Purification of the crude residue by column chromatography (silica gel, 10–30% EtOAc–hexanes) gave a colorless oil; yield: 17.3 mg (50%, 72% based on recovered starting material); *R<sub>f</sub>* = 0.12 (40% EtOAc–hexanes); [ $\alpha$ ]<sub>D</sub><sup>25</sup> +66.8 (c 0.2, MeOH). IR (thin film): 3422, 2929, 1717, 1255, 1062, 948 cm<sup>-1</sup>. <sup>1</sup>H NMR (300 MHz, CD<sub>3</sub>OD):  $\delta$  = 6.93 (dd, *J* = 15.3, 6.9 Hz, 1 H), 6.08 (d, *J* = 15.6 Hz, 1 H), 5.65 (dd, *J* = 11.4, 4.5 Hz, 1 H), 5.49 (td, *J* = 11.1, 3.3 Hz, 1 H), 5.27 (td, *J* = 11.7, 2.4 Hz, 1 H), 5.17–5.10 (m, 2 H), 5.01–4.91 (m, 1 H), 4.70 (t, *J* = 9.6 Hz, 1 H), 3.27 (s, 3 H), 2.62–2.48 (m, 1 H), 2.04–1.85 (m, 2 H), 1.81–1.67 (m, 1 H), 1.51–1.40 (m, 1 H), 1.28 (d, *J* = 6.3 Hz, 3 H), 1.11–1.06 (m, 1 H). <sup>13</sup>C NMR (75 MHz, CD<sub>3</sub>OD):  $\delta$  = 168.3, 149.9, 136.3, 135.1, 130.4, 128.6, 121.5, 74.3, 73.4, 69.6, 55.4, 35.6, 30.7, 26.8, 20.7. HRMS (ESI): *m/z* [M + Na]<sup>+</sup> calcd for C<sub>15</sub>H<sub>22</sub>NaO<sub>4</sub>: 289.1416; found: 289.1410.

#### Pestalotioprolide D (2)

A 1.0 M solution of TBAF in THF (150  $\mu$ L, 0.15 mmol, 5.0 equiv) was added dropwise to a solution of macrolactone **20** (15 mg,

0.03 mmol) in anhyd THF (1.2 mL, 0.025 M) at 0 °C, and the mixture was stirred from 0 °C to rt for 1.5 h. The reaction was quenched with sat. aq NaHCO<sub>3</sub> (3 mL) and H<sub>2</sub>O (2 mL). The aqueous phase was extracted with EtOAc (4 × 5 mL) and the organic phase was washed with brine and dried (Na<sub>2</sub>SO<sub>4</sub>). Purification of the crude residue by column chromatography (silica gel, 5–20% EtOAc–hexanes) gave a colorless oil; yield: 5.8 mg (75%); *R<sub>f</sub>* = 0.21 (20% EtOAc–hexanes); [ $\alpha$ ]<sub>D</sub><sup>26</sup> –35.6 (c 0.1, MeOH).

IR (thin film): 2931, 1724, 1406, 1237, 1085, 953 cm<sup>-1</sup>. <sup>1</sup>H NMR (300 MHz, CD<sub>3</sub>OD):  $\delta$  = 6.31 (d, *J* = 11.1 Hz, 1 H), 5.89 (dd, *J* = 11.1, 9.6 Hz, 1 H), 5.79 (app t, *J* = 9.6 Hz, 1 H), 5.71–5.63 (m, 1 H), 5.22 (app t, *J* = 9.6, 1 H), 4.94–4.90 (m, 1 H), 3.29 (s, 3 H), 2.96 (ddd, *J* = 17.4, 10.8, 2.7, 1 H), 2.79 (ddd, *J* = 15.0, 10.5, 2.7, 1 H), 2.73 (ddd, *J* = 17.4, 6.6, 2.4 Hz, 1 H), 2.40 (ddd, *J* = 15.3, 6.9, 3.0 Hz, 1 H), 2.19–2.05 (m, 1 H), 1.91–1.79 (m, 1 H), 1.70–1.61 (m, 1 H), 1.59–1.47 (m, 1 H), 1.38–1.26 (m, 1 H), 1.24 (d, *J* = 6.3 Hz, 3 H), 0.98–0.83 (m, 1 H). <sup>13</sup>C NMR (75 MHz, CD<sub>3</sub>OD):  $\delta$  = 201.5, 174.6, 145.5, 134.9, 129.8, 127.4, 73.2, 73.0, 56.0, 40.9, 37.3, 30.0, 29.9, 28.2, 20.3. HRMS (ESI): *m/z* [M + Na]<sup>+</sup> calcd for C<sub>15</sub>H<sub>22</sub>NaO<sub>4</sub>: 289.1416; found: 289.1410.

# Total Synthesis and Biological Evaluation of Mutolide and Analogues

Aticha Thiraporn,<sup>[a]</sup> Nongluk Saikachain,<sup>[b]</sup> Rungtiwa Khumjiang,<sup>[b]</sup> Chatchai Muanprasat,<sup>[b]</sup> and Kwanruthai Tadpetch\*<sup>[a]</sup>

**Abstract:** The convergent total syntheses of three 14-membered macrolide natural products, mutolide, nigrosporolide and (4S,7S,13S)-4,7-dihydroxy-13-tetradeca-2,5,8-trienolide have been achieved. The key synthetic features include Shiina macrolactonization to assemble the 14-membered macrocyclic core, Wittig or Still-Gennari olefination and selective reduction of propargylic alcohol to construct the *E*- or *Z*-olefins. Cross metathesis was also highlighted as an

efficient tool to forge the formation of *E*-olefin. The three synthetic macrolides were evaluated for their cytotoxic activity against three human cancer cell lines as well as for inhibitory effect on CFTR-mediated chloride secretion in human intestinal epithelial (T84) cells. Mutolide displayed significant cytotoxic activity against HCT116 colon cancer cells with an  $IC_{50}$  of  $\sim 12 \mu M$  as well as a potent CFTR inhibitory effect with an  $IC_{50}$  value of  $\sim 1 \mu M$ .

## Introduction

The 14-membered macrolides are a class of polyketide secondary metabolites that have attracted considerable interest of the scientific community due to their broad structural variations and exceptional biological activity.<sup>[1]</sup> Prominent examples of this group of metabolites are erythromycin<sup>[2]</sup> (1) and oleandomycin<sup>[3]</sup> (2), of which the structures contain a 14-membered macrolactone core with glycoside residues and are currently used as antibiotic medication (Figure 1A). Another group of 14-membered unsaturated macrolides are those lacking the sugar moieties which are relatively underexplored and underutilized. This group of metabolites has been shown to exhibit significant and diverse biological activities. Selected examples of this macrolide subclass are illustrated in Figure 1B. Albocycline<sup>[4]</sup> (3) displays a remarkable inhibitory activity against methicillin-resistant *Staphylococcus aureus* (MRSA) as potently as vancomycin.<sup>[5]</sup> Sch 725674 (4) isolated from *Aspergillus* sp. exhibits antifungal activity against *Saccharomyces cerevisiae* (PM503) and *Candida albicans* (C43) with MICs of 8 and 32  $\mu g/mL$ , respectively.<sup>[6]</sup> 7-O-Methylnigrosporolide (5) and pestalotioprolide E (6) display potent cytotoxic activity against the L5178Y murine lymphoma and A2780 human ovarian cancer cell lines.<sup>[7]</sup>

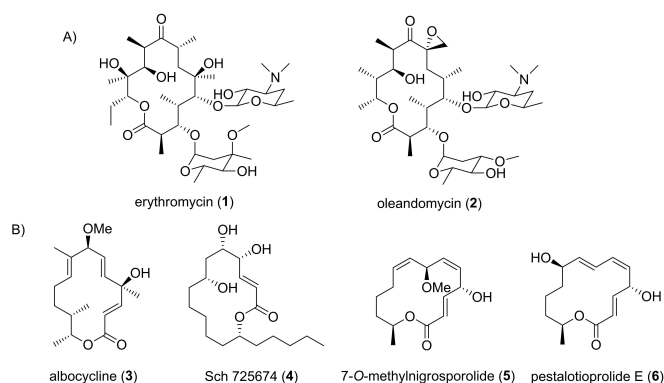


Figure 1. Selected examples of biologically active 14-membered macrolides.

In 2000, Zeeck and co-workers disclosed the isolation of a novel 14-membered macrolactone, mutolide (7) from the culture broth of a fungus strain derived from UV mutagenesis of the fungus *Sphaeropsidales* sp. (strain F-24'707) which displayed weak antibacterial activity against *B. subtilis* and *E. coli* (Figure 2).<sup>[8]</sup> Macrolide 7 was later identified from the coprophilous fungus *Lepidosphaeria* sp. (PM0651419) by Kulkarni-Almeida et al. in 2015.<sup>[9]</sup> This work discovered for the first time the anti-inflammatory properties of 7. Mutolide mitigated secretion of pro-inflammatory cytokines TNF- $\alpha$ , IL-6 and IL-17 in various cells. Mechanistic investigation suggested that mutolide may exert its anti-inflammatory effect via NF- $\kappa$ B inhibition. Recently in 2020, the Liu and Proksch group reported the isolation of mutolide from the endophytic fungus *Aplosporella javeedii*.<sup>[10]</sup> It was discovered that mutolide exhibited a very potent cytotoxic activity against the L5178Y mouse lymphoma cells with an  $IC_{50}$  value of 0.4  $\mu M$  after 72 hours of incubation. Notably, this was ten-fold more potent than that of the positive control kahalalide F ( $IC_{50} = 4.3 \mu M$ ). In addition, macrolide 7 also displayed significant cytotoxicity against the human leukemia (Jurkat J16) and lymphoma (Ramos) cell lines with  $IC_{50}$  values of 5.8 and 4.4  $\mu M$ , respectively after 24 hours of incubation which

[a] A. Thiraporn, Dr. K. Tadpetch  
Division of Physical Science and Center of Excellence  
for Innovation in Chemistry, Faculty of Science,  
Prince of Songkla University, Hat Yai,  
Songkhla 90110 (Thailand)  
E-mail: kwanruthai.t@psu.ac.th

[b] N. Saikachain, R. Khumjiang, Prof. Dr. C. Muanprasat  
Chakri Naruebodindra Medical Institute,  
Faculty of Medicine Ramathibodi Hospital,  
Mahidol University, Bang Pla, Bang Pli,  
Samut Prakan 10540 (Thailand)

Supporting information for this article is available on the WWW under  
<https://doi.org/10.1002/asia.202200329>

This manuscript is part of a special collection highlighting Women in  
Chemistry.



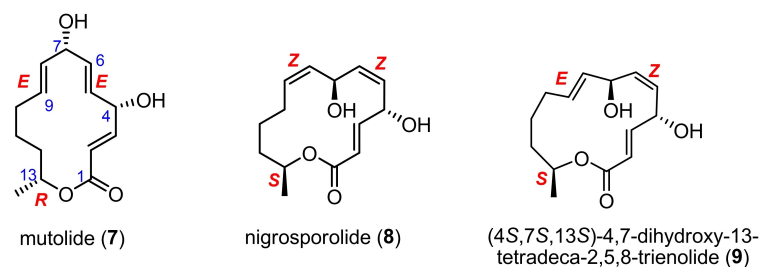


Figure 2. Structures of mutolide (7), nigrosporolide (8) and (4S,7S,13S)-4,7-dihydroxy-13-tetradeca-2,5,8-trienolide (9).

was comparable to that of staurosporine ( $IC_{50}$  = 2.5  $\mu$ M). Remarkably, these  $IC_{50}$  values against these two cell lines dropped to 1.4 and 0.8  $\mu$ M, respectively after 72 hours of incubation.

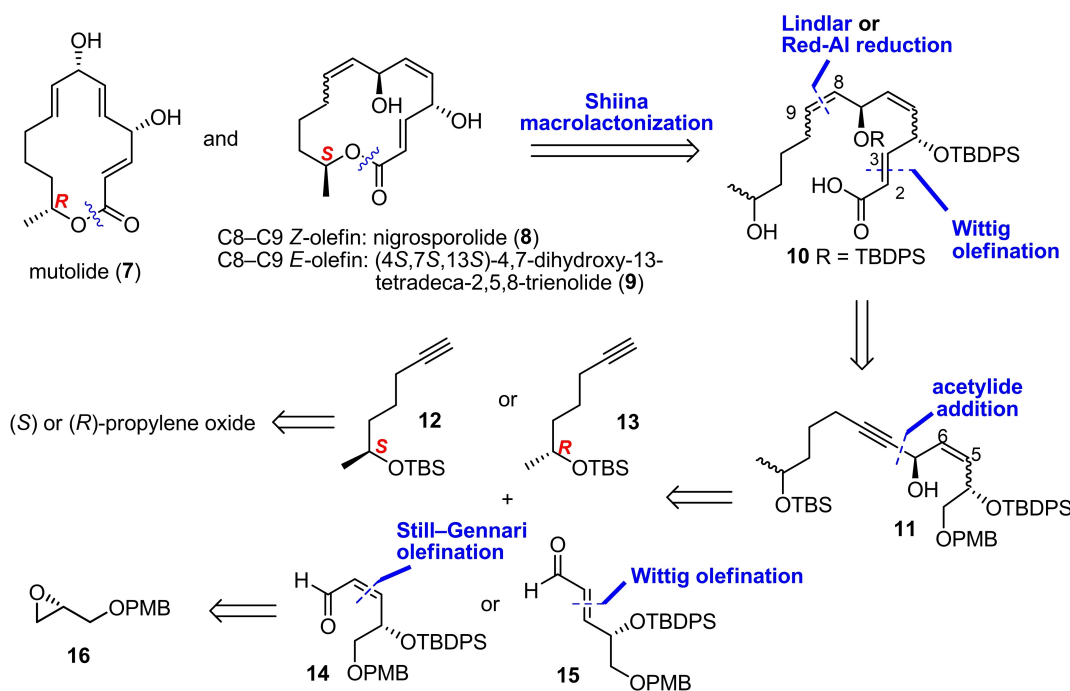
There are known natural analogues of 7 namely nigrosporolide (8) and (4S,7S,13S)-4,7-dihydroxy-13-tetradeca-2,5,8-trienolide (9) (Figure 2). Structurally, macrolides 8 and 9 differ from 7 only by the stereochemistry of the C-13 stereogenic center as well as C5–C6 and C8–C9 olefins. Interestingly, however, biological activity studies of macrolactones 8 and 9 are much less precedented compared to mutolide. Nigrosporolide (8), originally isolated from the mold *Nigrospora sphaerica* in 1995, was reported to show plant-growth inhibitory activity.<sup>[11]</sup> Macrolide 8 was reisolated by the Liu and Proksch group from *P. microspora* and showed weak cytotoxic activity against the L5178Y murine lymphoma and the A2780 human ovarian cancer cell lines with  $IC_{50}$  values of 21 and 43  $\mu$ M, respectively.<sup>[7]</sup> Macrolide 9 was first isolated from the phytopathogen fungus *Colletotrichum acutatum* in 2009<sup>[12]</sup> and reisolated from a marine-derived fungus *Diaportheaceae* sp. PSU–SP2/4 in 2014.<sup>[13]</sup> Compound 9 showed no antibacterial activity against *S. aureus* and MRSA. However, it was mildly active against human breast adenocarcinoma (MCF-7) cells with an  $IC_{50}$  value of 30.76  $\mu$ g/mL and non-cytotoxic to noncancerous Vero cells.<sup>[13]</sup> It should be noted that compound 9 was previously synthesized as an advanced intermediate in the total synthesis of aspergillide C by Shishido and co-workers.<sup>[14]</sup> Owing to very promising anti-inflammatory and anticancer activities of mutolide as well as its unprecedented total chemical synthesis, we set out a synthetic program aimed at developing a unified synthesis of mutolide and its natural analogues 8 and 9 in order to further evaluate other biological activities. Herein, we reported the total synthesis of macrolides 7–9 as well as evaluation of their cytotoxic activity against three human cancer cell lines and inhibitory effect on cystic fibrosis transmembrane conductance regulator (CFTR)-mediated chloride secretion, a process known to cause secretory diarrheas, in human intestinal epithelial (T84) cells.

## Results and discussion

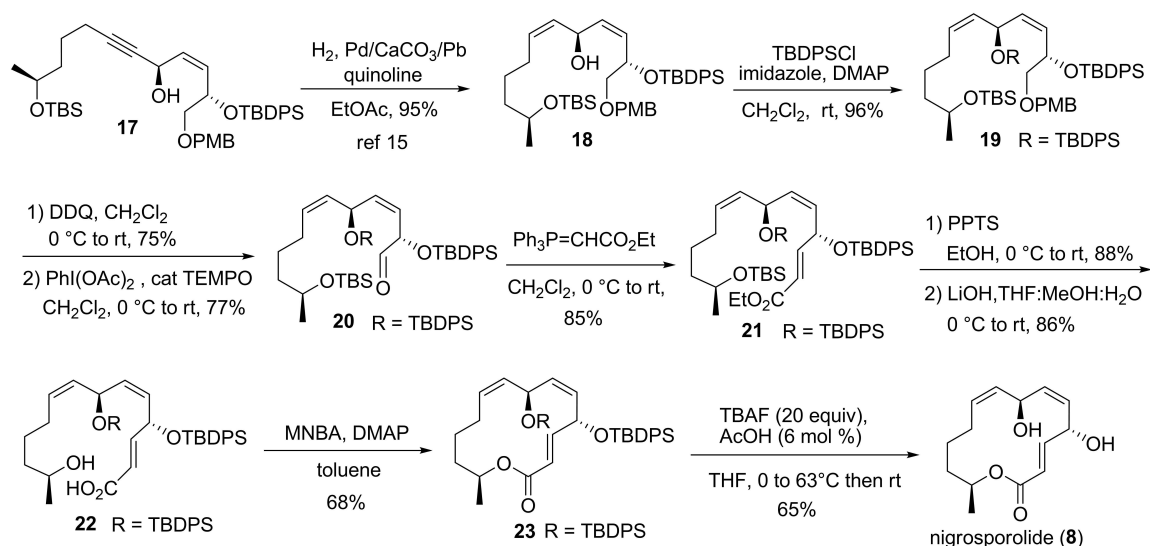
Our research group has recently reported the first total synthesis of 7-O-methylnigrosporolide (5).<sup>[15]</sup> Since nigrosporolide (8) possesses the same core skeleton as 5 and the macrolide targets 7–9 are structurally similar, we envisioned

that we could utilize our previously described key bond formation strategy for the syntheses of 7–9. The retrosynthetic analysis of macrolides 7–9 is outlined in Scheme 1. The reliable Shiina macrolactonization of seco acid 10 would be employed to assemble the macrocycle. The C2–C3 *E*-olefin moiety in macrolides 7–9 would also be constructed via Wittig olefination. The C8–C9 *Z*-olefin of 10 required for the synthesis of 8 would be generated by Lindlar reduction of propargylic alcohol 11, whereas the C8–C9 *E*-olefin of 10 required for the synthesis of macrolides 7 and 9 would be affected by Red-Al reduction of 11. The known propargylic alcohol 11 necessitated for the synthesis of macrolides 8 and 9 would be prepared via the key acetylide addition of (*S*)-alkyne 12 and *Z*-enal 14. Propargylic alcohol 11 needed for the synthesis of mutolide (7) would be assembled by acetylide addition of (*R*)-alkyne 13 and *E*-enal 15. The alkyne (12 or 13) and enal (14 or 15) coupling precursors would be obtained from commercially available (*S*)- or (*R*)-propylene oxide and (*S*)-benzyl glycidyl ether (16) via a protocol previously reported by our group.<sup>[15]</sup>

We started with the synthesis of nigrosporolide (8) following our previously reported synthesis of 7-O-methylnigrosporolide (5) starting from alcohol 18 prepared via Lindlar reduction of known propargylic alcohol 17 (Scheme 2).<sup>[15]</sup> C7–Alcohol of 18 was protected with *tert*-butyldiphenylsilyl (TBDPS) group to furnish silyl ether 19 in 96% yield. We chose this protecting group for the purpose of global deprotection in the final step. Next, compound 19 was converted to aldehyde 20 in 2 steps via PMB deprotection with DDQ followed by oxidation of the corresponding primary alcohol with  $PhI(OAc)_2$  in the presence of catalytic TEMPO. It should be noted that oxidation using Dess-Martin periodinane previously employed in the synthesis of 5 was very sluggish with this substrate. Next, Wittig olefination of 20 using (carbethoxymethylene)triphenylphosphorane furnished (*E*)- $\alpha,\beta$ -unsaturated ester 21 in 85% yield. The *E*-geometry of the newly created C2–C3 double bond was verified by the  $^1H$ - $^1H$  coupling constant of 15.3 Hz. Selective removal of the TBS protecting group of 21 using 3 equivalents of PPTS exclusively produced the corresponding secondary alcohol in 88% yield. Subsequent hydrolysis of the ethyl ester functional group was affected with LiOH in THF and aqueous methanol to deliver seco acid 22, which was subjected to Shiina macrolactonization using 2-methyl-6-nitrobenzoic anhydride (MNBA) and DMAP in toluene to furnish the macrocycle 23 in 68% yield. Finally, global deprotection of both TBDPS groups of 23 was smoothly accomplished upon



**Scheme 1.** Retrosynthetic analysis of mutolid (7), nigrosporolide (8) and (4S,7S,13S)-4,7-dihydroxy-13-tetradeca-2,5,8-trienolide (9).

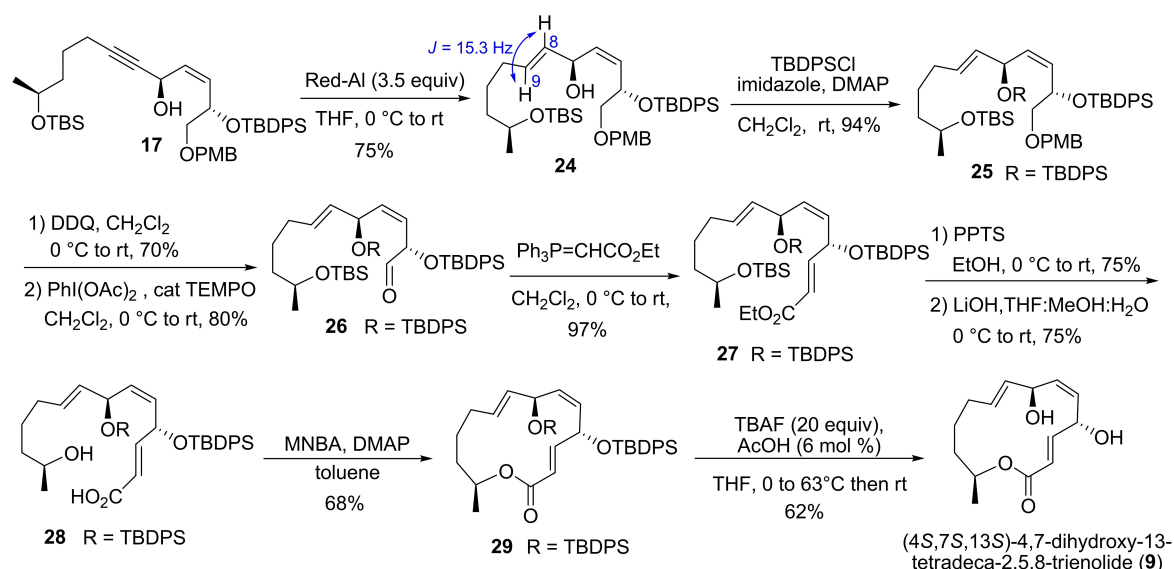


**Scheme 2.** Completion of the synthesis of nigrosporolide (8).

treating with large excess of TBAF (20 equiv) buffered with acetic acid (6 mol%) in THF from 0 °C to 63 °C to afford nigrosporolide (8) in 65% yield. The <sup>1</sup>H and <sup>13</sup>C NMR spectroscopic data of 8 were in excellent agreement with those reported for the natural product 8<sup>[11]</sup> (see Table S11 in Supporting Information). The specific rotation of synthetic 8 ( $[\alpha]_D^{26} = +89.0$ , *c* 0.90, MeOH) was in accordance with the reported value for natural 8 ( $[\alpha]_D^{20} = +81.0$ , *c* 0.90, MeOH).<sup>[7]</sup>

We next focused on the synthesis of (4S,7S,13S)-4,7-dihydroxy-13-tetradeca-2,5,8-trienolide (9) as depicted in Scheme 3. The synthesis commenced with selective reduction of known propargylic alcohol 17 using 3.5 equivalents of

sodium bis(2-methoxyethoxy)aluminum hydride (Red-Al) in THF from 0 °C to room temperature to smoothly give (E)-olefin 24 in 75% yield (Scheme 3).<sup>[16]</sup> The E-geometry of the newly formed olefin was confirmed by the coupling constant of 15.3 Hz between H8 and H9. Alcohol 24 was then transformed to macrocyclic intermediate 29 in 7 steps via the same synthetic approach employed in the synthesis of 8. Similarly, removal of TBDPS groups of 29 under the same conditions used for 8 delivered targeted macrolactone 9 in 62% yield. The <sup>1</sup>H and <sup>13</sup>C NMR spectroscopic data of 9 were in good agreement with those reported for Shishido's intermediate (see Table S12 in Supporting Information).<sup>[14]</sup> The specific rotation of synthetic 9



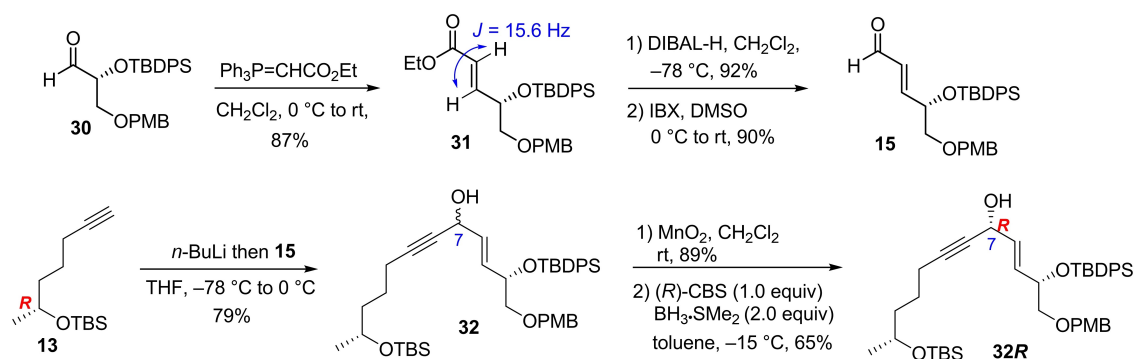
Scheme 3. Completion of the synthesis of (4S,7S,13S)-4,7-dihydroxy-13-tetradeca-2,5,8-trienolide (9).

was observed as  $[\alpha]_D^{24} = +148.8$  ( $c$  0.68, CHCl<sub>3</sub>), which was closely similar to that of natural product 9 ( $[\alpha]_D^{25} = +156.0$ ,  $c$  0.68, CHCl<sub>3</sub>).<sup>[13]</sup>

Having accomplished the syntheses of macrolides 8 and 9 via the proposed disconnection, we proceeded to synthesize mutolide (7) following the same strategy (Scheme 4). The synthesis began with preparation of *E*-enal 15 from our previously reported aldehyde intermediate 30. Wittig olefination of 30 mediated with (carbethoxymethylene)triphenylphosphorane delivered (*E*)- $\alpha,\beta$ -unsaturated ester 31 as a single isomer in 87% yield (verified by the <sup>1</sup>H-<sup>1</sup>H coupling constant of 15.6 Hz). Conversion of the ester moiety of 31 to *E*-enal 15 was accomplished in 2 steps via DIBAL-H reduction, followed by IBX oxidation. Enal 15 was then subjected to addition of the acetylide of (*R*)-alkyne 13 (prepared from commercially available (*R*)-propylene oxide) to furnish propargylic alcohol 32 as a mixture of inseparable diastereomers in 79% yield. Diastereomeric mixture of propargylic alcohols 32 was next subjected to oxidation with MnO<sub>2</sub>, followed by stereoselective ketone reduction using (*R*)-CBS oxazaborolidine

and BH<sub>3</sub>·SMe<sub>2</sub> in toluene at -15 °C to deliver 32R in 65% yield.<sup>[17]</sup>

With the requisite propargylic alcohol 32R in hand, we next proceeded with optimization of selective reduction of the alkyne moiety of 32R to the desired *E*-olefin 33 (Table 1). Disappointingly, reaction conditions successfully employed in the synthesis of 9 using Red-Al 3.5 or 5 equivalents in THF from 0 °C to room temperature gave no desired product and the starting material was recovered (entries 1 and 2).<sup>[16]</sup> Increasing the temperature to 50 °C in the presence of 4 equivalents of Red-Al also failed to furnish any desired product and only the starting material was observed (entry 3).<sup>[18]</sup> Further optimization was then performed by changing the solvent to toluene at 0 °C to room temperature and at -15 °C using 3 equivalents of Red-Al (entries 4 and 5).<sup>[19]</sup> These conditions led to undesired overreduced product 34 in 40% yield and 29% yield, respectively.

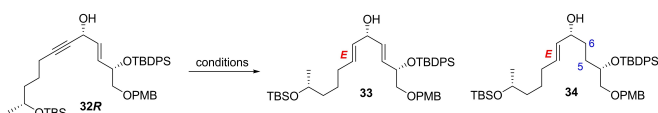


Scheme 4. Synthesis of propargylic alcohol 32R for the synthesis of mutolide (7).



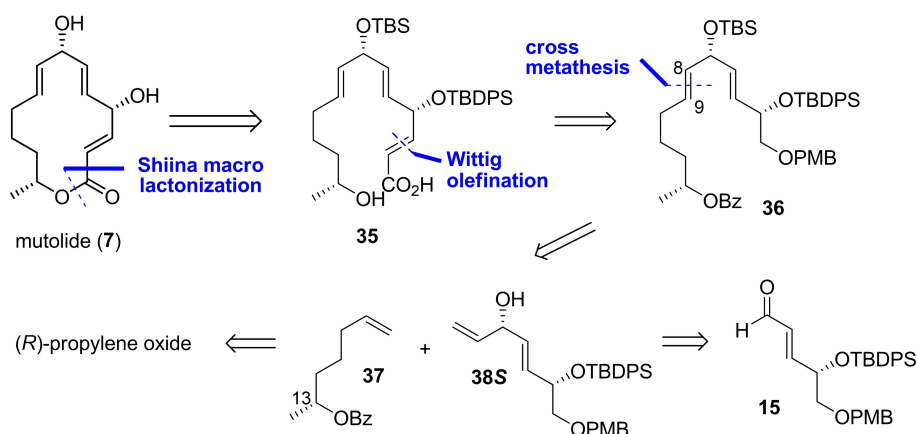
**Table 1.** Screening for Red-Al-mediated (*E*-selective reductions of alkyne **32R**. The ChemDraw Equation on page 5 (conversion of compound **32R** to **33** and **34**) should be inserted here

entry	Red-Al [equiv]	solvent	temp	time [h]	results
1	3.5	THF	0 °C to rt	5	no reaction
2	5.0	THF	0 °C to rt	18	no reaction
3	4.0	THF	0 °C to 50 °C	8	no reaction
4	3.0	toluene	0 °C to rt	3	<b>34</b> (40% yield, 58% brsm)
5	3.0	toluene	−15 °C	6	<b>34</b> (29% yield, 65% brsm)

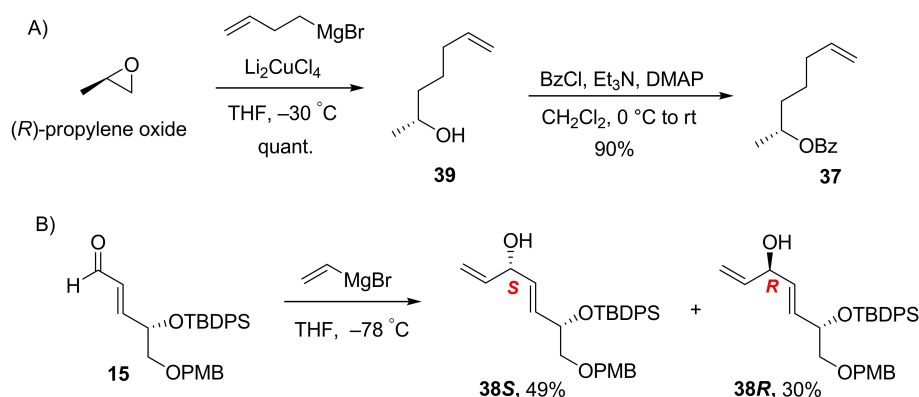


Problematic over-reduction of alkyne intermediate **32R** led us to revise the retrosynthesis of **7** as shown in Scheme 5. Shiina macrolactonization of seco acid **35** would still be utilized to assemble the macrocyclic core of **7**. The *E*-double bond at C8–C9 would be forged via cross-metathesis between (*R*)-hept-6-en-2-yl benzoate (**37**) and chiral allylic alcohol **38S** which would be prepared from (*R*)-propylene oxide and *E*-enal **15**, respectively. The benzoate group was chosen as a protecting group at C13–alcohol of **37** instead of TBS group in order to shorten the synthetic sequence since it could be simultaneously removed in the hydrolysis step.

Preparation of cross metathesis precursors **37** and **38S** is illustrated in Scheme 6. The synthesis of known (*R*)-propylene oxide with 3-butenylmagnesium bromide in the presence of catalytic dilithium copper(II) chloride to give chiral alcohol **39**,<sup>[20]</sup> which was immediately protected with benzoyl group to provide **37** in excellent yield (Scheme 6A). The requisite allylic alcohol **38S** was prepared by treatment of *E*-enal **15** with vinylmagnesium bromide in THF at −78 °C. The chiral allylic alcohols **38S** and **38R** were obtained in 79% yield as a 1.6:1 mixture of diastereomers which could be separated by column chromatography (Scheme 6B). The absolute configuration of the alcohol chiral center of each diastereomer was confirmed by Mosher's ester analysis. Attempts to convert **38R** to the desired **38S** via oxidation followed by CBS reduction



**Scheme 5.** Revised retrosynthesis of mutolide (**7**).



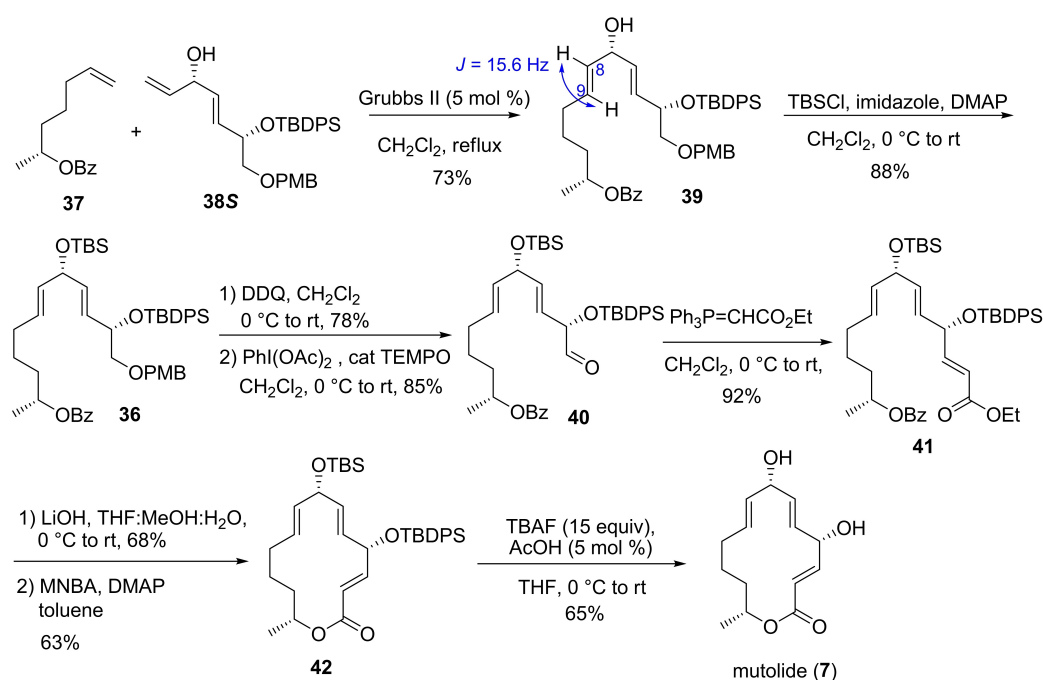
**Scheme 6.** A) Preparation of (*R*)-hept-6-en-2-yl benzoate (**37**). B) preparation of chiral allylic alcohol **38S**.

were unsuccessful with this substrate as poor stereoselectivity was observed. Mitsunobu inversion also resulted in poor stereoselectivity as both **38S** and **38R** were obtained presumably via epimerization in the methanolysis step.<sup>[21]</sup>

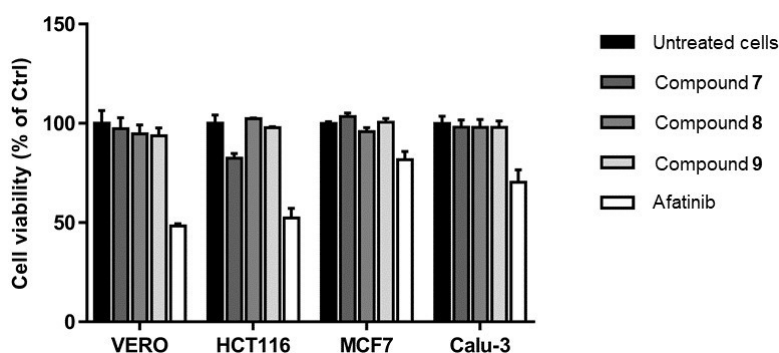
Having achieved both key fragments **37** and **38S**, the stage was then set for the key cross metathesis and completion of the synthesis of **7** (Scheme 7). Gratifyingly, treatment of alkenes **37** and **38S** with 5 mol% of second-generation Grubbs catalyst in refluxing  $\text{CH}_2\text{Cl}_2$  (0.1 M) smoothly and stereoselectively produced *E*-alkene product **39** in 73% yield (Scheme 7).<sup>[22]</sup> The *E*-geometry of the new olefin was verified by the coupling constant of 15.6 Hz between H8 and H9. Next, C-7 hydroxyl group of **39** was protected with TBSCl to give **36** in 88% yield. The TBS protecting group was chosen in this case for the purpose of the ease in desilylation step and selective desilylation was not required in this synthetic sequence. Compound **36** was further elaborated to (*E*)- $\alpha,\beta$ -unsaturated ester **41** in 3 high-yielding steps using the similar synthetic sequence as that of **9**. The newly generated C2–C3 double bond of ester **41** was again verified by the  $^1\text{H}$ - $^1\text{H}$  coupling constant of 15.3 Hz. Simultaneous removal of ester functional group and the benzoyl group was mediated with 4 equivalents of LiOH in THF and aqueous methanol to provide the corresponding seco acid, which was subsequently exposed to Shiina macrolactonization conditions to give macrocycle **42** in 63% yield. Global deprotection of both silyl protecting groups of **42** using 15 equivalents of TBAF buffered with acetic acid (5 mol%) in THF smoothly delivered mutolide (**7**) in 65% yield. The  $^1\text{H}$  and  $^{13}\text{C}$  NMR spectroscopic of synthetic **7** were nearly identical to those reported for natural **7** (see Table S13 in Supporting Information).<sup>[8,9]</sup> The specific rotation of synthetic **7**

( $[\alpha]_{\text{D}}^{23} = -59.8$ ,  $c$  1.79,  $\text{CH}_3\text{CN}$ ) was in accordance with the reported value for natural **7** ( $[\alpha]_{\text{D}}^{25} = -61.0$ ,  $c$  1.79,  $\text{CD}_3\text{CN}$ ).<sup>[8]</sup>

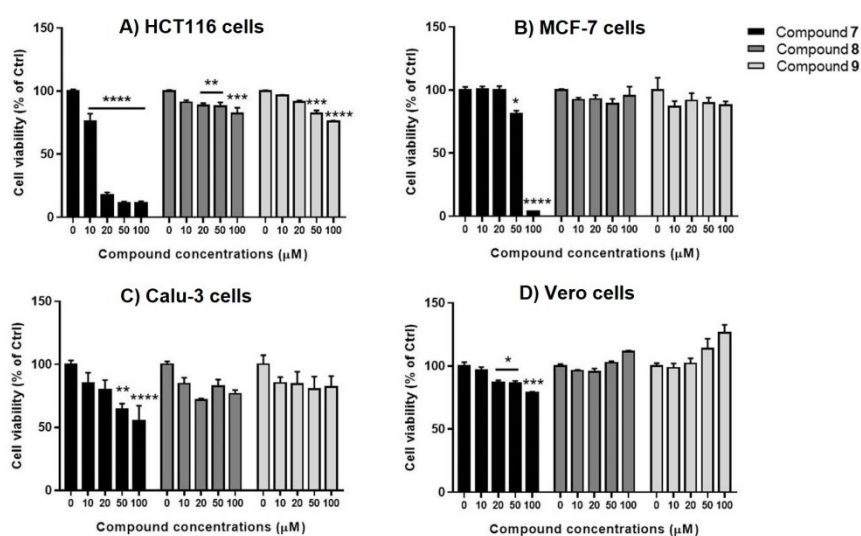
The three synthetic macrolides **7–9** were evaluated for their *in vitro* cytotoxic activity against three human cancer cell lines, including HCT116 colorectal carcinoma, MCF-7 breast adenocarcinoma and Calu-3 lung adenocarcinoma, as well as non-cancerous (Vero) cells using MTT assay. Viability of cells after 24 hours of treatment with 10  $\mu\text{M}$  of compounds **7–9** were measured and compared with untreated cells using afatinib as a positive control (Figure 3). We observed that compounds **7–9** were non-cytotoxic to Vero cells and macrolactones **8** and **9** showed no cytotoxic effects on the three cancer cell lines tested at 10  $\mu\text{M}$ . However, mutolide (**7**) displayed inhibition of viability of HCT116 cells at this concentration (~82% cell viability), albeit in lower extent compared to afatinib (~52% cell viability). Therefore, the dose-response experiments of **7–9** were performed at 0, 10, 20, 50 and 100  $\mu\text{M}$  at 24 hours of incubation (Figure 4). It was found that mutolide significantly inhibited the viability of HCT116 cells in a concentration-dependent manner with an  $\text{IC}_{50}$  value of ~12  $\mu\text{M}$  (Figure 4A). Notably, at 20  $\mu\text{M}$ , the percentage of HCT116 cell viability dropped to ~18% and further dropped to ~11% at 50 and 100  $\mu\text{M}$ . Mutolide also inhibited the viability of MCF-7, Calu-3 and Vero cells in a concentration-dependent manner with less potency ( $\text{IC}_{50} > 50 \mu\text{M}$ ) compared to the HCT116 cells (Figures 4B, 4C and 4D). Macrolactones **8** and **9** did not show significant inhibition of cell viability in all cell lines. It is worth noting that our findings are in accordance with Liu and Proksch's reports<sup>[7,10]</sup> that mutolide showed higher antiproliferative effect compared to their analogues **8** and **9**. In addition, we found that the viability of HCT116 cells treated with mutolide or analogues **8** and **9** with longer incubation times (48 and 72 h) remained



**Scheme 7.** Completion of the synthesis of mutolide (**7**).



**Figure 3.** Viability of cells treated with synthetic compounds 7–9 or afatinib at 10  $\mu\text{M}$  for 24 h determined by the MTT assay. Results are shown in percentage of cell viability relative to untreated cells.

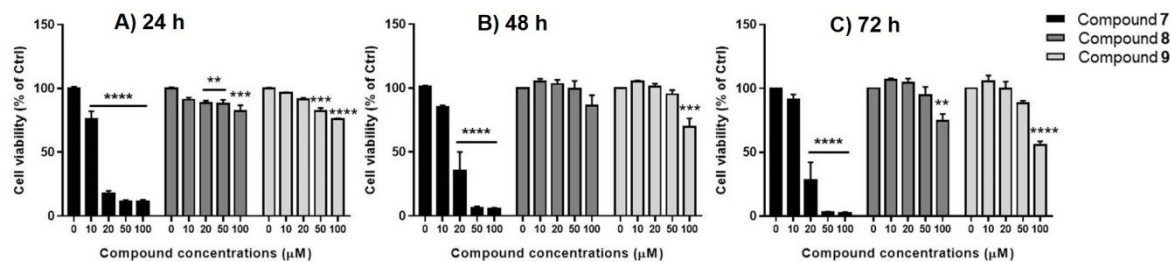


**Figure 4.** Viability of A) HCT116 cells, B) MCF-7 cells, C) Calu-3 cells and D) Vero cells treated with synthetic compounds 7–9 at indicated concentrations for 24 h determined by the MTT assay. \*, \*\*, \*\*\* and \*\*\*\* indicated the  $p$ -values of  $<0.05$ ,  $<0.01$ ,  $<0.005$  and  $<0.001$ , respectively ( $n=3$ ) (One-way analysis of variance).

relatively unchanged (Figure 5,  $\text{IC}_{50}$  values of  $\sim 16 \mu\text{M}$  for mutolide), suggesting that prolonged incubation times did not significantly affect the potency of mutolide on inhibition of HCT116 cells.

Synthetic compounds 7–9 were further assessed for their inhibitory activity of cystic fibrosis transmembrane conductance regulator (CFTR)-mediated chloride secretion in human intesti-

nal epithelial (T84) cells. Overstimulation of CFTR-mediated chloride secretion is known to be involved in the pathogenesis of secretory diarrhea which is one of the major health problems that causes morbidity and mortality worldwide. Our research group has recently reported that zearalenone, a 14-membered resorcylic acid lactone fungal metabolite, is a potent CFTR inhibitor with nanomolar potency.<sup>[23]</sup> In this work, three

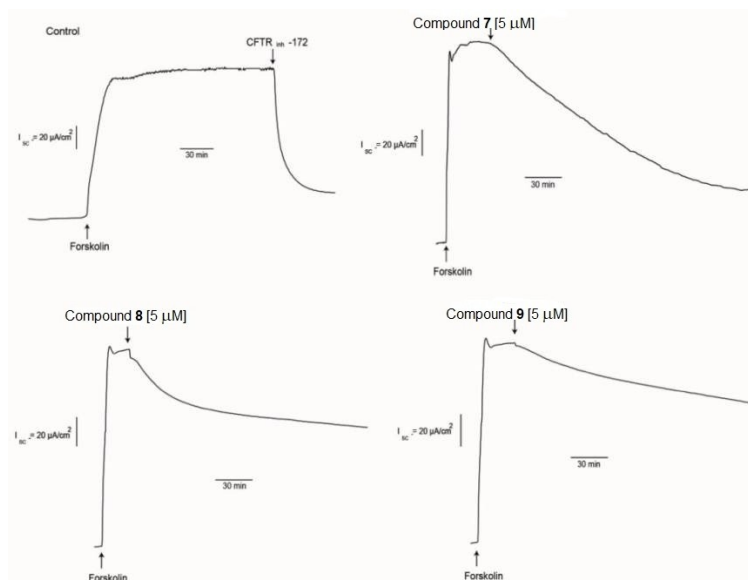


**Figure 5.** Viability of HCT116 cells treated with synthetic compounds 7–9 after A) 24 h, B) 48 h and C) 72 h of incubations at indicated concentrations for 24 h determined by the MTT assay. \*, \*\*, \*\*\* and \*\*\*\* indicated the  $p$ -values of  $<0.05$ ,  $<0.01$ ,  $<0.005$  and  $<0.001$ , respectively ( $n=3$ ) (One-way analysis of variance).

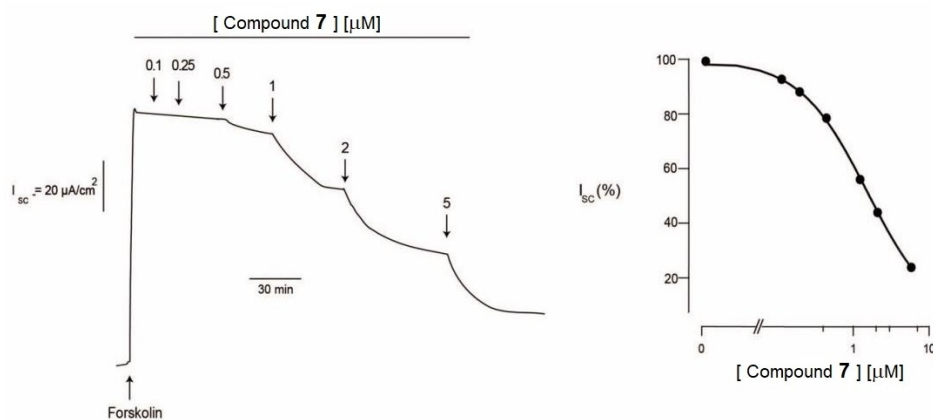
synthetic 14-membered macrolides lacking resorcylic acid moieties **7–9** were screened for their inhibitory effects on the CFTR channels using short-circuit current analysis (Figure 6). It was found that at 5  $\mu\text{M}$ , mutolide showed the most significant inhibition ( $\sim 70\%$  inhibition) compared to macrolides **8** and **9** (40% and 30% inhibition, respectively). Thus, compound **7** was further evaluated in concentration-inhibition studies, which revealed that **7** concentration-dependently inhibited CFTR-mediated chloride secretion in T84 cells stimulated by forskolin (a cAMP donor) with an  $\text{IC}_{50}$  of  $\sim 1 \mu\text{M}$  (Figure 7). It should be noted that this potent inhibitory activity of **7** is comparable to that of zearalenone, suggesting the potentials of this class of 14-membered macrolactones in drug discovery for treatment of secretory diarrheas.

In conclusion, we have completed the total synthesis of mutolide (**7**), nigrosporolide (**8**) and (4*S*,7*S*,13*S*)-4,7-dihydroxy-13-tetradeca-2,5,8-trienolide (**9**) starting from commercially

available (*S*)- or (*R*)-propylene oxide and previously described (*S*)-benzyl glycidyl ether. The synthetic **7** was accomplished in a longest linear sequence of 16 steps and a total of 18 steps in 1.5% overall yield, whereas **8** and **9** were achieved in a longest linear sequence of 17 steps and a total of 22 steps, in 1.8 and 1.1 and % overall yields, respectively. The key features of our synthesis involved Shiina macrolactonization to assemble the 14-membered macrocyclic core, Wittig olefination to construct the C2–C3 (*E*)- $\alpha,\beta$ -unsaturated ester moiety and selective reduction of propargylic alcohol to generate *Z*- or *E*-alkene at C8–C9 for macrolides **8** and **9**. Cross metathesis was successfully exploited to forge the formation of C8–C9 (*E*)-olefin in the synthesis of **7**. The three synthetic macrolides **7–9** were evaluated for their cytotoxic activity against three human cancer cell lines as well as their inhibitory effect on CFTR-mediated chloride secretion in human intestinal epithelial (T84) cells. Mutolide was found to display significant cytotoxic activity



**Figure 6.** Evaluation of effects of compounds **7–9** (5  $\mu\text{M}$ ) on CFTR-mediated chloride secretion in T84 cells. Forskolin (20  $\mu\text{M}$ ) was used to stimulate the CFTR-mediated chloride secretion. CFTR<sub>inh</sub>-172 (20  $\mu\text{M}$ ) was used as a positive control. Representative tracings of 3 experiments are shown.



**Figure 7.** Evaluation of potency of synthetic mutolide (**7**) on CFTR-mediated chloride secretion on human intestinal epithelial (T84) cells. (Left) A representative current tracing of 3 experiments. (Right) Summary of the data. Data were fitted to Hill's equation.

against HCT116 colon cancer cells with an  $IC_{50}$  of  $\sim 12 \mu\text{M}$ . In addition, macrolide **7** exhibited potent CFTR inhibitory effect with an  $IC_{50}$  value of  $\sim 1 \mu\text{M}$ .

## Acknowledgements

This work was financially supported by Prince of Songkla University (Grant No. SCI6104385) and the Faculty of Science Research Fund. We also acknowledge partial support from the Thailand Science Research Innovation supported through the Direct Basic Research Grant (DBG6280007), Center of Excellence for Innovation in Chemistry (PERCH-CIC), Ministry of Higher Education, Science, Research and Innovation. Additional support was generously provided by the Graduate School, Prince of Songkla University, the Science Achievement Scholarship of Thailand (SAST), Faculty of Science, Prince of Songkla University and the Thesis Research Grant under the Scholarship Supports for the Potential scholar in research and innovation to enhance the economic, social and community sectors (Talent Utilization) for A. Thiraporn. C. M. acknowledges support from Mahidol University (Basic Research Fund: fiscal year 2022).

## Conflict of Interest

The authors declare no conflict of interest.

## Data Availability Statement

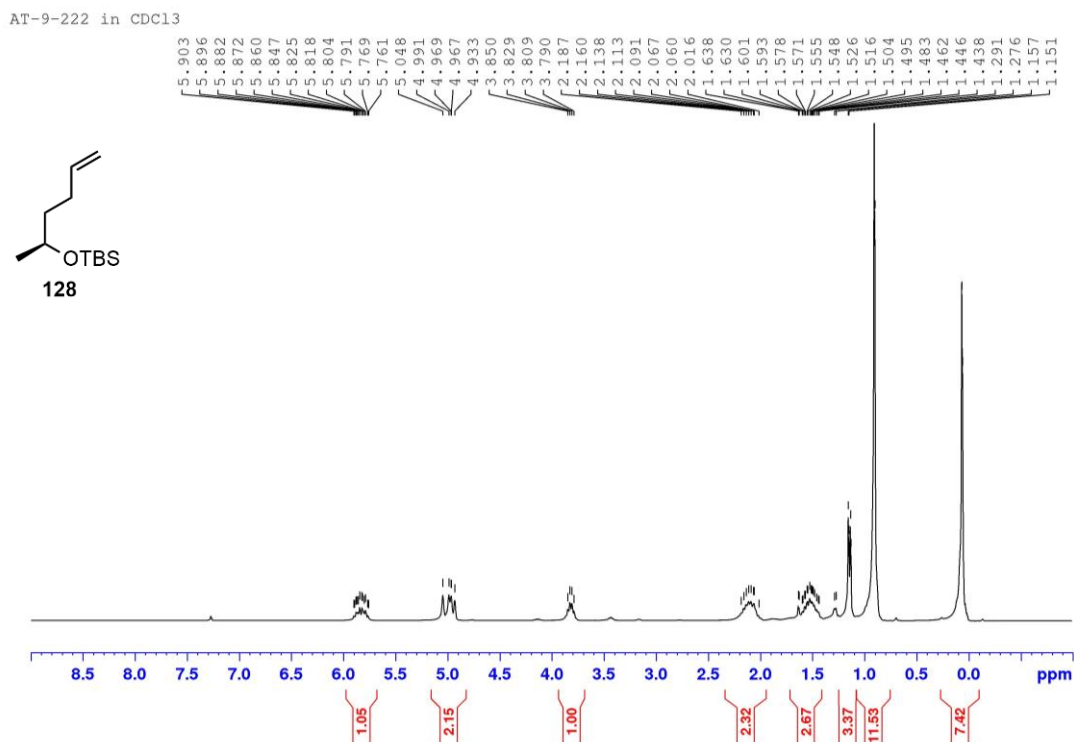
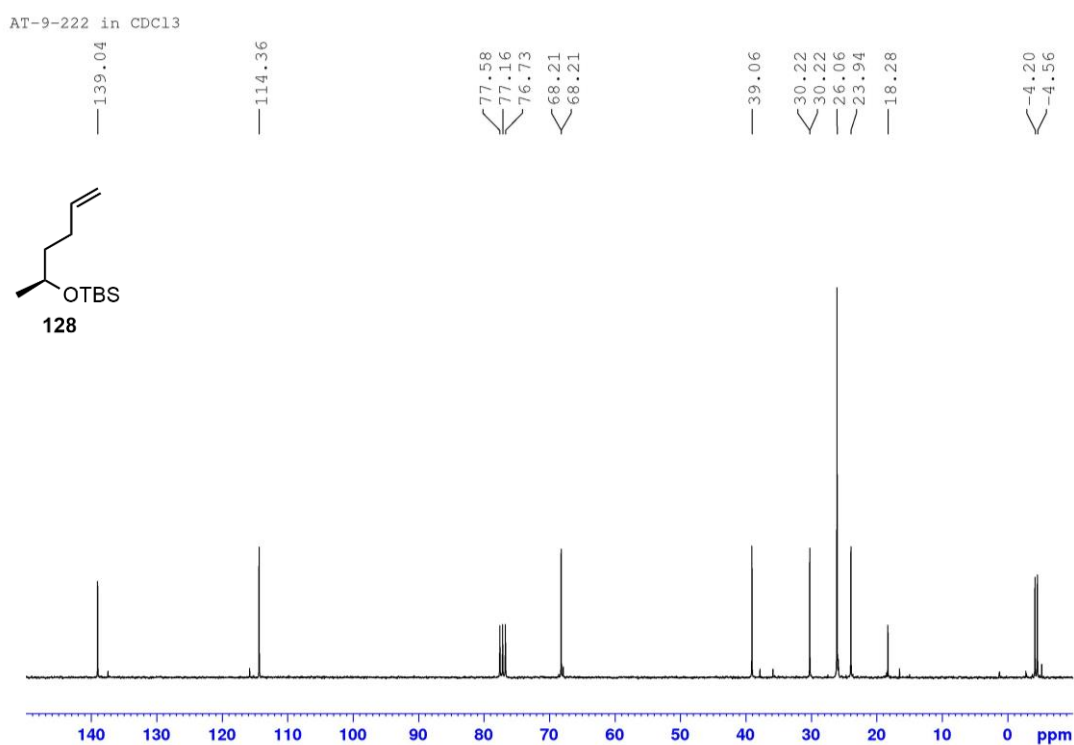
The data that support the findings of this study are available from the corresponding author upon reasonable request.

**Keywords:** CFTR inhibitory activity · Cytotoxic activity · 14-Membered macrolactones · Mutolide · Total synthesis

- [1] a) D. T. W. Chu, *Expert Opin. Invest. Drugs* **1995**, *4*, 65–94; b) G. G. Zhanel, M. Dueck, D. J. Hoban, L. M. Vercaigne, J. M. Embil, A. S. Gin, J. A. Karlowsky, *Drugs* **2001**, *61*, 443–498; c) A. Janas, P. Przybylski, *Eur. J. Med. Chem.* **2019**, *182*, 111662; d) H. Zhang, J. Zou, X. Yan, J. Chen, X. Cao, J. Wu, Y. Liu, T. Wang, *Mar. Drugs* **2021**, *19*, 180.

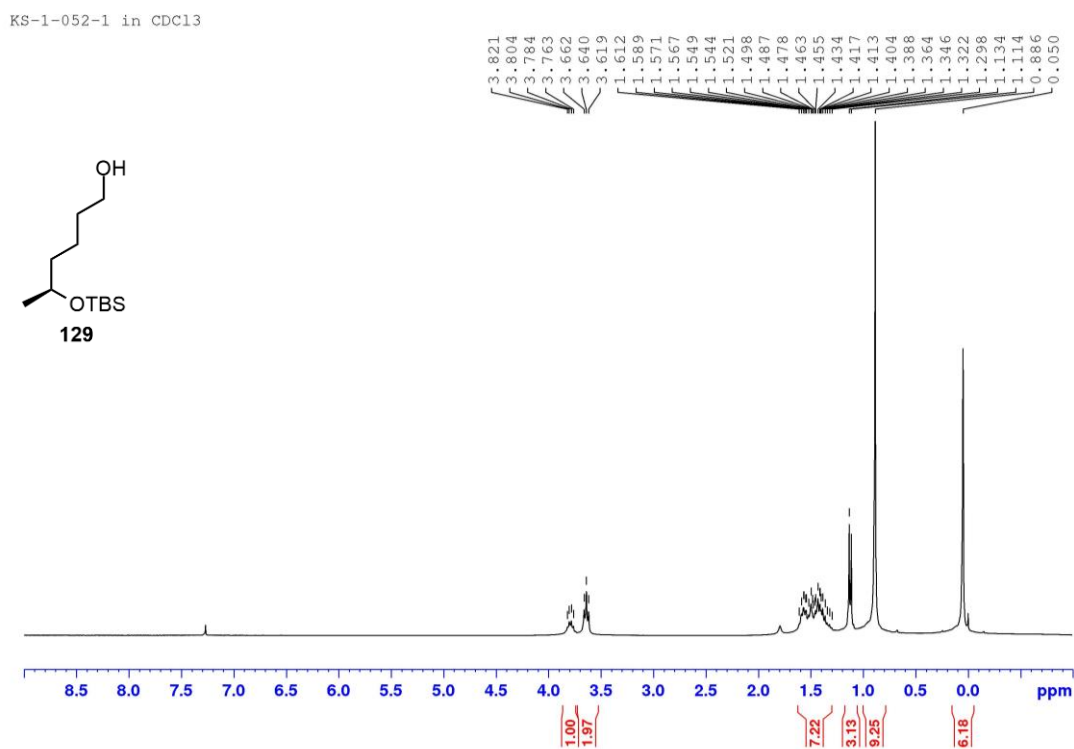
- [2] J. M. McGuire, R. L. Bunch, R. C. Anderson, H. E. Boaz, E. H. Flynn, H. M. Powell, J. W. Smith, *Antibiot. Chemother.* **1952**, *2*, 281–283.  
 [3] H. Els, W. D. Celmer, K. Murai, *J. Am. Chem. Soc.* **1958**, *80*, 3777–3782.  
 [4] a) N. Nagahama, M. Suzuki, S. Awataguchi, T. Okuda, *J. Antibiot. Ser. A* **1967**, *20*, 261–266; b) T. Furamai, N. Nagahama, T. Okuda, *J. Antibiot. Ser. A* **1968**, *21*, 85–90.  
 [5] N. Koyama, M. Yotsumoto, H. Onaka, H. Tomoda, *J. Antibiot.* **2013**, *66*, 303–304.  
 [6] S.-W. Yang, T.-M. Chan, J. Terracciano, D. Loebenberg, M. Patel, M. Chu, *J. Antibiot.* **2005**, *58*, 535–538.  
 [7] S. Liu, H. Dai, G. Makhloufi, C. Heering, C. Janiak, R. Hartmann, A. Mandi, T. Kurtan, W. E. G. Müller, M. U. Kassack, W. Lin, Z. Liu, P. Proksch, *J. Nat. Prod.* **2016**, *79*, 2332–2340.  
 [8] H. B. Bode, M. Walker, A. Zeeck, *Eur. J. Org. Chem.* **2000**, *2000*, 1451–1456.  
 [9] M. Shah, S. K. Deshmukh, S. A. Verekar, A. Gohil, A. S. Kate, V. Rekha, A. Kulkarni-Almeida, *Springerplus* **2015**, *4*, 706, DOI 10.1186/s40064-015-1493-6.  
 [10] Y. Gao, F. Stuhldreier, L. Schmitt, S. Wesselborg, L. Wang, W. E. G. Müller, R. Kalscheuer, Z. Guo, K. Zou, Z. Liu, P. Proksch, *Fitoterapia* **2020**, *146*, 104652.  
 [11] J. S. Harwooda, H. G. Cutler, J. M. Jacyno, *Nat. Prod. Lett.* **1995**, *6*, 181–185.  
 [12] G. Mancilla, D. Jiménez-Teja, M. Femenía-Ríos, A. J. Macías-Sánchez, I. G. Collado, R. Hernández-Galán, *Nat. Prod. Commun.* **2009**, *4*, 395–398.  
 [13] N. Khamthong, V. Rukachaisirikul, S. Phongpaichit, S. Preedanon, J. Sakayaroj, *Phytochem. Lett.* **2014**, *10*, 5–9.  
 [14] H. Kobayashi, M. Kanematsu, M. Yoshida, K. Shishido, *Chem. Commun.* **2011**, *47*, 7440–7442.  
 [15] A. Thiraporn, P. lawsipo, K. Tadpetch, *Synlett* **2022**, *33*, 1341–1346, DOI: 10.1055/a-1792-8402.  
 [16] a) B. Crousse, M. Mladenova, P. Ducept, M. Alami, G. Linstrumelle, *Tetrahedron* **1999**, 4353–4368; b) A. Yajima, Y. Oona, R. Nakagawa, T. Nukada, G. Yabuta, *Bioorg. Med. Chem.* **2009**, *17*, 189–194.  
 [17] a) K. A. Parker, I. A. Katsoulis, *Org. Lett.* **2004**, *6*, 1413–1416; b) B. Zhang, Y. Wang, S. P. Yang, Y. Zhou, W. B. Wu, W. Tang, J. P. Zuo, Y. Li, J. M. Yue, *J. Am. Chem. Soc.* **2012**, *134*, 20605–20608.  
 [18] M. Egi, T. Kawai, M. Umemura, S. Akai, *J. Org. Chem.* **2012**, *77*, 7092–7097.  
 [19] a) M. Morita, Y. Kobayashi, *J. Org. Chem.* **2018**, *83*, 3906–3914; b) K. A. Keaton, A. J. Phillips, *Org. Lett.* **2008**, *10*, 1083–1086.  
 [20] E. W. Tate, D. J. Dixon, S. V. Ley, *Org. Biomol. Chem.* **2006**, *4*, 1698–1706.  
 [21] Y. Ochi, S. Yokoshima, T. Fukuyama, *Org. Lett.* **2016**, *18*, 1494–1496.  
 [22] E. G. Nolen, A. J. Kurish, J. M. Potter, L. A. Donahue, M. D. Orlando, *Org. Lett.* **2005**, *7*, 3383–3386.  
 [23] P. Muangnil, S. Satitsri, K. Tadpetch, P. Saparpakorn, V. Chatsudthipong, S. Hannongbua, V. Rukachaisirikul, C. Muanprasat, *Biochem. Pharmacol.* **2018**, *150*, 293–304.

Manuscript received: March 31, 2022  
 Revised manuscript received: June 20, 2022  
 Accepted manuscript online: June 21, 2022  
 Version of record online: July 6, 2022

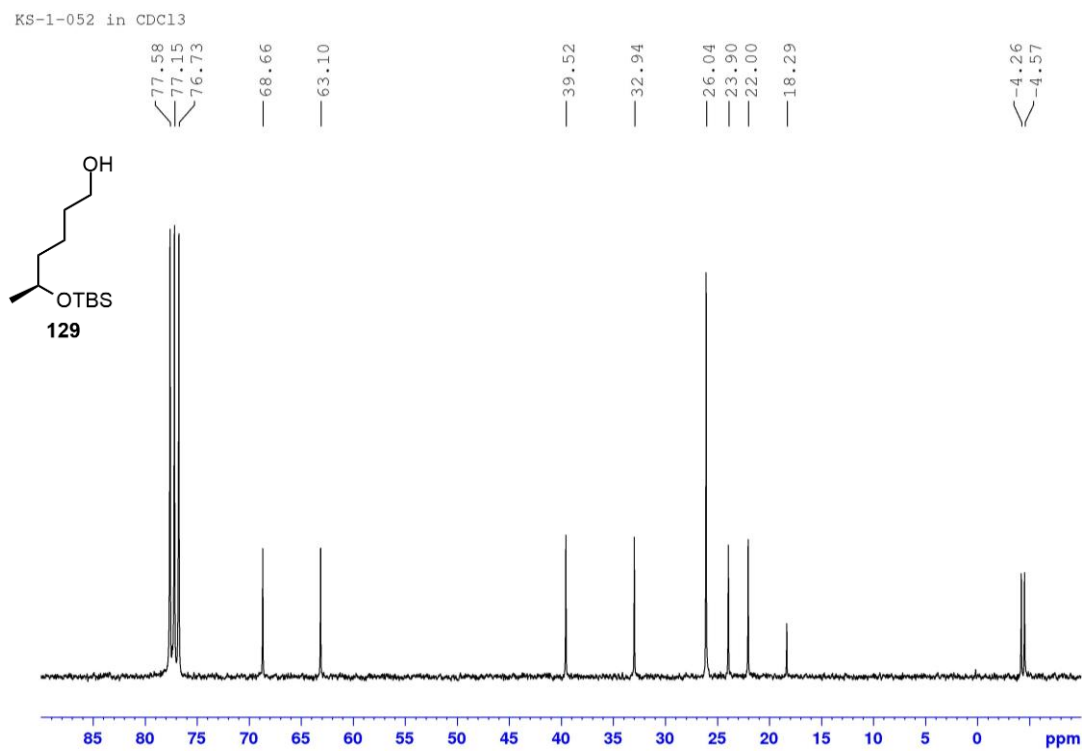
**$^1\text{H}$  and  $^{13}\text{C}$  NMR Spectra****Figure 11**  $^1\text{H}$  NMR (300 MHz,  $\text{CDCl}_3$ ) spectrum of compound **128****Figure 12**  $^{13}\text{C}$  NMR (75 MHz,  $\text{CDCl}_3$ ) spectrum of compound **128**



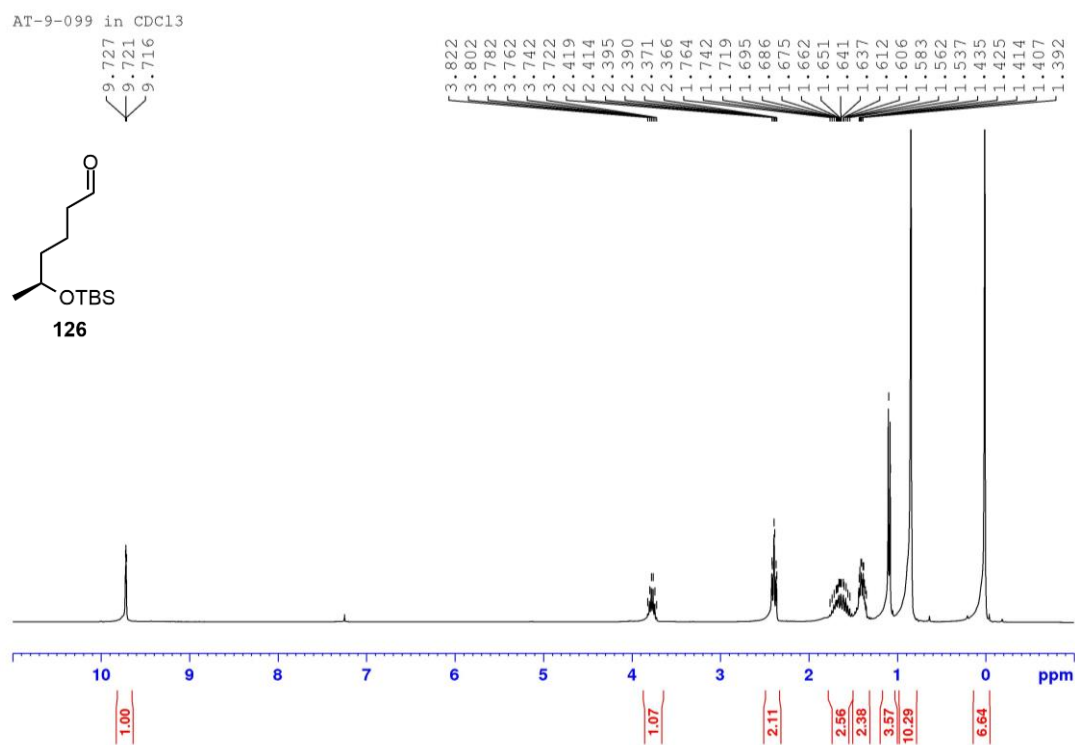
**Figure 13**  $^1\text{H}$  NMR (300 MHz,  $\text{CDCl}_3$ ) spectrum of compound **129**



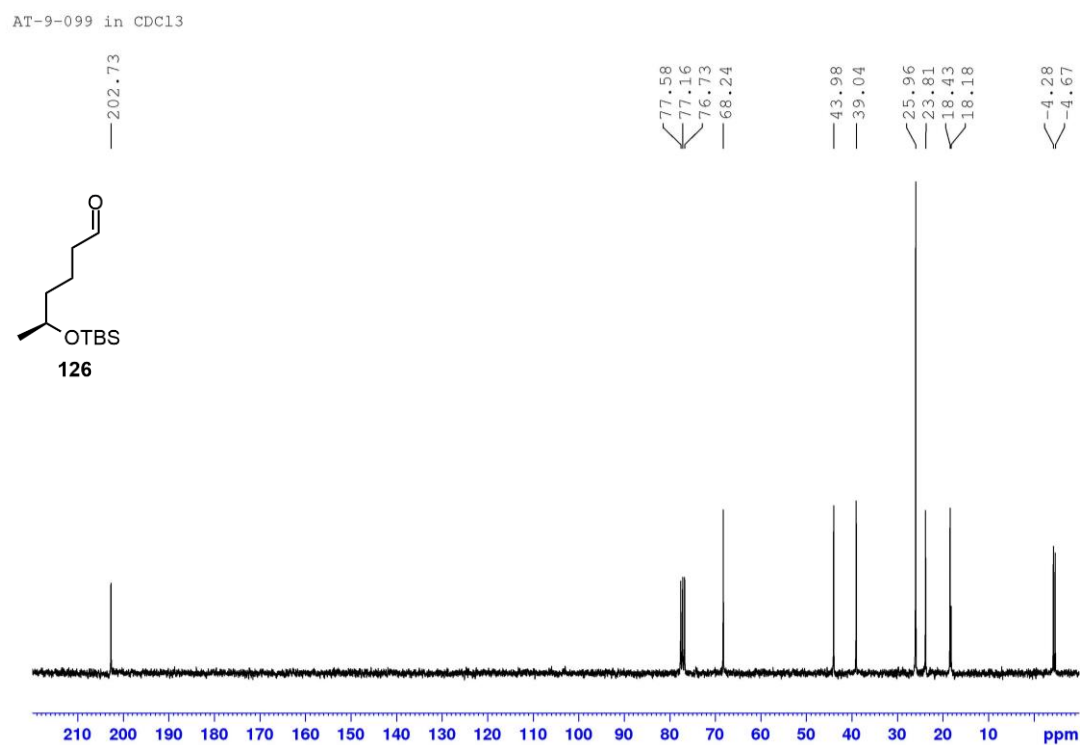
**Figure 14**  $^{13}\text{C}$  NMR (75 MHz,  $\text{CDCl}_3$ ) spectrum of compound **129**



**Figure 15**  $^1\text{H}$  NMR (300 MHz,  $\text{CDCl}_3$ ) spectrum of compound **126**

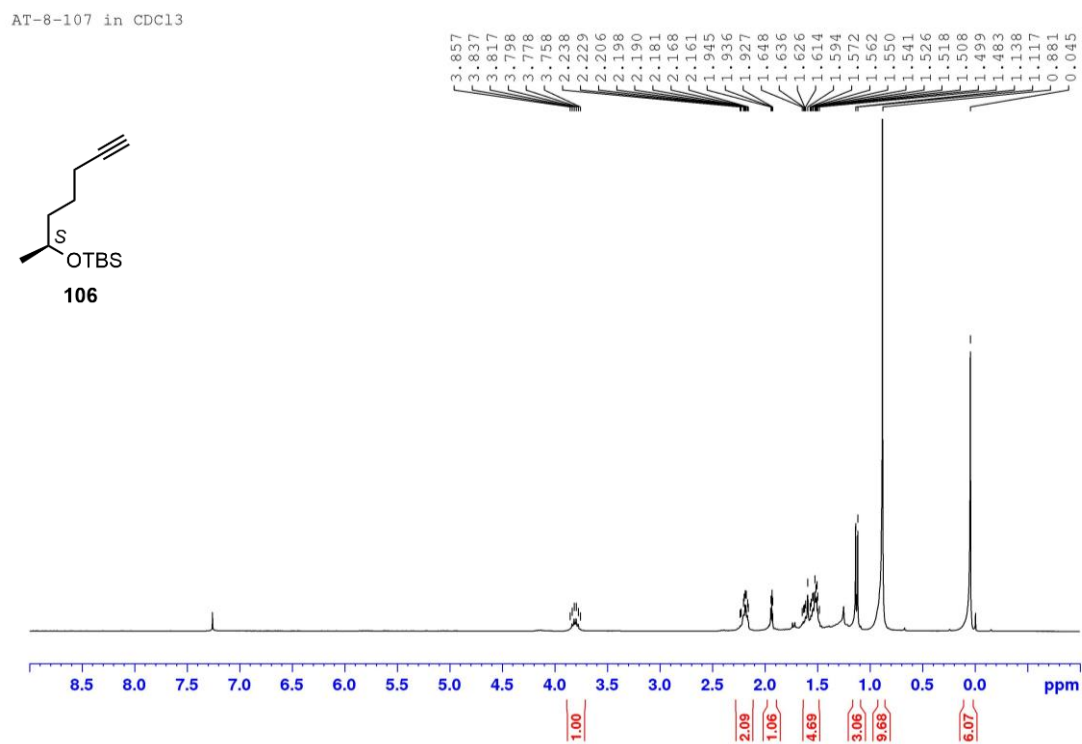


**Figure 16**  $^{13}\text{C}$  NMR (75 MHz,  $\text{CDCl}_3$ ) spectrum of compound **126**

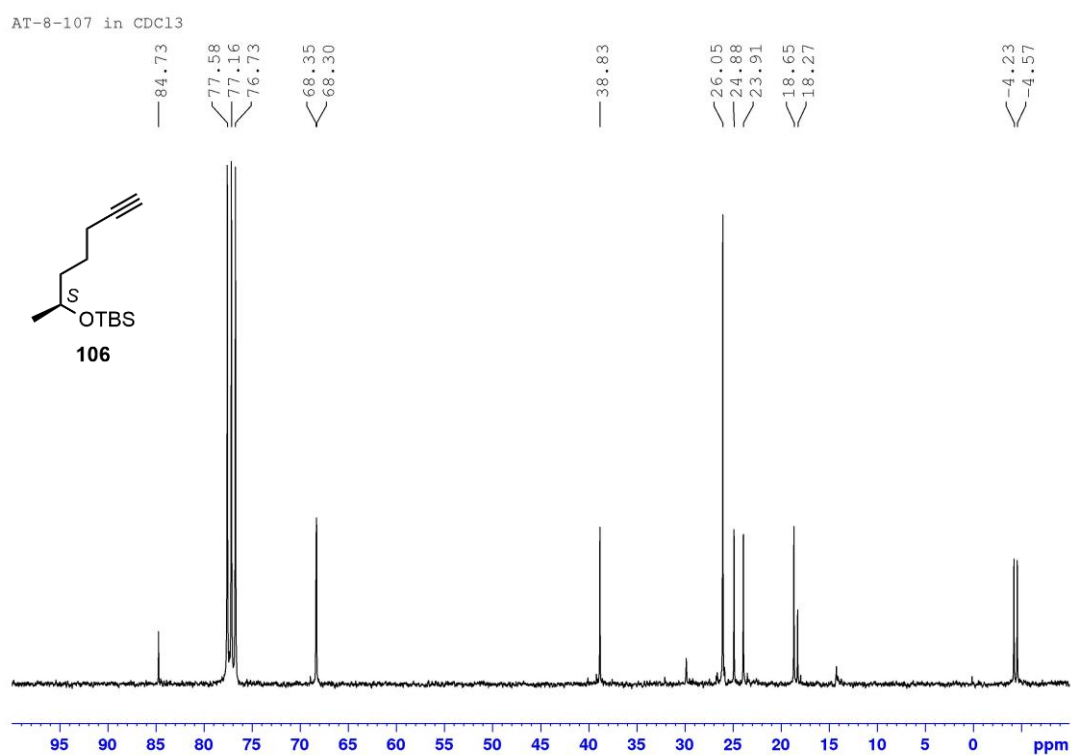


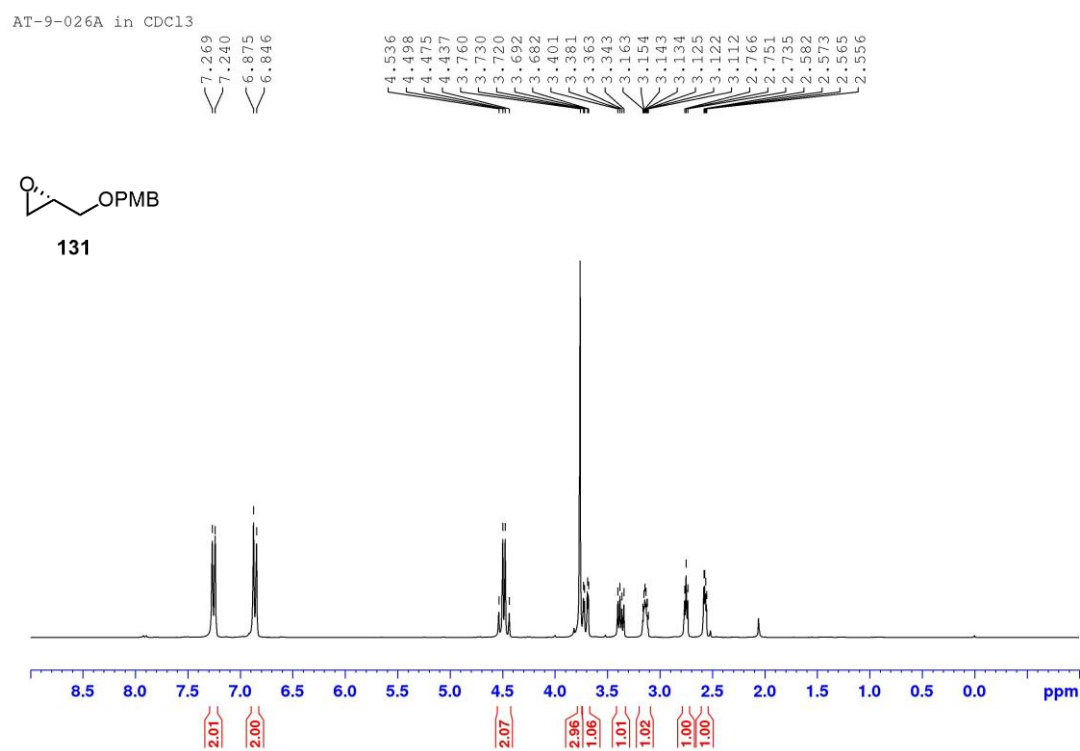
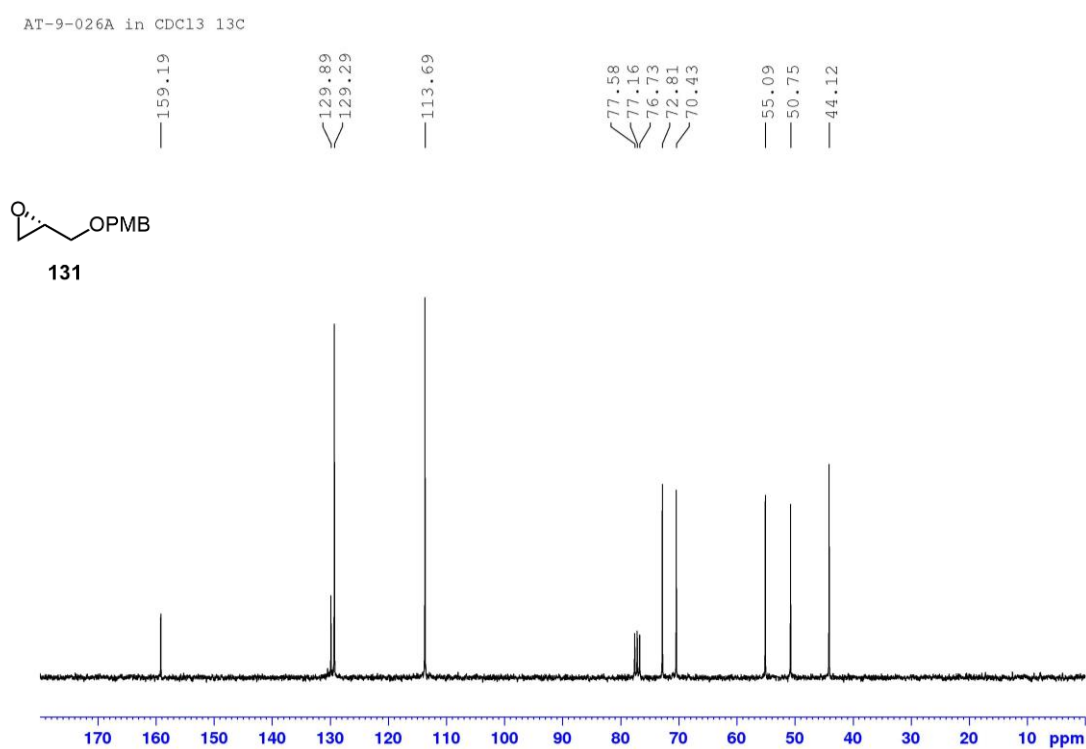


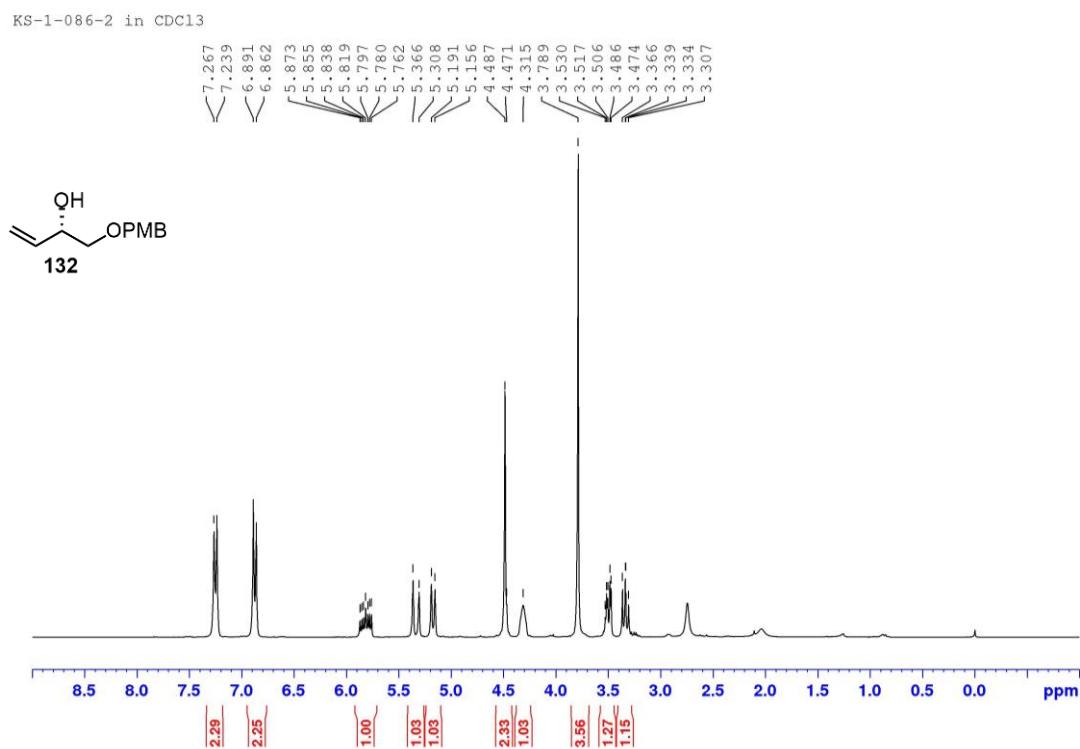
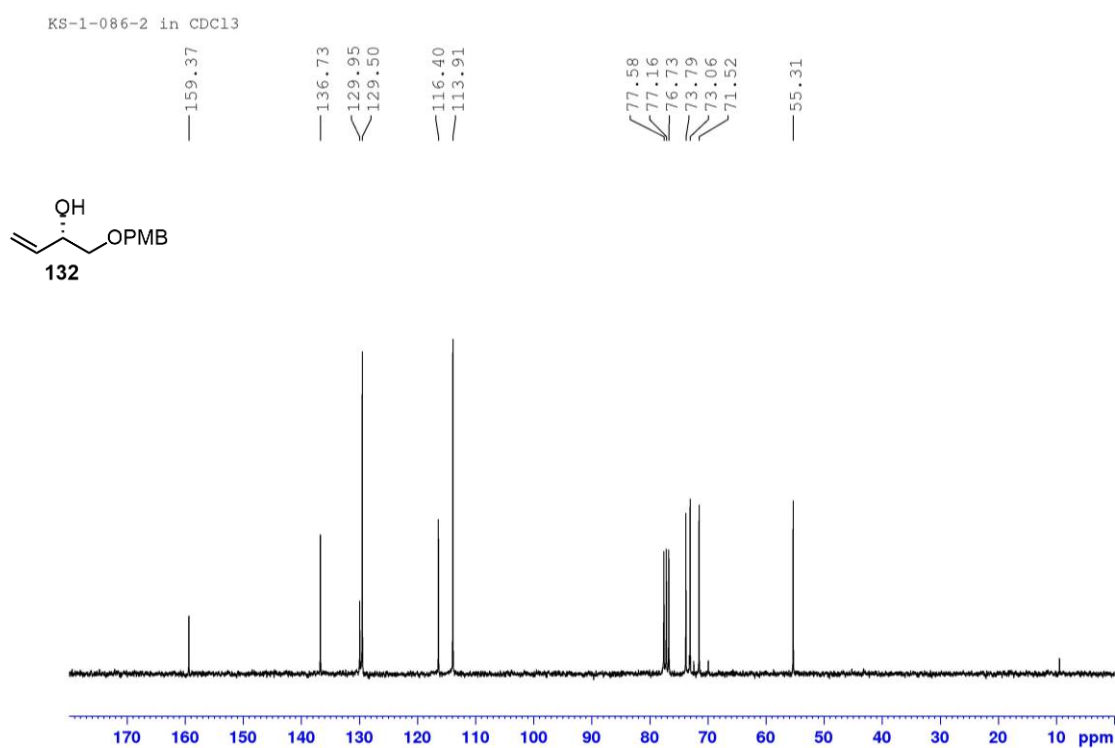
**Figure 17**  $^1\text{H}$  NMR (300 MHz,  $\text{CDCl}_3$ ) spectrum of compound **106**



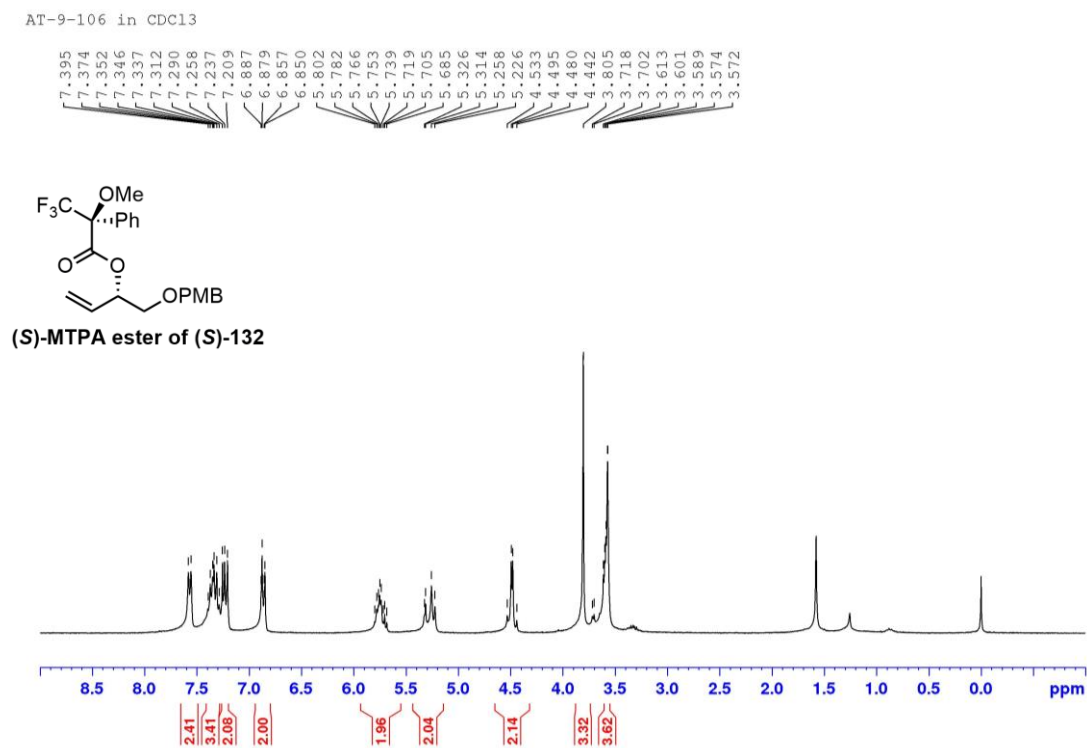
**Figure 18**  $^{13}\text{C}$  NMR (75 MHz,  $\text{CDCl}_3$ ) spectrum of compound **106**



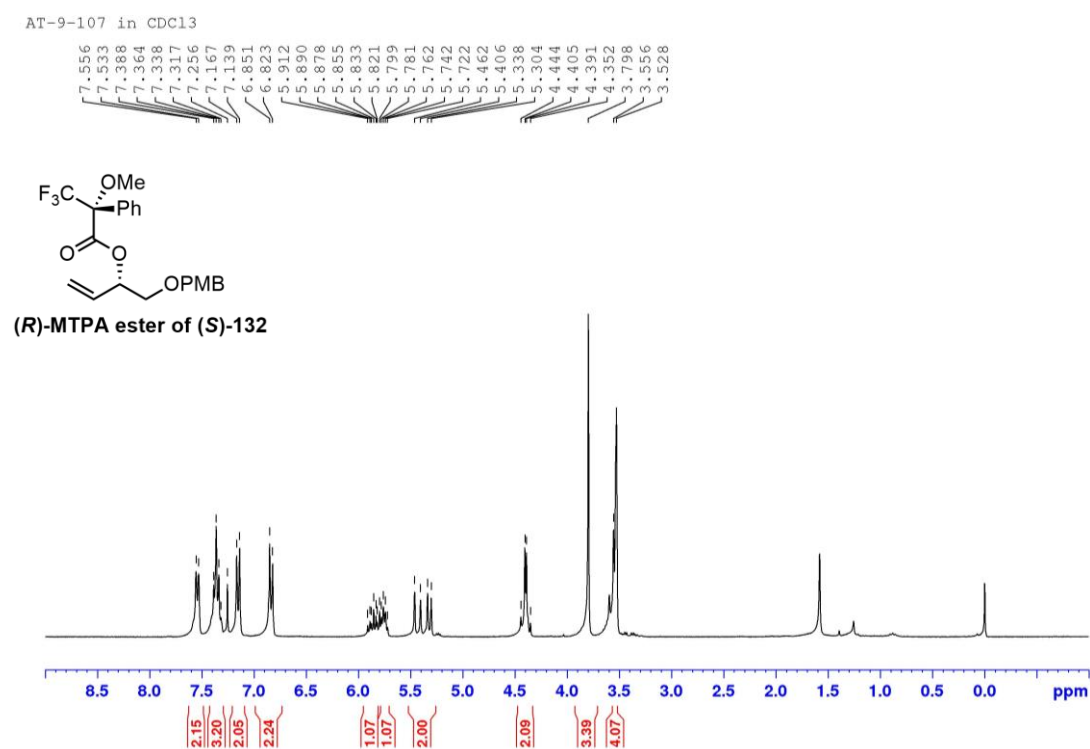
**Figure 19**  $^1\text{H}$  NMR (300 MHz,  $\text{CDCl}_3$ ) spectrum of compound **131****Figure 20**  $^{13}\text{C}$  NMR (75 MHz,  $\text{CDCl}_3$ ) spectrum of compound **131**

**Figure 21**  $^1\text{H}$  NMR (300 MHz,  $\text{CDCl}_3$ ) spectrum of compound **132****Figure 22**  $^{13}\text{C}$  NMR (75 MHz,  $\text{CDCl}_3$ ) spectrum of compound **132**

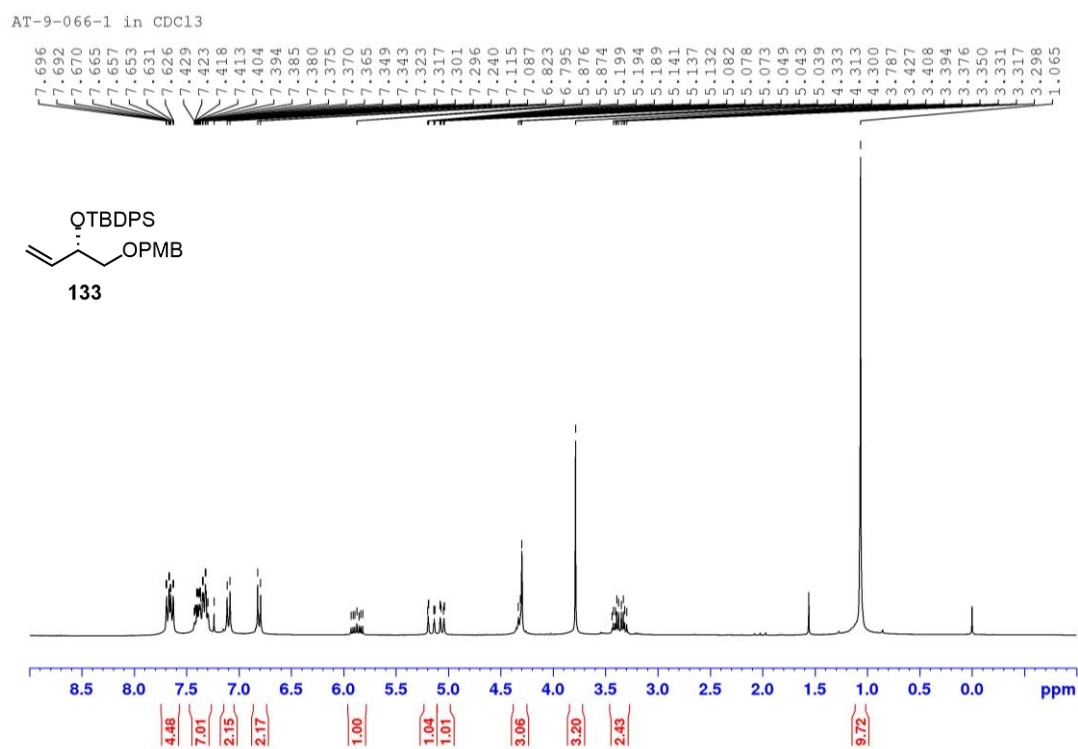
**Figure 23**  $^1\text{H}$  NMR (300 MHz,  $\text{CDCl}_3$ ) spectrum of (*S*)-MTPA ester of (*S*)-132



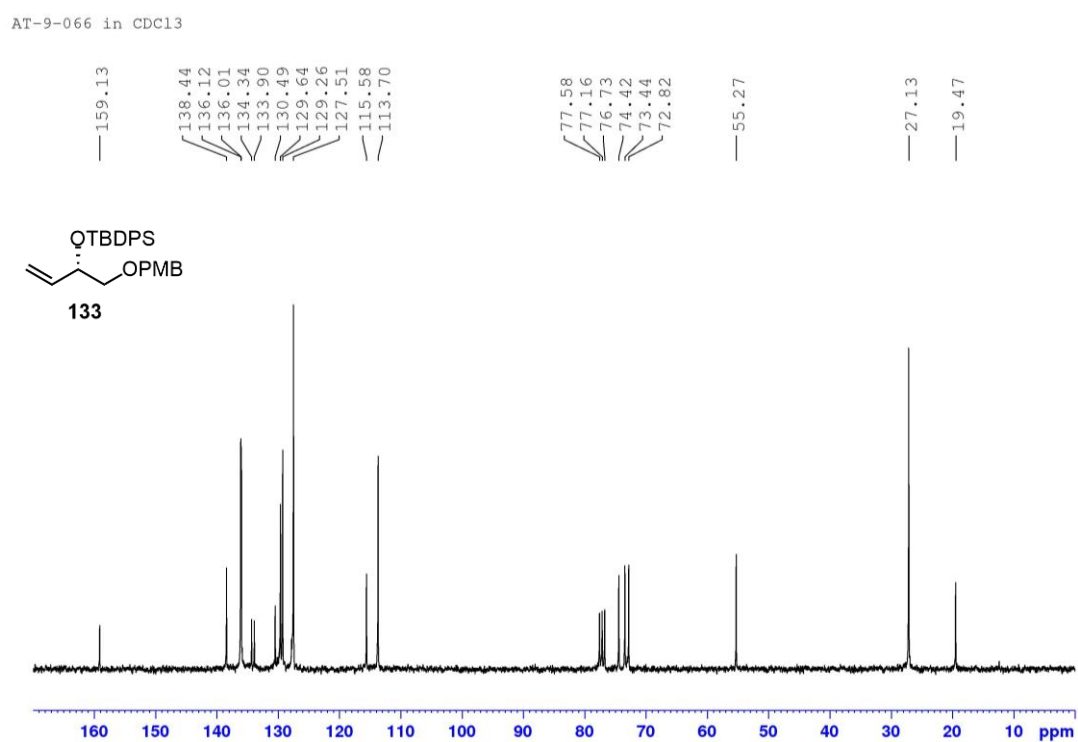
**Figure 24**  $^1\text{H}$  NMR (300 MHz,  $\text{CDCl}_3$ ) spectrum of (*R*)-MTPA ester of (*S*)-132

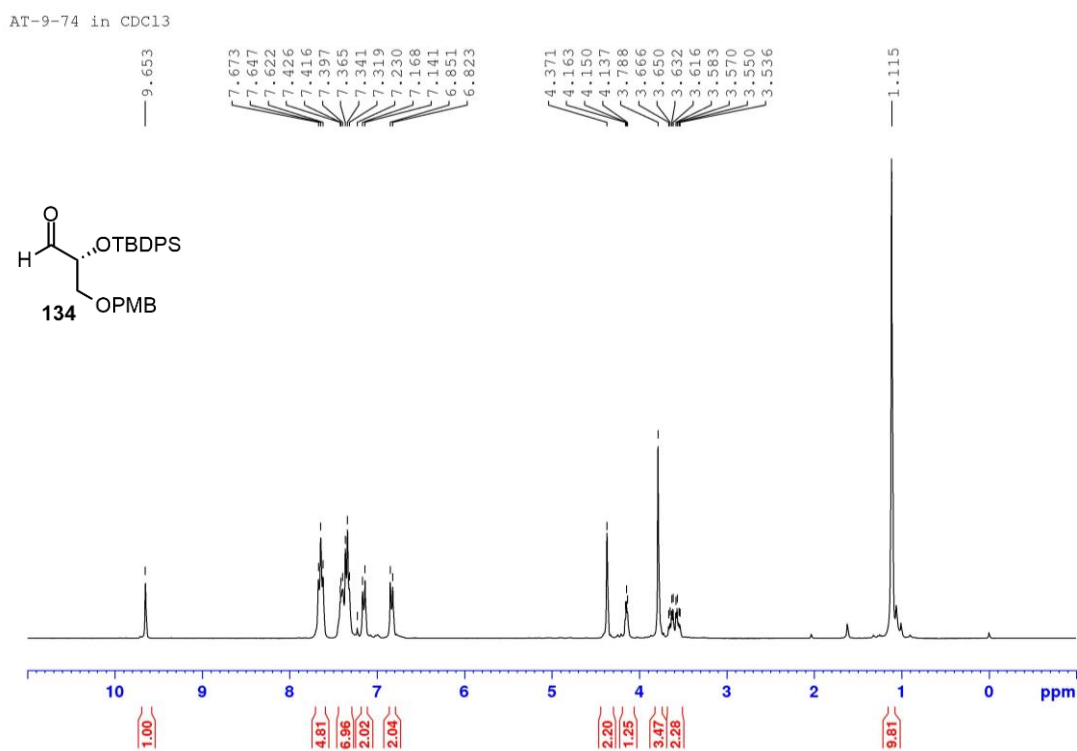
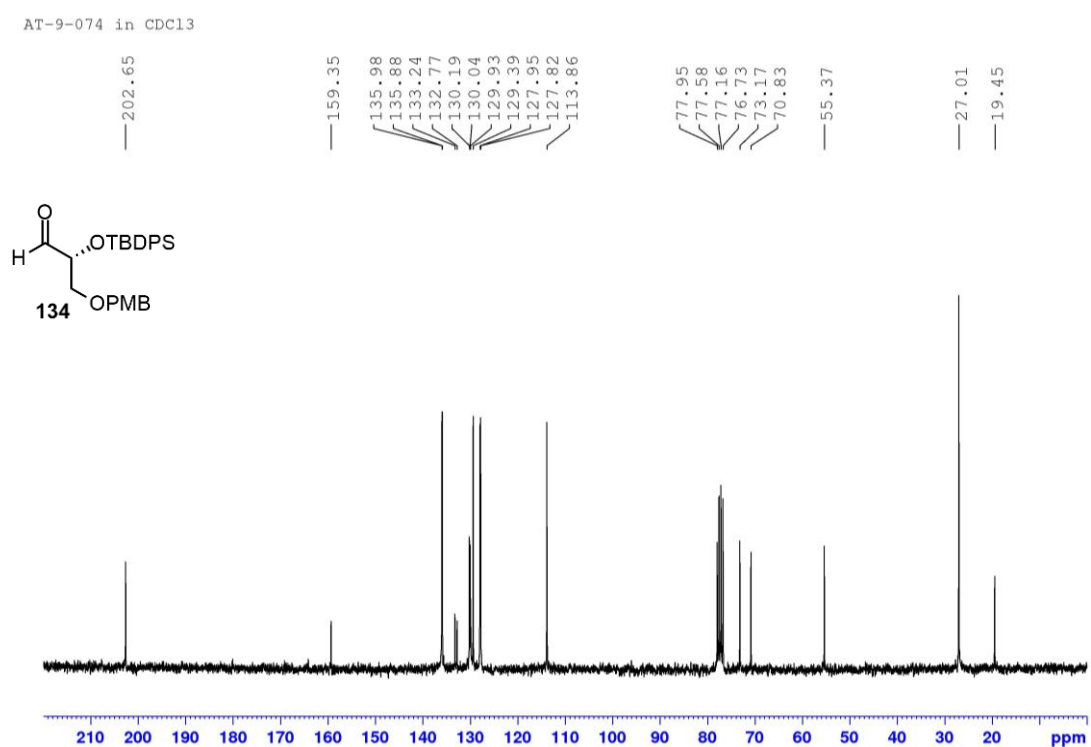


**Figure 25**  $^1\text{H}$  NMR (300 MHz,  $\text{CDCl}_3$ ) spectrum of compound **133**

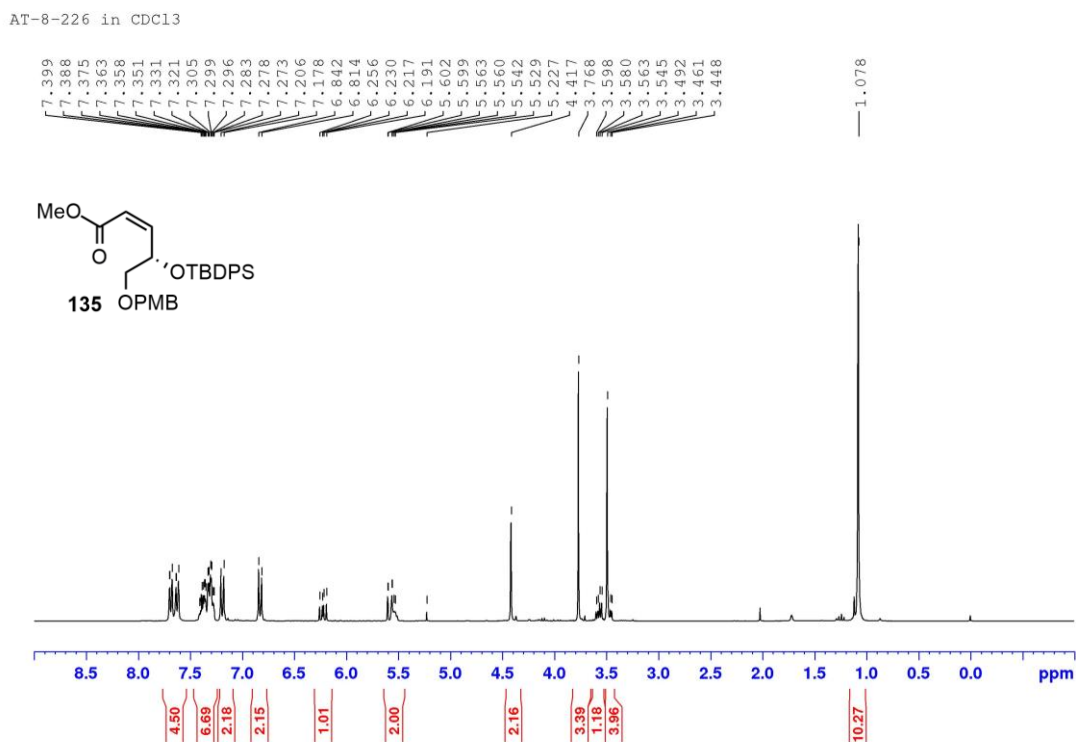


**Figure 26**  $^{13}\text{C}$  NMR (75 MHz,  $\text{CDCl}_3$ ) spectrum of compound **133**

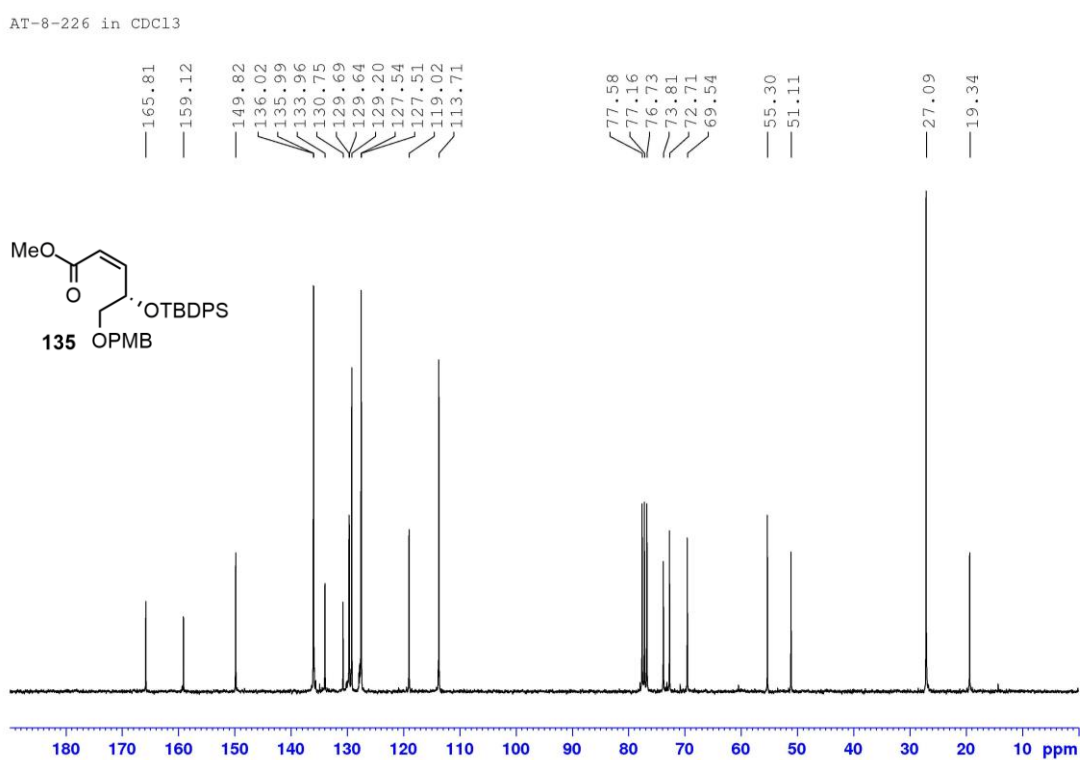


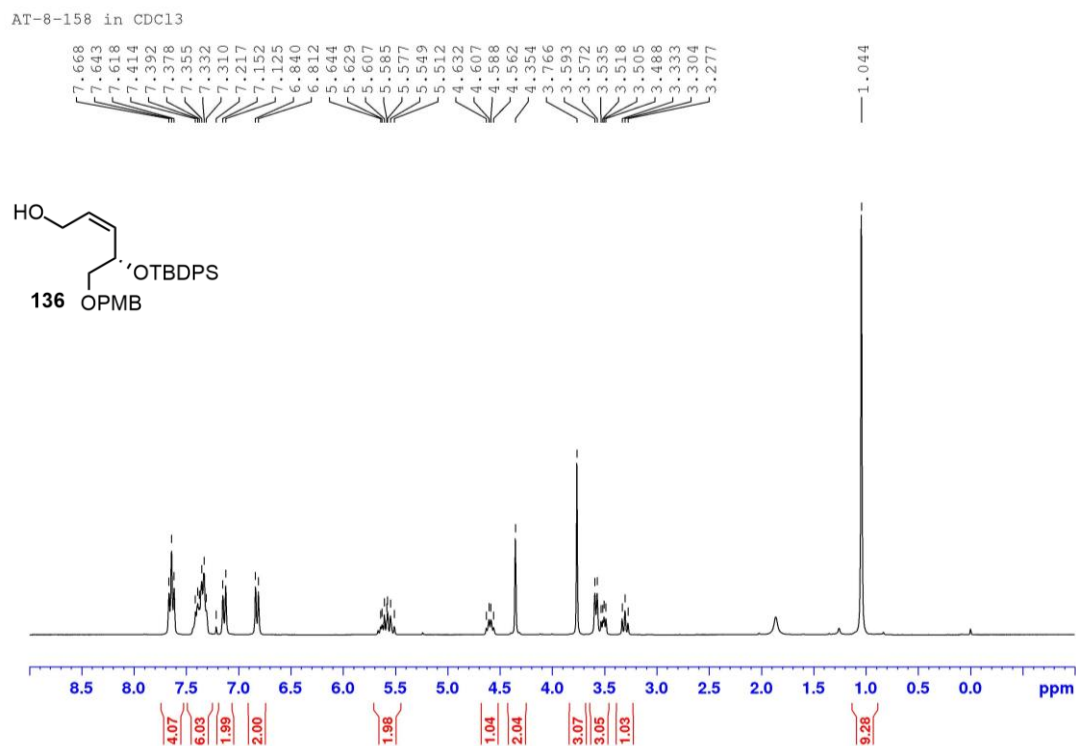
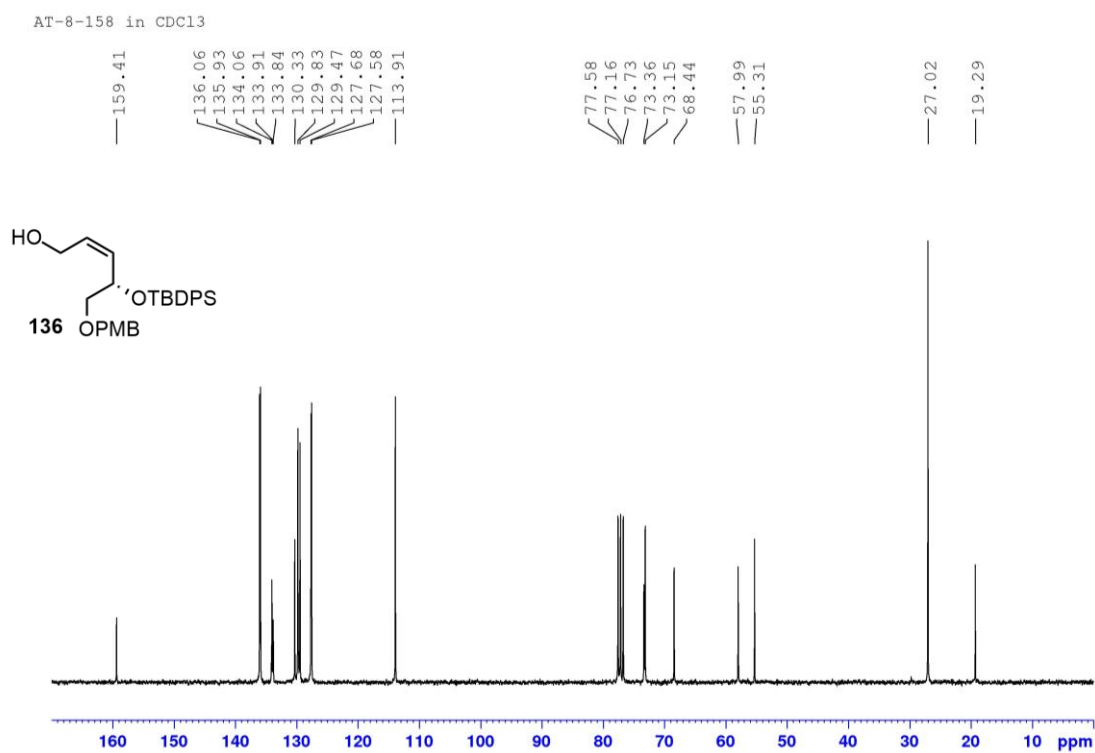
**Figure 27**  $^1\text{H}$  NMR (300 MHz,  $\text{CDCl}_3$ ) spectrum of compound **134****Figure 28**  $^{13}\text{C}$  NMR (75 MHz,  $\text{CDCl}_3$ ) spectrum of compound **134**

**Figure 29**  $^1\text{H}$  NMR (300 MHz,  $\text{CDCl}_3$ ) spectrum of compound **135**

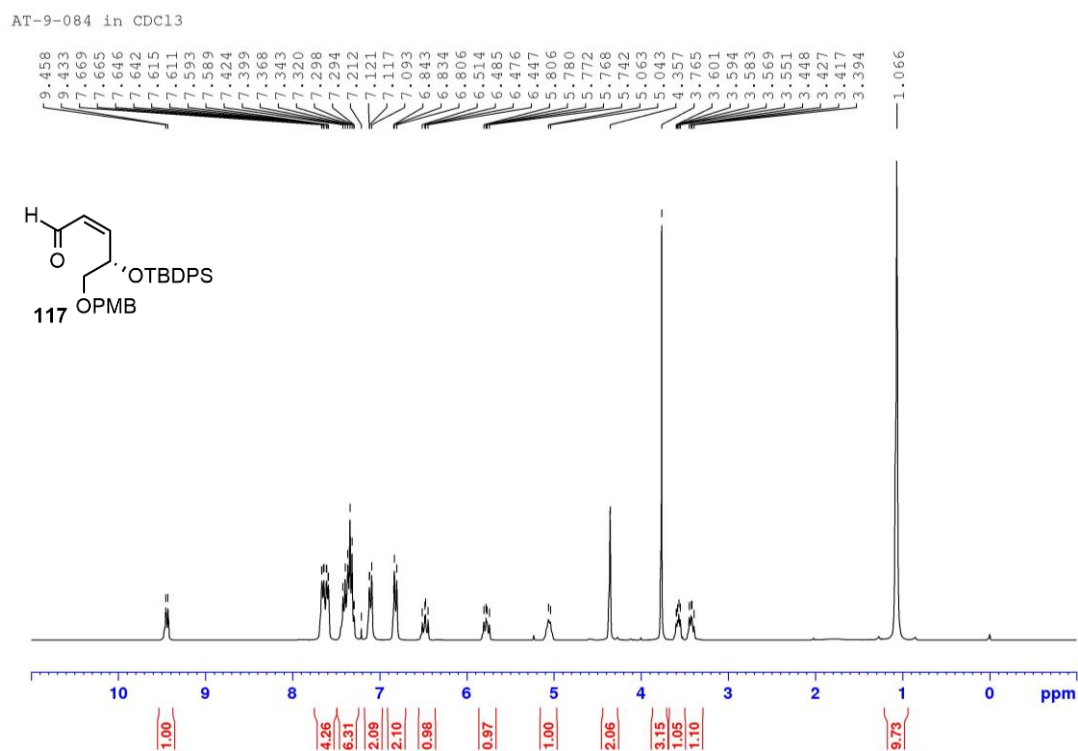
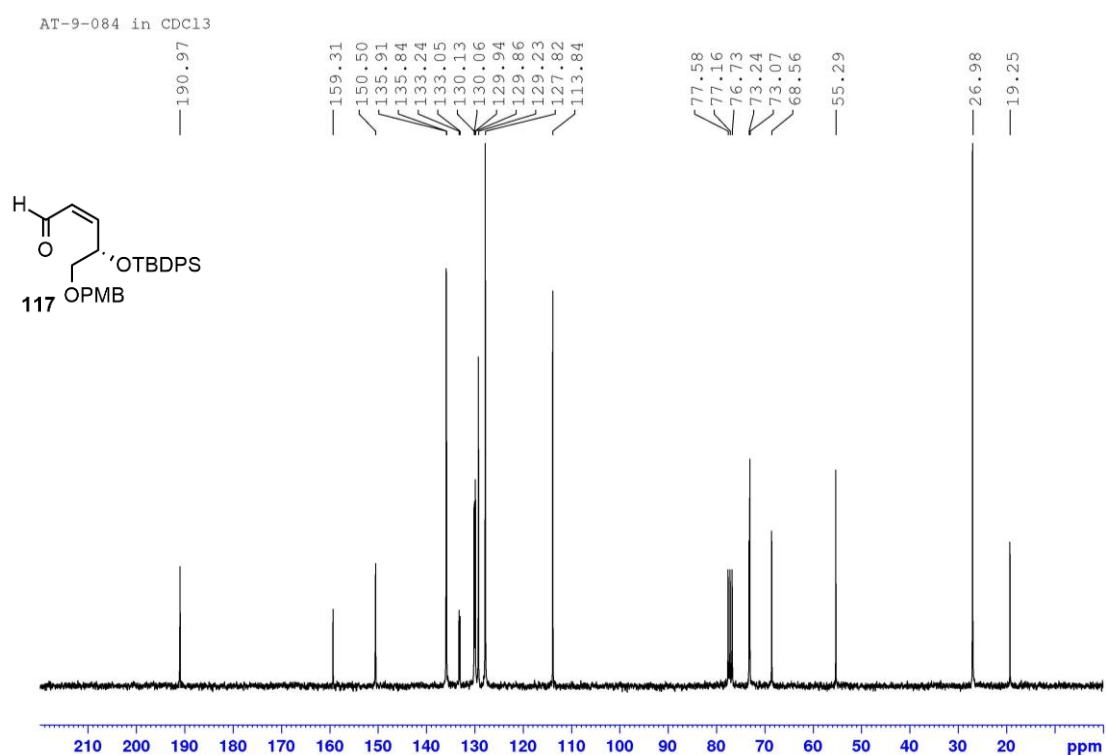


**Figure 30**  $^{13}\text{C}$  NMR (75 MHz,  $\text{CDCl}_3$ ) spectrum of compound **135**

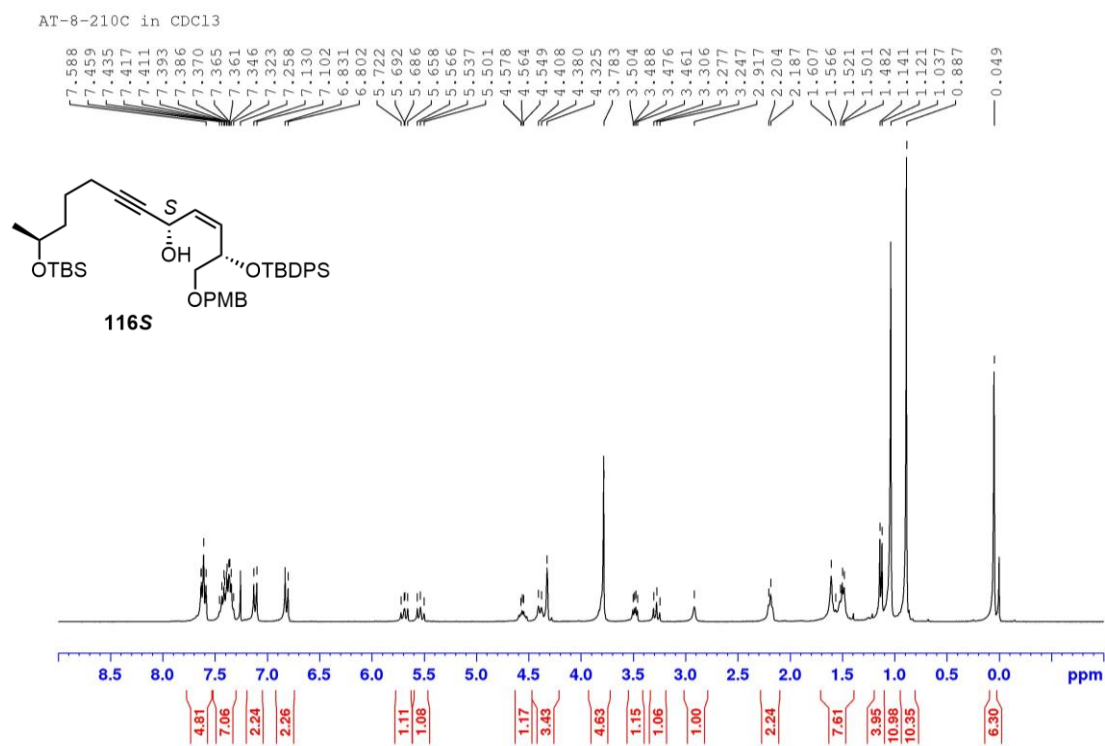


**Figure 31**  $^1\text{H}$  NMR (300 MHz,  $\text{CDCl}_3$ ) spectrum of compound **136****Figure 32**  $^{13}\text{C}$  NMR (75 MHz,  $\text{CDCl}_3$ ) spectrum of compound **136**

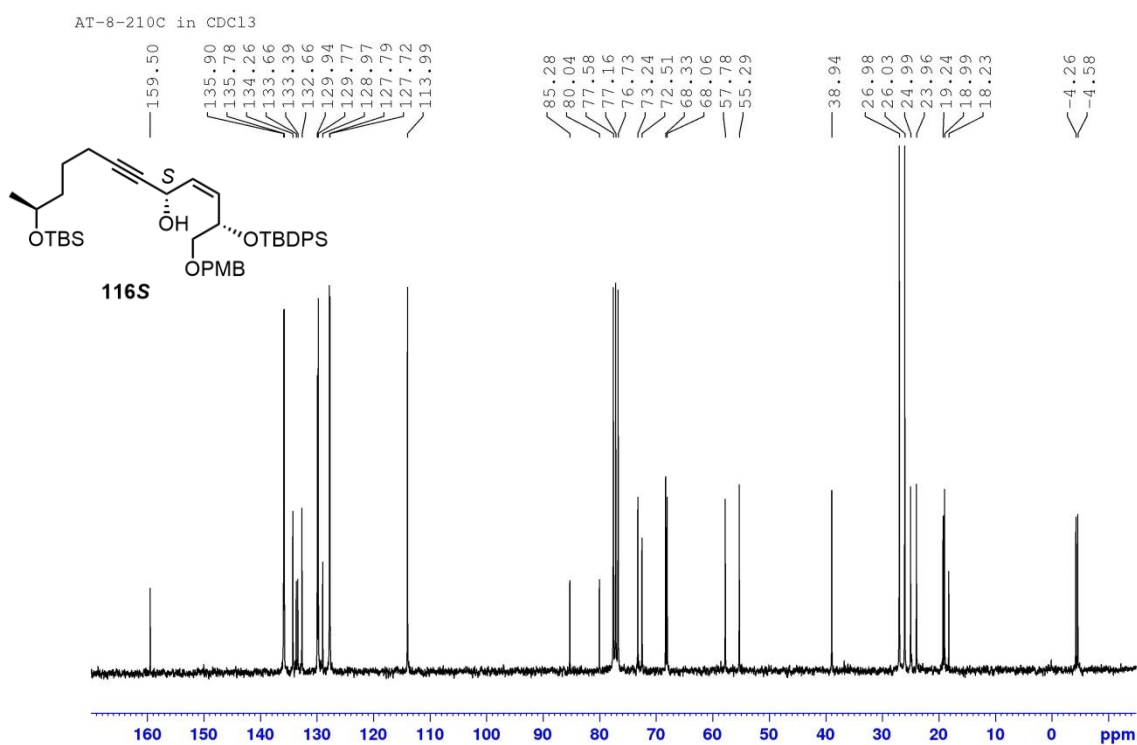


**Figure 33**  $^1\text{H}$  NMR (300 MHz,  $\text{CDCl}_3$ ) spectrum of compound **117****Figure 34**  $^{13}\text{C}$  NMR (75 MHz,  $\text{CDCl}_3$ ) spectrum of compound **117**

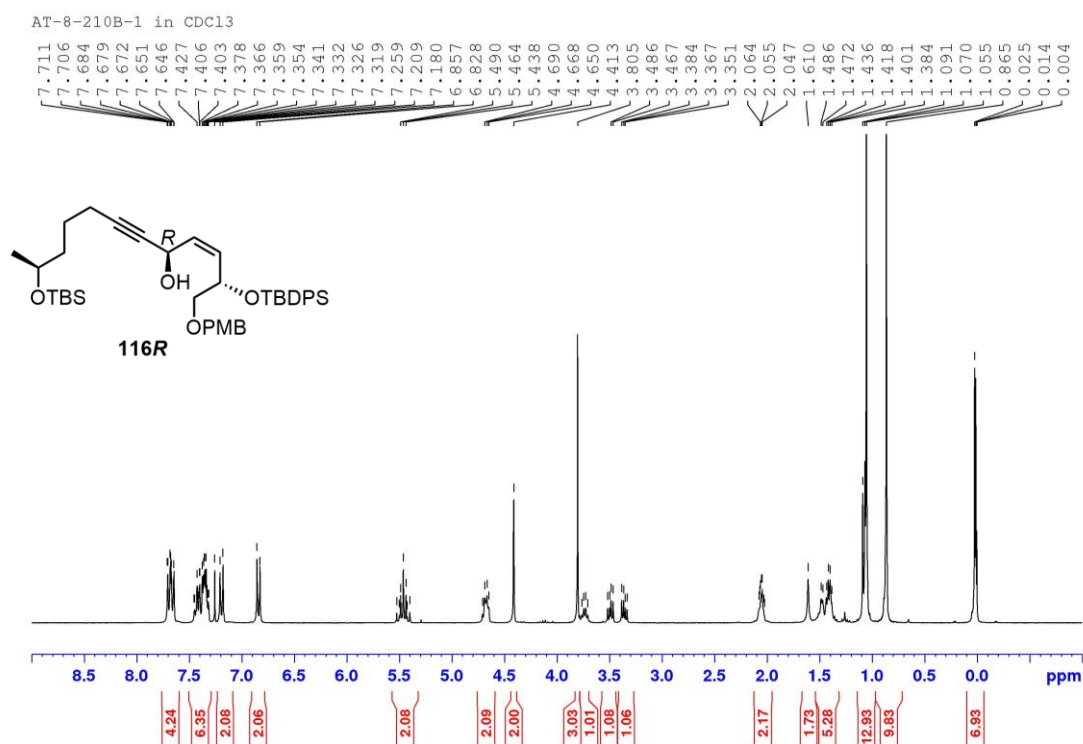
**Figure 35**  $^1\text{H}$  NMR (300 MHz,  $\text{CDCl}_3$ ) spectrum of compound **116S**



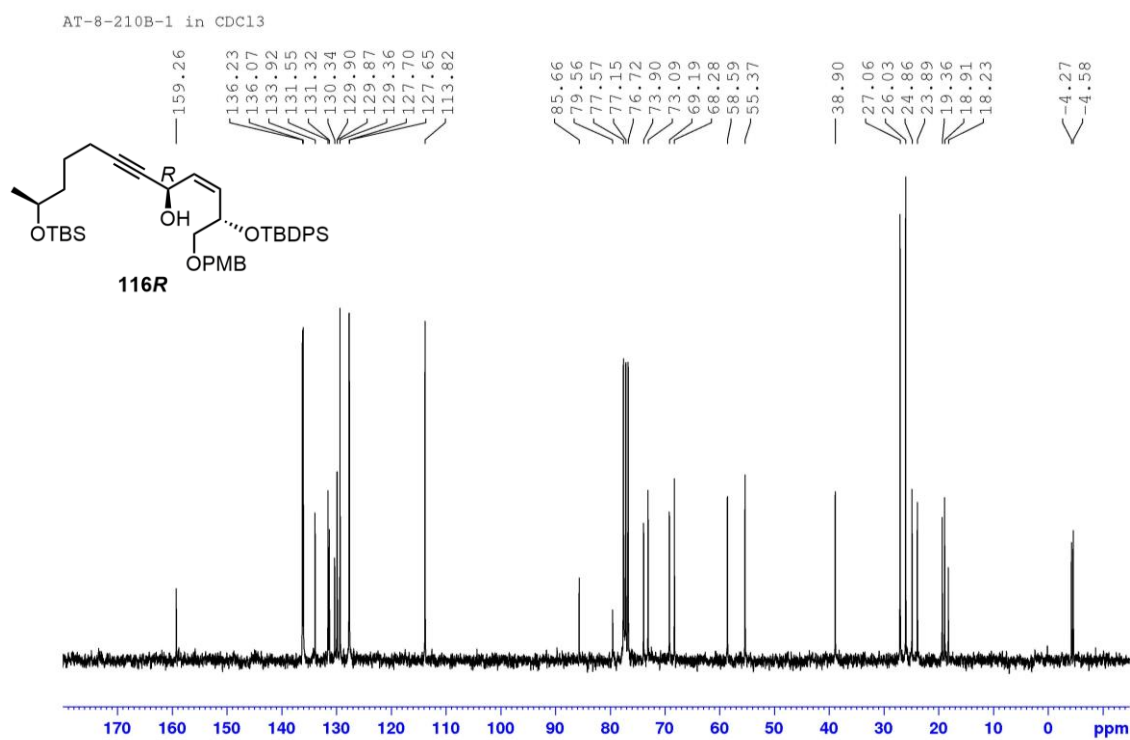
**Figure 36**  $^{13}\text{C}$  NMR (75 MHz,  $\text{CDCl}_3$ ) spectrum of compound **116S**



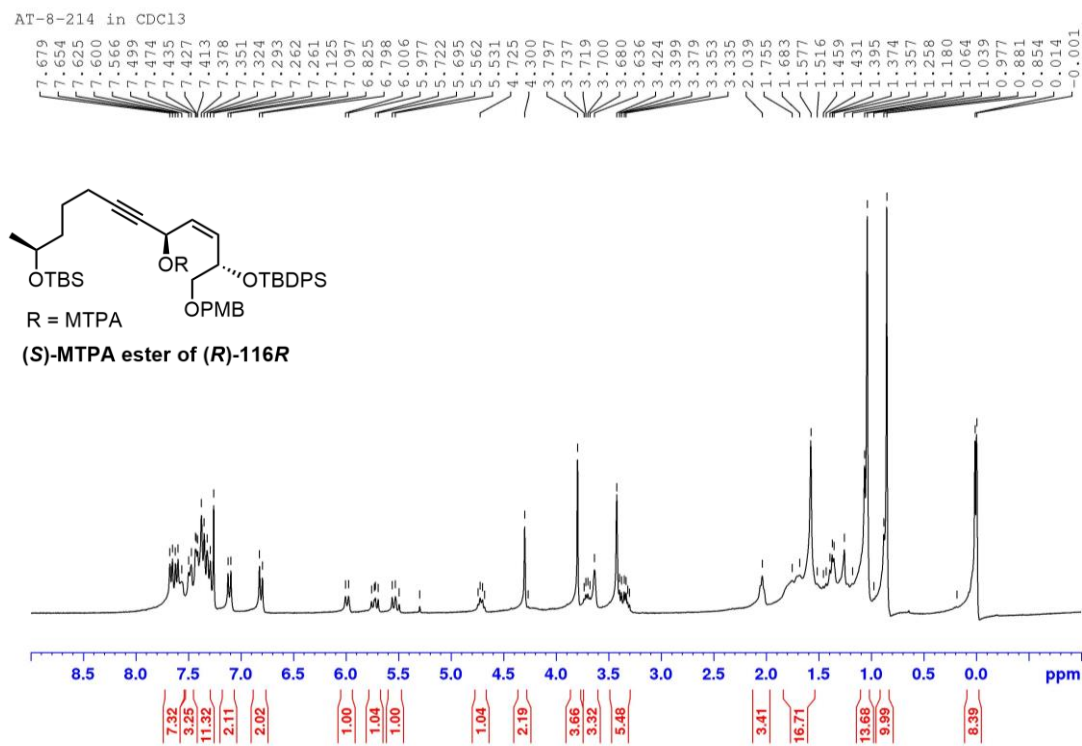
**Figure 37**  $^1\text{H}$  NMR (300 MHz,  $\text{CDCl}_3$ ) spectrum of compound **116R**



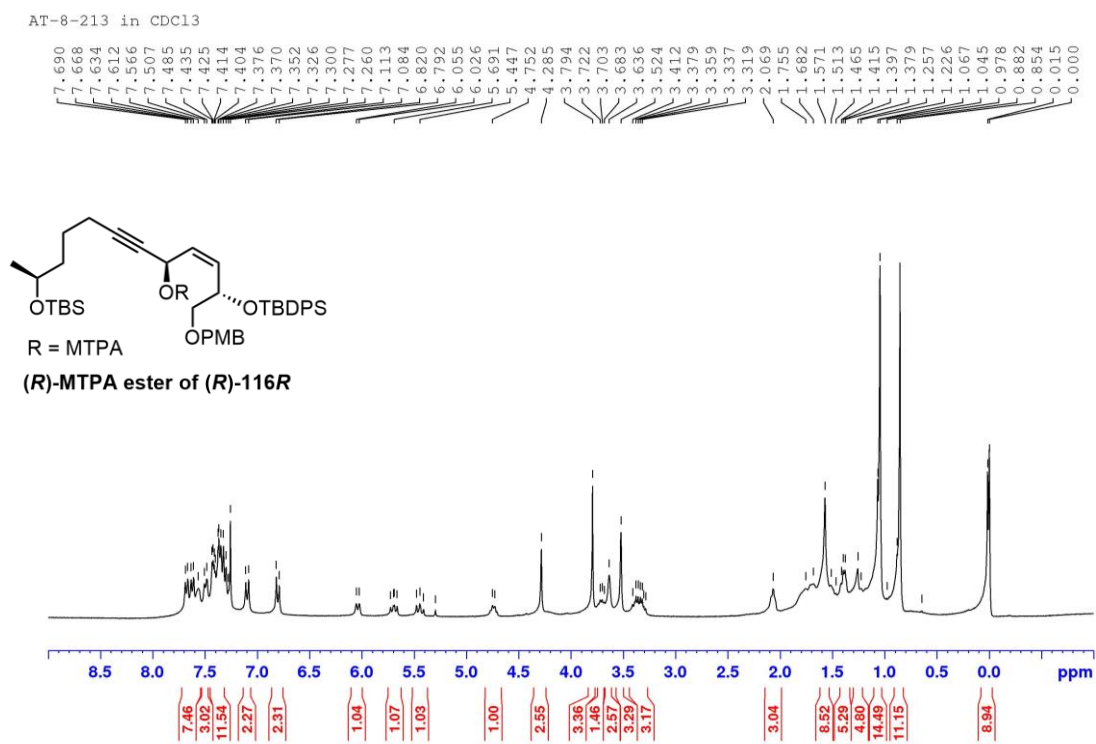
**Figure 38**  $^{13}\text{C}$  NMR (75 MHz,  $\text{CDCl}_3$ ) spectrum of compound **116R**



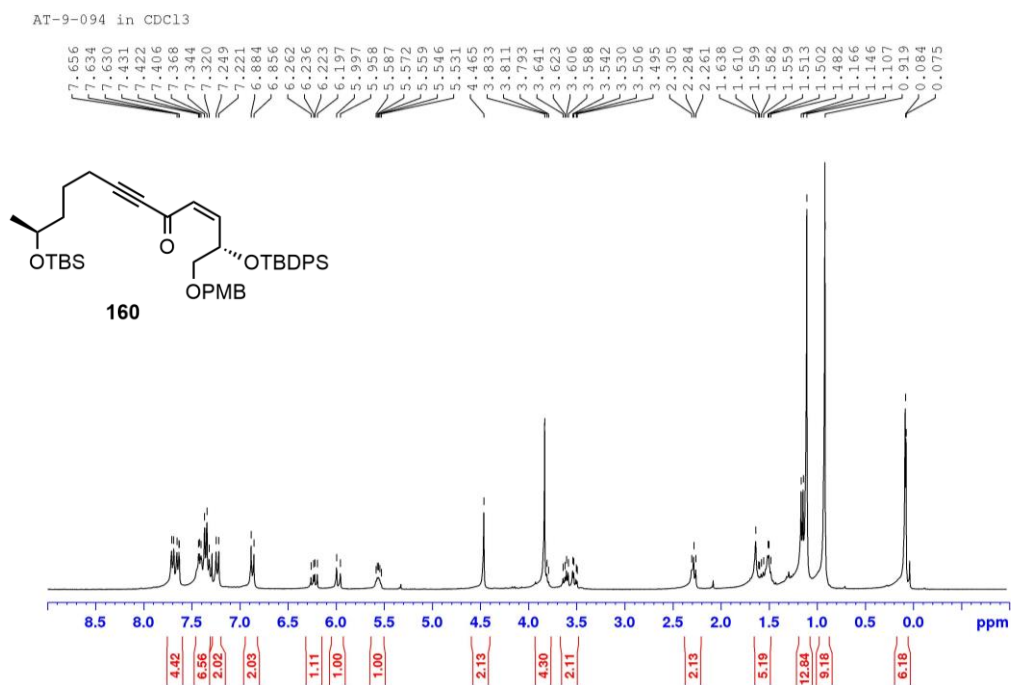
**Figure 39**  $^1\text{H}$  NMR (300 MHz,  $\text{CDCl}_3$ ) spectrum of (*S*)-MTPA ester of **116R**



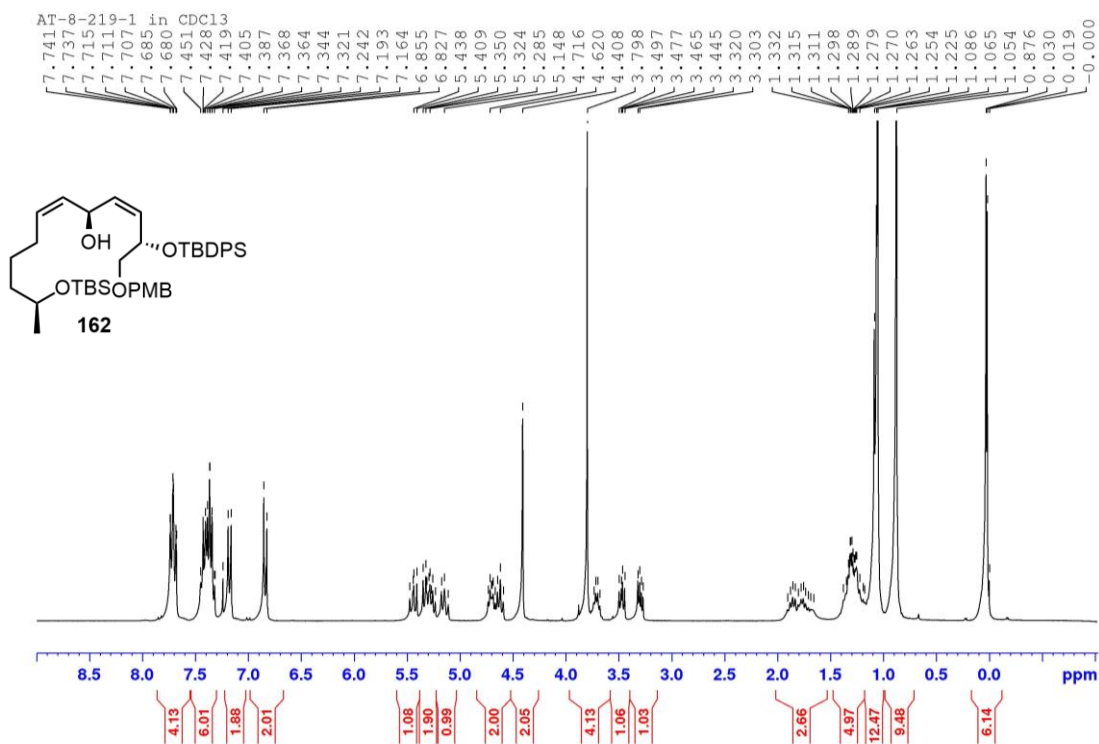
**Figure 40**  $^1\text{H}$  NMR (300 MHz,  $\text{CDCl}_3$ ) spectrum of (*R*)-MTPA ester of **116R**



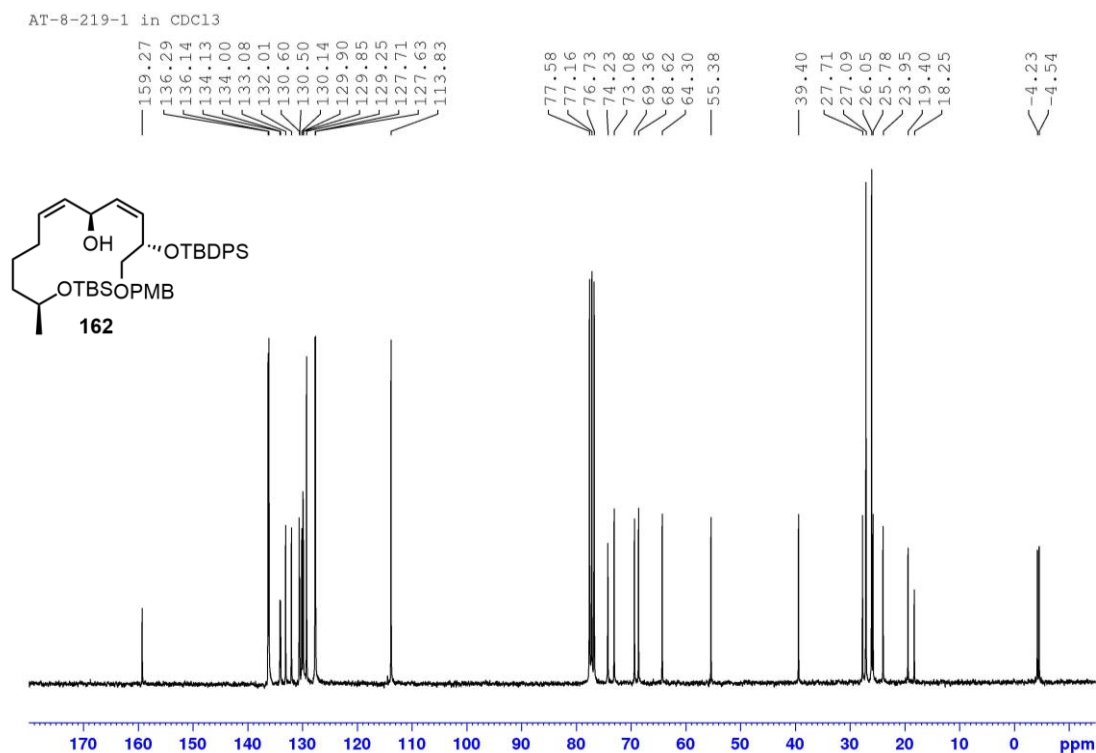
**Figure 41**  $^1\text{H}$  NMR (300 MHz,  $\text{CDCl}_3$ ) spectrum of compound **160**



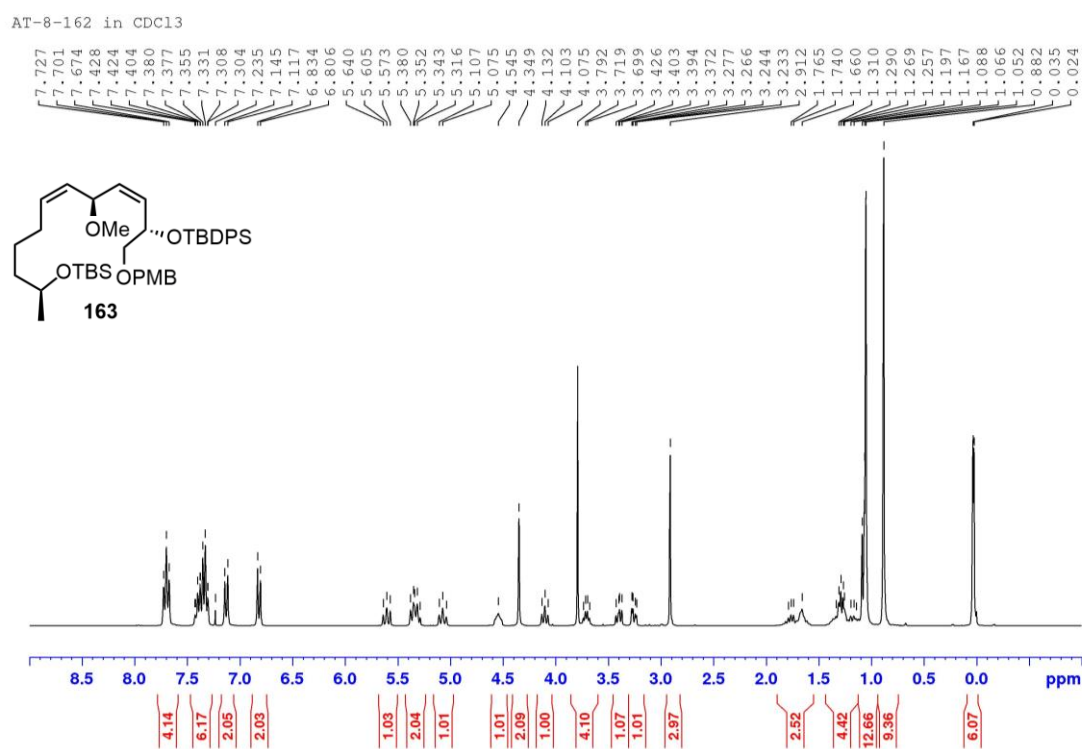
**Figure 42**  $^1\text{H}$  NMR (300 MHz,  $\text{CDCl}_3$ ) spectrum of compound **162**



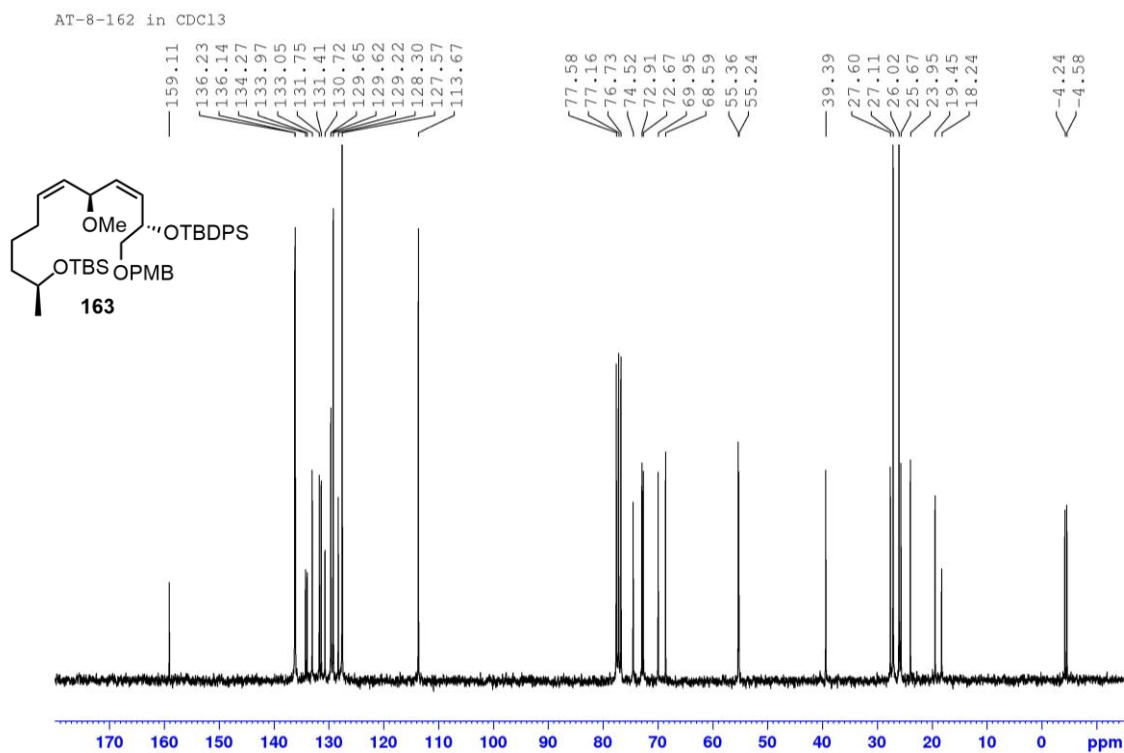
**Figure 43**  $^{13}\text{C}$  NMR (75 MHz,  $\text{CDCl}_3$ ) spectrum of compound **162**



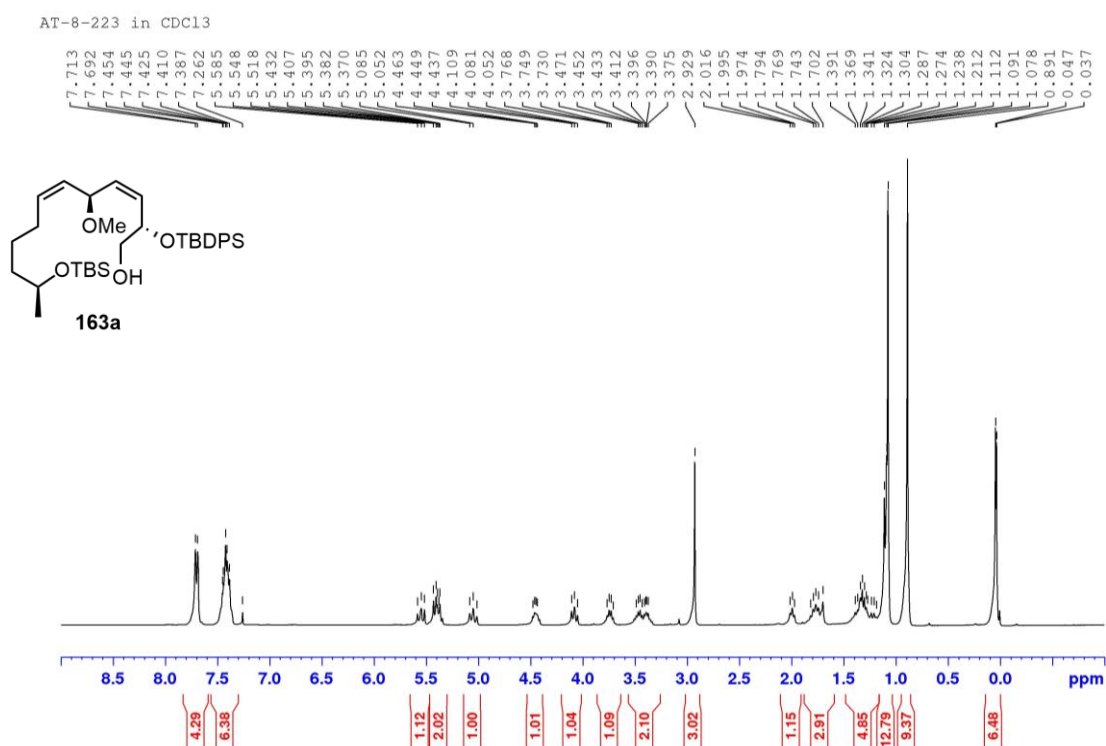
**Figure 44**  $^1\text{H}$  NMR (300 MHz,  $\text{CDCl}_3$ ) spectrum of compound **163**



**Figure 45**  $^{13}\text{C}$  NMR (75 MHz,  $\text{CDCl}_3$ ) spectrum of compound **163**

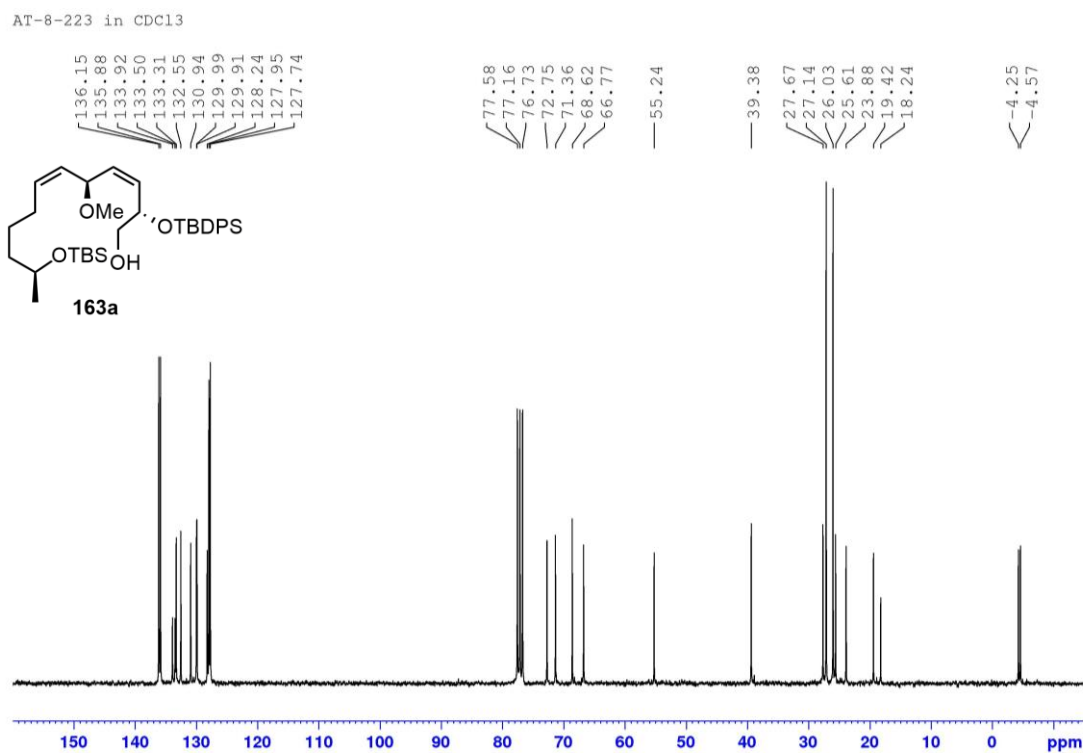


**Figure 46**  $^1\text{H}$  NMR (300 MHz,  $\text{CDCl}_3$ ) spectrum of compound **163a**

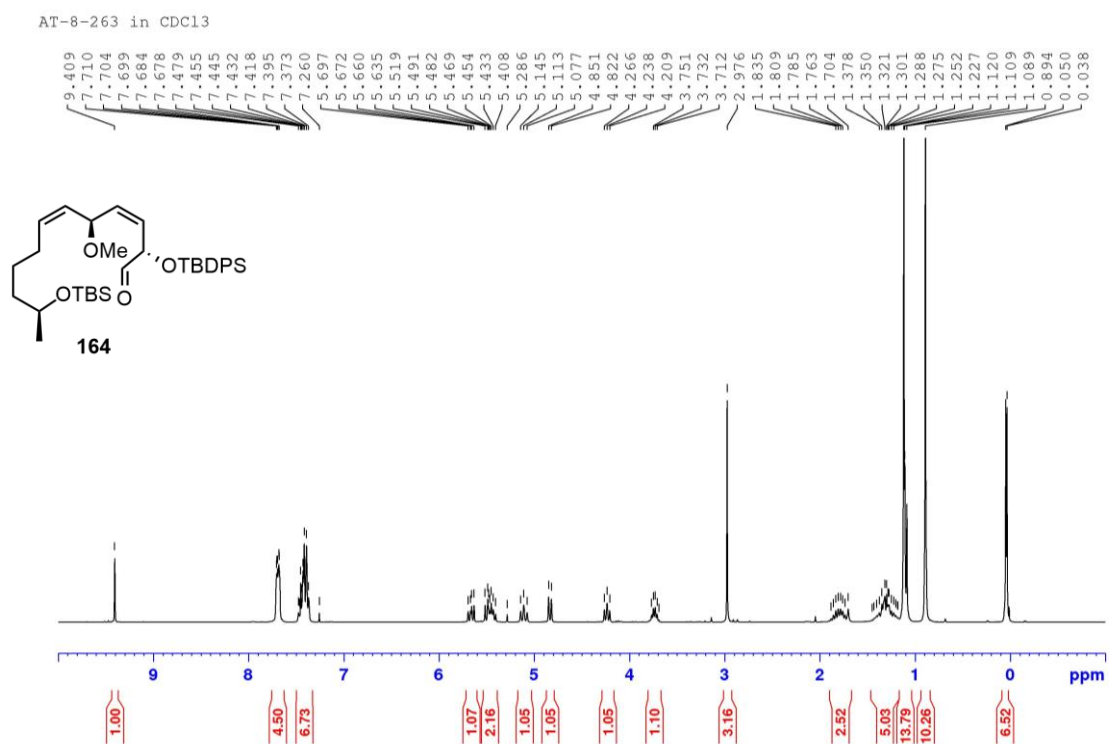




**Figure 47**  $^{13}\text{C}$  NMR (75 MHz,  $\text{CDCl}_3$ ) spectrum of compound **163a**

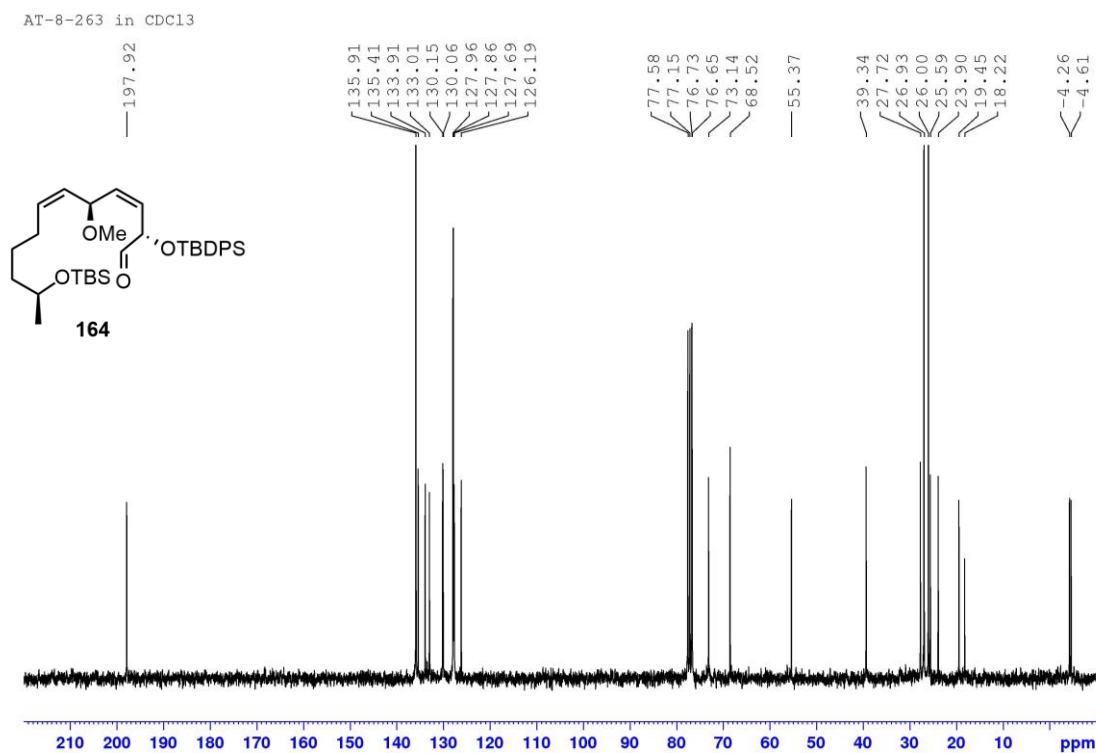


**Figure 48**  $^1\text{H}$  NMR (300 MHz,  $\text{CDCl}_3$ ) spectrum of compound **164**

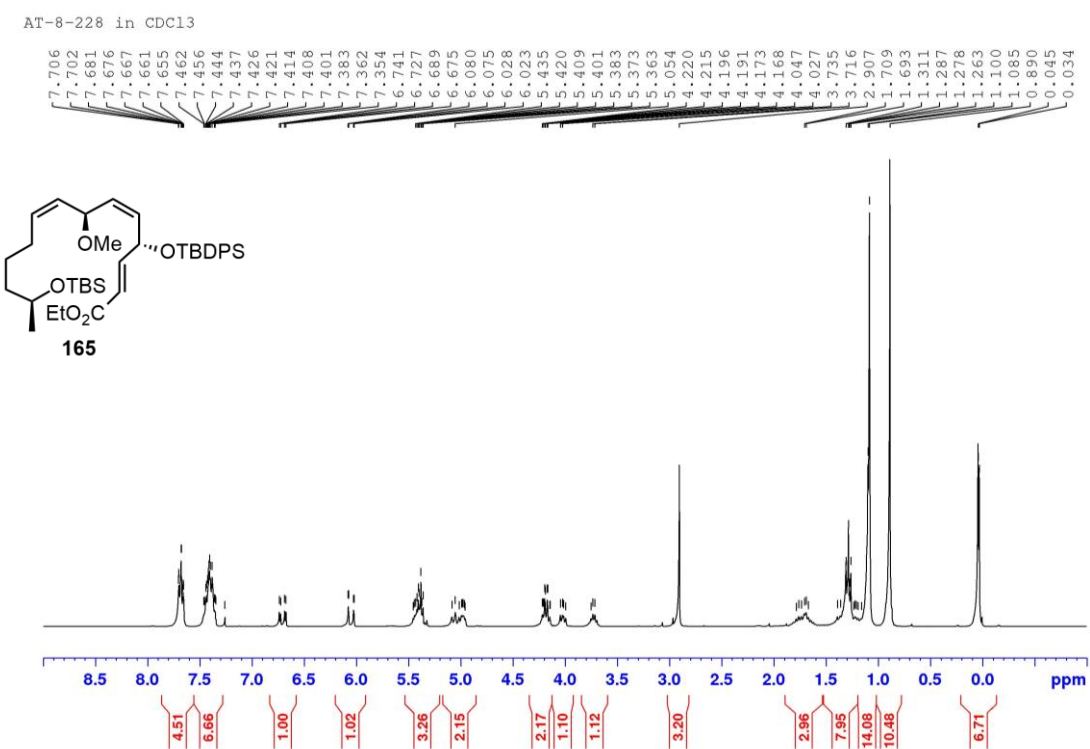




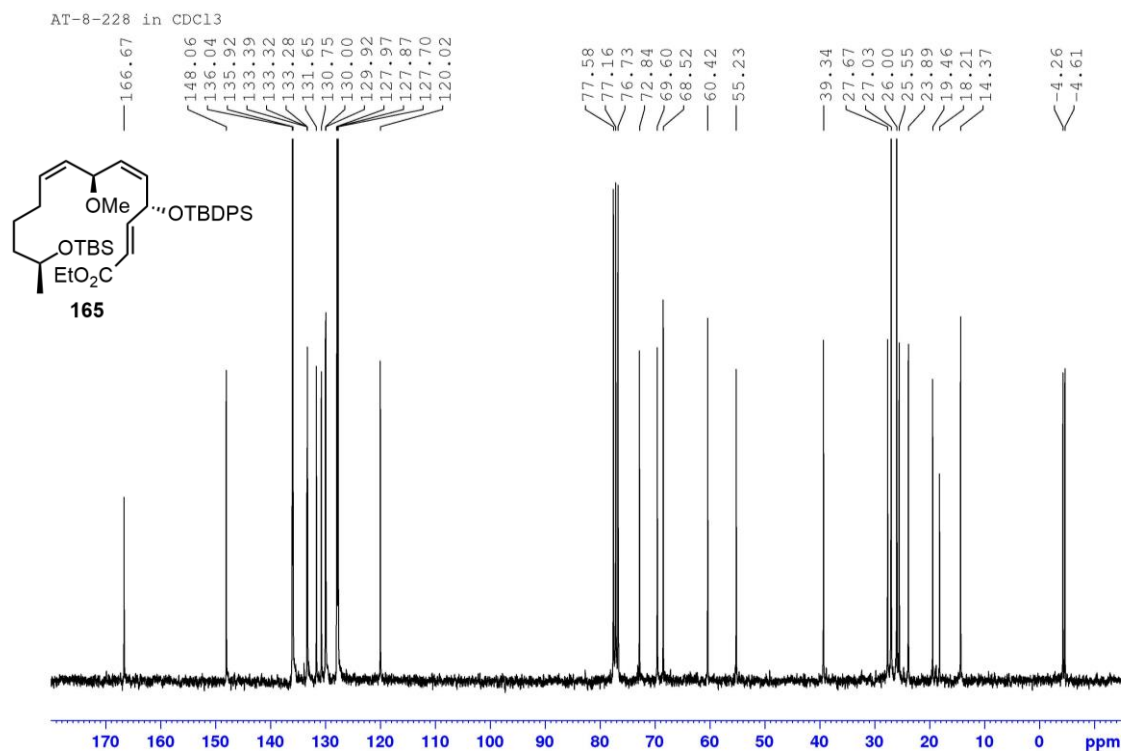
**Figure 49**  $^{13}\text{C}$  NMR (75 MHz,  $\text{CDCl}_3$ ) spectrum of compound **164**



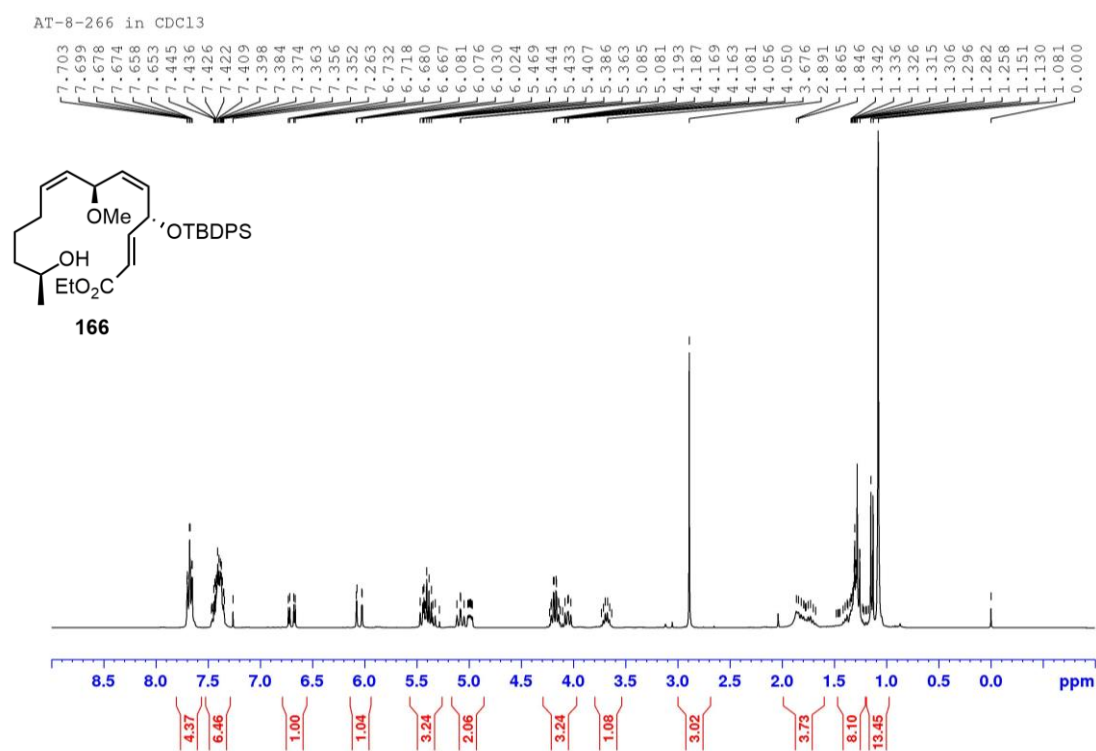
**Figure 50**  $^1\text{H}$  NMR (300 MHz,  $\text{CDCl}_3$ ) spectrum of compound **165**



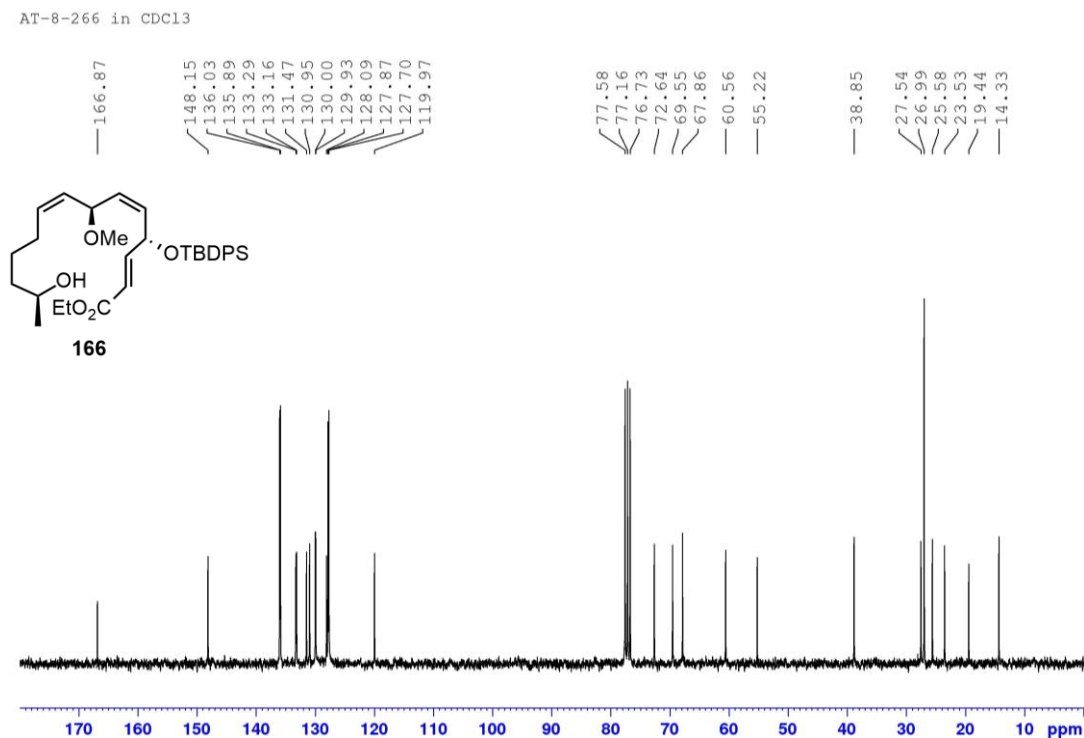
**Figure 51**  $^{13}\text{C}$  NMR (75 MHz,  $\text{CDCl}_3$ ) spectrum of compound **165**



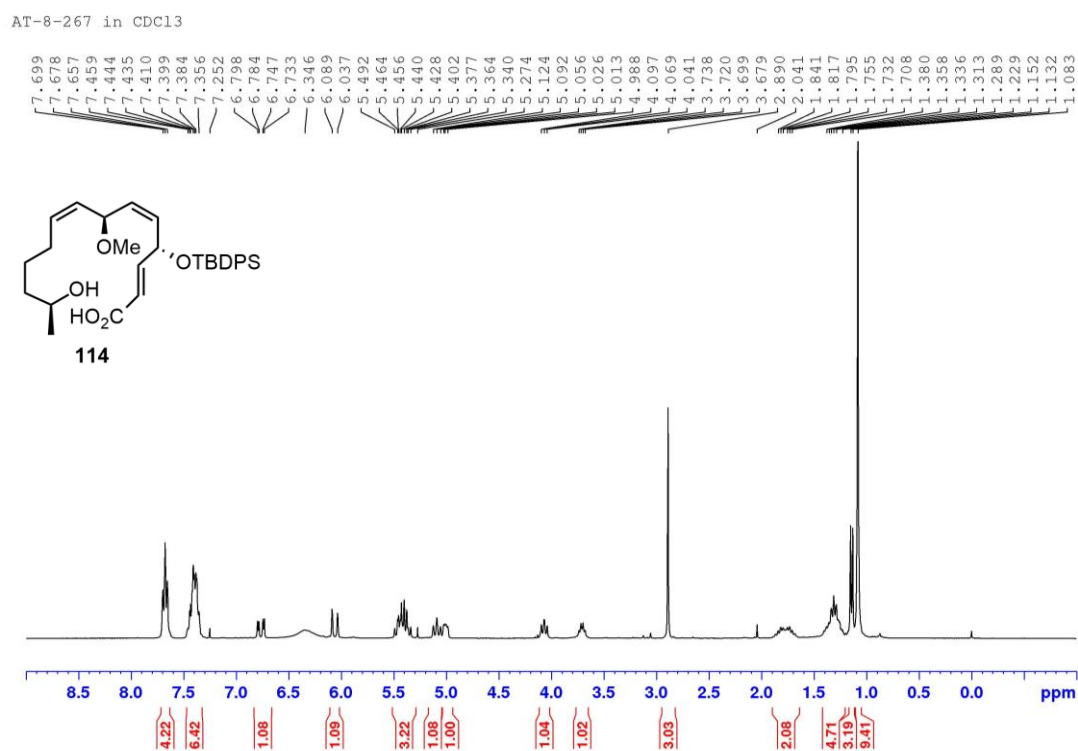
**Figure 52**  $^1\text{H}$  NMR (300 MHz,  $\text{CDCl}_3$ ) spectrum of compound **166**



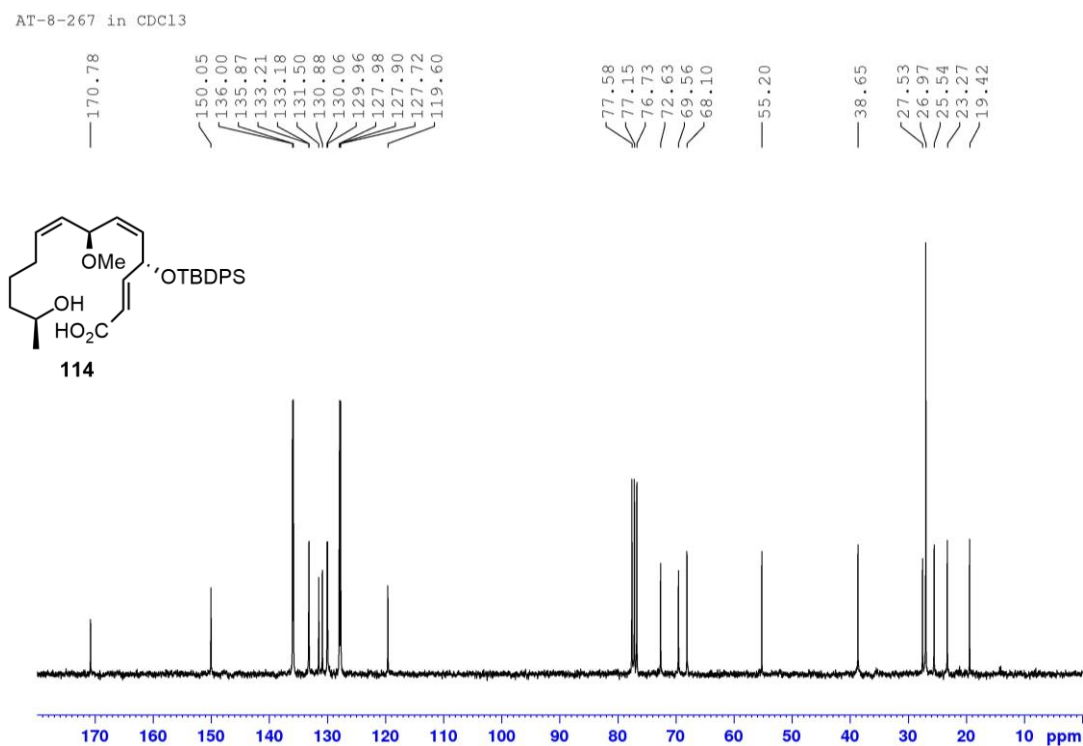
**Figure 53**  $^{13}\text{C}$  NMR (75 MHz,  $\text{CDCl}_3$ ) spectrum of compound **166**



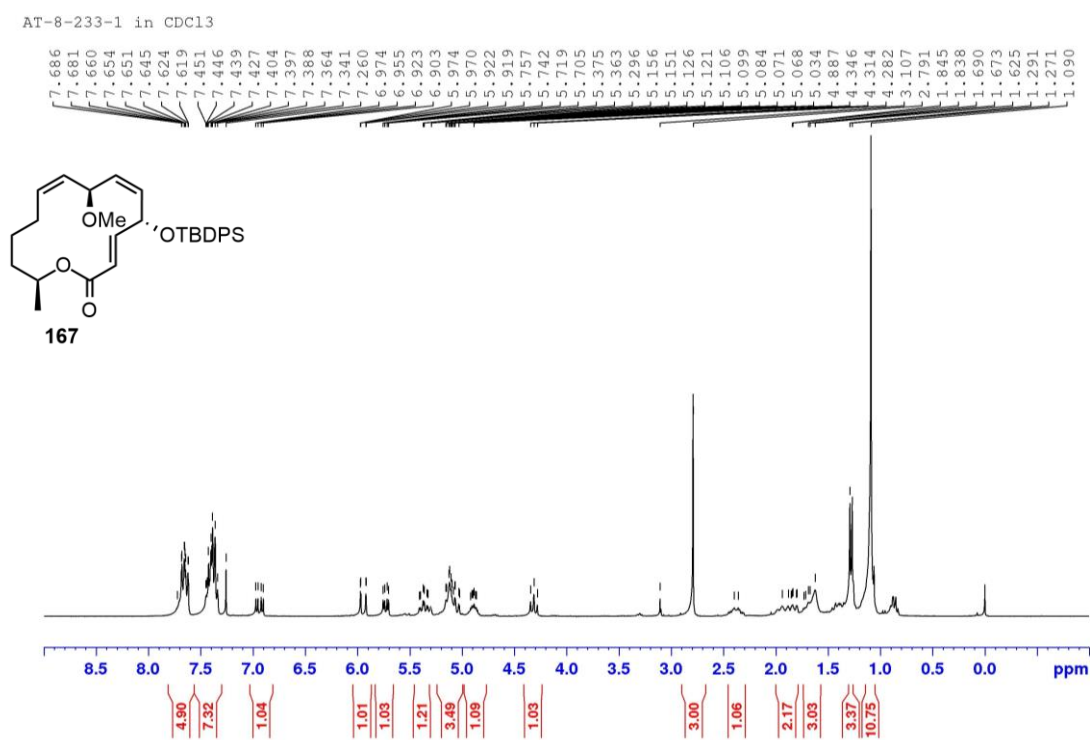
**Figure 54**  $^1\text{H}$  NMR (300 MHz,  $\text{CDCl}_3$ ) spectrum of compound **114**



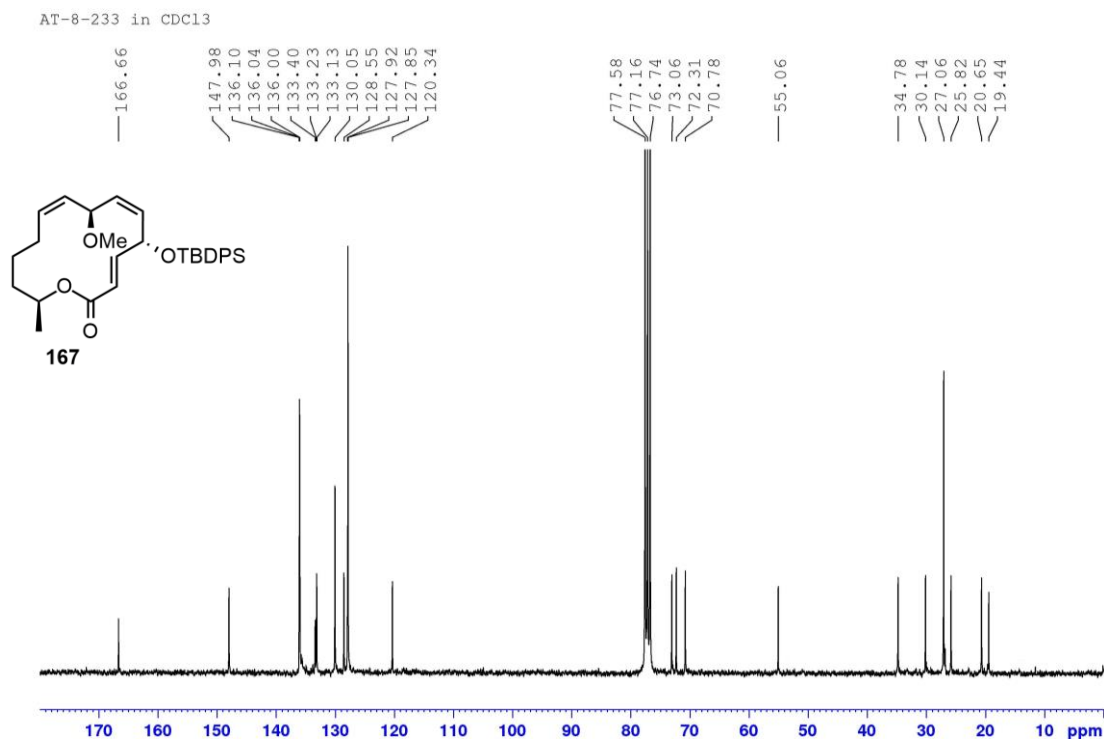
**Figure 55**  $^{13}\text{C}$  NMR (75 MHz,  $\text{CDCl}_3$ ) spectrum of compound **114**



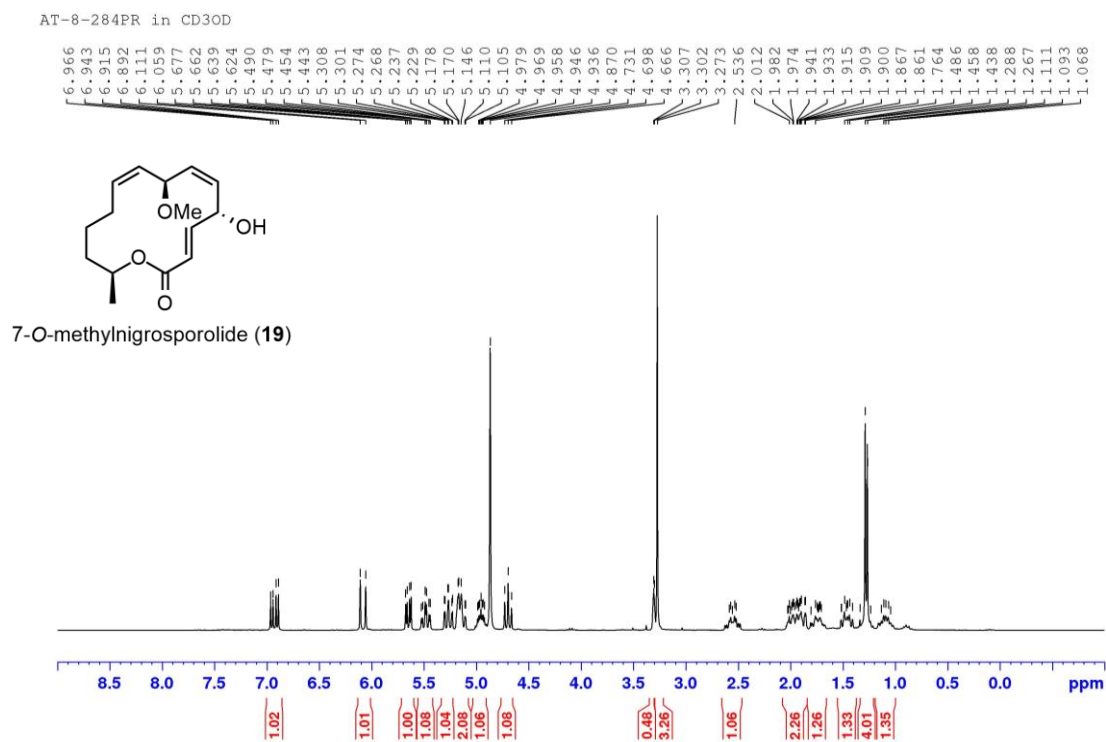
**Figure 56**  $^1\text{H}$  NMR (300 MHz,  $\text{CDCl}_3$ ) spectrum of compound **167**



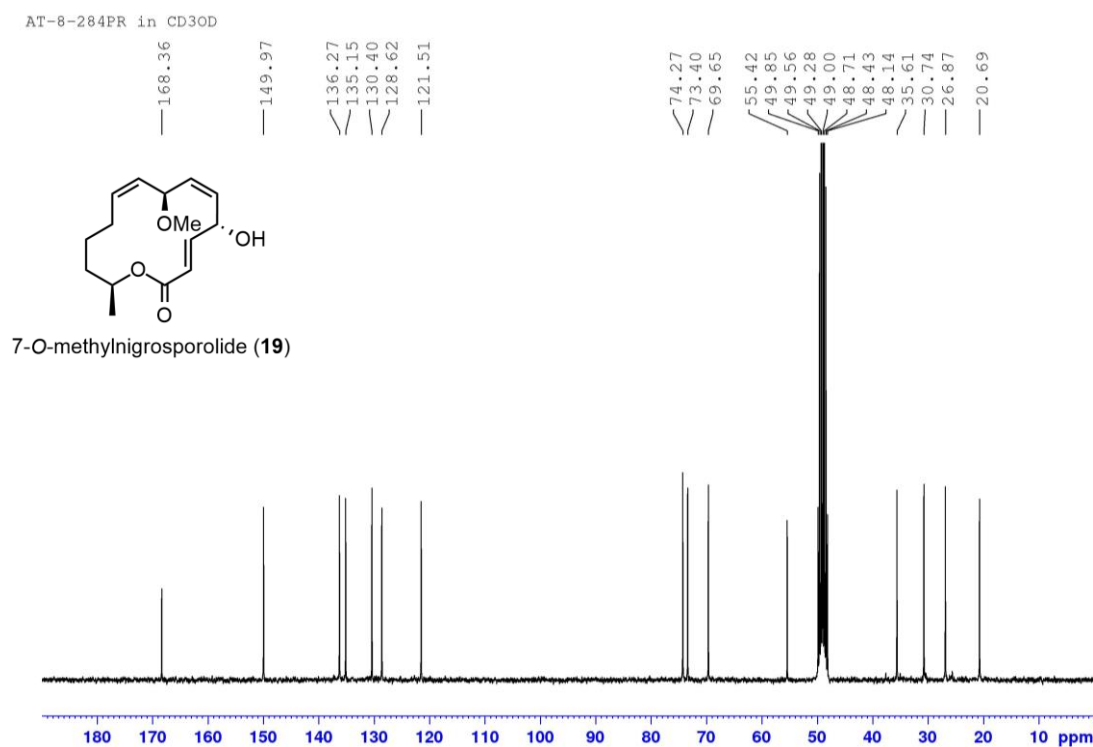
**Figure 57**  $^{13}\text{C}$  NMR (75 MHz,  $\text{CDCl}_3$ ) spectrum of compound **167**



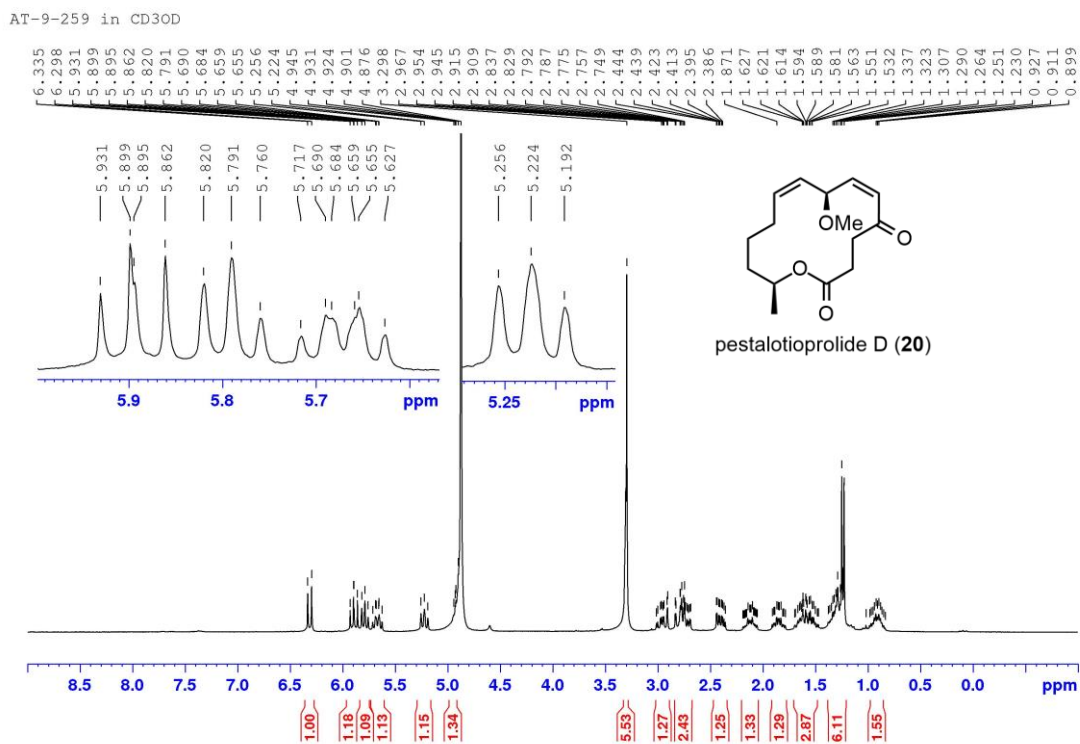
**Figure 58**  $^1\text{H}$  NMR (300 MHz,  $\text{CD}_3\text{OD}$ ) spectrum of 7-*O*-methylnigrosporolide (**19**)



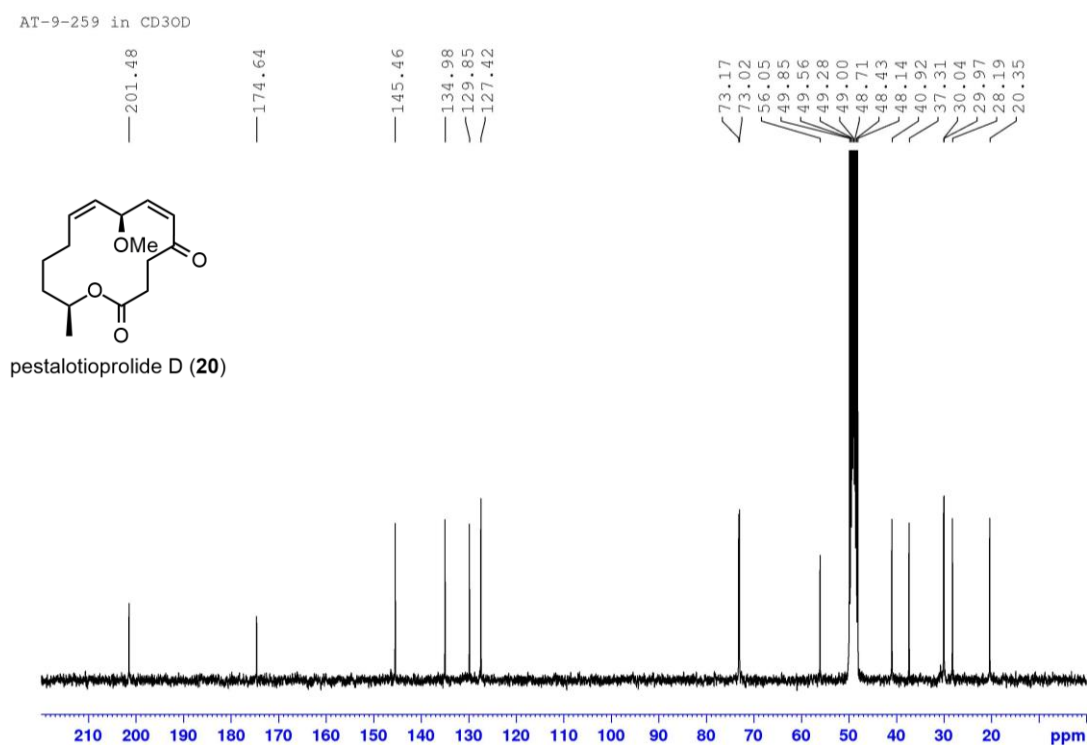
**Figure 59**  $^{13}\text{C}$  NMR (75 MHz,  $\text{CD}_3\text{OD}$ ) spectrum of 7-*O*-methylnigrosporolide (**19**)



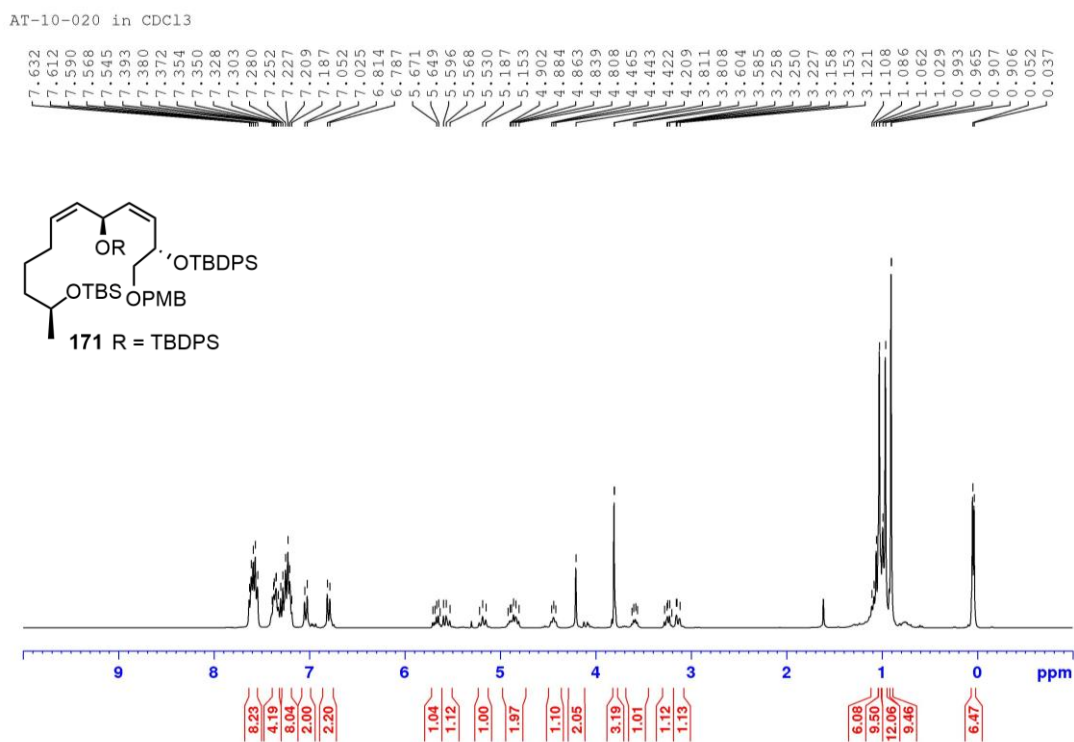
**Figure 60**  $^1\text{H}$  NMR (300 MHz,  $\text{CD}_3\text{OD}$ ) spectrum of pestalotioprolide D (**20**)



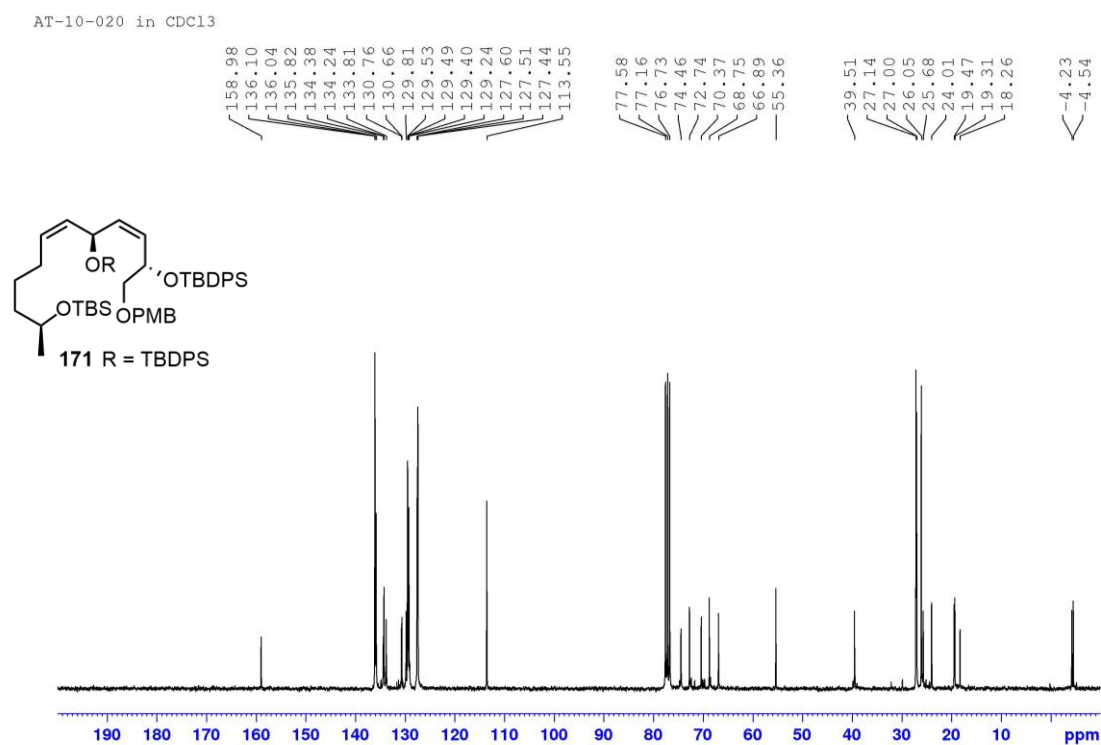
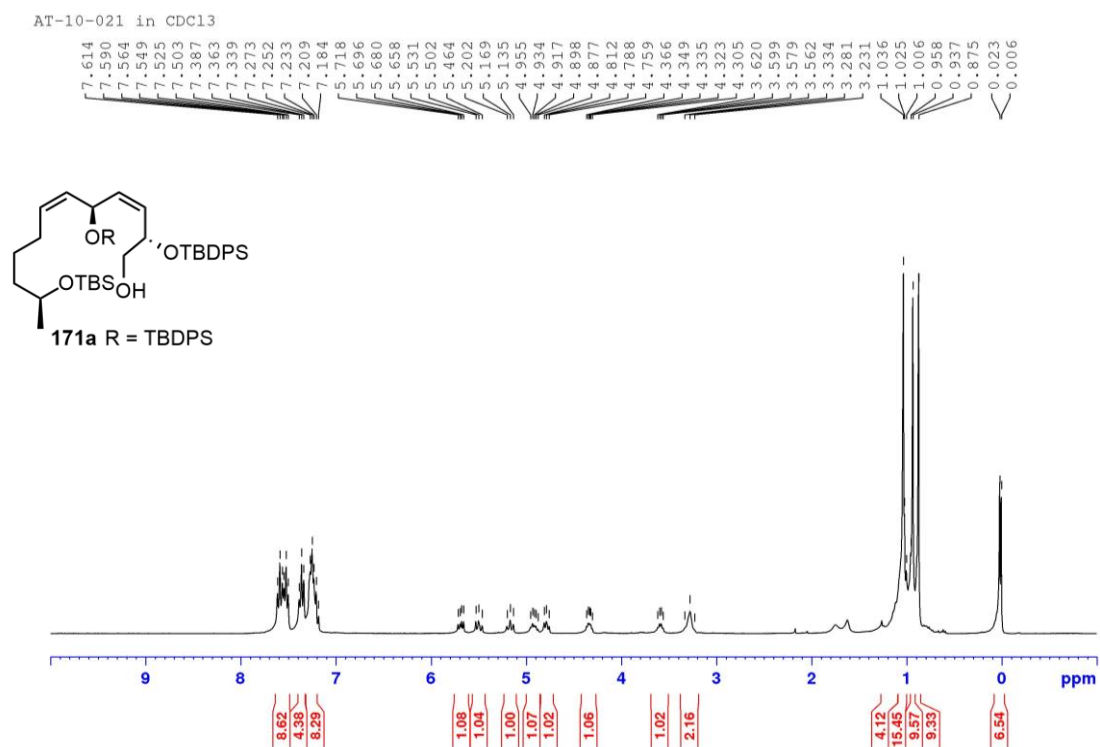
**Figure 61**  $^{13}\text{C}$  NMR (75 MHz,  $\text{CD}_3\text{OD}$ ) spectrum of pestalotioprolide D (**20**)



**Figure 62**  $^1\text{H}$  NMR (300 MHz,  $\text{CDCl}_3$ ) spectrum of compound **171**

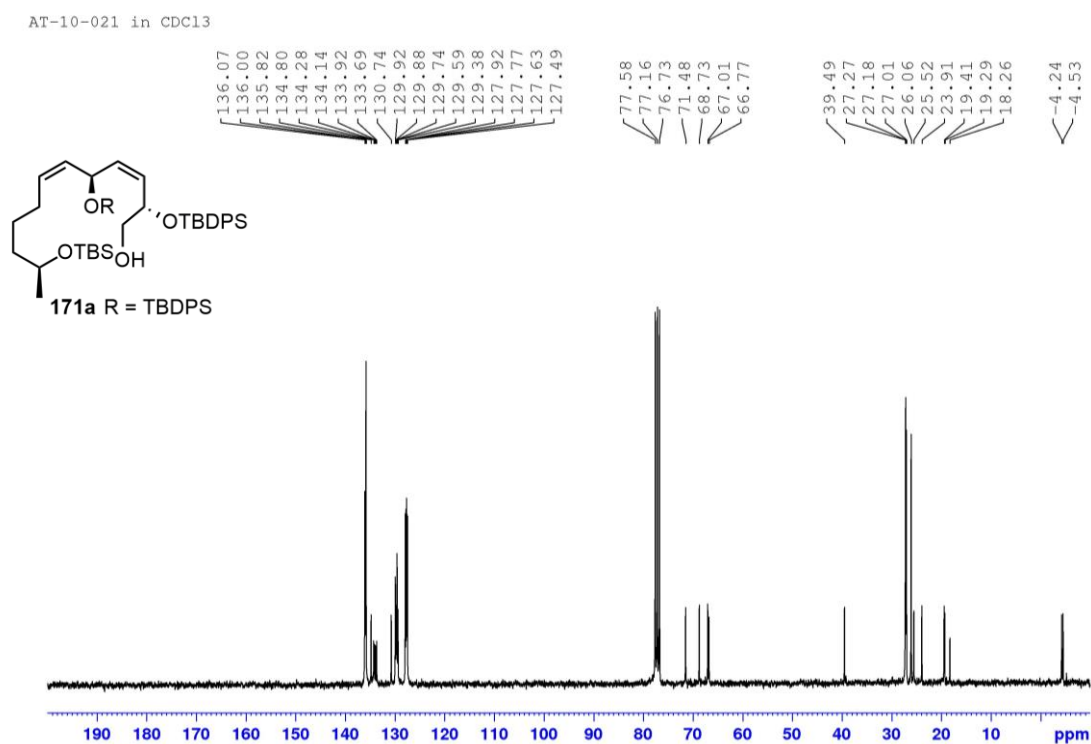




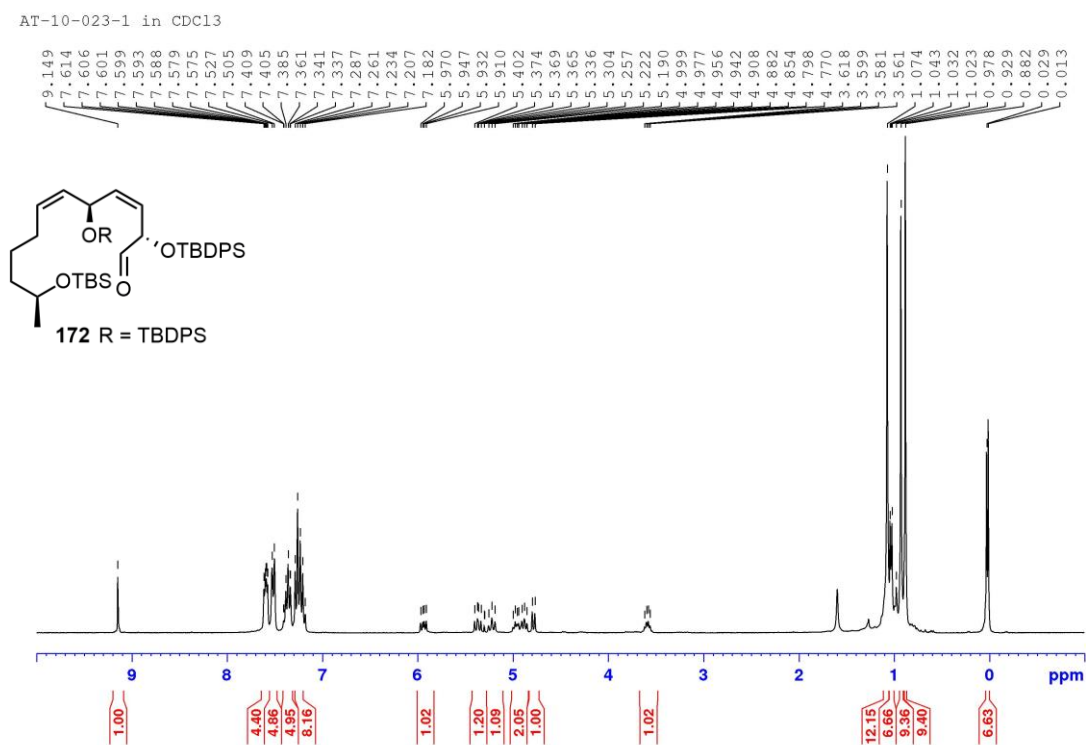
**Figure 63**  $^{13}\text{C}$  NMR (75 MHz,  $\text{CDCl}_3$ ) spectrum of compound **171****Figure 64**  $^1\text{H}$  NMR (300 MHz,  $\text{CDCl}_3$ ) spectrum of compound **171a**



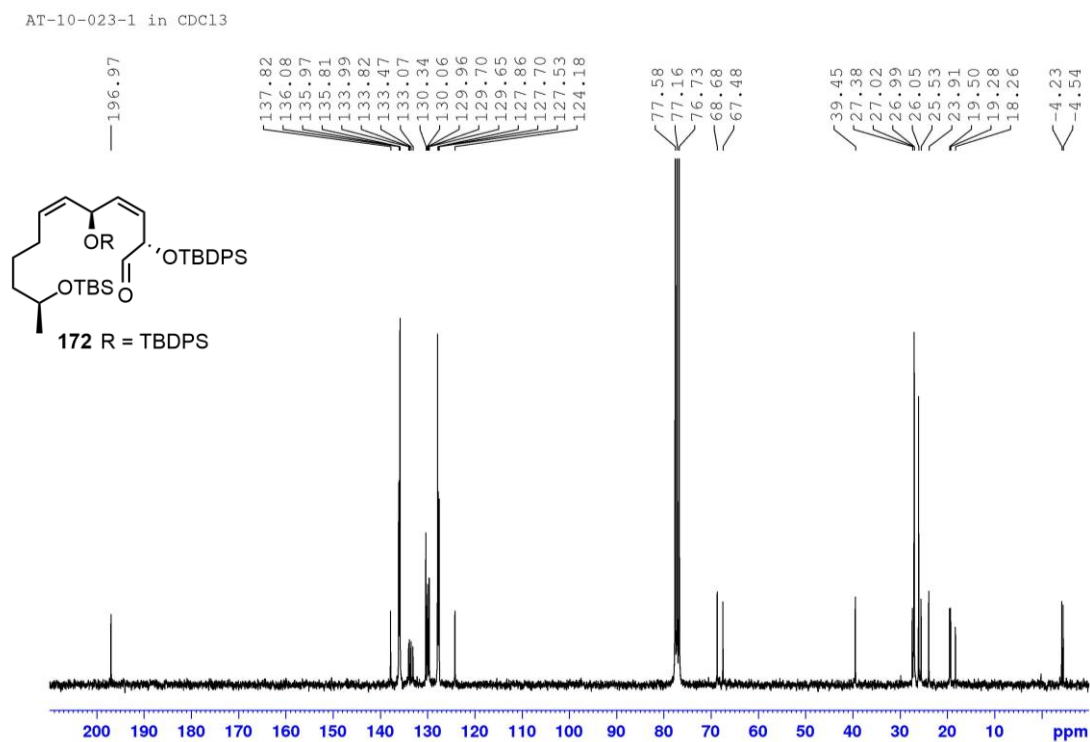
**Figure 65**  $^{13}\text{C}$  NMR (75 MHz,  $\text{CDCl}_3$ ) spectrum of compound **171a**



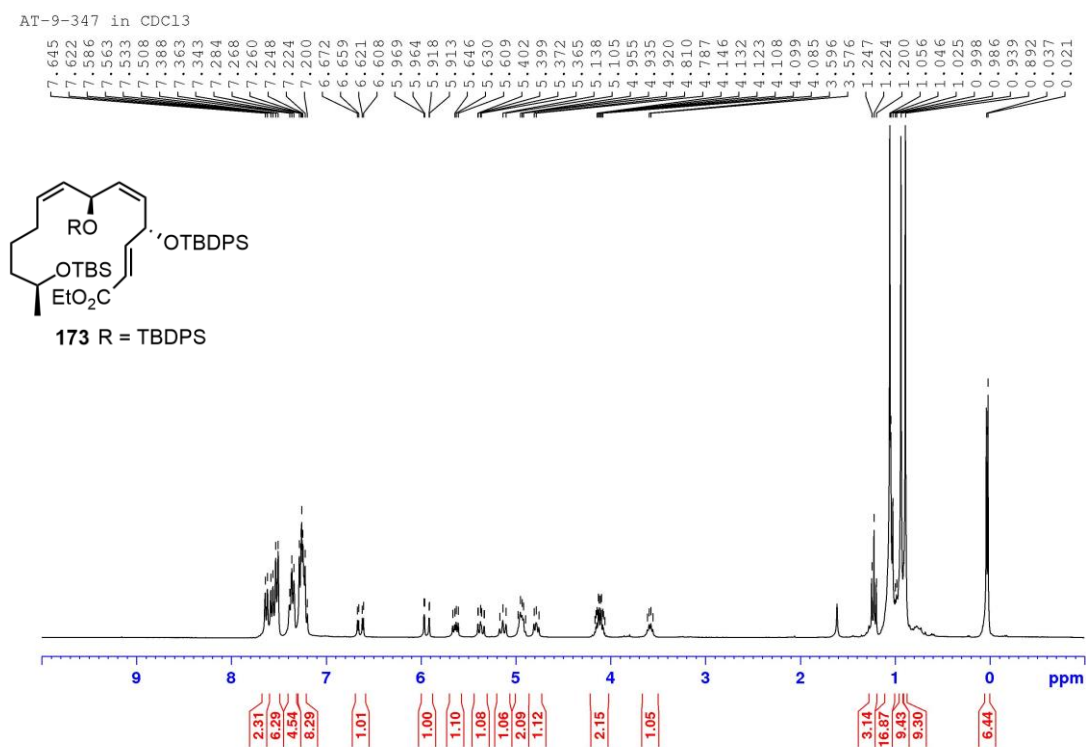
**Figure 66**  $^1\text{H}$  NMR (300 MHz,  $\text{CDCl}_3$ ) spectrum of compound **172**



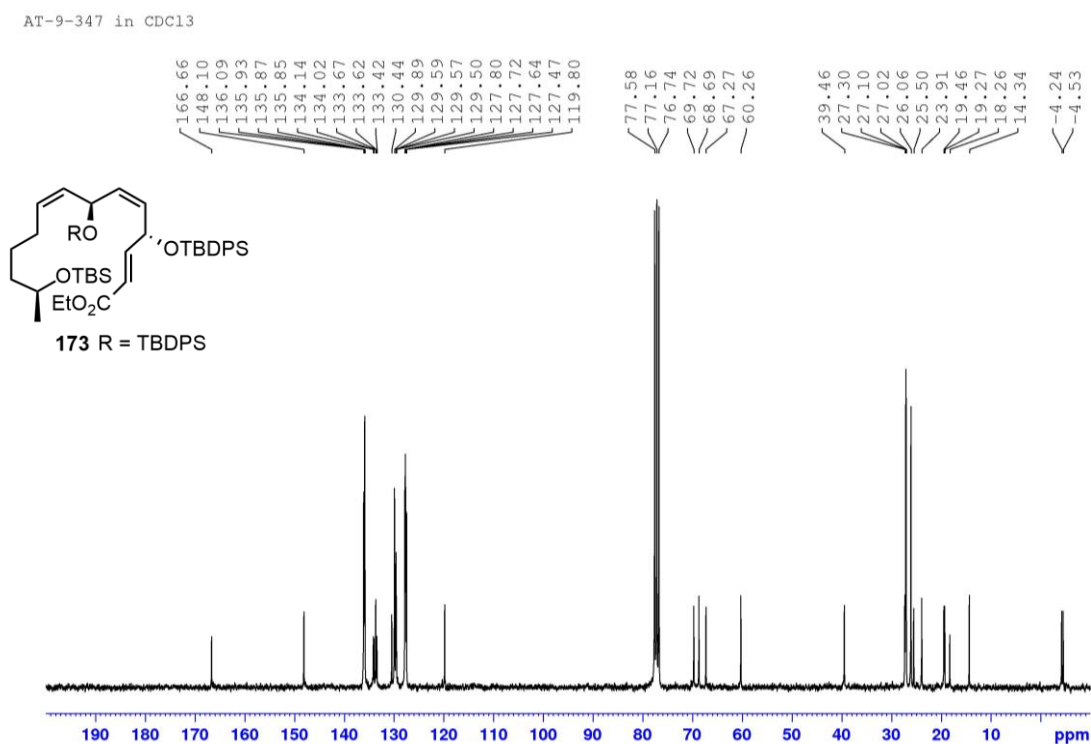
**Figure 67**  $^{13}\text{C}$  NMR (75 MHz,  $\text{CDCl}_3$ ) spectrum of compound **172**



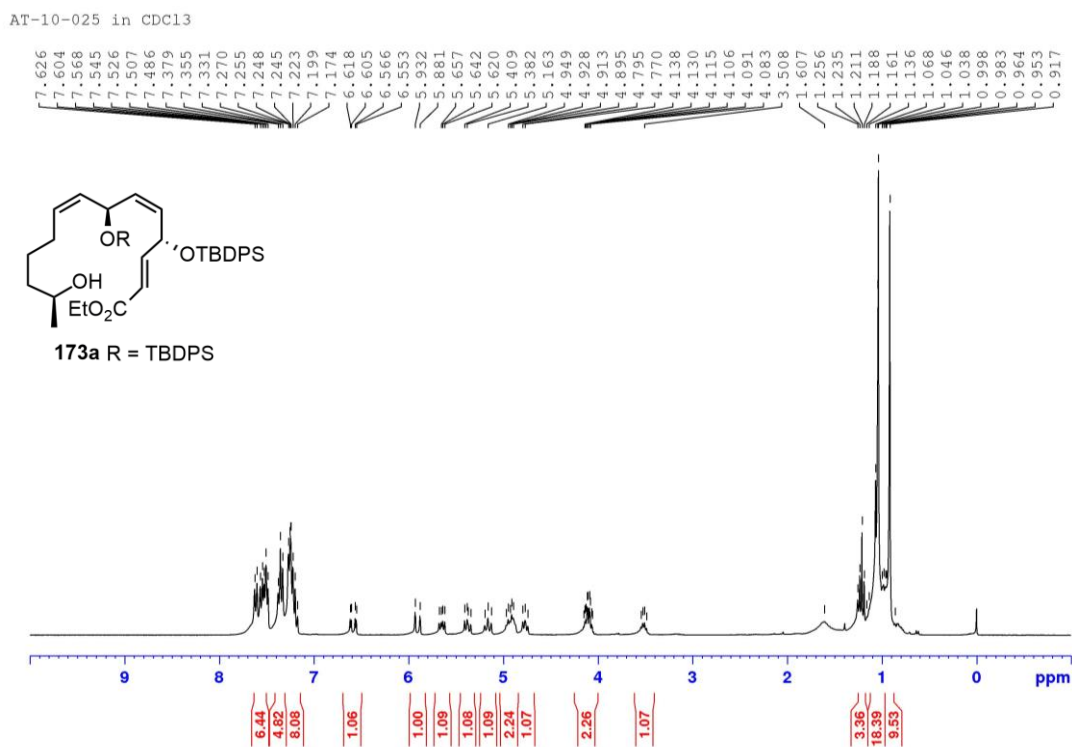
**Figure 68**  $^1\text{H}$  NMR (300 MHz,  $\text{CDCl}_3$ ) spectrum of compound **173**



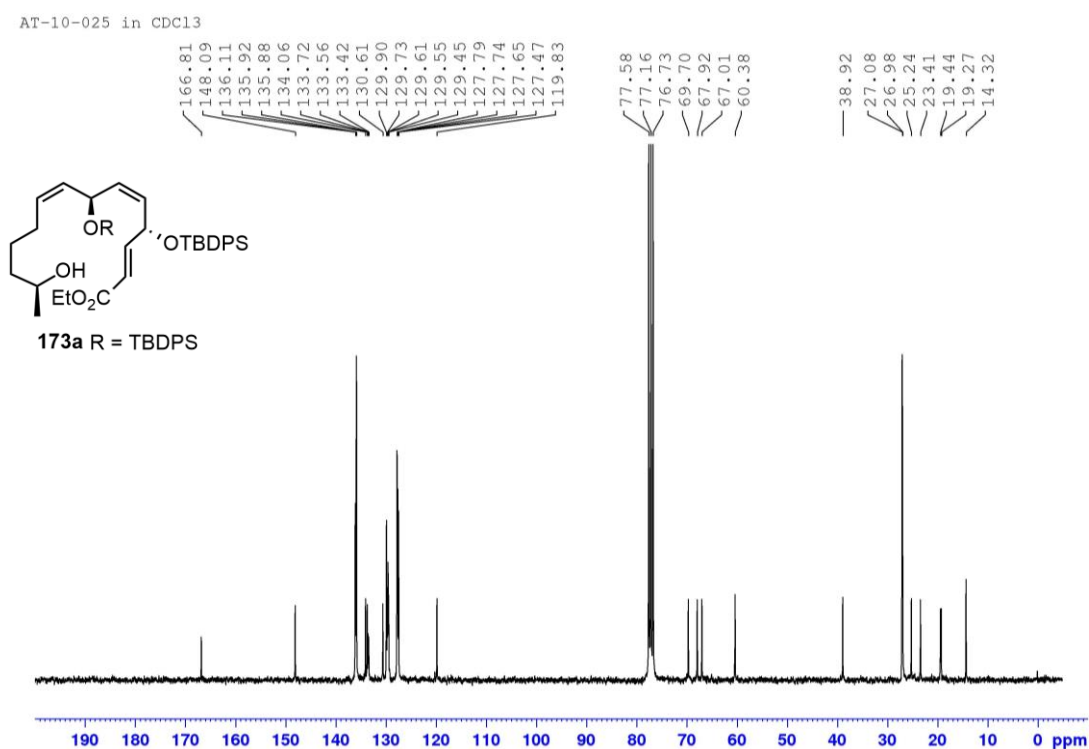
**Figure 69**  $^{13}\text{C}$  NMR (75 MHz,  $\text{CDCl}_3$ ) spectrum of compound **173**



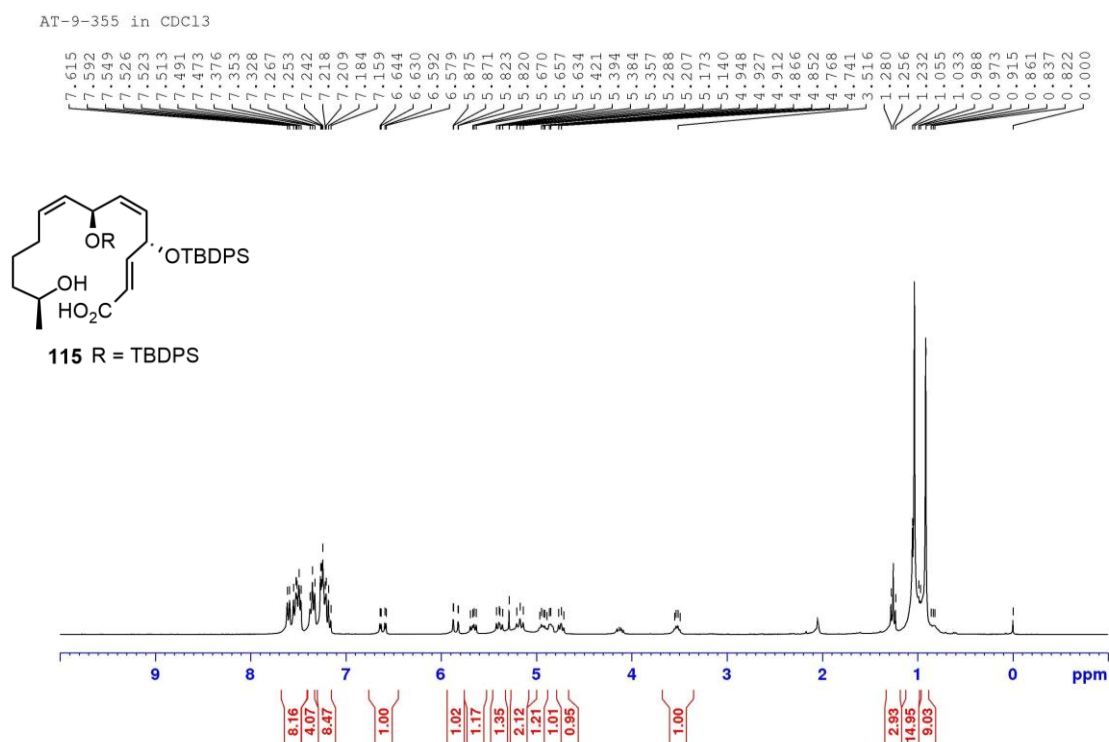
**Figure 70**  $^1\text{H}$  NMR (300 MHz,  $\text{CDCl}_3$ ) spectrum of compound **173a**

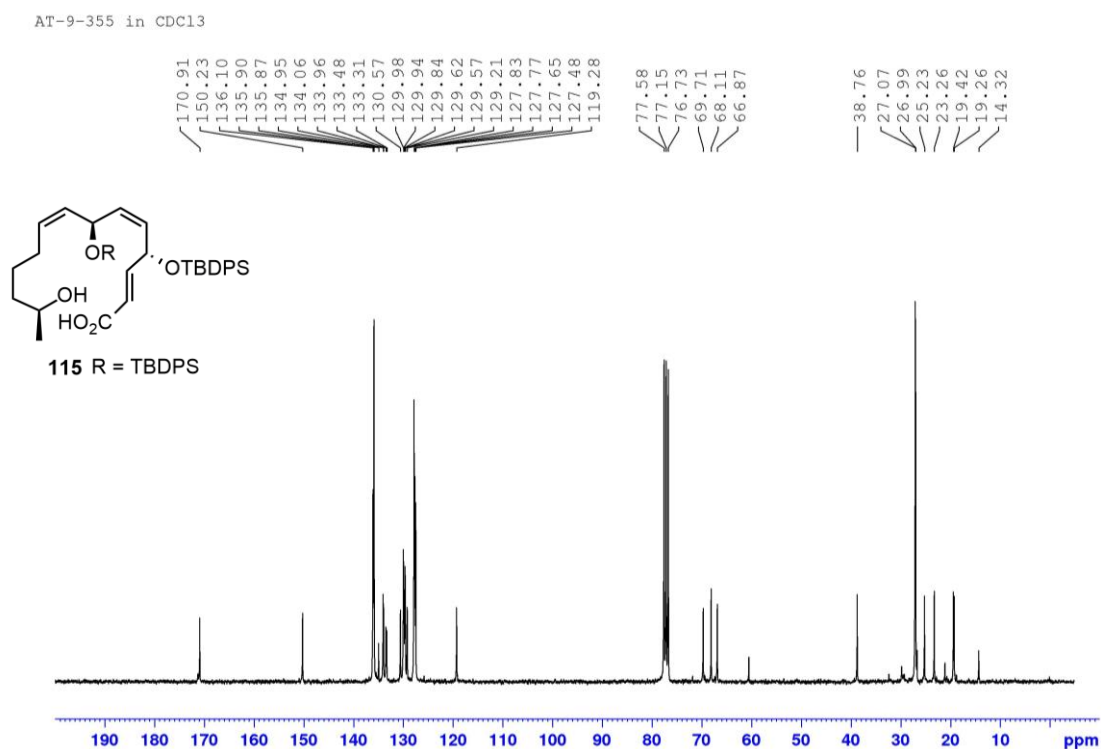
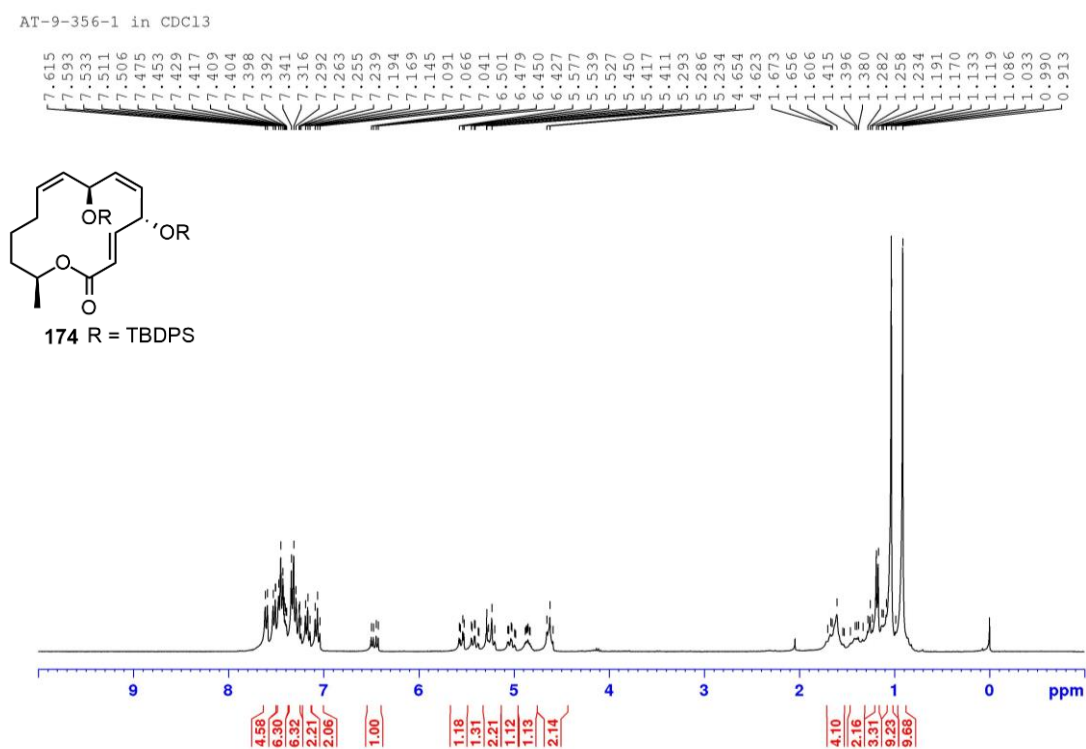


**Figure 71**  $^{13}\text{C}$  NMR (75 MHz,  $\text{CDCl}_3$ ) spectrum of compound **173a**

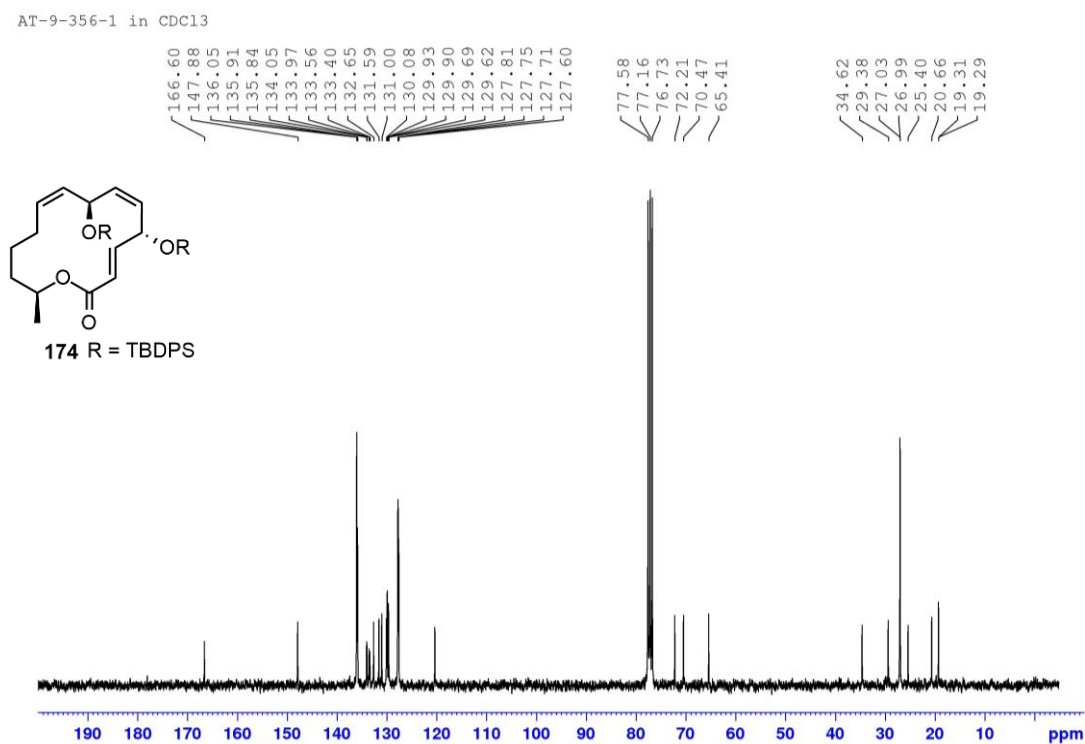


**Figure 72**  $^1\text{H}$  NMR (300 MHz,  $\text{CDCl}_3$ ) spectrum of compound **115**

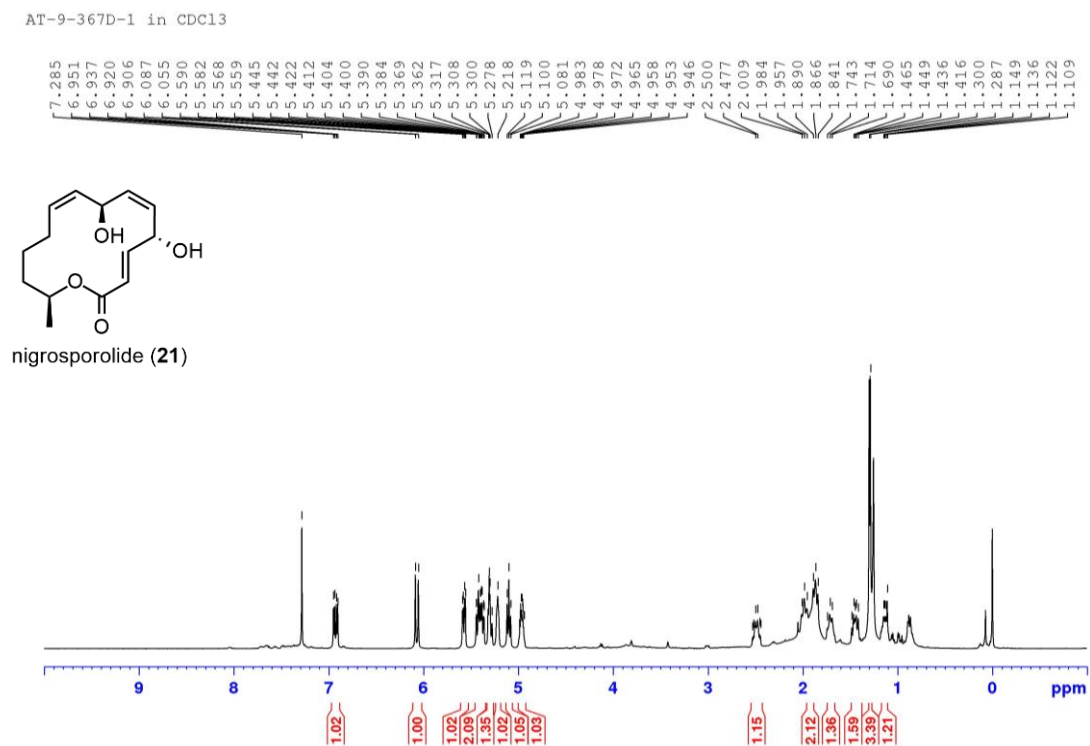


**Figure 73**  $^{13}\text{C}$  NMR (75 MHz,  $\text{CDCl}_3$ ) spectrum of compound **115****Figure 74**  $^1\text{H}$  NMR (300 MHz,  $\text{CDCl}_3$ ) spectrum of compound **174**

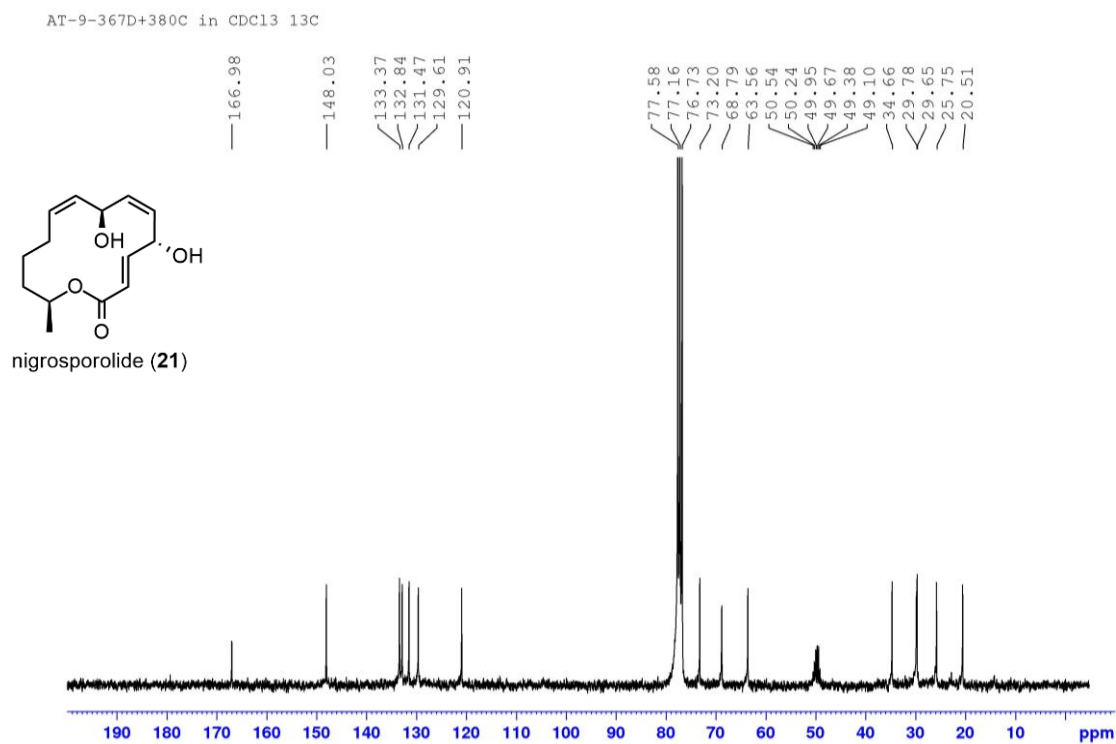
**Figure 75**  $^{13}\text{C}$  NMR (75 MHz,  $\text{CDCl}_3$ ) spectrum of compound **174**



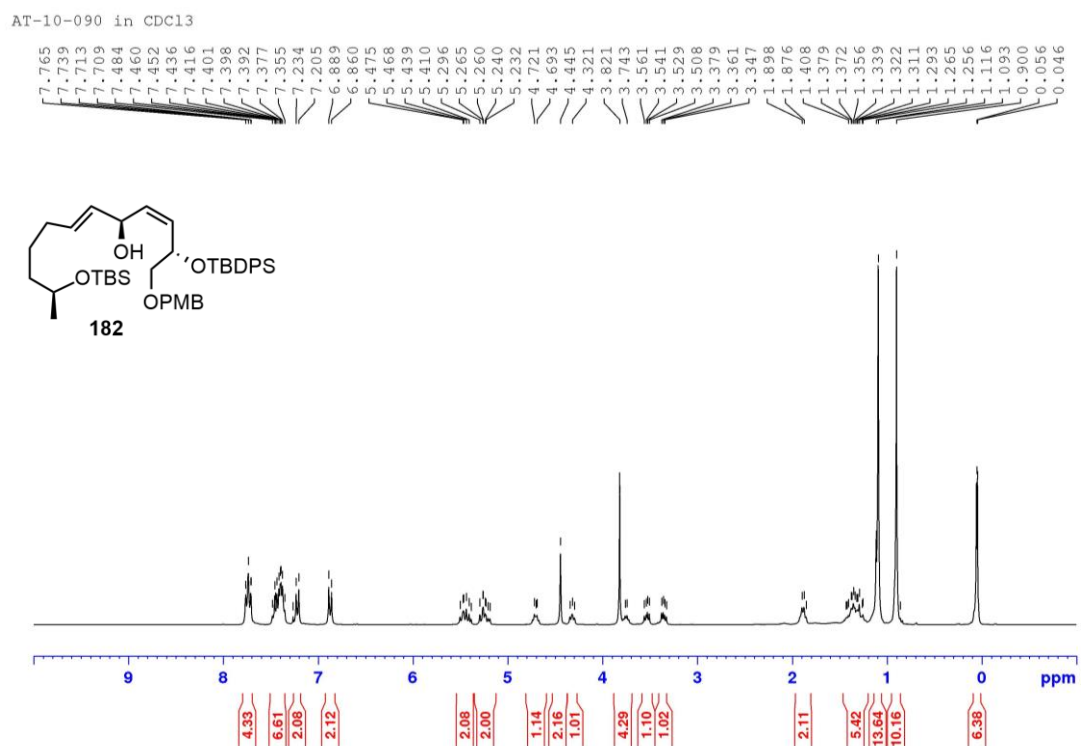
**Figure 76**  $^1\text{H}$  NMR (500 MHz,  $\text{CDCl}_3$ ) spectrum of nigrosporolide (**21**)



**Figure 77**  $^{13}\text{C}$  NMR (75 MHz,  $\text{CDCl}_3$ ) spectrum of nigrosporolide (**21**)

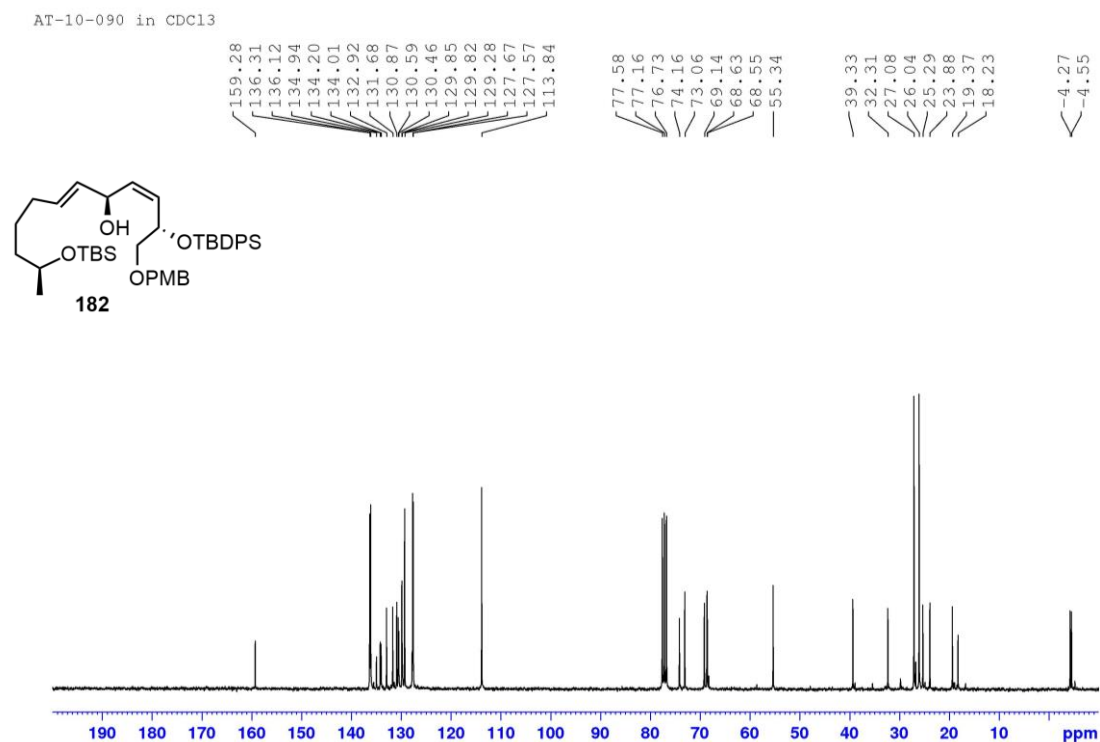


**Figure 78**  $^1\text{H}$  NMR (300 MHz,  $\text{CDCl}_3$ ) spectrum of compound **182**

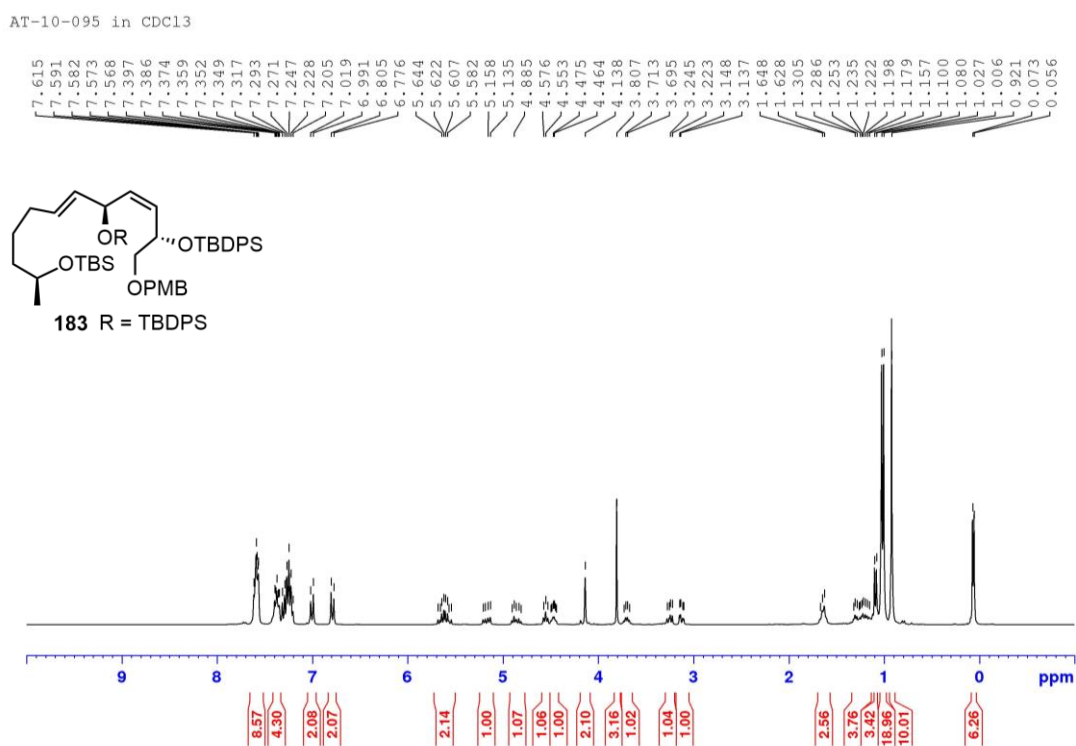




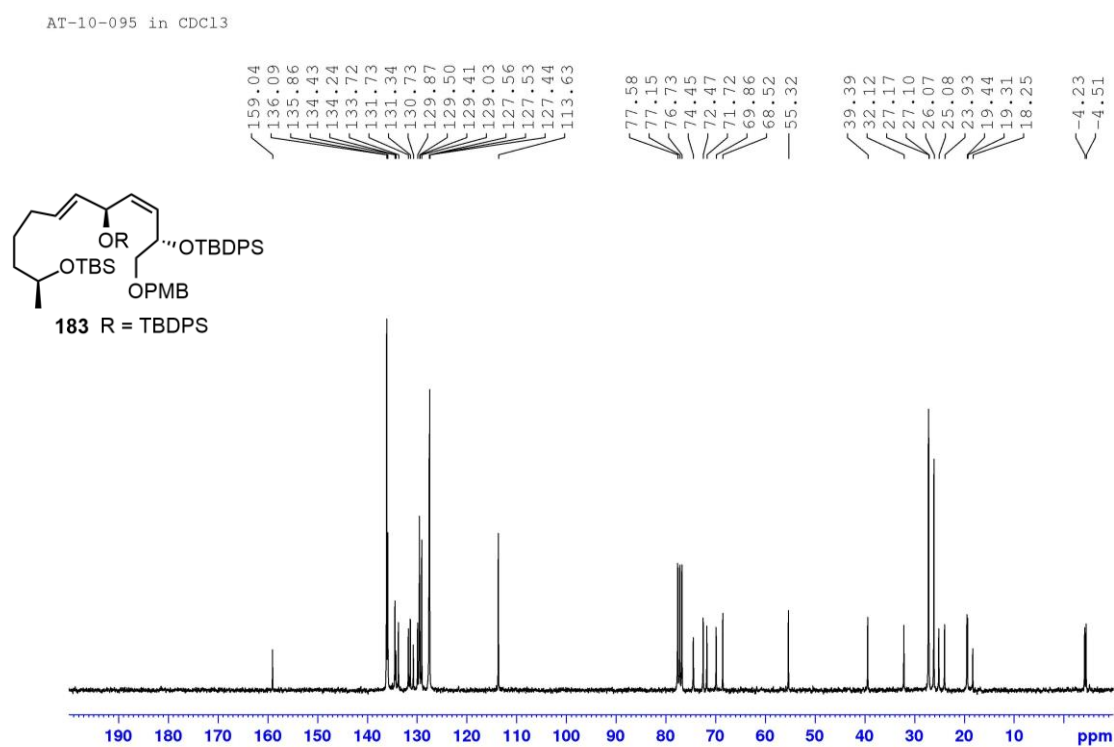
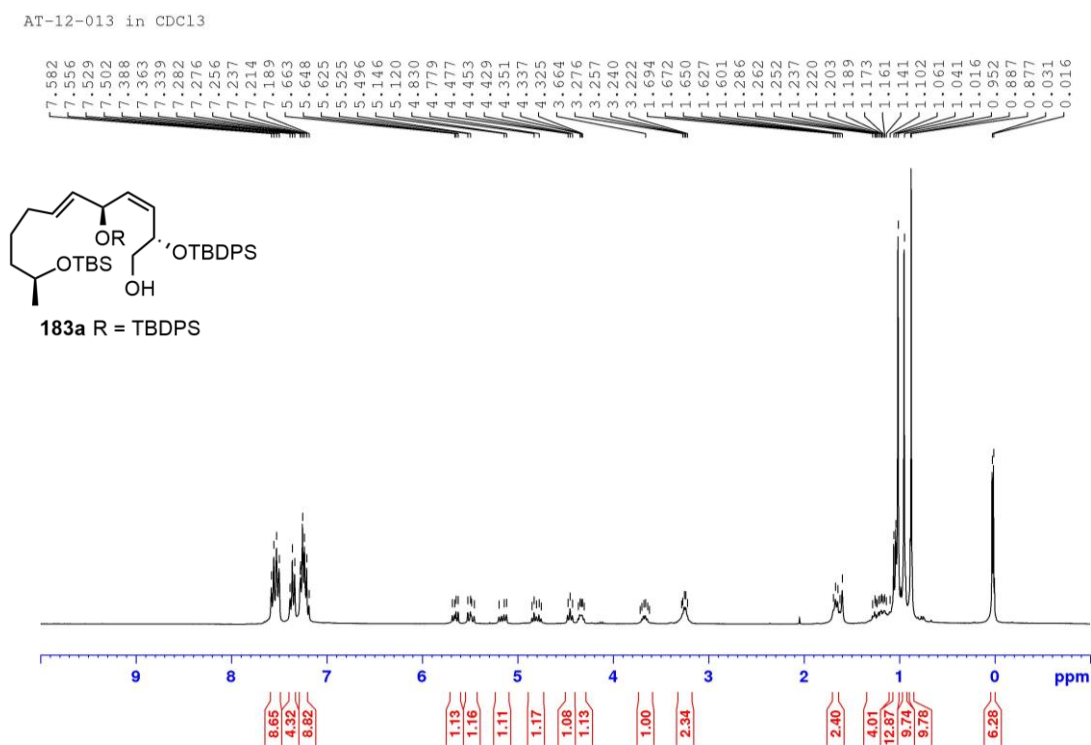
**Figure 79**  $^{13}\text{C}$  NMR (75 MHz,  $\text{CDCl}_3$ ) spectrum of compound **182**



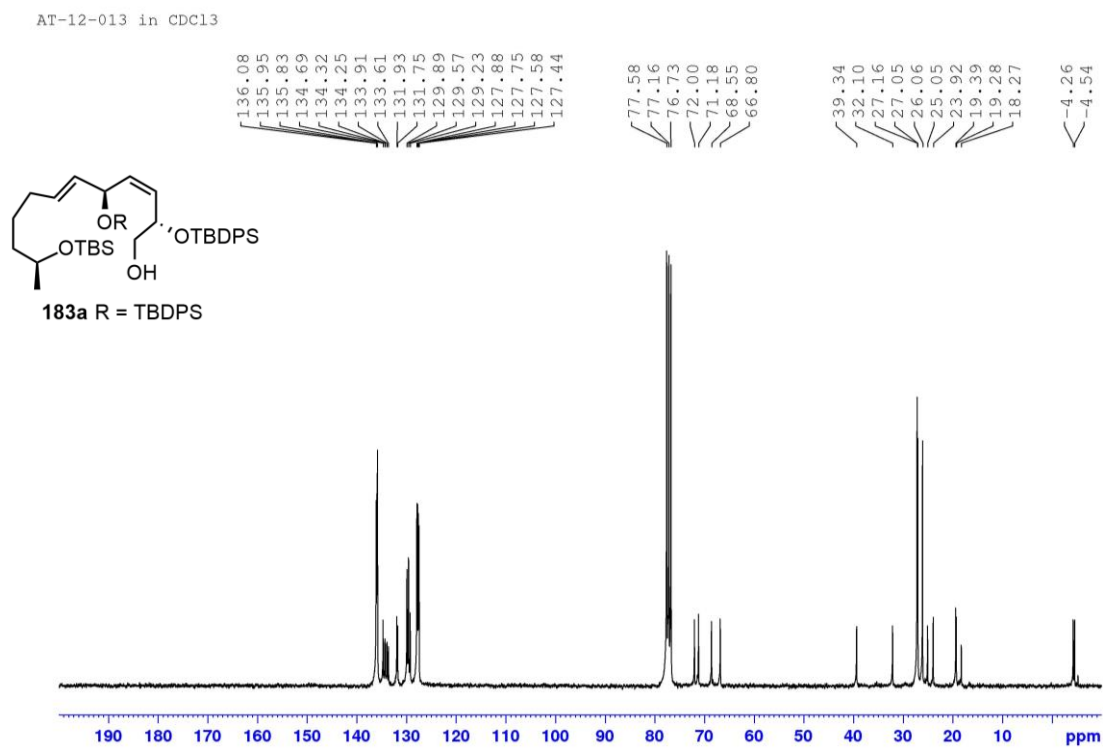
**Figure 80**  $^1\text{H}$  NMR (300 MHz,  $\text{CDCl}_3$ ) spectrum of compound **183**



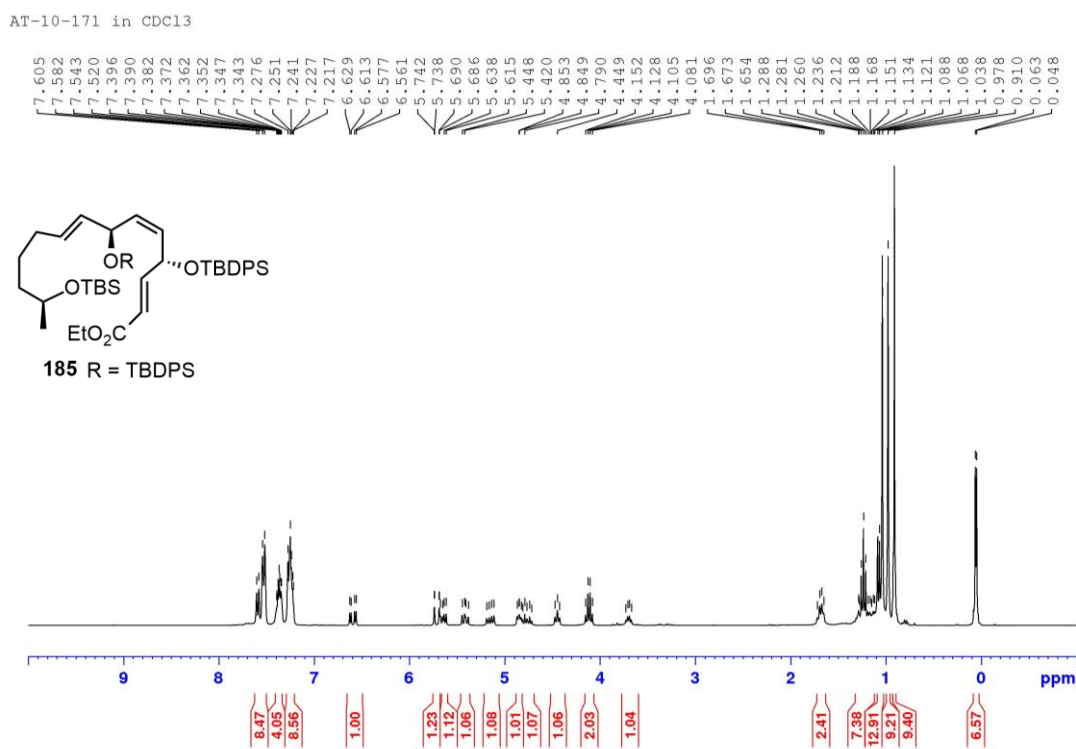


**Figure 81**  $^{13}\text{C}$  NMR (75 MHz,  $\text{CDCl}_3$ ) spectrum of compound **183****Figure 82**  $^1\text{H}$  NMR (300 MHz,  $\text{CDCl}_3$ ) spectrum of compound **183a**

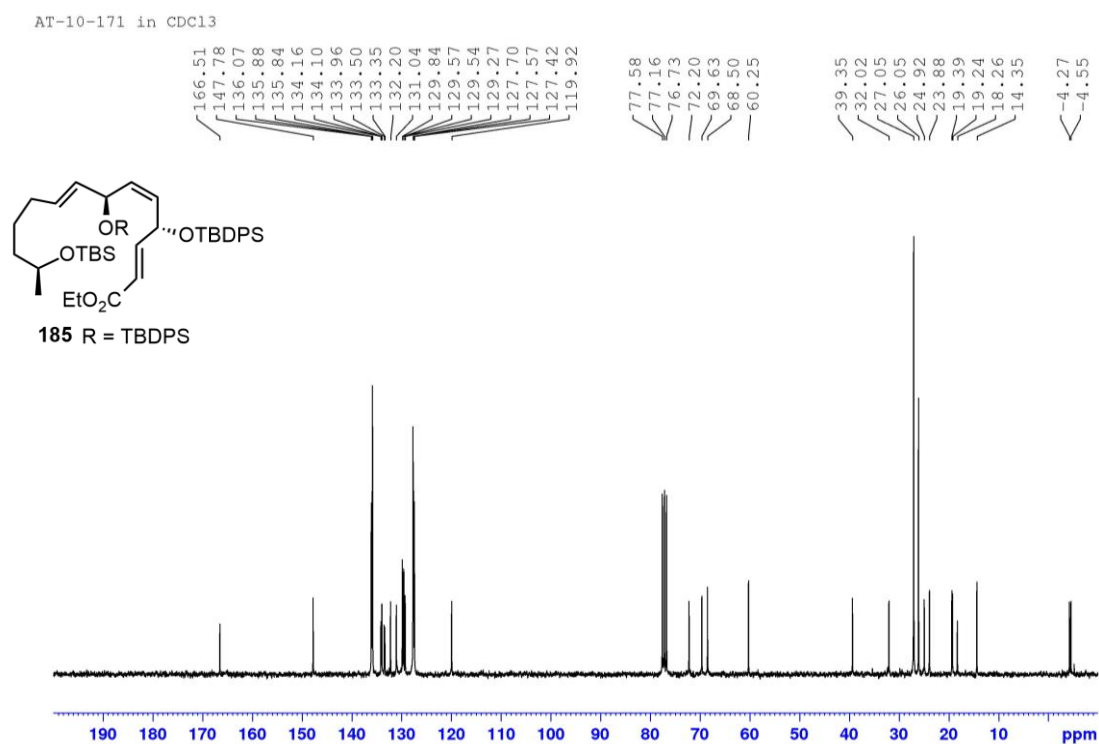
**Figure 83**  $^{13}\text{C}$  NMR (75 MHz,  $\text{CDCl}_3$ ) spectrum of compound **183a**



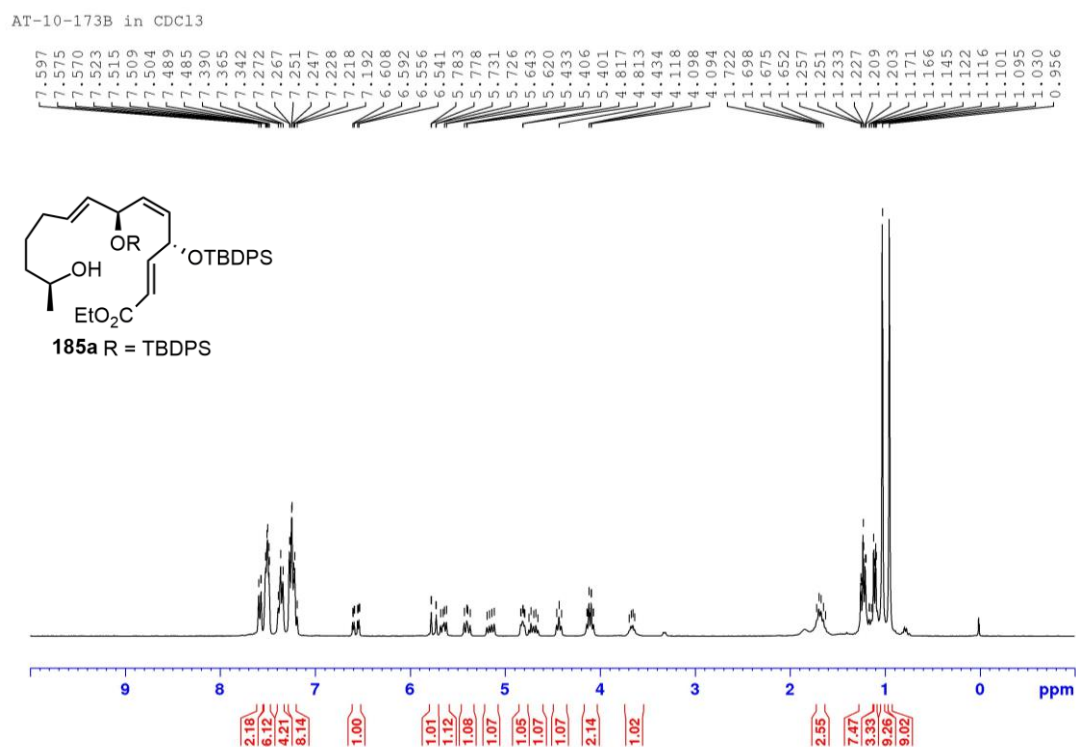
**Figure 84**  $^1\text{H}$  NMR (300 MHz,  $\text{CDCl}_3$ ) spectrum of compound **185**



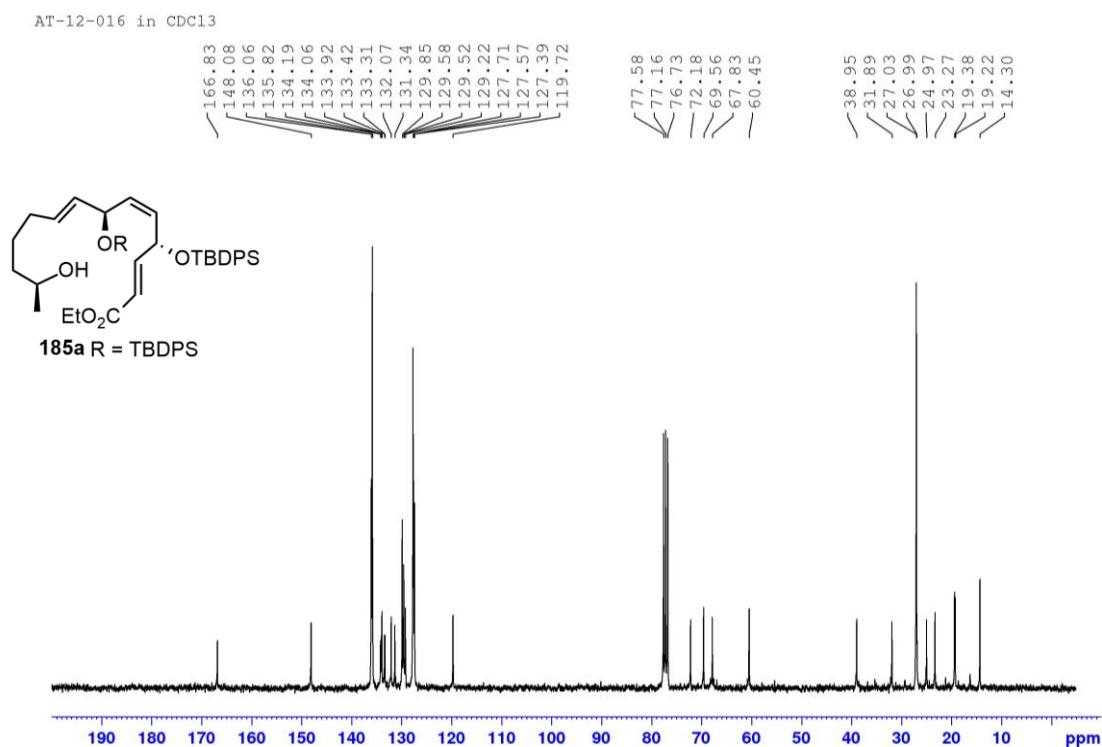
**Figure 85**  $^{13}\text{C}$  NMR (75 MHz,  $\text{CDCl}_3$ ) spectrum of compound **185**



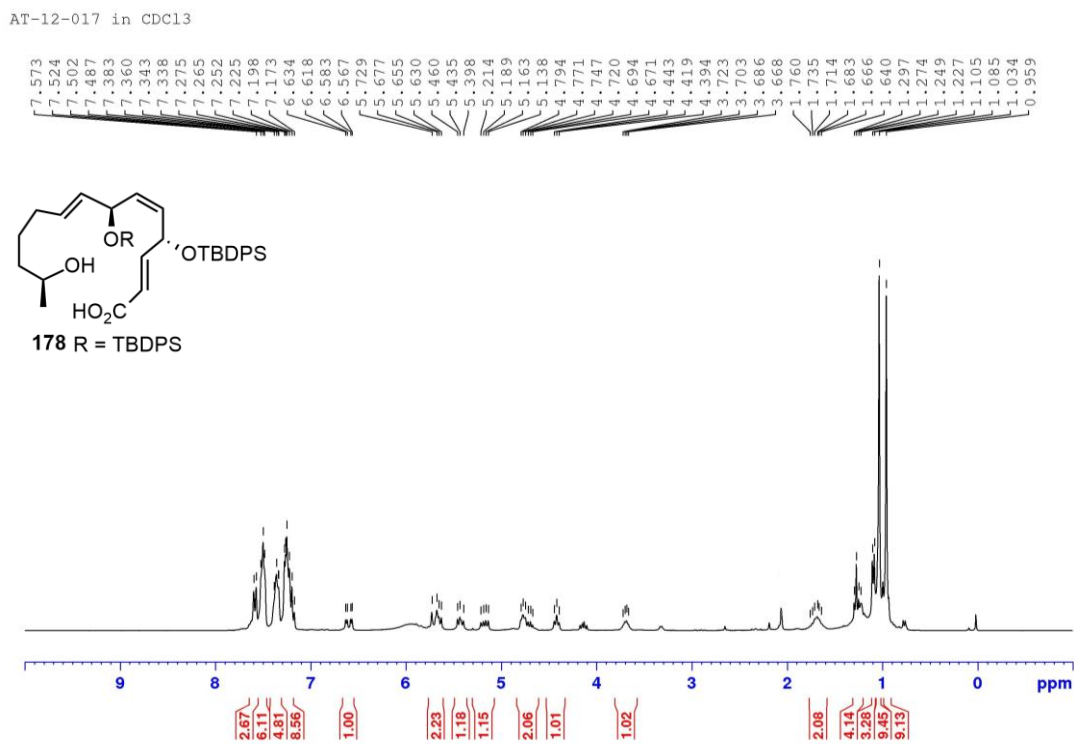
**Figure 86**  $^1\text{H}$  NMR (300 MHz,  $\text{CDCl}_3$ ) spectrum of compound **185a**



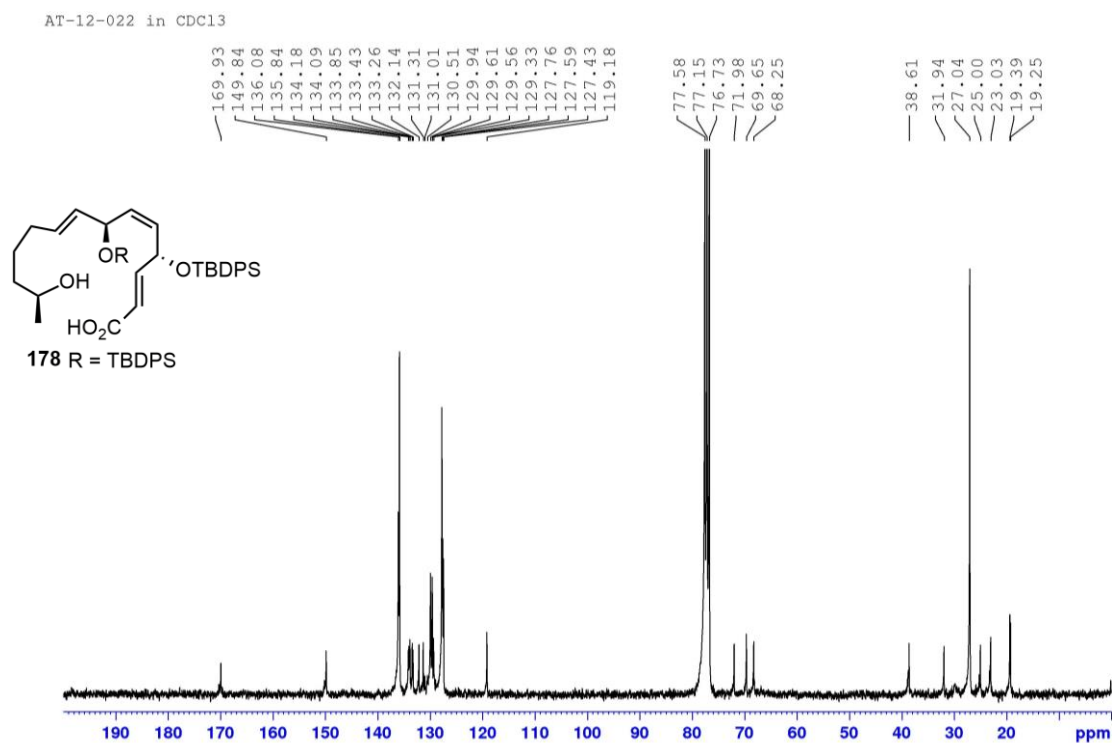
**Figure 87**  $^{13}\text{C}$  NMR (75 MHz,  $\text{CDCl}_3$ ) spectrum of compound **185a**



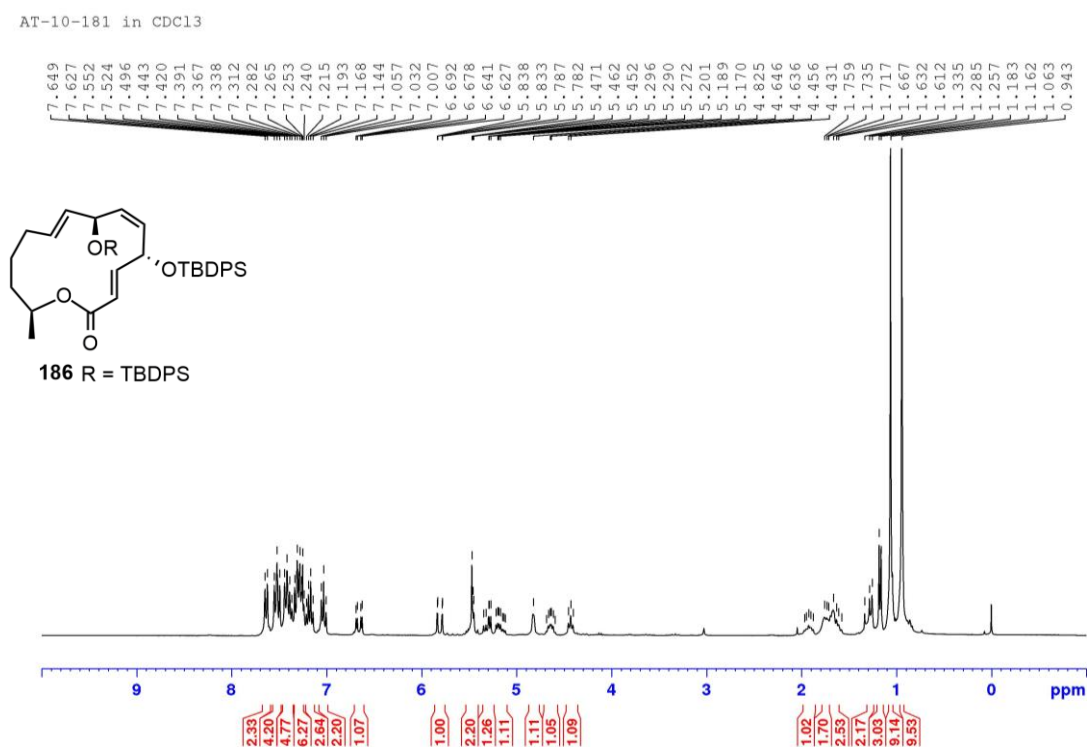
**Figure 88**  $^1\text{H}$  NMR (300 MHz,  $\text{CDCl}_3$ ) spectrum of compound **178**



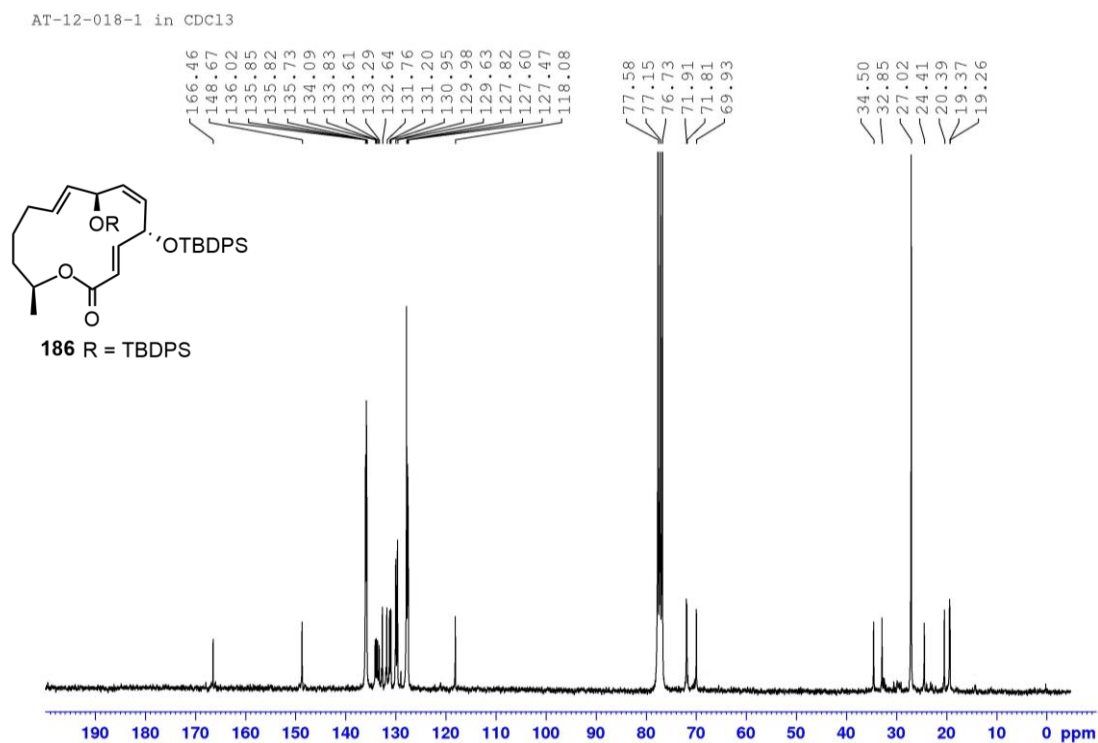
**Figure 89**  $^{13}\text{C}$  NMR (75 MHz,  $\text{CDCl}_3$ ) spectrum of compound **178**



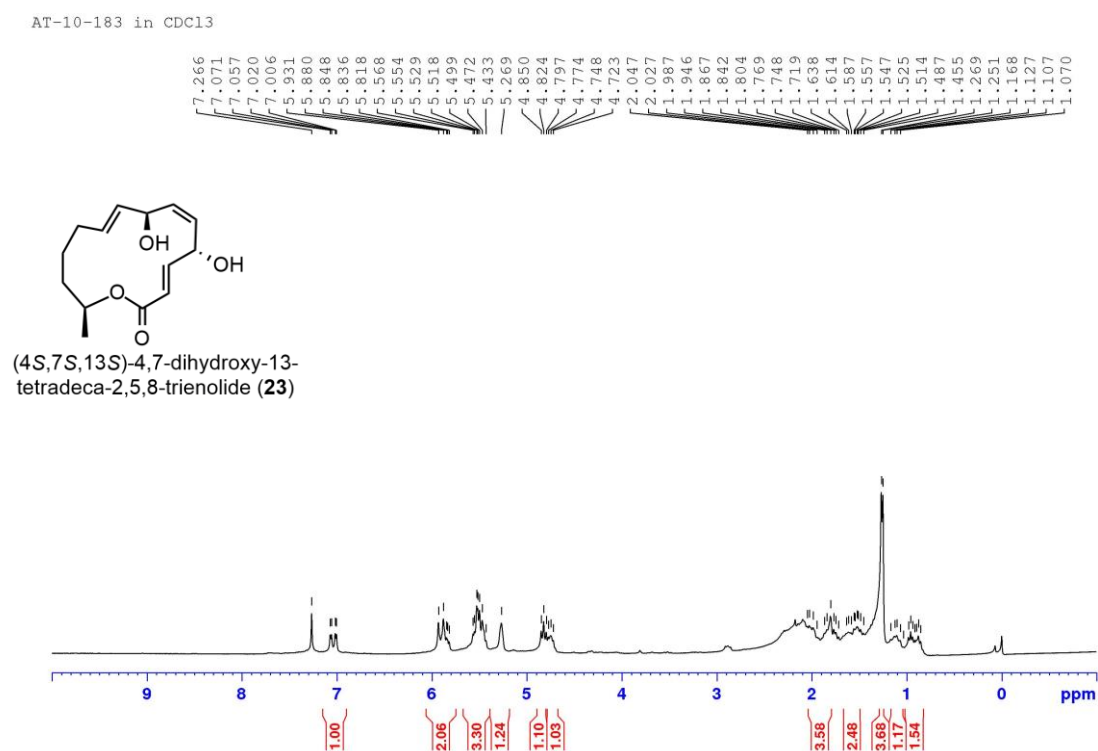
**Figure 90**  $^1\text{H}$  NMR (300 MHz,  $\text{CDCl}_3$ ) spectrum of compound **186**



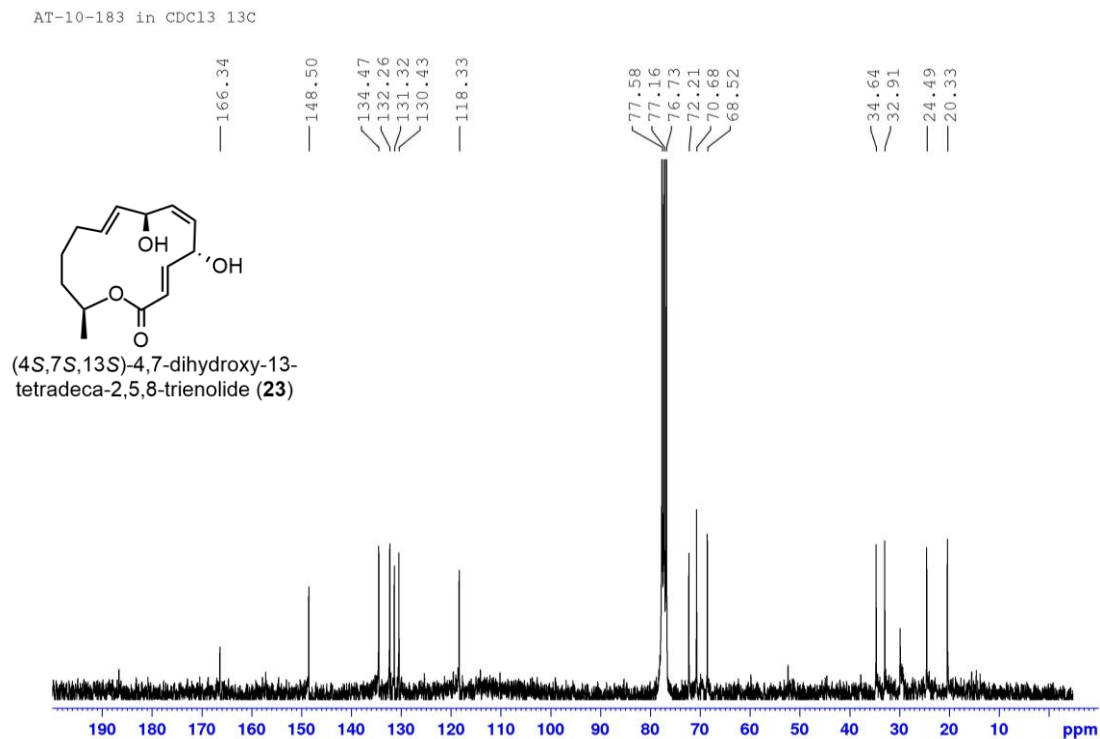
**Figure 91**  $^{13}\text{C}$  NMR (75 MHz,  $\text{CDCl}_3$ ) spectrum of compound **186**



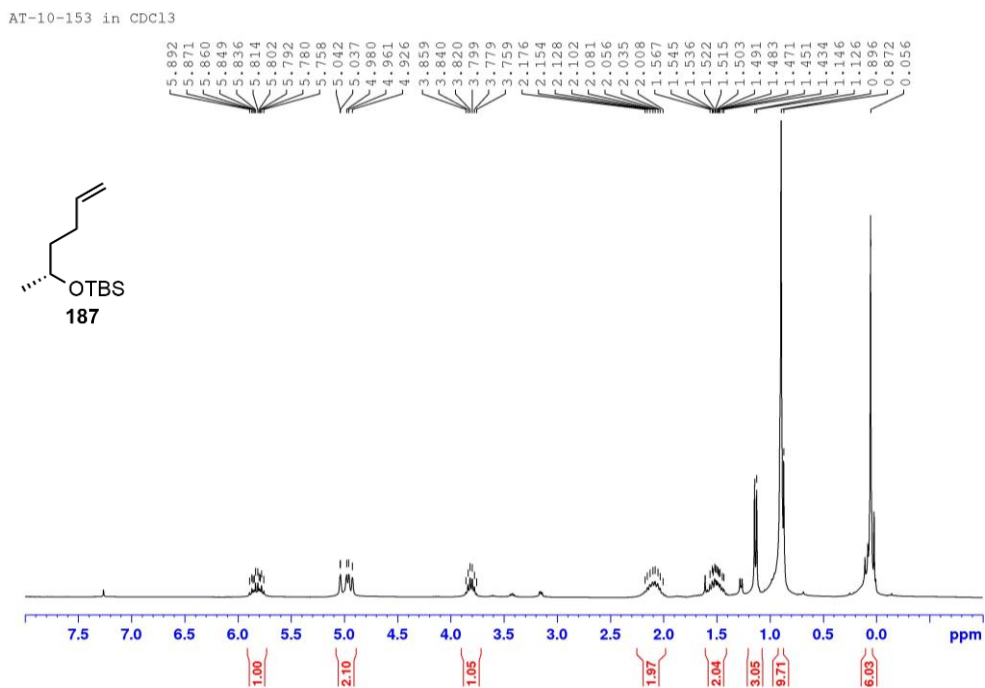
**Figure 92**  $^1\text{H}$  NMR (300 MHz,  $\text{CDCl}_3$ ) spectrum of (4*S*,7*S*,13*S*)-4,7-dihydroxy-13-tetradeca-2,5,8-trienolide (**23**)



**Figure 93**  $^{13}\text{C}$  NMR (75 MHz,  $\text{CDCl}_3$ ) spectrum of (4*S*,7*S*,13*S*)-4,7-dihydroxy-13-tetradeca-2,5,8-trienolide (**23**)

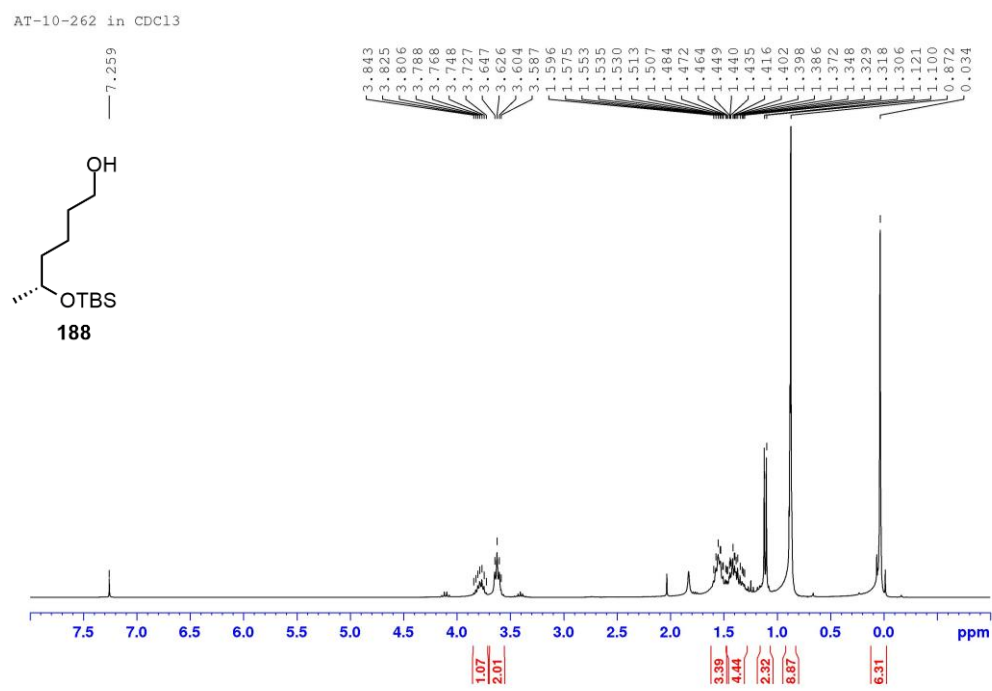


**Figure 94**  $^1\text{H}$  NMR (300 MHz,  $\text{CDCl}_3$ ) spectrum of compound **187**

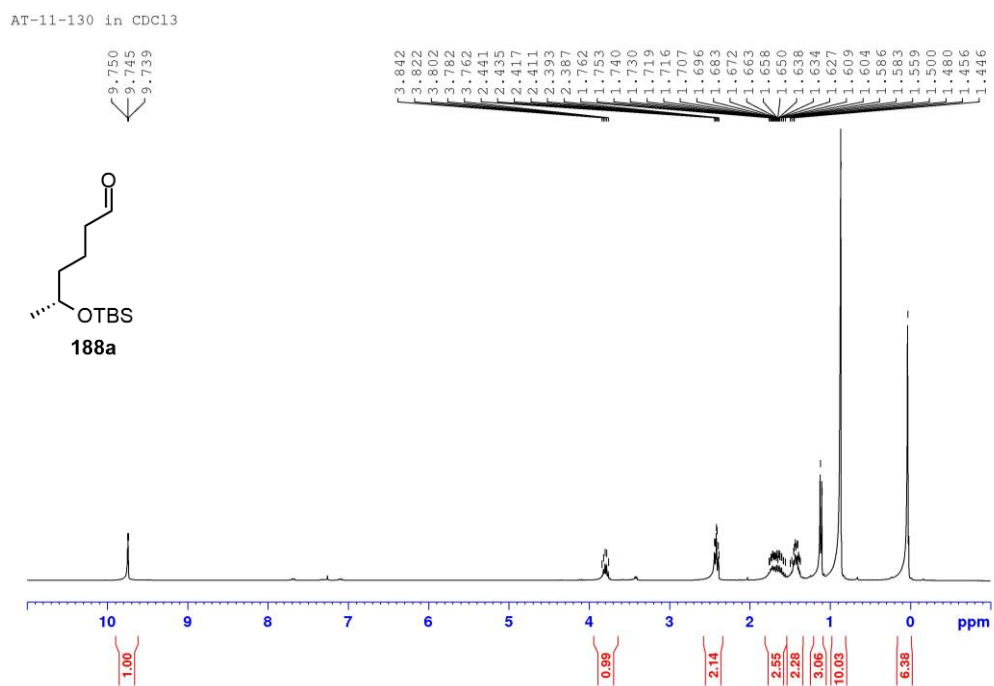




**Figure 95**  $^1\text{H}$  NMR (300 MHz,  $\text{CDCl}_3$ ) spectrum of compound **188**

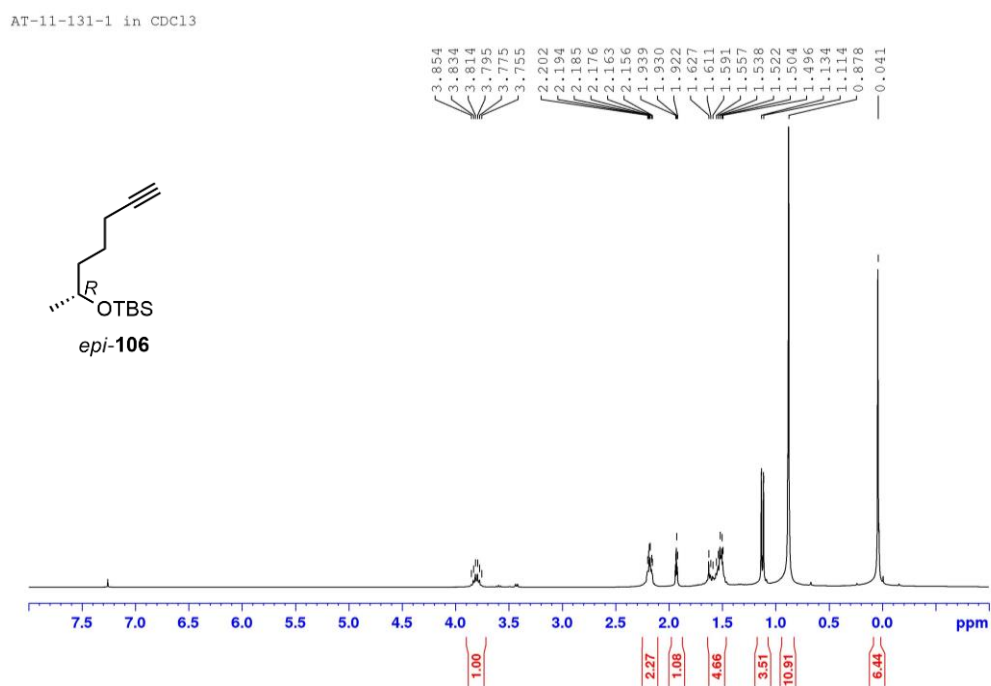


**Figure 96**  $^1\text{H}$  NMR (300 MHz,  $\text{CDCl}_3$ ) spectrum of compound **188a**

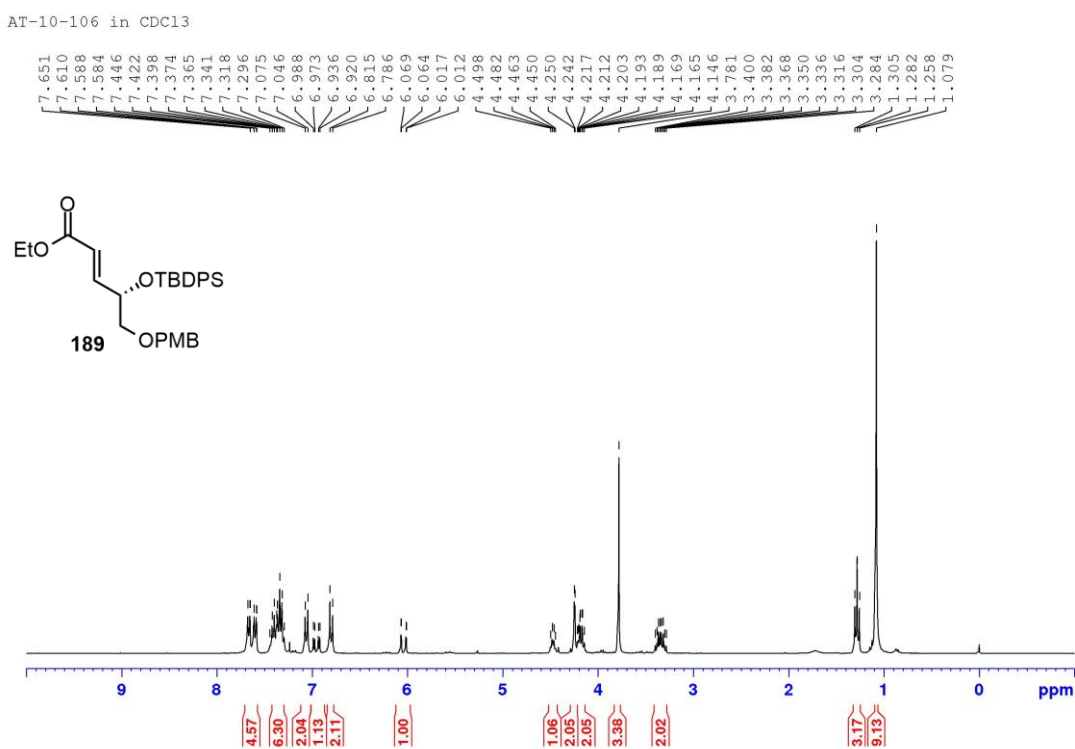




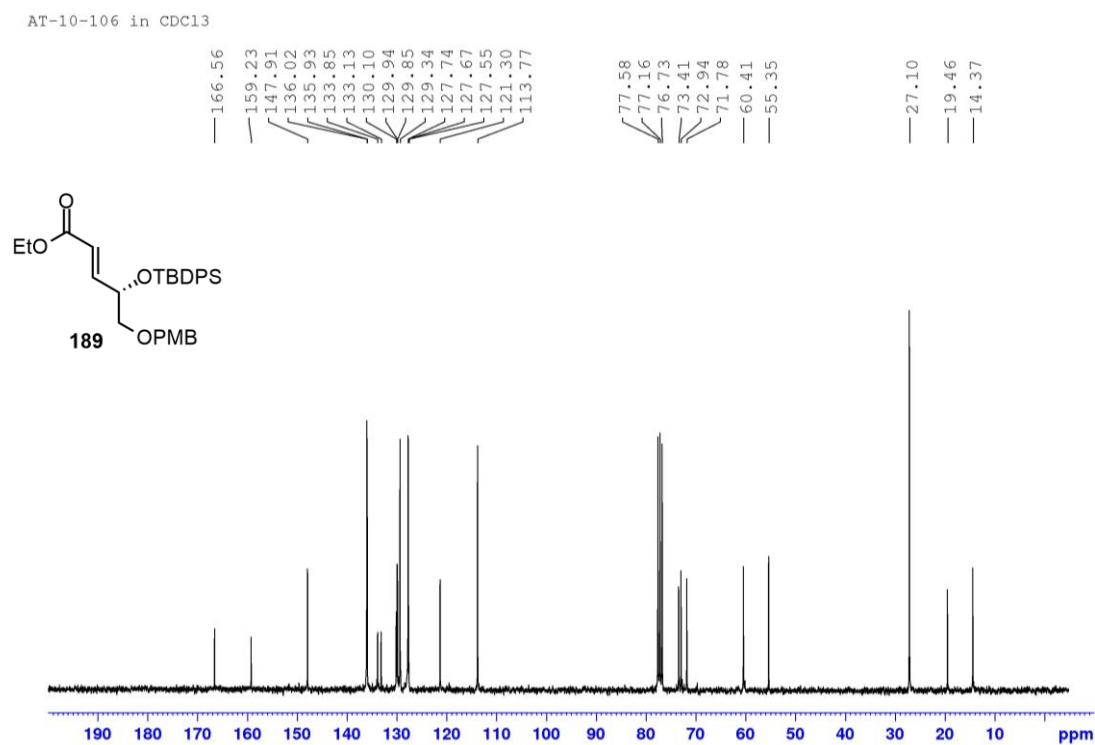
**Figure 97**  $^1\text{H}$  NMR (300 MHz,  $\text{CDCl}_3$ ) spectrum of compound *epi-106*



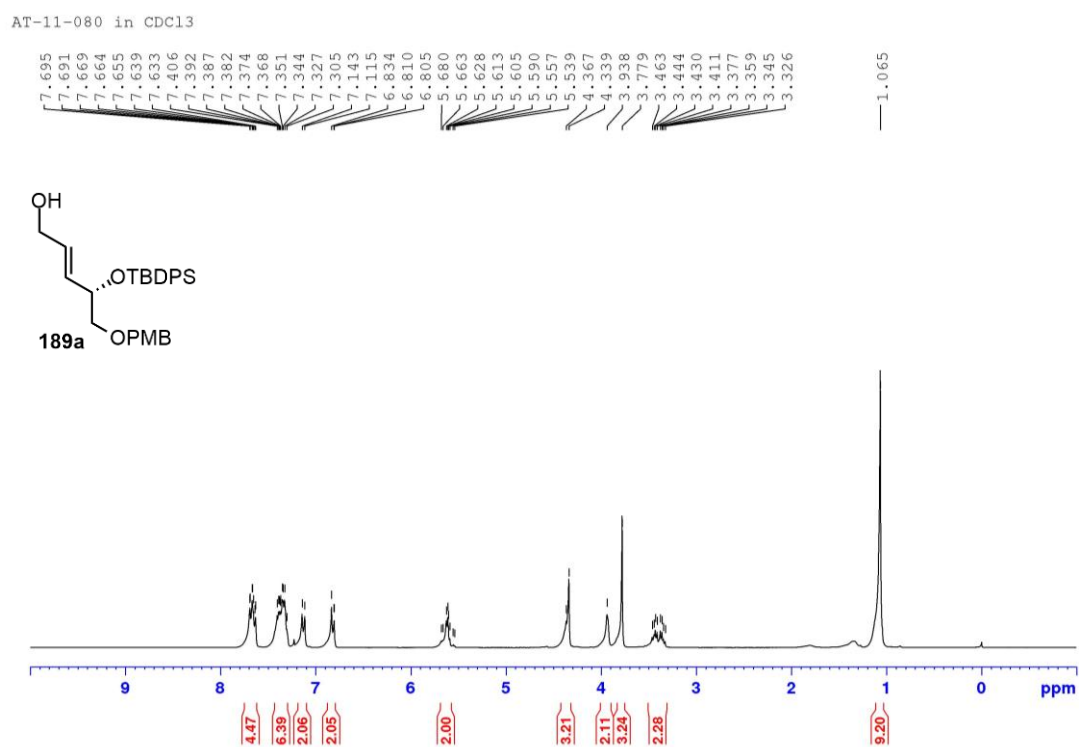
**Figure 98**  $^1\text{H}$  NMR (300 MHz,  $\text{CDCl}_3$ ) spectrum of compound **189**



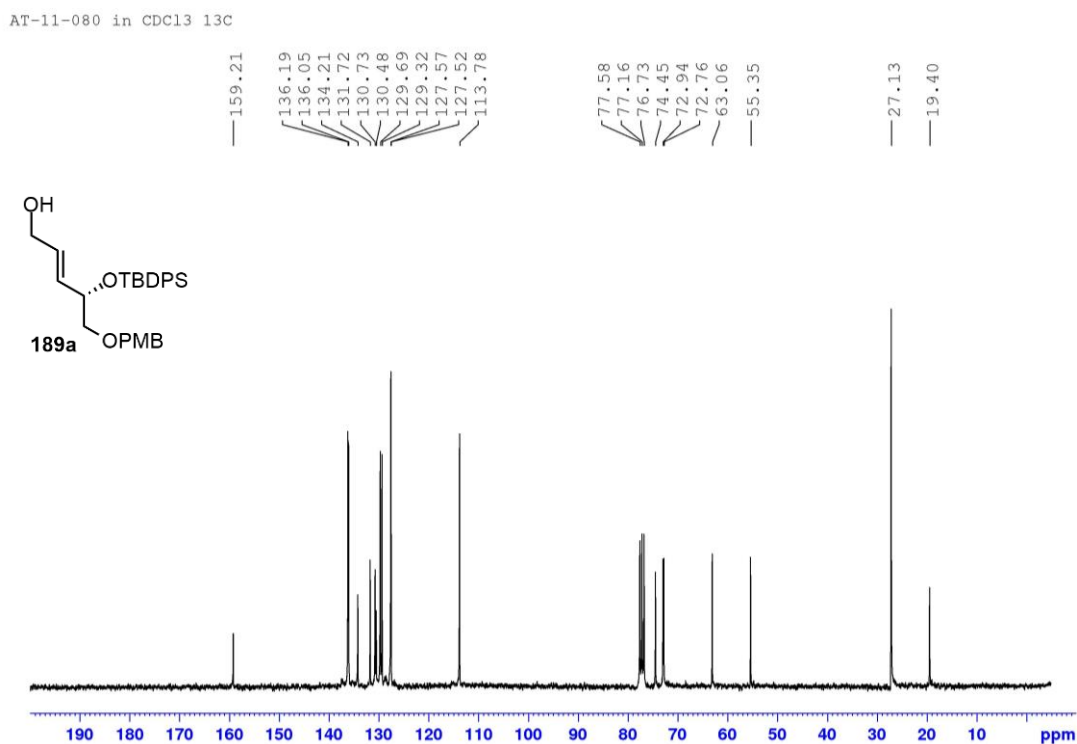
**Figure 99**  $^{13}\text{C}$  NMR (75 MHz,  $\text{CDCl}_3$ ) spectrum of compound **189**



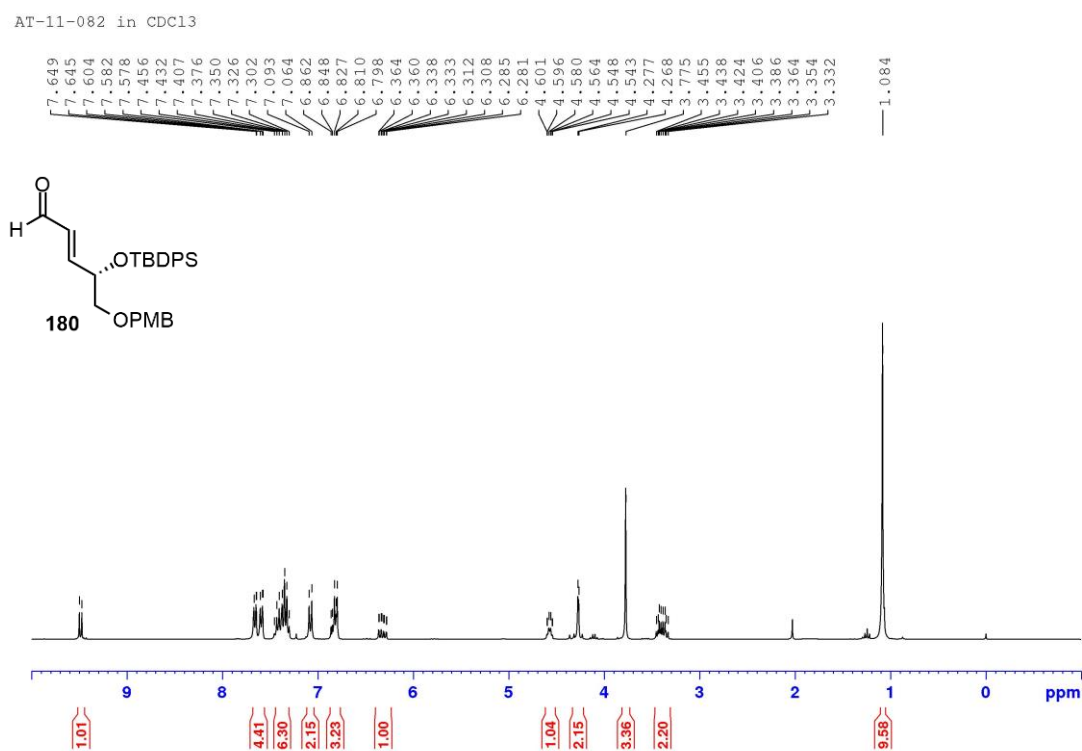
**Figure 100**  $^1\text{H}$  NMR (300 MHz,  $\text{CDCl}_3$ ) spectrum of compound **189a**

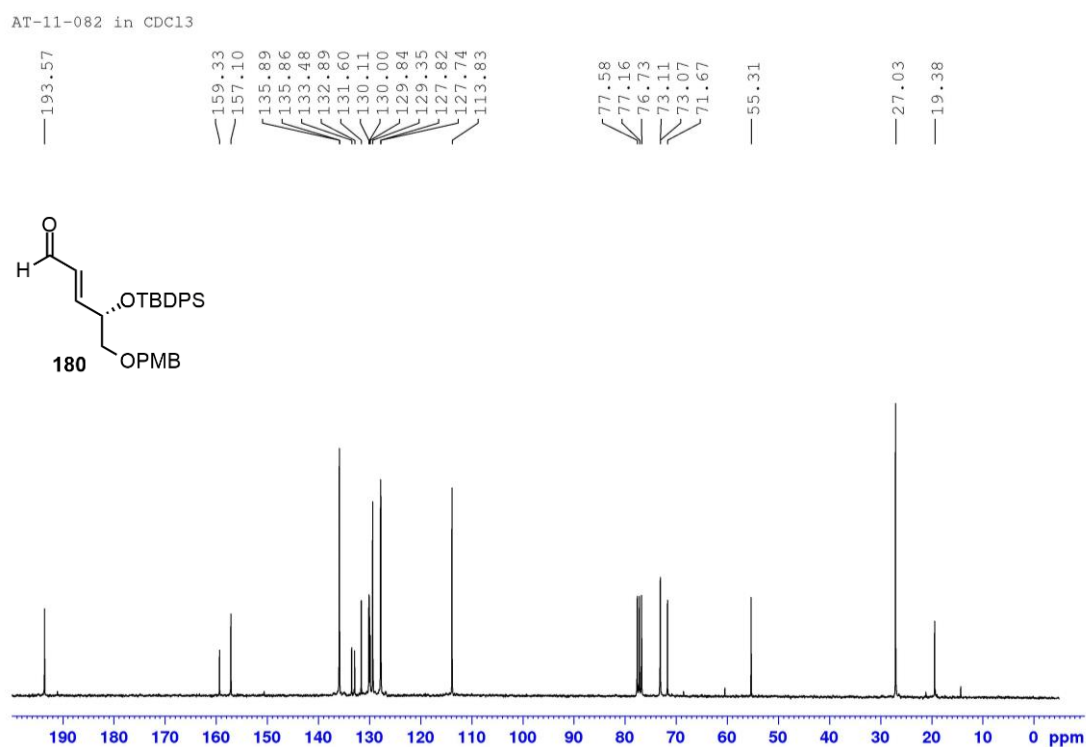
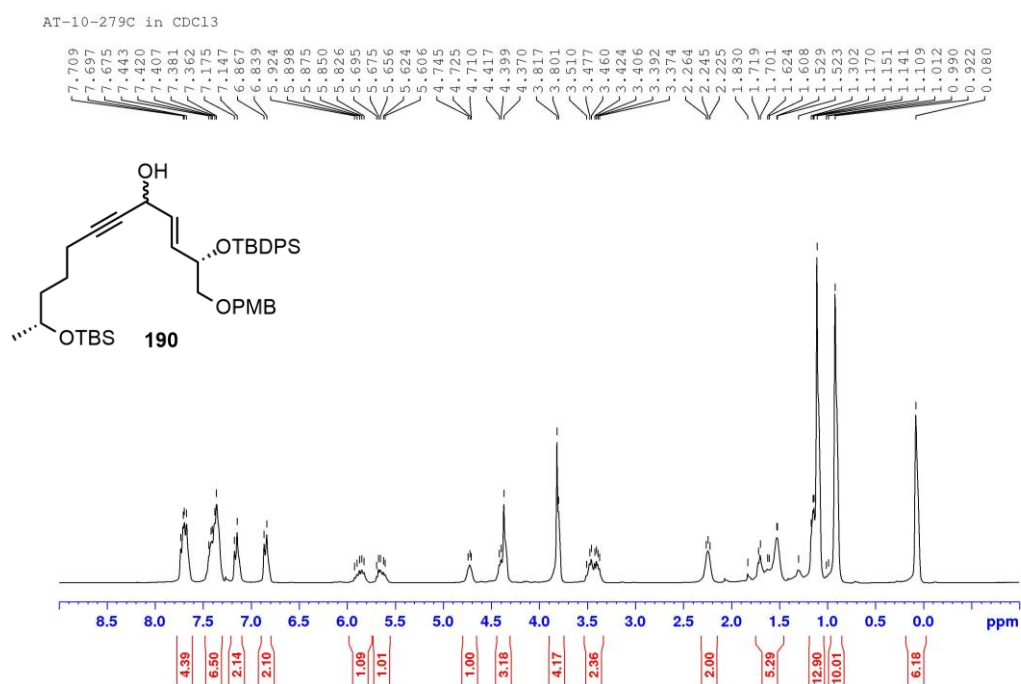


**Figure 101**  $^{13}\text{C}$  NMR (75 MHz,  $\text{CDCl}_3$ ) spectrum of compound **189a**

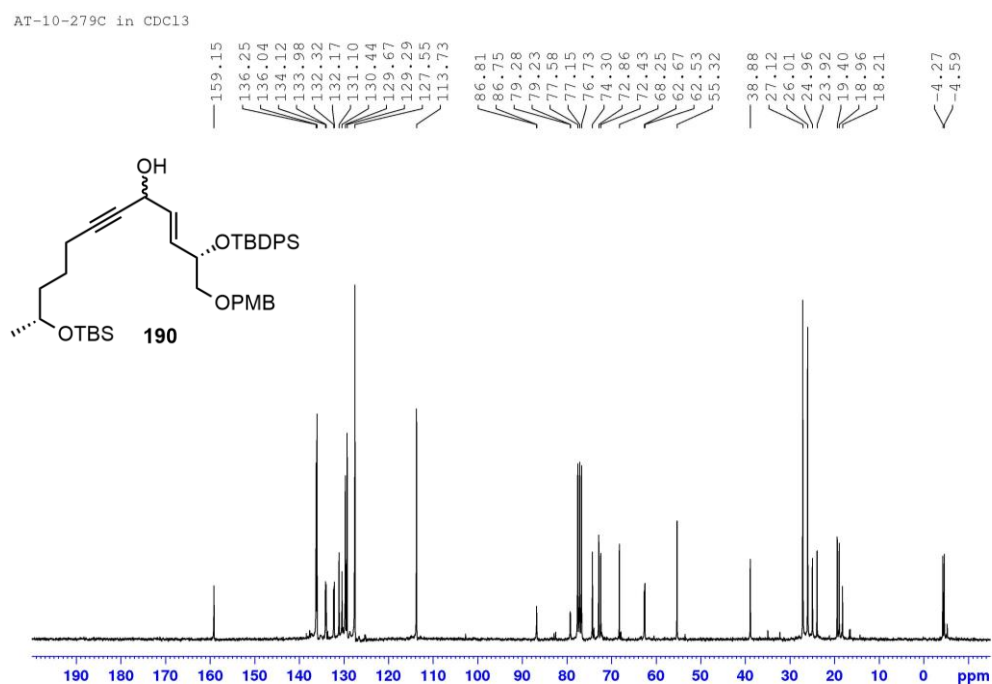


**Figure 102**  $^1\text{H}$  NMR (300 MHz,  $\text{CDCl}_3$ ) spectrum of compound **180**

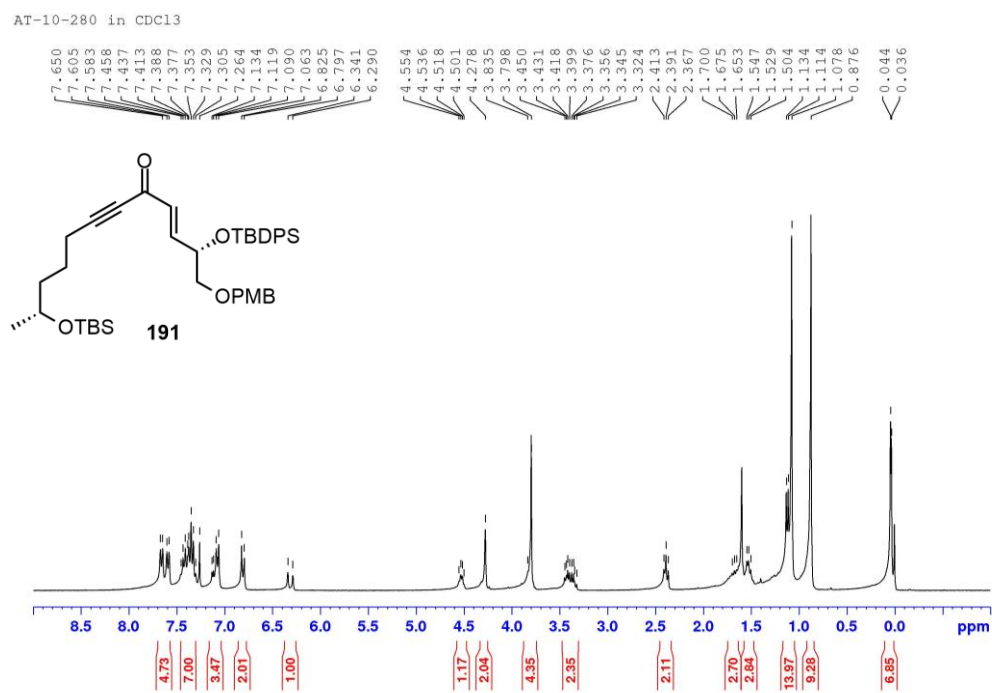


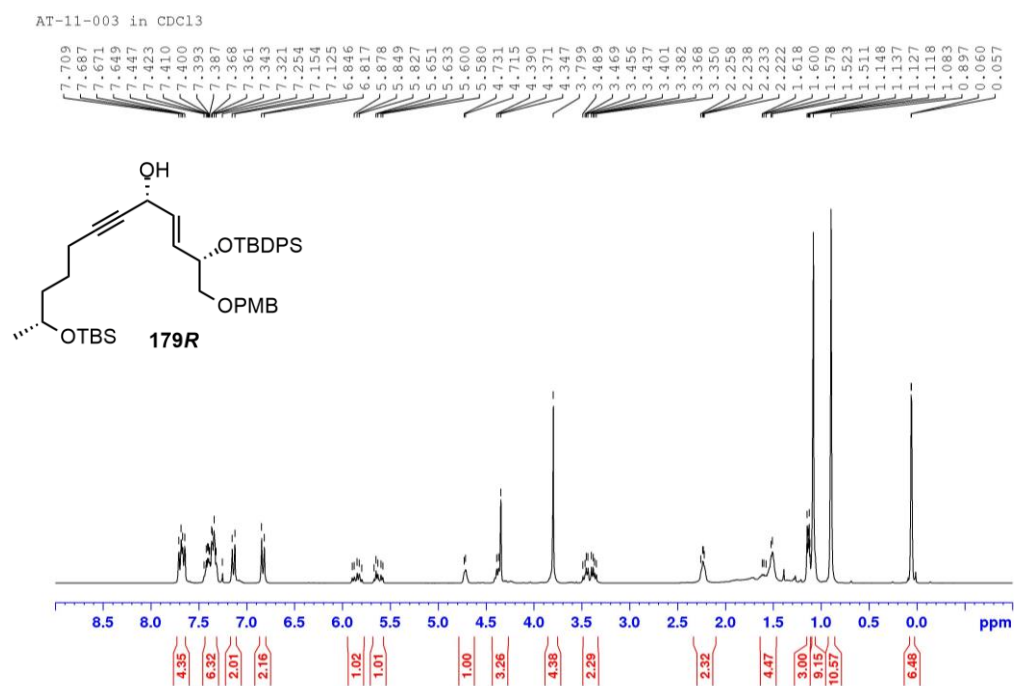
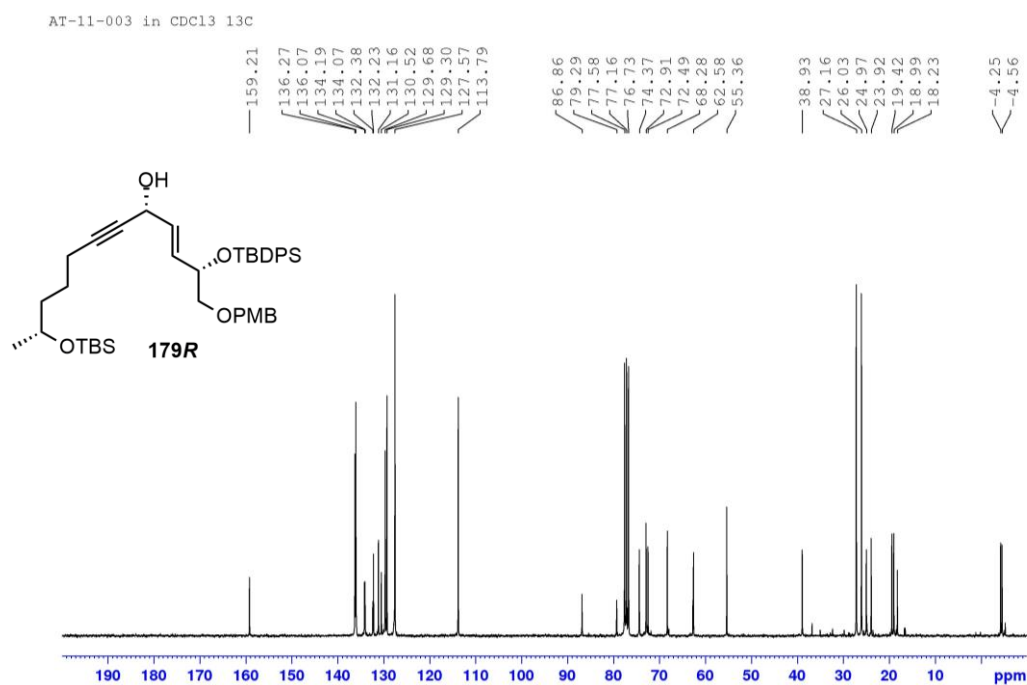
**Figure 103**  $^{13}\text{C}$  NMR (75 MHz,  $\text{CDCl}_3$ ) spectrum of compound **180****Figure 104**  $^1\text{H}$  NMR (300 MHz,  $\text{CDCl}_3$ ) spectrum of compound **190**

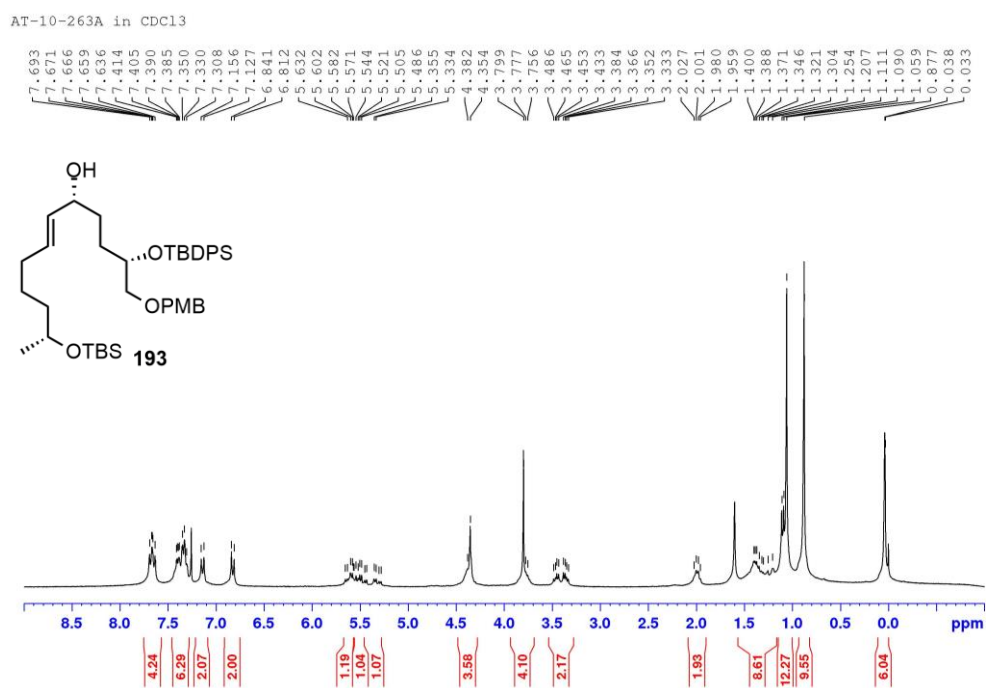
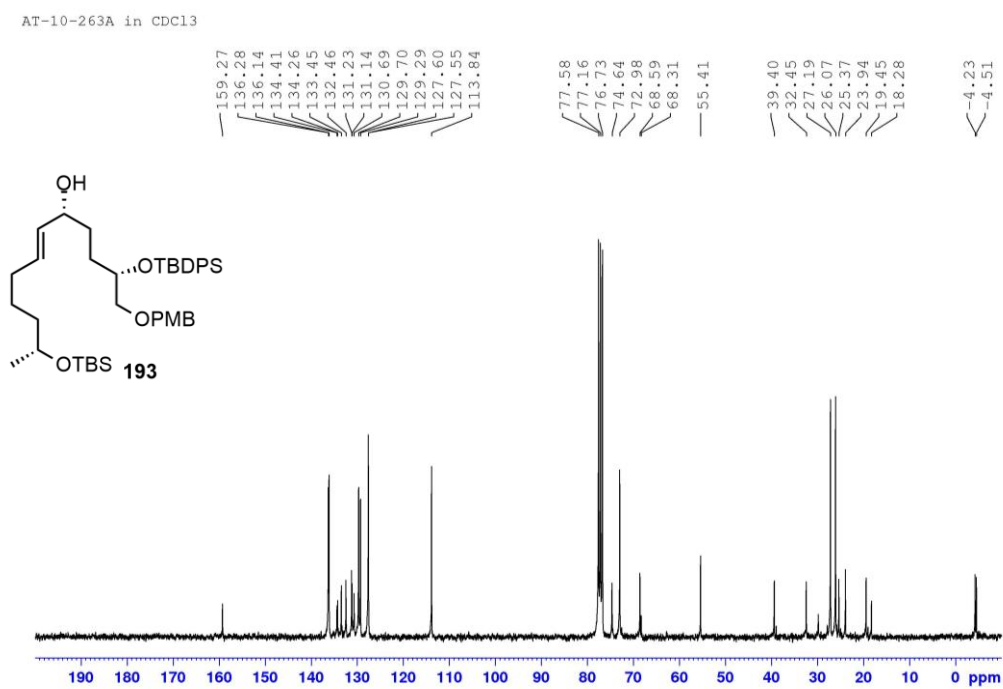
**Figure 105**  $^{13}\text{C}$  NMR (75 MHz,  $\text{CDCl}_3$ ) spectrum of compound **190**

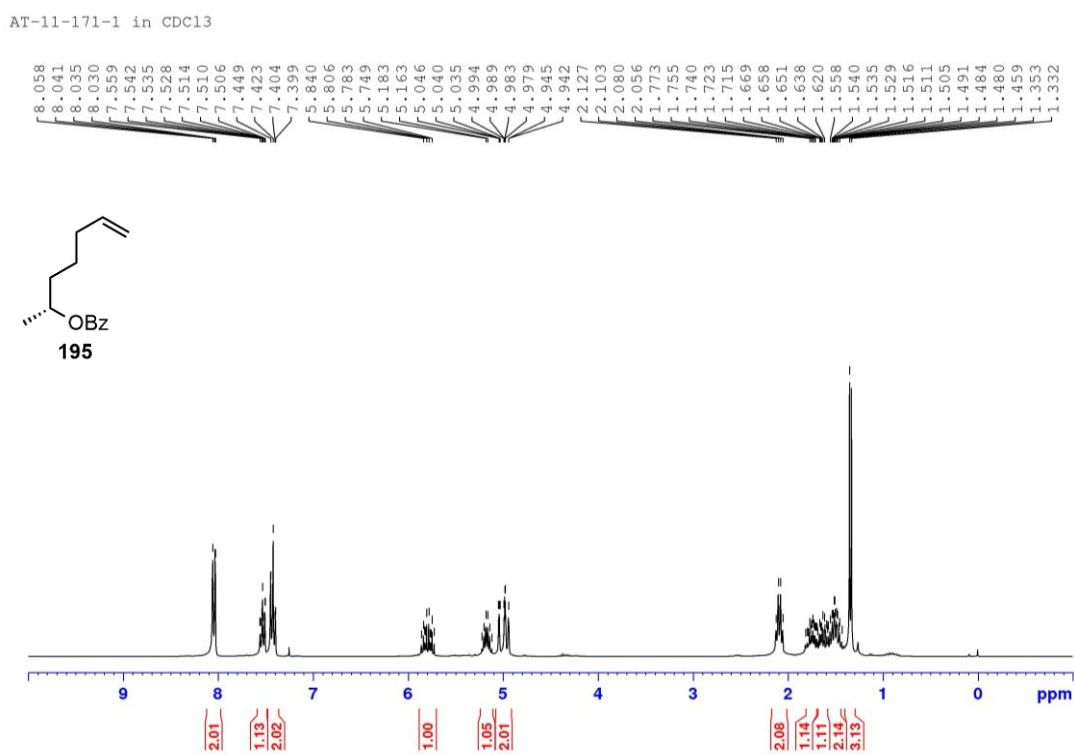
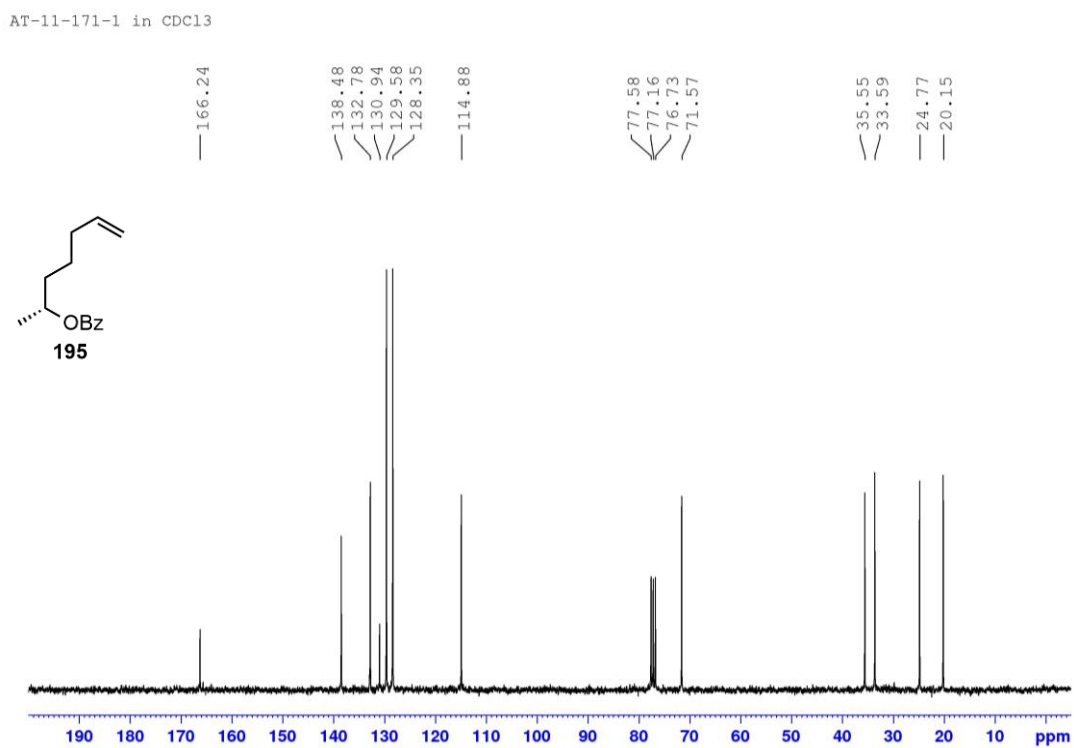


**Figure 106**  $^1\text{H}$  NMR (300 MHz,  $\text{CDCl}_3$ ) spectrum of compound **191**

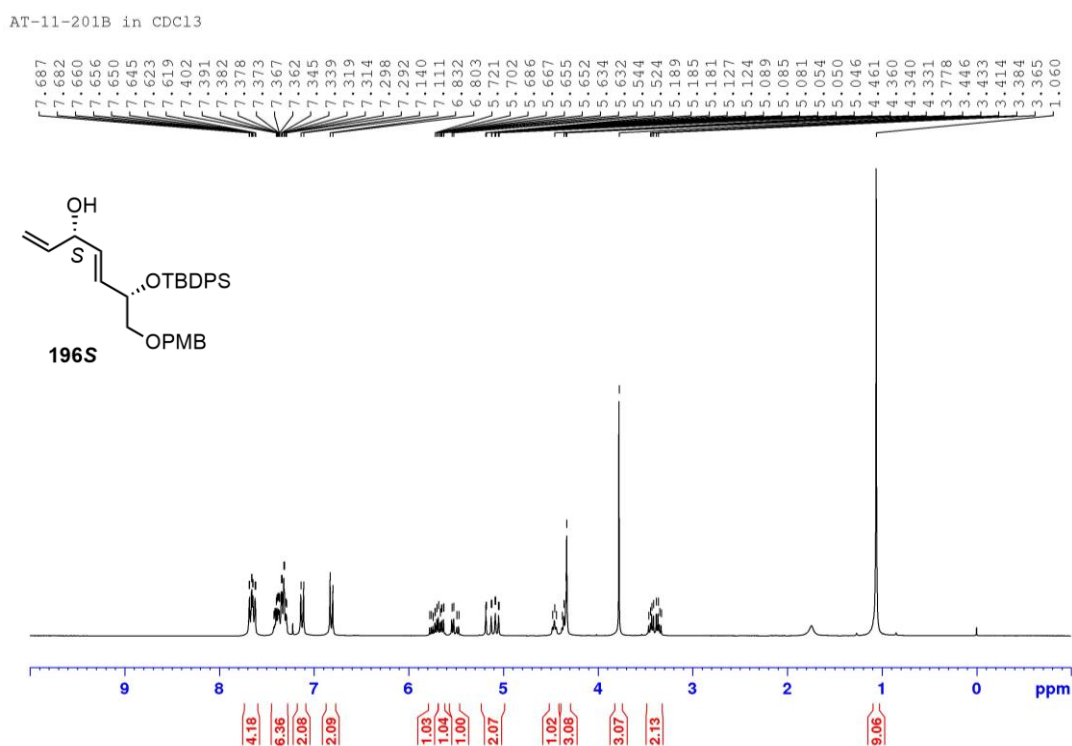
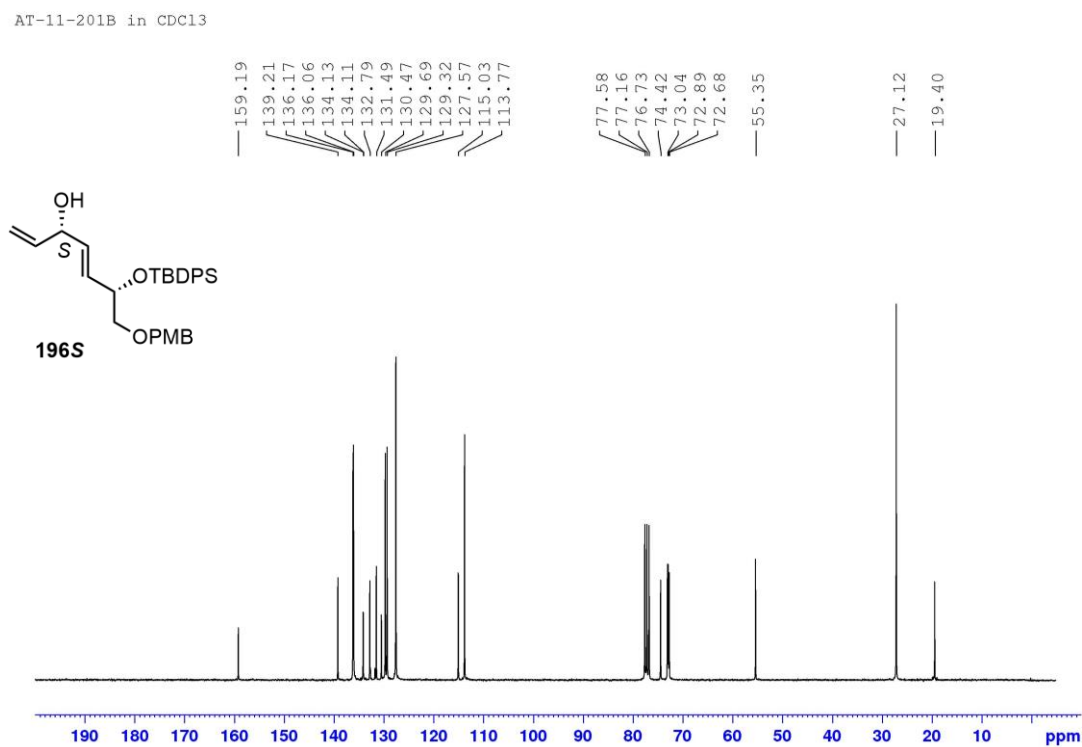


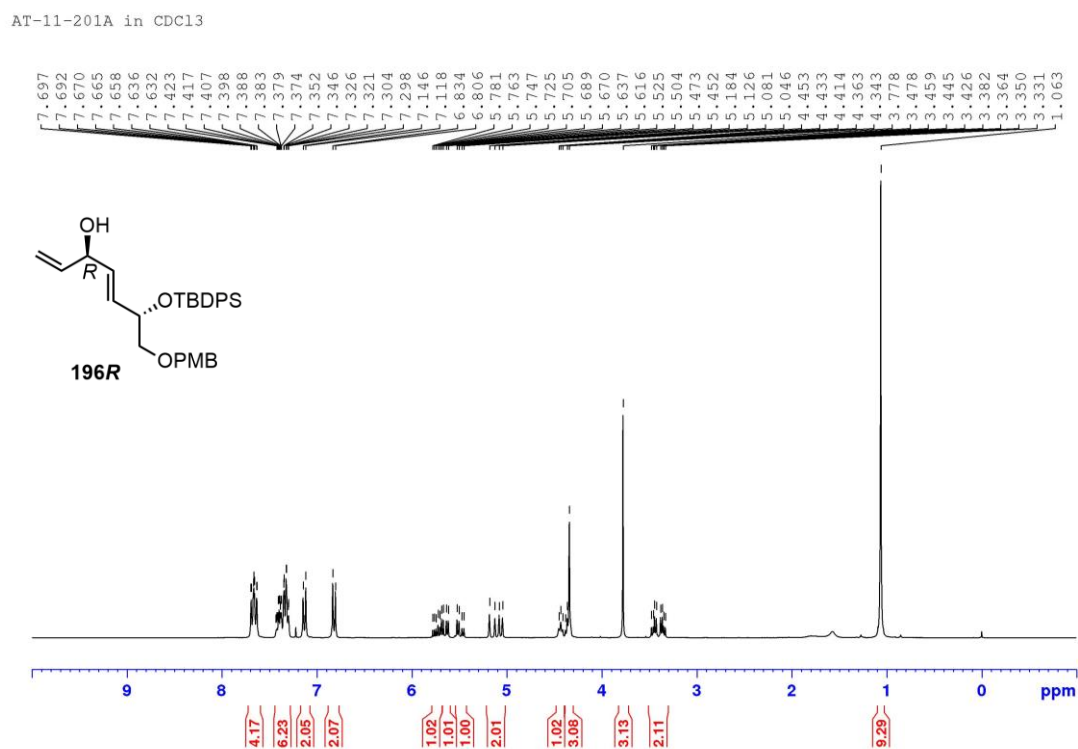
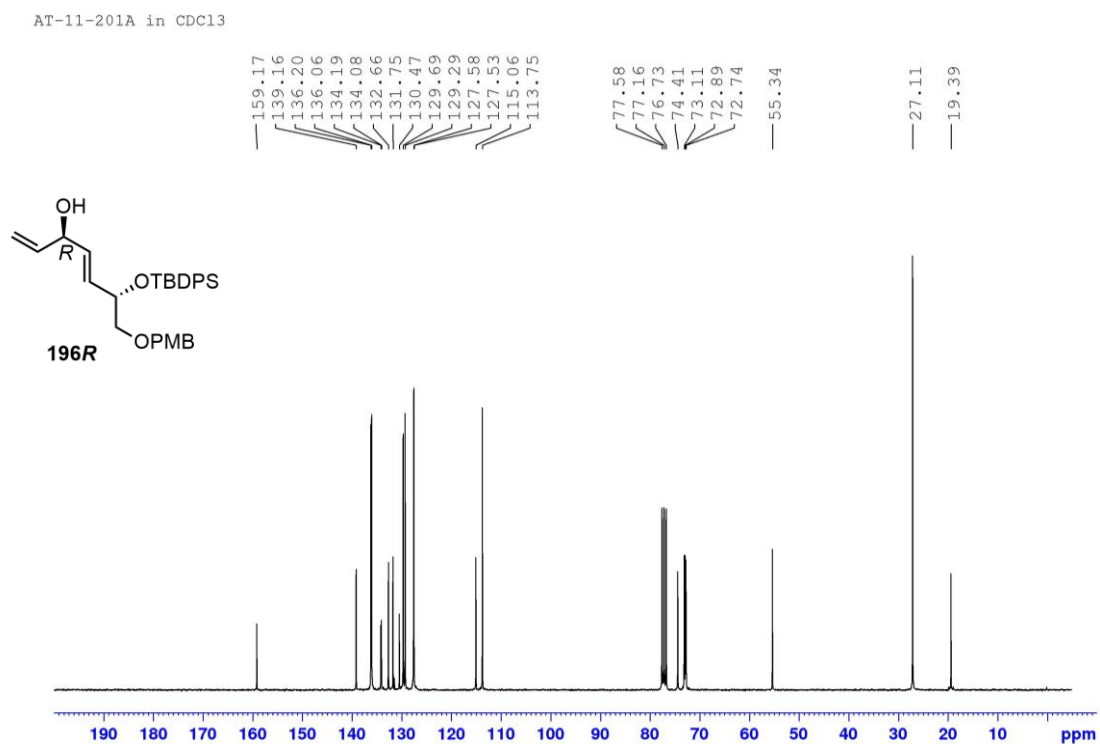
**Figure 107**  $^1\text{H}$  NMR (300 MHz,  $\text{CDCl}_3$ ) spectrum of compound **179R****Figure 108**  $^{13}\text{C}$  NMR (75 MHz,  $\text{CDCl}_3$ ) spectrum of compound **179R**

**Figure 109**  $^1\text{H}$  NMR (300 MHz,  $\text{CDCl}_3$ ) spectrum of compound **193****Figure 110**  $^{13}\text{C}$  NMR (75 MHz,  $\text{CDCl}_3$ ) spectrum of compound **193**

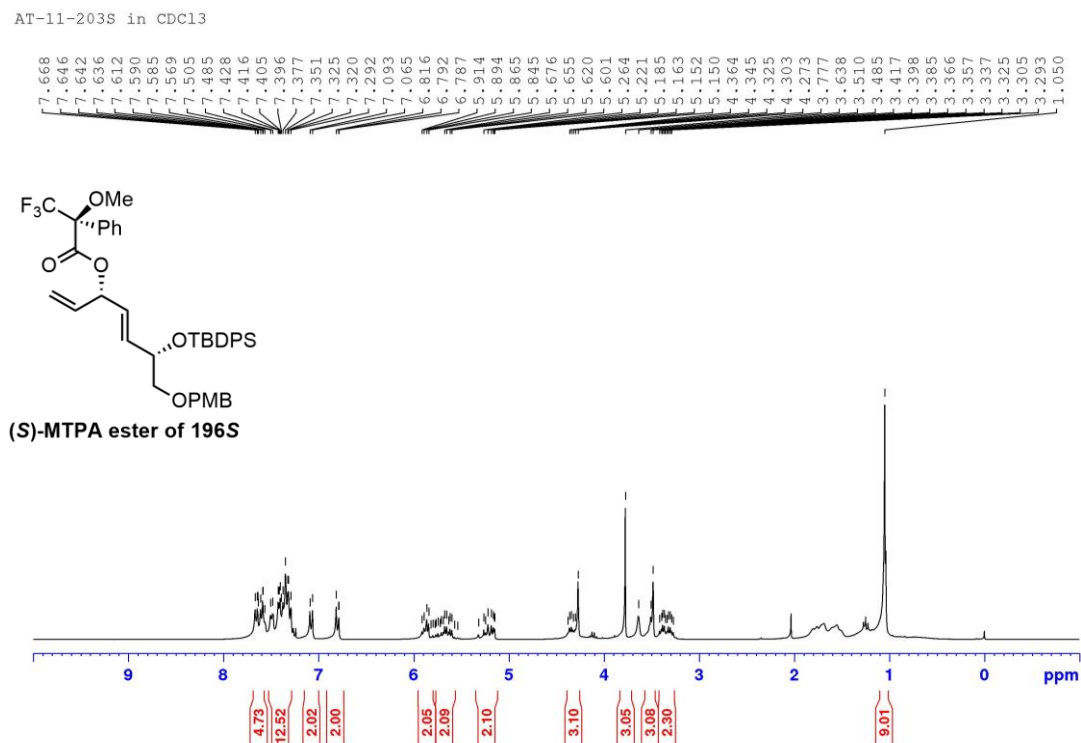
**Figure 111**  $^1\text{H}$  NMR (300 MHz,  $\text{CDCl}_3$ ) spectrum of compound **195****Figure 112**  $^{13}\text{C}$  NMR (75 MHz,  $\text{CDCl}_3$ ) spectrum of compound **195**



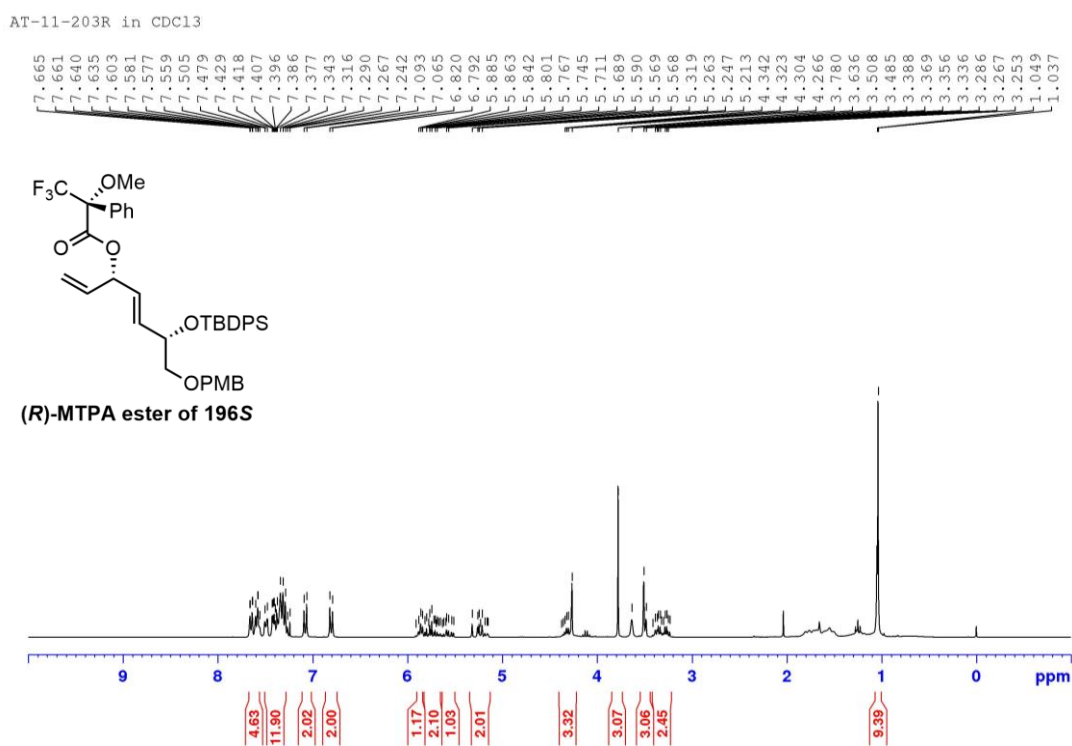
**Figure 113**  $^1\text{H}$  NMR (300 MHz,  $\text{CDCl}_3$ ) spectrum of compound **196S****Figure 114**  $^{13}\text{C}$  NMR (75 MHz,  $\text{CDCl}_3$ ) spectrum of compound **196S**

**Figure 115**  $^1\text{H}$  NMR (300 MHz,  $\text{CDCl}_3$ ) spectrum of compound **196R****Figure 116**  $^{13}\text{C}$  NMR (75 MHz,  $\text{CDCl}_3$ ) spectrum of compound **196R**

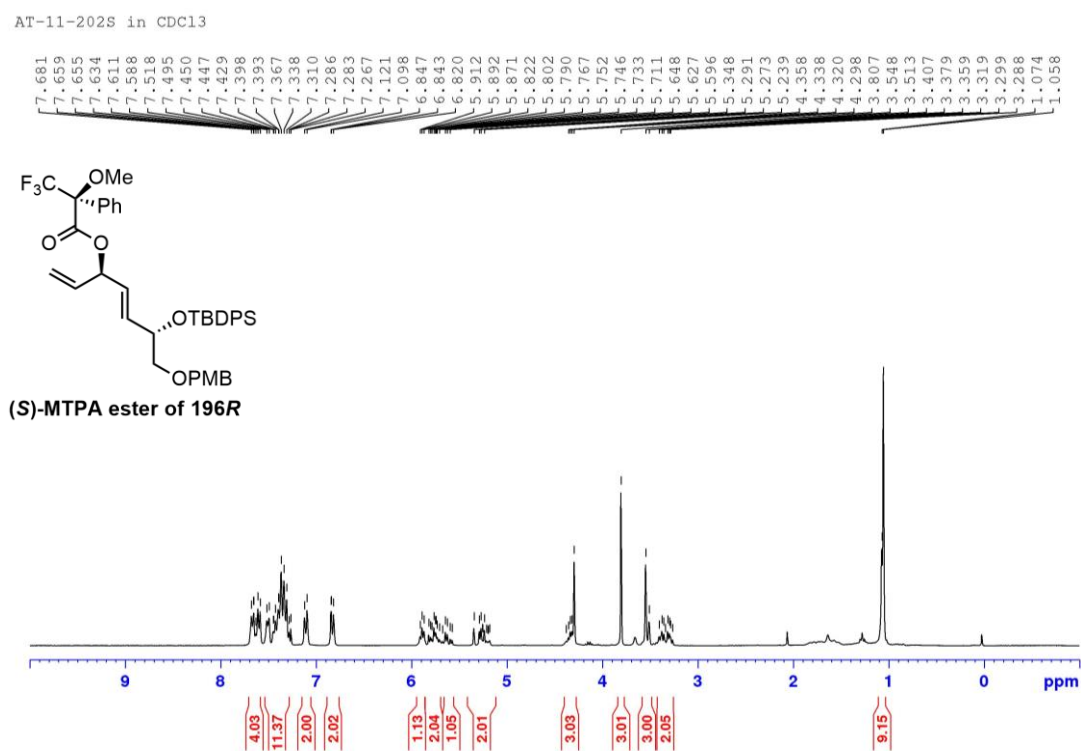
**Figure 117**  $^1\text{H}$  NMR (300 MHz,  $\text{CDCl}_3$ ) spectrum of (*S*)-MTPA ester of **196S**



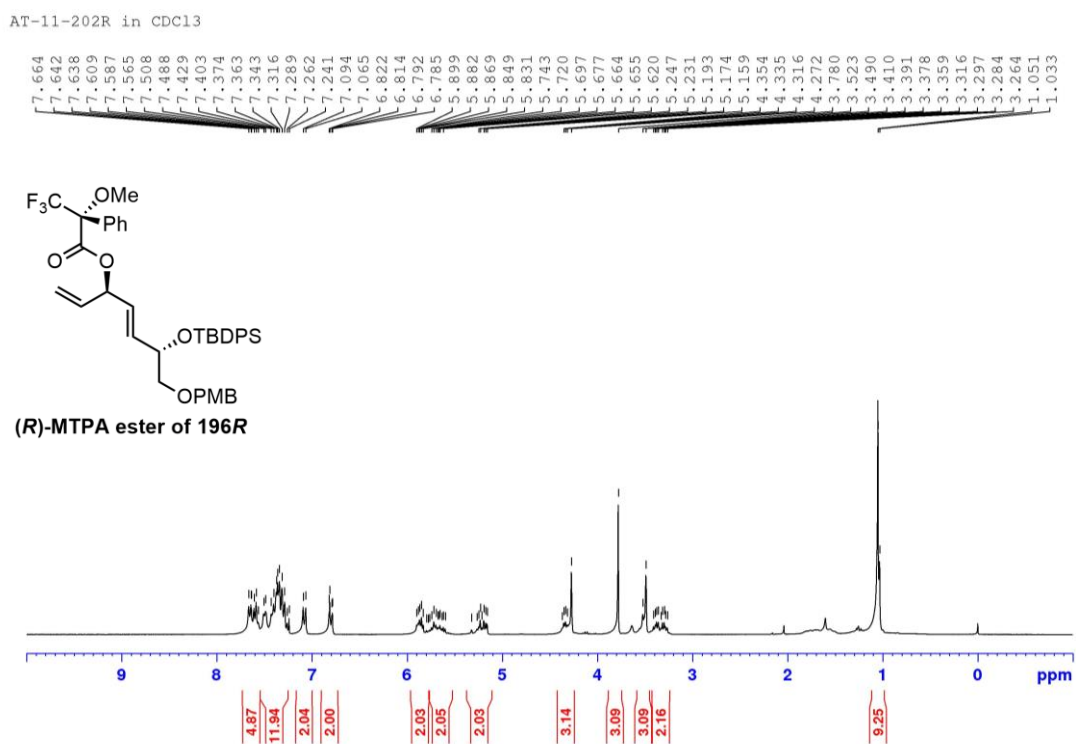
**Figure 118**  $^1\text{H}$  NMR (300 MHz,  $\text{CDCl}_3$ ) spectrum of (*R*)-MTPA ester of **196S**



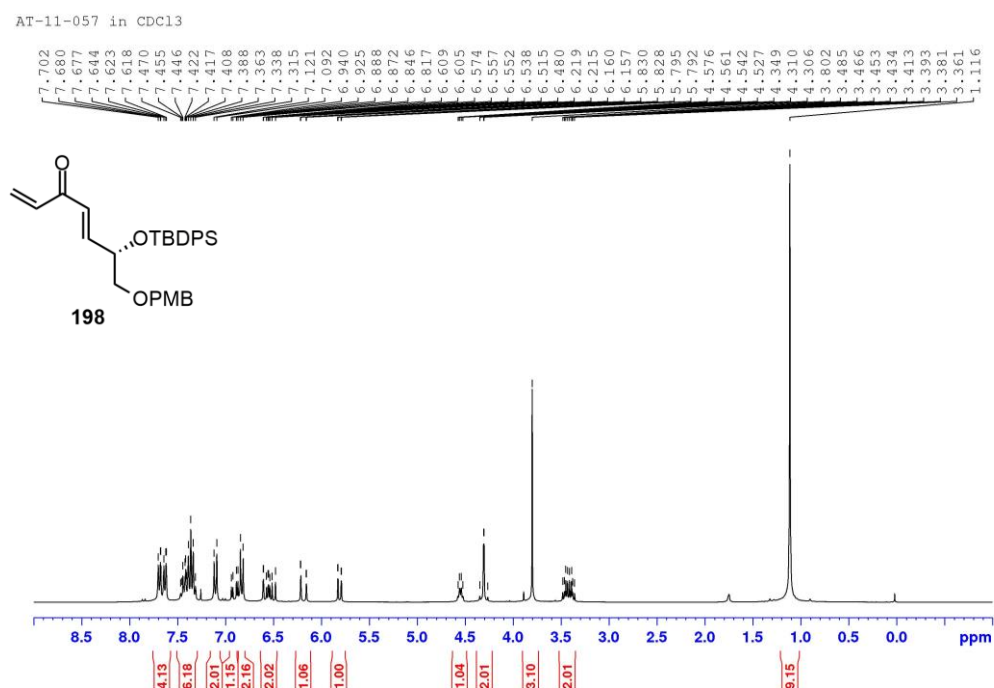
**Figure 119**  $^1\text{H}$  NMR (300 MHz,  $\text{CDCl}_3$ ) spectrum of (*S*)-MTPA ester of **196R**



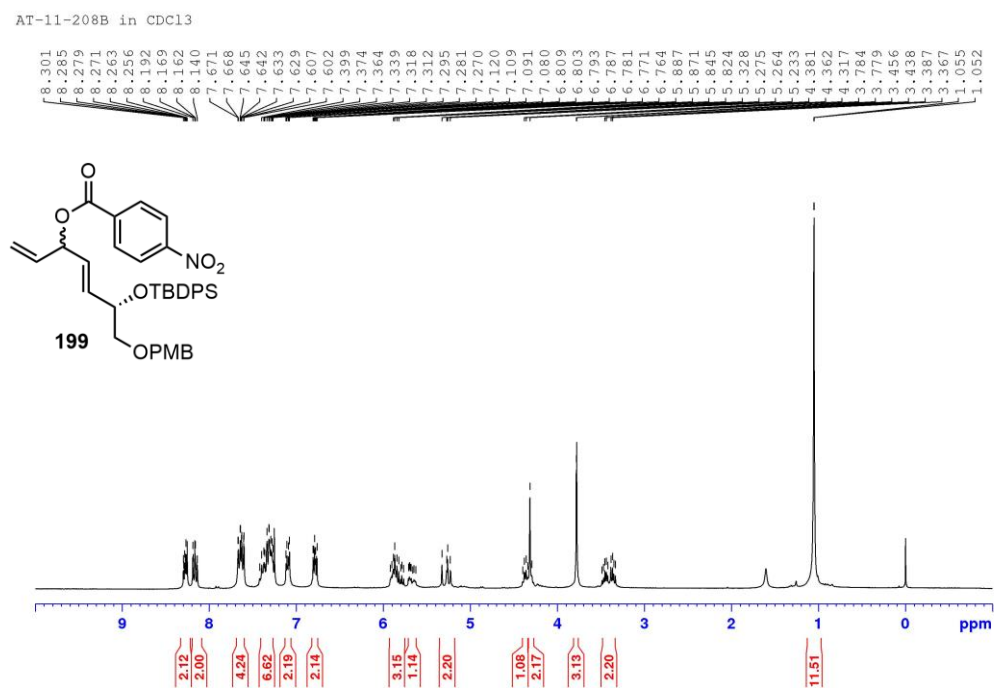
**Figure 120**  $^1\text{H}$  NMR (300 MHz,  $\text{CDCl}_3$ ) spectrum of (*R*)-MTPA ester of **196R**

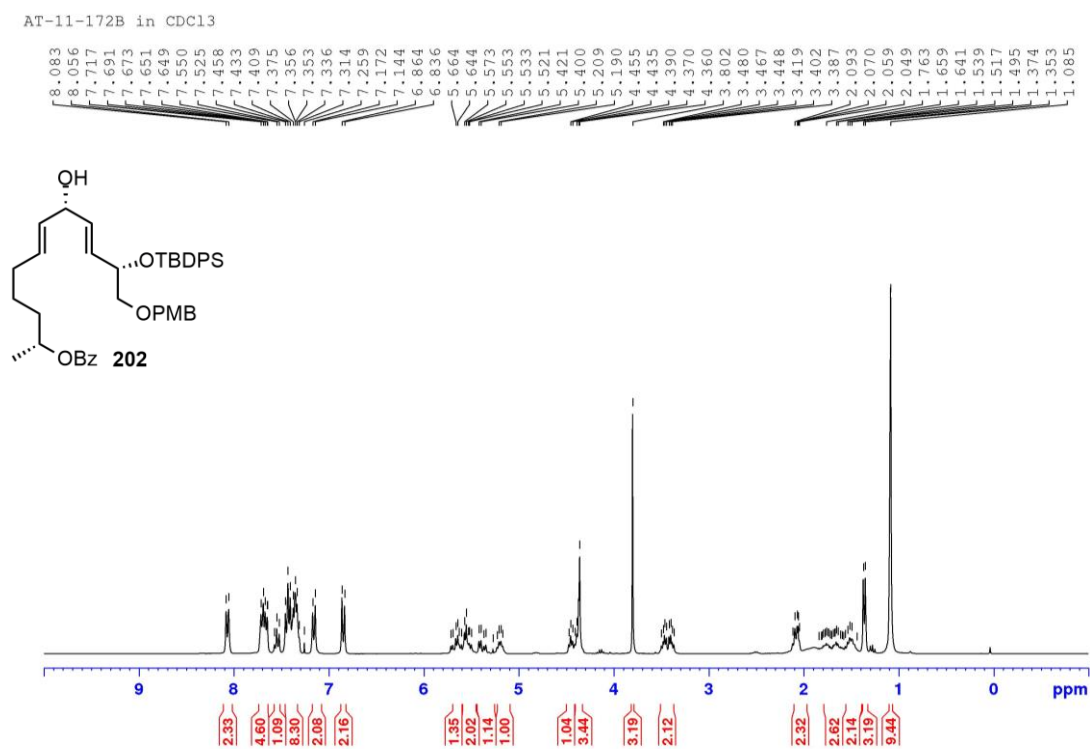
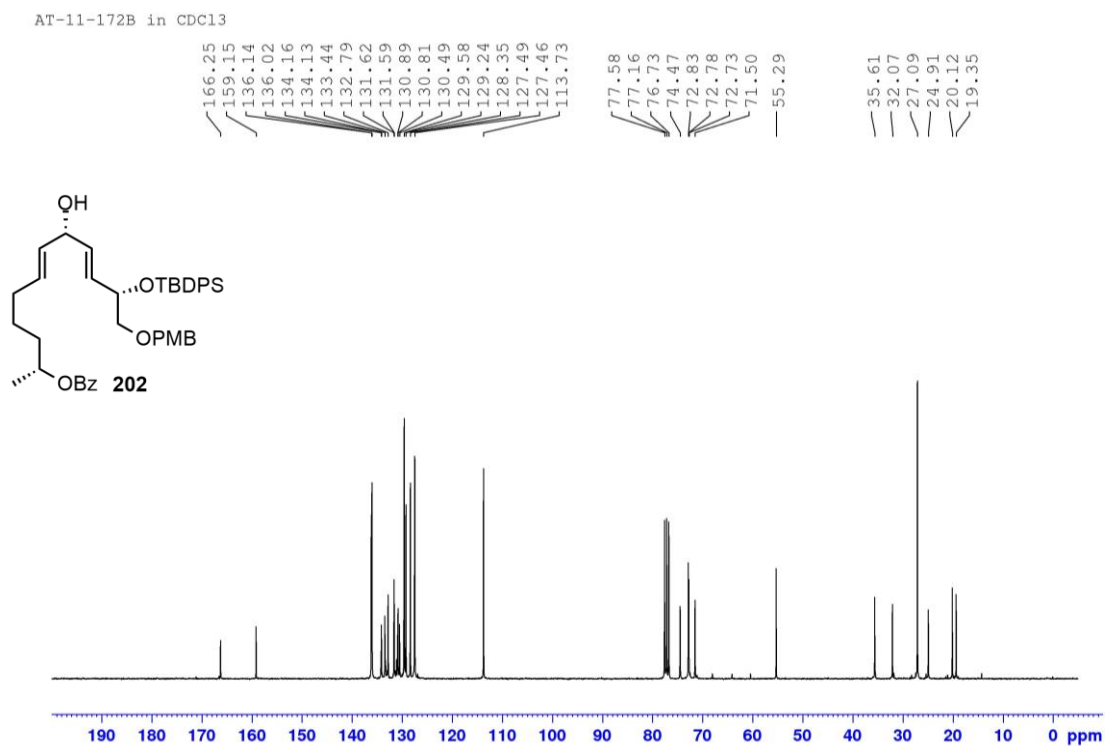


**Figure 121**  $^1\text{H}$  NMR (300 MHz,  $\text{CDCl}_3$ ) spectrum of compound **198**

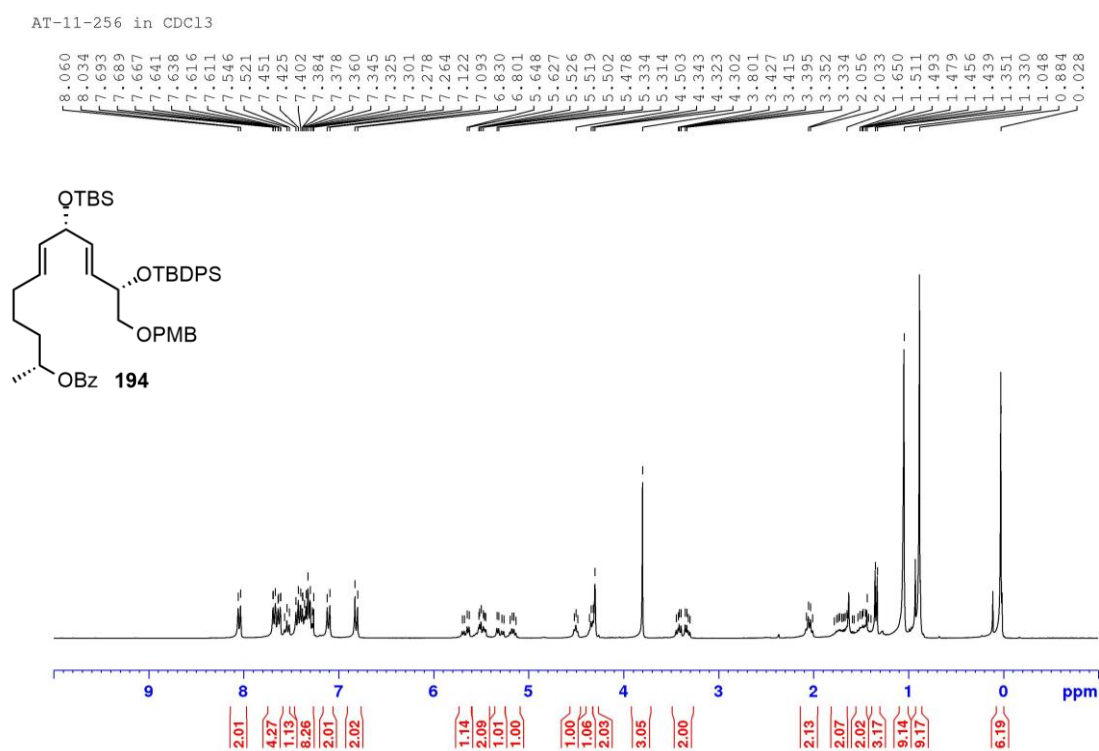


**Figure 122**  $^1\text{H}$  NMR (300 MHz,  $\text{CDCl}_3$ ) spectrum of compound **199**

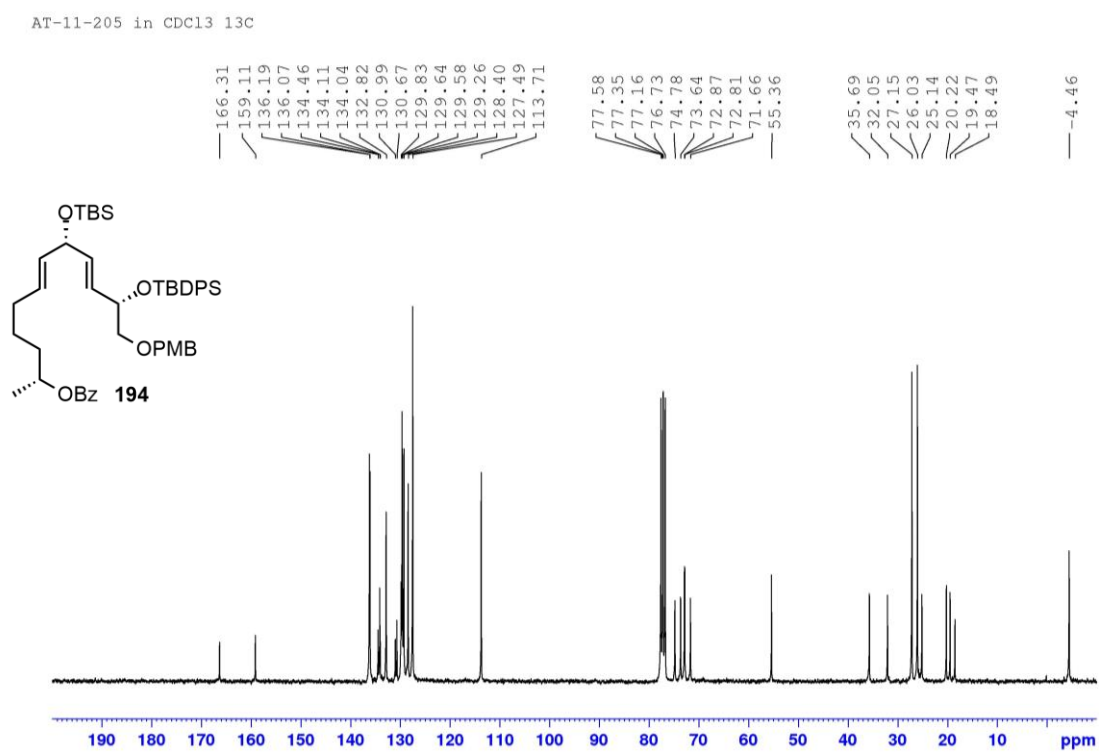


**Figure 123**  $^1\text{H}$  NMR (300 MHz,  $\text{CDCl}_3$ ) spectrum of compound **202****Figure 124**  $^{13}\text{C}$  NMR (75 MHz,  $\text{CDCl}_3$ ) spectrum of compound **202**

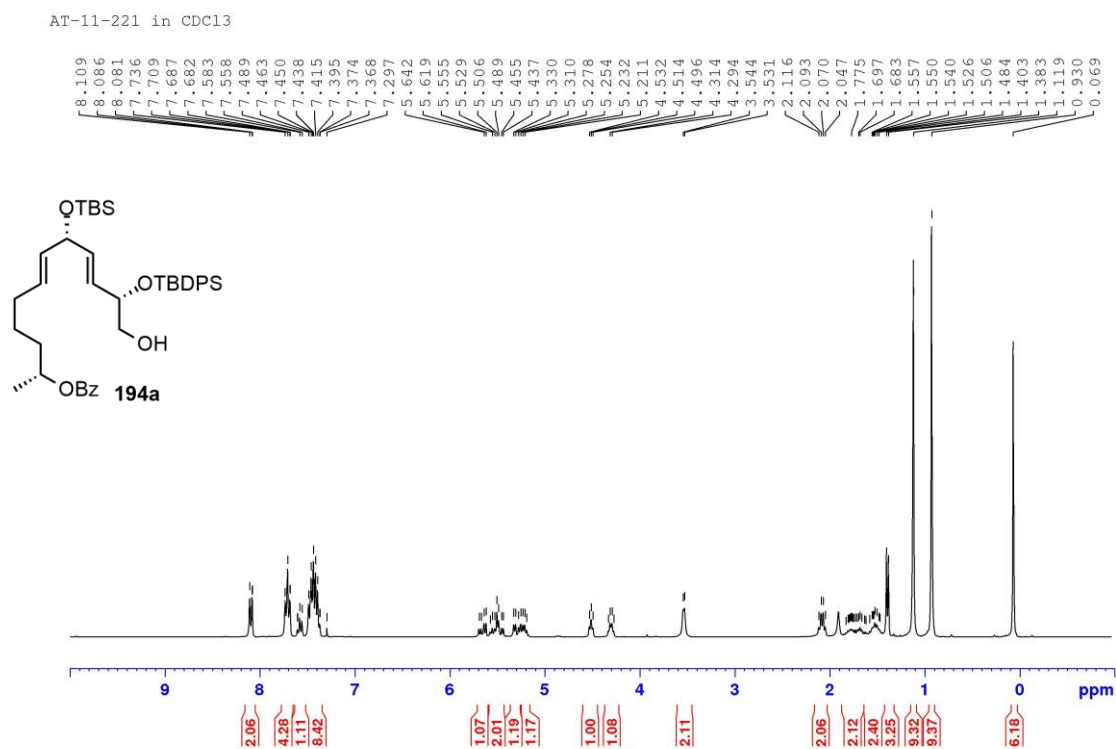
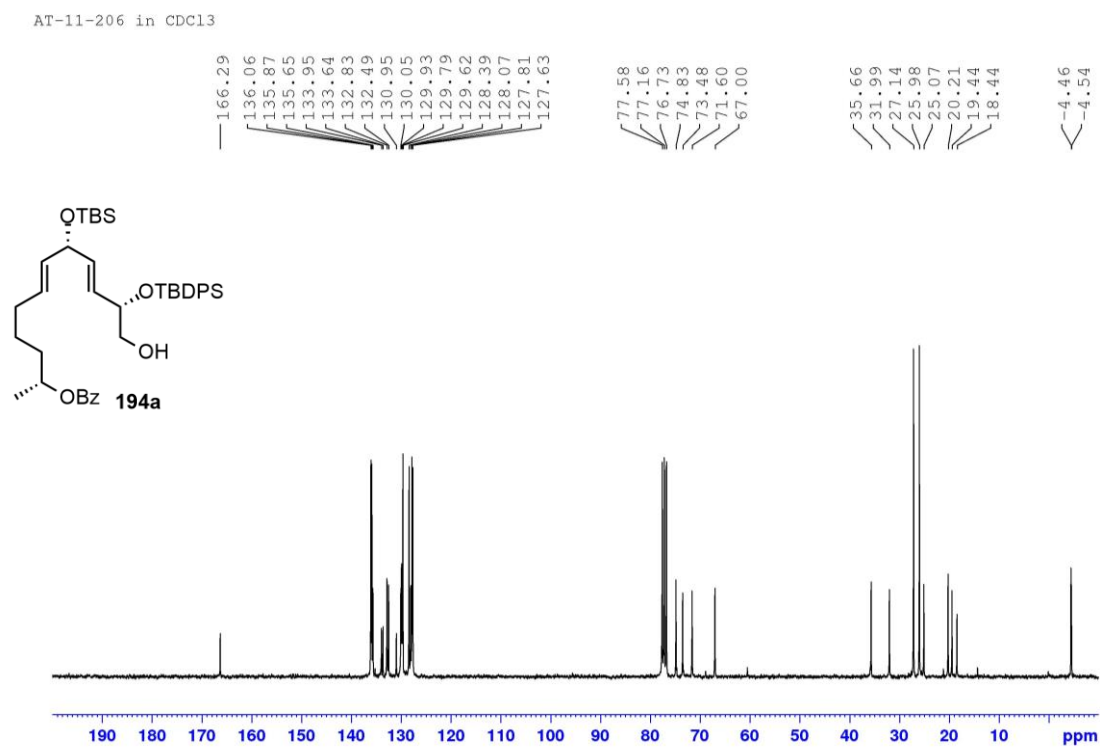
**Figure 125**  $^1\text{H}$  NMR (300 MHz,  $\text{CDCl}_3$ ) spectrum of compound **194**



**Figure 126**  $^{13}\text{C}$  NMR (75 MHz,  $\text{CDCl}_3$ ) spectrum of compound **194**

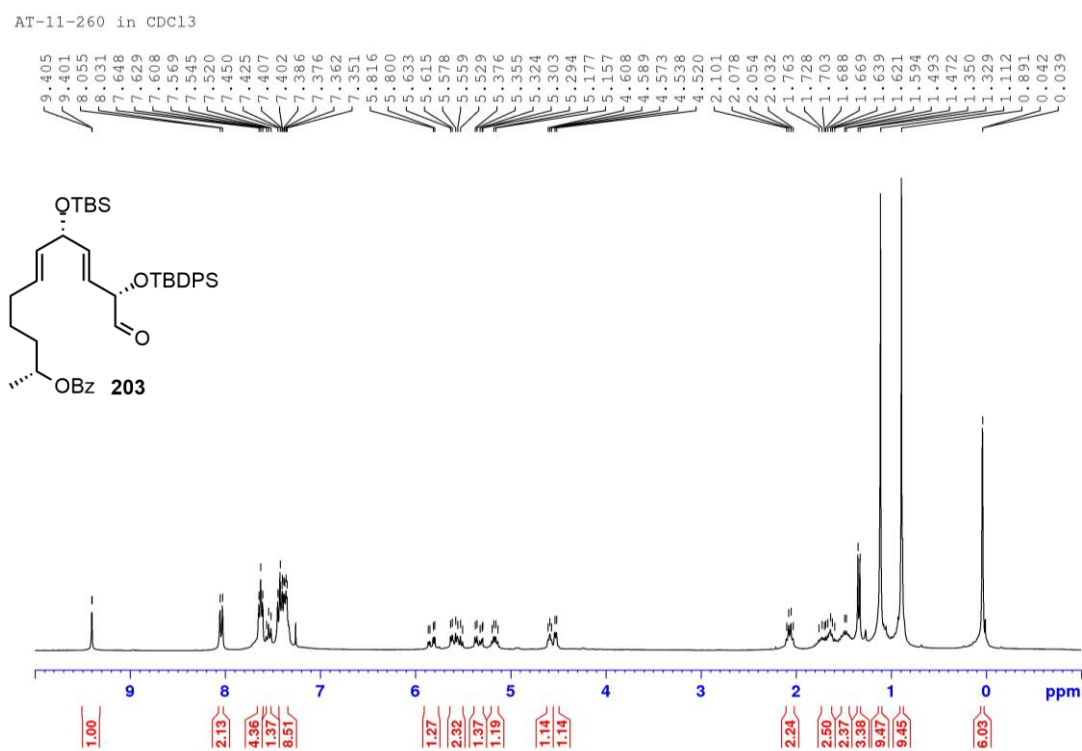




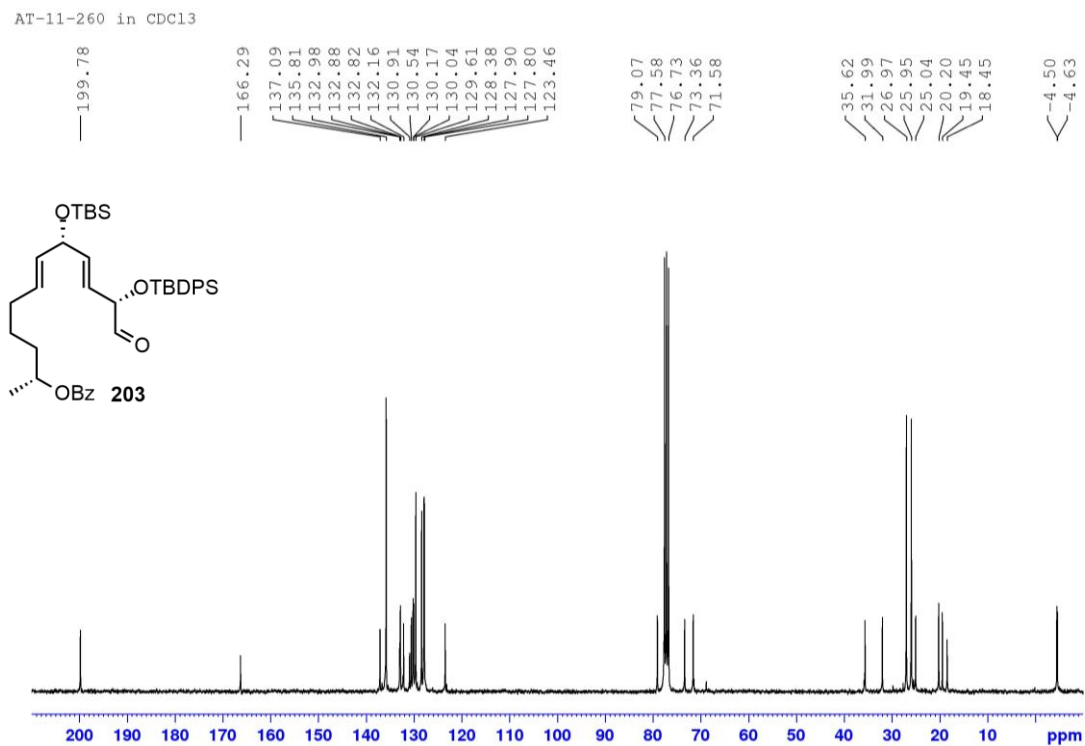
**Figure 127**  $^1\text{H}$  NMR (300 MHz,  $\text{CDCl}_3$ ) spectrum of compound **194a****Figure 128**  $^{13}\text{C}$  NMR (75 MHz,  $\text{CDCl}_3$ ) spectrum of compound **194a**

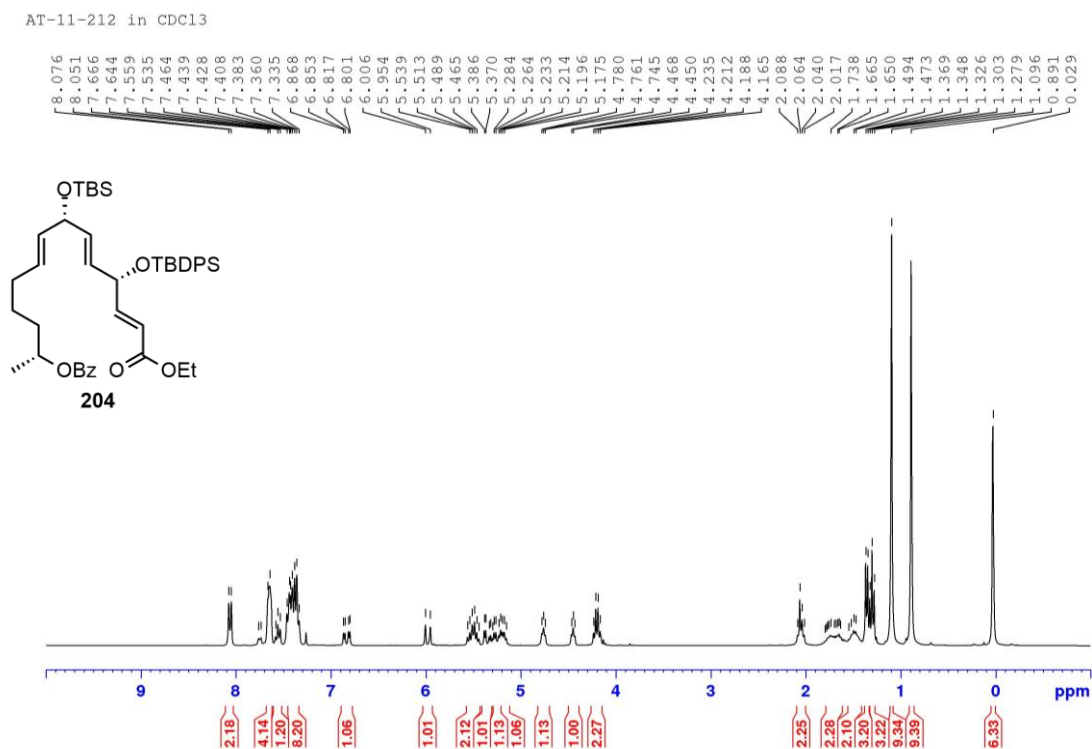
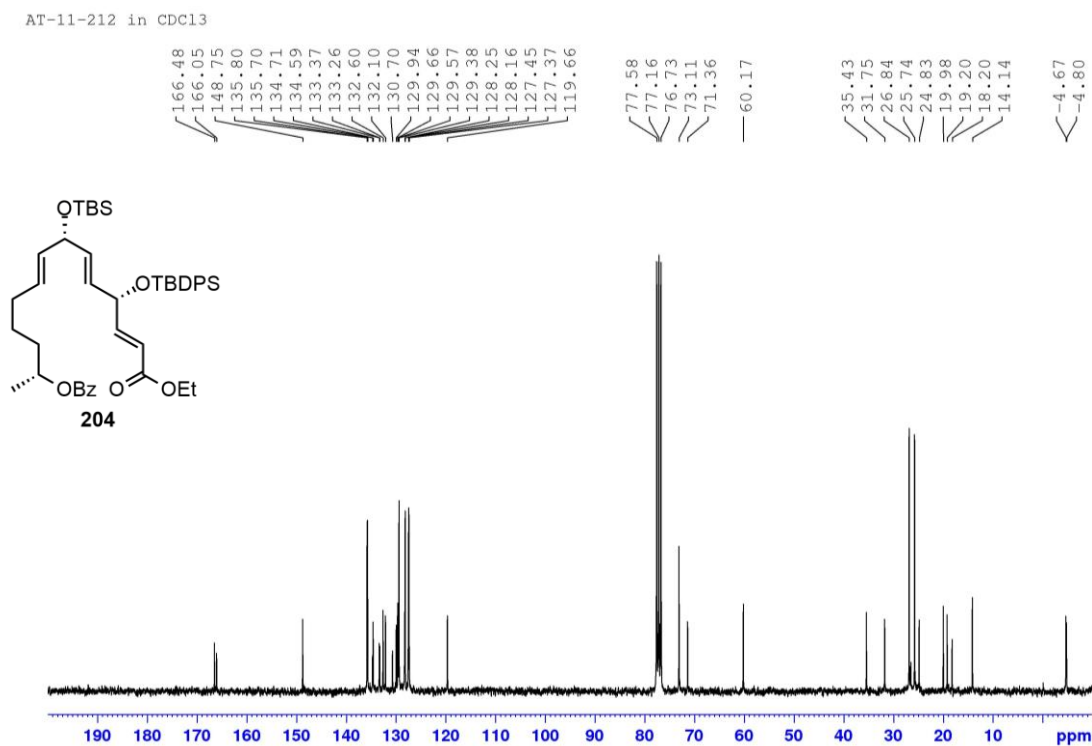


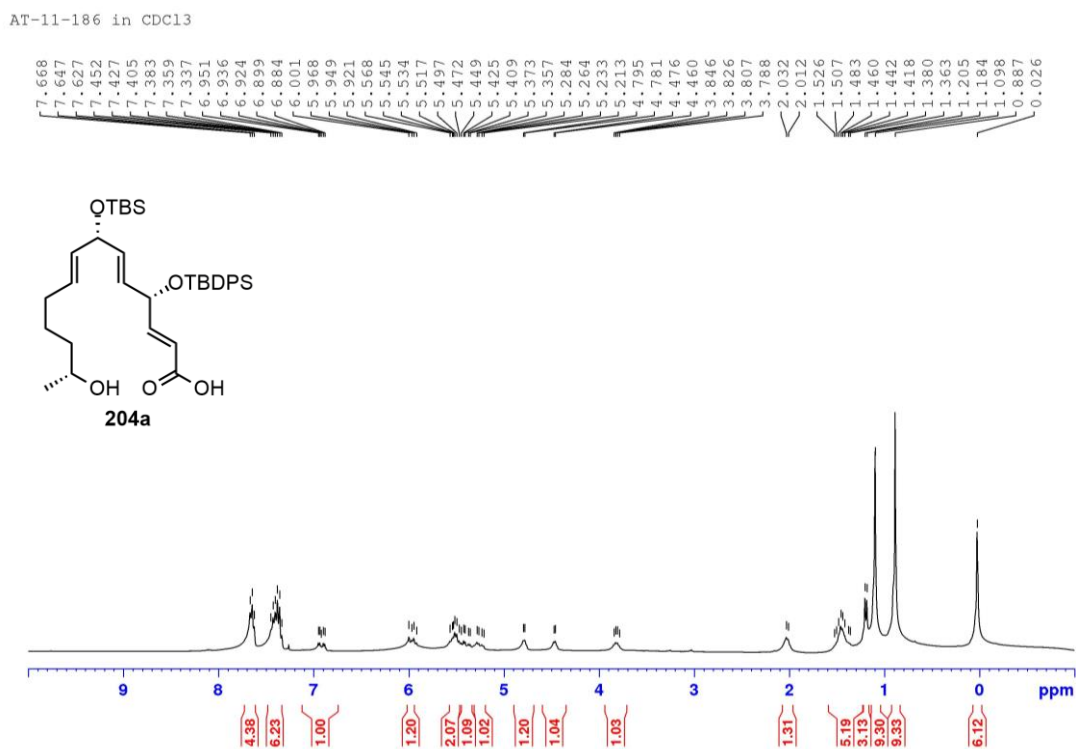
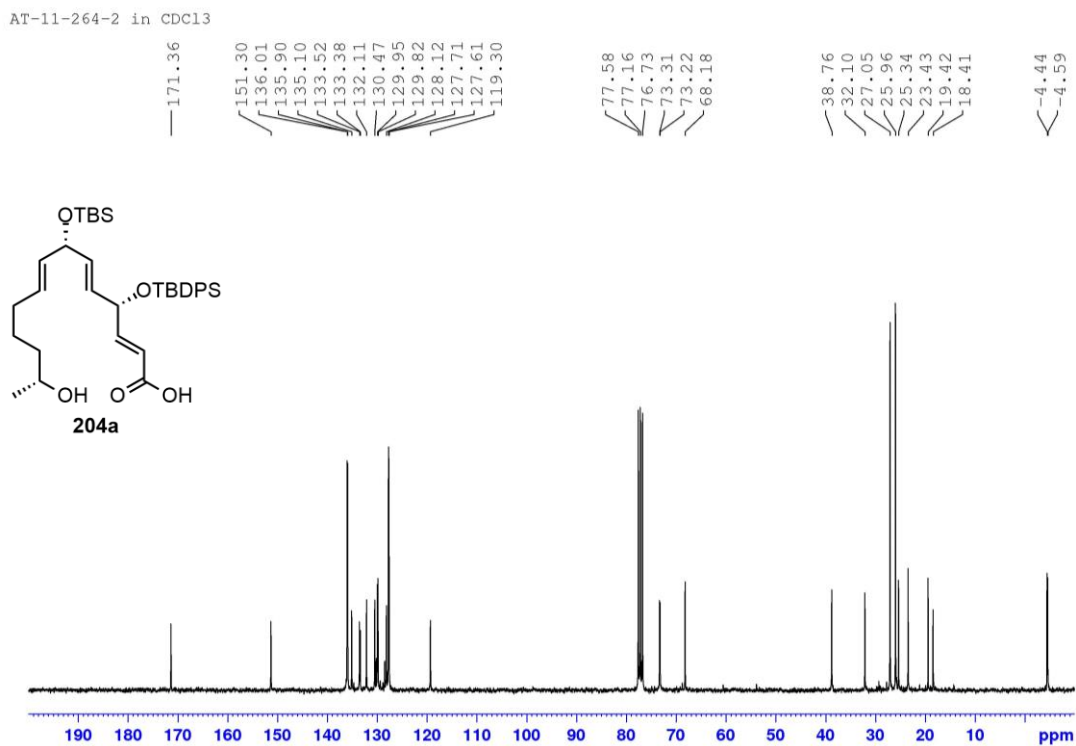
**Figure 129**  $^1\text{H}$  NMR (300 MHz,  $\text{CDCl}_3$ ) spectrum of compound **203**



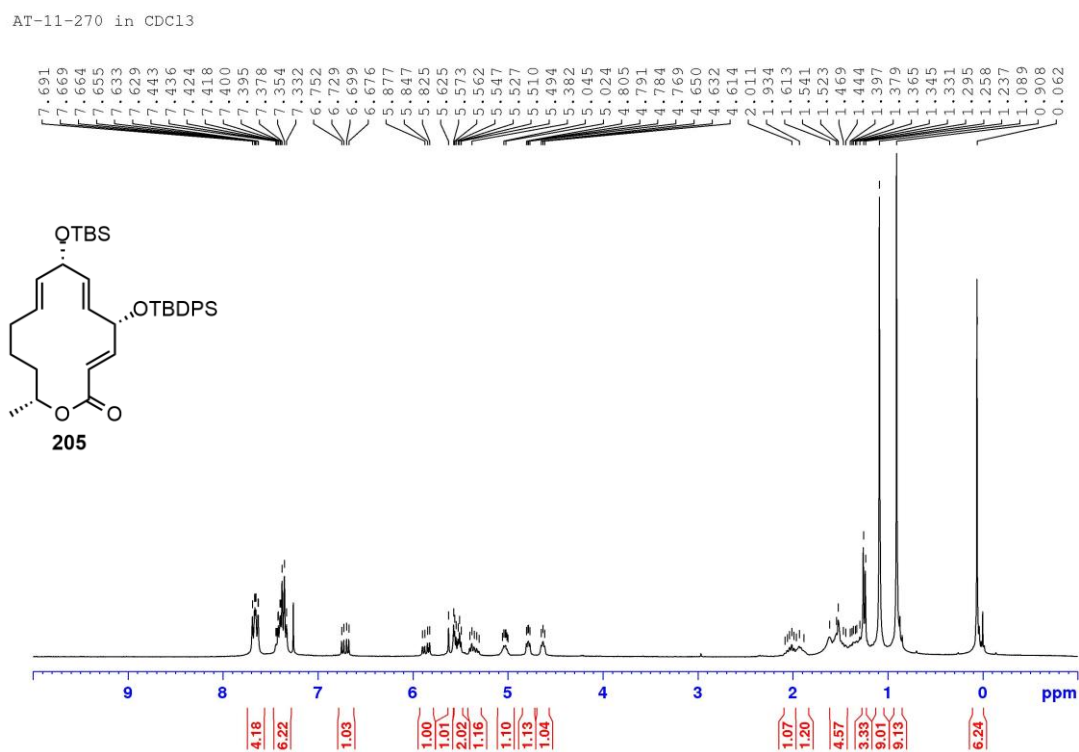
**Figure 130**  $^{13}\text{C}$  NMR (75 MHz,  $\text{CDCl}_3$ ) spectrum of compound **203**



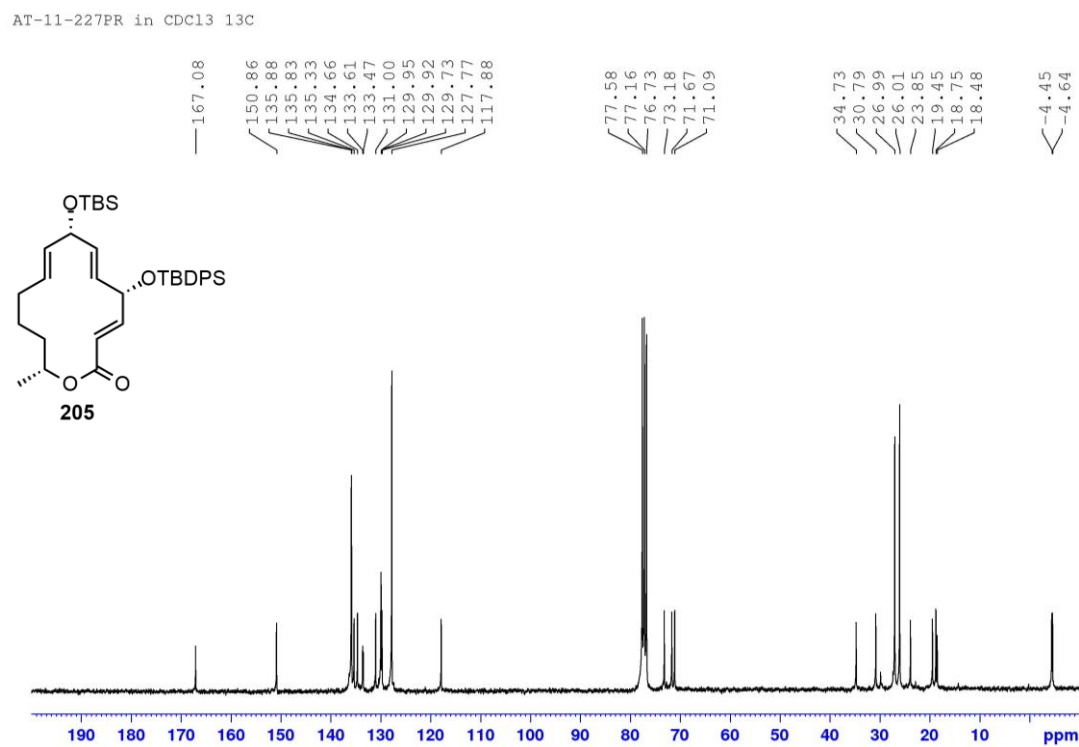
**Figure 131**  $^1\text{H}$  NMR (300 MHz,  $\text{CDCl}_3$ ) spectrum of compound **204****Figure 132**  $^{13}\text{C}$  NMR (75 MHz,  $\text{CDCl}_3$ ) spectrum of compound **204**

**Figure 133**  $^1\text{H}$  NMR (300 MHz,  $\text{CDCl}_3$ ) spectrum of compound **204a****Figure 134**  $^{13}\text{C}$  NMR (75 MHz,  $\text{CDCl}_3$ ) spectrum of compound **204a**

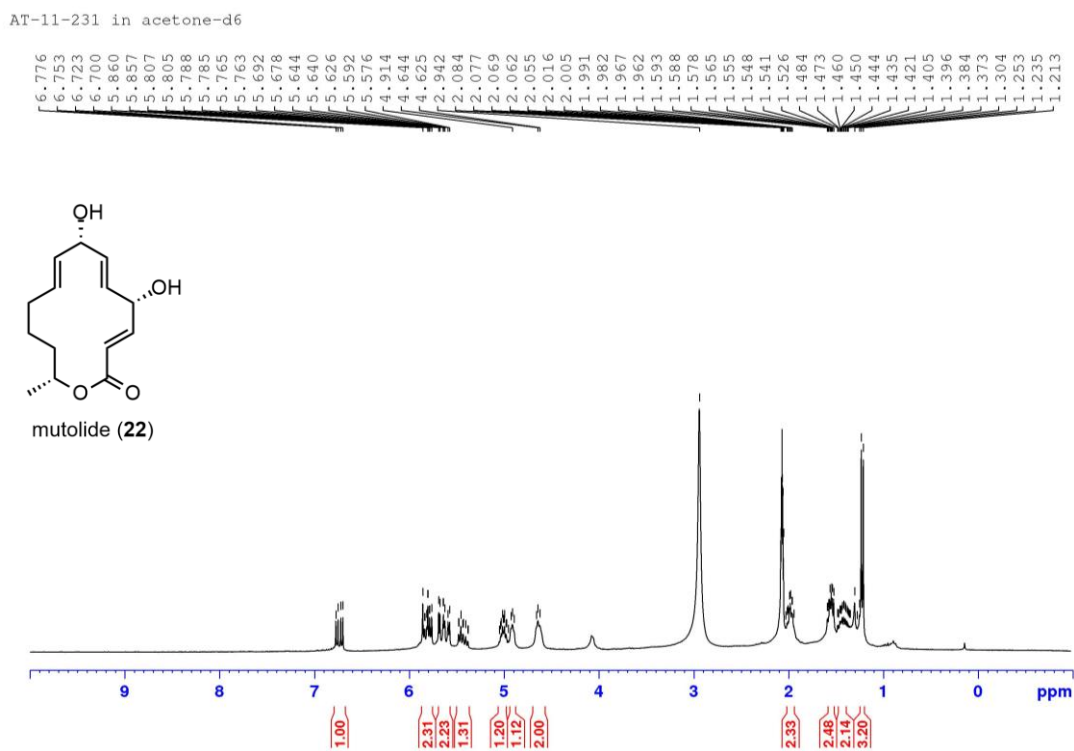
**Figure 135**  $^1\text{H}$  NMR (300 MHz,  $\text{CDCl}_3$ ) spectrum of compound **205**



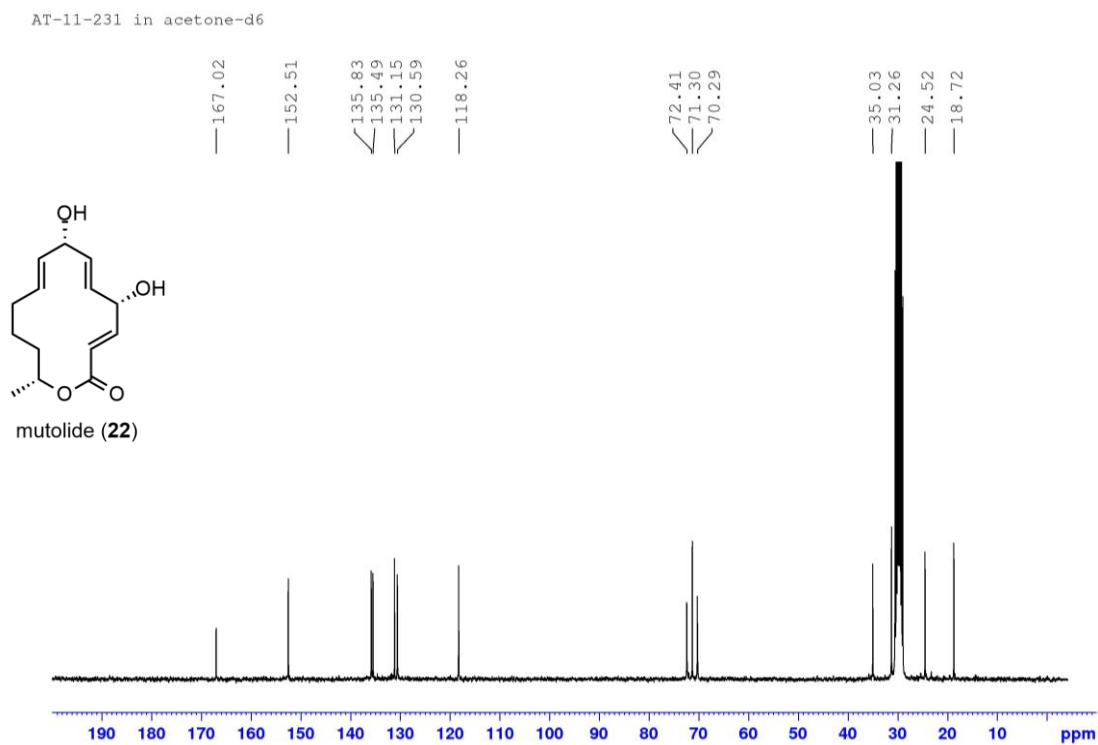
**Figure 136**  $^{13}\text{C}$  NMR (75 MHz,  $\text{CDCl}_3$ ) spectrum of compound **205**



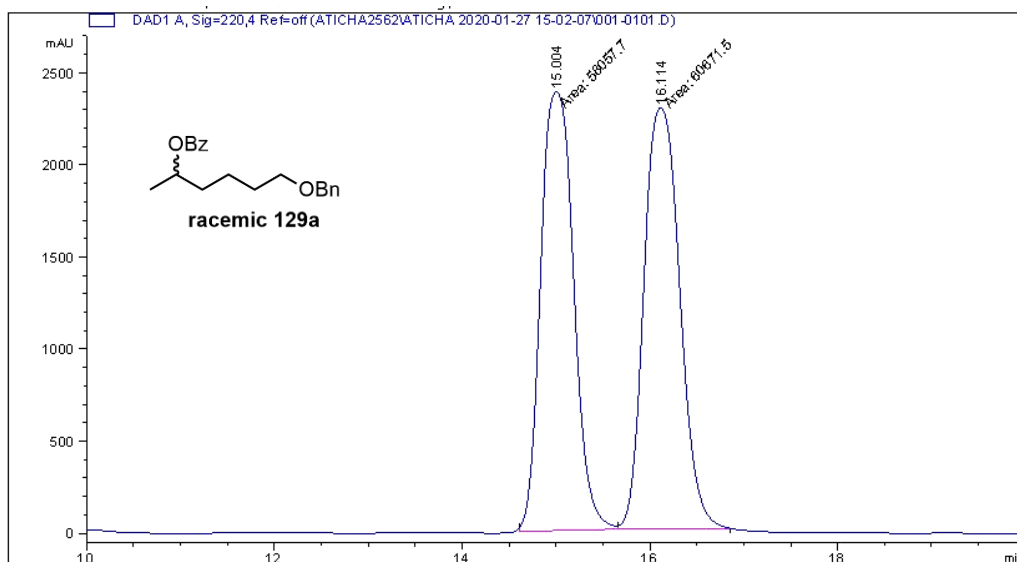
**Figure 137**  $^1\text{H}$  NMR (300 MHz, acetone- $d_6$ ) spectrum of mutolide (22)



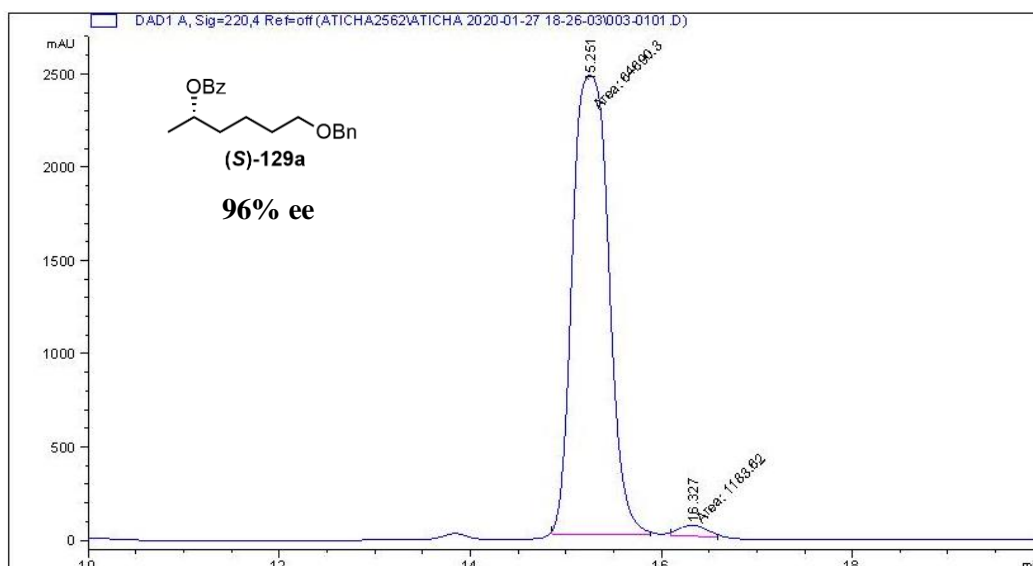
**Figure 138**  $^{13}\text{C}$  NMR (75 MHz, acetone- $d_6$ ) spectrum of mutolide (22)



## HPLC traces

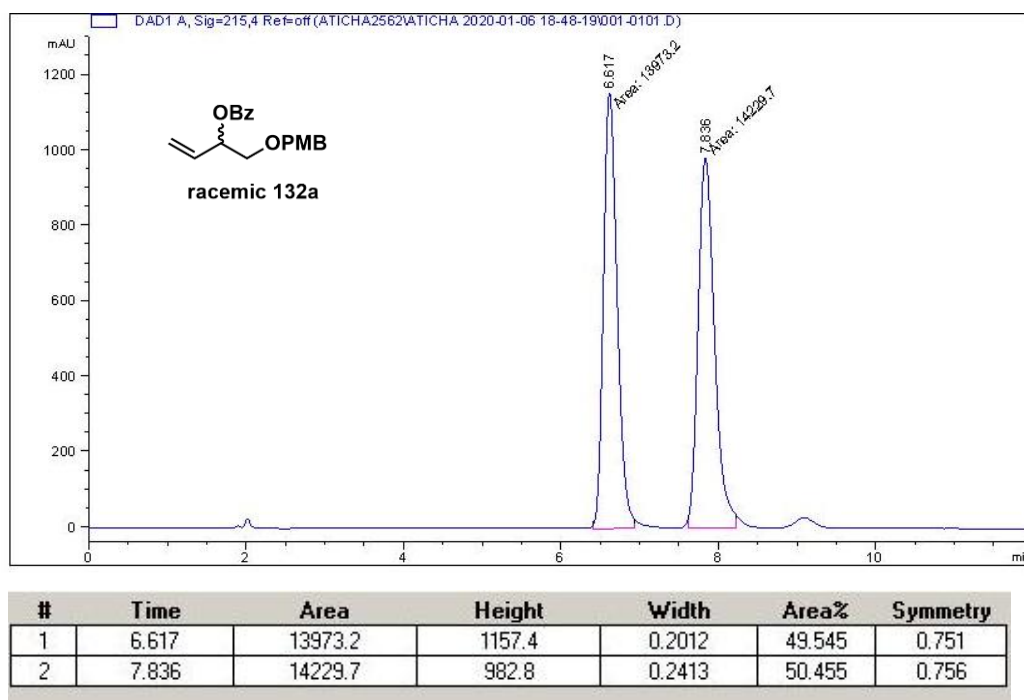
Figure 139 Chromatogram of racemic benzoate ester **129a**

#	Time	Area	Height	Width	Area%	Symmetry
1	15.004	58057.7	2380.6	0.4065	48.899	0.869
2	16.114	60671.5	2288	0.442	51.101	0.834

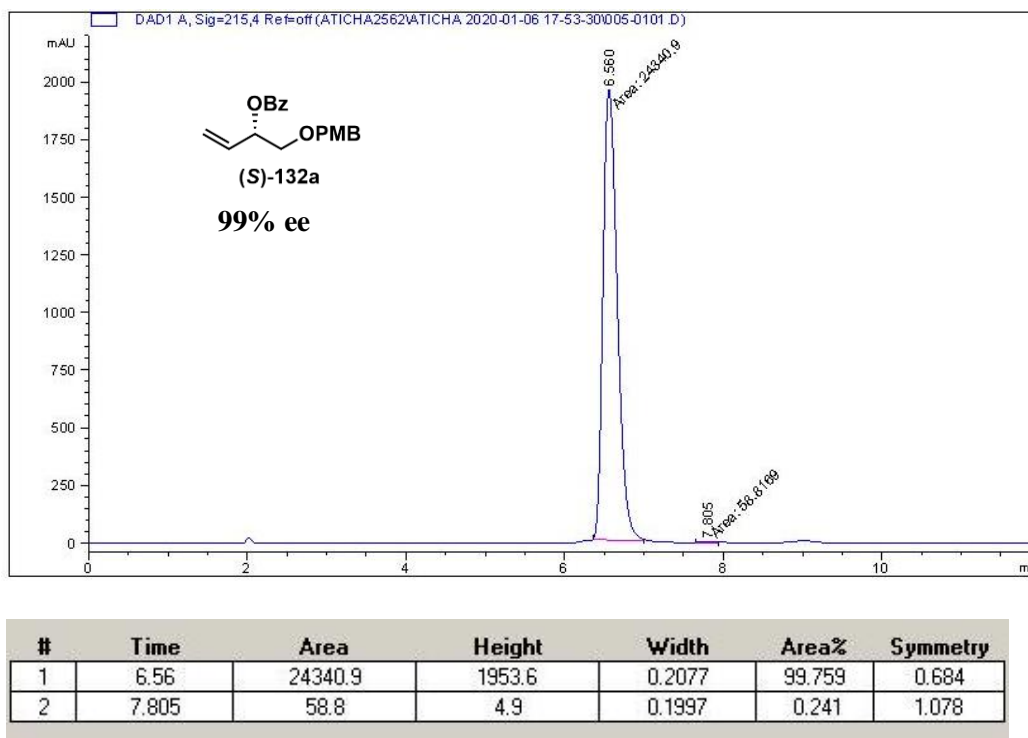
Figure 140 Chromatogram of (*S*)-benzoate ester **129a**

#	Time	Area	Height	Width	Area%	Symmetry
1	15.251	64690.3	2460.7	0.4382	98.203	0.88
2	16.327	1183.6	57.5	0.3433	1.797	0.843

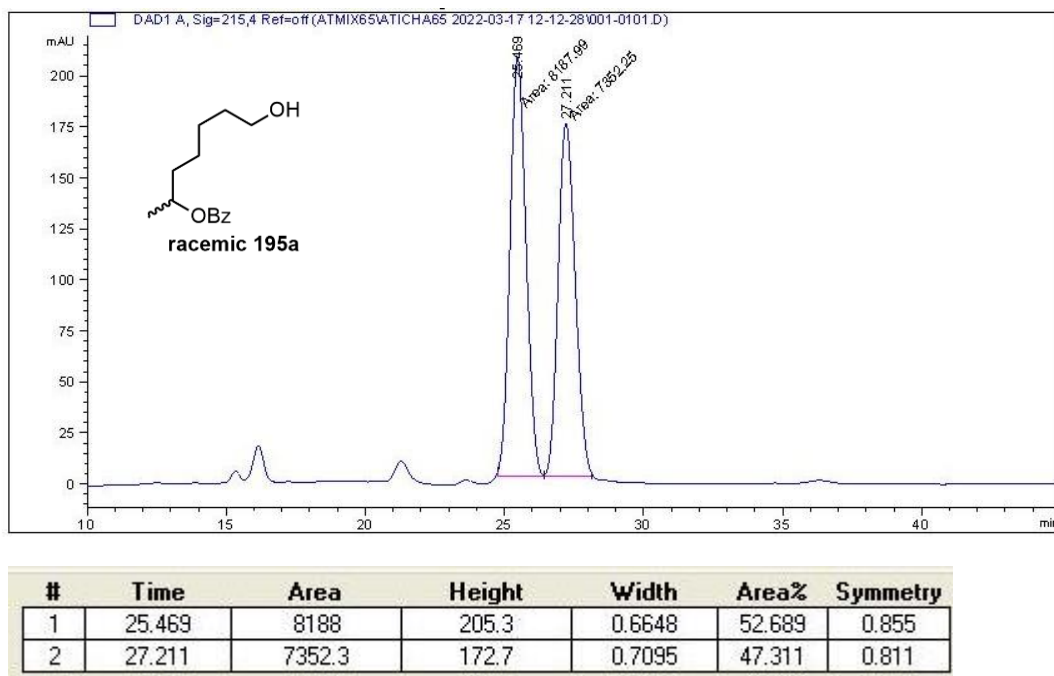
**Figure 141** Chromatogram of racemic benzoate ester **132a**



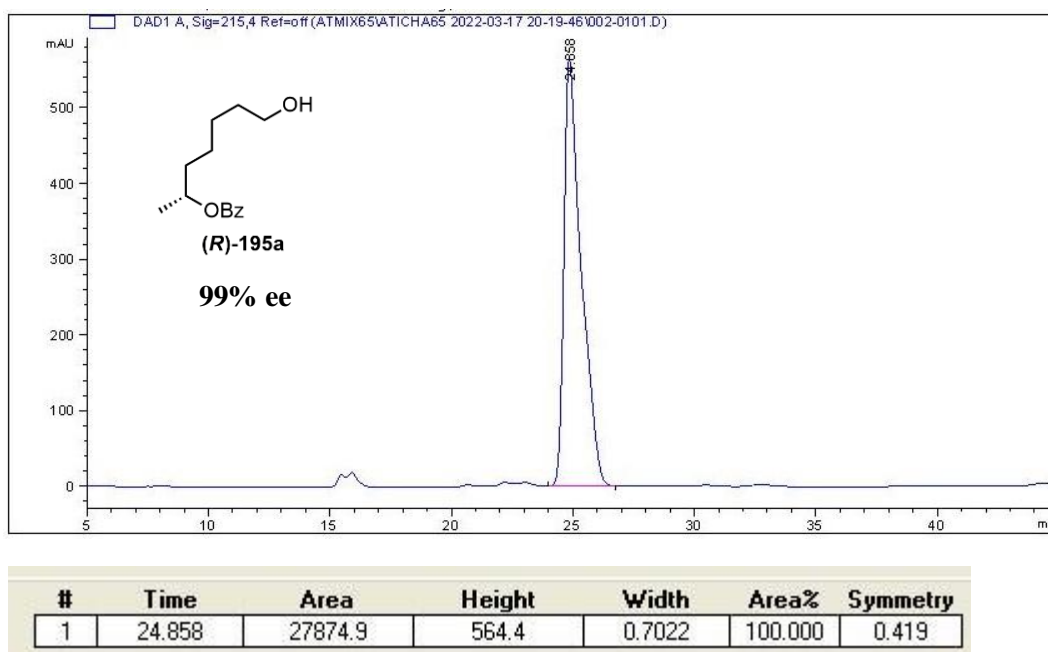
**Figure 142** Chromatogram of (*S*)-benzoate ester **132a**



**Figure 143** Chromatogram of racemic alcohol **195a**



**Figure 144** Chromatogram of (*R*)-alcohol **195a**





## VITAE

**Name** Miss Aticha Thiraporn

**Student ID** 6010230052

### Education Attainment

Degree	Name of Institution	Year of Graduation
B.Sc. (Chemistry) (2 <sup>nd</sup> Hons.)	Prince of Songkla University	2014
M.Sc. (Organic Chemistry)	Prince of Songkla University	2017

### Scholarship Awards during Enrolment

The Science Achievement Scholarship of Thailand (SAST)

### List of Publication

- Tadpetch, K.; Chukong, C.; Jeanmard, L.; Thiraporn, A.; Rukachaisirikul, V.; Phongpaichit, S.; Sakayaroj, J. 2015. Cytotoxic Naphthoquinone and a New Succinate Ester from the Soil Fungus *Fusarium Solani* PSU-RSPG227. *Phytochemistry Lett.* 11, 106–110.
- Thiraporn, A.; Rukachaisirikul, V.; Iawsipo, P.; Somwang, T.; Tadpetch, K. 2017. Total Synthesis and Cytotoxic Activity of 5'-Hydroxyzearelenone and 5 $\beta$ -Hydroxyzearelenone. *Eur. J. Org. Chem.* 7133–7147.
- Thiraporn, A.; Iawsipo, P.; Tadpetch, K. 2022. Total Synthesis and Cytotoxic Activity of 7-O-Methylnigrosporolide and Pestalotioprolide D. *Synlett.* 33 (14), 1341–1346.
- Thiraporn, A.; Saikachain, N.; Khumjiang, R.; Muanprasat, C.; Tadpetch, K. 2022. Total Synthesis and Biological Evaluation of Mutolide and Analogues. *Chem. Asian J.* 17, e202200329.
- Tadpetch, K.; Vijitphan, P.; Kaewsen, S.; Thiraporn, A.; Rukachaisirikul, V. 2022. Direct synthesis of tetrahydropyran-4-ones via O<sub>3</sub>ReOH-catalyzed Prins cyclization of 3-chlorohomoallylic alcohols. *Org. Biomol. Chem.* 20, 9618–9624.